

**Springer**

*Tokyo*

*Berlin*

*Heidelberg*

*New York*

*Barcelona*

*Budapest*

*Hong Kong*

*London*

*Milan*

*Paris*

*Santa Clara*

*Singapore*

N. Ogata · S.W. Kim · J. Feijen · T. Okano (Eds.)

# Advanced Biomaterials in Biomedical Engineering and Drug Delivery Systems

With 364 Figures



Springer

NAOYA OGATA, PH.D.  
Professor, Department of Chemistry, Sophia University  
7-1 Kioi-cho, Chiyoda-ku, Tokyo, 102 Japan

SUNG WAN KIM, PH.D.  
Professor and Director, Center for Controlled Chemical Delivery, Department of Pharmaceutics  
and Pharmaceutical Chemistry, University of Utah  
Salt Lake City, UT 84112, USA

JAN FEIJEN, PH.D.  
Professor, Department of Chemical Technology and Institute of Biomedical Technology,  
University of Twente  
P.O. Box 217,7500 AD Enschede, The Netherlands

TERUO OKANO, PH.D.  
Professor, Institute of Biomedical Engineering, Tokyo Women's Medical College  
8-1 Kawada-cho, Shinjuku-ku, Tokyo, 162 Japan

ISBN 978-4-431-65885-6      ISBN 978-4-431-65883-2 (eBook)  
DOI 10.1007/978-4-431-65883-2

© Springer-Verlag Tokyo 1996

Softcover reprint of the hardcover 1st edition 1996

This work is subject to copyright. All rights are reserved, whether the whole or part of the material is concerned, specifically the rights of translation, reprinting, reuse of illustrations, recitation, broadcasting, reproduction on microfilms or in other ways, and storage in data banks.

The use of registered names, trademarks, etc. in this publication does not imply, even in the absence of a specific statement, that such names are exempt from the relevant protective laws and regulations and therefore free for general use.

Product liability: The publisher can give no guarantee for information about drug dosage and application thereof contained in this book. In every individual case the respective user must check its accuracy by consulting other pharmaceutical literature.

# Foreword



First of all, I would like to share the great pleasure of the successful five-day symposium with every participant in the 5th Iketani Conference which was held in Kagoshima from April 18 (Tuesday) to 22 (Saturday), 1995.

Outstanding speakers enthusiastically presented their up-to-the-minute results. Relatively little time was allotted for each presentation to ensure as much time as possible for intensive discussions on the particular topics that had just been presented. I was delighted to see that the lectures were of high quality, and the discussions were lively, exciting, and productive in a congenial atmosphere. We also had 92 papers in the poster session, in which young (and relatively young) scientists made every effort to present the novel results of their research in advanced biomaterials and drug delivery systems (DDS). I believe some of the research is most promising and will become noteworthy in the twenty-first century.

It was a privilege for me to deliver a lecture at the special session of the symposium. In my introductory remarks, I pointed out five key terms in multifaceted biomaterials research: materials design, concept or methodology, devices, properties demanded, and fundamentals. I am confident that innovative progress in device manufacturing for end-use, e.g., artificial organs, vascular grafts, and DDS, can be brought about only through properly designed advanced materials that exhibit the desired functionality at the interface with any living body. Fundamentals must be studied to elucidate the structure-property relationship in the nature of the interaction of materials with biological elements from the standpoint of molecular and cellular levels. Indeed, this was a guiding principle all through the sessions of the 5th Iketani Conference.

The three days of sessions were most pleasurable ones for me. A number of innovative devices were reported on the basis of a new concept or methodology. These devices will no doubt enhance the quality of human life enormously. There were also several outstanding studies on fundamentals, which, I believe, are now exploring new frontiers of basic science.

Thus, I regard this international symposium as a significant milestone which will surely open for us a new age of science and technology of advanced biomaterials and DDS.

At this time, let me advise young scientists to respect fundamentals and devote themselves to achieving the best background possible in a particular field of basic science. Innovative progress in interdisciplinarily cooperative sciences can be achieved only by cooperation between scientists of different fields when all of them are top-rank specialists in basic science.

This book is an official record of all the papers presented at the three days of sessions of the 5th Iketani Conference. The pleasure I felt at the conference is doubled by this publication, because it will convey exactly to colleagues throughout the world the essence of the presentations and discussions at this milestone symposium.

I would like to take this opportunity to express my heartfelt gratitude to Professor Naoya Ogata and every member of the Triangle Research Collaboration for their enthusiastic efforts to organize this superb international symposium. I also express most sincere appreciation to the Iketani Science and Technology Foundation for their generous financial support to the symposium.

The distinguished contributions of Kagoshima University are highly appreciated. Especially, the Inamori Auditorium provided us a marvelous space and setting for the symposium. Finally, I extend my hearty thanks to all the participants, who found time in their busy schedule to come and join this symposium to celebrate my 75th birthday.

A handwritten signature in black ink, appearing to read 'Teiji Tsuruta', with a long horizontal line extending to the right.

Teiji Tsuruta, Ph.D.  
Professor, Science University of Tokyo  
Professor Emeritus, University of Tokyo

# Preface

The 5th Iketani Conference on Biomedical Polymers was held at the Inamori Hall of Kagoshima University from April 18 to 22, 1995. This international conference focused on advanced biomaterials in biomedical engineering and drug delivery systems and was in honor of Professor Teiji Tsuruta's 75th birthday.

Synthetic polymers have been developed mainly as structural materials such as fibers, films, or plastics since their production began on a large scale as Nylon in 1938. However, other new applications of polymers have been developed since 1980 in terms of high value added materials. Biomedical polymers and drug delivery systems have been developed as intelligent applications of polymeric materials. Such intelligent polymers as biocompatible or stimuli-responsive polymers opened new areas of application. Since 1980, many international conferences on multifunctional polymers have been held in various parts of the world. This conference, however, had a slightly different flavor.

The 5th Iketani Conference was to promote and stimulate the progress of biomedical polymers. The focus was on biomedical engineering and drug delivery systems, which have been moving toward great contributions in the fields of artificial organs and human health care.

Animals or plants are composed mainly of proteins or cellulose, called natural polymers in contrast to synthetic polymers. Both natural and synthetic polymers belong to the same category in terms of macromolecules, but synthetic polymers are generally considered environmentally nonadaptive materials. Recent developments in molecular design have led to more sophisticated and intelligent polymers, especially in biomedical applications of synthetic polymers. This international conference was organized around the concept of making more intelligent approaches through good molecular design to match synthetic polymers with natural polymers.

The conference was also organized in honor of Professor Teiji Tsuruta on his 75th birthday. Professor Tsuruta is one of the pioneers in the field of biomedical polymers and has promoted research on biomedical polymers since 1970, following his marvelous work on anionic polymerizations, especially the asymmetric polymerization of propyleneoxide. The organizing committee wanted to celebrate his 75th birthday at this meeting to promote further progress on biomedical polymers and to motivate and encourage young research scientists.

Kagoshima is located in the southern part of Japan. Some people in Kagoshima say their city is located at the heart of Japan. Modern Japan began in Kagoshima when the Meiji Restoration, the Japanese revolution of 1868, opened a new era and brought an end to the old feudal age. The energy of the fresh, young *samurai* of Kagoshima was able to destroy the old Tokugawa clan and open a new era for Japan. We believed that Kagoshima was an ideal place

to ferment a revolution in biomedical polymers, and the organizing committee decided on Kagoshima as the conference site.

This 5th Iketani Conference attracted about 250 scientists from 11 countries and included 40 invited speakers and 92 poster papers. All participants made a lasting impression at the conference. We believe the conference made a great contribution to progress in biomedical polymers worldwide. We note that many poster contributors presented their excellent papers in the poster session and two young scientists, Dr. Yasuo Suda of Osaka University and Mr. Yuzo Kaneko of Waseda University, received the Triangle Research Collaboration Award for their outstanding presentation. Finally, we would like to acknowledge the Iketani Science and Technology Foundation for their full support of the conference. Without their support our goal could not have been achieved. Many thanks are also due to the members of the Organizing Committee, to Dr. A. Kikuchi, Tokyo Women's Medical College, and Dr. T. Aoki, Sophia University, and to the secretaries who made the conference a success.

Naoya Ogata  
Sung Wan Kim  
Jan Feijen  
Teruo Okano

# Contents

Foreword .....	V
Preface .....	VII
The Organizing and Program Committee.....	XIX
Professor Teiji Tsuruta—Biographical Data .....	XXI
Memories of the Iketani Conference.....	XXIII

## Advanced Biomaterials

Controlled Release Systems Using Swellable Random and Block Copolymers and Terpolymers N.A. PEPPAS, S. VAKKALANKA, C.S. BRAZEL, A.S. LUTTRELL, and N.K. MONGIA .....	3
Polymer Gel—A New Type of Soft Energy Transducer Y. OSADA and J. GONG .....	8
Communicating with the Building Blocks of Life Using Advanced Macromolecular Transducers G.G. WALLACE .....	13
Water-Soluble Nucleic Acid Analogs—Preparation and Properties— K. TAKEMOTO .....	18
Intelligent Materials T. OKANO, A. KIKUCHI, Y. KANEKO, K. SAKAI, M. MATSUKATA, N. OGATA, and Y. SAKURAI.....	23
Functional Synthetic and Semisynthetic Polymers in Biomedical Applications E. CHIPELLINI and R. SOLARO.....	28
Bioconjugates from Synthetic Polymers—How They Can Be Married?— N. OGATA .....	32
Plasma Modification of Polymeric Surfaces for Biomedical Applications J.G.A. TERLINGEN, A. BRUIL, A.S. HOFFMAN and J. FEIJEN .....	38
New Polymeric Materials Design for Biomedical Applications T. TSURUTA .....	43



## Novel Approaches to Drug Delivery Systems and Future Trends

New Oral Drug Delivery System R.M. OTTENBRITE, R. ZHAO and S. MILSTEIN . . . . .	51
Penetration of Polymeric Drug Carriers into K562 Cells K. ABDELLAOUI, M. BOUSTTA, H. MORJANI, M. MANFAIT, and M. VERT . . . . .	57
Novel Bioadhesive, pH- and Temperature-Sensitive Graft Copolymers for Prolonged Mucosal Drug Delivery A.S. HOFFMAN, G.H. CHEN, S.Y. KAANG, Z.L. DING, K. RANDERI, and B. KABRA. . . . .	62
Enhanced Intestinal Absorption of Peptides by Complexation of the Partially Denatured Peptide J.R. ROBINSON and G.M. MLYNEK . . . . .	67
Controlled Drug Delivery Formulation with Safe Polymers T. NAGAI, M. MORISHITA, I. MORISHITA, Y. SUZUKI, and Y. MAKINO . . . . .	71
Supramolecular Assemblies for Improved Drug Delivery System J. SUNAMOTO . . . . .	76
Biodegradable Polyphosphazenes for Biomedical Applications E. SCHACHT, J. VANDORPE, J. CROMMEN, and L. SEYMOUR . . . . .	81
Receptor-Mediated Cell Specific Delivery of Drugs to the Liver and Kidney M. HASHIDA, M. NISHIKAWA, and Y. TAKAKURA . . . . .	86
Biorecognizable Biomedical Polymers J. KOPEČEK, P. KOPEČKOVÁ, and V. OMELIANENKO . . . . .	91
Nanosopic Vehicles with Core-Shell Structure for Drug Targeting K. KATAOKA. . . . .	96
Third Phase in Polymer Drug Development—SMANCS As a Prototype Model Drug for Cancer Treatment— H. MAEDA . . . . .	101
Development of a Tetracycline Delivery System for the Treatment of Periodontal Disease Using a Semisolid Poly(ortho ester) J. HELLER, K.V. ROSKOS, B.K. FRITZINGER, S.S. RAO, and G.C. ARMITAGE. . . . .	106
Mechanistic Aspects of Transdermal Drug Transport W.I. HIGUCHI, K. YONETO, A.-H. GHANEM, S.K. LI, D.J.A. CROMMELIN, J.N. HERRON, and Y.-H. KIM . . . . .	111
Transbuccal Delivery of Polar Compounds B. YANG and K. KNUTSON . . . . .	116
Receptor-Mediated Targeting of Peptides and Proteins Y. SUGIYAMA and Y. KATO. . . . .	121
Temperature Sensitive Polymers for Delivery of Macromolecular Drugs S.W. KIM . . . . .	126

**Biomedical Engineering**

Novel Biomaterials As Artificial Cornea via Plasma Induced Grafted Polymerization  
 G.-H. HSIUE, S.-D. LEE, C.-Y. KAO, and P.C.-T. CHANG . . . . . 137

Ultrathin Polymeric Films As Biomedical Interfaces of Controlled Chemical Architecture  
 D.W. GRAINGER, G. MAO, and D.G. CASTNER . . . . . 142

Randomness and Biospecificity: Random Copolymers Are Endowed with Biospecific Properties  
 M. JOZEFOWICZ and J. JOZEFONVICZ . . . . . 147

Strategy and Bionic Design of Vital Functioning Vascular Wall Reconstruction  
 T. MATSUDA . . . . . 153

Surface Modification of Biomaterials by Topographic and Chemical Patterning  
 A. CURTIS and S. BRITLAND . . . . . 158

Interleukin-4 Mediated Foreign Body Giant Cell Formation and Cytoskeletal Rearrangement on Poly(etherurethane urea) In Vivo and In Vitro  
 J.M. ANDERSON, W.J. KAO, K.M. DEFIFE, A.K. McNALLY, and C. JENNEY . . . . . 163

Polymer-Supported Tissue Engineering  
 Y. IKADA . . . . . 168

New Frontier of Biomimetic Glycotechnology for Cellular and Tissue Engineering  
 T. AKAIKE, M. GOTO, H. YURA, A. KOBAYASHI, C.-S. CHO, A. MARUYAMA, and K. KOBAYASHI . . . . . 173

Control of Healing with Photopolymerizable Biodegradable Hydrogels  
 J.A. HUBBELL, J.L. WEST, and S.M. CHOWDHURY . . . . . 179

A Novel Biomaterial: Aramid-Silicone Resin  
 M. AKASHI, T. FURUZONO, T. MATSUMOTO, A. KISHIDA, and I. MARUYAMA . . . . . 183

Gradient Surfaces As Tools to Study Biocompatibility  
 H.B. LEE, B.J. JEONG, and J.H. LEE . . . . . 188

Preparation of Self-Assembled Biomimetic Membranes and Their Functions  
 N. NAKABAYASHI . . . . . 193

Synthesis and Cell-Adhesion Properties of Polyurethanes Containing Covalently Grafted RGD-Peptides  
 H.-B. LIN and S.L. COOPER . . . . . 198

**Biomaterials and Biomedical Engineering**

One Pot Synthesis of Poly(ethylene oxide) with a Cyano Group at One End and a Hydroxyl Group at the Other End  
 M. IJIMA, Y. NAGASAKI, M. KATO, and K. KATAOKA . . . . . 205

Creation of New Si-Containing Block Copolymer Membrane with Both High Gas Permeability and Blood Compatibility H. ITO, A. TAENAKA, Y. NAGASAKI, K. KATAOKA, M. KATO, T. TSURUTA, K. SUZUKI, T. OKANO, and Y. SAKURAI .....	207
Surface Modification of Poly(lactic acid) with Bioactive Peptides T. YAMAOKA, Y. TAKEBE, and Y. KIMURA .....	209
Adsorption of Biomolecules onto Multiblock Copolymer Consisting of Aromatic Polyamide and Poly(dimethylsiloxane) T. FURUZONO, A. KISHIDA, T. MATSUMOTO, I. MARUYAMA, T. NAKAMURA, and M. AKASHI .....	211
Hemocompatible Cellulose Dialysis Membrane Modified with Phospholipid Polymer K. ISHIHARA and N. NAKABAYASHI .....	213
Artificial Glycoconjugate Polymers: Cell-Specific Biomedical Materials Using Carbohydrates As Recognition Signals K. KOBAYASHI, T. USUI, and T. AKAIKE .....	215
Preparation of Acrylamide Coated PVC Tube by APG Treatment and Its Characterization Y. BABUKUTTY, M. KODAMA, H. NOMIYAMA, M. KOGOMA, and S. OKAZAKI .....	217
Anticoagulant Properties of Sulfonated Glucoside-Bearing Polymer N. SAKAMOTO, K. SUZUKI, A. KISHIDA, and M. AKASHI .....	219
Histological and Morphological Comparison of Explanted Small Diameter PU and ePTFE Vascular Prostheses: A Preliminary Study Z. WANG, Z. ZHANG, and M. KODAMA .....	221
Poly(acrylamides) Containing Sugar Residues: Synthesis, Characterization and Cell Compatibility Studies R. BAHULEKAR, J. KANO, and M. KODAMA .....	223
Molecular Design of Artificial Lectin; Recognition and Killer Cell Induction of Lymphocytes by a Novel Water Soluble Polymer Having Phenylboronic Acid Moiety H. MIYAZAKI, K. KATAOKA, T. OKANO, and Y. SAKURAI .....	225
Selective Adhesion and Spontaneous Fusion of Platelets on Polyion Complex Composed of Phospholipid Polymers K. ISHIHARA, H. INOUE, K. KURITA, and N. NAKABAYASHI .....	227
Thermo-Responsive Polymer Surfaces for Cell Culture: Analysis of the Surfaces and Control of the Cell Attachment/Detachment H. SAKAI, Y. DOI, T. OKANO, N. YAMADA, and Y. SAKURAI .....	229
RGDS-Carrying Latex Particles for Cell Activation and Integrin Separation Y. KASUYA, Y. INOMATA, H. GAKUMAZAWA, K. FUJIMOTO, and H. KAWAGUCHI .....	231
Estimation of the Secondary Structure of Fibronectin Adsorbed to Polystyrene and Deprotected Poly( $\epsilon$ - <i>N</i> -benzyloxycarbonyl-L-lysine) by FTIR ATR Spectroscopy K. KUGO, K. MATSUTANI, and J. NISHINO .....	233

Hybrid Biomaterials Comprising Double-Helical DNA. Covalent Coupling Between $\lambda$ Phage DNA and Poly( <i>N</i> -isopropylacrylamide) M. MAEDA, D. UMEMO, and M. TAKAGI .....	235
Preparation of Glucose-Sensitive Hydrogels by Entrapment or Copolymerization of Concanavalin A in a Glucosyloxyethyl Methacrylate Hydrogel T. MIYATA, A. JIKIHARA, K. NAKAMAE, T. URAGAMI, A.S. HOFFMAN, K. KINOMURA, and M. OKUMURA .....	237
Complexation of Neocarzinostatin Chromophore with a Hydrophobized Polysaccharide As an Apoprotein Model M. KUBOYAMA, T. UEDA, K. AKIYOSHI, and J. SUNAMOTO .....	239
Hydrolytic Degradation of Poly(L-lactide-co- $\epsilon$ -caprolactone)s A. NAKAYAMA, I. ARVANITTOYANNIS, N. KAWASAKI, K. HAYASHI, and N. YAMAMOTO	241
Selective Adsorption of Plasma Protein onto Phase-Separated Domain of Immobilized Organosilane Monolayer Surfaces A. TAKAHARA, K. KOJIO, S. GE, and T. KAJIYAMA .....	243
The Possibility of the Constitution of an Artificial Thymus by Utilizing Keratinocytes N. NEGISHI, M. NOZAKI, J. OHNO, T. TODA, and H. MATSUSHITA .....	245
Improved Nonthrombogenicity of Heparin Immobilized and Sulfonated Polyurethane: In Vitro Evaluation Using Epifluorescent Video Microscopy C. NOJIRI, S. KURODA, T. KIDO, K. HAGIWARA, K. SENSHU, K.D. PARK, Y.H. KIM, K. SAKAI, and T. AKUTSU .....	247
Evaluation of a Newly Developed Biological Patch H.-W. SUNG, Y. CHANG, Y.-T. CHIU, J.-H. LU, H.-L. HSU, and C.-C. SHIH .....	249
Application of HEMA-St Block Copolymer Coated Small Caliber Vascular Graft for Veins K. SUZUKI, T. OKANO, Y. SAKURAI, S. TERADA, M. NOZAKI, and N. TAKEMURA .....	251
Transfer and Surface Fixation of Gels by an Excimer Laser Ablation Y. NAKAYAMA and T. MATSUDA .....	253
PVA Hydrogel As an Artificial Vitreous Body M. KODAMA, B. WANG, G. MU, A. YAMAUCHI, T. MATSUURA, Y. HARA and M. SAISHIN .....	255
Analysis of Plasma Membrane Glycocalyx and/or of Quantitative Computerized Cytological Image of Platelets Adhered to HEMA-St ABA Type Block Copolymer Surfaces with Good Antithrombogenicity K. ABE, M. SUGAWARA, T. HORIE, K. SUZUKI, T. OKANO, and Y. SAKURAI .....	257
Immobilization of Human Thrombomodulin onto Biomaterials: Evaluation of Antithrombogenicity Using Small Dialyzer A. KISHIDA, Y. AKATSUKA, Y. UENO, I. MARUYAMA, and M. AKASHI .....	259
Surface Characterization of HEMA-Styrene Block Copolymer Using Transmission Electron Microscopy K. SENSHU, C. NOJIRI, T. KIDO, S. YAMASHITA, A. HIRAO, and S. NAKAHAMA .....	261

Induction of Endothelial Cell Differentiation on Copolymer Surfaces Having Phenylboronic Acid Groups T. AOKI, Y. NAGAO, E. TERADA, K. SANUI, N. OGATA, N. YAMADA, A. KIKUCHI, T. OKANO, Y. SAKURAI, and K. KATAOKA .....	263
Immobilization of Biosignal Proteins to Control Cellular Functions Y. ITO, J. ZHENG, and Y. IMANISHI .....	265
Temperature-Modulated Surface Hydrophilic/Hydrophobic Alterations for Novel Recovery of Cultured Cells A. KIKUCHI, M. OKUHARA, F. OGURA, Y. SAKURAI, and T. OKANO .....	267
Cell Cultures on Plasma-Modified Nylon Meshes and Collagen/Nylon Composite Biomatrix S.M. KUO, S.W. TSAI, and Y.J. WANG .....	269
Direct Extraction of Taste Receptor Proteins by Liposome from Intact Epithelium of Bullfrog Tongue M. NAKAMURA, K. TSUJII, and J. SUNAMOTO .....	271
The Influence of Serum on the Spreading of Tumor Cells on Synthetic Glycolipid Films T. SATO, M. ENDO, and Y. OKAHATA .....	273
Transfer of Membrane Proteins from Human Erythrocytes to Liposomes Y. OKUMURA, K. SUZUKI, M. GOTO, and J. SUNAMOTO .....	275
Reconstitution of Bovine Placental Insulin Receptor on Artificial Vesicles by Using Direct Protein Transfer Techniques T. UEDA and J. SUNAMOTO .....	277
Protein Reconstitution from Cell Membrane to Monolayer Using Direct Transfer Technique G. GLÜCK, Y. OKUMURA, and J. SUNAMOTO .....	279
Glucose Responsive Inter-Polymer Complex Gel Based on the Complexation Between Boronic Acid and Polyols—Mechanism of Gelation and Glucose Exchange— I. HISAMITSU, K. KATAOKA, T. OKANO, and Y. SAKURAI .....	281
Synthesis of Ionic Polyurethane Elastomers As Chemomechanical Materials T. SHIIBA and M. FURUKAWA .....	283
A Synthetic Polyanion Polymer As a Growth Promoter for L929 Mouse Fibroblast T. SAWA, Y. OKUMURA, J.-L. DING, R.M. OTTENBRITE, and J. SUNAMOTO .....	285
Adhesion of Fibroblast onto Poly( $\gamma$ -benzyl L-glutamate)/Poly(ethylene oxide) Diblock Copolymer Langmuir-Blodgett Films C.-S. CHO, A. KOBAYASHI, M. GOTO, K.-H., PARK, and T. AKAIKE .....	287
New Bioactive Macromolecular Glycolipids from Bacterial Cell Surface Y. SUDA, H. TAKADA, T. HAYASHI, T. TAMURA, S. KOTANI, and S. KUSUMOTO .....	289
$^{13}\text{C}$ -Labeling in Methionine Methyl Groups of Glycophorin A <sup>M</sup> and Its Effect on the Secondary Structure Z. ZHOU, Y. OKUMURA, and J. SUNAMOTO .....	291

Stabilization of Enzyme by Polymer with Pendant Monosaccharide K. NAKAMAE, T. NISHINO, Y. SAIKI, Y. YOSHIDA, M. OKUMURA, K. KINOMURA, and A.S. HOFFMAN . . . . .	293
Molecular Architecture of Temperature-Responsive Bioconjugates M. MATSUKATA, T. AOKI, K. SANUI, N. OGATA, A. KIKUCHI, Y. SAKURAI, and T. OKANO. . . . .	295
Stabilization of L-Asparaginase by Chemical Modification with Poly(ethylene glycol) Derivatives M. HIROTO, A. MATSUSHIMA, H. NISHIMURA, Y. KODERA, and Y. INADA . . . . .	297
New Polymeric Hydrogels for the Removal of Uraemic Toxins G. BARSOTTI, E. CHIellini, E. DOSSI, D. GIANNASI, S. GIOVANNETTI, G. MAZZANTI, and R. SOLARO . . . . .	299
Estimation of Biocompatibility of Polymeric Materials Using RT-PCR Method S. KATO, K. OHMURA, A. KISHIDA, K. SUGIMURA, and M. AKASHI. . . . .	301
Temperature Responsive Swelling-Deswelling Kinetics of Poly( <i>N</i> -isopropylacrylamide) Grafted Hydrogels Y. KANEKO, K. SAKAI, R. YOSHIDA, A. KIKUCHI, Y. SAKURAI, and T. OKANO. . . . .	303
Temperature-Sensitive Changes in Surface Properties of a Poly( <i>N</i> -isopropylacrylamide) Hydrogel Layer K. MAKINO, K. SUZUKI, Y. SAKURAI, T. OKANO, and H. OHSHIMA. . . . .	305
Effect of Anion-Exchange Capacity and Porosity of Polyethyleneimine-Immobilized Cellulose Fibers on Selective Removal of Endotoxin S. MORIMOTO, T. IWATA, A. ESAKI, M. SAKATA, H. IHARA, and C. HIRAYAMA. . . . .	307
Cellular Communication with Conducting Electroactive Polymers A.J. HODGSON, M.J. JOHN, M. KELSO, and G.G. WALLACE . . . . .	309
 <b>Drug Delivery Systems</b>	
Stimuli-Sensitive Release of Lysozyme from Hydrogel Containing Phosphate Groups K. NAKAMAE, T. NIZUKA, T. MIYATA, T. URAGAMI, A.S. HOFFMAN, and Y. KANZAKI. . . . .	313
Slow Release of Heparin from a Hydrogel Made from Polyamine Chains Grafted to a Temperature-Sensitive Polymer Backbone Y. NABESHIMA, Z.L. DING, G.H. CHEN, A.S. HOFFMAN, H. TAIRA, K. KATAOKA, and T. TSURUTA . . . . .	315
Formation of Core-Shell Type Nano-Associates Through Electrostatic Interaction Between Peptide and Block Copolymer with Poly(ethylene glycol) Segment A. HARADA and K. KATAOKA. . . . .	317
PEG-Poly(lysine) Block Copolymer As a Novel Type of Synthetic Gene Vector with Supramolecular Structure S. KATAYOSE and K. KATAOKA . . . . .	319

Development of Polymeric Micelles for Drug Delivery of Indomethacin S.B. LA, K. KATAOKA, T. OKANO, and Y. SAKURAI .....	321
Synthesis of Heterobifunctional Poly(ethylene glycol) with a Reducing Monosaccharide Residue at One End for Drug Delivery T. NAKAMURA, Y. NAGASAKI, M. KATO, and K. KATAOKA .....	323
Functional Polymeric Micelles: Synthesis and Characterization S. CAMMAS, Y. NAGASAKI, K. KATAOKA, T. OKANO, and Y. SAKURAI .....	325
Micelle Forming Polymeric Anticancer Drug Containing Chemically Bound and Physically Incorporated Adriamycin T. SETO, S. FUKUSHIMA, H. EKIMOTO, M. YOKOYAMA, T. OKANO, Y. SAKURAI, and K. KATAOKA .....	327
Pharmaceutical Aspects of Block Copolymer Micelles G.S. KWON, M. NAITO, M. YOKOYAMA, T. OKANO, Y. SAKURAI, and K. KATAOKA ....	329
Nanosize Hydrogel Formed by Self-Assembly of Hydrophobized Polysaccharides K. AKIYOSHI, S. DEGUCHI, I. TANIGUCHI, and J. SUNAMOTO .....	331
Novel Design of Supramolecular-Structured Biodegradable Polymer for Drug Delivery N. YUI and T. OOYA .....	333
Interaction of Poly(ethylene oxide)-Bearing Lipid Reconstituted Liposomes with Murine B16 Melanoma Cells M. HARATAKE and J. SUNAMOTO .....	335
Physical Stabilization of Insulin Through Chemical Modification: Site-Specific Glycosylation or PEGylation M. BAUDYŠ, T. UCHIO, S.C. SONG, D.C. MIX, and S.W. KIM .....	337
Therapeutic Effects of the Soybean Trypsin Inhibitor and Its Gelatin Conjugate on the Pseudomonal Elastase Induced Shock in Guinea Pig Y.-H. SHIN, T. AKAIKE, and H. MAEDA .....	339
The Pulsatile Release System of Macromolecular Drugs from Alginate Gel Beads M. KAWABUCHI, A. WATANABE, M. SUGIHARA, A. KIKUCHI, Y. SAKURAI, and T. OKANO. ....	341
Albumin Release from Bioerodible Hydrogels Based on Semi-Interpenetrating Polymer Networks Composed of Poly( $\epsilon$ -caprolactone) and Poly(ethylene glycol) Macromer J.-H. HA, S.-H. KIM, and C.-S. CHO .....	343
A Novel Drug Delivery System of Hepatocyte Growth Factor (HGF): Utilization of Heparin-HGF Complex Y. KATO, K.-X. LIU, T. TERASAKI, T. NAKAMURA, and Y. SUGIYAMA .....	345
New Polymeric Hydrogel Formulations for the Controlled Release of Proteic Drugs: DSC Investigation of Water Structure E.E. CHIellini, E. CHIellini, D. GIANNASI, E. GRILLO FERNANDES, and R. SOLARO .....	347

Degradation Mechanism of Azo-Containing Polyurethanes by the Action of Intestinal Flora Y. KIMURA, T. YAMAOKA, T. UEDA, S.-I. KIM, and H. SASATANI .....	349
Novel Immunoliposomes Modified with Amphipathic Polyethyleneglycols Conjugated at Their Distal Terminals to Monoclonal Antibodies K. MARUYAMA, T. TAKIZAWA, and M. IWATSURU .....	351
Photo-Induced Drug Release from Liposome Using Photochromic Lipid Having Spiropyran Group Y. OHYA, Y. OKUYAMA, and T. OUCHI .....	353
New Structurally Modified Cyclodextrins for Controlled Release of Antihypertensive Drugs M.C. BRESCHI, E. CHIELLINI, F. MORGANTI, and R. SOLARO .....	355
Development of Delivery Systems for Antisense Oligonucleotides Y. TAKAKURA, R.I. MAHATO, T. NOMURA, K. SAWAI, M. YOSHIDA, T. KANAMARU, and M. HASHIDA .....	357
Transfection to Smooth Muscle Cells Using Terplex of LDL, DNA, and Hydrophobized Cationic Polymers A. MARUYAMA, J.-S. KIM, T. AKAIKE, and S.W. KIM .....	359
Preparation of Ammonio-Terminated Polyoxyethylene/Polydimethylsiloxane Block Copolymer and Application to Transdermal Penetration Enhancer T. AOYAGI, T. AKIMOTO, and Y. NAGASE .....	361
Theoretical Design of Skin Penetration Enhancement via Prodrug-Enhancer Combination Based on a Diffusion Model H. BANDO, F. YAMASHITA, Y. TAKAKURA, and M. HASHIDA .....	363
Preparation of Biodegradable Microspheres Containing Water-Soluble Drug, $\beta$ -Lactam Antibiotic J.H. KIM, I.C. KWON, Y.H. KIM, Y.T. SOHN, and S.Y. JEONG .....	365
Effect of Micropore Structure on Drug Release Form Self-Setting Calcium Phosphate Cement Containing Anti-Cancer Agent M. OTSUKA, Y. MATSUDA, J. HSU, J.L. FOX, and W.I. HIGUCHI .....	367
Amine Effect on Controlled Release of Insulin from Phenylboronic Acid Gel in Physiological pH D. SHIINO, K. MATSUYAMA, Y. KOYAMA, K. KATAOKA, Y. SAKURAI, and T. OKANO ..	369
Drug Releasing Mechanism from Redox Active Micelles Y. TAKEOKA, T. AOKI, K. SANUI, N. OGATA, T. OKANO, Y. SAKURAI, and M. WATANABE .....	371
<b>Author Index</b> .....	373
<b>Key Word Index</b> .....	377



# The Organizing and Program Committee

## *Chairman*

N. Ogata (Sophia University)

## *Vice Chairmen*

J. Feijen (University of Twente)

S.W. Kim (University of Utah)

T. Akaike (Tokyo Institute of Technology)

M. Akashi (Kagoshima University)

M. Hashida (Kyoto University)

T. Kajiyama (Kyushu University)

K. Kataoka (Science University of Tokyo)

J. Kopeček (University of Utah)

T. Okano (Tokyo Women's Medical College)

Y. Sakurai (Tokyo Women's Medical College)

Y. Sugiyama (University of Tokyo)

J. Sunamoto (Kyoto University)

K. Takemoto (Ryukoku University)

# Professor Teiji Tsuruta—Biographical Data

**Date of Birth:** January 1, 1920

**Present Address:** 1-1-1 Shimodacho, #609, Kohoku-ku, Yokohama, Kanagawa, 223 Japan

## **Education:**

Kyoto University, Faculty of Engineering, Department of Industrial Chemistry

B.S., Organic Chemistry, 1941; Ph.D., Organic Chemistry, 1953

(Ph.D. Dissertation: “Studies on Organic Reaction Mechanisms with Active Methylene Compounds”)

## **Professional Career:**

- Kyoto University, Faculty of Engineering and Institute for Chemical Research  
Research Associate (1945–1951)  
Associate Professor (1951–1962)  
Professor (1962–1964)
- University of Tokyo, Faculty of Engineering, Department of Synthetic Chemistry  
Professor (1964–1980)  
Professor Emeritus (1980–present)
- Science University of Tokyo, Faculty of Engineering, Department of Industrial Chemistry  
Professor (1980–present)  
Dean of Faculty of Engineering (1984–1985)  
Director of Research Institutes for Science and Technology (1985–1990)  
Director of Research Institute for Biosciences (1989–1994)

## **Student Supervision (1962–1990):**

45 students for Ph.D., 104 students for M.S., and 90 students for B.S.

## **Visiting Professorships:**

USA, Russia, Poland, and China

## **Some Professional Activities:**

President of the Society of Polymer Science, Japan (1980–1982)

President of the Chemical Society of Japan (1985)

Congress Chairman of the Third World Biomaterials Congress (1988)

- Regional Editor (Eastern Asia) of *Die Makromolekulare Chemie* (1979–1989)  
Regional Editor (Eastern Asia) of *Reactive Polymers* (1982–1988)  
Editor of the *Journal of Biomaterials Science, Polymer Edition* (1988–present)  
Editorial Board Member of the *Journal of Macromolecular Science–Chemistry* (1966–1993)  
Editorial Board Member of *Polymer Bulletin* (1988–1993)  
Titular Member of the Nomenclature Commission, IUPAC Macromolecular Division (1968–1979)  
Research Coordinator-in-Chief, “Design of Multiphase Biomedical Materials,” a special research project supported by the Ministry of Education, Science, and Culture, Japan (1982–1984)  
Research Coordinator-in-Chief, “New Functionality Materials—Design, Preparation, and Control,” priority area research program supported by the Ministry of Education, Science, and Culture, Japan (1987–1992)

**Awards:**

- The G. Stafford Whitby Memorial Lecturer Award (1973)  
29th Chemical Society of Japan Award (1977)  
Award for Distinguished Service to the Advancement of Polymer Science, Society of Polymer Science, Japan (1985)  
The Japanese Society for Biomaterials Award for Distinguished Service to Biomaterials Science (1988)  
Docteur Honoris Causa from the Pierre and Maire Curie University in Paris (1990)

**Publications (1942–1995):**

Nearly 300 original papers and books as well as chapters in books.

Major topics of research in these publications are:

- Organometallics-initiated vinyl polymerizations
- Stereoselective polymerizations of oxiranes
- Amino-functional macromonomers and polymers
- Organosilicone-containing monomers and polymers
- Biomedical applications of novel polymeric materials (1976–present)

# Memories of the Iketani Conference

## 1. Special Lecture by Professor Teiji Tsuruta

Prof. Teiji Tsuruta delivered his special lecture, titled “New Polymeric Materials Design for Biomedical Applications,” on April 20, 1995. The lecture was concerned with the syntheses of amino-containing polymers and their biomedical applications, such as cell separation, pH-responsive hydrogel systems, and gas separation membranes. The work was carried out over the past two decades with his collaborators. Prof. Tsuruta’s stimulating words encouraged all the participants, especially younger scientists. After the lecture, Dr. Sandrine A. Cammas of Tokyo Women’s Medical College presented a bouquet of beautiful flowers to Prof. Tsuruta.



## 2. From the Banquet

1) A symposium banquet was held at the Shiroyama Kanko Hotel on the evening of April 20, 1995, with more than 200 participants. Prof. Naoya Ogata, Congress Chairman, presented an honorary plaque and a gift of Satsuma Kiriko, famous glass art of Kagoshima Prefecture, to Prof. Tsuruta.



2) Prof. Tsuruta awarded memorial plaques to all invited speakers for their distinguished contributions. Prof. James M. Anderson, Case Western Reserve University, USA, received his plaque from Prof. Tsuruta on behalf of all invited speakers.



3) Professor Allan S. Hoffman, University of Washington, USA, delivered a special address and toast at the banquet.

Kagoshima, April 20, 1995



### Toast

It is my great privilege and pleasure to have the opportunity to toast Prof Tsuruta sensei. This wonderful and extraordinary man, who has such a rare combination of scholarship and humanity, has touched so many of us, and has left a lasting impression and effect on our lives and our careers.

I thought about how to describe him and his many varied and interesting qualities.

With his personal interactions with people he is always

- pleasant and happy,
- gentle and kind,
- helpful and encouraging.

With his ideas and research concepts and goals, he is always

- thoughtful and thorough
- patient and persistent
- precise and decisive
- creative and productive.

Tsuruta sensei never pushes, always leads, always teaches, always inspires.

So let us toast this wonderful man, and wish him a happy 75<sup>th</sup> birthday, and many more years of happiness and continued creativity and success.

Allan Hoffman

# **Advanced Biomaterials**

# CONTROLLED RELEASE SYSTEMS USING SWELLABLE RANDOM AND BLOCK COPOLYMERS AND TERPOLYMERS

Nicholas A. Peppas\*, Sarah Vakkalanka, Christopher S. Brazel, Amy S. Luttrell, and Neena K. Mongia

*Biomaterials and Drug Delivery Laboratories, School of Chemical Engineering, Purdue University, West Lafayette, Indiana 47907-1283, USA*

## ABSTRACT

Recent advances on the use of N-isopropyl acrylamide-containing random and block copolymers and terpolymers are presented. Such systems are shown to be dependent on temperature and pH (if acrylic acid is an added comonomer). Their temperature-dependence is significantly increased in the presence of block domains prepared by co- or terpolymerization. They are suited for release of fibrinolytic enzymes and antithrombotic agents. Ultrapure poly(vinyl alcohol) gels are also studied for release of ketansarin and related wound healing enhancers.

**KEY WORDS:** Swellable polymers, temperature-sensitive gels, pH-sensitive gels, epidermal growth factors, fibrinolytic enzymes.

## INTRODUCTION

Recent advances in the development of neutral and ionic swellable polymers have concentrated on several aspects of their synthesis, characterization and behavior. Major questions that have been addressed in recent work include:

- synthetic methods of preparation of hydrophilic polymers with desirable functional groups;
- synthetic methods of preparation of multifunctional or multiarm structures including branched or grafted copolymers and star polymers.;
- understanding of the criticality and the swelling/syneresis behavior of novel anionic or cationic polymers;
- development of ultrapure polymers, such as crosslinker-free poly(vinyl alcohol) gels produced by freezing-thawing of aqueous solutions;
- synthesis and characterization of biomimetic hydrogels;
- understanding of the relaxational behavior during dynamic swelling; and
- modeling of any associated dissolution or biodegradation.

## CRITICAL BEHAVIOR OF NIPAAm-CONTAINING RANDOM AND BLOCK COPOLYMERS

Hydrogels composed of lightly crosslinked N-isopropylacrylamide (NIPAAm) and methacrylic acid (MAA) were synthesized and characterized for their sensitivity to external conditions and their ability to control release of two antithrombotic agents, heparin and streptokinase. PNIPAAm is noted for its sharp change in swelling behavior across the lower critical solubility temperatures of the polymer, while PMAA shows pH-sensitive swelling due to ionization of the pendant carboxylic groups in the polymer. Hydrogel copolymers of NIPAAm and MAA with appropriate composition were designed to sense small changes in blood stream pH and temperature to deliver antithrombotic agents, such as streptokinase or heparin, to the site of a blood clot.

Experiments were performed to show that hydrogels with certain compositions could show both temperature- and pH- sensitivity, and that these changes could control release of heparin or

streptokinase. Equilibrium and pulsatile swelling studies were performed on all polymers to determine to what extent the hydrogels would respond to changes in environmental temperature and pH, and how fast that response would be.

### Synthesis of Temperature and pH-Sensitive, Swellable Co- and Terpolymers

NIPAAm (Eastman Kodak, Rochester, NY) was purified by recrystallization in benzene/hexane. The polymers were synthesized either by free-radical copolymerization of MAA (Aldrich, Milwaukee, WI) and NIPAAm, or by free radical terpolymerization of AA (Aldrich, Milwaukee, WI), NIPAAm, and HEMA (Aldrich, Milwaukee, WI). The monomers were combined in various molar ratios and ethylene glycol dimethacrylate (EGDMA) was added at 1 mol% of monomers to form crosslinked networks. When preparing the P(MAA-co-NIPAAm) **random copolymers** (1), deionized water and methanol were necessary to dissolve high concentrations of NIPAAm monomer. A 50/50 mixture of the solvents was added in a total amount of 50 wt% of total monomers. 2,2'-Azobis(isobutyronitrile) (AIBN) (Aldrich, Milwaukee, WI) at an amount of 1 wt% (of the total final weight) was used as an initiator. Nitrogen was then bubbled through the mixture to remove dissolved oxygen. The reacting mixture was then transferred to cylindrical polypropylene vials and sealed, and reacted for a period of 24 hours at 50°C.

The **random terpolymers** could be prepared using only deionized water as a solvent. Water was added at a total amount of 50 wt% (of the monomers-NIPAAm, AA, and HEMA). Ammonium persulfate at 1 wt% (of the total weight-monomers, water, and EGDMA) and sodium metabisulfite at 1 wt% (of the total weight) were used as initiators. Nitrogen was bubbled through the mixture following initiator addition and the contents were transferred to cylindrical polypropylene vials and sealed. The terpolymerization was carried out in a 37°C constant temperature water bath. The ensuing hydrogels were removed from the vials and allowed to dry at 25°C. When the cylindrical samples became rigid, they were sliced into thin discs by the use of a diamond-blade rotary saw.

**Block terpolymers** consisting of NIPAAm, AA, and HEMA were prepared by a free radical polymerization. NIPAAm at 10 mol% (of the total monomers-NIPAAm, AA, HEMA) was then homopolymerized at room temperature in a beaker in deionized water, 1 mol% (of the total monomers) ammonium persulfate, and 1 mol% sodium metabisulfite. This mixture was stirred for approximately ten minutes, or until the viscosity increased slightly. In a separate beaker, 80 mol% (of the total monomers) HEMA, 10 mole% (of the total monomers) AA, and 1 mole% (of the total monomers) EGDMA were mixed and then added dropwise to the NIPAAm mixture. During this addition, the reacting mixture was constantly stirred by a magnetic stir bar. Following the addition of the monomers, the contents were immediately transferred to 10 mL polypropylene vials which were sealed and allowed to react for 24 hours in a 37°C constant temperature water bath. The gels were subsequently recovered and sliced into thin discs as above.

Thin discs (diameter of approximately 14 mm and a thickness of 0.8 mm) of the previously prepared copolymers and terpolymers were dried to a constant weight in a vacuum oven at 37°C. They were then placed in vials containing a pH=6 buffered solution and immersed in a water bath at 32°C for at least three days in order to attain their corresponding equilibrium swollen state. The gel samples (pH=6) were transferred to a pH=5 buffered solution at 37°C for 30 minutes and returned to the pH=6 buffered solution at 32°C for 30 minutes. This pattern was repeated for several cycles. The typical swelling behavior of a random terpolymer containing molar ratio of 10:10:80 NIPAAm:AA:HEMA is shown in Figure 1, as a function of oscillating pH from 5 to 6. The abrupt swell/deswelling process is accompanied by significant changes in the swelling/deswelling rates from 0.23 to 0.44 min<sup>-1</sup>.

The very important temperature dependence of the same terpolymer, both in its random and block form is shown in Figure 2 which shows that block terpolymers with just 10% NIPAAm behave in a significantly different way. This is in agreement with the recent studies of Chen and Hoffman (2) with grafted gels and Yoshida et al. (3) with comb-type gels.



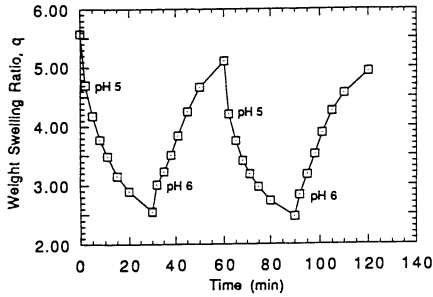


Figure 1. Pulsatile pH Swelling of Hydrogels with a 10:10:80 NIPAAm:AA:HEMA Molar Ratio

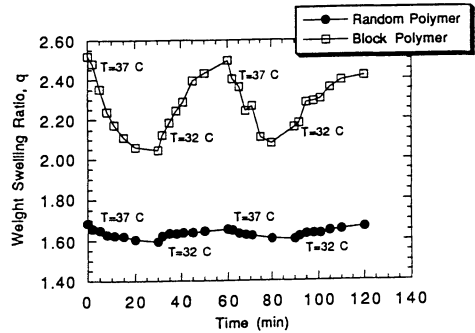


Figure 2. Comparison of Pulsatile Temperature Swelling of Random and Block Polymers with a 10:10:80 NIPAAm:AA:HEMA Molar Ratio

### Antithrombotic Agent Release

Streptokinase (Calbiotech, La Jolla, CA) and heparin (Sigma, St. Louis, MO) loading and release were carried out either by imbibition or by direct, low temperature co- or terpolymerization in presence of the active agent. A typical release behavior for the same gel as before is shown in Figure 3 where instantaneous streptokinase release is placed in a pH=6 solution at 32°C, whereas the release is significantly reduced when the same gel is placed at pH=5 and 37°C. Yet the system is still releasing streptokinase due to the hydrophilic, "neutral" HEMA component. It must be noted that all these systems have significant *bioadhesive behavior* as tested by the classical tensiometric technique.

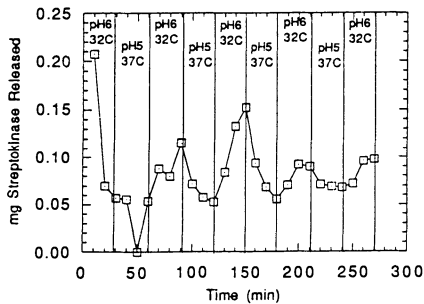


Figure 3. Streptokinase Release under Conditions of Pulsatile Temperature and pH from Hydrogel with a 10:10:80 NIPAAm:AA:HEMA Molar Ratio which was Loaded by Swelling in the Presence of Drug.

### ULTRAPURE POLY(VINYL ALCOHOL) GELS WITH MUCOADHESIVE BEHAVIOR

Recent work on the use of ultrapure poly(vinyl alcohol) (PVA) gels has concentrated on their application for epidermal growth factor release. Ultrapure hydrogels were prepared by exposing an aqueous solution of 15 or 20 wt% PVA to repeated cycles of freezing for 6 or 12 hours at -20°C and thawing for 2 hours at 25°C. The resulting gels are desirable in that they do not contain any leachable toxic crosslinked agents. The properties of the PVA gels make them important biomaterials for a variety of applications, including bioadhesive drug delivery systems.

The adhesive and surface characteristics of the PVA gels produced by the freezing/thawing technique were examined using tensile techniques and contact angle measurements (Figure 4). As the number of freezing/thawing cycles increased, the value of the work of adhesion decreased due to the increase in the PVA sample degree of crystallinity. The PVA gels prepared from the 20 wt% solution that were exposed to 2 cycles of freezing/thawing exhibited the greatest value of the work of adhesion. Surface contact angle measurements of the PVA gel in contact with water were used to evaluate the wettability of the PVA samples. The results showed that as the number of freezing/thawing cycles was increased, there was a decrease in the contact angles. Therefore, increasing the crystallinity of the PVA gel decreased the contact angle and increased the wettability of the PVA gels.

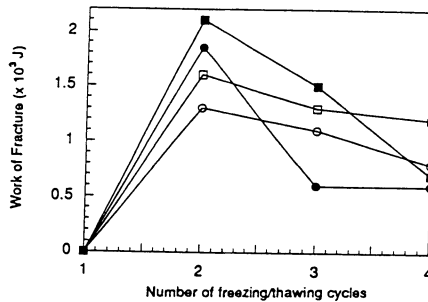


Figure 4. Work of fracture as a function of number of freezing/thawing cycles. PVA samples were exposed to freezing followed by thawing for 2 hours. 15 wt% PVA, 6 hours freezing (○); 15 wt% PVA, 12 hours freezing (□); 20 wt% PVA, 6 hours freezing (●); 20 wt% PVA, 12 hours freezing (■).

Crystallinity of these PVA gels was calculated using differential scanning calorimetry. Crystallinity was determined by comparing the heat required to melt a PVA sample to the heat required to melt a 100% crystalline sample. The average degree of crystallinity of a PVA sample prepared from a 20 wt% solution that was exposed to 3 cycles of freezing/thawing was 8.7% on a dry basis.

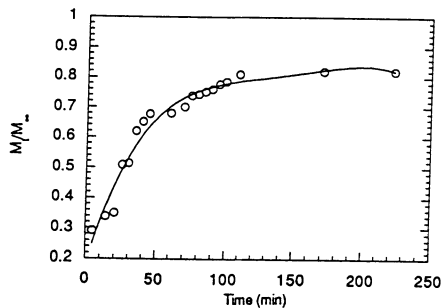


Figure 5. Fractional ketansarin release from a PVA sample prepared from a 20 wt% solution exposed to 2 cycles of freezing for 12 hours followed by thawing for 2 hours.

Drug delivery studies were also conducted with ketansarin, a wound healing enhancer. Release studies were conducted using PVA samples prepared from a 20 wt% solution that were exposed to 2 or 3 cycles of freezing for 12 hours followed by thawing for 2 hours (Figure 5). Results from the release of the drug from the PVA sample exposed to 2 cycles showed that approximately 80% of the ketansarin was released within 4 hours, with the majority being released within the first 100 minutes. Ketansarin was released more slowly from the PVA gel that was exposed to 3 cycles, with only approximately 70% of the drug being released within the first 4 hours. Overall, approximately the same fraction of ketansarin was released from both of the PVA gels.

**Acknowledgment**

This work was supported by grants from the National Science Foundation and the National Institutes of Health.

**REFERENCES**

1. Brazel CS and Peppas NA (1995) Synthesis and characterization of thermo- and chemo-mechanically responsive poly(*N*-isopropylacrylamide-co-methacrylic acid) hydrogels. *Macromolecules*, submitted.
2. Chen G, Hoffman AS (1995) Graft copolymers that exhibit temperature induced phase transitions over a wide range of pH. *Nature* 373: 49-52.
3. Yoshida R, Uchida K, Kaneko Y, Sakai K, Kikuchi A, Sakurai Y, Okano T (1995) Comb-type grafted hydrogels with rapid deswelling response to temperature changes. *Nature* 374: 240-242.

# POLYMER GEL-A NEW TYPE OF SOFT ENERGY TRANSDUCER

*Yoshihito Osada and Jianping Gong*

Division of Biological Sciences, Graduate School of Science,  
Hokkaido University, Sapporo 060, Japan

## Summary

The cooperative binding of a linear as well as a cross-linked polyelectrolyte with an oppositely charged surfactant has been theoretically analyzed. The hydrophobic interaction has been treated using the nearest neighbor interaction model, while the electrostatic interaction has been calculated using the rod-like model. The general formulas derived on the basis of the free energy minimum principle predicted that the cross-linkage enhances the initiation process but strongly suppresses the cooperativity due to the osmotic pressure in the network domain. The theoretical results showed fairly good agreement with the experimental data, confirming the essential features of the theory.

**Key words:** Gel, polyelectrolyte, cooperativity, electrostatic interaction, hydrophobic interaction

## Introduction

Biological materials are usually composed of soft and wet materials in the body. This is in contrast with most of industrial materials such as metal, ceramics and plastics that are dry and hard. Thus, arises the problem of how to design a mobile machine using soft and wet materials, or how to afford the soft material to make shape changes or to generate tensile stresses that can lead to motility without the requirement of a rigid structure. One should notice that there are suitable materials which largely satisfy these requirement. They are wet and soft and look like a solid material but are capable of undergoing large deformation. That is the *polymer gel*.

The system which undergoes shape change and produce contractile force in response to environmental stimuli is called a "chemomechanical system". This system can transform chemical free energy directly into mechanical work to give isothermal energy conversion and this can be seen in living organisms, for example, in muscle, flagella and in ciliary movement. Synthetic polymer network, "gel", is the only artificial system able to convert chemical energy directly into mechanical work. Gels are *soft* with respect to their environments. Machines made of metal or silicon operates as closed systems. They do not adapt to changes in their operating conditions unless a separate sensor system or a human operator is at the controls. Gels, in contrast, are thermodynamically "*open*": they exchange chemicals with the solvent surrounding them and alter their molecular state in the process of accomplishing work. Such materials could be used wherever power for more conventional devices is limited or difficult to obtain: underwater, in space or in the human body.

We have recently developed a new type of electrically-driven chemomechanical system which shows quick responses with worm-like motility. The principle of motility of this system is based upon an electrokinetic molecular assembly reaction of surfactant molecules on the hydrogel caused by both electrostatic and hydrophobic interactions. We have made a comparative study on the surfactant binding with oppositely charged linear and network polymers<sup>1,2</sup> and found that the cross-linkage enhances the initiation process but strongly suppresses the cooperativity due to the osmotic pressure in the network domain.

### Theory

We consider the electrostatic interaction between a solubilized linear polyelectrolyte with negative charges and positively charged surfactants capable of forming micellar-like complexes. The free energy of the system,  $F$ , can be written as a sum of three terms

$$F = F_{\text{int}} + F_{\text{mobile}} + F_{\text{comp}} \quad (1)$$

where  $F_{\text{int}}$  is the free energy of the volume interaction of monomer links,  $F_{\text{mobile}}$  the free energy of motion of micro ions in the solution,  $F_{\text{comp}}$  the free energy of surfactants bound with polyions. We denote  $\Delta F_e$  as the free energy change due to the electrostatic binding, which equals the electrostatic potential energy on the surface of the macroion, and  $\Delta F_h$  as that through the hydrophobic interaction. For simplification, we supposed that  $\Delta F_e$  does not change with respect to the progress of binding.  $\Delta F_h$  depends on the chemical structure of the surfactant, particularly on the size of alkyl chains. If we take account of the nearest neighbor interaction between surfactant molecules, the binding of surfactant should occur in a continuous sequence but not in a random distribution along the polymer chain.

The equilibrium value of  $\beta$ , which is the ratio of the molar number of bound surfactants to the total monomeric units, can be determined by minimization of the total free energy of the system  $\frac{\partial F}{\partial \beta} = 0$ . Thus, we have

$$\ln C_s^p v_c = \frac{\Delta F_e + \Delta F_h}{kT} - 1 + \ln \frac{\sqrt{4\beta(1-\beta)[\exp(-\frac{\Delta F_h}{kT}) - 1] + 1} + 2\beta - 1}{\sqrt{4\beta(1-\beta)[\exp(-\frac{\Delta F_h}{kT}) - 1] + 1} + 1 - 2\beta} \quad (2)$$

where  $C_s^p$  is the equilibrated molar concentration of surfactant in the polymer solution. The second term of the above equation is a transition function that becomes steeper with an increase in the value of  $\Delta F_h$ .

Eq.2 indicates that the binding isotherm of the surfactant onto the linear polyelectrolyte consists of two terms: the first term characterizes the transition concentration (initiation process) and the second term characterizes the steepness of the transition (cooperative process). The initiation process of the binding is determined not only by the electrostatic interaction, but also by the hydrophobic interaction, while the cooperative process of the binding is determined only by the hydrophobic interaction, which is obtained from the slope of the binding curve at  $\beta=0.5$ . If we denote the cooperativity parameter  $u$  and the initiation constant  $K()$  as

$$\left. \frac{d \ln C_s^p}{d\beta} \right|_{\beta=0.5} = \frac{4}{\sqrt{u}} \quad (3)$$

and

$$\left(\frac{1}{C_s^g}\right)_{\beta=0.5} = K_0 u \quad (4)$$

we have

$$u = \exp\left(-\frac{\Delta F_h}{kT}\right) \quad (5)$$

and

$$K_0 = \epsilon v_c \exp\left(-\frac{\Delta F_e}{kT}\right) \quad (6)$$

Thus, the slope of the isotherm curve increases exponentially with an increase in  $\Delta F_h$ . It is clear that  $K_0$  characterizes the electrostatic interaction of the surfactant with the polyelectrolyte that corresponds to the binding constant of the surfactant molecule to sit to an isolated binding site on a polymer.  $u$  characterizes the aggregation process of surfactant molecules already bound to the polyelectrolyte. Since  $\Delta F_h < 0$  for the hydrophobic interaction,  $u > 1$  when the hydrophobic interaction contributes to the binding. For the case of binding through a simple salt formation,  $\Delta F_h = 0$  and  $u = 1$ .

In the case of a cross-linked polyelectrolyte immersed in an oppositely charged surfactant solution, the free energy of the system,  $F$ , is the sum of the free energy of the outer solution,  $F_s$ , and the free energy of the polymer network,  $F_g$ :

$$F = F_s + F_g \quad (7)$$

$F_g$  can be expressed as follows:

$$F_g = F_{int} + F_{mobile} + F_{comp} + F_{el} \quad (8)$$

where  $F_{int}$  and  $F_{comp}$  are the same as those used before,  $F_{mobile}$  is the free energy of motion of microions in the network and  $F_{el}$  the elastic free energy of the network.

By minimizing the total free energy of the system  $\frac{\partial F}{\partial \beta} = 0$ , we get the equilibrium value of  $\beta$ :

$$\ln C_s^g v_c = \frac{\Delta F_e + \Delta F_h}{kT} - 1 + \ln \frac{\sqrt{4\beta(1-\beta)[\exp(-\frac{\Delta F_h}{kT})-1]+1} + 2\beta - 1}{\sqrt{4\beta(1-\beta)[\exp(-\frac{\Delta F_h}{kT})-1]+1} + 1 - 2\beta} + \ln \frac{(\alpha+\beta-\gamma)V_g}{[1-(\alpha+\beta-\gamma)](V-V_g)} \quad (9)$$

where  $C_s^g = \frac{M-N(\alpha+\beta)}{V-V_g}$  is the molar concentration of the surfactant in the outer solution. The differentiation of the isotherm curve at  $\beta=0.5$  now becomes

$$\left(\frac{d \ln C_s^g}{d \beta}\right)_{\beta=0.5} = 4 \exp\left(\frac{\Delta F_h}{2kT}\right) + \frac{4}{1-4(\alpha-\gamma)^2} + \frac{1}{V_g} \frac{dV_g}{d\beta} \quad (10)$$

and

$$(\ln C_s^g v_c)_{\beta=0.5} = \frac{\Delta F_e + \Delta F_h}{kT} - 1 + \ln \frac{[0.5+(\alpha-\gamma)]V_g}{[0.5-(\alpha-\gamma)](V-V_g)} \quad (11)$$

where  $V_g$ ,  $\alpha$ , and  $\gamma$  are the values at  $\beta=0.5$ . In a manner similar to the linear polymer, we define

$$\left(\frac{d \ln C_s^g}{d \beta}\right)_{\beta=0.5} = \frac{4}{\sqrt{u^g}} \quad (12)$$

and 
$$\left(\frac{1}{C_s^g}\right)_{\beta=0.5} = K_0^g u^g \quad (13)$$

For the surfactant with strong hydrophobic interaction

$$\exp\left(\frac{\Delta F_h}{2kT}\right) \approx 0 \quad (14)$$

and 
$$-1 << \frac{1}{4V_g} \frac{dV_g}{d\beta} \leq 0 \quad (15)$$

which indicates that when the polyelectrolyte is cross-linked to form a network, it behaves like a rigid polymer with respect to the binding, therefore  $u^g \approx 1$ . This shows that the surfactant-polymer network binding is not cooperative regardless of the strong hydrophobic interaction.

Thus, it is seen that the presence of the cross-linkage introduces an extra ionic osmotic pressure difference inside and outside the network. When  $\beta$  is small,  $[P_s^+] \ll [P_g^+]$ , and the network always tends to swell which is balanced by the elastic force. This swelling ionic osmotic pressure enhances the initial binding process but suppresses the surfactant aggregation compared with those of the linear polyelectrolyte. If we regard the polymer network as a cross-linked three-dimensional polymer chain in water, the presence of the locally concentrated counter ions, which originate the swelling osmotic pressure, makes the network expand in competition with the conformational shrinkage on binding and thus strongly reduces the cooperativity.

The described theoretical approach was compared with the experimental data for the binding of dodecylpyridinium chloride (C<sub>12</sub>PyCl) with a linear and a cross-linked poly(2-acrylamido-2-methylpropane sulfonic acid)(PAMPS). PAMPS is a strong polyacid with fully ionized sulfonic groups as macroions and H<sup>+</sup> as counterions.

Fig.1 shows the theoretical binding isotherms(solid line) calculated from eq. 6 and the observed data (solid triangular) obtained for C<sub>12</sub>PyCl bound with a linear PAMPS. The theoretical calculation was carried out using the following values:  $N=3 \times 10^{-5}M$ ,  $V_0=6 \times 10^{-6}L$ ,  $V=0.01L$ ,  $v_c=0.018L/M$ ,  $\Delta F_h/kT=-6.2$ , and  $\Delta F_c/kT=-7.0$ . We see that the theoretical curve fits quite well with the observed data when  $\beta$  is less than 0.7. However, a deviation was observed when  $\beta$  exceeds 0.7. This could be associated with the drastic conformational change of polymer chain from the extended random coil to globules, which should occur at a certain  $\beta$  value. This conformational change would largely decrease the surface potential energy  $\Delta F_c$  and alter the binding equilibrium to give decreased binding of the surfactant.

The results of the theoretical (solid line) and the observed data (open circles) for a polymer network are also shown in Fig.1. Again, the theoretical curve fits well with the observed data in the range of  $\beta$  less than 0.7.

Figure 2 shows the theoretical and experimental binding isotherms of the surfactants with different alkyl chain length bound to a network of  $q=50$ . Increasing the alkyl size of the surfactant shifts the binding curves toward lower surfactant concentrations, while it does not enhance the cooperativity. Deviation from the experimental data is also observed at  $\beta=0.7$  or higher.

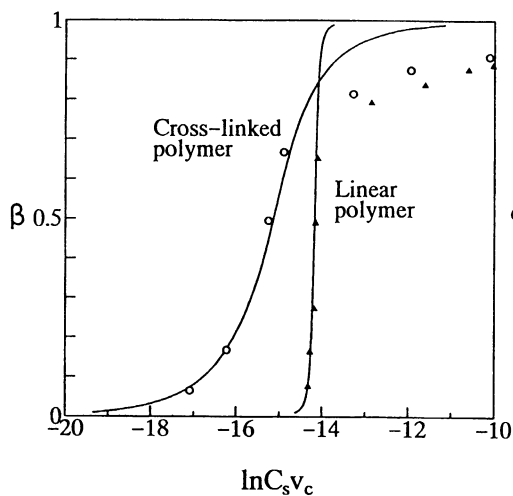


Fig. 1 Binding isotherms of dodecylpyridinium chloride ( $C_{12}PyCl$ ) with a linear and a cross-linked poly(2-acrylamido-2-methylpropane sulfonic acid) (PAMPS). Solid lines are calculated curves and open circles (cross-linked polymer) and triangles (linear polymer) are experimental data quoted from reference 1.

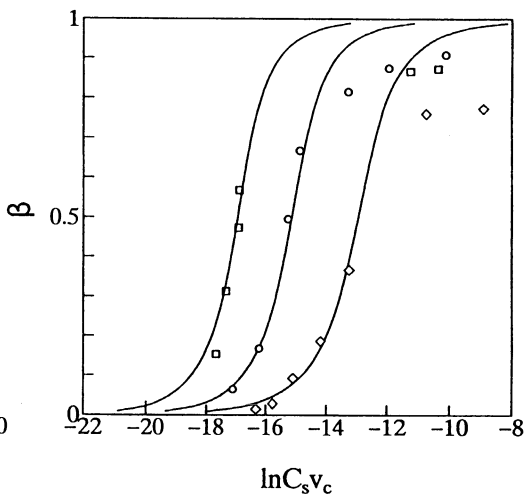


Fig. 2 Binding isotherms of surfactant with different alkyl chain length to a network of  $q=50$ . Solid lines are calculated curves using  $\Delta F_h/kT = -8.0, -6.2, -4.0$  from left to right. Experimental data ( $\square$ :  $C_{18}PyCl$ ,  $\circ$ :  $C_{12}PyCl$ ,  $\diamond$ :  $C_{10}PyCl$ ) were quoted from reference 1.

In the above numerical calculation, we simply assumed that  $\alpha \approx 0$  and  $\gamma \approx 0$ , which means that all of the surfactant ions in the polymer network have bounded with the polyions, and we did not consider the equilibrium between the free surfactant ions and the bound surfactant in the network domain. This is true only when the surfactant has a very strong hydrophobic interaction and the polymer network has a high cross-linking density. A numerical calculation of the general situation in which the equilibrium of surfactants inside the network is considered should be performed for the polymer network having a high degree of swelling. Nevertheless, the calculated isotherms showed fairly good agreement with the experimental data, which confirms the essential feature of the theory.

## References

- (1) Okuzaki, H.; Osada, Y. *Macromolecules* Sept., **1995**, in press.
- (2) Gong, J. P.; Osada, Y. *J. Phys. Chem.* **1995**, in press.



# COMMUNICATING WITH THE BUILDING BLOCKS OF LIFE USING ADVANCED MACROMOLECULAR TRANSDUCERS

Prof. Gordon G. Wallace

*Intelligent Polymer Research Laboratory, Department of Chemistry, University of Wollongong, Northfields Avenue, Wollongong, NSW, 2522, Australia*

## ABSTRACT

This paper reviews the use of conducting electroactive polymers (CEPs) in biomolecular communications. That is the use of CEPs in situations that demonstrate controlled interactions with moieties of biological interest and the ability to monitor such interactions via the electronic signals generated. As examples, the ability to manipulate CEP interactions with water, simple electrolyte ions, amino acids, proteins and mammalian cells is discussed.

**KEY WORDS:** Conducting electroactive polymers, water interactions, ionic interactions, amino acid interactions, mammalian cells.

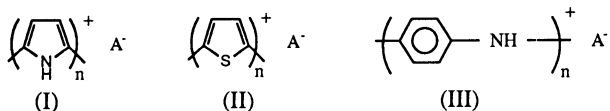
## INTRODUCTION

The ability to communicate enables us to monitor and stimulate other systems to achieve enhanced performance. Such **intersystem** communications (especially those based on sight and sound) have been revolutionised in recent years due to the development of new communication tools (telephone, facsimile, video systems etc.). However, the development of **intrasystem** communications has proven more difficult. We still, for example, have difficulty in retrieving information from, and modifying the behaviour of the human system at the molecular level.

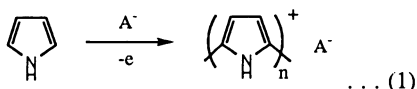
Just as the development of **intersystem** communications required breakthroughs in new materials it appears that **intrasystem** communication demands the same. The recent development of materials that are biocompatible and that when combined with appropriate communication systems have properties that can be used to monitor and stimulate molecular events is poised to make a significant impact on how we communicate with biosystems. This new class of materials is based on conductive electroactive polymers.

## PROPERTIES OF CONDUCTING ELECTROACTIVE POLYMERS

Conducting electroactive polymers (CEPs) such as polypyrrole, polythiophenes and polyaniline (I-III) shown below:



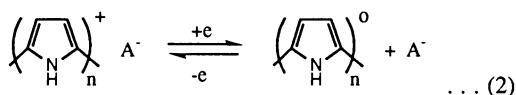
are readily synthesised according to:  
eg:



[n is normally between 2 and 4 and A<sup>-</sup> is a counterion incorporated during synthesis].

This simple polymerisation process can be used to provide materials with a diverse array of molecular properties. For example, A<sup>-</sup> may be a metal complexing agent, a polyelectrolyte, an enzyme, antibody or even living cells. Each of these imparts their chemical functionality to the resulting material.

CEPs, as the name implies, are electrically conducting materials. They are also electroactive, being oxidised and reduced according to:



This latter property enables the chemical functionality of the polymer system to be controlled in-situ. As stated above, conducting polymers are capable of a diverse array of molecular interactions and this can be modified by the A<sup>-</sup> incorporated during synthesis. The imposition of electrical stimuli adds a further dimension in that this can be used to control the molecular functionality. This is discussed below using examples of interest to biomolecular communications.

**Water:** The interaction of CEPs with water is perhaps foremost in determining biocompatibility. Our studies using dynamic contact angle analyses [1] revealed that the strength of the interaction of CEPs with water can be controlled by attaching functional groups to the polymer backbone or by incorporation of appropriate counterions. In fact in some specific cases (eg. the incorporation of polyelectrolytes - see later) the interaction with water is modified to such an extent that the materials become hygroscopic. The application of stimuli to electrochemically reduce the polymer (Equation 2) modifies the strength of polymer-water interactions since the material, in general, becomes more hydrophobic. Such interactions (water/conducting polymer) can be monitored since the water content of these materials influences the electronic properties. It is well known for example that the resistivity of conducting polymers is dependent on the water content.

**Electrolytes:** Conducting polymers can be oxidised and reduced in a reversible manner (Equation 2). These processes induced by electrical stimuli, involve ion movement and hence control the interactions between CEPs and electrolyte ions. Using stand alone CEP membranes, it is possible to use these phenomena to induce and control transport of electrolytes across CEPs. In our laboratories [2] we have developed systems that demonstrate that the controlled transport of simple ions such as Na<sup>+</sup>, K<sup>+</sup> and Ca<sup>2+</sup> is possible. Using a simple electromembrane cell design (Figure 1) the electrically stimulated transport of ions can be demonstrated (Figure 2).

**Amino Acids:** The interaction of amino acids has been studied by us [3] using inverse thin layer chromatography (ITLC). This involves the use of the polymer to be studied as a coating on the TLC plate. Using appropriate molecular probes (in this case amino acids), the strength of molecular interactions can then be quantified. The effect of applied potential on such interactions has also been studied and has been shown to have a dramatic effect on amino acid polymer interactions. In work on sensors we have demonstrated that the interaction of amino acids gives rise to electronically useful signals. This can be used to monitor interactions of amino acids with CEPs in-situ, again confirming the use of these materials as *two-way* biocommunication systems.

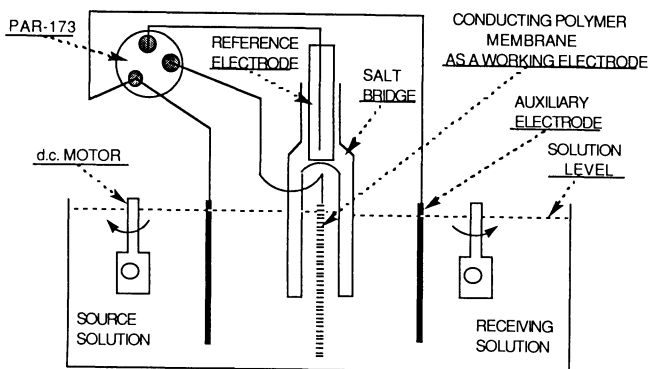


Figure 1 The electrotransport cell.

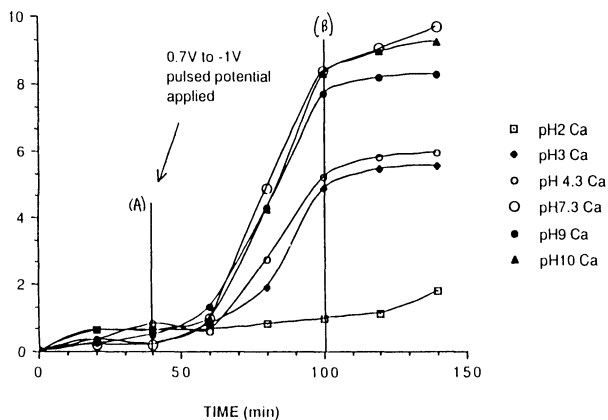
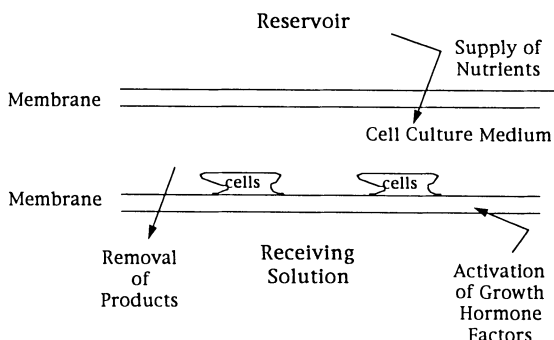


Figure 2 Electrically stimulated transport of  $\text{Ca}^{2+}$  across a polypyrrole paratoluene sulfonate membrane. Stimulus applied point (A) and removed point B.

Experiment carried out in different pH media as indicated and  $C(\text{E} - 5\text{M})$  is concentration of  $\text{Ca}^{2+}$  in receiver side.

**Proteins:** Using electrochemical quartz crystal microbalance experiments we have demonstrated that the interaction of proteins with conducting electroactive polymers can be controlled electrochemically. The EQCM technique enables the mass of a conducting polymer to be monitored in-situ as electrical stimuli are applied. We have also verified the ability to control such interactions in-situ using electrochemically controlled affinity chromatography [4]. The ability to control such interactions has been studied and used by us in the development of new sensing technologies [5]. With all systems considered it has been shown that the use of oscillating potential routines can ensure the control of protein-polymer interactions. This is true even when antibodies are incorporated into the polymer to induce specific protein interactions. As with all of the above interactions electronic signals can be generated as a consequence of protein-polymer interactions.

**Mammalian Cells:** Mammalian cells (eg. human carcinoma, PC-12, fibroblast cells) can be grown on conducting polymers and events within these cells can be stimulated using appropriate electrical stimuli (Schematic 1). Again, the communication system is two way since these molecular events give rise to electronic signals that can be used to monitor them.



Schematic 1 Communicating with mammalian cells using advanced macromolecular transducers.

## BIOCOMPATIBILITY AND A LINE OF COMMUNICATION

An additional requirement of a material suitable for biocommunication is that it be biocompatible. Over the last two decades much work has been focussed on the development of synthetic materials that are biocompatible. Traditionally these systems, such as hydrogels, are dynamic at the molecular level but provide no obvious conduit for communication.

Conducting electroactive polymer (eg. polypyrroles/polyelectrolyte composites) have been shown to be "biocompatible" in that they can sustain mammalian cell growth. The incorporation of polyelectrolytes (PE<sup>0</sup>) into conducting polymers during synthesis according to:

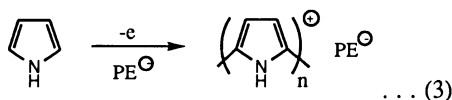
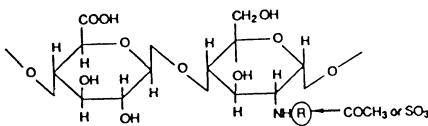
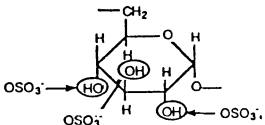


Table 1 Polyelectrolytes incorporated into conducting polymers.

Polymer	Structure
Heparin	
Dextran sulfate	

results in materials with some unexpected and useful properties. The structures of some of the polyelectrolytes used in this work are shown in Table 1. All of the composite polymer systems are conductive and electroactive undergoing the expected oxidation/reduction reaction according to equation 2.

They also have unexpectedly high water contents (up to 90%) and are hygroscopic. It is presumably this hydrogel like property that enables the materials to interact with mammalian cells and in fact sustain cell growth. To date we have considered the growth of human carcinoma, fibroblasts, endothelial and PC-12 cells. This aspect of our work is discussed in more detail elsewhere in this volume.

## CONCLUSION

As with all communication systems biomolecular communications require materials that can transduce events of importance (in this case molecular events). There must also be a line of communication that permits behaviour (in this case molecular events) to be altered by application of appropriate stimuli. As with all systems the materials used for communication must be compatible with the environment in which they are to be used.

It appears that conductive electroactive polymers will now provide these capabilities and we are poised to enter a new world of communications.

## REFERENCES

- [1] Teasdale, P.R.; Wallace, G.G. (1995). In-situ characterisation of conducting polymers by measuring dynamic contact angles with Wilhemy's plate technique. *React. Polym.* 24: 157-164.
- [2] Mirmohseni, A.; Price, W.E.; Wallace, G.G.; Zhao, H. (1993). Adaptive membrane systems based on conductive electroactive polymers. *J. Int. Mat. Sys. Structures.* 4: 43-49.
- [3] Teasdale, P.R.; Wallace, G.G. (1994). Characterising the chemical interactions that occur on polyaniline with Inverse Thin Layer Chromatography. *Polymer International.* 35: 197-205.
- [4] Hodgson, A.J.; Lewis, T.W.; Maxwell, K.M.; Spencer, M.J.; Wallace, G.G. (1990). New conducting polymer affinity chromatography phases. *Journal Liq. Chromatography.* 13: 3091-3110.
- [5] Wallace, G.G. (1993). Dynamic conduct (and references cited therein). *Chemistry in Britain.* Nov. 967-970.

Kiichi Takemoto

Faculty of Science and Technology, Ryukoku University, 520-21 Seta-Otsu, Shiga, Japan

#### SUMMARY

For the purpose of preparing water-soluble natural and synthetic polymers, which contain nucleic acid base units as the functional side groups, a different sorts of polymers, such as polyethyleneimine, polyamino acids and so on were used as the base materials. The properties of the polymers derived, as well as the specific interaction between nucleic base containing complementary polymers were studied in detail. Introduction of such nucleic acid base units onto hyaluronic acid was also carried out. Applicabilities of these polymers obtained, for example those as the controlled release system by using reversible photodimerization reaction of thymine bases were also shown.

#### KEY WORDS

water solubility, nucleic acid base, polyethyleneimine, polyamino acid, hyaluronic acid

#### INTRODUCTION

The chemistry of functional nucleic acid analogs has received considerable attention in recent years, and numerous works have been contributed on this field [1-3]. On this line, we have been extending a comprehensive work in particular on the preparation, properties and functionalization of a large variety of such analogs.

Very recently, we have been concerning the preparation of water-soluble nucleic acid analogs. As well known, the nucleic acid bases such as adenine, thymine and so on are relatively hydrophobic, and therefore such base-containing analogs are generally soluble in common organic solvents, but rather insoluble in water. On the other hand, natural nucleic acids are hydrophilic and denatured in organic solvents. For aiming the new material target to natural nucleic acids, it seems to be necessary to synthesize water-soluble analogs.

In the present paper, synthesis of water-soluble polyethyleneimine, polyamino acids, for example poly-L- and -D-lysine derivatives containing nucleic acid bases with spacers was shown. Besides of them, we studied further the synthesis of hyaluronic acid derivatives conjugated with nucleic acid bases. The studies on their properties, interaction of these polymers and applicabilities were also done.

#### RESULTS AND DISCUSSION

Preparation of homoserine derivatives of nucleic acid bases

For example, starting from nucleic acid bases, the carboxyethyl derivatives of the bases were prepared by a Michael type addition reaction of ethyl acry-

late followed by the hydrolysis. The carboxyethyl derivatives of the bases were reacted with ( $\pm$ )- $\alpha$ -amino- $\gamma$ -butyrolactone hydrobromide to afford  $\gamma$ -butyrolactone derivatives of the bases. For the coupling reaction, pentachlorophenyl ester derivatives were used with imidazole as a catalyst [ 4 ] .

#### Grafting onto polyethyleneimine

The grafting of nucleic acid base derivatives with a hydroxyl group onto polyethyleneimine polymer backbone was also carried out by the activated ester method. Since the reactivity of the  $\gamma$ -lactone is low, direct reaction of the lactone derivative with polyethyleneimine was ineffective. Therefore, the lactone derivatives were at first hydrolyzed to 3-hydroxybutyric acid derivatives, followed by the condensation with polyethyleneimine using the activated ester method. The grafting reaction was carried out in N,N-dimethylformamide, to which a small amount of 4-pyrrolidinopyridine was added as an effective catalyst. Nucleic acid base contents of the polymers were determined by UV spectroscopy of hydrolyzed samples. A quantitative calculations were done by using the corresponding carboxyethyl derivatives as the standards. The base units ( unit mole per cent ) on the polymer were tabulated in Table 1. ( PEI: polyethyleneimine, Hse: homoserine )

#### Interaction study on the base containing PEI-Hse derivatives

The interaction study between water-soluble polyethyleneimine derivatives containing thymine ( PEI-Hse-Thy ) and adenine ( PEI-Hse-Ade ) was at first studied at pH 7.0, with continuous variation techniques. The hypochromicity values for PEI-Hse-Thy and PEI-Hse-Ade system ( 1:1 base unit ) were determined at pH 2.2 and 5.5. At pH 2.2, the hypochromicity was found to be negligible even after 3 days, while the value at pH 5.5 was obtained as 7.1 %, which was comparable to the value at pH 7.0. Adenine base has a pKa value at 4.15, and exists in a protonated form at pH 2.2, and the protonated adenine base cannot form a complex with its complementary thymine base. This may be the reason for the negligible hypochromicity value at pH 2.2 and the high value at pH 5.5. From the facts, the polymer complex between PEI-Hse-Thy and PEI-Hse-Ade at pH 7.0 can be concluded to be due to the complementary base-base interaction.

The interaction study was then done for the system of PEI-Hse-Ura ( Ura: uracil ) and PEI-Hse-Ade at pH 7.0. The system showed the highest hypochromicity value when the base unit ratio is about 1:1 ( Uracil:adenine ), suggesting that the formation of a stable 1:1 polymer complex due to the specific base-base interaction. The hypochromicity value obtained ( 15.2 % ) was higher than that for the PEI-Ade and PEI-Thy systems, which had no spacer groups. The interaction between cytosine and hypoxanthine containing polymers, that is, PEI-Hse-Cyt and PEI-Hse-Hyp was further studied. In this case, the formation of a stable 1:1 polymer complexes was also observed, which is due to complementary base-base interaction.

In the case of the interaction between PEI-Hse-Hyp and poly C, the complex formation by base-base specific interaction was clearly seen in aqueous solution at pH 7.0. The overall stoichiometry of the complex based on the nucleic acid base units was approximately 2:1 ( hypoxanthine:cytosine ) under the condition used. The maximum hypochromicity value, obtained as 26 %, was smaller than that of poly I and poly C system ( 33 % ), but higher than those of other synthetic polymer analogue - polynucleotide systems. The interaction of PEI-Hse-Ura and PEI-Hse-5 FU ( FU: fluorouracil ) with poly A was also studied.

#### Applicability of the polymer complexes

An exciting subject of the synthetic nucleic acid analogs in the field of polymeric drugs appears to be the interferon inducing activity. The most effective synthetic inducers of  $\gamma$ -interferon are found on the polymeric complexes between nucleic acids and polynucleotides, such as a double-stranded helix of

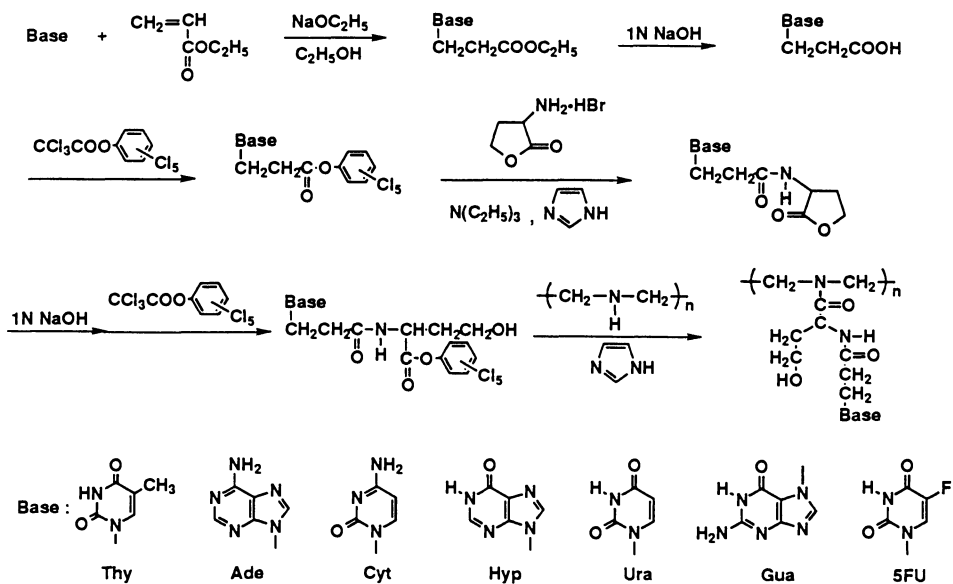


Table 1. Composition of Water-Soluble Nucleic Acid Analogs

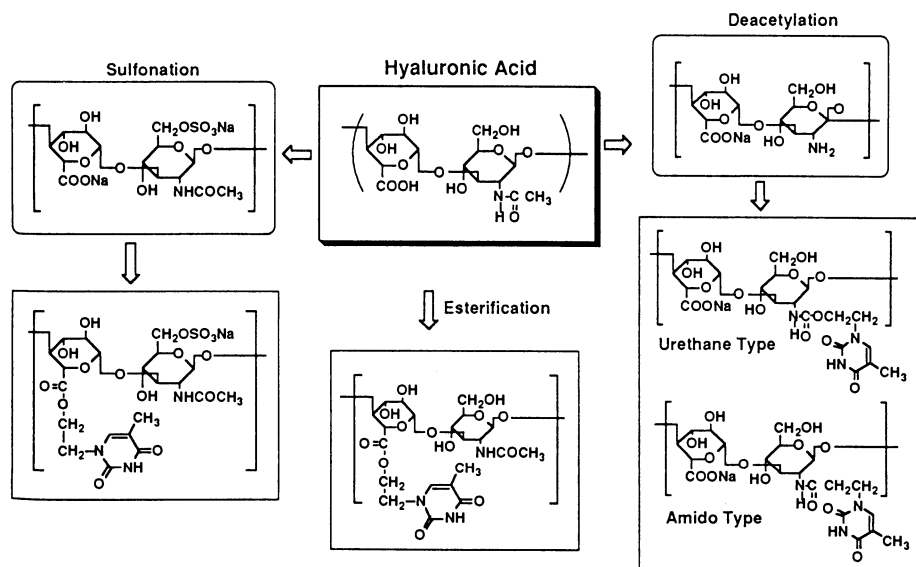
Base	Polymer	Content of the bases, %	Yield, %
Adenine	PEI-Hse-Ade	92	80
Cytosine	PEI-Hse-Cyt	86	78
5-Fluorouracil	PEI-Hse-5FU	91	68
Hypoxanthine	PEI-Hse-Hyp	92	68
Thymine	PEI-Hse-Thy	97	78
Uracil	PEI-Hse-Ura	94	78



poly C - poly I complex. It is known that the synthetic nucleic acid analogs are incapable of inducing interferon in human fibroblast cell in nature. On the other hand, it was found that the complexes of water-soluble polyethyleneimine derivatives containing cytosine and homoserine as a spacer, that is PEI-Hse-Cyt, with poly I is a highly effective  $\gamma$ -interferon inducer in human fibroblast cell. A reason for such high effectivity may be caused by the stability of PEI-Hse-Cyt with poly I complex, and the high uptake of the complexes by cells [ 2 ].

New polymers of hyaluronic acid derivatives containing nucleic acid bases [ 5 ]

Hyaluronic acid is a natural polymer of great interest in the pharmaceutical and clinical practice. However, only a few studies on its chemical modification of hyaluronan seem to have been reported. It is expected that the conjugation of nucleic acid base with hyaluronic acid derivatives is a good strategy to obtain a new type of biocompatible nucleic acid analogs.



The conjugation of nucleic acid base with sulfonated hyaluronan was achieved by the ring opening reaction of 1,2-O-ethano derivatives of nucleic acid bases. Thymine and 5-bromouracil bases were quantitatively conjugated to sulfonated hyaluronan in 15 % and 24 %, respectively [ 6 ].

An alternative method to get nucleic base containing hyaluronan includes its synthesis via deacetylation of hyaluronic acid, though the problem of its degradation cannot be avoided. Nucleic acid base conjugation with deacetylhyaluronic acid was achieved in high content by the activated esterification, which affords water-soluble derivatives. Content of the bases introduced could be controlled by the variation of the ratio of bases and deacetylated hyaluronic acid [ 7 ]. By the investigation of CD and UV spectra, deacetylated hyaluronic acid derivatives conjugated with thymine base were found to form polymer complex with poly A in neutral aqueous solution, through a specific interbase interaction between thymine and adenine.

Studies on the applicability of such hyaluronic acid derivatives conjugated with nucleic acid bases are also the subjects of great interest. Such deriva-

tives were studied as a new concept of controlled release system, that is, the photoresponsive controlled releasing system [ 8 ]. Deacetylated hyaluronic acid conjugated with thymine base was prepared as a drug releasing membrane, and sucrose was used as a model drug substance. Thymine moiety in the membrane was applied as the functional group, which provided reversible crosslinks: i.e., formation and cleavage of thymine dimer structure, induced by UV light photoreaction. The rate of sucrose releasing from the membrane was controlled by the degree of photodimerization reaction at UV light ( 280 nm ), which led to the slow release of sucrose. The results indicated that hyaluronic acid conjugated with thymine base can be applied as an effective material for the photoresponsive controlled releasing system.

The hyaluronic acid derivatives conjugated with thymine base was then studied from another concept of controlled releasing system, that is, the specific interaction and photoresponsive controlled release system. Again, deacetylated hyaluronic acid conjugated with thymine base was applied for a drug release membrane [ 9 ].

#### ACKNOWLEDGEMENT

I wish to express my hearty thanks to Dr. T. Wada and Dr. Y. Inaki of Osaka University, Japan, and Dr. S. Chirachanchai of Chulalongkorn University, Bangkok, Thailand, for their helpful assistance of a series of the work.

#### REFERENCES

1. Takemoto K. and Inaki Y. ( 1981 ) Synthetic nucleic analogs. *Adv.Polymer Sci* 41: 1-51
2. Pitha J.( 1983 ) Polymeric Drugs. *Adv.Polymer Sci* 50: 1
3. Takemoto K., Inaki Y. and Ottenbrite, Eds. ( 1987 ) *Functional Monomers and Polymers*, Marcel Dekker, Inc. New York
4. Inaki Y., Sakuma Y., Suda Y. and Takemoto K. ( 1982 ) *J.Polymer Sci.Polymer Chem.Ed.*20: 1917
5. Chirachanchai S.( 1995 ) Dissertation
6. Wada T., Chirachanchai S., Izawa N., Inaki Y. and Takemoto K. ( 1994 ) *Chem.Lett.*: 2027
7. Wada T., Chirachanchai S., Izawa N., Inaki Y. and Takemoto K. ( 1994 ) *J.Bioactive and Compatible Polymers* 9: 429
8. Chirachanchai S. Wada T., Inaki Y. and Takemoto K.: *J.Controlled Release*, to be published
9. Chirachanchai S., Wada T., Inaki Y. and Takemoto K.: *J.Controlled Release*, to be published

# INTELLIGENT MATERIALS

Teruo Okano, Akihiko Kikuchi, Yuzo Kaneko\*, Kiyotaka Sakai\*, Miki Matsukata<sup>†</sup>,  
Naoya Ogata<sup>†</sup>, and Yasuhisa Sakurai

Institute of Biomedical Engineering, Tokyo Women's Medical College,  
8-1 Kawadacho, Shinjuku, Tokyo 162, JAPAN

\* Department of Chemical Engineering, Waseda University  
3-4-1 Okubo, Shinjuku, Tokyo 169, JAPAN

<sup>†</sup> Department of Chemistry, Sophia University,  
7-1 Kioicho, Chiyoda 102, JAPAN

## SUMMARY

Poly(*N*-isopropylacrylamide) (PIPAAM) is well-known to change its structure in response to temperature in aqueous solutions [1,2]. Polymer chains of IPAAm hydrate to form expanded structures in water at lower solution temperatures (<32°C). At temperatures above 32 °C, however, the chains form compact structures by dehydration manifested as a lower critical solution temperature (LCST) [2]. Telomerization chemistry is expected to control oligomer molecular weight and create synthetic routes to semitelechelic oligomers averaging one functional end group per oligomer chain [6]. Thiol compounds having functional groups as telogens are known to be effective in introducing functional groups to the ends of growing polymeric chains and regulating polymer molecular weight by radical telomerization via chain-transfer reactions [7]. The research described in this paper is directed toward development and fundamental studies of biomedically relevant modulation systems using the temperature-responsive polymer, PIPAAm with a functional end group, as switching sequence. Temperature responsive semitelechelic PIPAAm polymer was attached to biomolecules, crosslinked hydrogels and solid surfaces to create new, modified bioconjugates, graft type gels and grafted surfaces, respectively.

Key Words : Poly(*N*-isopropylacrylamide), surface modification, hydrogels, biomolecule conjugates, temperature-responsibility.

## INTRODUCTION

Considerable research attention has been focused recently on materials which change their structure and properties in response to external stimuli. These materials, termed "intelligent materials", sense a stimulus as a signal (sensor function), judge the magnitude of this signal (processor function), and then alter their function in direct response (effector function). Introduction of stimuli-responsive polymers as switching sequences into both artificial materials and bioactive molecules would permit external, stimuli-induced modulation of their structures and "on-off" switching of their respective functions at molecular levels[1-3].

Intelligent materials embodying these concepts would contribute to the establishment of basic principles for fabricating novel systems which modulate their

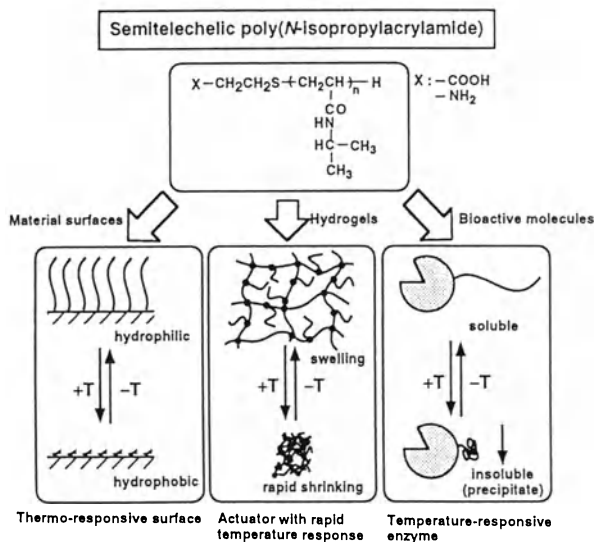


Fig.1 Temperature-responsive intelligent biointerfaces. Semi-telechelic poly(*N*-isopropylacrylamide) can be introduced into solid surfaces, hydrogels and proteins (enzyme and bioactive peptides) as on-off switches for hydrophilic/hydrophobic, swelling/shrinking, soluble/insoluble and active/inactive alterations.

structural changes and functional changes in response to external stimuli. These materials are attractive not only as new, sophisticated biomaterials but also utility in protein biotechnology, medical diagnosis and advanced site-specific delivery systems. We have been studying the design of molecular architecture of intelligent materials. PIPAAm was used to introduce a reversible switching function correlated to hydration-dehydration changes of polymer chains in response to changes in temperature, as shown in Figure 1.

## INTELLIGENT MATERIALS SURFACE

We have reported hydrophilic/hydrophobic surface property alterations in response to temperature changes using solid surfaces[4-7]. These surfaces demonstrated hydrophobic properties above the LCST where PIPAAm chains existed as collapsed conformation. Both hepatocytes and endothelial cells readily attached and multiplied on these grafted surfaces. When temperature is decreased below the LCST to 4°C, the surface swells and becomes hydrophilic. Cells detached from these surfaces in response to the hydration of grafted PIPAAm chain. Consequently, cultured cells could be easily recovered from these surfaces by low temperature treatment with improved viability compared to those harvested typically by enzymatic treatment. Since PIPAAm physical structures and properties are readily controlled by simple changes in temperature without changing any chemical structure of the polymer, temperature-responsive PIPAAm is unique and attractive as the molecular switching component for the "biointerface" by altering interfacial properties and functions in response to external temperature changes.

Two types of PIPAAm were used as surface modifiers: an end-functionalized PIPAAm with a carboxyl end group (Fig.2a) and a poly(IPAAm-*co*-acrylic acid) polymer (Fig.2b). By means of dynamic contact angle measurements in water, the wettability of terminally polymer grafted surfaces using end-functionalized PIPAAm with an end carboxyl group were compared with that of multipoint polymer grafted surfaces using PIPAAm copolymers containing carboxyl groups along the polymer chain. Each PIPAAm grafted surface showed completely hydrophilic properties under 20 °C. Although multipoint grafted surfaces demonstrated surface property changes near 24°C, the extent of decrease in the hydrophilic property was small compared to that of the terminal grafted surfaces. Terminal grafted surfaces demonstrated hydrophilic/hydrophobic surface property changes at 24°C with small temperature increases. The value of  $\cos\theta$  changes from 0.63 at 20°C to 0.05 at 26°C. Temperature responsive surface property changes which terminal grafted surfaces demonstrated were more rapid and significant than that of multipoint grafted surfaces demonstrated. These features were

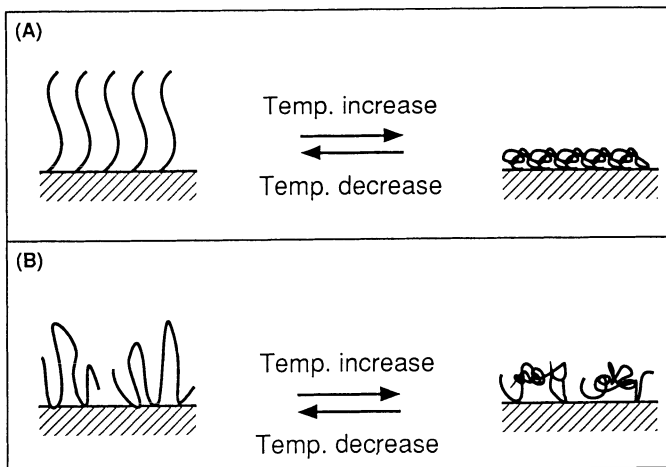


Fig. 2. Schematic illustration of phase transition corresponding to temperature response for PIPAAm grafted surfaces; a) terminally PIPAAm grafted, and b) multipoint graft PIPAAm surfaces, in aqueous media

suggested to be due to more effective restricted conformational freedom for PIPAAm graft chains which influence polymer dehydration and hydrogen bonding with water molecules. Also, these surfaces are shown to achieve on-off regulation of platelet contact-induced activation. These results suggest a new concept wherein PIPAAm grafted surfaces could be concentrated at specific site in the body by external temperature modulation.

## INTELLIGENT HYDROGELS

In contrast to conventional crosslinked PIPAAm hydrogels, we have prepared a thermosensitive hydrogel with a comb structure in which PIPAAm chains are grafted onto crosslinked networks (Fig.1). Within the gel, terminally grafted chains have freely mobile ends, distinct from the typical network structure in which both ends of the PIPAAm chains are crosslinked and relatively immobile. With increasing temperature, grafted PIPAAm chains begin to collapse from their expanded (hydrated) form to compact (dehydrated) forms. This collapse occurs before the PIPAAm network begins to shrink, because of the mobility of the grafted chains. The grafted polymer chains dehydrate to create hydrophobic nuclei which enhance aggregation of the crosslinked chains. Disks of comb-type graft PIPAAm gels and IPAAm homopolymer gels with identical thickness and diameters show different de-swelling kinetics when the temperature is increased from below to above the phase transition temperature (Fig.3a). Conventional IPAAm homopolymer gels shrunk very slowly after the temperature was increased from 10°C to 40°C, requiring more than a month to reach equilibrium. This gel shrunk gradually from the surface inwards, mediated by diffusion of the collapsing polymer network and the release of entrapped water from the collapsing gel. As a dense, collapsed polymer layer impermeable to water was formed near the gel surface before bulk gel collapse was initiated (thermal convection is more rapid than mass transfer), gel shrinking was hindered after the initial stages by internal hydrostatic pressure. As a result, the PIPAAm homopolymer gel shrinkage rate was limited by water permeation from the gel interior through the collapsed polymer skin, keeping water within the gel for longer periods.

In contrast to the IPAAm homopolymer gel, the comb-type PIPAAm graft gel shrunk rapidly to its equilibrium state. In the process, the gel underwent large, rapid volume changes with marked mechanical buckling, indicative of the much greater aggregation forces operating within the grafted gel. Trapped water was rapidly squeezed out from the gel interior. This result is supported by the changes in the amount of freezable water within two types of gel matrices determined by DSC. As can be seen in Fig.3b, almost 90% of the freezable water was desorbed from the graft-type PIPAAm gel within 20 min after the temperature was increased to 40°C, although non-freezable water content remained nearly constant and fairly low. Therefore, we attribute the marked swelling changes observed for graft-type PIPAAm gel to the large change in freezable water

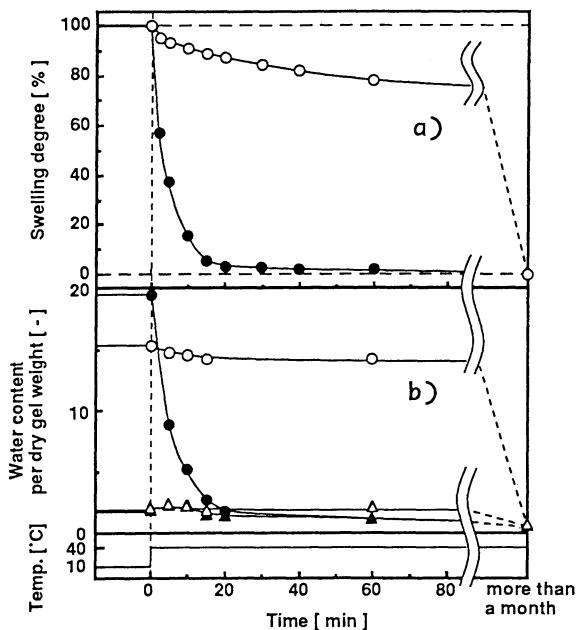


Fig.3a) Shrinking kinetics of PIPAAm homopolymer (○) and comb-type grafted (●) PIPAAm gels after temperature increase from 10°C to 40°C.

Fig.3b) Changes in water structure inside of shrinking PIPAAm homopolymer (○, freezable water; ●, non-freezable water) and comb-type grafted PIPAAm (Δ, freezable water; ▲, non-freezable water) gels.

content in the gel. In contrast to the graft-type PIPAAm gel, only 5% of the freezable water was desorbed from the IPAAm homopolymer gelafter 60 min. Rapid shrinking of the graft-type PIPAAm gel was due to the immediate dehydration of PIPAAm grafted chains in the gel matrix followed by subsequent hydrophobic interaction between dehydrated grafted chains preceding shrinkage of the PIPAAm network, affecting rapid expulsion of water from the gel matrix. The rapid shrinking and release of most of the freezable water resulted in a large volume change, suggesting that a skin structure that would reduce the de-swelling rate is not formed in this case. An increase in void volume within the grafted PIPAAm network resulting from collapsed grafted chains may also contribute to rapid release of water to the gel exterior.

In the case of a gel swelling in water at 10 °C from an equilibrium shrunken state (40° C), the swelling rate was slower than the de-swelling rate, and no difference in swelling rate was observed between the two types of gel. In both cases the amount of absorbed water increases in proportion to the square root of time. These results indicate that polymer network diffusion is rate-determining for swelling. The details of this process are currently under investigation.

### INTELLIGENT BIOMOLECULES

Using PIPAAm, polymer-enzyme conjugates of lipase[9] and polymer-protein conjugates[10,11] by covalent couplin were synthesized. Polymer-enzyme conjugates retained their native enzymatic activities below the critical temperature, white these conjugates precipitated and their catalytic function

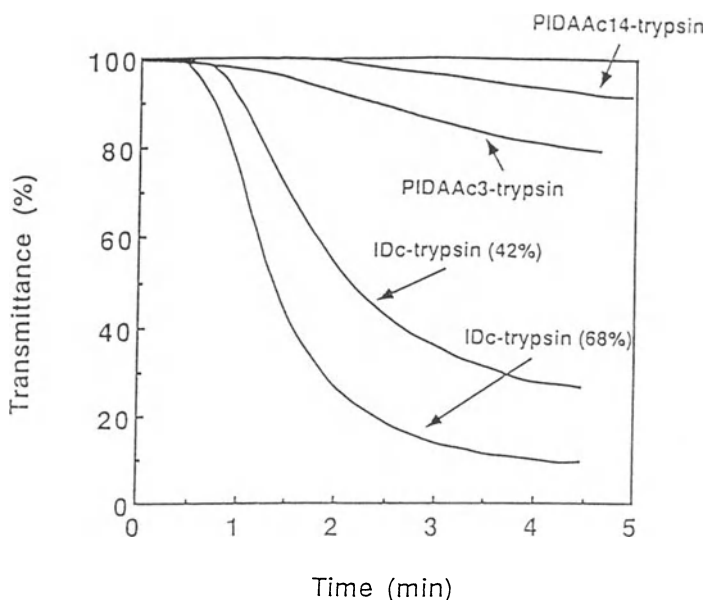


Figure 4. Speed of response towards temperature changes (35 to 45°C) of PIPAAm-trypsin conjugate solutions, whose concentration was normalized by protein concentration; 250  $\mu\text{g/ml}$ .

IDc-trypsin (single end attachment)

PIDAAc-trypsin (multi-point attachment)



were shut off above the critical temperature. These conjugates can be readily separated from reactive mixtures as a precipitate by simple temperature changes after reaction and reused in cycles without denaturation. In particular, the role of free mobile PIPAAm grafted chains were discussed from the results of the rate of precipitation of the conjugate. Fig.4 shows the rate of transmittance change of bioconjugate solution, clearly demonstrating the rapid temperature response of free mobile PIPAAm grafted chains.

These new intelligent biointerface is an important basis to achieve drug targeted delivery at temperature modulated targeted site.

## REFERENCES

- [ 1 ] Okano T, Yoshida R (1993) Intelligent Polymeric Materials for Drug Delivery. In: Tsuruta T, Hayashi T, Kataoka K, Ishihara K, Kimura Y, (eds) Biomedical Applications of Polymeric Materials. CRC Press, Boca Raton, pp.407-428
- [ 2 ] Okano T (1993) Molecular Design of Temperature-Responsive Polymers as Intelligent Materials. In: Dusek K, (eds) Advances in Polymer Science. Springer-Verlag, Berlin, 110:pp.179-197
- [ 3 ] Okano T, Yoshida R (1993) Thermo-responsive property of poly (N-isopropylacrylamide-co-alkyl methacrylate). In: Tsuruta T, Doyama M, Seno M, Imanishi Y, (eds) New Functionality Materials, Volume B Synthesis and Function Control of Biofunctionality Materials, Elsevier Science Publishers B.V., Amsterdam, pp.189-196
- [ 4 ] Yamada N, Okano T, Sakai H, Karikusa F, Sawasaki Y, Sakurai Y (1990) Thermo-responsive polymeric surfaces: control of attachment and detachment of cultured cells. Makromol. Chem., Rapid Commun. 11: 571-576
- [ 5 ] Okano T, Yamada N, Sakai H, Sakurai Y (1993) A novel recovery system for cultured cells using plasma-treated polystyrene dishes grafted with poly(N-isopropylacrylamide). J. Biomed Mater Res, 27: 1243-1251
- [ 6 ] Takei YG, Aoki T, Sanui K, Ogata N, Sakurai Y, Okano T (1995) Temperature-modulated platelet and lymphocyte interactions with poly(N-isopropylacrylamide)-grafted surfaces. Biomaterials (in press)
- [ 7 ] Takei YG, Aoki T, Sanui K, Ogata N, Sakurai Y, Okano T (1994) Dynamic contact angle measurement of temperature-responsive surface properties for poly(N-isopropylacrylamide) grafted surfaces. Macromolecules 27: 6163-6166
- [ 8 ] Yoshida R, Uchida K, Kaneko Y, Sakai K, Kikuchi A, Sakurai Y, Okano T (1995) Comb-type grafted hydrogels with rapid de-swelling response to temperature changes. Nature, 374: 240-242
- [ 9 ] Matsukata M, Takei Y, Aoki T, Sanui K, Ogata N, Sakurai Y, Okano T (1994) Temperature modulated solubility-activity alterations for Poly(N-isopropylacrylamide)-lipase conjugates. J. Biochem. 116: 682-686
- [ 10 ] Takei YG, Aoki T, Sanui K, Ogata N, Okano T, Sakurai Y (1993) Temperature-responsive bioconjugates. 1. Synthesis of temperature-responsive oligomers with reactive end groups and their coupling to biomolecules. Bioconjugate Chem 4: 42-46
- [ 11 ] Takei YG, Aoki T, Sanui K, Ogata N, Okano T, Sakurai Y (1993) Temperature-responsive bioconjugates. 2. Molecular design for temperature-modulated bioseparation. Bioconjugate Chem. 4 : 341-346

# FUNCTIONAL SYNTHETIC AND SEMISYNTHETIC POLYMERS IN BIOMEDICAL APPLICATIONS

E. Chiellini, R. Solaro

*Dept. of Chemistry and Industrial Chemistry, University of Pisa, via Risorgimento 35, 56126 Pisa, Italy*

## SUMMARY

A survey is reported on our activity performed in the last few years on the preparation of new synthetic and semisynthetic polymeric materials endowed with bioerodible-biodegradable characters and designed for applications in the practice of drug controlled release. The presentation will be arranged into the following sections: 1) hydroxyl containing polyesters, that comprise polymers of racemic and optically active glyceric acid, and copolymers of cyclic anhydrides, including also carbon dioxide, with monoglycidyl ethers of reversibly protected polyols. 2) bioerodible polycarboxylates as derived from the alternating copolymerization of maleic anhydride with alkyl vinyl ethers followed by partial esterification of maleic anhydride groups. 3) multihydroxyl grafted polysaccharides, including cyclodextrins. Typical examples of their applications in the release of drugs are also presented.

**KEY WORDS:** hydrogels, hydroxyl containing polyesters, hydroxyl containing polycarbonates, cyclodextrin derivatives, drug release

## INTRODUCTION

Over the years an ever growing interest has focused attention of polymer chemists on the design of polymeric materials aimed at the fulfilment of special needs in agrochemical, pharmaceutical and biomedical exploitation areas. Flourishing information is currently available in single and multiauthored books as well as on journals specifically addressed to the various areas of interest whose disciplinary borderlines are getting increasingly narrower helping to overcome the barrier between fundamental and applied research.

We got involved in the scientific activity pertaining to the present International Symposium almost two decades ago<sup>1</sup> and thus we had been able to witness and appreciate the quantitative and qualitative growth of the interdisciplinary field of Biomedical Polymers to which Prof. Tsuruta and his school gave outstanding contributions and leading inputs.

In keeping with the ongoing research trend in the above mentioned area, in the present contribution, we wish to report on the results attained in the preparation and characterization of multifunctional synthetic and semisynthetic polymers and oligomers specifically designed for the practice of controlled delivery of conventional and macromolecular drugs.

In particular attention will be focused on three types of polymeric materials that for convenience can be classified as: 1) *hydroxyl containing polyesters*; 2) *carboxyl containing alternating copolymers*; 3) *multihydroxyl grafted polysaccharides*. Examples will be also presented of their utilization in the formulation of polymeric drug delivery systems.

## METHODS

Details on the synthetic procedures and descriptions of the characterization of the mentioned three classes of multifunctional polymeric materials have been already reported in specific publications that at any convenience can be quoted by following in that order. One can refer to ref. 2 for polymeric materials of class **1**, to refs. 3 and 4 for class **2**, and to ref. 5 for class **3**.



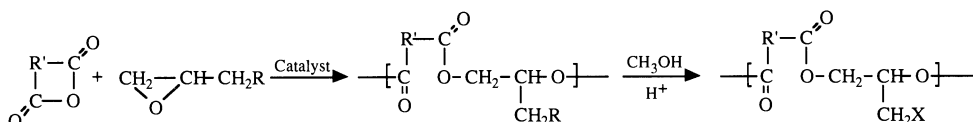
## RESULTS AND DISCUSSION

### 1. Hydroxyl containing polyesters

Linear polyesters including polycarbonates that contain from one to four free hydroxyl groups in the repeating units were prepared according to a two-step process. This consists of the polymerization of suitable derivatives of protected polyols followed by the controlled removal of the protecting groups. The preparation of monomeric precursors is critical to the success of the overall process. These precursors must contain selectively and reversibly protected hydroxyl moieties that do not conflict with the polymerization process and are capable of remaining unaltered during the polymer workup. Among the several routes that usually apply to the synthesis of polyesters, we adopted pathways based on hydroxyacid self-condensation, the condensation of bishydroxyl compounds with diacid chlorides, and ring-opening alternating addition of epoxides to cyclic anhydrides or carbon dioxide. Accordingly, we prepared polyesters with free hydroxyl groups directly attached to the polymer backbone or in pendant residues at various distances from the main chain.

Polyglycerates of moderate molecular weights, were prepared by internal transesterification reaction of the corresponding 2- or 3-O-protected glycerates<sup>6,7</sup>.

Series of new polyesters and polycarbonates containing free hydroxyl groups in the side chain have been prepared by ring opening polymerization of cyclic anhydrides, including carbon dioxide, with the glycidyl ethers of protected sequential polyols consisting of an odd number of carbon atoms, followed by controlled removal of the protecting groups under mild conditions<sup>8-10</sup>.



R' = CH=CH, (CH<sub>2</sub>)<sub>2</sub>, (CH<sub>2</sub>)<sub>3</sub>, C<sub>6</sub>H<sub>4</sub>, C<sub>6</sub>H<sub>10</sub>;

R = isopropylidenediglyceryl, diisopropylidenedexylitoyl, diisopropylideneribitolyl, diisopropylidene-L-arabitolyl

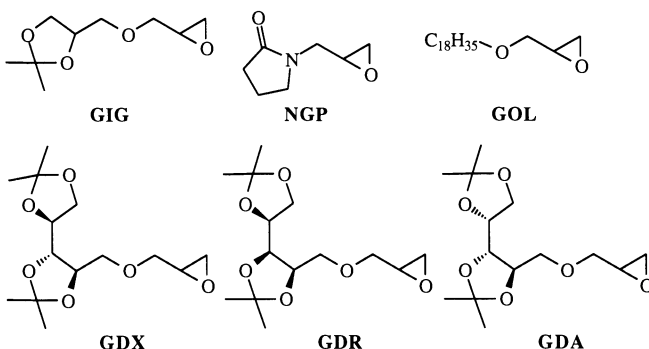
X = glyceryl, xylitolyl, ribitolyl, L-arabitolyl

New functional polyesters were obtained by copolymerization of cyclic anhydrides, such as maleic, succinic, glutaric, phthalic, and hexahydrophthalic anhydride, with glycidyl derivatives of protected polyols, such as glycidylisopropylidenediglycerol (GIG), glycidyl diisopropylidenedexylitol (GDX), glycidyl diisopropylideneribitol (GDR), glycidyl diisopropylidene-L-arabitol (GDA), glycidyl oleol (GOL), and N-glycidylpyrrolidone (NGP), in the presence of organoaluminum derivatives such as bis(diethylaluminum) sulphate, triisobutylaluminum, and hexaisobutylalumoxane as catalysts.

NGP and GOL were obtained as racemic enantiomers mixtures, whereas in the other cases rather complex isomeric mixtures of optically inactive (GIG, GDX and GDR) and optically active (GDA) diastereomers were obtained.

By following the same reaction principles, a series of new polycarbonates was prepared by copolymerization of carbon dioxide with the above reported glycidyl ethers at 35°C in the

presence of the diisobutylzinc/pyrogallol catalytic system. Polymerization products, soluble in moderately polar organic solvents, such as acetone and chloroform, and characterized by molecular weights included between 8·10<sup>3</sup> and 7·10<sup>4</sup>, are obtained in medium-low conversions, depending on the chemical composition of the reaction mixture.

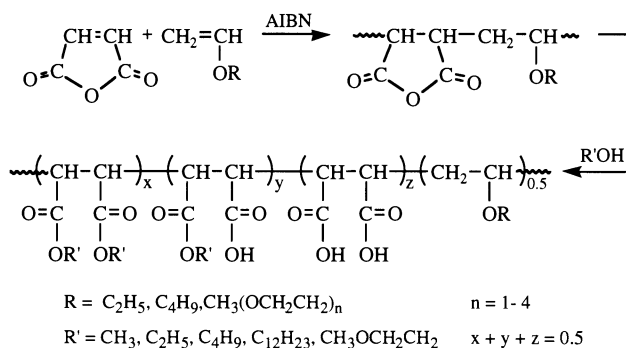


The almost exclusive formation of cyclic carbonates was observed when an equimolar mixture of tetraphenylporfinealuminum monochloride and tetrabutylammonium bromide was used as polymerization catalyst.

Complete removal of the protecting isopropylidene groups was attained under mild conditions, by stirring a polymer solution in 1:1 chloroform/methanol, at moderate temperature in the presence of a catalytic amount of hydrochloric acid or a sulphonic ion-exchange resin.

## 2. Carboxyl containing alternating copolymers

Alternating copolymerization of maleic anhydride with alkyl vinyl ethers of monomethyl endcapped polyethyleneglycols, followed by hemiesterification reactions of the anhydride moieties, led to a series of carboxyl containing functional polyhydrocarbons with an hydrophilic/hydrophobic balance and reactivity that make them particularly suitable for giving rise to new hybrid polymeric materials by combination with proteins<sup>3</sup>.



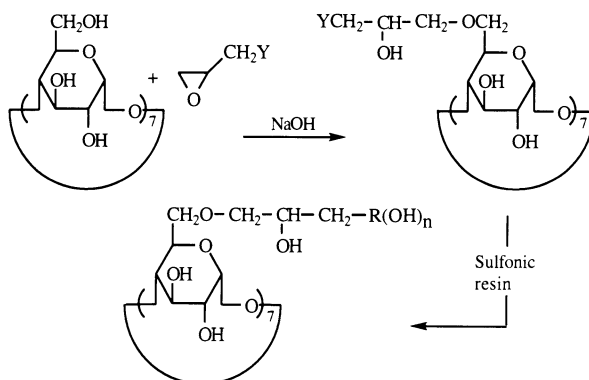
These new formulations have been found very promising in the controlled release of proteic drugs such as  $\alpha$ -interferon<sup>4</sup> and continuous research is currently undergoing in this area.

## 3. Multihydroxyl grafted polysaccharides

By grafting of glycidyl ethers of protected sequential polyols to polysaccharides, it has been possible to attain a wide variety of new multihydroxyl containing polysaccharides including cyclodextrins.

New functional derivatives of  $\beta$ -cyclodextrin were prepared by grafting either the reported glycidyl ethers of the mono- and diacetonides of alditols with 3 and 5 carbon atoms or N-glycidylpyrrolidone<sup>5,11</sup>. Grafting reactions were carried out at 60°C under alkaline conditions by using 1-2 moles of glycidyl ether per glucose residue. The reaction products resulted in all cases soluble in chloroform and were characterized by a content of 0.5-1.0 glycidyl residue per glucose unit.

The isopropylidene groups of the grafted products derived from protected alditols were removed at 45°C in methanol or in water/methanol mixtures in the presence of an acid catalyst. By suitably tuning reaction time and temperature, it was possible to stop the reaction at various degrees of deprotection thus allowing for the realization of complex mixtures of cyclodextrin derivatives with interesting rheological behavior. The prepared derivatives, both partially protected or totally deprotected, were in any case amorphous in nature.



Their solubility in water generally increased with increasing the degree of deprotection to reach values larger than 3 g/g water, whereas their solubility in chloroform decreased from an upper value of more than 1.5 g/ml to a practical insolubility at 100% deprotection.. It is also interesting to note that  $\beta$ -cyclodextrin grafted with glycidyl diisopropylideneribitol (grafting degree 0.5) presented a water solubility that decreased with temperature. Investigation of the effect of inherent structural parameters of the modified  $\beta$ -cyclodextrin on its solubility and the dependence on temperature is at present object of further attention.

New drug conjugates of antihypertensive drugs were prepared by complexation of nifedipine, corynanthine, and oxprenolol with modified or commercially available cyclodextrins. Some of the prepared drug/cyclodextrin formulations were preliminary tested "in vivo" on spontaneously hypertensive rats to evaluate their pharmacological activity. Improvement of drug absorption and bioavailability and increased antihypertensive efficacy was obtained when corynanthine and nifedipine were used as complexes with cyclodextrin derivatives<sup>12,13</sup> (Fig. 1). Research is in progress as aimed at the evaluation of the uptake of complexes of other conventional hydrophobic and proteic drugs with  $\beta$ -cyclodextrin derivatives as a function of type and extent of functionalization.

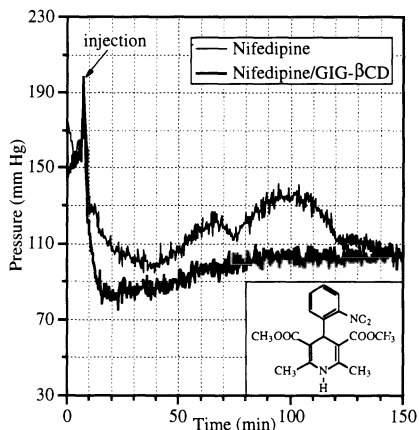


Figure 1. Variation of blood pressure in hypertensive rats by intraperitoneal administration of 5 mg nifedipine, alone or complexed with  $\beta$ -cyclodextrin derivatives

## CONCLUDING REMARKS

The potential has been stressed of new synthetic methods useful for the preparation of new versatile multifunctional polymeric materials that appear to be valuable candidates for various applications in biomedical and pharmaceutical fields<sup>14</sup>.

## REFERENCES

1. E. Chiellini, G. Galli, F. Ciardelli, R. Palla, F. Carmassi, *Inf.Chem.*, **176**, 221 (1978)
2. E. Chiellini, L. Bemporad, R. Solaro, *J. Bioact. Compat. Polym.*, **9**, 152 (1994)
3. E. Chiellini, G. Leonardi, D. Giannasi, R. Solaro, *J. Bioact. Compat. Polym.*, **7**, 161 (1992)
4. E. Chiellini, R. Solaro, G. Leonardi, D. Giannasi, R. Lisciani, G. Mazzanti, *J. Control. Release*, **22**, 273 (1992)
5. R. Solaro, S. D'Antone, L. Bemporad, E. Chiellini, *J. Bioact. Compat. Polym.*, **8**, 236 (1993)
6. E. Chiellini, S. Faggioni, R. Solaro, in *Polymers in Medicine and Surgery*, PRI, London, p. 39/1 (1989)
7. E. Chiellini, S. Faggioni, R. Solaro, *J. Bioact. Compat. Polym.*, **5**, 16 (1990)
8. R. Solaro, L. Bemporad, E. Chiellini, in *Synthetic Polymers as Drug Carriers. Interactions with Blood*, A. Baszkin, P. Ferruti, M.A. Marchisio, M.C. Tanzi, Eds., ALFA, Brescia, p. 71 (1991)
9. E. Chiellini, R. Solaro, *Makromol. Chem., Macromol. Symp.*, **54/55**, 483 (1992)
10. E. Chiellini, R. Solaro, L. Bemporad, *Eur. Pat. Appl.* 91830485.8 (1991).
11. E. Chiellini, E., R. Solaro, S. D'Antone, L. Bemporad, *Eur. Pat. Appl.* 91830497.3 (1991)
12. F. Morganti, *Thesis*, University of Pisa (1993).
13. F. Morganti, M.C. Breschi, L. Bemporad, R. Solaro, E. Chiellini, *ESB - 11th European Conference on Biomaterials*, Pisa - Italy, Sept 10-14 (1994)
14. E. Chiellini, R. Solaro, *ChemTech*, 29 (1993)

# Bioconjugates from Synthetic Polymers -How they can be married?-

N. Ogata

Department of Chemistry, Sophia University  
7-1 Kiioi-Cho, Chiyoda-Ku, Tokyo 102, Japan

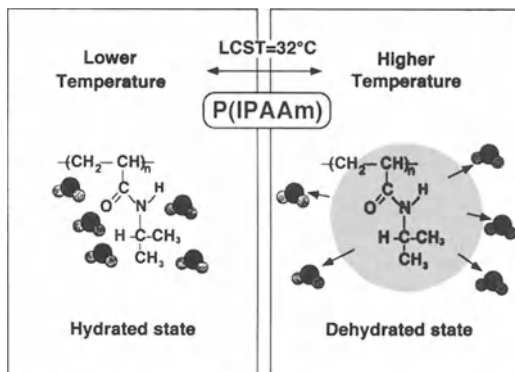
**SUMMARY:** Chemical modifications of biopolymers such as blood proteins or enzymes were carried out to prepare novel bioconjugates which led to new separation or recovery systems, by using temperature-responsive poly(N-isopropylacrylamide)(PIPAAm) which showed reversible dissolution-precipitation behaviors in water. Novel optical resolutions were developed to separate racemic mixtures of  $\alpha$ -amino acids by means of selective adsorptions of these racemes to temperature-responsive and optically active PIPAAm derivatives. Complete optical resolutions were attained by the optically active PIPAAm derivatives.

**KEY WORDS:** Bioconjugate, Enzyme, Trypsine, Optical resolution, Poly(N-isopropylacrylamide)

## 1. INTRODUCTION

Poly(N-isopropylacrylamide) (PIPAAm) is a well-known water soluble polymer which show unique and reversible hydration-dehydration changes in response to small temperature changes(1). An aqueous solution of PIPAAm causes phase separation to precipitate PIPAAm out of the aqueous solution at a certain temperature which is called as a lower critical solution temperature (LCST), as illustrated in scheme 1. The LCST of PIPAAm is 32°C and can be controlled from lower to higher temperatures by changing compositions of copolymers of IPAAm and other comonomers such as butyl methacrylate (BMA) or N,N-dimethylacrylamide (DMA).

**Poly(N-isopropylacrylamide)(P(IPAAm))is a water-soluble polymer at room temperature. Aqueous solutions of this polymer exhibit a lower critical solution temperature(LCST)around 32°C.**



Scheme 1 Phase transition of poly(N-isopropylacrylamide(PIPAAm) in water

Temperature-responsive hydrogels derived from PIPAAm have been extensively studied in terms of *intelligent polymers* to apply to biotechnological process control such as drug-release systems (2-4), recovery of cultured cells (5,6), and immobilized enzymes (7).

Telechelic oligo(IPAAm) (OIPAAm) having end carboxylic acid group was synthesized by a radical polymerization of IPAAm in the presence of  $\beta$ -mercaptopropionic acid as a chain transfer agent(8). The OIPAAm could be combined with biomolecules such as blood proteins (9) or enzymes (10) and a novel separation and recovery systems was established. This paper deals with further extension of the application of the temperature-responsive PIPAAm for the recovery of enzymes and for optical resolutions of racemes of  $\alpha$ -amino acids.

## 2. MODIFICATION OF ENZYME

Modification of Lipase by PIPAAm which was reported in a previous paper (11) led to study on the modification of Trypsine by PIPAAm by using the same condensation reaction of OIPAAm with Trypsine as the case of Lipase. N- $\alpha$ -benzoyl-D,L-arginine hydrochloride (BAONA) was used as a substrate for the hydrolysis reaction by Trypsine. Fig. 1 indicates LCST behaviors of native and IDC-modified ( copolymer from 90 mol% IPAAm and 10 mol% DMA of molecular weight 5,000, abbreviated as IDC 10). The IDC-Trypsine exhibited the same LCST behavior as that of the IDC-10 and native Trypsine did not show changes of transmittance in the aqueous solution. Dissolution and precipitation changes of the IDC-modified Trypsine was reversible by temperature changes.

Enzymatic activities of the IDC-modified Trypsine were measured as functions of temperatures, as shown in Fig. 2. Fig. 2 indicates that the enzymatic activity of the IDC-modified Trypsine rather increased in comparison with that of native Trypsine, possibly owing to specific adsorption of the substrate onto PIPAAm chains through hydrogen bonding. Table I summarizes values of  $K_m$  and  $V_{max}$  obtained from Lineweaver-Burk plots of the hydrolysis reaction.  $K_m$  of the IDC-modified Trypsine was much smaller than that of native Trypsine, while  $V_{max}$  values were almost similar, indicating that IDC-modified Trypsine could strongly adsorb substrates to enhance the enzymatic reactions.

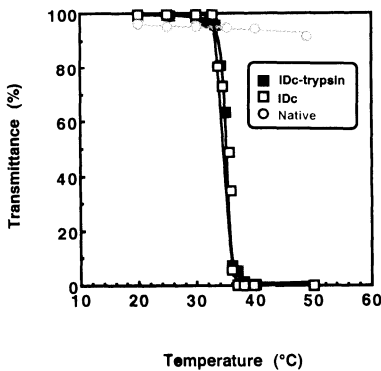


Fig. 1

Temperature dependence of transmittance of aqueous solutions of IDC and IDC-modified trypsin (1wt%, 500nm light)

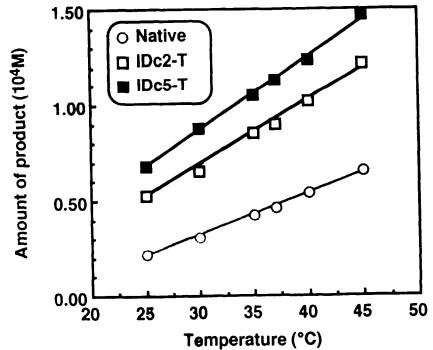


Fig. 2

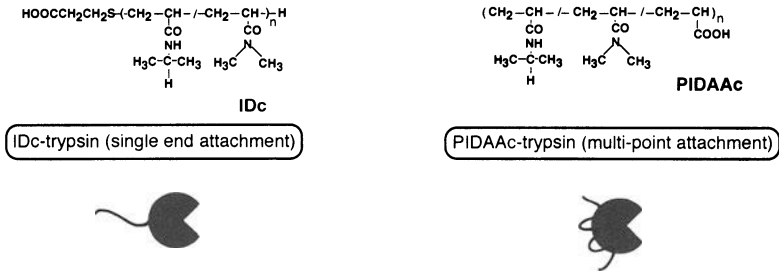
Effect of temperature on enzymatic activity of PIPAAm-conjugate trypsins (IDC2-T; modified by poly(IPAAm-co-DMA(2mol%)), IDC5-T; modified by poly(IPAAm-co-DMA(5mol%)), trypsin concentration=6.67 $\mu$ g/ml)

Table I Kinetic constants if IDc-trypsin conjugates

	$K_m(10^3M)$	$V_{max} (10^4M/sec)$
Native	1.320	1.75
IDc-5T	0.278	1.77
IDc-2T	0.461	1.75

It is interesting to incorporate PIPAAm chains as multi-point attachment on the surface of enzymes in order to compare enzymatic activities between single and multi-point attachments of the temperature-responsive PIPAAm. The multi-point PIPAAm abbreviated as PIDAAc was obtained by a radical terpolymerization of IPAAm, DMA and acrylic acid. The concept of enzyme modifications either by single or multi-point attachments of IPAAm is schematically shown in Scheme 2.

Fig. 3 indicate stabilities of the enzymatic activities of IDc- and PIDAAc-modified Trypsine, which show that the IDc-modified Trypsine is stable with much improvements of the enzymatic activity in comparison with that of native Trypsine, while that of PIDAAc-modified slightly decreased with time. Single-point attachments of PIPAAm on the surface of Trypsine might cause a protection of denaturation, while multi-point attachments of PIPAAm might induce some morphological change of Trypsine so that the enzymatic stability might decrease. Nevertheless, the modification of Trypsine by temperature-responsive PIPAAm resulted in a great improvements of both enzymatic activity and thermal stability of Trypsine.



Scheme 2 Concept of enzyme modification by single or multi-points attachments of temperature-responsive PIPAAm

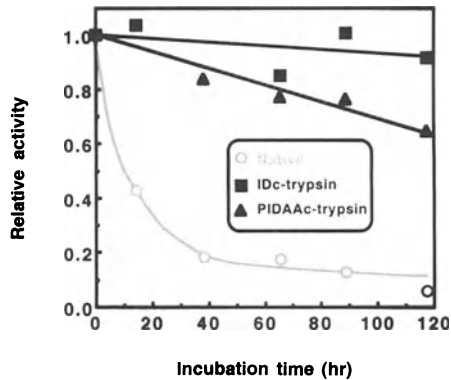


Fig.3 Stability of PIPAAm-trypsin/Tris-HCl buffer (pH8.15) solutions, incubating at 35°C

Since IDc-modified enzymes precipitate as droplets at temperatures above the LCST, these conjugates can be easily separated from the reaction phase by applying centrifugal separation, followed by a simple removal of supernatant after temperatures of the reaction phase raised above the LCST. Fig. 4 indicates relative enzymatic activities of IDc- or PIDAAc-modified Trypsine as functions of repeated number of cycles. The IDc-modified Trypsine slightly decreased the enzymatic activity which was superior to that of native Trypsine, while the enzymatic activity of the PIDAAc-modified Trypsine was inferior to native Trypsine. These results suggest that the single-point attachment of PIPAAm is better to maintain the enzymatic activity of Trypsine.

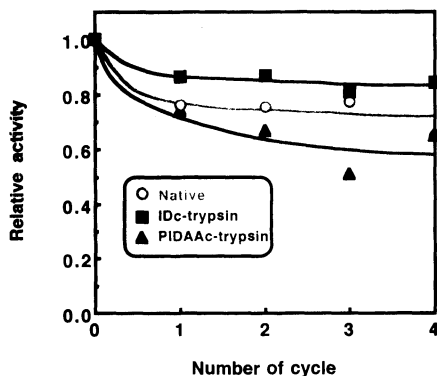
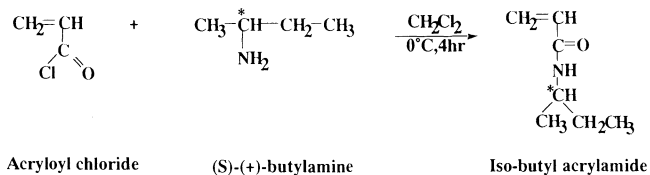
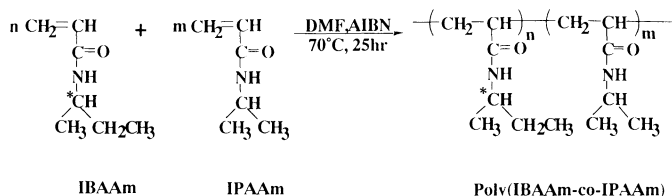


Fig. 4 Enzymatic activities of PIPAAm-trypsin after recycling by temperature change between 4° and 50°C.

### 3. OPTICAL RESOLUTION BY OPTICALLY ACTIVE PIPAAm

Optical resolution of racemic mixtures is very important in pharmaceutical and agricultural drugs since optical isomers are normally very difficult to separate by conventional separation methods such as distillation or recrystallization because they have almost similar chemical and physical properties, yet their biological and medical responses are different. These optical isomers are separated by chromatographic methods by utilizing small differences in absorption and desorption behaviors of these optical isomers onto various adsorbents. When optically active groups are incorporated into the temperature-responsive PIPAAm, it is expected that chiral interactions of the optically active sites in PIPAAm with substrates may lead to optical resolution owing to a strong adsorption of one side of isomers, when the IPAAm is dissolved with racemic mixtures of substrates in an aqueous solution and the dissolved PIPAAm starts to precipitate out of the aqueous solution by heating above LCST. Base on this expectation, optically active N-isobutylacrylamide (IBAAm) was synthesized, followed by copolymerization with IPAAm, in order to obtain optical active PIPAAm derivatives. Synthetic route is shown as below:





Poly(IBAAm) (PIBAAm) and poly(IPAAm-co-IBAAm) containing more than 30 mol% of IBAAm did not dissolve in water. LCST behaviors of poly(IPAAm-co-IBAAm) having 20 mol% of IBAAm are shown in Fig. 5, which also indicates LCST behaviors of the copolymer in the presence of L-Tryptophan (L-Try). Fig. 5 also shows LCST behavior of optically inactive (raceme of isobutyl moiety) poly(IPAAm-co-IBAAm) in the absence and in the presence of L-Try. LCST of optically inactive copolymer was 29°C, while that of the optically active copolymer shifted to 45°C, some 16°C higher temperatures. When L-Try was added to the aqueous solution, the LCST shifted to higher temperatures than that of copolymers themselves, some 10°C higher temperatures, respectively. The shift of LCST to higher temperatures can be ascribed to the increase of hydrophilicity of the copolymers owing to the adsorption of L-Try, indicating a strong chiral interaction between the copolymer and L-Try.

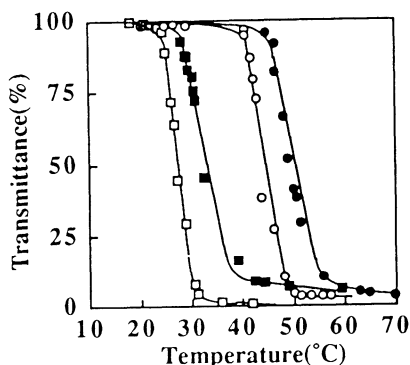


Fig. 5 LCST behaviors of 1wt% aqueous solution of poly(IBAAm-co-IPAAm) (light=500nm)

● : Chiral polymer+L-Try ,      ■ : Racemic polymer+L-Try  
 ○ : Chiral polymer+water,      □ : Racemic polymer+water

Racemic Try was dissolved in an aqueous solution of the optically active copolymer below LCST and temperature was increased above LCST so that the copolymer precipitated simultaneously with adsorption of L-Try. Supernatant of the solution was analyzed to identify the ratio between L- and D-Try in the solution. Results are summarized in Table II, which indicates that optical resolution of racemic Try was attained. Thus, a novel optical resolution method was developed by using optical active PIPAAm derivatives. This novel separation method is very useful for large scale optical resolutions.

Table II

Adsorption of Try to poly(IBAAm-co-IPAAm) in aqueous solution

Code	D-Trp / mmol l <sup>-1</sup>	L-Trp / mmol l <sup>-1</sup>
Chiral moiety	1.2×10 <sup>-2</sup> (5.3 %)	0.00 (0.0 %)
Racemic moiety	2.1×10 <sup>-2</sup> (9.2 %)	3.1×10 <sup>-2</sup> (13.2 %)



## References

- 1) M.Heskins, J.E.Guillet, and E.James, *J.Macromol. Chem.*, **A2**,1441(1968).
- 2) Y.H.Bae, T.Okano, R.Hsu, and S.W.Kim, *Makromol., Rapid Commun.*, **8**, 481(1987).
- 3) Y.H.Bae, T.Okano, R.Hsu, and S.W.Kim, *J.Polym.Sci., Polym. Phys.*, **28**, 923(1990).
- 4) T.Okano, N.Yui, M.Yokoyama, and R.Yoshida, *Advances in Polymeric Systems for Drug Delivery. Japanese Technology Reviews Section E: Biotechnology*, Vol. **4**, No.1, Gordon and Breach Science Publishers SA, Yverdon, Switzerland.
- 5) T.Okano, N.Yamada, H.Sakai, and Y.Sakurai, *J. Biomed. Mater. Res.*, **27**, 1243(1993).
- 6) N.Yamada, T.Okano, H.Sakai, F.Kurikusa, Y.Sawasaki, and Y.Sakurai, *Makromol. Chem., Rapid Commun.*, **11**, 571(1990).
- 7) L.C.Dong and A.S.Hoffman, *J. Controlled Release*, **4**, 223(1986).
- 8) Y.G.Takai, T.Aoki, K.Sanui, N.Ogata, T.Okano, and Y.Sakurai, *Bioconjugate Chem.*, **4**, 42(1993).
- 9) Y.G.Takai, T.Aoki, K.Sanui, N.Ogata, T.Okano, and Y.Sakurai, *Bioconjugate Chem.*, **4**, 341(1993).
- 10) M.Matsukata, Y.G.Takai, K.Sanui, N.Ogata, Y.Sakurai, and T.Okano, *J. Biochem.*, **116**, 682(1994).

# PLASMA MODIFICATION OF POLYMERIC SURFACES FOR BIOMEDICAL APPLICATIONS.

J.G.A. Terlingen, A. Bruil, A.S. Hoffman, J. Feijen,

Department of Chemical Technology, University of Twente, P.O. Box 217, 7500 AE Enschede, The Netherlands, \* Center for Bioengineering FI-20, University of Washington, Seattle, Washington 98195, USA.

## SUMMARY

In general the chemical composition of surfaces of biomaterials has to be tailored for a specific application. Using different types of glow discharge techniques it is possible to achieve a well defined chemical composition of the surface. Using the plasma immobilization technique it is possible to selectively introduce functional groups or poly(ethylene oxide) chains on the surface. By using a tetrafluoromethane (CF<sub>4</sub>) plasma fluorinated surfaces can be obtained. Poly(tetrafluoro ethylene)-like surfaces can be obtained by treating polymer surfaces covered with glass with a CF<sub>4</sub> plasma. Furthermore the fluorine introduced by a CF<sub>4</sub> plasma treatment can be etched off by an argon plasma treatment in a controlled way. This yields polymer surfaces with a wide range in surface wettability. These surfaces have been evaluated with respect to the adhesion of granulocytes and lymphocytes.

Key words: Glow discharge treatment, plasma immobilization, fluorination, teflon-like surfaces, leukocyte adhesion

## INTRODUCTION

The success of a polymeric material in biomedical applications is not only determined by its mechanical properties, but also to a large extent by its surface properties. Therefore an increasing demand to tailor the surface properties of polymeric materials exists. Surface modification is generally applied for three purposes; changing the barrier properties especially of membranes, adjustment of the surface free energy or introduction of functional groups which can be used for further covalent coupling of bioactive compounds. Several methods like wet oxidation and surface grafting have been developed to modify the surface properties of polymers. Among the most promising methods in this respect are glow discharge techniques, in which a partially ionized gas (a plasma) is used to alter the surface chemistry of polymeric materials.

The use of plasma techniques to modify polymeric surfaces has some distinct advantages. Firstly using these techniques only the outermost surface is modified leaving the bulk properties unaffected, in contrast to techniques like gamma induced grafting. Furthermore solvents are not required, which is environmentally favorable. The surface modification procedure is generally a fast single step. Due to the fact that the modifying phase is a gas these techniques can be used to modify surfaces of objects with complex three dimensional shapes. Plasma techniques can be operated batch wise or on-line and can be applied on a large industrial scale. However these techniques have also some drawbacks. Glow discharge processes are operated at reduced pressure and require a good process control, e.g. by optical emission or mass spectrometry. This translates directly into a relatively high investment in equipment. The operational costs however are low.

The main feature of plasma modified polymeric surfaces is that they possess a unique surface chemistry. This is inherently due to the complex nature of the plasma phase. A plasma consists of neutrals, excited neutrals, electrons and ions. Furthermore a wide spectrum of electromagnetic radiation is emitted, including short wave UV radiation. All these constituents affect the chemical composition of the surface. A plasma is thus a highly reactive medium. On the other hand the action of many different reactive species in the plasma leads to a complex surface chemistry. This situation is further complicated by some post plasma phenomena as post plasma oxidation, e.g. quenching of radicals by oxygen [1] and ageing [2].

In this paper we want to discuss some strategies to use plasma techniques in order to obtain surfaces with a predefined surface composition. We will focus on plasma treatment techniques although considerable progress is made in the plasma polymerization field, e.g. by plasma polymerization at

low substrate temperatures [3]. Two approaches will be discussed, plasma immobilization and plasma fluorination.

## PLASMA IMMOBILIZATION

In order to selectively introduce one type of functional group on polymer surfaces, which can be used for further covalent coupling, we have developed the plasma immobilization process (Figure 1). In this process a pre-adsorbed layer of a surface active agent is immobilized on a polymeric substrate by a treatment with an inert gas plasma. The pre-adsorbed layer is most likely crosslinked to the substrate by short wave UV radiation emitted from the plasma phase. By selecting a proper surfactant the required functionality can be introduced.

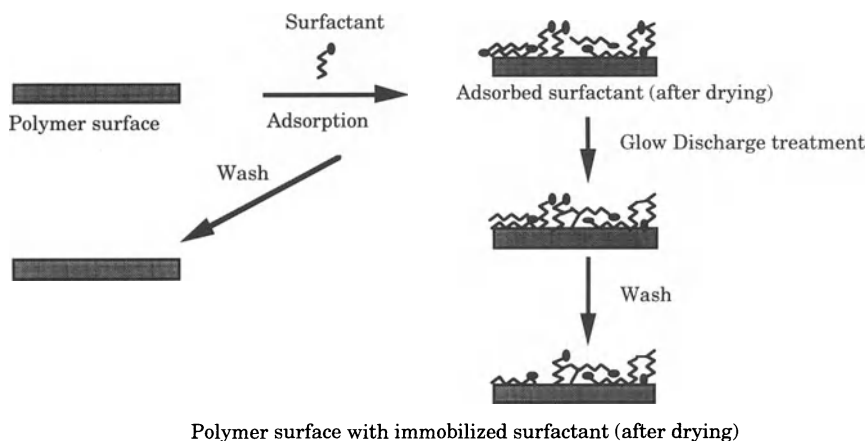


Figure 1: Schematic presentation of the plasma immobilization method. A layer of a surfactant pre-adsorbed on a polymeric surface is plasma treated to immobilize this layer to the substrate [4].

The feasibility of the plasma immobilization method was shown by immobilizing a layer of sodium dodecylsulfate on poly(propylene) (PP) [5]. Using this method 25 % of the pre-adsorbed layer was immobilized and intact sulfate groups, available for ion exchange were introduced on the PP surface. Furthermore this method has successfully been used for the introduction of amine groups on poly(ethylene) (PE) [6]. Approximately 50 % of a pre-adsorbed (mono)layer of decylamine hydrochloride was immobilized on PE by an argon plasma treatment of 2 seconds. The presence and the reactivity of the introduced amine groups was checked by reactions with different aldehyde containing compounds.

The plasma immobilization technique was also used to immobilize different poly(ethylene oxide) containing surfactants on PE in order to obtain non-fouling surfaces [7,8]. The PEO containing surfactants were successfully immobilized by argon or helium plasma treatments and showed a remarkable decrease in fibrinogen adsorption. Also in this case an optimal treatment time was observed. By treating the pre-adsorbed layer too long, the PEO chains are probably degraded, which renders the surface less non-fouling. Furthermore it was shown that unsaturated surfactants are more efficiently immobilized, which is readily explained by the assumed UV induced crosslinking of the surfactant to the surface.

In order to introduce carboxylic acid groups on PE the plasma immobilization method was also applied to a pre-adsorbed layer of polyacrylic acid (PAAc) on PE. It was not possible to immobilize this layer to the PE substrate [9]. Before the pre-adsorbed PAAc layer could be immobilized it was etched off. The large difference in etching rates of PAAc (200 Å/min) and PE (6 Å/min) during argon plasma treatments illustrate this effect. A detailed investigation showed that PAAc is selectively decarboxylated during argon plasma treatments by short wave UV radiation (wavelength < 150 nm) emitted from the plasma [10].

In order to introduce carboxylic acid groups a different approach was followed. PE films were treated directly with an oxidizing carbon dioxide plasma. This yields highly wettable, oxidized

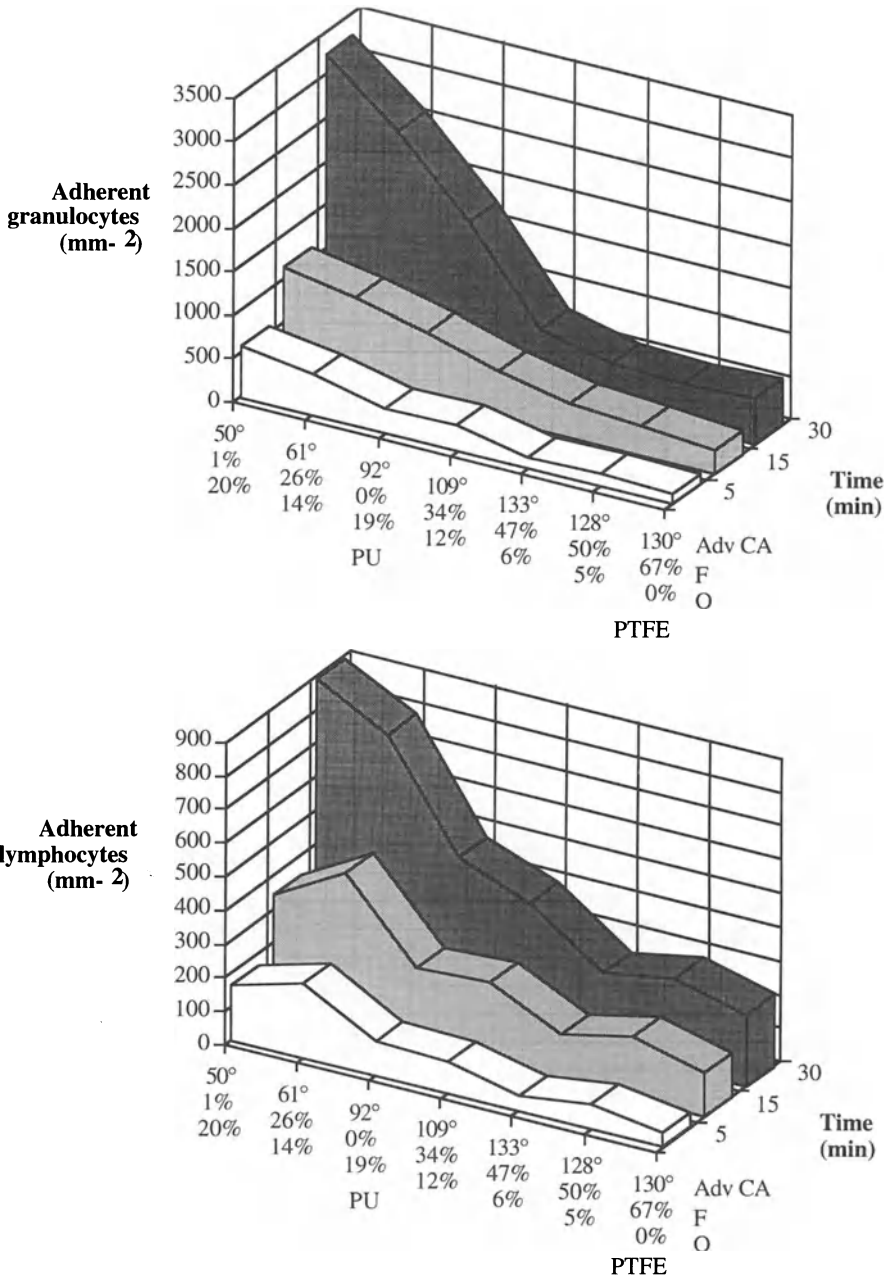


Figure 2: In vitro adhesion of purified granulocytes and lymphocytes under static conditions on surfaces with different hydrophilicities [12]. The surfaces were obtained by fluorination of PU films followed by etching of the fluorinated layer by an argon plasma treatment. The surface composition, amounts of fluorine and oxygen as determined by XPS measurements and the advancing contact angle measured in water with the Wilhelmy Plate technique are noted for all surfaces. The unmodified control surfaces (PTFE and PU) are also shown in this figure.

surfaces with a large variety of oxygen containing groups (epoxide, hydroxyl, ketone/aldehyde and carboxylic acid groups) [11]. These groups were detected and quantified by selective gas phase reactions followed by XPS (X-Ray Photoelectron Spectroscopy). In contrast to the plasma immobilization method, the surface chemistry obtained by the direct oxidation contains a wide variety of functional groups. One aspect of these oxidized surfaces should however be mentioned. Oxidized polymer surfaces are very dynamic systems which are sensitive to their storage conditions e.g. storage in air or in water, storage time and temperature [2]. Generally their surface wettability decreases with increasing storage time and temperature.

## CONTROLLED FLUORINATION OF POLYMERIC SURFACES

One of the best ways to obtain a low surface energy polymeric surface is fluorination. Especially when the degree in fluorination can be controlled a range of surface energies can be obtained, which can be utilized for the study of e.g. cellular adhesion to solid surfaces. We have applied tetrafluoromethane (CF<sub>4</sub>) plasma treatments to fluorinate different types of polymer surfaces (PE [9], PAAc [10] and polyurethane (PU) [12]). From kinetic studies it was shown that the degree of fluorination can be controlled by changing the plasma treatment time. In the treatment time window from 0.01-10 s. (in our treatment system) the amount of fluorine incorporated on the surface is directly proportional to the logarithmic of the treatment time. At longer treatment times the surface composition reaches an equilibrium. This equilibrium is the result of the balance between fluorination and etching of the surface. Etching of the surface is due to chemical etching and sputtering. A mathematical model has been derived to describe the kinetics for the CF<sub>4</sub> plasma treatment of PAAc. Using this model the surface composition over 5 decades of plasma treatment times could be fitted [10].

By covering the polymer surface during the CF<sub>4</sub> plasma treatment, e.g. with a glass cover, it was possible to obtain totally fluorinated surfaces [10]. XPS measurements showed that the surface chemistry of CF<sub>4</sub> plasma treated covered PAAc is comparable to that of poly(tetrafluoro ethylene) (PTFE). For instance the C1s envelope was similar to that of PTFE. This indicates that the surface modification is primarily due to fluorine containing radicals (e.g. F radicals) and that the etching is due to sputtering. By covering the surface, the sputter component of the process is blocked, rendering the surface PTFE like.

The possibility to fluorinate and defluorinate surfaces was used to obtain a set of polymer surfaces with different surface hydrophilicity. The primary aim of this study was to investigate the effect of the surface wettability of poly(urethane) (PU) films on the adhesion of leukocytes [12]. The PU films were fluorinated with a CF<sub>4</sub> plasma and subsequently treated with an argon plasma to etch the fluorinated layer away. In a in-vitro adhesion study with either purified granulocytes or lymphocytes it was shown that the adhesion of both types of cells increased with increasing surface hydrophilicity. Although surface wettability and the chemical composition of the surface are directly related, the increase of the adhesion seems primarily governed by the wettability and less by the surface composition. This is illustrated by the fact that the two control surfaces (PTFE and PU) used in this study fit nicely in the adhesion curves.

## CONCLUSIONS

Although plasmas are very reactive systems, capable of modifying inert polymer surfaces, they can also be used to obtain tailor-made polymer surfaces. The plasma immobilization method offers opportunities to selectively introduce functional groups or poly(ethylene oxide) chains. Furthermore by using CF<sub>4</sub> plasma treatments, especially on covered samples, it is possible to obtain well defined, even PTFE-like, surfaces.

## ACKNOWLEDGEMENTS

The authors like to thank DSM (Geleen, The Netherlands) and the NPBI (Emmer-Compascuum, The Netherlands) for financial support for this research.

## REFERENCES

- [1] Gerenser L.J. (1987) X-ray photoemission study of plasma modified polyethylene surfaces. *J. Adhesion Sci. Tech.*, 1: 303-318.
- [2] Takens G.A.J., Terlingen J.G.A., Feijen J. (1993) Ageing of carbon dioxide plasma treated polyethylene surfaces. International Symposium on Plasma Chemistry ISPC-11, Loughborough, UK, August 22-27 1993, 1236-1241.
- [3] Lopez G.P., Ratner B.D. (1992) Substrate temperature effects on film chemistry in plasma deposition of organics. II. Polymerizable precursors. *J. Polym. Sci.: Part A: Polym. Chem.*, 30: 2415-2425.
- [4] Terlingen J.G.A., Feijen J., Hoffman A.S. (1992), Immobilization of surface active compounds on polymer supports using a gas discharge process. *J. Biomater. Sci. Polymer Edn.*, 4: 31-33 .
- [5] Terlingen J.G.A., Feijen J., Hoffman A.S. (1993) Immobilization of surface active compounds on polymer supports using glow discharge processes. 1. Sodium dodecyl sulfate on poly(propylene) *J. Colloid Interface Sci.*, 155: 55-65.
- [6] Terlingen J.G.A., Brenneisen L.M., Super H.T.J., Pijpers A.P., Hoffman A.S., Feijen J. (1993) Introduction of amine groups on poly(ethylene) by plasma immobilization of a preadsorbed layer of decylamine hydrochloride. *J. Biomater. Sci. Polym Edn.*, 4: 165-181.
- [7] Shue M.S., Hoffman A.S., Feijen J. (1992) A glow discharge treatment to immobilize poly(ethylene oxide)/poly(propylene oxide) surfactants for wettable and non-fouling biomaterials *J. Adhesion Sci. Technol.*, 6: 995-1009.
- [8] Shue M.-S., Hoffman A.S., Terlingen J.G.A., Feijen J. (1993) A new gas discharge process for preparation of non-fouling surfaces on biomaterials. *Clinical Materials*, 13: 41-45.
- [9] Terlingen J.G.A., Hoffman A.S., Feijen J. (1993) Effect of glow discharge treatment of poly(acrylic acid) preadsorbed onto poly(ethylene) *J. Appl. Polym. Sci.*, 50: 1529-1539 .
- [10] Terlingen J.G.A., Takens G.A.J., Gaag van der F.J., Hoffman A.S., Feijen J. (1994) On the effect of treating poly(acrylic acid) with argon and tetrafluoromethane plasmas: kinetics and degradation mechanism *J. Appl. Polym. Sci.*, 52: 39-53.
- [11] Terlingen J.G.A., Gerritsen H.F.C., Hoffman A.S., Feijen J. (1995) Introduction of functional groups on poly(ethylene) surfaces by a carbon dioxide plasma treatment. *J. Appl. Polym. Sci.*, in press.
- [12] Bruil A., Brenneisen L.M., Terlingen J.G.A., Beugeling T., Aken van W.G., Feijen J. (1994) In vitro leukocyte adhesion to modified polyurethane surfaces II Effect of wettability. *J. Colloid Interface Sci.*, 165: 72-81.

# NEW POLYMERIC MATERIALS DESIGN FOR BIOMEDICAL APPLICATIONS

Teiji Tsuruta

Department of Industrial Chemistry, Faculty of Engineering, Science University of Tokyo,  
Kagurazaka 1-3, Shinjuku-ku, Tokyo 162, Japan

## SUMMARY

Multifaceted aspects of biomedical materials researches were discussed in terms of five key words: devices, properties demanded, concept or methodology, materials design, and fundamentals. Properly designed poly(HEMA)-graft-polyamine copolymers(HA) were found to form microdomain structure and exhibit unique biomedical behavior at the interface with living cell, such as different adhesivity against lymphocyte subpopulations, B cell and T cell. The conformational transition of polyamine chains under physiological pH-range was closely related with the cell recognition mechanism. Some of HA copolymer surfaces containing a small amount of polyamine portions became inert enough against lymphocytes as well as blood platelets to reject their attachment. This behavior was discussed in terms of random network concept of water molecules on material surface. The excellent *in vivo* blood compatibility of HEMA-STY triblock copolymer was explained by a similar mechanism. Results of microdomain formation of poly[4-bis(trimethylsilyl)methylstyrene] poly(HEMA) diblock copolymer were discussed referring to its physicochemical and biomedical properties. Discontinuous 270-fold change of swelling degree in response to pH changes was observed in a newly designed segmented polyamineurea. Another multiblock polyurea was also designed using poly(sil-amine) segments which showed LCST behavior in addition to the pH-sensitivity.

## KEY WORDS

materials design, polyamine copolymers, microdomain structure, conformational transition, inert surface

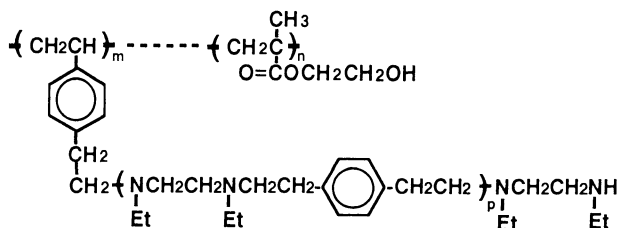
## INTRODUCTION

Multifaceted aspects of biomedical materials researches are discussed in terms of five key words: devices, properties demanded, concept or methodology, materials design, and fundamentals. A majority of researches focused on device-manufacturing for end-use. Innovative devices are manufactured on the basis of a new concept or methodology. To approach the target device, new materials designs should be carried out by utilizing synthetic-, biologically derived-, and/or hybridized-materials. Fundamentals must be studied to elucidate structure-property relationship in the nature of interaction of materials with biological elements from the standpoint of molecular and cellular levels. Thus, it is evident that the aforementioned five elements play complementary role with one another in the progress in biomedical materials researches.

Two decades ago, we found a new and convenient method for syntheses of a series of amino-containing monomers, oligomers and polymers. This finding prompted us to search new opportunities as materials for biomedical applications, under the cooperation with Professor Sakurai and his group. Newly designed polyamine-graft copolymers were found to form microdomain structure and exhibit unique biomedical behavior at the interface with living cells, e.g. blood platelets or lymphocytes. Scanning electron micrographs of adhering platelets or lymphocytes on the surface of polyamine-graft copolymers showed that most of the adhering cells keep their native shape, in contrast with the extensive shape change observed for cells binding to the surface of polystyrene or poly(HEMA) [1, 2]. Our intention was to elucidate structure-property relationship in the nature of interaction between the microdomain-structured polyamine-graft copolymers and living cells such as platelets and lymphocytes.

## DESIGN OF POLY(HEMA)-graft-POLYAMINE COPOLYMERS(HA) AS MATERIAL FOR CELL SEPARATION

In the course of our biomedical studies on interaction between cells and various amino-containing polymers, we became interested in different adhesion properties of lymphocyte subpopulations, B cell and T cell, on the surface of poly(HEMA)-graft-polyamine copolymers(HA):



Properly-designed HA surfaces exhibited preferential adhesivity to B cell over T cell under physiological conditions, which enabled us to achieve an effective cell separation by utilizing HA surfaces[3, 4]. Further studies showed that origin of the cell recognition by the HA surface comes from the conformational transition(followed by phase transition) of polyamine chains on the copolymer surface in response to pH difference under physiological conditions. The length of the polyamine chains and their density on the surface are the most influential factors determining the phase transition process. After detailed studies on materials design, the most effective condition was established with HA 13(3750), which contains 13 wt% polyamine of molecular weight(Mn) being 3750. Here, the recovery of T cell at pH7.3 was almost quantitative.

It was previously confirmed that the lymphocyte adhesion on HA surface was caused primarily by ionic interaction at the cell materials interface[5]. A higher value(4.6) of isoelectric point for T cell than that(3.8) for B cell may explain the higher susceptibility of T cell adhesion to the decrease in ionic character of HA surface which resulted from the sharp transition to the aggregate state[6-8]. On HA 13(1 1000) surface, the efficacy of B/T separation was very low because of the high retention of T cells on this surface even at  $\alpha < 0.5$ . To know ionic character of HA surface in operative in contact with cell in aqueous media, the streaming potential measurements were carried out. The  $\zeta$  potential of HA copolymers was extremely sensitive to the change in chain length of polyamine grafts. Especially, the  $\zeta$  potential of HA 13(1 1000) was significantly more positive at pH7.4. It is probably reasonable to assume that the slipping plane having enough positive charge exhibits adhesivity to T cell as well as B cell[4]. In contrast with HA copolymer, another block copolymer, poly(HEMA)-graft-poly(4-diethylaminoethylstyrene)(HME), exhibited only inferior characteristics in recognition of the lymphocyte subpopulations because of the low dependency of the phase transition process of HME upon its surrounding pH variation[9].

## DESIGN OF BIOINERT SURFACES USING HA-COPOLYMERS WHICH CONTAIN A SMALL AMOUNT OF AMINO GROUPS

It has long been believed that water-soluble polymers, e.g. poly(ethylene oxide), poly-acrylamide and poly(vinyl alcohol), are inert to any of biological elements. A number of trial were carried out to improve biocompatibility of polymeric materials by conjugating water soluble polymers, especially poly(ethylene oxide), onto the base-material surfaces. It is to be noted, however, that the PEO-modification does not always bring about good biocompatible surfaces[10].

In the course of our study with HA copolymer columns, we observed frequently that some of HA copolymer surfaces having a small number of polyamine grafts became inert enough against blood platelets as well as lymphocytes to reject their attachment[8, 9, 11, 12]. For instance, platelet attachment scarcely took place on the surface of HA2(containing N<sup>+</sup> in 0.1-0.3wt%) in contrast with poly(HEMA), where more than 90 percent cell attachment was observed on the surface. A similar cell-retention profile was also observed on the surface of poly[N-methyl-N-(4-vinylphenethyl)ethylenediamine(AVEMA)-co-HEMA](HAV)[13, 14].



The inertness of poly(HEMA) surfaces, which contain a small amount of amino group, was confirmed also by analysing results of frontal chromatograms of lymphocytes[2]. Another quantitative evaluation for affinity of lymphocyte subpopulations toward HAV copolymer surfaces was carried out by using a novel technique, hybrid field-flow fractionation/adhesion chromatography(FFF/AC)[14, 15].

Besides the aforementioned examples, there are available several other ones which show the unique biomedical effect as surface modifier of a small quantity of amino groups: e.g. Sepacell-PL, Hemophan and DIPAM(or Methacrol)[16-18].

Interesting swelling behavior was found in the HAV copolymers containing AVEMA in one and two mole% [13, 14]. The total water content of the swollen copolymers, HAV1 and HAV2, were increased by 150% and 175%, respectively, compared with that of poly(HEMA) itself. Free water content of the HAV copolymers was found 4 to 5 times larger than that of poly(HEMA). This result is probably explained by the instabilization of the random network structure [19, 20] of water molecules by introducing a small amount of amino groups to the poly(HEMA) matrix. Protonated amino groups destroy their surrounding hydrogen bonds to produce deficient spot in the networks [21]. Thus, the network structures become unstable, so that the resident time of trapped proteins will be shorter compared with the case of poly(HEMA). Recent study [22, 23] revealed that the surface of polyamine-graft-polystyrene copolymer(SA) containing 6wt% of polyamine portion exhibited a minimal adsorptive property against bovine plasma fibronectin(FN) and vitronectin(VN), the both of which are known to mediate cell-adhesion processes.

The random network concept may probably be applicable, in principle, to an elucidation of the excellent *in vivo* blood compatibility of HEMA-STY copolymer [24, 25]. The random network structure of water molecules on HEMA-STY surface must be very labile under the influence of hydrophilic-hydrophobic lamella structure, where protein residence time will be too short to cause conformational change of trapped protein molecules. The Vroman effect will be operated easily on the surface. This may be the reason why albumin, a blood protein of the biggest population, was found in the form of monomolecular layer keeping its native conformation. Since albumin is not a cell-adhesive protein, there was presumably no chance for blood cells to adhere to the HEMA-STY surface.

We synthesized poly[4-bis(trimethylsilyl)methylstyrene(BSMS)]-poly(HEMA) diblock copolymer to approach new materials possessing both excellent blood compatibility and oxygen permeability. Anionic polymerization of BSMS was carried out with BuLi as initiator in THF at -75°C. Then, a 1.5-molar amount of 1, 1-diphenylethylene(DPH) was added to the reaction system to stabilize the living end of poly(BSMS), whereupon a THF solution of LiCl and 2-(trimethylsiloxy)ethyl methacrylate(ProHEMA) were added, successively. We prepared a series of block-copoly(BSMS/HEMA) samples, BH(30), BH(58) and BM(80), in which the mole ratio BSMS/HEMA was 30/70, 58/42, and 80/20, respectively.

TEM examination of BH(30) film prepared by casting from DMF solution showed "island/sea" like microdomain structure. DSC measurement of BH(30) and BH(58) films supported also the formation of microdomain structure. Another unique property of the block-copoly(BSMS/HEMA) is its remarkably higher water absorbing capacity compared with the corresponding random copolymer. SEM observation revealed that rat platelets adhered to BH(30) surface scarcely suffered shape change in contrast with the serious shape change with formation of pseudopods on the surface of poly(BSMS). Studies on gas permeation through the block-copoly(BSMS/HEMA) as well as more details on the mode of interaction with living cells are now under way.

#### **DESIGN OF STIMULI-SENSITIVE SEGMENTED POLYAMINEUREA AND POLY(SIL-AMINEUREA)**

The pH-dependent morphology change which had been observed on the surface of poly(HEMA)-graft-polyamine copolymers(HA) prompted us to explore another novel polymeric materials: segmented polyamineurea(SPAU) having repetitive array of polar(ethylenediamine) and apolar(1, 4-diethylenephylene) units in the main chain [26]. The SPAU-EDA(EDA as chain extender) exhibited reproducible swelling/deswelling in response to a slight change of the surrounding pH-value. For instance, SPAU-EDA maintained at 30°C a high swelling degree of 40 below pH5.2, whereas drastic shrinking took place to decrease the swelling degree down to 0.15 at pH5.5 which is 1/270 of the initial value at pH5.2. The shift of ethylenediamine units from the doubly protonated trans conformation to the deprotonated random coil conformation is presumably the trigger for this phase transition [27].

We recently found a convenient method to prepare poly(sil-amine) telechelic oligomers through anionic polyaddition reaction between divinylsilane (e.g. dimethyldivinylsilane) and diamine (e.g. N, N'-diethylethylenediamine) [28]. Comparative studies of poly(sil-amine) (PSiA) and polyamine were carried out. Similarly to the case of polyamine, remarkable pH-dependency of turbidity of PSiA solution was observed. On the other hand, PSiA exhibited much higher temperature sensitivity than polyamine in the turbidity point. DSC measurements of PSiA solution showed that the solution at pH 7.4 gave an extremely sharp endothermic peak ( $\Delta H$  26.6 kcal/monomeric unit) at 57°C which coincided with the turbidity point. This can be regarded as LCST. The corresponding  $\Delta H$  for polyamine was only 11.5 kcal/monomeric unit. It is to be noted that only 0.2 increase in pH (7.2-7.4) value caused more than 10°C decrease in the turbidity point of PSiA. Studies on synthesis and properties of poly[(sil-amine)urea] is now under way.

## REFERENCES

1. Kataoka K, Okano T, Sakurai Y, Nishimura T, Maeda M, Inoue S, Tsuruta T (1982) Effect of microphase separated structure of polystyrene/polyamine graft copolymer on adhering rat platelets in vitro. *Biomaterials* 3: 273-240
2. Maruyama A, Tsuruta T, Kataoka K, Sakurai Y (1988) Quantitative evaluation of rat lymphocyte adsorption on microdomain structured surfaces of poly(2-hydroxyethyl methacrylate)/polyamine. *Biomaterials* 9: 471-481
3. Tsuruta T (1987) Biomedical behavior of some amino-containing polymers in contact with blood constituents. *Makromol Chem, Macromol Symp* 12: 323-331
4. Tsuruta T (1990) Synthesis and evaluation of polyamine graft and block copolymers as novel biomaterials for cell separation. *Makromol Chem, Macromol Symp* 33: 243-251
5. Maruyama A, Tsuruta T, Kataoka K, Sakurai Y (1987) Polyamine graft copolymer column for separation of rat B and T lymphocytes: Role of ionic interaction between matrices and lymphocyte. *Makromol Chem Rapid Comm* 8: 27-30
6. Nabeshima Y, Tsuruta T, Kataoka K, Sakurai Y (1989) Structural control of poly(2-hydroxyethyl methacrylate)-graft-polyamine copolymers for differential retention of rat lymphocyte subpopulations. *J Biomater Sci Polymer Edn* 1: 85-97
7. Kikuchi A, Mizutani S, Kataoka K, Tsuruta T (1991) Resolution of lymphocyte subpopulations derived from rat spleen by polyamine-graft-PHEMA copolymer. *Polymers for Advanced Technologies* 2: 245-251
8. Kikuchi A, Kataoka K, Tsuruta T (1992) The role of protonation and conformation transition of polyamine-graft-PHEMA copolymer surfaces. *J Biomater Sci Polymer Edn* 3: 355-374
9. Kataoka K, Sakurai Y, Nabeshima Y, Sasaki Y, Maruyama A, Tsuruta T (1991) Selective retention of lymphocyte subpopulations on polyHEMA-graft-polyamine copolymer: Effect of chemical structure of polyamine graft. *Kobunshi Ronbunshu* 48: 201-209 (in Japanese)
10. Llanos GR, Sefton MV (1993) Does polyethylene oxide possess a low thrombogenicity? *J Biomater Sci Polymer Edn* 4: 381-400
11. Kataoka K, Sakurai Y, Hanai T, Maruyama A, Tsuruta T (1988) Immunoaffinity chromatography of lymphocyte subpopulations using tert-amine derived matrices with adsorbed antibodies. *Biomaterials* 9: 218-224
12. Maruyama A, Tsuruta T, Kataoka K, Sakurai Y (1989) Elimination of cellular active adhesion on microdomain-structured surface of graft-polyamine copolymers. *Biomaterials* 10: 291-298
13. Kikuchi A, Karasawa M, Kataoka K, Okuyama K, Tsuruta T (1993) Amino-containing polymers as non-adsorbable surface for platelets. Akutsu T, Koyanagi H (eds) *Artificial Heart* (Springer-Tokyo) 4: 29-32
14. Kikuchi A, Karasawa M, Tsuruta T, Kataoka K (1993) Differential affinity of Lymphocyte subpopulations toward PHEMA surface derivatized with a small amount of amino groups--evaluation under the regulated shear stress. *J Colloid Interface Sci* 158: 10-18
15. Bigelow JC, Gidding JC, Nabeshima Y, Tsuruta T, Kataoka K, Okano T, Yui N, Sakurai Y (1989) Separation of B and T lymphocytes by a hybrid field-flow fractionation/adhesion chromatography technique. *J Immunological Methods* 117: 289-293
16. Renier M, Anderson JM, Hiltner A, Lodoen GA, Payet CR (1993) Infrared spectral analysis of extractables from poly(etherurethane urea) (PEUU) elastomers. *J Biomater Sci Polymer Edn* 5: 231-244

17. Brunstedt MR, Ziats NP, Schubert M, Hiltner PA, Anderson JM (1993) Protein adsorption onto poly(ether urethane ureas) containing Methacrol 2138F: a surface-active amphiphilic additive. *J Biomed Mater Res* 27: 255-267
18. Brunstedt MR, Ziats NP, Robertson SP, Hiltner A, Anderson JM (1993) Protein adsorption to poly(ether urethane ureas) modified with acrylate and methacrylate polymer and copolymer additives. *J Biomed Mater Res* 27: 367-377
19. Stillinger FH (1980) Water revisited. *Science* 209: 451-457
20. Rice SA, Sceats MG (1981) A random network model for water. *J Phys Chem* 85: 1108-1119
21. Maeda Y, Tsukida N, Kitano H, Terada T, Yamanaka J (1993) Raman spectroscopic study of water in aqueous polymer solutions. *J Phys Chem* 97: 13903-13906
22. Taira H, Tanaka A, Kataoka K, Tsuruta T, Hayashi M (1994) Adhesion and growth behavior of bovine aortic endothelial cells on polyamine graft copolymer. *Jpn J Artif Organs* 23: 695-699 (in Japanese)
23. Taira H, Kataoka K, Tsuruta T, Hayashi M (1995) Bovine aortic endothelial cells culture on polyamine graft copolymer surfaces: Influences and roles of adsorbed fibronectin and vitronectin from serum in cell culture. *Jpn J Artif Organs* 24: 42-47 (in Japanese)
24. Nojiri C, Okano T, Jacobs HA, Park KD, Mohammad SF, Olsen DB, Kim SW (1990) Blood Compatibility of PEO grafted polyurethane and HEMA/styrene block copolymer surfaces. *J Biomed Mater Res* 24: 1151-1171
25. Nojiri C, Okano T, Koyanagi H, Nakahama S, Park KD, Kim SW (1992) In vivo protein adsorption on polymers: visualization of adsorbed proteins on vascular implants in dogs. *J Biomater Sci Polymer Edn* 4: 75-88
26. Koyo H, Tsuruta T, Kataoka K (1993) Synthesis of novel types of segmented polyamineurea and polyamine-poly(ethylene oxide) block copolymer. *Polymer J* 25: 141-152
27. Kataoka K, Koyo H, Tsuruta T (1995) Novel pH-sensitive hydrogels of segmented poly(amineureas) having a repetitive array of polar and apolar units in the main chain. *Macromolecules* 28 (in press)
28. Nagasaki Y, Honzawa E, Kato M, Kataoka K, Tsuruta T (1994) Novel stimuli-sensitive telechelic oligomers. pH and temperature sensitivities of poly(silamine) oligomers. *Macromolecules* 27: 4848-4850

# **Novel Approaches to Drug Delivery Systems and Future Trends**

## NEW ORAL DRUG DELIVERY SYSTEM

Raphael M. Ottenbrite and Ruifeng Zhao, Center for High Technology Materials, Chemistry Department, Virginia Commonwealth University Richmond, VA 23284-2006, USA

Sam Milstein, Emisphere Technologies Inc., 15 Skyline Drive, Hawthorne, NY 10595, USA

**ABSTRACT:** A new oral drug delivery system is discussed with respect to its specific dependence on pH and ability to enhance absorption of pharmaceutical agents. This technique not only can be used to deliver the protein and polar macromolecular drugs which are currently administered by injection, but also can be used to administer antigens and vaccines.

**KEY WORDS:** oral drug delivery, proteinoid microsphere, chaperon, heparin, inteferon.

### INTRODUCTION

Oral administration of protein and polar macromolecular drugs has been considered one of the greatest challenges in oral drug delivery since these drugs are easily hydrolyzed and digested by acids and enzymes in the gastrointestinal (GI) tract. In addition, oral administration of these drugs usually results in extremely low to no bioavailability due to their poor membrane permeability in the GI tract [1-3].

Many small molecules are chemically and structurally stable and remain unchanged by oral delivery. However, macromolecular drugs such as heparin, insulin and human growth hormone are very sensitive to the environmental components in the GI tract since their activity is directly related to specific molecular structures. Successful oral drug delivery requires that the drug-carrier be resistant both to the attack by enzymes and to the impact of pH gradients (pH changing from ~1-3 in the stomach to ~6-7 in the intestine), and also be capable of passing through the intestinal membrane without permanently altering its structure or function. Specific digestive processes can efficiently transform proteins and polysaccharides into smaller molecular fragments that are pharmacologically ineffective [1]. Currently these drugs and newly developed biotechnology drugs have to be administered via injection.

Recently, oral drug delivery research has focused on using natural or synthetic polymers as drug carriers to protect these drugs through the GI tract [2-3]. Meanwhile, the use of microsphere or nanoparticles to protect these drugs from degradation is being investigated [4-5].

### PROTEINOID MICROSPHERES

Thermally synthesized copoly(amino acids), or proteinoids, are known to form microspheres. These proteinoid microspheres have been studied mainly by Fox *et al* as protocellular models [6]. Recently, an application of these proteinoid microspheres as a delivery system for pharmaceutical agents was patented by Steiner and Rosen [7]. The merit of this application is the oral delivery

and release of an encapsulated active pharmacological agent. This novel drug delivery system has been demonstrated to be viable for several different kinds of pharmacological agents including insulin and heparin.

The core of this technology involves delivering therapeutical agents such as polysaccharides and proteins which are being presently administrated via injection. Small amino acid-based compounds called proteinoids, made simply by thermal condensation of specific amino acids, are used. The solid material obtained, after the condensation process, is finely ground and extracted with sodium hydrogen carbonate solutions. The extracts are lyophilized to yield a lightly colored product. This proteinoid material is composed of small peptide molecules ranging in size from 300 to 800 daltons, mostly consisting of tri- and tetrapeptides. The structures of these proteinoids are complex mixtures of diastereomerically linear, cyclic and branched chained peptides [1].

These proteinoids spontaneously form microspheres with pharmaceutical agents at low pH conditions (pH~1-3), which are insoluble and can be isolated. Under higher pH conditions (pH~6-7), the microspheres disassemble, releasing the encapsulated material [1]. To encapsulate a drug, the proteinoid material is dissolved in water at pH 7. This solution is added to a therapeutically desirable drug dissolved in a low pH solution with vigorous shaking. Under these acidic conditions, the proteinoids form microspheres with encapsulated drugs ranging in size from 5 to 10 microns [8]. The size is usually dependent on the proteinoid used and the agitation methods, i.e., the microspheres produced from handy agitation ranges from 10 to 15 microns while smaller spheres are formed by ultrasonic sound agitation (0.5 microns). The unique characteristic of these microspheres is that they remain intact in the acidic environment of the stomach (pH~1). In upper GI tract, the higher pH (pH~6-7) causes the microspheres to solubilize and disassemble, allowing the drug to be released for absorption [1]. In this manner, the proteinoid microspheres are able to protect a therapeutic agent from gastric acids and enzymes in the stomach and then release it into the intestinal absorption area.

The ability of these proteinoid materials to inhibit the activity of proteases in the intestine has been examined by *in vitro* assays. The results indicate that some proteinoids permit a competitive inhibition process of both trypsin and chymotrypsin at concentrations in the millimolar range. The  $K_i$  values have been seen for these proteinoids in the 10-400 mM range. Interestingly, most of the proteinoid carriers studied show inhibition of both trypsin and chymotrypsin within this range even though the structures of the proteinoids would suggest greater specificity for one enzyme over another.

Standard heparin and low molecular weight heparin (LMWH) microspheres were chosen as the model system. Heparin is a well-known anticoagulant and widely used for the prevention and treatment of thrombic diseases. Currently, both standard heparin and LMWH have to be administered intraparenterally to evaluate clinical efficacy. *In vivo* evidence indicates that the LMWH delivered by this technique was rapidly absorbed. It was found that heparin orally administered in proteinoid spheres resulted in a significant increase in clotting time, which was detectable 30 minutes after dosing. This same phenomenon has been observed in all of the species that have been tested [1]. Data on six different animal species, which include mice, rats, guinea pigs, dogs, and primates, as well as a completed phase I human trial, with LMWH encapsulated in proteinoid microspheres also demonstrated successful oral delivery with this system (Figure 1) [1].

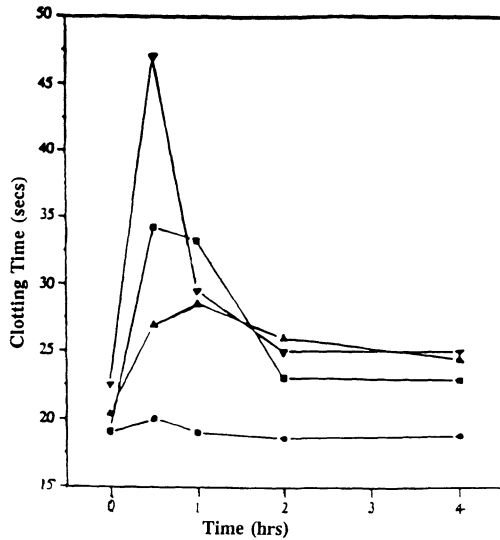


Figure 1. Oral Dosing of Heparin in Rats; ● baselines, ▲ subcutaneous injection, ■ heparin + carrier I, ▼ heparin + carrier II. (*Unpublished Results, Emisphere Technologies Inc.*)

## CHAPERONED ORAL DELIVERY

In the development of new pharmaceutical reagents, the initial design is usually focused on the therapeutic functions and the physicochemical requirements. Only secondarily are design features devoted to characteristics that are related to drug delivery to the biological target. Consequently, innumerable therapeutic compounds have been eliminated due to the inability to achieve therapeutic levels of reagent in appropriate anatomical compartments. This is a design fault which neglects blood and membrane transport requirements. Consequently, this compromise provides optimal bioactivity but due to low delivery efficiency, very high doses to achieve therapeutic effects are usually necessary.

As discussed earlier, oral delivery, from a practical viewpoint, is the best mode of administration. Presently, an effective way to deliver proteins, glycoproteins, glycosaminoglycans, and new technology macromolecules, is of prime interest. The main problem resides in the fact that due to enzymatic and hydrolytic digestion, their structural properties are altered which affects their physicochemical properties. Furthermore, poor absorption or delivery to the necessary biocompartments is common. The ideal oral delivery system would involve an agent that could associate with the drug so as to protect it from the hostile environment of hydrolytic and enzymatic degradation while in the stomach as well as enhance the rate of absorption from the GI tract. This mode of activity would entail a chaperon-like conduct by the carrier with respect to the drug, i.e., serve as a protector from hostile environments while presenting the drug to the absorption site.

Protein transport modes in and out, through and between cells, is observed in Nature. To effect these modes of transport nature causes a transient protein conformational change into a "transportable state". This "transportable state" is different from the native conformation, and

after being transported, the drug returns to the native state. For example, liposomes and synthesized proteins are translocated to appropriate cellular organelles by a variety of mechanisms including chaperons [9]. The current understanding of protein conformation suggests that there exist a number of discrete conformations ranging from the native to the denatured state [10]. A current model of the protein suggests that the folding, after the establishment of the secondary structures, involves sequential steps to achieve the native state [11]. The available data on chaperons indicate that part of their functions is to keep the proteins in their nonactive (partially-folded) state. Furthermore it has been demonstrated that partially unfolded proteins pass through membranes more readily than in the native state [12].

Milstein [13] has recently postulated that oral drug delivery can occur under the following conditions: a) the drug exists in an intermediate conformation that is neither the native state nor the fully denatured state; b) the conformational intermediate is readily reversible to the native state with the full biological activity when in systematic circulations and/or at its biological target. Evidences supporting this theory is described by Rosen[7] with respect to effective oral delivery of both proteins and nonproteins. It is clear that sphere formation and drug encapsulation by proteinoids is a non-covalent process. It is only recently that evidence has been obtained that enhanced drug uptake from the GI tract is the result of drug complexation with the carriers.

It has been found that specific synthetic proteinoid materials (Mw 300-800) can effect therapeutic uptake of drugs such as interferon, growth hormone and calcitonin within minutes after ravage administration. Shown in Figure 2 is the effect of a synthetic chaperon with interferon (IFN). No IFN absorption is indicated by normal oral ingestion, however, in conjunction with the chaperon the absorption from the GI tract is very rapid and is similar to the profile experienced by an intramuscular injection of IFN. These data indicate that a synthetic carrier may mimic the behavior of natural chaperons, that is, change the conformation of a protein such that its adsorption from the GI tract is enhanced. Therefore, by combining the appropriate carrier with a specific drug, a complex can be formed with physicochemical properties that effect membrane transport.

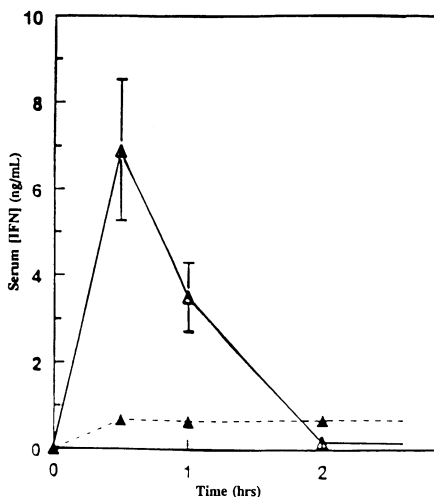


Figure 2. Oral Administration of  $\alpha$ -IFN with and without Chaperon in Rats; ▲ 1.0 mg/kg IFN,  $\Delta$  1.0 mg/kg IFN with 800 mg/kg Chaperon. (Unpublished Results, Emisphere Technologies Inc.)



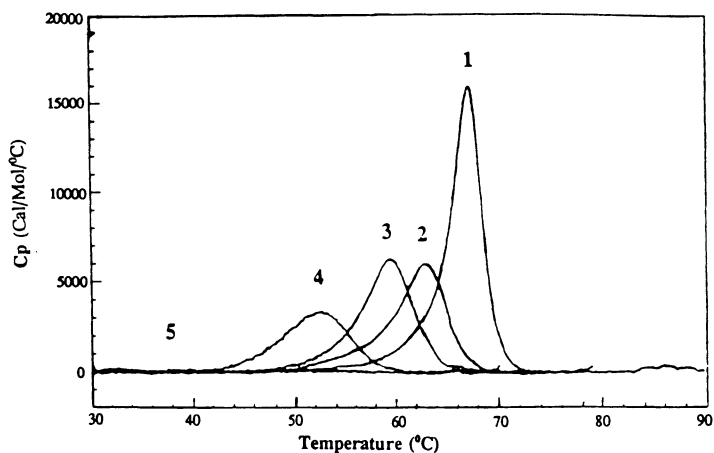


Figure 3. Chaperon Induced Conformational Change of  $\alpha$ -IFN; 1)  $\alpha$ -IFN without the Chaperon, 2)  $\alpha$ -IFN with 5 mg/mL Chaperon, 3)  $\alpha$ -IFN with 10 mg/mL Chaperon, 4)  $\alpha$ -IFN with 25 mg/mL Chaperon, 5)  $\alpha$ -IFN with 100 mg/mL Chaperon. (Unpublished Data, E. Friere, The Johns Hopkins University)

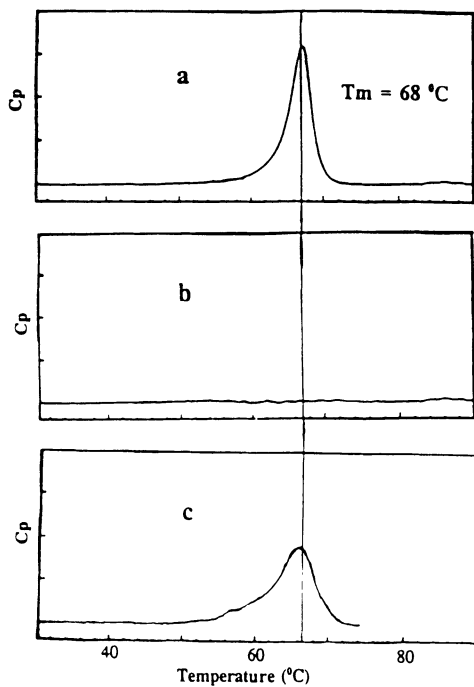


Figure 4. Reversible Denaturation of  $\alpha$ -IFN By A Synthetic Chaperon, a) Nature  $\alpha$ -IFN alone, b)  $\alpha$ -IFN with a Chaperon, c)  $\alpha$ -IFN with the Chaperon after Dialysis. (Unpublished Results, Emisphere Technologies Inc.)

Physical evidence for complex formation which would be related to partial denaturation of protein drugs has been obtained by differential scanning calorimetry (DSC), circular dichroism, isothermal titration and NMR techniques. Shown in Figure 3 are the effects of a synthetic chaperon on the DSC transition for  $\alpha$ -interferon ( $\alpha$ -IFN). As the concentration of the synthetic chaperon was increased, the transition peak (1) migrated to lower temperatures and decreased intensity (2-4) until the chaperon concentration was 100 mg/mL when the transition was completely suppressed (5). This change was attributed to complexation of the chaperon with the drug in a non-native state. This complexation is reversible, as shown in Figure 4. Without the chaperon present, the DSC for the native state of  $\alpha$ -interferon is very clear and sharp (Figure 4a). After addition of the chaperon, no transition is observed due to denaturation (Figure 4b). However, after dialysis by which the chaperon material was removed, the IFN returned to its native state to produce its characteristic DSC transition (Figure 4c). Present studies are being carried out with chaperons made from amino acid residues and with respect to their influences on heparin *in vivo* and by physicochemical evaluation.

#### REFERENCES:

1. Emisphere Technologies Inc. Report, May, 1994.
2. O'Hagan D. T., CRC Crit. Rev. in Ther. Drug Carrier Syst., 1987, 4, 197-220.
3. Smith P. L., Adv. Drug Deliv. Rev., 1992, 8, 253-90.
4. Damge C., J. Contr. Release, 1990, 13, 233-9.
5. Morishita I., Int. J. Pharm., 1992, 78, 9-16.
6. Fox S. W., Origins of Life, 1976, 7, 49.
7. Steiner S. and Rosen R., U.S. Patent, 1990, 4925673.
8. Santiago N., Phar. Res., 1993, 10(8), 1243-7.
9. Gething M-J. and Sambrook, J. Nature, 1992, 355, 33-45.
10. Baker D. and Agard D. A., Biochemistry, 1994, 33, 7505-9.
11. Bychkova V. E. and Berni R., Biochemistry, 1992, 31, 7566-71.
12. Haynie D. T. and Freire E., Proteins: Structure, Function and Genetics, 1993, 16, 115-40.
13. Milstein S., Unified Mechanism for Oral Drug Delivery, 1995, unpublished.

# PENETRATION OF POLYMERIC DRUG CARRIERS INTO K562 CELLS

Khadija Abdellaoui, Mahfoud Boustta, Hamid Morjani\*, Michel Manfait\* and Michel Vert

*C.R.B.A. URA C.N.R.S. 1465, Faculty of Pharmacy, Montpellier I University, 34060, Montpellier, France*

*\*Laboratory of Biomolecular Spectroscopy, Faculty of Pharmacy, 51096, Reims, France*

## ABSTRACT

Poly( $\beta$ -malic acid), PMLA, is known as a worthwhile degradable and bioresorbable drug carrier, which bears pendent reactive carboxylic acid groups usable to tailor make macromolecular prodrugs. Fluoresceinamine (Fl), has been covalently bound to poly(malic acid) as a model of a drug molecule to prospect the fate of poly(malic acid)-drug conjugate in contact with living cells, and especially cell uptake. For this, Fl was bound to poly( $\beta$ -malic acid) through amide bond using DCC as the coupling agent. Three partially benzylated Fl-PMLA conjugates were also synthesized by attachment of benzyl alcohol residues to pendent carboxylic acid groups via ester bonds. LASER-microspectrofluorometry (L-MSF) and fluorescence microscopy were used to evaluate the *in vitro* uptake of the conjugates by tumor cells K562 (A human erythroleukemia). It is shown that cell uptakes are polymer-dependent, molecular weight-dependent and hydrophobe-dependent.

**KEY WORDS:** macromolecular prodrug, fluorescent labelling, intracellular uptake, laser-microspectrofluorometry (L-MSF)

## INTRODUCTION

During the past two decades, increasing attention has been paid to the concept of high molecular weight prodrugs to transport drugs from one body compartment to the other, to decrease the side effects of toxic drugs and to achieve a more selective administration of the active molecules to cells [1-4]. During the pionering phase, people have used common water-soluble polymers as carriers. However, the need to conceive bioresorbable macromolecular carriers which could be eliminated from the body after the liberation of the drug, was recognized very soon [5]. On the other hand, drug-polymer conjugates should liberate the drug only after being within the cells. Ideally, degradation of the conjugate should take place in the lysosomal compartments by exposure to a number of digestive enzymes at an acidic pH (4-5) in order to release the parent drug *in situ* [6-8]. Based on these remarks, poly( $\beta$ -malic acid), PMLA<sup>50H<sub>100</sub></sup>, was synthesized and the properties of this polymer and of its derivatives were investigated in detail according to the list of specifications of bioresorbable polymeric drug carriers [9]. The methods available to monitor the fate of polymeric prodrugs in living cells are limited. For the last two years, we have prospected the use of LASER-microspectrofluorometry (L-MSF) to investigate the behavior of fluorescent poly( $\beta$ -malic acid) derivatives in contact with living cells [10-12], according to a new methodology previously used for the study of fluorescent drugs (Doxorubicin and Daunorubicin for example).

In the past years, an important progress has been made in microspectrofluorometry by the use of LASERS as excitation source and by the advent of optical multichannel analyzers (OMA) for the detection of fluorescence signal. LASER excitation permits a spatial resolution of about 1 $\mu$ m and high excitation efficiency. Spectrographic dispersion on optical multichannel analyzers has eliminated monochromator scanning of a fluorescence spectrum, thus considerably reducing acquisition time. This arrangement decreases excitation power requirement, thus reducing heating effect, photodamage and photobleaching of the sample which are severe inconveniences during *in vitro* studies. L-MSF can then study weak signals from volumes of a few cubic micrometers in single cell compartments, with good spectral resolution, signal to noise ratio and stability.

In this paper, we wish to report the synthesis of fluorescent polymeric conjugates by coupling fluoresceinamine (Fl) to racemic poly( $\beta$ -malic acid) (PMLA<sup>50H<sub>100</sub></sup>). The resulting models of polymeric prodrugs were characterized and their intracellular fate was investigated in cultures of tumor cells K562 (a

human erythroleukemia) by LASER-microspectrofluorometry and fluorescence microscopy. Data are discussed in terms of cell penetration and of the hydrophobization of the drug-polymer conjugates.

## MATERIALS AND METHODS

Poly( $\beta$ -benzyl  $\beta$ -malate) (PMLA,Be<sub>100</sub>) (M<sub>w</sub>  $\approx$  30 000; M<sub>w</sub>/M<sub>n</sub> = 1.5) was obtained from  $\beta$ -benzyl malolactonate as previously described in literature [13]. After hydrogenolytic cleavage of the benzyl ester protecting groups to liberate the pendent COOH groups, PMLA<sup>50</sup>H<sub>100</sub> (M<sub>SEC</sub>  $\approx$  37 000 in aqueous solvents, with reference to polystyrene sulfonate standards) was obtained. Fluoresceinamine isomer II was purchased from Aldrich-Chem. Co. N,N'-dicyclohexylcarbodiimide, 99%, and benzyl alcohol, 99%, were purchased from Janssen Chimica. These materials were used without further purification. The synthesis of poly( $\beta$ -benzyl malate-co- $\beta$ -malic acid) copolymers and the coupling of the dye were made in two steps : first, activation of carboxylic acid groups of the poly( $\beta$ -malic acid) with DCC to form a reactive polyanhydride, and secondly, nucleophilic attack of the benzyl alcohol hydroxyl group and of the fluoresceinamine amino group on anhydride groups to form respectively an ester and an amide bond.

**Cells :** Human K562 leukemic cells [14] were grown in DMEM supplemented as described above. The sensitive K562 cell lines were provided by the biochemistry laboratory of the Pharmacy Departement (Reims University, France). Uptake studies were carried out with cells which had been in exponential phase since the day before experiment, then centrifuged, transferred in 15 ml tubes suitable for cell culture at a density of 10<sup>5</sup> cells/ml and incubated in DMEM containing FI or a labelled polymer (PMLA,FI<sub>v</sub> or PMLA,Be<sub>x</sub>FI<sub>v</sub>) at 37°C in a moisted air/CO<sub>2</sub> incubator. The cells were then washed three times with fresh PBS to remove adherent conjugate from their surface, the drug free medium was then added. The cells were seeded on a cover - slide in a Petri dish containing PBS for the microspectrofluorometric and fluorescence microscopic analyses. The first sampling was carried out at a incubation time of 3h.

**L-MSF :** Fluorescent emission spectra from a volume within a living cell were recorded with a microspectrofluorometer (modified Raman Spectrometer OMARS 89, DILOR, Lille, France) as already described [15]. By means of an optical microscope (Olympus BH2) equipped with a 100x water phase contrast immersion objective (Leitz Fluotar), a laser beam was focused on a spot of less than 1 $\mu$ m in diameter. Sample observation and collection of fluorescence emission were obtained through the same optics. The actual fluorescence sampling was restricted by means of a suitable pinhole diaphragm on the image plane of the microscope objective. The emission light signal, spectrally dispersed by a diffraction grating, was detected with an optical multichannel analyzer, made of a cooled 512-diode array and optically coupled to an image intensifier. Data were collected locally, and then transferred to a computer for analysis with a lab-developed software. Laser power and instrumental response were controlled by the daily use of rhodamine B as an external standard. Following different treatments, including free FI; PMLA,FI<sub>v</sub> or PMLA,Be<sub>x</sub>FI<sub>v</sub>, the cells were scraped from the culture dish and seeded in a dish containing PBS. At least 20 spectra from the same intracellular location were accumulated in order to obtain a signal to noise ratio of about 30. The reported data were collected from 20 different cell nuclei within the first 15 min following transfer of the cells into PBS. Sample heating, photobleaching and photodamage were checked and found to be negligible under our experimental conditions. The laser power on the sample was 4  $\mu$ W and the illumination time 1 sec. Phase contrast microscopy was used to show that cells remained viable after repeated fluorescence determinations.

**Fluorescence Microscopy of K562 cells treated with free FI; PMLA,FI<sub>v</sub> or PMLA,Be<sub>x</sub>FI<sub>v</sub>:** To determine the cellular site at which the free FI or labelled polymer is localized, the treated cells were examined and photographed by microscopy using fluorescence excitation.

## RESULTS

### Qualitative analysis

Photomicrographs of K562 cells incubated with (a) free FI, (b) poly( $\beta$ -malic acid)/FI (PMLA,FI<sub>v</sub>) conjugates and (c) hydrophobized poly( $\beta$ -benzyl malate)/FI (PMLA,Be<sub>x</sub>FI<sub>v</sub>) conjugates were taken at 24h (Fig.1). Weak fluorescence diffuse and homogeneous was observed for free FI in (a). FI is a molecule which can hardly penetrate in the cells. An opposite behavior was noticed with the conjugates. Indeed the

later are able to penetrate in the cells via a pinocytic phenomenon, thus leading to an intense intracellular fluorescence (b) or a localized cytoplasmic fluorescence (c).

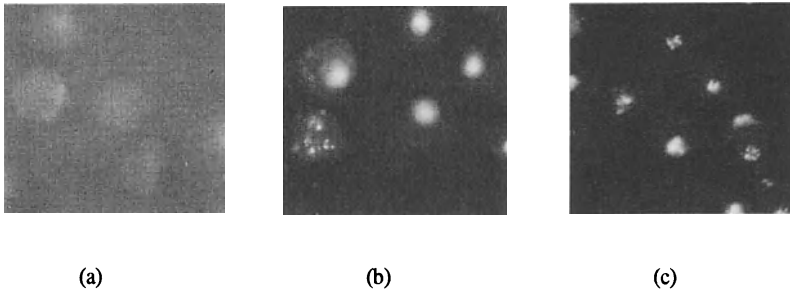


Fig.1 Photomicrographs of cells incubated with free FI (a), PMLA,FI<sub>y</sub> (b) and PMLA,Be<sub>x</sub>FI<sub>y</sub> (c) after 24 hours

### Quantification of fluorescence

The fluorescence spectra of conjugates appeared to be different from that of free FI. The intracellular uptake of FI was determined after incubation of cells with free FI, with PMLA,FI<sub>y</sub> or with PMLA,Be<sub>x</sub>FI<sub>y</sub> at identical concentrations ( $10^{-5}M$ ) and for various incubation times. Cells were studied for FI content 3h and 24h after the addition of drugs to the medium. The fluorescence emissions arising from the nucleus or the cytoplasm of a cell treated with FI or conjugates polymer/FI were expressed as the sum of corresponding spectral contributions of FI and intracellular autofluorescence (Fig.2).

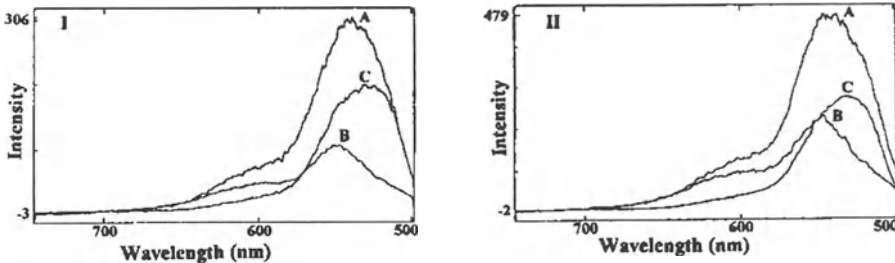


Fig.2 Nuclear I and cytoplasmic II intracellular spectra of the cells incubated with polymer/FI conjugate after 3 hours. A: Intracellular experimental spectra; B: Intracellular autofluorescence; C: Fluorescence of FI or polymer/FI conjugates

The intracellular fluorescence of FI after 3h of incubation with free FI was diffuse and identical in nucleus and cytoplasm. Intracellular FI levels increased with the incubation time as shown by data at 24h post inoculation. In K562 cells incubated with PMLA,FI<sub>y</sub>, the intranuclear fluorescence of FI, after three hours of incubation, was 2-3 times higher and the cytoplasmic fluorescence was 3-5 times higher, compared with the same cells incubated with free FI. It can be seen that the polymer/FI conjugates became associated with the cells rapidly (even at 1h of incubation time), and over a 3h incubation period there was a little progressive accumulation of fluorescence in both the nucleus and the cytoplasm. In the case of PMLA/FI conjugates, no significant increase in intracytoplasmic fluorescence was observed 24 hours post-ncubation, while a clear increase of intranuclear fluorescence was observed as a function of the incubation time (Fig.3).

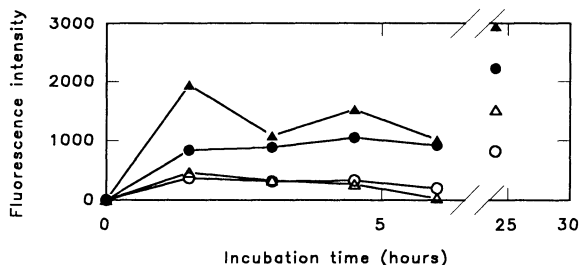


Fig.3 Drug uptake in K562 cells as a function of time : intranuclear fluorescence with free FI (○) or polymer/FI conjugate (●) and intracytoplasmic fluorescence with free FI (△) or polymer/FI conjugate(▲)

Using conjugate fractions of different molecular weight, experiments were carried out to investigate the effect of the size of PMLA/FI and PMLABex/FI conjugates on the rate of pinocytic capture and intracellular hydrolysis (Fig.4).

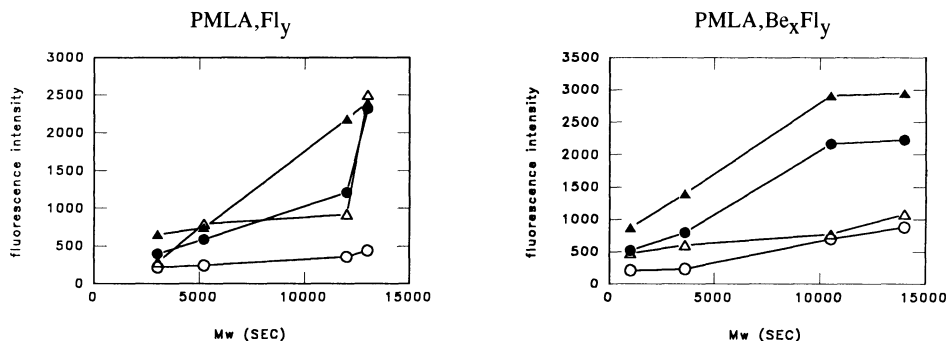


Fig.4 Drug uptake in K562 cells as a function of molecular weight of various conjugates after 3 hours of incubation in nucleus (○) and cytoplasm (△) and after 24 hours of incubation in nucleus (●) and cytoplasm(▲)

Whereas the rate of pinocytic capture of the different fractions was clearly related to size, the proportion of captured conjugate subject to intracellular hydrolysis after three hours of incubation was independent of the size (the intranuclear fluorescence after 3hr of incubation was identical for all fractions of conjugates). Also, the intracellular fluorescence (nuclear and cytoplasmic) after 24 hr of incubation, with poly( $\beta$ -benzyl malate)/FI conjugates was higher than with poly( $\beta$ -malic acid)/FI conjugates. This feature shows that the incorporation of hydrophobic residues (benzyl residues) into PMLA/FI conjugate increased the affinity for the plasma membrane and consequently dramatically enhanced the rate of pinocytic uptake by cells.

## CONCLUSION

The use of fluoresceinamine as a marker allowed us to use LASER-microspectrofluorometry to evaluate the polymer uptake by K562 cells. The internalization process of adsorptive pinocytosis, in which bulk extracellular fluid is constitutively engulfed by the cell, occurred at variable rates between cell types, and appeared to be dependent on the metabolic state of the cell. The results of the present study demonstrate that, compared with free FI, the covalent attachment of FI to polymers led to an increase in the uptake of

the FI by the cells; this enhanced uptake was still apparent after prolonged periods of incubation. Fluorescently labeled polymers were found to accumulate in the cytoplasm. The kinetics of intranuclear accumulation of FI (FI released from the conjugates localized into the lysosomal vesicles), as a function of time, was rapid in sensitive K562 cells. The uptake of polymer/FI conjugates by the cells was five fold greater than that of free FI. Further work is under way to investigate the behavior of PMLA/doxorubicin conjugates by the same techniques.

## REFERENCES

- [1].Zunino F, Savi G, Giuliani F, Gambetta R, Supino R, Tinelli S and Pezzoni G. (1981) Comparison of antitumor effects of daunorubicin covalently linked to poly-L-amino acid carriers. *Eur J Cancer Clin Oncol* 20: 121-125
- [2].Daussin F, Boschetti E, Delmotte F and Monsigny M. (1988) p-Benzylthiocarbamoyl-aspartyl-daunorubicin-substituted polytrisacryl: a new drug acid-labile arm-carrier conjugate. *Eur J Biochem* 176: 625-628
- [3].Yokoyama M, Miyauchi M, Yamada N, Okano T, Sakurai Y, Kataoka K and Inoue S. (1990) Polymer micelles as novel drug carrier: adriamycin-conjugated poly(ethylene glycol)-poly(aspartic acid) block copolymer. *J Control Rel* 11: 269-278
- [4].Shih LB, Goldenberg DM, Xuan H, Lu H, Sharkey RM and Hall TC. (1991) Anthracycline immunoconjugates prepared by a site-specific linkage via an amino-dextran intermediate carrier. *Cancer Res* 51: 4192-4198
- [5].Vert M. (1986) Polyvalent polymeric drug carriers. *CRC Crit Rev The. Drug Carrier Syst* 2: 291-327
- [6].Seymour LW, Duncan R, Kopecek P and Kopecek J. (1987) Daunomycin-and adriamycin-N-(2-hydroxypropyl)methacrylamide copolymer conjugates; toxicity reduction by improved drug-delivery *Cancer Treatment Rev* 14: 319-327
- [7].Dumitriu S, Popa M and Dumitriu M. (1989) Polymeric biomaterials as enzyme and drug carriers. Part IV: polymeric drug carriers systems. *J Bioact Compat Polym* 4: 151-197
- [8].Ohya Y, Hirai K and Ouchi T. (1992) Synthesis and cytotoxic activity of doxorubicin bound to poly( $\alpha$ -malic acid) via ester or amide bonds. *Makromol Chem* 193: 1881-1887
- [9].Braud C and Vert M. (1993) poly( $\beta$ -malic acid) based biodegradable polyesters aimed at pharmacological uses. *Trends in Polymer Science* 3: 57-65
- [10].Gigli M, Doglia SM, Millot JM, Valentini L and Manfait M. (1988) Quantitative study of doxorubicin in living cells nuclei by microspectrofluorometry. *Biochem Biophys Acta* 950: 13-20
- [11].Gigli M, Rosoanaivo TWD, Millot JM, Jeannesson P, Rizzo V, Jardillier JC, Arcamone F and Manfait M. (1989) Correlation between growth inhibition and intranuclear doxorubicin and 4'-deoxy-4'-iododoxorubicin quantitated in living K562 cells by microspectrofluorometry. *Cancer Res* 49: 560-566
- [12].Delplace F, Flan B, Montreuil J, Lenain B, Barbillat J and Delhaye M. (1990) Analysis of fluorescent products and study of their interaction with cells by means of laser-microspectrofluorometry. *Analisis* 18: 27
- [13].Vert M and Lenz RW. (1981) Malic acid polymers. *US Patent* 4: 265, 247
- [14].Lozzio CB and Lozzio BB. (1975) Human chronic myelogenous leukemia cell-line with positive philadelphia chromosome. *Blood* 45: 321-334
- [15].Ginot L, Jeannesson P, Angiboust JF, Jardillier JC and Manfait M. (1984) Interactions of adriamycin in sensitive and resistant leukemic cells: a comparative study by microspectrofluorometry. *Studia Biophys* 9: 45-48

# NOVEL BIOADHESIVE, PH- AND TEMPERATURE-SENSITIVE GRAFT COPOLYMERS FOR PROLONGED MUCOSAL DRUG DELIVERY

A. S. Hoffman<sup>1</sup>, G. H. Chen<sup>1</sup>, S. Y. Kaang<sup>1</sup>, Z. L. Ding<sup>1</sup>, K. Randeri<sup>2</sup> and B. Kabra<sup>2</sup>

<sup>1</sup>Center for Bioengineering, FL-20, University of Washington, Seattle, WA 98195, USA

<sup>2</sup>Alcon Laboratories, Ft. Worth, TX 76134, USA

## INTRODUCTION

In this paper we describe the synthesis of new bioadhesive polymer structures and compositions that have been designed for application as vehicles for prolonged ophthalmic drug delivery. The major polymer component in these studies is high molecular weight PAAc, which is a well-known bioadhesive polymer.<sup>1</sup> PAAc is often incorporated into a delivery formulation in order to increase the residence time of a drug delivery vehicle in contact with mucosal surfaces. If the residence time of a drug formulation is prolonged by increased adherence to a mucosal surface, such as the eye, then it would also be desirable to slow down the release of the drug, so that it would be delivered over the period of retention of the formulation on the eye surface. In order to accomplish this, we have incorporated a more hydrophobic component, in this case a temperature-sensitive polymer, into the drug formulation.

There are three ways that a temperature-sensitive component can be incorporated together with a bioadhesive component (PAAc) in a formulation: (1) as a physical mixture with PAAc, (2) in a random copolymer with AAc, or (3) as segments in graft or block copolymers with PAAc.<sup>2,3</sup> Physical mixtures of PAAc and PNIPAAm tend to physically separate and release drug too rapidly at body temperature and pH. Random copolymers of the two are not satisfactory because they lose temperature-sensitivity and do not have sufficient hydrophobic character when the content of the AAc component reaches levels where bioadhesive properties are observed. The graft copolymer structure is most effective because (a) it combines both bioadhesive and hydrophobic properties in one single molecule, (b) retains both behaviors independently over a wide pH range, and (c) doesn't permit physical separation. This is the rationale for the work described in this paper, which will include the synthesis, physical properties and drug delivery kinetics of this unusual family of graft copolymer matrices.

## METHODS

### Synthesis of graft copolymers

Graft copolymers having PAAc as the backbone and grafted side chains of NIPAAm or NIPAAm-BMA copolymers may be prepared in two ways: 1) by copolymerization of the macromonomer of oligomers of polyNIPAAm or copolyNIPAAm-BMA with AAc (e.g.<sup>4,5</sup>) or 2) by coupling oligomers of polyNIPAAm or poly(NIPAAm-co-BMA) onto the PAAc backbone through the reaction of amino terminal groups of the oligomers with the PAAc carboxyl group. Hydrogels may also be prepared by including crosslinker (MBAAm). Fig. 1 shows a schematic graft copolymer structure and Fig. 2 shows the synthesis of the graft copolymer by the second method, i.e., conjugation of the amino-terminated oligomer onto the PAAc backbone. The details of the synthesis of such graft copolymers have been reported elsewhere.<sup>2,3</sup>



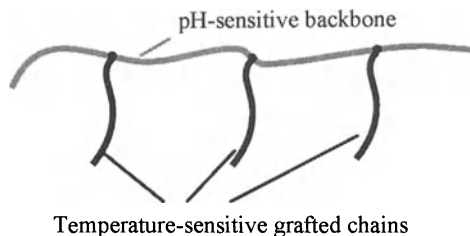


**Figure 1** Schematic structure of graft copolymer with a temperature-sensitive polymer grafted to a bioadhesive polymer backbone.

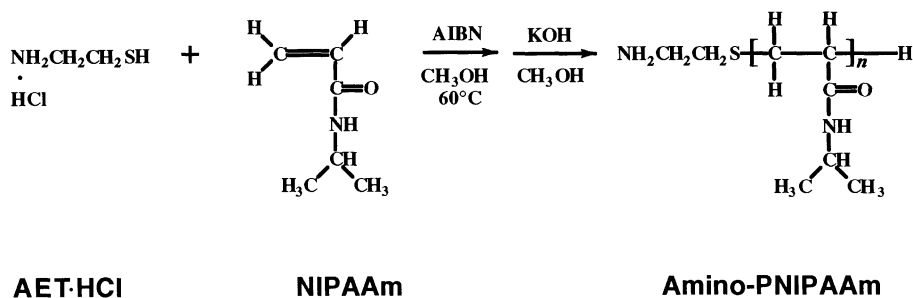


**Figure 2a** Synthesis of amino-terminated PNIPAAm

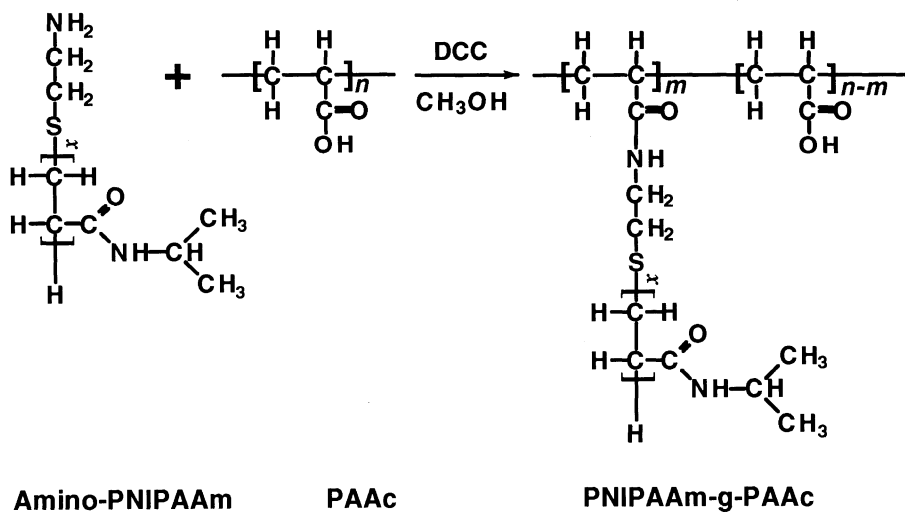


**Figure 2b** Synthesis of graft copolymer of PNIPAAm-g-PAAc by coupling amino-PNIPAAm to PAAc backbone

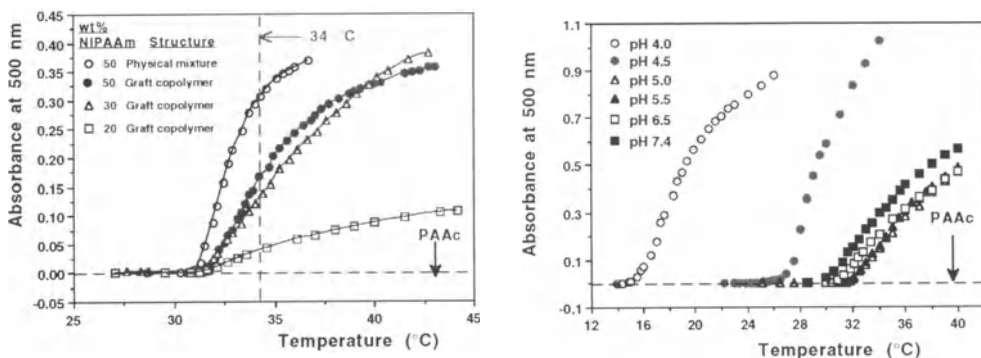


**Figure 3** Light absorbance of polymer solutions vs. temperature. Effect of (a) composition (at pH 7.4), and (b) pH (for the 50 wt% NIPAAm graft copolymer).

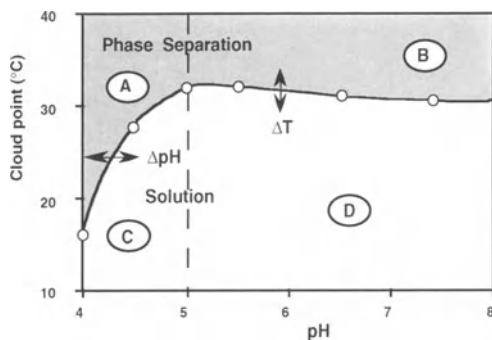


**Figure 4** The cloud points of the graft copolymer (50 wt% PNIPAAm) vs. pH, showing four regions A—D.

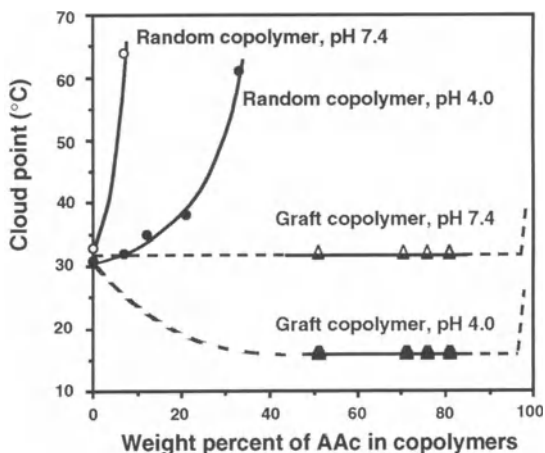


**Figure 5** The cloud points of random copolymers of NIPAAm and AAC, and of graft copolymers of PNIPAAm-g-PAAc plotted against the copolymer AAC content at pH 4.0 and 7.4

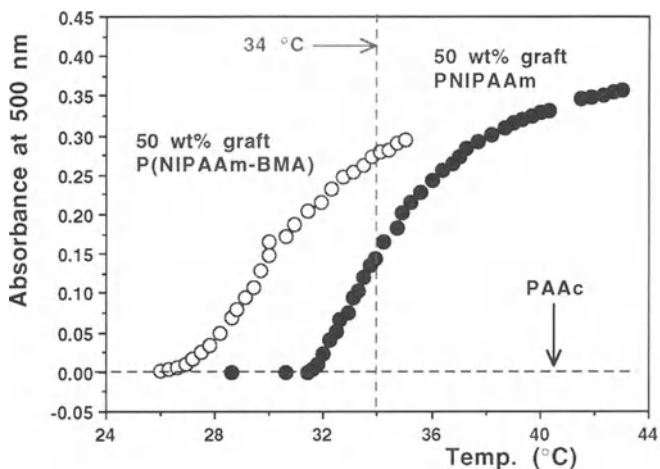


**Figure 6** Comparison of the phase transitions of the 50 wt% PNIPAAm graft copolymer with the 50 wt% P(NIPAAm-BMA) graft copolymer (at pH 7.4).

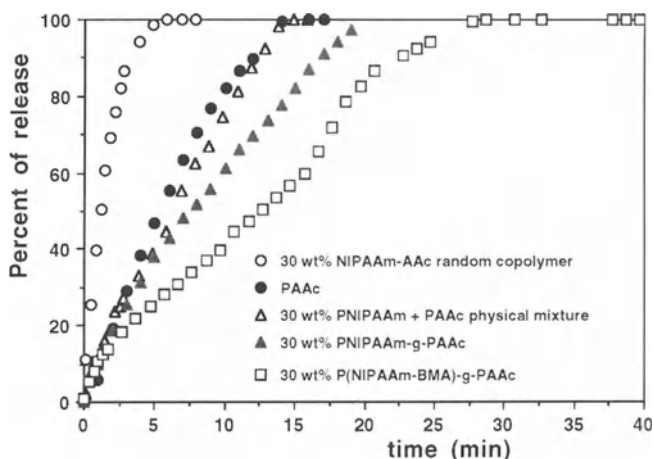


**Figure 7** Percent of timolol maleate release from various polymer matrices vs. time (PBS buffer, pH 7.4, 34 °C)

Timolol maleate, an ophthalmic drug (D), was used as a model drug to evaluate the copolymers as matrices for controlled drug release. The polymer solutions plus the drug (5 wt% drug, 95 wt% polymer) in methanol (10% w/v) were cast onto glass discs and dried to form films. These discs were immersed in PBS buffer, pH 7.4 at 34°C with vigorous stirring, and the amount of the drug released from the polymer films at various times was measured by a UV spectrophotometer at 294 nm.

## RESULTS AND DISCUSSION

Fig. 3a shows the effect of temperature on the light absorbance of aqueous solutions of different NIPAAm graft copolymer compositions and one physical mixture and Fig. 3b shows the effect of pH on the transition temperature. Even though the carboxyl groups in PAAc are ionized at pH 7.4, the graft copolymers all start to show an LCST phase transition at almost the same temperature as PNIPAAm, independent of the overall composition. With as high as 80 wt% of AAc, the graft copolymer still shows the onset of turbidity at pH 7.4. The presence of the ionized PAAc backbone seems only to reduce the magnitude of the turbidity and to widen the temperature range of the response, indicating that even when it is ionized, the PAAc backbone does not change the phase transition property of the polyNIPAAm graft chain. However, as pH is lowered, it can be seen that the LCST is also lowered, possibly due to H-bonding between the -CONH- groups of PNIPAAm with the -COOH groups of the PAAc. Fig. 4 shows the cloud points of the 50% graft copolymer of PNIPAAm-g-PAAc as a function of pH and temperature. Fig. 5 shows clearly how the cloud points of random and graft copolymers dramatically differ as a function of composition, at two different pHs. Fig. 6 shows that the copoly(NIPAAm-co-BMA) oligomer and its graft copolymer exhibited a cloud point in PBS around 26°C, which is 6°C lower than PNIPAAm.

The release of timolol maleate from the two different graft copolymers at 34°C and pH 7.4 is significantly retarded in comparison to release from matrices of PAAc, random copolymers of AAc and NIPAAm, or physical mixtures of PAAc and PNIPAAm. These data are shown in Fig. 7. These interesting graft copolymers should be useful as sustained-release, bioadhesive drug delivery vehicles at physiologic conditions. Such dual-sensitivity, "hybrid intelligent" graft and block copolymers may also have many exciting new uses.

## ACKNOWLEDGEMENTS

The authors would like to dedicate this paper to Prof. Teiji Tsuruta, on the occasion of his 75th birthday. Prof. Tsuruta has been a special inspiration over the past ten years to one of the authors (ASH). We also want to gratefully acknowledge the support of the Alcon Inc. for this research. Prof. Kaang is now back at Chonnam National University, Korea.

## REFERENCES

- [1] Park H, and Robinson JR (1987) *Pharmaceutical Res.* **4**: 457-464
- [2] Chen GH, and Hoffman AS (1995) *Nature* **373**: 49-52
- [3] Chen GH, and Hoffman AS (1995) *Macromol. Rapid Commun.* **16** (in press)
- [4] Takeuchi S, Oike M, Kowitz C, Shimasaki C, Hasegawa K, and Kitano H (1993) *Makromol. Chem.* **194**: 551-558
- [5] Klier J, Scanton AB, and Peppas NA (1990) *Macromolecules* **23**: 4944-4949

# ENHANCED INTESTINAL ABSORPTION OF PEPTIDES BY COMPLEXATION OF THE PARTIALLY DENATURED PEPTIDE

Joseph R. Robinson and Gwen M. Mlynek

*School of Pharmacy, University of Wisconsin, 425 N. Charter Street, Madison, Wisconsin 53706 U.S.A.*

## SUMMARY

Protein synthesized within a living cell must be transported across biological membranes to reach their target site. This transport is accomplished through the use of a class of carrier, termed chaperones, and involves binding of the protein, which is in an intermediate state, to the carrier. Using this natural model as a conceptual starting point, evidence is presented that, in a fully aqueous solution, certain small molecular weight compounds can be added to proteins which will significantly enhance membrane penetration of the protein. Using iodinated human growth hormone, in isolated tissue and perfusion studies of the rabbit intestine, small molecular weight compounds, termed proteinoids, cause a five-fold increase in the permeability coefficient. Evidence is presented that this is a passive absorption process with no demonstrable changes in the absorbing membrane.

**KEY WORDS:** chaperones, proteinoids, human growth hormone, molten globular state, stress proteins

## INTRODUCTION

Oral delivery of peptides continues to be an unachieved goal although significant advances have been made during the past five-ten years. The major issues inhibiting absorption across mucosal tissue, especially intestinal tissue, appear to be self-association of the peptide; proteolytic destruction of the drug by luminal, brush-border, and tissue proteases; and low permeability across the intestinal tissue. The first two of these three issues can be addressed through fairly conventional formulation approaches, including microencapsulation. The latter issue of permeability appears much more intractable and has classically been addressed through the use of penetration enhancers or by covalently modifying the peptide. Each of these approaches can create significant regulatory problems and are much more difficult to develop into a commercial product. An alternative novel approach to improve penetration has been suggested by Milstein (1). In this case, modelled after the normal biological approach of protein absorption across biological membranes, the non-fully active peptide, which exists in solution in equilibrium with the fully active peptide, is complexed with a low molecular weight carrier. The complexed peptide is much more permeable across biological tissues.

### Cellular Movement of Recently Synthesized Peptides

How does a recently synthesized peptide cross a biological membrane to reach its site of action? To answer this question it is worthwhile examining the relatively brief history of

heat shock proteins (2). Thirty years ago it was noted that following a sudden increase in temperature all cells increase production of a class of molecules that protects them from further damage. The phenomena was referred to as the heat shock response and the class of molecules produced were referred to as heat shock proteins (HSP). Subsequently, we have learned that a wide variety of environmental assaults, such as alcohols, metabolic poison, and stress, produce HSP. HSP's are now commonly referred to as stress proteins and it is known that they are far more than just defensive molecules and, indeed, participate in a variety of metabolic processes, including the pathway of protein synthesis and transport across biological membranes. Stress proteins bind to newly synthesized proteins as they are being folded and assembled into their mature form. This prevents premature folding. The stress protein may dissociate from the protein and allow it to fold into its functional shape or to associate with other proteins. These HSP or stress proteins are now commonly referred to as molecular chaperones (3). By definition (4), molecular chaperones are a family of unrelated classes of proteins that mediate the correct assembly of other polypeptides but that are not components of the functional assembled structures.

The proposed function of chaperone proteins is to assist polypeptides to self-assemble by inhibiting alternative assembly pathways that produce incorrect structures. Naturally, the peptide-chaperone complex allows movement of the peptide across a biological barrier. Whether the chaperone-peptide complex moves together across the membrane or the chaperone merely presents the partially folded peptide to the membrane surface, varies on a case by case basis.

Milstein (1) began with the premise that peptides in solution exist in equilibrium in a variety of states, one of which is the fully active form. Support for this assumption of various

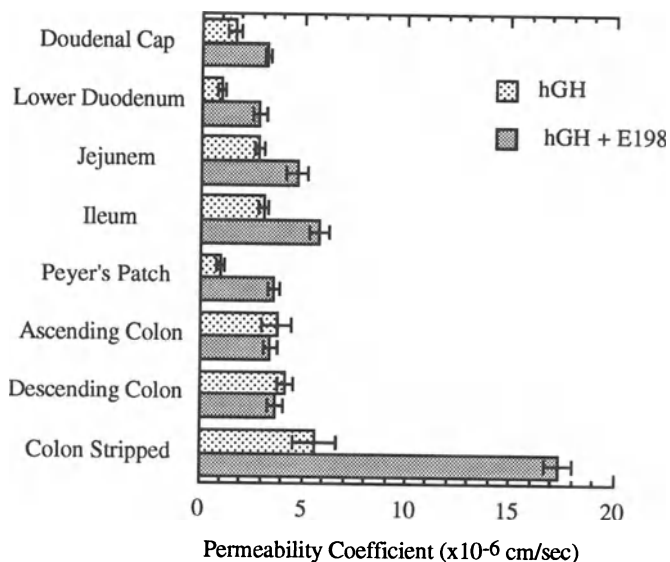


Fig. 1

Effect of E198 on hGH permeability in various regions of the rabbit intestine.

states of the peptide have been recently reported for the enzyme lactate dehydrogenase (5). He further identified specific small molecules that would non-covalently bind to certain peptides. The bound form would entail the non-fully active peptide and a number of these small molecules. Thus, for example, he found that the following sulfonamide,



referred to as E198, would bind to human growth hormone. Evidence for the binding is through Differential Scanning Calorimetry. We have examined the permeability characteristics of iodinated human growth hormone in the presence and absence of E198, using isolated rabbit intestinal tissue studies.

Figure 1 shows the influence of E198 on  $^{125}\text{I}$ -hGH permeability across rabbit intestinal tissue. A variety of metabolic agents to test for the presence of an active transport process, including ouabain and amiloride, confirmed that the process involved passive diffusion. Evidence that E198 is not a classic penetration enhancer is found by examining the influence of this agent on the permeability of mannitol, which classically employs the paracellular route for drug permeation and progesterone, an agent that uses the transcellular route, as

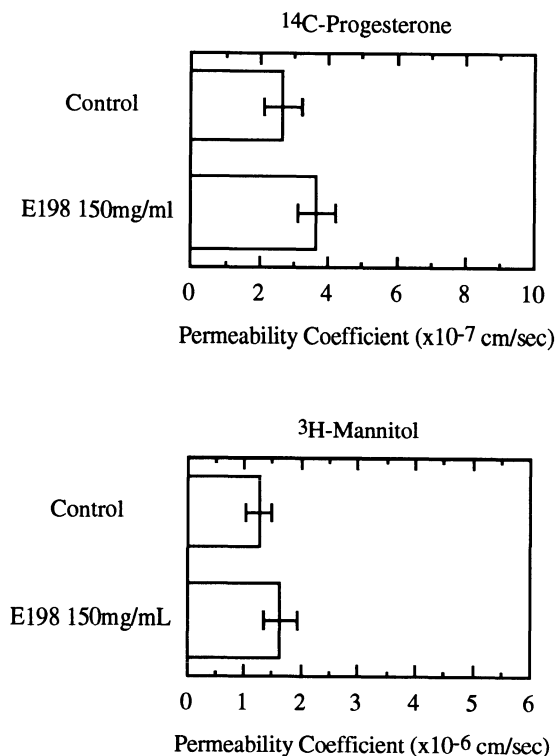


Fig. 2  
Effect of E198 on absorption of  $^{14}\text{C}$ -progesterone and  $^3\text{H}$ -mannitol through rabbit duodenal tissue.

shown in Fig. 2. Further evidence that E198 is not a classic penetration enhancer was the absence of tissue damage or change as judged by enzymatic markers and dyes.

The precise mechanism of membrane penetration, i.e., does E198 penetrate across the tissue with hGH or does it simply present hGH to the tissue, is not yet known but is actively being pursued in this laboratory. What is clear, however, is that small and large molecular weight substances can bind and stabilize intermediate peptide conformers whose physicochemical properties allow for improved intestinal absorption.

## REFERENCES

1. Milstein, S, Emisphere Corporation, Patent Pending
2. Welch, WJ (1993) How do cells respond to stress? Sci Amer 56-64 (May issue)
3. Beckman, RP, Mizzen, LA and Welch, WJ (1990) Interaction of HSP with newly synthesized proteins: implications for protein folding and assembly. Sci 248: 850-853
4. Ellis, JR, Hemmingsen, SM (1989) Molecular chaperones. Trends Biochem Sci 14: 339-42
5. Xue, Q and Yeung, ES (1995) Differences in the chemical reactivity of individual molecules of an enzyme. Nat 373: 681-683



# CONTROLLED DRUG DELIVERY FORMULATION WITH SAFE POLYMERS

Tsuneji Nagai<sup>a</sup>, Mariko Morishita<sup>a</sup>, Isao Morishita<sup>b</sup>, Yoshiki Suzuki<sup>c</sup>, and Yuji Makino<sup>c</sup>

<sup>a</sup>Department of Pharmaceutics, Hoshi University, Ebara 2-4-41, Shinagawa-ku, Tokyo 142, Japan, <sup>b</sup>Tsumura & Co., Yoshiwara 3586, Ami-machi, Inashiki-gun, Ibaraki 300-11, Japan and <sup>c</sup>DDS Research Laboratories, Teijin Ltd., Asahigaoka 4-3-2, Hino, Tokyo 191, Japan

## SUMMARY

From the pharmaceutical point of view, the bioavailability, that is the amount and rate of absorption, is the most important factor determining the drug quality with respect to its efficacy and safety. Then, the bioavailability is controlled by well-designed dosage forms, for which interactions with surrounding components are applicable. Practically there are afforded various possibilities of modification of the interaction and then of control of drug delivery by a design of dosage forms, using polymers. The present talk will contain, as example, enteral delivery of insulin by Eudragit microspheres with protease inhibitors, topical mucosal drug delivery systems with adhesive polymers, and nasal delivery of salmon calcitonin by functional powder preparations using microcrystalline cellulose. These polymers are guaranteed already as pharmaceutically safe ones.

**KEY WORDS** : safe polymer, microspheres, adhesive tablet, nasal powder

## INTRODUCTION

Researches in controlled drug delivery with view to development of new drugs are getting quite active internationally, as it is shown by noticeable recent advances in drug delivery systems (DDS) which includes transdermal therapeutic systems (TTS) and targeting therapies.

The basic technology of DDS is concerned with enhancement and control of bioavailability of drugs, which is in relation with the efficacy and safety of drugs. The bioavailability is controlled by well designed dosage forms. DDS or TTS are the most advanced dosage forms which afford the control of bioavailability. For the control of bioavailability, there are two main approaches. One is concerned with chemical modifications of active ingredients, for example, prodrug, antedrug, conjugation and immobilizing. The other is with the formulation approach by applications of interaction of drug with the surrounding components, such as: (a) at molecular level, that is, intermolecular interactions (for example, complex formation, molecular dispersions and so on); (b) at particle level, that is, particle-particle (and/or molecular-particle) interactions (for example, matrix, microcapsules, particle coating, tablets, capsules, and so on); and c) miscellaneous (combinations of the above two, or with a devise). The surrounding components thereby include body tissues and organs, and thus a triple interaction among drug, dosage form and body components should be considered. Practically there are afforded various possibilities of modification of the triple interaction and control of drug delivery by a design of dosage forms, especially using polymers, as some examples will be shown.

## ENTERAL DELIVERY OF INSULIN BY EUDRAGIT MICROSPHERES WITH PROTEASE INHIBITORS<sup>1)</sup>

As a new pharmaceutical approaches to design an oral dosage form of insulin, we developed insulin microspheres (IMS) prepared with polyacrylic polymer (Eudragit L 100), which contained such protease inhibitors as aprotinin, Bowman-Berk inhibitor, soybean trypsin inhibitor and chymostatin. These preparations were administered orally with a 20 U/kg insulin dose to normal and diabetic rats. IMS without protease inhibitor and with soybean trypsin inhibitor or chymostatin produced no

marked hypoglycemic response in both groups of rats (Fig. 1). A significant continuous hypoglycemic effect was obtained after oral administration of microspheres containing aprotinin or Bowman-Berk inhibitor in both groups of rats when compared with controls. The efficacy order of four protease inhibitors incorporated into the microspheres was aprotinin  $\geq$  Bowman-Berk inhibitor  $>$  chymostatin = soybean trypsin inhibitor.

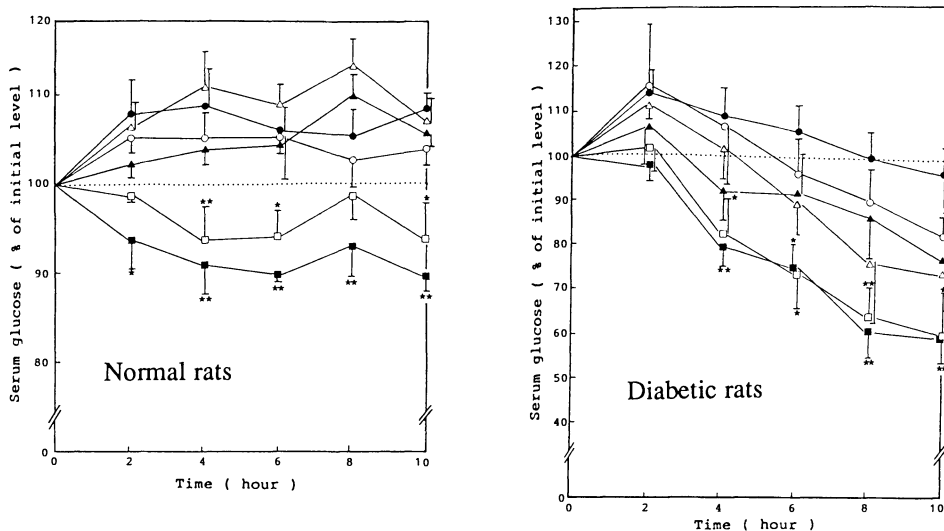


Fig. 1. Hypoglycemic effect of insulin microspheres (IMS) administered orally to normal and diabetic rats. (●) Control; (○) IMS without protease inhibitor; (▲) IMS containing soybean trypsin inhibitor; (△) IMS containing chymostatin; (■) IMS containing aprotinin; (□) IMS containing Bowman-Birk inhibitor. Each point represents the mean  $\pm$  S.E. Comparisons calculated at each period against controls: \* $p < 0.05$ , \*\* $p < 0.01$ .

Since we found aprotinin is a good material for our experimental purpose, next we found by *in situ* loop method, in the use of aprotinin, there is a site dependency of the enzyme inhibitory activity of aprotinin, on the absorption of insulin from gastrointestinal tract. We made 6 to 7 cm loops in the intestines and made experiments on duodenum, jejunum, ileum and colon. Regarding the serum glucose level when we administered insulin in the different segment loops of gastrointestinal tract, it decreased in jejunum a little bit, and in the ileum, it decreased most. In ileum, the level decreased depending on the dose, as the AUC and the cumulative change in glucose clearly depended on the dose of aprotinin. The result mentioned already suggests there is a possibility that insulin can be administered orally if insulin and the inhibitor in a high concentration can be released from the microspheres in the distal small intestine.

As the next step we designed the microspheres which makes both the concentrations of insulin and aprotinin at the absorption site. Three types of IMS were prepared using copolymers having pH-dependent solubility, Eudragit L100 (L), Eudragit S100 (S), and a 1:1 mixture of these (LS). In a release study, the insulin release rate from S-IMS was much slower than that from L-IMS at pH below 7.0.

We investigate the distribution of insulin microspheres of two different types of Eudragit after oral administration, at seven different sections of gastrointestinal tract where No. 1 is stomach as the starting point. No. 2 to 7 correspond to the small intestine (Fig. 2). In the case of Eudragit L which usually dissolves over pH 6, the microspheres dissolves between duodenum and jejunum. In the

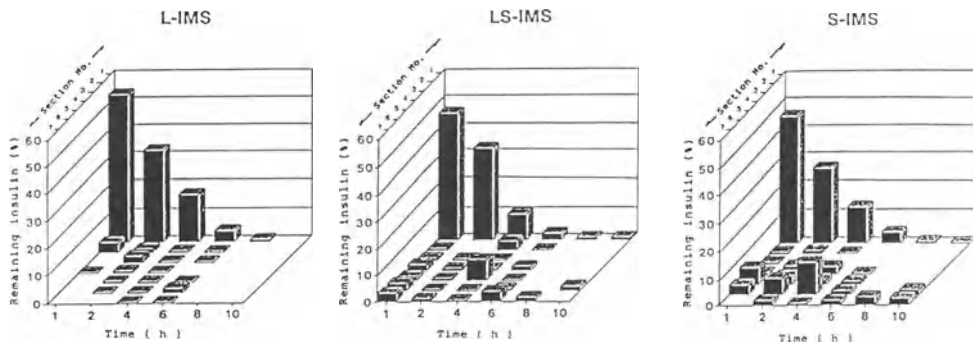


Fig. 2. Distribution of L-, LS- and S-IMS in the intestinal tract of rats. Each column represents the mean of 4-6 determinations.

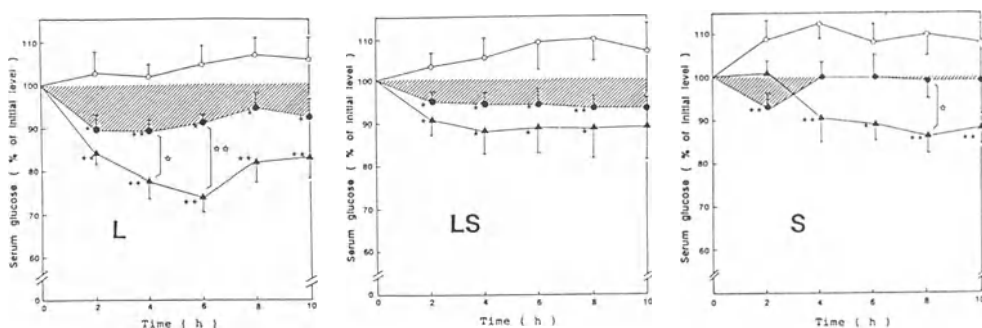


Fig. 3. Hypoglycemic effects of L-, LS- and S-IMS administered orally to rats. (O) Control (insulin-free microspheres); (●) IMS; (▲) IMS containing aprotinin. Each point represents the mean  $\pm$  S.E. Comparisons calculated at each period against controls: \* $p$ <0.05, \*\* $p$ <0.01. Comparisons calculated at each period for IMS vs IMS containing aprotinin: \* $p$ <0.05, \*\* $p$ <0.01.

case of Eudragit S which usually dissolves over pH 7, the microspheres dissolve between ileum and colon. In the one-to-one mixture of Eudragit L and S, it dissolves between jejunum and ileum. These results suggest the insulin microspheres dissolved slower *in vivo* than *in vitro*, and this may be due to the low water content and high viscosity conditions in the intestinal tracts. Conclusively, Eudragit S dissolves a little too late to make the concentration of insulin and aprotinin high around ileum and the microspheres of Eudragit L seem better.

In an *in vivo* experiment, the decrease in serum glucose was the highest in the insulin microspheres of Eudragit L (Fig. 3). The relative hypoglycemic efficacy compared with an intravenous administration hereby obtained was 3.6% by the insulin microspheres containing aprotinin in use of Eudragit L. As you understand, the hypoglycemic effect by our enteric insulin microspheres for oral administration is still insufficient compared with those in intravenous administration. However, our data may afford a kind of technology of targeting, as to ileum, not only of insulin but also of other peptide drugs. Our present trial has been on a use of enzyme inhibitors, but this technology may be extended to a use of absorption enhancers, or a combination of inhibitors and enhancers. Anyway, we should investigate much more to increase the bioavailability of insulin.

## TOPICAL MUCOSAL DRUG DELIVERY SYSTEMS WITH ADHESIVE POLYMER<sup>2)</sup>

In our series of studies of several topical mucosal adhesive dosage forms containing hydroxypropyl cellulose (HPC), first we tried to design a new topical dosage form for *carcinoma colli*. For this study, we combined HPC and carbomer (CM) to make disks or sticks by compression. In order to design a suitable formulation, we preliminarily investigated the release rate of drug and the water absorption (related to the adhesiveness). The release rate of drug increased with the concentration of HPC (Fig.4), while the water absorption increased with the concentration CM (Fig.5). When placed on *portio vaginalis* of voluntary patients, this preparation swelled well with the body fluid, sticking to the disease part with a good adhesiveness.

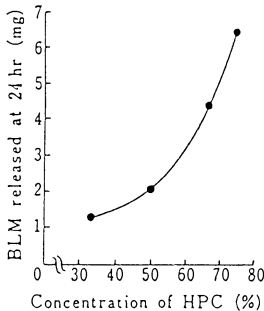


Fig. 4. Relation between release of drug (BLM) and concentration of HPC. Data are expressed as the mean of 3 determination.

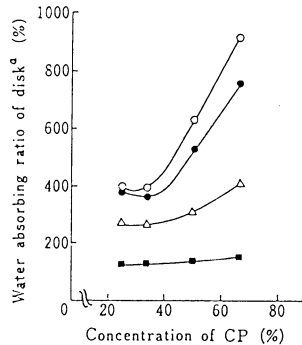


Fig. 5. Relation between water absorption of the disk and concentration of CM.  
Key: ■, 6 h; △, 24 h; ●, 48 h; ○, 72 h

Following this work, we tried an oral mucosal dosage form for the absorption of insulin; an adhesive tablet for *aphthous stomatitis*, the product of which is on market on the brand name of "Aftach," and adhesive powder spray for extensive *stomatitis* which is on market on the brand name of "Salcoat."

As the third ones, we tried to apply the adhesive dosage forms to nasal application and a powder dosage form for nasal absorption of insulin resulted in about one-third bioavailability in comparison with intravenous administration in beagle dogs; this dosage form has been applied to the one for nasal allergy, which is on market on the brand name of "Rhinocort".

## NASAL DELIVERY OF SALMON DELIVERY OF SALMON CALCITONIN BY FUNCTIONAL POWDER PREPARATIONS USING MICROCRYSTALLINE<sup>3)</sup>

Salmon calcitonin was administered into rabbit nostrils as powder mixtures with base materials and the effects of the materials on plasma calcitonin levels were compared. The results showed that microcrystalline cellulose, which is water-absorbing and water-insoluble but not mucosa adhesive, gave the highest absorption, whereas hydroxypropyl cellulose, which is water-absorbing and gel-foaming, or lactose, which is water-soluble, failed in significant absorption. Plasma calcitonin levels were neither detected with a liquid formulation.

In an *in vitro* study, microcrystalline cellulose didn't cause any disturbance in ciliary movement of mouse nasal mucosa. In an *in vivo* study, little irritation was observed in histopathological examinations of rabbit nasal mucosa after microcrystalline cellulose administrations. Then the salmon

calcitonin powder preparation was applied to humans (Fig. 6). The results so far showed that the bioavailability was excellent (5-10%) and the dose-respondered absorption with less variations were observed. The preparations are well tolerated by patients and better therapeutic effects than an existing liquid formulation are expected.

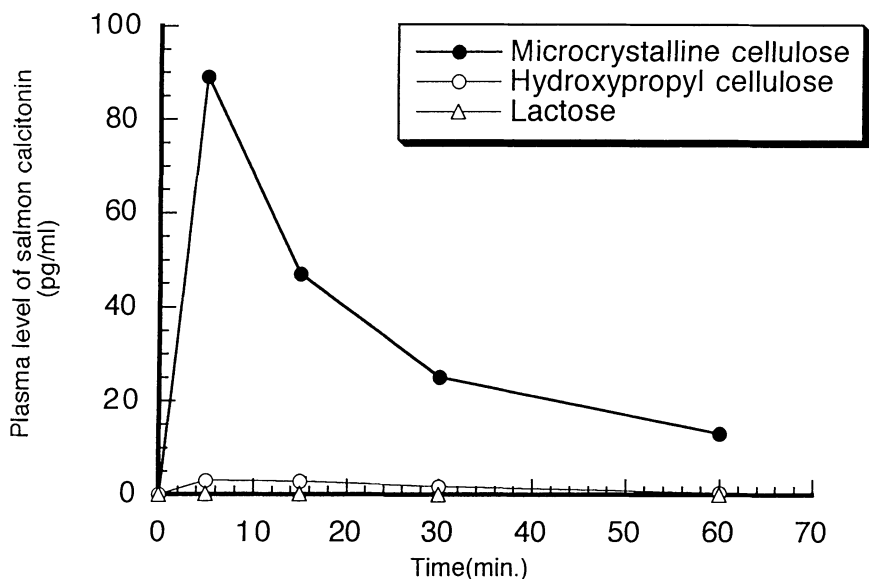


Fig. 6. Plasma salmon calcitonin level after nasal administration of powder preparations with different base materials.

It is clear that calcitonin can be fairly effectively absorbed through the human nasal membrane without using absorption promoters such as surfactants. The exact mechanism of this absorption is still under investigation, but at least the high deposition, local high concentration, rapid drug release and local residence are the reasons why the high bioavailability is shown.

## REFERENCES

- 1) Novel oral microspheres of insulin with protease inhibitor protecting from enzyme degradation: M. Morishita, I. Morishita, K. Takayama, Y. Machida and T. Nagai, *Int. J. Pharm.*, **78**, 1-7 (1992); Hypoglycemic effect of novel oral microspheres of insulin with protease inhibitor in normal and diabetic rats: I. Morishita, M. Morishita, K. Takayama, Y. Machida and T. Nagai, *Int. J. Pharm.*, **78**, 9-16 (1992); Enteral insulin delivery by microspheres in 3 different formulations using Eudragit L100 and S100: I. Morishita, M. Morishita, K. Takayama, Y. Machida and T. Nagai, *Int. J. Pharm.*, **91**, 29-37 (1993).
- 2) Adhesive topical drug delivery system: T. Nagai, *J. Controlled Release*, **2**, 121 (1985); Topical mucosal adhesive dosage forms: T. Nagai, *Med. Res. Rev.*, **6**, 227 (1986).
- 3) Therapeutic possibilities for nasal delivery: T. Nagai and Y. Suzuki, *Topics in Pharmaceutical Sciences 1991 (Proceedings of the 51st International Congress of Pharmaceutical Sciences of FIP, Washington, D.C., USA, 1-6 September 1991)*, p.83-93 (1992); Drug delivery to respiratory tracts by functional powder preparations: Y. Makino, K. Sakon, M. Dohi, M. Sakagami, Y. Nishibe, *Proceedings of France-Japan DDS Symposium: Advances in Novel Science and Technology of Drug Delivery and Targeting, Hakone, Japan, 7-10, December, 1994*, p11-12.

# SUPRAMOLECULAR ASSEMBLIES FOR IMPROVED DRUG DELIVERY SYSTEM

Junzo Sunamoto

*Division of Synthetic Chemistry & Biological Chemistry, Graduate School of Engineering, Kyoto University, Sakyo-ku Yoshida Hommachi, Kyoto 606, and Supermolecules Project, JRDC, Keihanna Plaza, Seika-cho 1-7, Soraku-gun, Kyoto 619-02, Japan*

## SUMMARY

For past two decades, we have been developing various kinds of drug delivery systems such as liposomes and O/W-emulsions those are coated by cell specific polysaccharide, biologically labile drugs stabilized by complexation with hydrophobized polysaccharides, cell-fusogenic liposome, and liposomal vaccines. In this article, basic concept for establishing these systems, methodologies for making them, and practical examples using these systems will be briefly described.

**KEY WORDS:** drug delivery system (DDS), liposome, emulsion, protein drug, liposomal vaccine

## INTRODUCTION

Different from ordinary molecules consisted of totally covalent bonds, *supermolecule* is defined as a molecule that is consisted of weak and noncovalent bonds such as hydrogen bond, ionic bond, dipole-dipole interaction and/or hydrophobic interaction. In the "Ringsdorf model", macromolecular prodrugs are designed and formed by chemical conjugation of totally covalent bonds. Different from the macromolecular prodrugs, in the supramolecular assembly system, we do not need worry about chemical and/or biochemical cleavage of the linkage between the true drug and its carrier after *in vivo* administration or cell uptake. Since 1982, we have been developing various kinds of drug delivery systems based on the concept of supramolecular assembly. Active targeting of drugs to a specific cell or tissue is the most important problem for developing an intelligent drug delivery system (DDS). For past two decades, we have made effort to establish a system of the active targeting DDS using several supramolecular assembly systems. With biologically labile drugs such as protein drugs or antisense, in addition, direct introduction of these drugs into cytosol of target cell is required to escape the digestion by lysosomal enzymes in endosome. For this purpose, a fusogenic liposome, which is modified by poly(ethylene oxide)-bearing lipid, was newly developed. In medicine, not only diagnosis and treatment but prophylaxis, especially preventive treatment, also is important. In this sense, a potent liposomal vaccine also was newly developed. These new concepts and methodologies will be introduced.

## SITE SPECIFIC DELIVERY USING CELL SPECIFIC POLYSACCHARIDE-COATED LIPOSOMES

Saccharide determinants play an important role in biological recognition, such as antigen-antibody interaction and cell-cell adhesion. Since 1982, we have developed a methodology to achieve receptor-mediated targeting in a liposomal DDS. For this purpose, we have synthesized several polysaccharide derivatives that were partially modified by chemical conjugation of an additional amino sugar or sialic acid, and we found that coating the liposomal surface by these polysaccharide derivatives was also able to control the cell specificity of the liposome. Using such specifically modified liposomes, we could succeed treatment of several infectious and cancer diseases in experimental animals.

## Synthesis of hydrophobized polysaccharide

For example, a cholesterol derivative as activated using a dicyanate spacer was reacted at 80 °C for 8 h with pullulan ( $M_w$  55000,  $M_w/M_n = 1.54$ ) in dry DMSO containing pyridine. Ethanol was added to the reaction mixture, and the suspension was kept overnight at 4.0 °C. The precipitates were separated, purified by dialysis against water using Seamless Cellulose Tube (VISKASE SALES Corp.), and lyophilized to give white powder. The degree of substitution of cholesterol group was determined by  $^1\text{H-NMR}$ . When pullulan ( $M_w$  55000) was substituted by 2.0 cholesterol groups per 100 anhydroglucoside units, for instance, it was coded as CHP-55-2.0 [1,2].

## Coating of liposomal surface with hydrophobized polysaccharides

The cholesterol-bearing polysaccharide effectively coated the liposomal surface [1, 3-6]. The polysaccharide-coated liposomes are physicochemically stable against the external stimuli such as pH, ionic strength, and *in vivo* biodegradation by lipases, lipooxidases, and serum proteins compared with the conventional liposome [6].

Effective delivery of drugs to a target cell or tissue largely diminishes the toxic side effect and increases the pharmacological activity. Targeting of drugs to a specific cell or tissue is the most important problem for developing useful drug delivery system (DDS). The polysaccharide-coated liposomes are expected to be an excellent drug carrier.

Amylopectin- or mannan-coated liposomes showed a unique specificity to phagocytes such as macrophages, monocytes, and neutrophils [6]. We have synthesized also several pullulan derivatives those were chemically modified in part additional sugars such as galactose, glucose, mannose, and sialic acid which show high affinity for specific cells. The uptake of these polysaccharide-coated liposomes by various cells was controlled by changing only the terminal sugar residue of the polysaccharide [7,8]. For example, 1-aminolactose-bearing pullulan-coated liposome was effectively internalized by rat and human liver cancer cells (AH66 and HuH7) [9].

Effective activation of macrophages by an immunomodulator is a basic requirement in immunotherapy. Anti-fungal drugs also must be delivered into cytosol of host phagocytes for perfect treatment of intracytoplasmic pathogens. In order to more effectively modulate the *in vivo* adjuvant activity of immunopotentiators and antimicrobial agents, macrophage-specific liposomes as coated with mannan or amylopectin derivatives (CHM or CHAp) were used as the targetable carrier to macrophages [5,10-12]. The CHM-coated liposome that is encapsulating poly(maleic acid-alt-7,12-dioxaspiro[5,6]dodec-9-ene) (MA-CDA) showed an effective activation of mouse peritoneal macrophages [10,11]. The maximum macrophage activation as induced by liposomal MA-CDA increased by 3.2 times in comparison with that of free MA-CDA. High cytostatic activity of mouse alveolar macrophages induced by *i.v.* was observed in the liposomal MA-CDA [5].

CHAp-coated liposomes were used to target to alveolar macrophages in the treatment of several animal models of infectious disease, experimental *Legionella pneumophila* in guinea pig [13], and *Pulmonary Candidiasis* in mice [14]. The CHAp-coated liposomes that were encapsulating antibiotics (sisomicin or amphotericin B) showed a remarkable treatment efficacy, which was much better than the conventional liposome at the same dosage [14].

CHP-coated egg PC liposomes were significantly accumulated at brain tumor in rat [15]. The accumulation of the CHP-coated liposome increased by 4.5 times at the tumor and by 2.1 times at the ipsilateral brain, and decreased by 4 times at the spleen compared with that of conventional liposome. Survival of 9L glioma-implanted rat was investigated by cis-platinum diamino dichloride-loaded liposome. Average survival (35.3 days for the group treated with the CHP-coated liposomes) was statistically ( $P < 0.05$ ) significant compared with that of the untreated group (20.3 days) [15].

We have developed also an improved technique for binding onto the liposomal surface a monoclonal antibody fragment specific to a target tumor cell. This method involves coating the outer surface of liposome with a pullulan derivative and subsequent covalent binding of the SH group bearing antibody fragment to the pullulan derivative on the liposomal surface [16,17]. The sialosylated Lewis<sup>x</sup> (CSLEX1)-conjugated liposome was prepared by introduction of SH-bearing anti-sialosylated

Lewis<sup>X</sup> fragment (IgMs) to the maleimide group-bearing pullulan-coated liposome. The binding of immunoliposome to human lung cancer cells (PC-9) drastically increased by factors as much as 447 compared with the binding of pullulan-coated liposome without antibody. PC-9 transplanted mice were treated with the immunoliposome. The adriamycin-loaded immunoliposome showed a strong tumor suppression for athymic mice in which human lung cancer PC-9 was subcutaneously implanted [18].

### Increased colloidal stability of O/W-emulsion of lipophilic drug

Cholesterol-bearing polysaccharide derivatives are unique amphiphilic polymers and show strong binding to hydrophobic substances and high colloidal stability. Therefore, the polysaccharide itself is a good stabilizer for O/W-emulsions [19,20]. A water-insoluble antitumor drug,  $\alpha$ -linolenic acid (ALA), was nicely emulsified by CHP in water. The emulsification of ALA by CHP gave a higher and improved anti-tumor activity compared with free ALA in both *in vitro* and *in vivo* experiments [21].

### Hydrophobized polysaccharides as a carrier for labile protein drugs

The CHP self-aggregates strongly interact with various soluble proteins and enzymes [22-24]. One CHP nanoparticle complexes with one protein for bovine serum albumin (BSA,  $M_w=67000$ ), one for  $\alpha$ -chymotrypsin dimer (Chy) ( $M_w=49000$ ), three for interferon  $\alpha$  ( $M_w=18750$ ), four for cytochrome c ( $M_w=12480$ ) and ten for insulin ( $M_w=5735$ ). The maximum amount of the protein bound to the CHP nanoparticle depended on the molecular weight (or the size) of protein. The complex showed an excellent colloidal stability without any precipitation. In addition, no dissociation of the protein from the complex was observed at all even after keeping for a week at pH 7.2 and 25 °C. Electrostatic interaction was not so important for the complexation. The CHP self-aggregate has hydrophilic hydrogen bondings domain and also hydrophobic cholesterol domain. Such an amphiphilic property of the nanosize hydrogel plays an important role for complexing soluble proteins that have both hydrophobic and hydrophilic patches on their surface.

The CHP self-aggregate complexed with Chy and formed colloiddally stable nanoparticles ( $R_G = 12$  nm), which was confirmed by high performance size exclusion column chromatography. The Chy dimer bound to one CHP nanoparticle at pH 4.2 and 25 °C. Chy was localized deeply inside the matrix of the CHP hydrogel, not in the region close to the surface of the hydrogel nanoparticle. The helix content of Chy increased from 9 % to 29 % upon the complexation, while the  $\beta$ -form content decreased from 34 % to 21 %. The enzymatic activity ( $V_{max}$ ) of complexed Chy decreased up to 1/88 at pH 8.0 compared with that of free Chy, while  $K_m$  did not change much. No dissociation of Chy from the complex was observed even after a week at 25 °C. However, Chy was released from the complex by the addition of BSA. Released Chy still kept almost the same enzymatic activity as that of free Chy before the complexation. This means that native conformation of Chy was recovered after the dissociation.

For free Chy, the CD ellipticity (at 222 nm) of complexed Chy was completely lost within 2 h at the elevated temperature. With the complexed Chy, on the other hand, its ellipticity still remained more than 85 % of the original value even after heating for 6 h at 92 °C. Regarding the secondary structure, the thermal denaturation of the protein was drastically prevented upon the complexation with the CHP self-aggregate. After heating the complex at 92 °C for 1 h, Chy was released from the complex by adding BSA. For released Chy, 74 % of the original enzyme activity was still kept. DSC measurement showed that no thermal unfolding of complexed Chy undergoes over a temperature range of 10 - 100 °C. Even at 90 °C, the helical content of complexed Chy little changed compared with that at 25 °C. The thermal unfolding of Chy was significantly retarded upon the complexation.

### FUSOGENIC LIPOSOME

For introduction of biologically active substances into cells, two possible paths have been considered; namely, endocytosis and fusion. In endocytosis, labile materials such as protein, enzyme, or nucleic acids are mostly and easily digested by lysosomal enzymes in endosome. Therefore, fusion of liposomal membrane with cytoplasm membrane is required for efficient and direct delivery of such the



fragile materials into cytosol. Recently, we provided a fusogenic liposome as prepared by mixing simple egg PC and an artificial lipid, 2-[ $\omega$ -hydroxy(oxyethylene) $_x$ - $\alpha$ -yl]-1,3-bis-(dodecyloxy)-propane (abbreviated as PEO-lipid( $n = x$ )). The PEO-lipid modified liposomes undergo the fusion with plant protoplast or mammalian cell such as tumor cells and lymphocytes [25].

## LIPOSOMAL VACCINE

Effective internalization of antigen into antigen presenting cells is most important process for the enhancement of immunogenicity by endogeneous antigen [26]. The adjuvant activity of liposome for inducing effective humoral and cellular immune responses have been demonstrated in several systems. The CHM-coated liposome that is loading a HTLV-1 related protein, (*gag-env* hybrid protein) was used *in vivo* immunization of WKA/H rats. WKA/H rats were subcutaneously immunized twice at one week interval by the *gag-env* hybrid protein-reconstituted liposomes. One week after the second and last immunization, HTLV-1<sup>+</sup> tumor cells (TARS-1) were intradermally challenged. In addition, splenic cells were simultaneously obtained for inspecting the generation of CTL. The splenic cells isolated were *in vitro* sensitized with mitomycin-C treated TARS-1 cells. Killer cell activity against TARS-1 was observed only by the case immunized with the CHM-coated *gag-env*-reconstituted liposome. The pretreatment of rats with carrageenan strongly inhibited the generation of CTL, and tumor rejection was not observed. These results indicate that the effective immunization require phagocytic process of CHM-coated *gag-env*-liposome most likely by macrophages.

Recently, we have developed an artificial boundary lipid, 1,2-dimyristoylamido-1,2-deoxyphosphatidylcholine (D<sub>14</sub>DPC). When such the D<sub>14</sub>DPC-containing liposome is coincubated with mammalian cells, several membrane proteins and/or enzymes are effectively and directly transferred from intact cell to the liposome. Both the activity and the native orientation of membrane proteins transferred were retained quite well even after transferred. Using this convenient technique, hence, a tumor surface antigen (TSA) from several tumor cells such as BALBRVD [27], B16 melanoma, and human lung cancer cell to D<sub>14</sub>DPC-containing liposomes was directly transferred for making a potent liposomal vaccine.

## REFERENCES

- [1] Sunamoto J, Sato T, Taguchi T, Hamazaki H (1992) Naturally Occurring Polysaccharide Derivatives Which Behave as an Artificial Cell Wall on Artificial Cell Liposomes. *Macromolecules* 25: 5665-5670
- [2] Akiyoshi K, Deguchi S, Moriguchi N, Yamaguchi S, Sunamoto J (1993) Self-aggregates of Hydrophobized Polysaccharides in Water. Formation and Characteristics of Nanoparticles. *Macromolecules* 26: 3062-3068
- [3] Takada M, Yuzuriha T, Katayama K, Iwamoto K, Sunamoto J (1984) Increased Lung Uptake of Liposomes Coated with Polysaccharides. *Biochem Biophys Acta* 802: 237-244
- [4] Sunamoto J, Iwamoto K (1986) Protein-Coated and Polysaccharide-Coated Liposomes as a Targetable Drug Carrier. *CRC Crit. Rev. Therapeutic Drug Carrier Systems* 2:117-136
- [5] Sunamoto J, Sato T (1989) Improved Drug Delivery Directed to Specific Tissue Using Polysaccharide-coated Liposomes. In: Tsuruta T, Nakajima A (eds) *Multiphase Biomedical Materials*. VSP, The Netherland, pp167-190
- [6] Sato T, Sunamoto J (1993) Site Specific Liposomes Coated with Polysaccharides. In: Gregoriadis G (ed) *Liposome Technology 2nd Edition Volume III*, CRC Press, Boca Raton FL, pp179-198
- [7] Sunamoto J, Sakai K, Sato T, Kondo H (1988) Molecular Recognition of Polysaccharide-coated Liposomes, Importance of Sialic Acid Moiety on Liposomal Surface. *Chem Lett* 1988:1781-1784
- [8] Akiyoshi K, Takanabe H, Sato T, Sato T, Kondo H, Sunamoto J (1990) Cell Specificity of Polysaccharide Derivatives on Liposomal Surface. *Chem Lett* 1990: 473-476
- [9] Yamamoto M, Iwata R, Kadohara T, Segawa T, Izawa K, Kadota T, Tuchiya R, Goto Y, Ohata N, Ishii N, Koji T, Moriguchi N, Sato T, Akiyoshi K, Sunamoto J (1991) Hepatoma Cell Targetability of Liposomes Coated with Polysaccharides Bearing Galactose Groups. *DDS Jpn* 6: 355-359

- [10] Sato T, Kojima K, Iida T, Sunamoto J, Ottenbrite RM (1986) Macrophage Activation by Poly(maleic acid-alt-2-cyclohexyl-1,3-dioxap-5-ene) as Encapsulated in Polysaccharide-coated Liposome. *J Bioactive and Compatible Polym* 1:448-460
- [11] Ottenbrite RM, Sunamoto J, Sato T, Kojima K, Sahara K, Hara K, Oka M (1988) Improvement of Immunopotentiator Activity of Polyanionic Polymers by Encapsulation into Polysaccharide-Coated Liposome. *J Bioactive and Compatible Polym* 3:184-190
- [12] Akashi M, Iwasaki H, Miyauchi N, Sato T, Sunamoto J, Takemoto K (1989) Potent Immunomodulating Activities of Polyvinyladenine and (Vinyladenine-alt-Maleic Acid) Copolymer. *J Bioactive and Compatible Polym* 4:124-136
- [13] Sunamoto J, Goto M, Iida T, Hara K, Saito A, Tomonaga A (1984) Unexpected Tissue Distribution of Liposomes Coated with Amylopectine Derivatives and Successful Use in the Treatment of Experimental Legionnaires' Diseases. In: Gregoriadis G, Poste G, Senior J, Trouet A (eds) *Receptor-Mediated Targeting of Drugs*, Plenum Publishing, New York, pp 359-372
- [14] Kohno S, Miyazaki T, Yamaguchi K, Tanaka H, Hayashi T, Hirota M, Saito A, Hara K, Sato T, Sunamoto J (1988) Polysaccharide-Coated Immunoliposomes Bearing Anti-CEA Fab' Fragment and Their Internalization by CEA-Producing Tumor Cells. *J Bioactive and Compatible Polym* 3:196-204
- [15] Ochi A, Shibata S, Mori K, Sato T, Sunamoto J (1990) Targeting Chemotherapy of Brain Tumor Using Liposome-Encapsulated Cisplatin— Part 2. Pullulan-Coated Liposomes to Target Brain Tumor. *DDS Jpn* 5: 261-265
- [16] Sunamoto J, Sato T, Hirota M, Fukushima K, Hiratani K, Hara K (1987) A Newly Developed Immunoliposome - An Egg Phosphatidylcholine Liposome Coated with Pullulan Bearing Both a Cholesterol Moiety and an IgMs Fragment. *Biochim Biophys Acta* 898: 323-330
- [17] Sato T, Sunamoto J, Ishii N, Koji T (1988) Polysaccharide-Coated Immunoliposomes Bearing Anti-CEA Fab' Fragment and Their Internalization by CEA-Producing Tumor Cells. *J Bioactive and Compatible Polym* 3: 196-204
- [18] Hirota M, Fukushima K, Hiratani K, Kadota J, Kawano K, Oka M, Tomonaga A, Hara K, Sato T, Sunamoto J (1989) Targeting Cancer Therapy in Mice by Use of Newly Developed Immunoliposomes Bearing Adriamycin. *J Liposome Res* 1:15-33
- [19] Carlsson A, Sato T, Sunamoto J (1989) Physicochemical Stabilization of Lipid Microspheres by Coating with Polysaccharide Derivatives. *Bull Chem Soc Jpn* 62:791-796
- [20] Iwamoto K, Kato T, Kawahara M, Koyama N, Watanabe S, Miyake Y, Sunamoto J (1991) Polysaccharide-Coated Oil-in-Water Emulsions as Targetable Carrier for Lipophilic Drugs. *J Pharm Soc* 80: 219-224
- [21] Fukui H, Akiyoshi K, Sato T, Sunamoto J, Yamaguchi S, Numata M (1993) Anticancer Activity of Polyunsaturated Fatty Acid Emulsion Stabilized by Hydrophobized Polysaccharide. *J Bioactive and Compatible Polym* 8:305-316
- [22] Akiyoshi K, Sunamoto J (1992) Physicochemical Characterization of Cholesterol-Bearing Polysaccharides in Solution. In: Friberg SE, Lindman B (eds) *Organized Solutions Surfactants in Science and Technology*. Marcel Dekker Inc, New York, pp 290-304
- [23] Akiyoshi K, Nagai K, Nishikawa T, Sunamoto J (1992) Self-aggregates of Hydrophobized Polysaccharide as a Host for Macromolecular Guests. *Chem Lett* 1992: 1727-1730
- [24] Nishikawa T, Akiyoshi K, Sunamoto J (1994) Supramolecular Assembly between Nanoparticles of Hydrophobized Polysaccharide and Soluble Protein. Complexation between the Self-Aggregate of Cholesterol-Bearing Pullulan and  $\alpha$ -Chymotrypsin. *Macromolecules* 27: 7654-7659
- [25] Okumura Y, Yamauchi M, Yamamoto M, Sunamoto J (1993) Interaction of a Fusogenic Liposome with HeLa Cell. *Proc Japan Acad* 69 (B):45-50
- [26] Sato T, Sunamoto J (1992) Recent Aspects in the use of Liposomes in Biotechnology and Medicine. In: Holman RT, Sprecher H, Harwood JL (eds) *Progress in Lipid Research*. Pergamon Press, Oxford, 31: 345-372
- [27] Noguchi Y, Noguchi T, Sato T, Yokoo Y, Itoh S, Yoshida M, Yoshiki T, Akiyoshi K, Sunamoto J, Nakayama E, Shiku H (1991) Priming for *In vitro* and *In vivo* Anti HTLV-1 Cellular Immunity by Virus Related Protein Reconstituted into Liposome. *J Immunol* 148:3599-3603

## Biodegradable Polyphosphazenes for Biomedical Applications

E. Schacht, J. Vandorpe and J. Crommen and L. Seymour\*

Biomaterial & Polymer Research Group, University of Ghent,  
Krijgslaan 281, B-9000 Ghent, Belgium

\*) Cancer Research Campaign Laboratory, Clinical Oncology, Queen Elizabeth Hospital,  
University of Birmingham, Birmingham B15 2TH (U.K.)

### SUMMARY

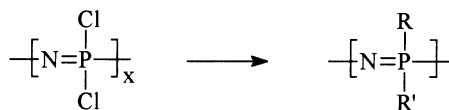
A series of biodegradable polyphosphazenes with amino acid ester side groups were prepared starting from the poly(dichlorophosphazene). It was demonstrated that the rate of hydrolytic degradation can be varied by introduction of small amounts of depsipeptide side groups. Some selected polyphosphazenes were used to prepare implant devices containing mitomycin C (MMC). In vitro release studies demonstrated that the release rate can be controlled by the amino acid side group composition. Initial in vivo data indicates that i.p. implanted devices show promise for the treatment of tumour bearing animals.

### KEYWORDS

Polyphosphazenes, biodegradation, mitomycin C.

### INTRODUCTION

Biodegradable polymers show great promise in the design of drug delivery systems. The specifications for the candidate polymer, i.e. their in vivo degradation rate, are conditional on the specific therapeutic application. Hence, there is a need for a variety of polymers with a variable range of degradabilities. A family of polymers where a large variability in properties is feasible are the polyphosphazenes. These are polymers with an inorganic backbone consisting of alternating nitrogen and phosphorous atoms linked by alternating single and double bonds. Starting from poly(dichloro phosphazene) a broad range of polymers with variable properties can be prepared by nucleophilic displacement reactions [1-4] :



It was reported before by Allcock and co-workers, who extensively explored the field of polyphosphazene synthesis, that amino-substituted polyphosphazenes (e.g. R-R' = ethyl esters of amino acids) are susceptible towards hydrolytic degradation [5-7] and hold promise as biodegradable materials.

Searching for biodegradable polymers with an adjustable rate of degradation we prepared a series of polyphosphazenes substituted with different amino acid ethyl esters and variable amounts (0-10%) of a depsipeptide [8,9]. The latter are hydrolysis sensitive and generate pendant carboxyl groups that can promote the backbone degradation [10]. Biodegradable polymers are of interest

for the preparation of implantable drug delivery systems. One application is the use of cytostatic containing matrices that can be implanted following surgical resection of primary carcinoma's [11].

A number of the polymer derivatives were selected for the preparation of small tablets containing the cytostatic agent mitomycin C. The effect of polymer composition on the drug release was evaluated in vitro. Finally, MMC-containing tablets were tested in vivo using tumour bearing mice.

## RESULTS AND DISCUSSION

Polyphosphazenes containing ethyl glycinate (GlyOEt) and a small number of depsipeptide side groups ethyl 2-[O-(glycyl)lactate] (gly-lacOEt) were prepared as described before [8]. Pellets, prepared by heat compression, were incubated in phosphate buffer pH 7.4 at 37°C. Mass loss with incubation time was determined. The results shown in Fig. 1 clearly demonstrate the remarkable effect of the depsipeptide side groups on the polymer degradation.

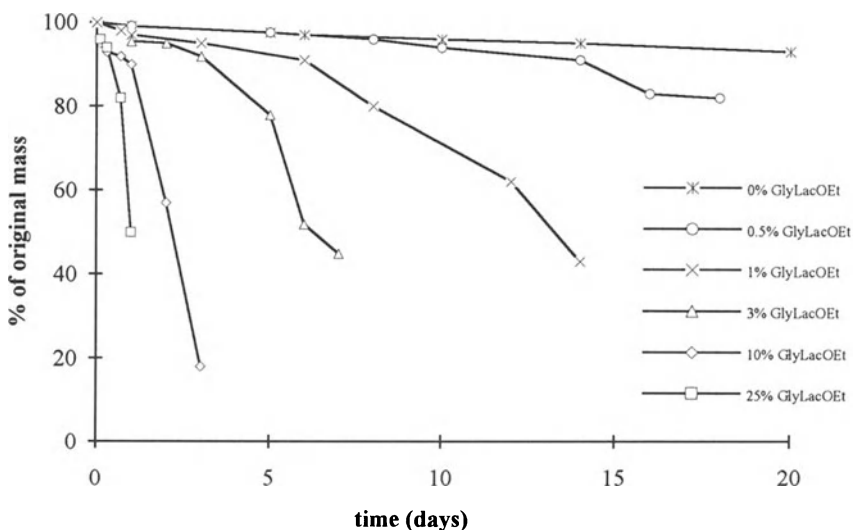


**Fig. 1** : percent mass loss of poly[(ethyl-2-(O-glycyl lactate ester)-co-(ethyl glycinate)phosphazenes] in PBS at 37°C.

Where as poly[bis(ethyl glycinate)phosphazene] degrades slowly over a period of several months, the introduction of 1% of Gly-lacOEt side groups results in a desintegration of the pellet after about 2 weeks. It was further observed that the introduction of the depsipeptides results in an increased hydrophilicity of the polymer matrix.

Polymers with different mechanical properties and hyrophilic/lipophilic balance can be prepared by proper selection of the amino acid ester side groups [8].

Polyphosphazenes containing ethyl phenylalanate (Phe) and/or ethyl glycinate (Gly) side groups were selected for the preparation of MMC containing tablets.

The composition of the selected polymers is summarized in Table 1.

**Table 1** : Composition of selected amino acid substituted polyphosphazenes  
 $[-N=P-(NHR_1)(NHR_2)-]$

Code	$R_1 = H_2N-CH_2COOEt$	$R_2 = H_2N-CH-COOEt$ $CH_2\emptyset$
Gly100	100	0
Phe25	75	25
Phe35	65	35
Phe50	50	50
Phe70	30	70

Tablets (5 mm x 2 mm, 60 mg) containing 0.3 mg, 1.6 mg or 3 mg MMC were prepared by heat compression of the drug with one of the selected copolymers or a blend of two polymers. The release characteristics were examined in vitro. The results of release experiments performed in PBS at 37°C are shown in Figs. 2 and 3.

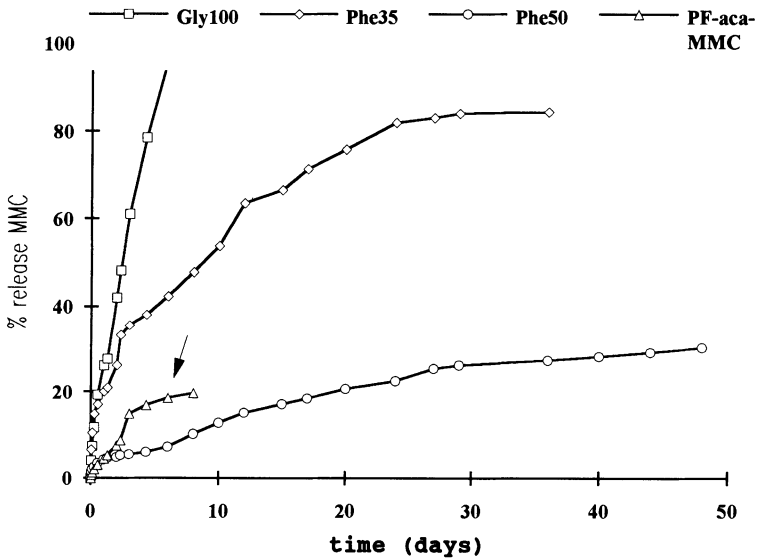


**Fig. 2** : In vitro release of MMC from polyphosphazene matrices prepared from polymers having different amino acid ester side groups.

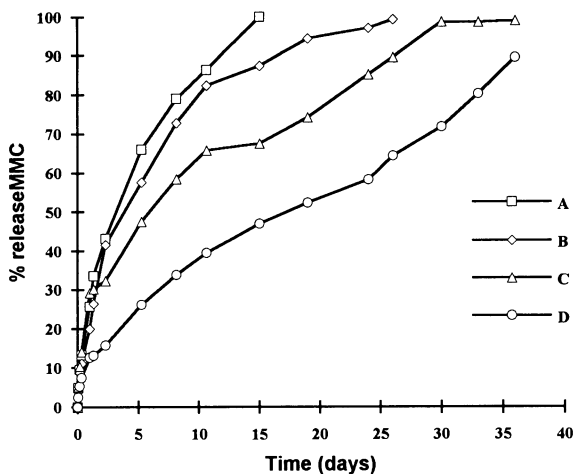


**Fig. 3 :** In vitro release of MMC from matrices prepared by blending polyphosphazenes with different side group composition (Phe25, Phe70).  
Percent Phe25 in blend : A = 100%, B = 60%, C = 40%, D = 0%.

From this data it can be seen that the rate of release depends on the polymer composition.

In one particular case (Fig. 2) MMC was substituted on its aziridine nitrogen with  $\epsilon$ -amino caproic acid and the prodrug was then coupled with poly(dichlorophosphazene). Remaining P-Cl groups were substituted with ethyl glycinate.

Release studies demonstrated a rapid desintegration of the tablets. This is most likely due to hydrolysis of the MMC resulting in pendant carboxyl groups that catalyse backbone degradation.

Tablets containing 0.3 mg, 1.6 mg or 3 mg of MMC in polyphosphazenes Gly100, Phe35 and Phe50 were implanted in the peritoneal cavity of mice bearing i.p. inoculated C26 murine colorectal cells. A preliminary study indicated that all implants containing 0.3 mg MMC were ineffective. Implants containing 3 MMC caused severe toxicity. Polyphosphazene matrices containing 1.6 MMC gave promising results.

**Table 2 :** Effect of MMC-containing matrices\* on the survival of mice bearing C26 colorectal cells.

Treatment	median survival (days)	T/C (%)
none	15.4	100
Gly100	4.0	26
Phe35	55.0	357
Phe50	22.6	146

\*Tablet of 60 mg containing 1.6 mg MMC.

As shown in table 2, the implant based on the polymer Phe35 resulted in a substantial increase of the median survival time. These matrices are at present evaluated in more detail.

## REFERENCES

1. H.R. Allcock, *Chem. Rev.* 72, 315 (1972).
2. H.R. Allcock, *Contemporary Topics, Polymer Sci.* 3, 55 (1979).
3. H.R. Allcock, *Makromol. Chem., Macromol. Symp.* 6, 101 (1986).
4. J.H. Goedemoed, J.H. Crommen and E.H. Schacht, in: *Polyphosphazene drug delivery systems for antitumor treatment*, ed. J.H. Goedemoed, V.U. University press, Amsterdam, Chapter I, (1990).
5. H.R. Allcock, T.J. Fuller, D.P. Mack, K. Matsumura and K.M. Smeltz, *Macromolecules* 10, 824 (1977).
6. H.R. Allcock, T.J. Fuller and K. Matsumura, *Inorg. Chem.* 21, 515 (1982).
7. H.R. Allcock, A.G. Scopelianis, *Macromolecules* 16, 715 (1983).
8. H.J. Crommen, J. Vandorpe and E.H. Schacht, *J. Controlled Release* 24, 167-180 (1993).
9. H.J. Crommen, E.H. Schacht and E.H. Mense, *Biomaterials* 13(8), 511 (1992).
10. H.J. Crommen, E.H. Schacht and E.H. Mense, *Biomaterials* 13(8), 601 (1992).
11. L.W. Seymour, R. Duncan, J. Duffy, S.Y. Ng and J. Heller, *J. Controlled Release* 31, 201-206 (1994).

# RECEPTOR-MEDIATED CELL SPECIFIC DELIVERY OF DRUGS TO THE LIVER AND KIDNEY

Mitsuru Hashida, Makiya Nishikawa, and Yoshinobu Takakura

Department of Drug Delivery Research, Faculty of Pharmaceutical Sciences, Kyoto University, Sakyo-ku, Kyoto 606-01, Japan

## SUMMARY

Effectiveness of several approaches aiming at hepatic and renal targeting of drugs and proteins is compared from various aspects. Receptor-mediated endocytosis of macromolecules with sugar moieties, scavenger receptor-mediated endocytosis of polyanions, and general electrostatic interaction of polycations with cell surfaces are characterized through pharmacokinetic analysis at a whole body level in order to evaluate their potentials in drug targeting. Based on the obtained results, superoxide dismutase (SOD) was derivatized to various forms and mannosylated SOD and cationized SOD showed inhibitory effect against injury induced by ischemia/reperfusion in the liver and kidney, respectively. Molecular design of a carrier system with galactose residue was further discussed and it was concluded that the cellular uptake rate of macromolecules was controlled by the density of galactose on the molecular surface. The maximal affinity was given at surface density of higher than  $1.0 \times 10^{-3}$  molecules/Å<sup>2</sup> in the case of globular proteins. However, higher extent of modification is required in the case of vitamin K<sub>3</sub> conjugate utilizing poly L-glutamic acid (PLGA) as a carrier backbone.

**KEY WORDS:** receptor-mediated endocytosis, superoxide dismutase, galactose receptor, targeting, molecular design

## INTRODUCTION

Chemical modification of drugs especially with macromolecular carriers would offer a promising way to optimize their delivery since diverse physicochemical and biological characteristics can be introduced to them through it [1]. In our series of investigation, systemic disposition characteristics of macromolecular drug carriers were explored in relation to their physicochemical and biological functions with the clearance concept-based pharmacokinetic analysis and a strategy for rational design of a targeting system was constructed as shown in Fig. 1 [2]. It was concluded that macromolecules with molecular weights larger than 70,000 and weak anionic nature would result in superior accumulation in the target site due to its large area under the plasma concentration-time curves (AUC). This approach had been successfully applied to the design of macromolecular prodrugs of anticancer agents aiming at passive and monoclonal antibody-mediated tumor targeting [3]. However, absolute targeted amounts of drug were still limited due to restriction in extravasation and interstitial diffusion of macromolecules as well as insufficiency in uptake capacity of the target cells. In contrast to solid tumors, the liver has some advantages for specific targeting



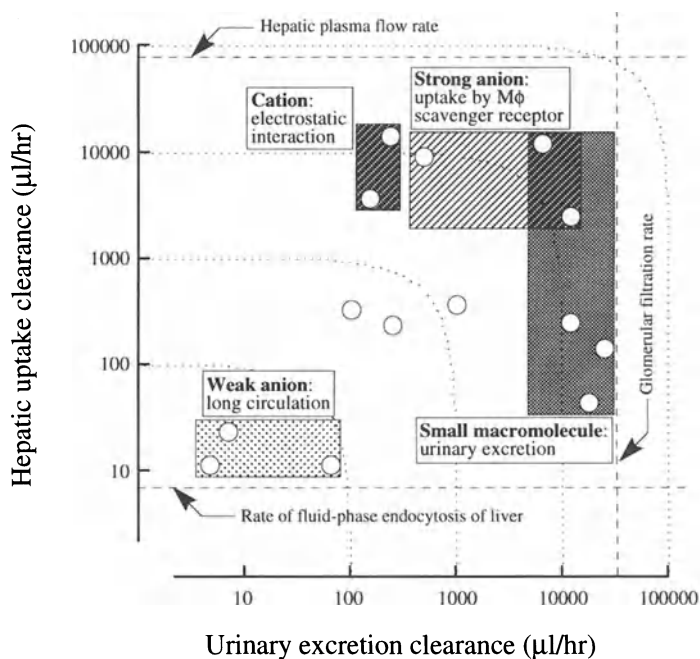


Fig. 1 Effect of physicochemical properties of macromolecules on their in vivo disposition

such as the discontinuous sinusoidal wall which enables macromolecules to gain free access to parenchymal cells and high and ligand-specific endocytic activity of parenchymal and non-parenchymal cells [4]. In the same way, the kidney would also be a good candidate for drug targeting [5].

In this presentation, various approaches which aim at hepatic and renal targeting will be compared by the pharmacokinetic analysis at the organ and the whole body levels. Discussion will be focused on the efficacy of a carbohydrate recognition mechanism in hepatic targeting of drugs and proteins and effect of modification extent is further examined for approaching to a rational design of a targeting system.

## MATERIALS AND METHODS

By way of targeting mechanisms to the liver, four types of biological interactions such as asialoglycoprotein receptor-mediated endocytosis by hepatocyte, mannose receptor-mediated endocytosis by nonparenchymal cells, scavenger receptor-mediated endocytosis of polyanions by nonparenchymal cells, and universal electrostatic interaction of polycations were adopted in our study. Bovine serum albumin (BSA; M.W.=67,000) was used as a model protein, and coupling of monosaccharides was carried out according to the method of Lee et al [6]. Two types of BSA conjugates with 1-thiogalactoside (Gal-BSA) and 1-thiomannoside (Man-BSA) were synthesized. Cationized BSA (Cat-BSA) was synthesized by coupling 1,6-hexamethylenediamine to the carboxyl groups of BSA by using 1-ethyl(3-dimethylaminopropyl)carbodiimide hydrochloride. Succinylated

BSA (Suc-BSA) was also synthesized by reacting with succinic anhydride and about 40 amino groups were modified per one BSA molecule. Similar approach was carried for recombinant human SOD (M.W.=32,000) including conjugation with polyethylene glycol (PEG), carboxymethyl dextran (CMD), and diethylaminoethyl dextran (DEAED). All SOD derivatives were confirmed to keep more than 50 % of original enzymatic activity of SOD. Gal-BSA and Gal-SOD with different modification extents, and galactosylated derivatives of immunoglobulin G (IgG; M.W.= 150,000) soybean trypsin inhibitor (STI; M.W.=20,000), and lysozyme (LZM; M.W.=14,000) were also tested. All protein derivatives were radiolabeled with  $^{111}\text{In}$  using diethylenetriaminepentaacetic acid anhydride. The galactosylated conjugate of vitamin K<sub>5</sub> was synthesized employing PLGA (M.W.=25,000) as a carrier backbone.

In vivo disposition profiles of these compounds were evaluated in mice and the obtained results were quantified by clearance concept-based pharmacokinetic analysis. Hepatic targeting efficacy of galactosylated derivatives with different modification extents was analyzed based on a physiological pharmacokinetic model including an uptake process with Michaelis-Menten kinetics and hepatic blood flow shown in Fig. 2. The targeting potentials were further studied in the isolated rat liver perfusion experiment. Isolated kidney perfusion experiment was also carried out and renal disposition characteristics of macromolecules were analyzed by separating into three processes, i.e., glomerular filtration, tubular reabsorption, and peritubular tissue uptake.

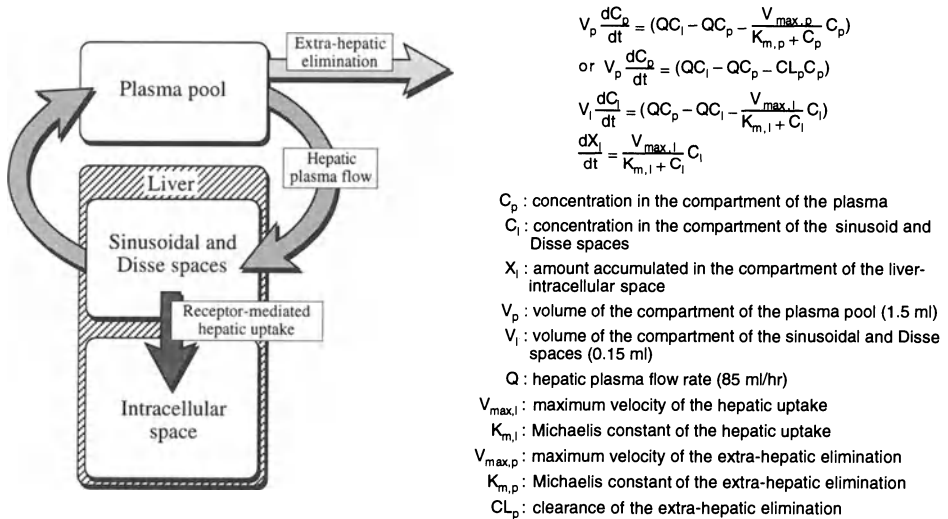


Fig. 2 Physiological pharmacokinetic model for analyzing the disposition of galactosylated proteins

## RESULTS AND DISCUSSION

### Cell-specific delivery of proteins by chemical modification

In mice, the hepatic uptake clearance of Gal-BSA achieved at 83.4 ml/hr at a dose of 0.1 mg/kg

which was approximately equal to the hepatic plasma flow, suggesting that Gal-BSA was almost completely taken up by the liver parenchymal cells during a single passage of the liver via receptor-mediated endocytosis. On the other hand, Man-BSA and Suc-BSA were accumulated preferentially in nonparenchymal cells. Unlike them, Cat-BSA showed non-specific distribution between these cell types simply depending on their effective surface area.

### Disposition and therapeutic characteristics of SOD derivatives

Among SOD derivatives which can be classified as 1) long circulating type (SOD-PEG, SOD-CMD); 2) cell-surface targeting type (Cat-SOD, SOD-DEAED); 3) intracellular targeting type for hepatocyte (Gal-SOD) and 4) resident macrophages and endothelial cells (Man-SOD) via carbohydrate-recognition mechanism; and 5) cellular targeting type via scavenger receptor (Suc-BSA), Man-SOD showed superior effect against hepatic ischemia/reperfusion injury. Protein derivatives also showed specific delivery patterns in the perfused kidney. In the kidney, Cat-SOD as well as SOD-PEG showed inhibitory effect against renal injury due to ischemia/reperfusion treatment.

### Molecular design of a carrier system with galactose as a homing device

Relationship between extent of modification with galactose residues and hepatic uptake clearances of proteins was studied at various doses as shown in Fig. 3. In this figure, the apparent values of hepatic uptake clearances are compared in relation to surface density of galactose residues and total numbers of galactose per one molecule. The effect of extent of galactose modification on affinity to hepatocyte was further elucidated in terms of Michaelis constant of the hepatic uptake ( $K_{m,1}$ ) and maximum velocity of uptake ( $V_{max,1}$ ) estimated by pharmacokinetic analysis with a physiological model (Fig. 2). It was concluded that the ligand-recognition by the receptor is controlled by the density of galactose on the protein surface and maximum affinity can be achieved at a density higher than  $1.0 \times 10^{-3}$  molecules/ $\text{\AA}^2$ .

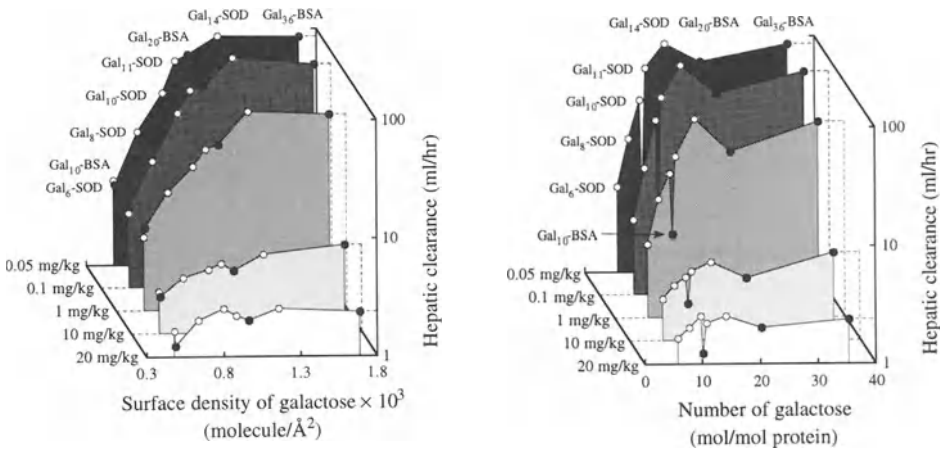


Fig. 3 Relationship between hepatic uptake clearances and the surface density of galactose residues (left) and the number of galactose residues (right) on Gal-BSA and Gal-SOD

### Preparation and pharmacological effect of vitamin K<sub>5</sub>-galactosylated PLGA conjugate

The conjugate of vitamin K<sub>5</sub> with galactosylated PLGA, a biodegradable backbone, shown in Fig. 4 exhibited remarkable accumulation in the hepatocytes as well as anti-hemorrhagic effect in mice having the warfarin pretreatment. However, the highest affinity was observed in the conjugate with 18-20 galactose molecules which is higher than the case of globular proteins, suggesting the effect of molecular shape of carrier backbone.

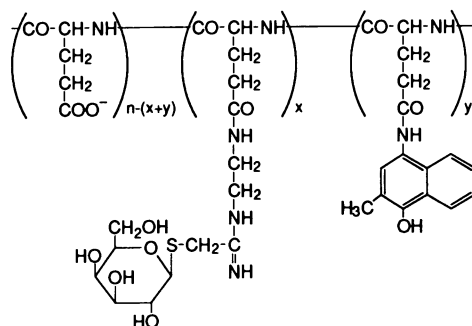


Fig. 4 Chemical structure of vitamin K<sub>5</sub>-galactosylated PLGA conjugate

### REFERENCES

1. Takakura Y and Hashida M. (1995) Macromolecular drug carrier systems in cancer chemotherapy: macromolecular prodrugs. *Crit. Rev. Oncol/Hepatol.* 18: 207-231.
2. Hashida M and Takakura Y. (1994) Pharmacokinetics in design of polymeric drug delivery systems. *J. Controlled Release* 31: 163-171.
3. Noguchi A, Takahashi T, Yamaguchi T, Kitamura K, Takakura Y, Hashida M, and Sezaki H. (1992) Preparation and properties of immunoconjugate composed of anti-human colon cancer monoclonal antibody and mitomycin C-dextran conjugate. *Bioconjugate Chem.* 3: 132-137.
4. Hashida M, Nishikawa M, and Takakura Y. (1995) Hepatic targeting of drugs and proteins by chemical modification. *J. Controlled Release*, in press.
5. Takakura Y, Mihara K, and Hashida M. (1994). Control of the disposition profiles of proteins in the kidney via chemical modification. *J. Controlled Release* 28: 111-119.
6. Lee Y, Stowell C, and Kranz M. (1976) 2-Imino-2-methoxyethyl 1-thioglycoside: new reagents for attaching sugars to proteins. *Biochemistry* 15: 3956-3963.

# BIORECOGNIZABLE BIOMEDICAL POLYMERS

Jindřich Kopeček, Pavla Kopečková, and Vladimir Omelyanenko

*Departments of Pharmaceutics and Pharmaceutical Chemistry/CCCD, and of Bioengineering, University of Utah, Salt Lake City, Utah 84112, U.S.A.*

**ABSTRACT** The design of biorecognizable biomedical polymers has to be based on a sound biological rationale. Using this rationale, the principles of the design, synthesis, and characterization of biorecognizable polymers are demonstrated on several examples including: targetable water-soluble carriers of bioactive compounds, the relationship between the supramolecular structure of polymer conjugates and their biorecognition, poly(ethylene glycol) conjugates, bioadhesive polymers for colon-specific drug delivery, and biodegradable hydrogels.

**KEY WORDS** Biorecognition of polymers; targetable polymeric prodrugs; supramolecular structure of polymers in solution; PEO - chymotrypsin conjugates; PEO - dextran conjugates; photocrosslinking of proteins; biodegradable hydrogels; oral delivery of proteins.

## INTRODUCTION

The synthesis, analysis, and characterization of biorecognizable polymers offers a great challenge. Energetically favorable interactions of polymer conjugates with recognition systems developed during evolution call for a high level of complementarity of the receptor and ligand structures. The characterization of the structure-property relationship of biorecognizable polymers requires an interdisciplinary approach. In addition to a detailed analysis of polymer structure, and characterization of their properties by physicochemical methods, a repertoire of sophisticated biological assays must be used to evaluate biological properties of the polymer conjugates. It is important to choose biological characterization methods which permit the correlation to be made between the chemical and supramolecular structures of the conjugates and their biological response. The principles of this approach to polymer design, synthesis, and characterization will be demonstrated on several examples described below.

## TARGETABLE WATER-SOLUBLE CARRIERS OF BIOACTIVE COMPOUNDS

These systems have to be biorecognizable on two levels [1]. First, on the cellular level at the plasma membrane to be internalized by a subset of cells by receptor-mediated pinocytosis. Second, they have to be recognized intracellularly in the lysosomal compartment on a molecular level by lysosomal enzymes to release the bioactive moiety. The design of such biorecognizable macromolecules was based on the behavior of natural systems. The differences in biorecognition of glycoproteins vs. asialoglycoproteins were a basis for the synthesis of N-(2-hydroxypropyl)methacrylamide (HPMA) copolymers, containing N-acylated galactosamine as the biorecognizable moiety. The detailed physicochemical characterization of these hybrid macromolecules is very important to avoid artifacts in the characterization of their biological properties. The binding, cell surface biorecognition, uptake and subcellular trafficking of HPMA copolymer conjugates with Hep G2 hepatocarcinoma cells has been characterized by confocal fluorescence microscopy. The intrinsic fluorescence of adriamycin, or the labeling of the macromolecules with fluorescein were used as tools for the detection of intracellular concentration levels [2]. The essential feature of confocal imaging of fluorescent specimens is that light from out-of-focus regions is eliminated from the detection system. Electronic processing of the stored images provides an accurate measure of fluorescence intensity and its 2-dimensional distribution. A three dimensional image representing the distribution of the fluorophore throughout the cells may be recreated from a series of two dimensional images [3]. The results

obtained permitted a detailed characterization of the biorecognition at the plasma membrane, cellular uptake, and subcellular trafficking of the polymers studied. Independent verification of the lysosomal localization of the polymer conjugates was obtained by the detection of the emission spectra of an intracellularly localized fluorescein label. The intracellular biorecognition of oligopeptide side-chains in HPMA copolymers by enzymes was studied with the aim to answer the following questions: a) what is the steric hindrance of the macromolecular backbone on the formation of the enzyme-substrate complex; b) is it possible to predict the structure of biorecognizable substrates from the data on the crystal structure of enzyme-inhibitor complexes? The determination of the kinetics of substrate cleavage permitted the quantitative characterization of biorecognition.

The lysosomal cleavage of adriamycin from a biorecognizable HPMA copolymer - adriamycin conjugate can be demonstrated microscopically. Two HPMA copolymer conjugates were incubated with Hep G2 cells. One contained tetrapeptide side-chains (Gly-Phe-Leu-Gly) degradable by lysosomal enzymes, the other a Gly-Gly sequence which is not susceptible to lysosomal cleavage [4]. After incubation with the HPMA copolymer - galactosamine - glycyglycyldriamycin conjugate the adriamycin fluorescence was visualized predominantly in the lysosomal compartment [2]. On the contrary, when Hep G2 cells were incubated with the HPMA copolymer - galactosamine - glycyphenylalanylleucylglycyldriamycin conjugate, fluorescence in the nuclear structures was observed (Fig. 1). Therefore, this technique permits the detection of the transport of the drug, released from the polymer carrier in the lysosomal compartment, across the lysosomal membrane, via the cytosol into the cell nucleus.

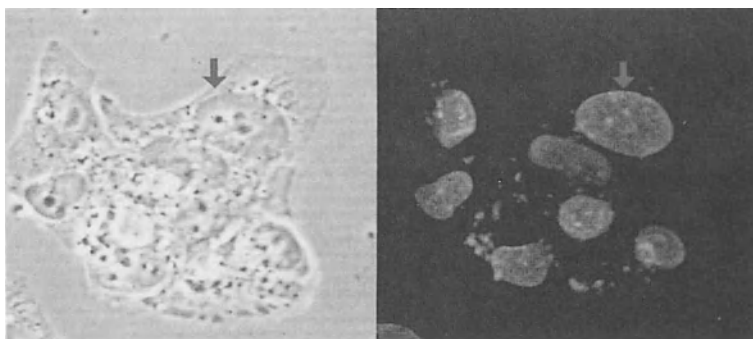


Fig. 1. Internalization of HPMA copolymer - galactosamine - glycyphenylalanylleucylglycyldriamycin conjugate by human hepatocarcinoma cells Hep G2.

The Hep G2 cell line (ATCC) was cultured in MEM medium supplemented with 10% fetal bovine serum at 37 °C in 5% CO<sub>2</sub> atmosphere. Cells were grown on a coverslip for 48 h. Before incubation with polymer conjugates they were rinsed by PBS, transferred into MEM medium without serum and incubated at 37 °C in 5% CO<sub>2</sub> for 1 h to permit the turnover of the asialoglycoprotein receptors, and the release of bound serum proteins. Polymer conjugates (100 µg/mL) were added to the medium and incubated for 20 h. After incubation, the cells were washed 4 x with PBS, fixed for 20 min with freshly prepared paraformaldehyde at room temperature, and rinsed with PBS. The inverted coverslip was mounted on a glass slide in PBS, pH 7.0, 50 mM NaN<sub>3</sub>, 90% glycerol. A Bio-Rad MRC 600 laser scanning confocal imaging system attached to a Zeiss Axioplan microscope with a x 63 objective was used. Excitation was achieved with a krypton/argon laser using the 488 nm line (BHS block filters).

Ovarian cancer has the highest mortality of any gynecological malignancy. Biorecognizable polymeric conjugates have a potential for the intraperitoneal treatment of ovarian cancer. Binding of drugs to macromolecular carriers should result in the decrease of their peritoneal permeability and permit sustained exposure of tumor cells to high concentrations of cytotoxic agents with, presumably, lower nonspecific toxicity when compared to free drugs. Monoclonal antibodies OV-TL 16 possess a high specificity against an antigen expressed on OVCAR-3 ovarian carcinoma cell line as well as on human ovarian tumors of different types. The potential of the OV-TL 16 antibody as a targeting

moiety of HPMA copolymer - cytotoxic drug (adriamycin or chlorin e<sub>6</sub>) conjugates was evaluated [5]. Various methods of binding the OV-TL 16 and its Fab fragments to HPMA copolymer-drug conjugates were studied. The affinity constant ( $K_a$ , M<sup>-1</sup>) of the wild OV-TL 16 antibody was  $4 \times 10^{-8}$ ; by covalent binding to the HPMA copolymer - drug conjugate the affinity constant decreased. In accordance with previous data [6], the decrease in the affinity constant was related to the chemistry of binding. A smaller decrease was observed when the antibody was bound to oxidized carbohydrate moieties near the hinge region when compared with binding via  $\epsilon$ -amino groups of lysine residues. The binding, biorecognition at the cellular surface, the uptake and subcellular trafficking of HPMA copolymer conjugates has been characterized by confocal fluorescence microscopy. Solution properties of polymer drug conjugates were assessed by fluorescence quenching. The affinity of the HPMA copolymer - drug - Ab conjugates to the OVCAR-3 cell line, their uptake and intracellular localization were determined [5].

## SUPRAMOLECULAR STRUCTURE OF POLYMER CONJUGATES

An important factor influencing the biorecognition of polymer conjugates are their solution properties. HPMA copolymers containing side-chains terminated in hydrophobic anticancer drugs may form aggregates by random association of macromolecules by point-like contacts. Formation of aggregates was characterized by quasielastic light scattering and the concomitant changes in biorecognition by physicochemical and biological methods. The results obtained by quasielastic light scattering correlated well with the enzymatic biorecognition of HPMA copolymers containing side chains terminated in a leaving group [7], as well as with the changes in the quantum yield of singlet oxygen formation [8] and fluorescence quenching [5] of copolymers containing covalently bound photosensitizers at the side-chain termini.

## SOLUBLE POLYMERS AS A TOOL IN ANALYZING BIOLOGICAL PROCESSES

Photodynamic therapy of tumors involves the delivery of a photosensitizing drug to the diseased tissue followed by illumination with light of a wavelength appropriate for absorption by the sensitizer. It is most widely believed that the generation of singlet oxygen is ultimately responsible for the phototoxic effects resulting in cell destruction, although other reactions, such as the formation of radicals may be involved [9]. Singlet oxygen generated by the illuminated photosensitizers may lead to the formation of crosslinks between protein molecules [10]. One suggested mechanism involves the photosensitized oxidation of histidine residues in one protein molecule followed by a nonphotochemical coupling with an amino group of another protein molecule to form covalent crosslinks. The mechanism of these reactions was evaluated on tailor-made synthetic model macromolecules. HPMA copolymers containing  $\epsilon$ -aminocaproic side-chains terminating in histidine or lysine were used to model the photosensitized crosslinking reactions of proteins. The amount of intermolecular crosslinking (the reaction did not reach the gel point) was calculated from the changes in molecular weight distribution upon illumination using the kinetic theory of rubber elasticity. The results obtained correlated well with photocrosslinking of a model protein, ribonuclease A [11].

## POLY(ETHYLENE GLYCOL) CONJUGATES

Covalent modification of proteins with semitelechelic hydrophilic polymers alters their biorecognition. The characterization of the degree of substitution, site of substitution, and conformational changes are extremely important in the determination of the structure-properties relationship. Conjugates of PEG with chymotrypsin were characterized by their ability to degrade low and high molecular weight substrates. The results obtained indicated that substrate-size-dependent specificity of PEG-modified enzymes cannot be explained solely by steric hindrance considerations. The decreased activity of PEG-modified enzymes toward protein substrates is consistent with the well documented ability of PEG to exclude proteins from its surroundings and with the influence of protein unfolding on the susceptibility to degradation [12].

Another example of PEG protein repulsion activity is the study of dextran and PEG modified dextran degradation [13]. PEG of molecular weight 2,000 as well as 5,100 were conjugated to dextran (T-40) yielding three different degrees of substitution. The biodegradation of six PEG-dextran

conjugates was evaluated, using dextranase, isolated rat cecum cell free extracts (CFE), and rat liver lysosomal enzymes. All the substrates were degraded by dextranase; however, the rate of the degradation decreased with an increase in the degree of modification as well as in the molecular weight of PEG. When incubated with CFE, these conjugates were degraded with reduced rates, but a similar trend was observed, indicating the presence of an endoacting dextranase in the rat cecum contents. The modified dextrans, however, resisted degradation by lysosomal enzymes *in vitro* during 36 h incubation at 37 °C. The results, as compared to those published on the modification of dextrans with low molecular weight reagents, demonstrated the PEGs' unique effects on the interaction of modified substrates with proteins. It appears that PEG conjugation reduced the enzymatic degradability of dextran conjugates not only due to the modification of dextran structure and the sterical hindrance to the formation of the enzyme-substrate complex, but also by the participation of PEG chains in the repulsion of enzyme molecules.

However, other hydrophilic polymers also possess protein repulsion properties. Recently, we have shown that the modification of polystyrene nanospheres with semitelechelic polyHPMA prevents their biorecognition by the reticuloendothelial system in mice [14].

### **BIOADHESIVE HPMA COPOLYMERS FOR COLON-SPECIFIC DRUG DELIVERY**

Water soluble HPMA copolymers were designed as bioadhesive colon-specific drug carriers [15]. Their design was based on the concept of site-specific binding of carbohydrate moieties complementary to colonic mucosal lectins [16] and on the concept of site-specific drug (5-aminosalicylic acid) release by the microbial azoreductase activity present in the colon [17]. A monomer containing 5-aminosalicylic acid was incorporated into the copolymer together with the fucosylamine (bioadhesive moiety) containing comonomer by radical copolymerization. The *in vitro* release rate of 5-ASA from HPMA copolymers by azoreductase activity in guinea pig cecum was approx. 2.5 times lower than from a low molecular weight analog. The azoreductase activities in cecum contents of guinea pig, rat, and rabbit as well as in human feces were determined [18]. The ratio of relative activities for rat : guinea pig : human : rabbit was 100 : 65 : 50 : 28. Both *in vitro* and *in vivo* HPMA copolymers containing side-chains terminated in fucosylamine showed a higher adherence to guinea pig colon when compared to HPMA copolymer without fucosylamine moieties. The incorporation of 5-ASA containing aromatic side-chains into HPMA copolymers further increased their adherence probably by combination of nonspecific hydrophobic binding with specific recognition [18].

### **RELATIONSHIP BETWEEN THE DETAILED STRUCTURE OF HYDROGELS AND THEIR BIODEGRADABILITY**

Novel hydrogels based on N,N-dimethylacrylamide copolymers which are pH-dependent and contain biodegradable azaromatic crosslinks are studied to achieve colon-specific peptide and protein delivery [15]. In the low pH of the stomach, the degree of swelling of gels is low and the drugs can be protected from digestion. As the gel passes down the GI tract, the swelling slowly increases due to the increased pH, however no drug is released in the small intestine. In the colon, the swelling reaches an extent that crosslinks become accessible to microbial azoreductase activities and mediators. The gel is then degraded and the drug is released from the gel.

To evaluate the influence of the detailed hydrogel structure on the rate of degradation, these hydrogels were synthesized by three synthetic methods: crosslinking copolymerization [19], crosslinking of polymeric precursors [20], and by a polymer - polymer reaction [21]. The detailed structure of the networks, i.e., content of crosslinks, unreacted pendent groups, and intramolecular cycles was determined. It was shown that the biodegradation of the hydrogels by gastrointestinal enzymes depends on their detailed structure. These structural changes may influence not only the rate of degradation, but can cause a change of degradation mechanism from bulk degradation to surface erosion [20].

The support of the NIH (CA 51578, DK 39544, GM 08393, GM 50839), Amgen, SmithKline Beecham, Hisamitsu, and Macromed is greatly acknowledged. This work would not have been possible without the contributions and support of our coworkers. Their names are mentioned in the references.



## References

- Putnam D, Kopeček J (1995) Polymer conjugates with anticancer activity. *Adv Polym Sci* 122: 55-123
- Omelyanenko V, Kopečková P, Rathi RC, Kopeček J, to be published
- Smith PJ, Sykes HR, Fox ME, Furlong IJ (1992) Subcellular distribution of the anticancer drug mitoxantrone in human and drug resistant murine cells analyzed by flow cytometry and confocal microscopy and its relationship to the induction of DNA damage. *Cancer Res* 52: 4000-4008
- Rejmanová P, Pohl J, Baudyš M, Kostka V, Kopeček J (1983) Polymers containing enzymatically degradable bonds. 8. Degradation of oligopeptide sequences in N-(2-hydroxypropyl)methacrylamide copolymers by bovine spleen cathepsin B. *Makromol Chem* 184: 2009-2020
- Omelyanenko V, Kopečková P, Shiah JG, Gentry C, Tully C, Poels L, Kopeček J (1995) Biorecognition of HPMA copolymer - drug - (OV-TL 16) antibody conjugates by OVCAR-3 ovarian carcinoma cell line. *Proc 22nd Int Symp Controlled Rel Bioact Mater*, Seattle, Washington, July 30 - August 2, Proceedings
- Krinick NL, Říhová B, Ulbrich K, Strohmalm J, Kopeček J (1990) Targetable photoactivatable drugs. Synthesis of N-(2-hydroxypropyl)methacrylamide copolymer - anti-Thy 1.2 antibodies - chlorin e<sub>6</sub> conjugates and a preliminary study of their photodynamic effect on mouse splenocytes in vitro. *Makromol Chem* 191: 839-856
- Ulbrich K, Koňák Č, Tuzar Z, Kopeček J (1987) Solution properties of drug carriers based on poly[N-(2-hydroxypropyl)methacrylamide] containing biodegradable bonds. *Makromol Chem* 188: 1261-1272
- Spikes JD, Krinick NL, Kopeček J (1993) Photoproperties of a mesochlorin e<sub>6</sub> - N-(2-hydroxypropyl)methacrylamide copolymer conjugate. *J Photochem Photobiol A: Chem* 70: 163-170
- Gu ZW, Spikes JD, Kopečková P, Kopeček J (1994) Synthesis and photoproperties of a substituted Zinc (II) phthalocyanine - N-(2-hydroxypropyl)methacrylamide copolymer conjugate. *Collection Czechoslov Chem Commun* 58: 2321-2336
- Spikes JD (1989) Photosensitization. In: *The Science of Photobiology*. Smith KC (ed). 2nd Ed. Plenum, New York, NY, pp 79-110
- Shen HR, Spikes JD, Kopečková P, Kopeček J (1995) Photosensitized crosslinking of proteins modeled by N-(2-hydroxypropyl)methacrylamide copolymers. *Proc 22nd Int Symp Controlled Rel Bioact Mater*, Seattle, Washington, July 30 - August 2, Proceedings
- Chiu HC, Zalipsky S, Kopečková P, Kopeček J (1993) Enzymatic activity of chymotrypsin and its poly(ethylene glycol) conjugates toward low and high molecular weight substrates. *Bioconjugate Chem* 4: 290-295
- Chiu HC, Koňák Č, Kopečková P, Kopeček J (1994) Enzymatic degradation of poly(ethylene glycol) modified dextran. *J Bioactive Compatible Polym* 9: 388-410
- Kamei S, Kopeček J (1995) Prolonged blood circulation in rats of nanospheres surface-modified with semitelechelic poly[N-(2-hydroxypropyl)methacrylamide]. *Pharmaceutical Res* in press
- Kopeček J, Kopečková P, Brøndsted H, Rathi R, Říhová B, Yeh PY, Ikesue K (1992) Polymers for colon-specific drug delivery. *J Contr Rel* 19: 121-130
- Říhová B, Rathi RC, Kopečková P, Kopeček J (1992) In vitro bioadhesion of carbohydrate containing N-(2-hydroxypropyl)methacrylamide copolymers to the GI tract of guinea pigs. *Int J Pharmaceutics* 87: 105-116
- Kopečková P, Kopeček J (1990) Release of 5-aminosalicylic acid from bioadhesive N-(2-hydroxypropyl)methacrylamide copolymers by azoreductases in vitro. *Makromol Chem* 191: 2037-2045
- Kopečková P, Rathi R, Takada S, Říhová B, Berenson MM, Kopeček J (1994) Bioadhesive N-(2-hydroxypropyl)methacrylamide copolymers for colon-specific drug delivery. *J Contr Rel* 28: 211-222
- Brøndsted H, Kopeček J (1991) Hydrogels for site-specific delivery. Synthesis and characterization. *Biomaterials* 12: 584-592
- Yeh PY, Kopeckova P, Kopecek J (1994) Biodegradable and pH sensitive hydrogels: Synthesis by crosslinking of N,N-dimethylacrylamide copolymer precursors. *J Polym Sci, Part A: Polym Chem* 32: 1627-1637
- Ghandehari H, Kopečková P, Yeh PY, Kopeček J (1995) Biodegradable and pH sensitive hydrogels: Synthesis by a polymer - polymer reaction. *Macromol Chem Phys* submitted

Kazunori Kataoka

Department of Materials Science, and Research Institute for Biosciences, Science University of Tokyo, 2641 Yamazaki, Noda, Chiba 278, JAPAN

**SUMMARY** Relevant properties of block copolymer micelles for the vehicles used in drug delivery were highlighted in this paper. These properties include (i) prolonged circulation time in blood compartment due to decreased RES uptake, (ii) considerable thermodynamic stability featured by low cmc value as well as by slow dissociation rate, (iii) loading of hydrophobic drug into the micelle core without precipitation, (iv) storage stability in both solution and freeze-dried form, and (v) passive accumulation to target site through direct extravasation. Further, structure and function of several types of polymeric micelle drugs were explained based on differences in the driving force of micellization. Hydrophobic and electrostatic interactions are two major basis for the formation of stable micelles in aqueous milieu. Impressive anti-cancer activity including the cure of solid tumor was evidenced for Adriamycin(ADR)-conjugated micelles prepared from block copolymer of poly(ethylene glycol) and poly( $\alpha,\beta$ -aspartic acid).

**KEY WORDS:** block copolymer, polymer micelle, long-circulating carrier, Adriamycin, polyion complex

## FEATURES OF BLOCK COPOLYMER MICELLES RELEVANT FOR DRUG DELIVERY

There has been a strong impetus for developing efficient systems for site-specific delivery of drugs by the use of appropriate vehicle systems. Nanoscopic vehicles having a microcontainer separate from the outer environment are promising for this purpose. Indeed, impressive results are reported for the use of natural vehicles, i.e., viruses and lipoproteins for delivery of drugs as well as of external genes, yet the tailoring process is rather complex and choice of incorporated substances is considerably restricted. Conceptual features of these natural vehicles is the self-assembly of macromolecules to form supramolecular structure (core-shell structure) in nanoscopic size. This feature can be modeled in a much simpler manner through the tailoring of the association of synthetic macromolecules with desired character. Block copolymers composed of hydrophobic and hydrophilic segments have the potential to form self-associates (micelles) in aqueous milieu[1]. The hydrophobic segment forms hydrophobic core of the micelle, while the hydrophilic segment surrounds the core as a hydrated outer shell. Since most drugs have a hydrophobic character, these drugs are easily incorporated in the inner core segment by covalent bonding or non-covalent bonding through hydrophobic interaction with core-forming segments. The features of block copolymer micelles relevant for drug delivery are summarized in Table 1.

Table 1 Properties of polymeric micelles relevant for drug delivery

Small size (~20nm)
Apparent thermodynamic stability
Solubilization of hydrophobic drugs
Low RES uptake (i.e.,stealth properties)
Modified biodistribution of drugs
Storage stability in freeze-dried form
Size of micelle may allow direct extravasation

Firstly, block copolymer micelle has a characteristic size range. In a ideal situation where both segments of the block copolymer undergoes clear phase separation in the micelle, core-shell structured micelle with diameter of several tens of nm should be formed as schematically shown in Fig. 1. This size range has a quite important meaning from a standpoint of drug targeting, because the drug vehicle should have a sufficient permeability into tissue to deliver the drug into the target located outside of the vasculature. Direct extravasation of the vehicle is a key process to achieve

sufficient drug accumulation to the target. It is known that endothelial linings of some of the capillaries are discontinuous, and macromolecules and small particles are possible to escape from the blood compartment to tissue interstitial space through small holes of the capillary. The size of the hole is in the range of 60-100nm. Capillaries in liver are the typical example of this type of capillaries with discontinuous endothelial linings lacking basement membrane (sinusoidal capillaries). Indeed, low density lipoprotein (LDL) with size of ca. 20nm easily penetrate these small holes of the liver

capillary to deliver cholesterol into liver parenchymal cells[2]. Discontinuous-typed capillary is also found in the tissue of solid tumors[3]: the fact gives rationale to deliver anti-cancer drug to solid tumor using vesicular carrier system including block copolymer micelle. In this way, direct extravasation of block copolymer micelle installing anti-cancer drug at solid tumor may be achieved.

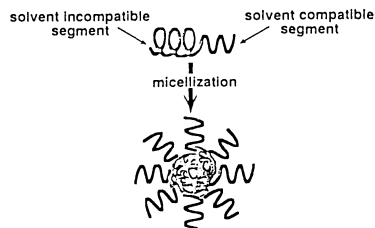


Fig. 1 Micellization of block copolymer in a selective solvent

It should be noted that, to achieve adequate accumulation of the carrier system into the localized target such as tumor, the carrier requires long-circulating property in the blood compartment. Thus, renal clearance of the carrier should be reduced to ensure prolonged circulation. As threshold molecular weight of renal clearance is reported to be ca. 50,000 for synthetic polymer with random-coil conformation[4], block copolymer micelle with apparent molecular weight over one million certainly shows negligible renal clearance, indicating its promising feature to work as long-circulating carrier. However, other than renal clearance, clearance through reticulo-endothelial system (RES) plays a substantial role in the disposition of particles in the blood compartment. Cells in RES locates in the organs such as liver and spleen, and these cells routinely uptake foreign substances, particularly, vesicles and particles. To achieve prolonged circulation in the bloodstream, carriers should escape from RES recognition. In the case of polymer micelle, property of the corona is substantially important to make the micelle stealth toward RES. Hydrophilic polymers with low interfacial free energy against water are preferable to be used as shell forming segments of polymer micelles. Further these hydrophilic polymer chains in the shell or the palisade of polymer micelles are fixed to the core as polymer brush through one-end with another end free in the solution. Thus, large steric repulsion is expected when the polymer brush has enough flexibility, allowing to prevent the strong interaction with cell and proteins.

While the block copolymer micelles generally have the association number of ca.200 with a considerably small (<10nm) core, highly dense palisade of polymer brush should surround the rigid-core to form soft-shell of the micelle. This soft-shell/rigid-core structure is a unique feature of the block copolymer micelles, and surely contributes the micelle to reveal stealth property toward RES recognition. Although a variety of hydrophilic polymer chain can be used to prepare the shell region of the micelle, poly(ethylene glycol)(PEG) is the most suitable for this purpose because of its high flexibility and low-toxicity.

Core of the block copolymer micelle serves as the drug microreservoir. Particularly, apparent solubility of highly hydrophobic drug can be increased dramatically, even higher than the solubility limit of free drug, through the incorporation into the micelle core. Once drug is successfully incorporated in the micelle core, the biodistribution of the drug is solely determined by the nature of the palisade of the micelle without the influence of the drug itself because the drug in the core should be segregated from the outer environment. Thus, modulation of drug biodistribution can be achieved by the use of block copolymer micelle as the carrier.

There are several advantages in block copolymer micelles from pharmaceutical view point[5]. For

example, high water solubility is ensured because drug-loaded core with hydrophobic property is effectively segregated from aqueous milieu by hydrophilic palisade, which contributes to increase the water solubility. Further, drug-loaded micelle can be stored in freeze-dried form, and is redissolved without any difficulties. Micelle sterilization is readily achieved by micro-filtration because the size of the micelle is smaller than the sieve of microfilters used for sterilization.

A unique physicochemical property of block copolymer micelles is their thermodynamic stability. Amphiphilic block copolymers with glassy hydrophobic segments form a considerably stable micelles with extremely low cmc in aqueous milieu. For example, micelles from poly(ethylene glycol)-poly( $\beta$ -benzyl L-aspartate)(PEG-PBCA) diblock copolymer were determined to have cmc values of 5-10mg/l[6], which are extremely low compared to cmc values of micelles from surfactant such as sodium dodecylsulfate. Strong cohesive force in the core may be responsible for these low cmc values. From a standpoint of using micelles for vehicles in drug targeting, dissociation rate of micelles has a critical meaning. It is well-known that dissociation rate of surfactant micelles is in the order of milliseconds. On the other hand, release rate of constituent polymer chains (unimers) from block copolymer micelles is expected to be quite slow when the micelles have a core associating through strong cohesive forces or having a glassy structure[7]. This feature allows polymer micelles to reach the target site before decaying into unimers in the bloodstream. Furthermore, polymer micelle system with a programmed decaying property can be designed by tailoring the chemical structure of the micelle-core.

It should be noted that polymer micelle may achieve both prolonged *in vivo* half-life and low chronic accumulation toxicity by controlling the decaying process of the micelle as schematically shown in Fig. 2. The most serious discrepancy of polymeric carriers is that extending half-life by increased molecular weight to avoid renal clearance results in the increased toxicity due to the non-specific tissue accumulation. This discrepancy may be overcome in polymer micelle system by regulating the molecular weight of the constituent block copolymers (unimers) to be lower than the threshold of renal clearance. In this way, unimers may be slowly dissociate from the micelle, lending themselves to excrete smoothly from the kidney.

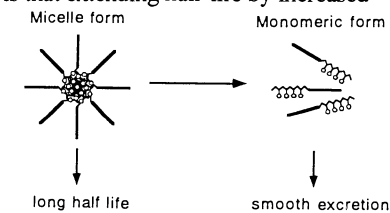


Fig. 2 Control of renal clearance through the programmed decay of the micelle

In the following sections, results from our research group will be briefly explained, focusing on some of the relevant properties of block copolymer micelles aforementioned[5,8].

## BLOCK COPOLYMER MICELLES FOR CANCER TREATMENT

We have prepared micelle-forming polymeric anti-cancer drug by conjugating hydrophobic anti-cancer drug, Adriamycin(ADR), to block copolymers of poly(ethylene glycol)-poly(aspartic acid)(PEG-PASP)[9,10]. Structural formula of the conjugate is shown in Fig. 3. Polymer micelle thus prepared exhibited advantageous pharmaceutical properties including high water solubility, prolonged storage in freeze-dried state, and simple sterilization by microfiltration. This polymer micelle-ADR has high potency to cure murine solid tumors by i.v. injection[11]. Further, prolonged *in vivo* half of the polymer micelle drug was evidenced through the study using the micelle labelled with radio isotope, indicating a relatively low RES uptake[12].

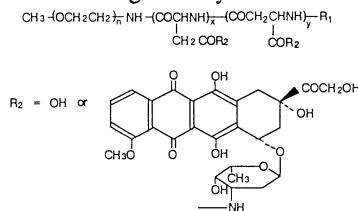


Fig. 3 Structural formula of ADR conjugate

Further, enhanced accumulation of the micelle into solid tumor was clearly observed. Of interest, the tumor accumulation ratios (tumor/heart and tumor/muscle) at 24h for the micelle-forming conjugate are an order of magnitude increase compared to free ADR as summarized in Table 2[12]. This remarkable selectivity is considered to be due to the enhanced vascular permeability as well as to the poor lymph transports in tumor as discussed by Maeda et al[3].

Table 2 Tumor/organ accumulation ratios of micelle-forming ADR-conjugate and free ADR at 24h

Sample	% dose per g tumor/% dose per g heart	% dose per g tumor/% dose per g muscle
	ADR	0.90
micelle-forming ADR-conjugate <sup>1)</sup>	12	40

1) Properties of the conjugate: Mw of PEG; 12,000, Mw of PAsp; 2,100, micelle diameter; 40nm. Carboxylate groups in PAsp segment of the block copolymer were almost quantitatively substituted by ADR.

Chemical conjugation of cisplatin to PEG-PAsp by ligand substitution reaction was successfully done recently to obtain cisplatin-conjugated micelles, which were very stable in aqueous solution[13]. In a sharp contrast with ADR-conjugated system, there was observed no micelle disruption upon the addition of sodium dodecyl sulfate, suggesting the

intermolecular complexation by diamineplatinum(II) bridges. Other than conjugated-form, free cisplatin may also be entrapped physically in the micelle core, which should be released from the micelle to give additional cytotoxicity. Indeed, the cisplatin micelle showed 1/8 to 1/5 *in vitro* cytotoxicity of intact cisplatin against murine B16 melanoma cells in 24-72h incubation.

Besides the micelles showing the passive accumulation at tumors, the preparation of micelles which are able to recognize specific sites is of interest. To achieve this goal, we have recently prepared block copolymer micelles having functional groups at the each chain ends of PEG palisade[15]. These micelles form through the association of PEG-PBLA block copolymers with functional groups at the  $\alpha$ -position of PEG. Targetable micelles can be prepared from these functionalized micelles by linking targeting moieties including sugars and proteins.

#### POLYION COMPLEX MICELLES FOR DELIVERY OF CHARGED COMPOUNDS

The formation of a palisade of hydrophilic segments surrounding the core of water-incompatible segments is the reason for prevention of progressive aggregation of the core and for stabilization of the monodispersive nano-associates (micelles) of amphiphilic block copolymers in aqueous milieu. Obviously, this concept of nano-associate stabilization by the hydrophilic palisade can be extended so as to include the case of macromolecular association through a force other than hydrophobic interaction; yet surprisingly, such attempts have not been reported. Recently, we were succeeded to prepare stable and monodispersive nano-associates through electrostatic interaction between a pair of oppositely-charged block copolymers with PEG segments[16]. We selected biodegradable poly(L-lysine) and poly(aspartic acid) as the polycation and polyanion segments in the block copolymer, respectively, with the intention of application of the nano-associates as novel drug carrier. The size of the nano-associates was determined to be 30nm by dynamic light scattering, being unchanged before and after freeze-drying. Viscosity measurement as well as laser-doppler electrophoresis provided evidence of the stoichiometry of the nano-associate formation. Worthy to mention is that charged drugs and proteins can be entrapped stably in this nano-associate. Further, stable nano-associates were found to form spontaneously between DNA and PEG/Poly(L-lysine) block copolymers. These results show a quite promising feature of these nano-associates based on block copolymer as vehicles used for site-specific delivery of charged drugs and biologically active compounds.

## ACKNOWLEDGEMENTS

The author is grateful to all the collaborators for their extensive contribution to this work. Part of this research is supported by a Grant-in-Aid for Scientific Research (Priority Area Research Program: No. 06282260), the Ministry of Education, Science, and Culture, Japan.

## REFERENCES

1. Tuzar Z, Kratochvil P (1976) Block and graft copolymer micelles in solution. *Adv. Colloid Interface Sci.* 6: 201-232
2. Firestone RA (1994) Low-density lipoprotein as a vehicle for targeting antitumor compounds to cancer cells. *Bioconj. Chem.* 5: 105-113
3. Maeda H, Seymour LW, Miyamoto Y (1992) Conjugates of anticancer agent and polymers: Advantages of macromolecular therapeutics in vivo. *Bioconj. Chem.* 3: 351-362
4. Seymour LW, Duncan R, Strohalm J, Kopecek J (1987) Effect of molecular weight (Mw) of N (2-hydroxypropyl)methacrylamide copolymers on body distribution and rate of excretion after subcutaneous, intraperitoneal, and intravenous administration to rats. *J. Biomed. Mater. Res.* 21: 1341-1358
5. Kataoka K, Kwon GS, Yokoyama M, Okano T, Sakurai Y (1993) Block copolymer micelles as vehicles for drug delivery. *J. Contr. Rel.* 24: 119-132
6. Kwon GS, Naito M, Yokoyama M, Okano T, Sakurai Y, Kataoka K (1993) Micelles based on AB block copolymers of poly(ethylene oxide) and poly( $\beta$ -benzyl L-aspartate). *Langmuir* 9: 945-949
7. Yokoyama M, Sugiyama T, Okano T, Sakurai Y, Kataoka K (1993) Analysis of micelle formation of an Adriamycin-conjugated poly(ethylene glycol)-poly(aspartic acid) block copolymer by gel permeation chromatography. *Pharm. Res.* 10: 895-899
8. Kataoka K (1994) Design of nanoscopic vehicles for drug targeting based on micellization of amphiphilic block copolymers. *J. Macromol. Sci.-Pure Appl. Chem.* A31: 1750-1769
9. Yokoyama M, Miyauchi M, Yamada N, Okano T, Sakurai Y, Kataoka K, Inoue S (1990) Polymer micelles as novel drug carrier: Adriamycin-conjugated poly(ethylene glycol)-poly(aspartic acid) block copolymer. *J. Contr. Rel.* 11: 269-278
10. Yokoyama M, Kwon GS, Okano T, Sakurai Y, Seto T, Kataoka K (1992) Preparation of micelle-forming polymer-drug conjugates. *Bioconj. Chem.* 3: 295-301
11. Yokoyama M, Okano T, Sakurai Y, Ekimoto H, Shibasaki C, Kataoka K (1991) Toxicity and antitumor activity against solid tumors of micelle-forming polymeric anticancer drug and its extremely long circulation in blood. *Cancer Res.* 51: 3229-3236
12. Kwon GS, Suwa S, Yokoyama M, Okano T, Sakurai Y, Kataoka K (1994) Enhanced tumor accumulation and prolonged circulation times of micelle-forming poly(ethylene oxide-aspartate) block copolymer-adriamycin conjugates. *J. Contr. Rel.* 29: 17-23
13. Yokoyama M, Okano T, Sakurai Y, Suwa S, Kataoka K Introduction of cisplatin into polymeric micelle, submitted for publication.
14. Kwon GS, Naito M, Yokoyama M, Okano T, Sakurai Y, Kataoka K (1995) Physical entrapment of adriamycin in AB block copolymer micelles, *Pharm. Res.* 12: 200-203
15. Cammas S, Kataoka K (1995) Functional poly(ethylene oxide)-co-( $\beta$ -benzyl-L-aspartate) polymeric micelles; block copolymer synthesis and micelles formation. *Macromol. Chem. Phys.* in press.
16. Harada A, Kataoka K Formation of polyion complex micelles in aqueous milieu from a pair of oppositely-charged block copolymer with poly(ethylene glycol) segments, submitted for publication.

## **THIRD PHASE IN POLYMER DRUG DEVELOPMENT: — SMANCS AS A PROTOTYPE MODEL DRUG FOR CANCER TREATMENT —**

Hiroshi Maeda

Department of Microbiology, Kumamoto University School of Medicine, Kumamoto 860, Japan

### **INTRODUCTION**

Tumor cells are essentially identical to the normal cells of the host in view of biochemical or molecular biological events and machineries thereof. However, I see a great difference between tumor and normal cells exists at the tissue level, particularly in tumor blood vessels. Therefore, it is a wise choice to develop a drug which will seek and find this unique character at the vascular level[1]. Macromolecules with biocompatible nature can be best utilized in this respect since we found that they leak out at the tumor blood vessels more selectively and remain uncleared in the tumor tissues for long time: i.e. extravasation into interstitial tumor tissue is much enhanced, but the clearance from tumor is greatly suppressed compared to the normal tissues. I coined this phenomenon as *enhanced permeability and retention (EPR) effect* of macromolecules and lipids in solid tumor[2-5].

Many genetically engineered proteins [as phase I polymer drug] of less than 50kDa have great potentials if their plasma half-life( $t_{1/2}$ ) is long enough and targeted to the diseased site. Because many cytokines or interleukines have extremely potent biological activity most of them need to be delivered selectively to the diseased site, otherwise systemic side effects overwhelms therapeutic value, as seen in TNF, IL-2 or even interferons. These problems can be solved simply by conjugating biocompatible polymers making the size above the renal threshold. This class of drugs can be classified as phase II polymer drugs which exhibiting longer plasma  $t_{1/2}$ .

In addition to the primary action of native molecules, the secondary functions may be added to the polymer-drugs such as metal chelating, immunopotentiating, free radical scavenging/resistant, anti-clot forming or oily formulability. This class may be classified as phase III polymer drugs, in which SMANCS [poly(styrene-co-maleic acid)[SMA]-conjugated neocarzinostatin (NCS)] belongs. Figure 1 shows the chemical structure of SMANCS.

### **Polymer Conjugation Results in Prolongation of Plasma Half-Life and Enhanced Tumor Targeting Effect**

SMA is used for car wax, floor polishing, and it is also used more recently for blending to the paper pulp. We conjugated two chain of SMA[1.6kDa] to a small antitumor protein NCS[12kDa]. NCS has highly potent biological activity but very rapid renal clearance( $t_{1/2}$  in mice: 1.9 min) made either too toxic or ineffective(Fig. 2)[5]. The conjugate showed about 10 times longer plasma  $t_{1/2}$ , and it also binds to plasma albumin, and exhibits EPR effect, which means highly tumor targeting; upto 10-30 fold accumulation in tumor over normal tissues, or drug concentration in tumor/blood ratio of 5-10. The same phenomenon, i.e. enhanced accumulation, was also observed at the inflammatory site[6] in many different macromolecular drug [e.g. ref. 6, 7]. These findings are now validated in HPMA-polymer-conjugated doxorubicin and PEG-conjugates of IL-2 and TNF[8-10]. These are examples of phase II polymer drugs.

### **New Properties Acquired by Polymer Conjugation**

SMANCS with half-*n*-butylester type exhibits high lipophilicity, which made oily formulation in Lipiodol (iodinated poppy seed oil ethylester) possible. SMANCS in Lipiodol can be arterially

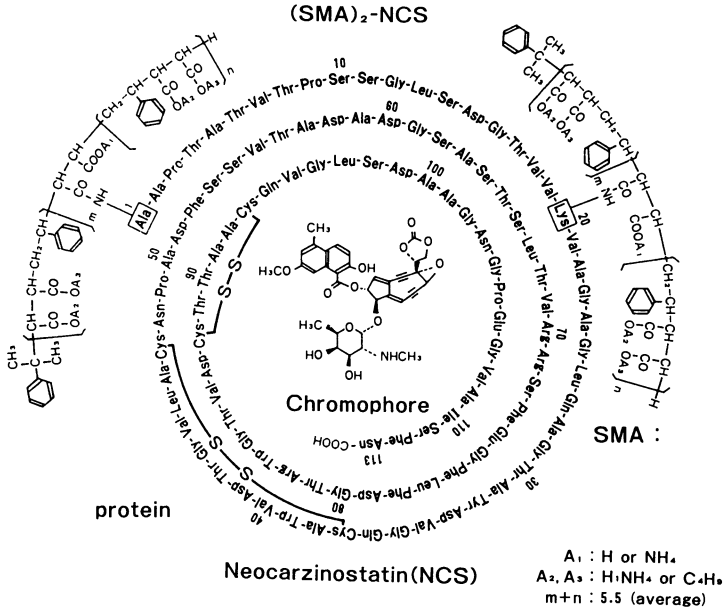


Figure 1. Chemical structure of SMANCS. SMA: poly(styrene-co-maleic acid)-half-*n*-butylate.

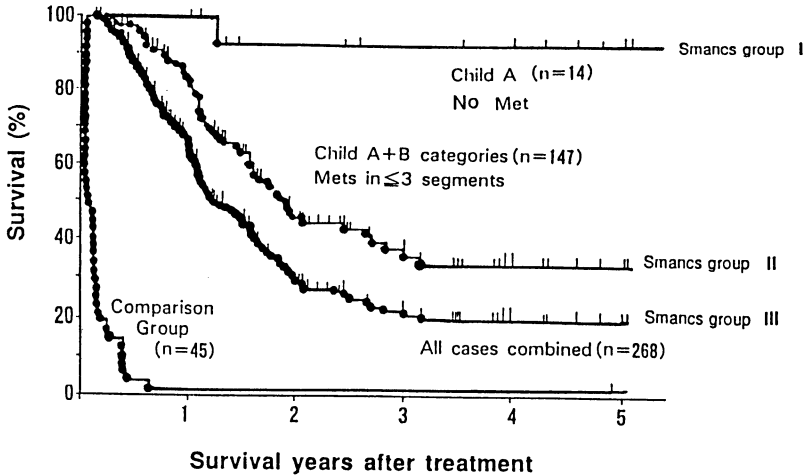


Figure 2. Survival profile of primary hepatoma patients. These patients are highly advanced and inoperable cases.



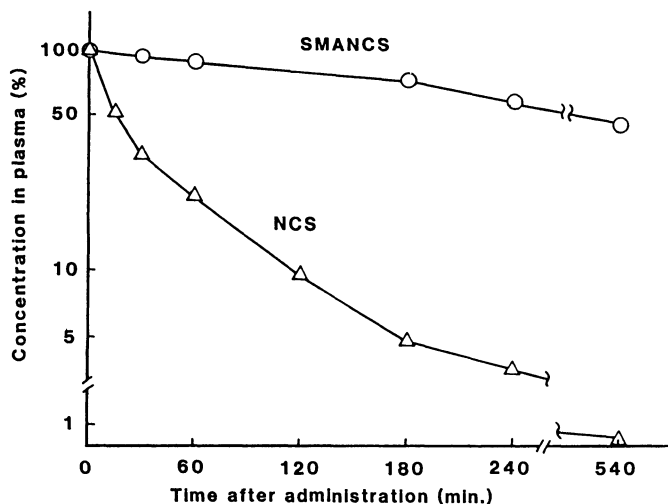


Figure 3. Plasma clearance of neocarzinostatin (NCS) and SMANCS in human cases[19]

administered (e.g. into the hepatic artery for hepatoma) with use of catheter, and extremely high tumor targeting is observed by this tactics (tumor/blood ratio of 2,000 or more, see Table I)[11]. Consequently excellent therapeutic effects but very few side effects were observed. In addition, tumor imaging become much sensitive and clearer under X-ray CT scan, and subsequent dosing regimen can be more quantitatively determined according to the tumor size[11]. Further, induction of interferon and activation of cellular immunity are observed which are not inherited characters in SMANCS from parent NCS [e.g. ref. 12, 13].

### Clinical Outcome: Present and Future

At present SMANCS is approved for use in primary hepatoma. Its efficacy is entirely depend on how adequately drug filled the tumor and condition of patients. Clinical efficacy as judged by survival span is unprecedentedly good for the patients with inoperable/advanced stage hepatoma otherwise they will die within 3-4 months; conventional treatments, either by surgery or chemotherapy, will have one year survival rate of less than 2-3% (Fig. 2). SMANCS treatment results in one year survival rate of 90% and that of five year survival of 35% if not with severe liver cirrhosis. Cause of death was usually liver cirrhosis (or hepatic failure) but not by tumor. Most frequent side effects is transitory fever in about 50% of the subjects. There is no toxicity in the liver, kidney, lung or in the bone marrow. Quality of life is better than any other cancer treatments. General clinical application of SMANCS therapy to other tumors such as those of kidney, gallbladder, bile-duct, pancreas, stomach and the lung await for further development although its efficacy has been demonstrated preliminary[14, 15].

Another use of macromolecular drug is intracavitary administration[16] via intraperitoneal or intrapleural route. The rationale of this route of administration is that macromolecules are retained in the tumor compartment much longer time than low molecular weight drugs such as mitomycin C or 5-FU. Free floating cancer cells are thus more accessible to the drug and readily killed, and ascites of Papanicolaou class V (with many definitely tumorous cells) become class I (all cells are normal and free of tumor cells) within one week[16 and unpublished data].

In conclusion, polymer conjugated anticancer drugs have many unique characters and they are much advantageous in pharmacokinetics and tumor targeting efficacy than conventional low molecular weight drugs. This notion can be now generalized with proteins and SMANCS[1], HPMA polymers[17] and other PEG-protein conjugates[e.g. 9, 10]. To enhance tumor delivery of

Table I. Accumulation of  $^{14}\text{C}$ -iodinated fatty acid. Intrahepatic arterial dose: 0.3 ml. Tumor implanted in the liver of rabbits. From Ref. 11 with permission.

Organs and tissues	Radioactivity DPM/g ( $\times 10^3$ )	
	15 min	3 days
Tumor	1252.58	130.94
Liver (adjacent)*)	56625	17.02
Liver (remote)	28.95	6.89
Small intestine	1.06	4.44
Lung	2.66	2.02
Kidney	1.61	2.57
Stomach	10.97	—
Heart	2.65	1.72
Large intestine	0.35	1.06
Spleen	2.39	3.28
Bladder	0.28	1.31
Brain	<0.1	0.38
Muscle	<0.1	0.46
Skin	<0.1	1.42
Mesenteric lymph node	0.15	2.21
Cervical lymph node	0.22	1.61
Thymus	0.22	0.93
Serum	0.58	1.03
Plasma cells	0.86	1.57
Bone marrow	<0.1	2.97
Urine (excreted)	—	1.14
Urine (vesical)	<0.1	1.06
Bile	70.91	1.78

\* To and from tumor.

polymer drugs further, angiotensin II induced hypertension will be practically feasible. At least two fold increased drug delivery to solid tumors and suppressing the drug delivery to normal tissues/organs such as the bone marrow and the kidney are observed due to contracted blood vessels in normal organs[18].

## REFERENCES

1. Matsumura Y, Maeda H (1986) A new concept for macromolecular therapeutics in cancer chemotherapy: Mechanism of tumoritropic accumulation of proteins and the antitumor agent smancs. *Cancer Res.* 46: 6387-6392
2. Maeda H (1991) SMANCS and polymer-conjugated macromolecular drugs: Advantages in cancer chemotherapy. *Adv. Drug Delivery Review* 6: 181-202
3. Maeda H, Matsumura Y (1989) Tumoritropic and lymphotropic principle of macromolecular drug. *Crit. Rev. Ther. Drug Carrier Syst.* 6: 193-210
4. Maeda H, Seymour L W, Miyamoto Y (1992) Conjugation of anticancer agents and polymers: advantages of macromolecular therapeutics in vivo. *Bioconj. Chem.* 3: 351-362
5. Maeda H, Matsumoto T, Konno T, Iwai K, Ueda M (1984) Tailor-making of protein drugs by polymer-conjugation for tumor targeting: A brief review on smancs. *J. Protein Chem.* 3: 181-193

6. Maeda H, Oda T, Matsumura Y, Kimura M (1988) Improved pharmacological properties of protein-drugs by tailoring with synthetic polymers. *J. Bioactive Compatible Polymers* 3: 27-43
7. Yamaoka T, Tabata Y, Ikada Y (1994) Accumulation of polyvinylalcohol at inflammatory site. *In: Polymeric Drugs and Drug Administration*. R.M. Ottenbrite (ed.) Am. Chem. Soc., pp 163-171
8. Duncan R (1992) Drug-polymer conjugates: potential for improved chemotherapy. *Anti-Cancer Drug* 3: 195-210
9. Tsutsumi Y, Kihara T, Yamamoto S, Kubo K, Nakagawa S, Miyake M, Horisawa Y, Kanamori T, Ikegami H, Mayumi T (1994) Chemical modification of natural human tumor necrosis factor  $\alpha$  with polyethylene glycol increased its antitumor potency. *Jpn. J. Cancer Res.* 5: 9-12
10. Katre NV, Knauf MJ, Laird WJ (1987) Chemical modification of recombinant interleukin 2 by polyethylene glycol increases its potency in murine Meth A sarcoma model. *Proc. Nat. Acad. Sci.* 84: 1487-1491
11. Iwai K, Maeda H, Konno T (1984) Use of oily contrast medium for selective drug targeting to tumor: Enhanced therapeutic effect and X-ray image. *Cancer Res.*, 44: 2115-2121
12. Suzuki F, Pollard RB, Maeda H (1989) Stimulation of non-specific resistance to tumors in the mouse using a poly(maleic acid-styrene)-conjugated neocarzinostatin. *Cancer Immunol. Immunother.*, 30: 97-104
13. Oda T, Morinaga T, Maeda H (1986) Stimulation of macrophage by polyanions and its conjugated proteins and effect on cell membrane. *Proc. Soc. Exp. Biol. Med.* 181: 9-17
14. Konno T, Maeda H, Iwai K, Maki S, Tashiro S, Uchida M, Miyauchi Y (1984) Selective targeting of anti-cancer drug and simultaneous image enhancement in solid tumors by arterially administered lipid contrast medium. *Cancer* 54: 2367-2374
15. Kobayashi M, Maeda H, Imai K, Konno T, Sugihara S, Yamanaka H (1991) Tumor-targeted chemotherapy with lipid contrast medium and macromolecular anticancer drug (SMANCS) for renal cell carcinoma. *Urology* 37: 288-294
16. Kimura M, Konno T, Oda T, Maeda H, Miyauchi Y (1993) Intracavitary treatment of malignant ascitic carcinomatosis with oily anticancer agents in rats. *Anticancer Res.* 13: 1287-1292
17. Seymour LW, Miyamoto Y, Maeda H, Brereton M, Strohaln J, Ulbrich K, Duncan R (1995) Influence of molecular weight on passive tumor accumulation of soluble macromolecular drug carrier. *Eur. J. Cancer* (May, in press)
18. Li CJ, Miyamoto Y, Kojima Y, Maeda H (1993) Augmentation of tumour delivery of macromolecular drugs with reduced bone marrow delivery by elevating blood pressure. *Br. J. Cancer* 67: 975-980
19. Maeda H, Miyamoto Y (1994) SMANCS approach - Oily formulations of protein drug for arterial injection and oral administration. *In: Drug Absorption Enhancement*. H.G.de Boer (ed) Harwood Academic Publs, pp 221-247

# Development of a Tetracycline Delivery System for the Treatment of Periodontal Disease Using a Semisolid Poly(Ortho Ester)

J. Heller<sup>1</sup>, K. V. Roskos<sup>2</sup>, B. K. Fritzing<sup>3</sup>, S. S. Rao<sup>3</sup> and G. C. Armitage<sup>4</sup>

<sup>1</sup> APS Research Institute, Redwood City, CA 94063; <sup>2</sup> Matrix Pharmaceuticals, Menlo Park, CA 94025; <sup>3</sup> SRI International, Menlo Park, CA 94025, <sup>4</sup> University of California, San Francisco, CA 94143

## SUMMARY

Poly(ortho esters) prepared by the condensation of 1,2,6-hexanetriol and an alkyl orthoacetate are viscous, semisolid materials at room temperature that can be injected using a blunt needle. The hydrolytic erosion of these materials can be controlled by varying the amount of Mg(OH)<sub>2</sub> incorporated into the polymer. When tetracycline was physically incorporated into the polymer, excellent, erosion-controlled, linear release was achieved with rates proportional to the amount of Mg(OH)<sub>2</sub>. Adhesion studies using bovine teeth with a polymer containing 10 wt% tetracycline and 1 wt% Mg(OH)<sub>2</sub> in a simulated oral environment demonstrated strong adhesion with cohesive failure of the polymer occurring at 118 mN/cm<sup>2</sup>. Toxicological studies have shown that the polymer is non-toxic in acute oral toxicity studies in rats when administered at 3.3g/Kg. Chronic oral dosing at 3.3 g/Kg for 4 weeks also had no effect. Acute intravenous studies using polymer hydrolysate administered at 1.0g/Kg also had no effect.

**KEY WORDS** Periodontitis, tetracycline, poly(ortho ester), bioerosion, drug release

## INTRODUCTION

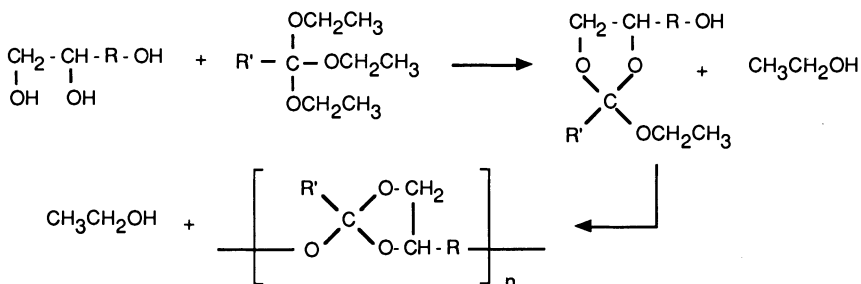
Periodontitis is a group of dentoalveolar infections that are one of the major causes of teeth loss. These infections are caused by a pathogenic flora established within the gingival sulcus which later deepens to form a periodontal pocket. The bacterial microflora deep within the periodontal pocket differs significantly from that in the supragingival environment in that it contains more anaerobes, more Gram-negative organisms and a greater proportion of motile species [1-8]. Treatments are based on strategies that shift the microflora within the periodontal pocket to that observed around healthy teeth and gingiva and a widely used treatment is to mechanically remove plaque and calculus followed by local treatment with antimicrobial agents. Clearly, controlled release devices that would maintain a therapeutically effective concentration of an antimicrobial agent within the pocket for the desired length of time would significantly improve treatment [9]. In this manuscript we describe the development of such a system.

## RESULTS

In previous manuscripts we have described the synthesis of a bioerodible polymer that at room temperature has an ointment-like consistency [10]. Because this material can be injected using a blunt needle, it is an interesting candidate for the treatment of periodontal disease provided that bioerosion and rate of tetracycline can be accurately controlled, the polymer is non-toxic and that sufficient bioadhesion to the tooth surface takes place to securely anchor the polymer in the periodontal pocket.

The structure of the polymer is shown in Scheme 1. When 1,2,6-hexanetriol is used in the synthesis, the hydrolysis products are 1,2,6-hexanetriol and a carboxylic acid whose identity is determined by the nature of the R-group [11]. The toxicology of 1,2,6-hexanetriol has been established and show to be nontoxic [12]. Because the polymer is comprised of highly flexible chains, it is a semisolid at room temperature even at molecular weights as high as 50 Kdaltons.

The structure of the polymer is shown in Scheme 1. When 1,2,6-hexanetriol is used in the synthesis, the hydrolysis products are 1,2,6-hexanetriol and a carboxylic acid whose identity is determined by the nature of the R-group [11]. The toxicology of 1,2,6-hexanetriol has been established and show to be nontoxic [12]. Because the polymer is comprised of highly flexible chains, it is a semisolid at room temperature even at molecular weights as high as 50 Kdaltons.



Scheme 1

Development of a clinically useful tetracycline delivery system for the treatment of periodontal disease based on the polymer shown in Scheme 1 requires the completion of the following tasks: (1) demonstration that the polymer can control the release of tetracycline at the desired rates and for the desired lengths of time, (2) demonstration that the drug-filled polymer can reside in the periodontal pocket for the desired 7 to 10 days, (3) demonstration that the polymer is non-toxic and (4) demonstration of efficacy by treatment of dogs with naturally occurring periodontal disease. Tasks 1, 2 and 3 have now been completed and the dog study is about to be initiated.

### Drug Release Studies

Because poly(ortho esters) contain a pH-sensitive linkage in the polymer backbone, acidic excipients can be used to accelerate polymer hydrolysis rates and basic excipients can be used to retard polymer hydrolysis rates [13]. This is one of the major advantages of poly(ortho esters) because very small changes in the concentration of the excipient dispersed in the matrix translate into significant changes in the rate of polymer hydrolysis and concomitant rate of drug release.

The ability to control hydrolytic erosion and rate of tetracycline release was determined by physically incorporating 10 wt% tetracycline and the desired amount of Mg(OH)<sub>2</sub> into the polymer, placing the mixture into a well within an erosion cell and pumping a phosphate buffer (pH 7.4) through the erosion cell at 10 ml/h. Samples (20 ml) were collected using an automatic fraction collector and assayed for tetracycline using reversed phase high performance liquid chromatography (HPLC).

Results of these studies are shown in Figure 1 which plots release of tetracycline from a propionate polymer (R' = CH<sub>3</sub>CH<sub>2</sub>) as a function of amount of Mg(OH)<sub>2</sub> dispersed in the polymer matrix [14]. Release of tetracycline in the absence of Mg(OH)<sub>2</sub> is extremely rapid, while the addition of as little as 0.5 wt% Mg(OH)<sub>2</sub> results in a sustained release over about 10 days. Addition of 1 wt% prolonged the release to about 25 days and 2 wt% produces a release estimated to last about 75 days. Because in all cases drug depletion and total polymer erosion was noted, satisfactory control over device lifetime and rate of tetracycline release is possible.

### Residence in the Periodontal Pocket

Prolonged residence of an ointment-like material in the periodontal pocket can only occur if there is sufficient bioadhesion between the polymer and the tooth surface. To determine the magnitude of this bioadhesion force, we have developed a microload cell and used extracted bovine anterior teeth as adhesive substrates [14]. Although human and bovine teeth give different average responses, the adhesiveness of both tooth surfaces for different adhesives are not significantly different [15,16].

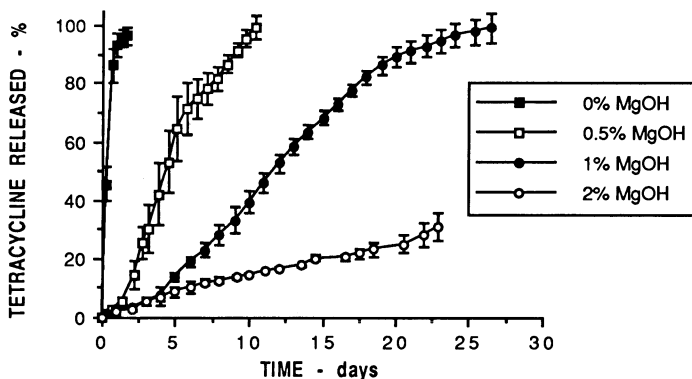


**Figure 1.** Cumulative release of tetracycline from a 27 kDa propionate polymer at pH 7.4 and 37°C as a function of Mg(OH)<sub>2</sub> concentration. 0.1M phosphate buffer, drug loading 10 wt%. Reproduced with permission from *Biomaterials*, 16 (1995) 313-317.

We have found that for the pure polymer, the required force of detachment was 392 mN cm<sup>-2</sup>. However, because the detachment occurs by cohesive failure of the polymer and not by failure of the bond between the polymer and the bovine tooth, this value is a minimal value and the true value of the adhesive bond is very likely significantly higher. However, this test was carried out on the neat polymer with no incorporated drug and excipient. Further, it was carried out on teeth surfaces that have not been exposed to proteins normally present in the oral environment. When the adhesion study was repeated using a formulation containing 10 wt% tetracycline and 1.0 wt% Mg(OH)<sub>2</sub> using teeth that had been exposed to dog serum (Sigma), rinsed with saline and kept wet with saline, the detachment force decreased to 118 mN cm<sup>-2</sup>. Again, as with the pure polymer, separation occurred by cohesive failure of the polymer and not between the bond between the specimen and polymer. The lower value indicates that polymer integrity has been weakened by the incorporation of tetracycline and Mg(OH)<sub>2</sub>. However, it is clear that the final formulation is also capable of strongly adhering to teeth.

### Sterilization

Due to the temperature and moisture sensitivity of poly(ortho esters) dry heat sterilization or steam sterilization is not a viable option. Ethylene oxide sterilization was also discarded as an option because this method could, despite extensive outgassing, leave toxic residues in the polymer. Thus, the only practical sterilization method is radiation sterilization. In this application, radiation sterilization is particularly attractive because the polymer-drug mixture can be sterilized as the final product in a hypodermic syringe.

However, radiation sterilization is not without problems because high energy radiation can lead to crosslinking and polymer chain cleavage. To determine the optimum radiation conditions, incremental doses of cobalt 60 radiation were used and the effect on polymer physico-chemical properties determined [17]. In these studies two different polymers having molecular weights of 33.3 and 17.4 kDa were exposed to radiation doses ranging from 0.5 to 4.0 Mrads. The results of these studies are shown in Table 1.

### Toxicology

Because there is the potential for ingestion of the polymer during treatment, acute and chronic feeding studies were carried out. Further, during bioerosion of the polymer, systemic absorption of hydrolysis products will take place so that acute intravenous toxicity studies using polymer hydrolysate were also carried out. All toxicological studies were carried out using adult Sprague Dawley rats using a doubly precipitated polymer which was then irradiated at 2.5 Mrad and stored in a dry-box at room temperature until use.

**Table 1.** Effect of Gamma-Sterilization on the Molecular Weight and the Dynamic Viscosity of Two Different Molecular Weights Poly(Ortho Esters)

Dose [Mrad]	POE - 33.3 kDa		POE - 17.4 kDa	
	M <sub>w</sub> [kDa]	Viscosity [Pa.s]	M <sub>w</sub> [kDa]	Viscosity [Pa.s]
0.5	21.6	7082.52	10.3	804.47
1.0	18.6	2212.78	9.5	579.43
1.5	15.3	919.59	8.5	445.92
2.0	11.9	508.98	8.4	321.25
2.5	11.0	294.50	7.3	146.44
3.0	7.9	254.19	5.7	94.82
3.5	6.6	294.41	6.2	313.26
4.0	6.3	251.44	5.9	170.49

Reprinted with permission from Pharm. Res. 11 (1994) 1485-1491

**Acute Oral Toxicity of Intact Polymer:** The intact polymer was emulsified in a vehicle consisting of 2 w/v % aqueous methyl cellulose solution with the aid of 1.6 w/v Tween 80 and administered to rats at a dose level of 3.3 g/Kg. No deaths or adverse clinical signs were observed during the study and no gross abnormalities were observed during necropsy. Thus, the polymer is non-toxic when administered as a single dose of 3.3 g/Kg to rats.

**28-Day Chronic Oral Toxicity of Intact Polymer:** The emulsified polymer prepared as already described was administered daily to rats at doses of 0.76, 1.64 or 3.27 g/Kg for 28 days. At necropsy, no gross abnormalities were observed in the tissues or external features. Histopathologic examination revealed no significant microscopic findings and no target organs for poly(ortho ester) toxicity. All hematology and clinical chemistry parameters were in the normal range. Thus, the polymer is non-toxic when administered daily at a maximum oral dose of 3.3 g/Kg for 4 weeks.

**Acute Intravenous Toxicity of Polymer Hydrolysate:** Sterile polymer was hydrolyzed by placing a known weight of the polymer in sterile buffered saline, pH 7.4 at 37°C for 15 days. The hydrolyzed polymer was filtered through sterile 0.2 micron filters and diluted as necessary. Rats were given 10 ml/Kg of sterile PBS containing hydrolyzed polymer equivalent to 0.5, 1.0 or 1.5 g/Kg, based on the weight of starting polymer. Rats given doses greater than 1.0 g/Kg had ataxia immediately following dosing, but recovered within 30 seconds and exhibited no other adverse clinical symptoms. The rats were kept under observation for 15 days. No gross abnormalities were observed following necropsy.

## ACKNOWLEDGEMENT

This work was supported by NIH Grant DE 10461. We wish to acknowledge the help of Mr. Steven Ng with polymer synthesis.

## REFERENCES

- [1] Socransky SS (1977) Microbiology of periodontal disease-Present status and future considerations J. Periodontol.: 48: 497-504
- [2] Listgarten MA, Hellden L (1978) Relative distribution of bacteria at clinically healthy and periodontally diseased sites in humans J. Clin. Periodontol. 5: 115-132
- [3] Slots J (1979) Subgingival microflora and periodontal disease J. Clin. Periodontol. 6: 351-382
- [4] Dzink JL, Tanner ACR, Haffajee AD, Socransky SS (1985) Gram-negative species associated with active destructive periodontal lesions J. Clin. Periodontol. 12: 648-659

- [5] Dzink JL, Socransky SS, Haffajee AD (1988) The predominant cultivable microbiota of active and inactive lesions of destructive periodontal diseases J. Clin. Periodontol. 15: 316-323
- [6] Haffajee AD, Socransky SS, Dzink JL, Taubman MA, Ebersole JL, Smith DJ (1988) Clinical, microbiological and immunological features of subjects with destructive periodontal diseases J. Clin. Periodontol. 15: 240-246
- [7] Loesche WJ.(1988) The role of spirochetes in periodontal disease Adv. Dent. Res. 2: 275-283
- [8] Slots J, Listgarten MA (1988), *Bacteroids gingivalis*, *Bacteroids intermedius* and *Actinobacillus actinomycetemcomitans* in human periodontal disease J. Clin. Periodontol. 15: 85-93
- [9] Urquhart, J., Rate-controlled drug dosage *Drugs*, 1982; **23**: 207-226
- [10] Heller J, Ng S, Fritzinger BK, Roskos KV (1990), Controlled drug release from bioerodible hydrophobic ointments *Biomaterials* 11: 235-237
- [11] Wuthrich P, Ng SY, Roskos KV, Heller J (1992) Pulsatile and delayed release of lysozyme from ointment-like poly(ortho esters) *J. Controlled Release* 21: 191-200
- [12] Smyth HF, Pozzani UC, Weil CS, Tallant MJ, Carpenter CP (1969) Experimental toxicity and metabolism of 1,2,6-hexanetriol *Tox. and Appl. Pharmacol.* 15: 282-286
- [13] Heller J (1993) Poly(ortho esters) *Adv. in Pol. Sci.* 107: 41-92
- [14] Roskos KV, Fritzinger BK, Rao SS, Armitage GC, Heller J (1995) Development of a drug delivery system for the treatment of periodontal disease based on bioerodible poly(ortho esters) *Biomaterials* 16:313-317
- [15] Nakamichi I, Iwaku M, Fusayama T (1983) Bovine teeth as possible substitutes in the adhesion test *J. Dent. Res.* 62:1076-1081
- [16] Cadwell DE, Johannessen B (1971) Adhesion of restorative materials to teeth *J. Dent. Res.* 50:1517-1525
- [17] Merkli A, Heller J, Tabatabay C, Gurny R (1994) Gamma sterilization of a semisolid poly(ortho ester) designed for controlled drug delivery-Validation and radiation effects *J. Pharm. Res.* 11:1485-1491



## MECHANISTIC ASPECTS OF TRANSDERMAL DRUG TRANSPORT

William I. Higuchi, Kunio Yoneto, Abdel-Halim Ghanem, S. Kevin Li, Daan J.A. Crommelin, James N. Herron, and Yong-Hee Kim

Department of Pharmaceutics and Pharmaceutical Chemistry, University of Utah, Salt Lake City, UT 84112, USA

### SUMMARY

The question of whether stratum corneum lipid liposomes (SCLL) might be a good model system for investigating the lipoidal pathway of the stratum corneum has been examined in two kinds of studies: (a) permeant release from SCLL and (b) fluorescence anisotropy experiments employing appropriate fluorescent probes. Semi-quantitative correlations were found, this suggesting SCLL may potentially be a good model for studying drug transport in the stratum corneum.

### KEY WORDS

Short chain n-alkanols; 1-alkyl-2-pyrrolidones; Enhancement factor; Fluorescence anisotropy; Stratum corneum lipid liposomes

### INTRODUCTION

As part of our research to gain mechanistic insights regarding the transport of drug molecules across skin, we have been studying the influences of chemical transport enhancers in a systematic fashion. Recently, [1,2] we completed the investigation of two homologous series, the short chain n-alkanols and the 1-alkyl-2-pyrrolidones (AP's) as enhancers for permeant transport across hairless mouse skin (HMS), especially as enhancers for the lipoidal pathway of the HMS stratum corneum. The important finding of this investigation (shown in Fig. 1) was the following: the potency of an enhancer for the lipoidal pathway of the stratum corneum was found, surprisingly, to be essentially the same in both homologous series when compared at equal alkyl group chain length, and the potency increased by around a factor of 3.5 per methylene group in both series. A main purpose of the present study was to examine whether or not SCLL would be a suitable model for gaining insights regarding the lipoidal pathway of the stratum corneum. The approach taken was (a) to determine SCLL bilayer transport enhancement induced by the AP's at iso-enhancement concentrations obtained with HMS stratum corneum and (b) to measure fluorescence anisotropies with fluorescent probes positioned in the SCLL bilayer in the presence of the n-alkanols and the AP's.

### MATERIALS AND METHODS

The SCLL (consisting of 55% by weight epidermal ceramides, 25% cholesterol, 15% free fatty acids, and 5% cholesteryl sulfate) were prepared as previously described [3]. Basically, two kinds of studies with the SCLL were carried out: 1, to perform SCLL bilayer permeability studies and to determine

whether there would be a correlation between the transport behavior of the SCLL bilayers and that of the lipoidal pathway of HMS; more specifically, the question studied was whether the same transport enhancement behavior seen with the AP's for HMS would be found with the SCLL bilayers; and 2, to perform fluorescent probe studies to determine whether or not there would be a correlation between steady-state fluorescence anisotropy changes (and therefore fluidity changes) with probes partitioned in the SCLL bilayers and the transport enhancement found in HMS when the comparisons are made under iso-enhancement concentration conditions, i.e., at concentrations of the n-alkanols or of the AP's giving the same lipoidal pathway transport enhancement with HMS.

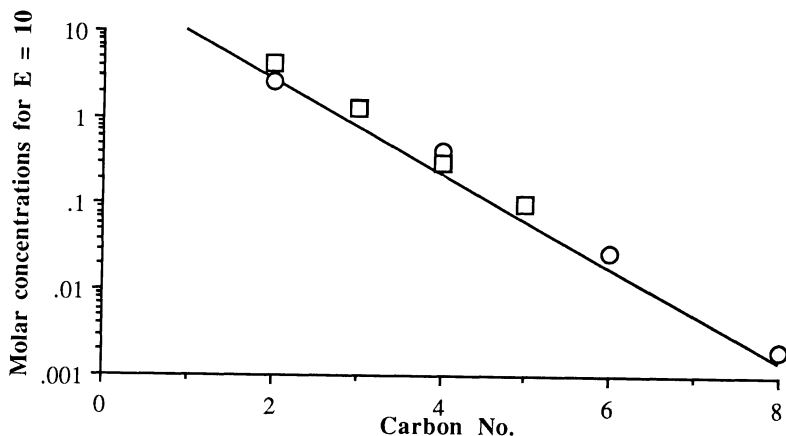


Fig. 1 Relationship between carbon number of the 1-alkyl-2-pyrrolidones (○) and the n-alkanols (□) and their "iso-enhancement" concentrations at  $E_{HMS} = 10$ . Here  $E_{HMS} = (P_{L,X}/P_{L,PBS}) \cdot F$  where  $P_{L,X}$  and  $P_{L,PBS}$  are the permeability coefficients of the solutes passing through the lipoidal pathway when X/PBS and PBS are the solvents, respectively. PBS is phosphate buffered saline and X/PBS is a solution of enhancer X in PBS.  $F$  is the solute activity coefficient ratio which can be obtained from the solute solubility ratio (if Henry's law is obeyed). Corticosterone was the probe permeant for the 1-alkyl-2-pyrrolidones and hydrocortisone for the n-alkanols. The line shows a 0.55 slope.

## RESULTS AND DISCUSSION

### SCLL bilayer permeability studies

The strategy employed was to determine the SCLL bilayer permeability increase (over the control) when each of the AP's was present as its iso-enhancement concentration (as established in the HMS studies). Model permeants employed were D-glucose, D-mannitol, 3-O-methyl-D-glucose, and raffinose. The release rates of the permeants from the SCLL were determined using an ultrafiltration technique. The results are shown for the case of  $E_{HMS} = 10$  in Fig. 2. Permeability coefficients calculated for the data in Fig. 2 and also for the case of  $E_{HMS} = 4.0$  were used to calculate the enhancement factor  $E_{SCLL}$ . Fig. 3 presents the relationship between  $E_{SCLL}$  and  $E_{HMS}$  for the AP's.

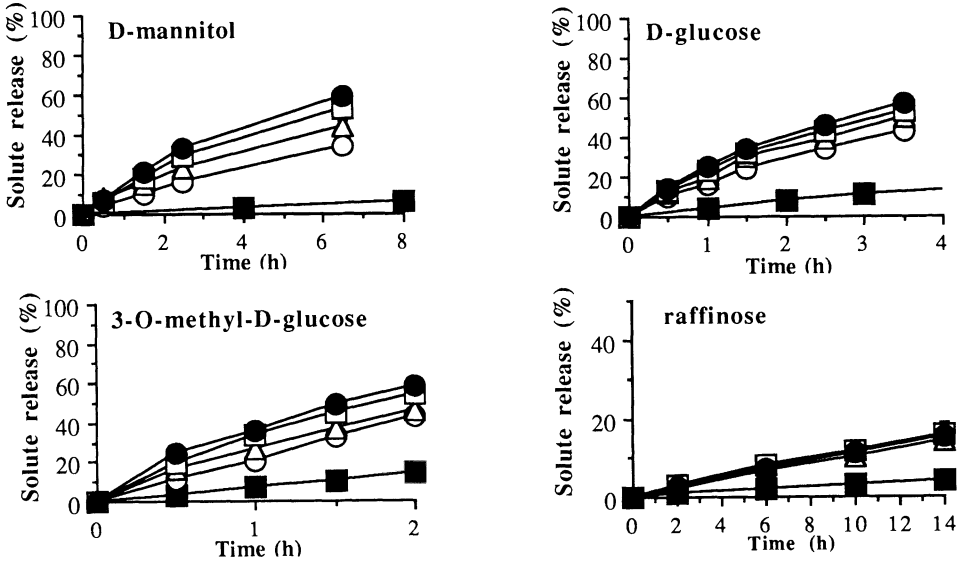


Fig. 2 Release of D-mannitol, D-glucose, 3-O-methyl-glucose and raffinose from SCLL in PBS (□) and for conditions of  $E_{HMS} = 10$  (i.e., ○, 30% EP; △, 6% BP; ■, 0.5% HP and ●, 0.05% OP) after correction for the burst effect. Each data point represents the mean and the standard deviation of three determinations.

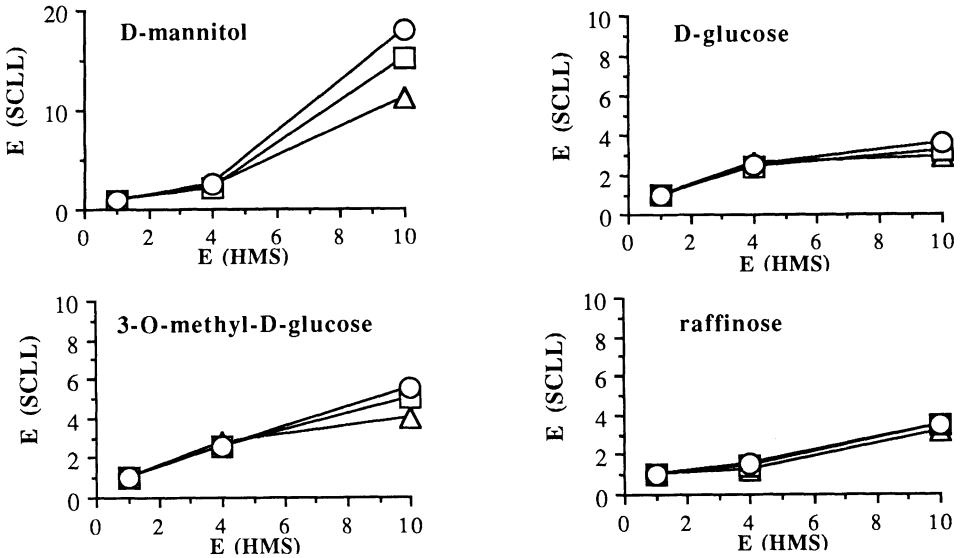


Fig. 3 Relationship between  $E_{SCLL}$  and  $E_{HMS}$  of D-mannitol, D-glucose, 3-O-methyl-glucose and raffinose.  $E_{SCLL} = (P_X/P_{PBS}) F$  where  $P_X$  and  $P_{PBS}$  are the SCLL permeability coefficients for the solute in a solution of enhancer X in PBS and in PBS, respectively. F and  $E_{HMS}$  are defined in the Fig. 1 caption. Symbols: △, BP; □, HP; ○, OP.

It should be noted that the SCLL bilayer and the lipoidal pathway of HMS compared in the present study are very different. Obviously, these two systems have very different macroscopic and possibly microscopic structures. While the release of solutes from the liposomes is trans-bilayer, some investigators believe that the diffusion in the stratum corneum is parallel to the bilayers (lateral diffusion) [4], implying that the mechanism of diffusion in the SCLL bilayer and that for the lipoidal pathway of HMS may be different (trans-bilayer vs. lateral). Moreover, the lipid compositions in SCLL and the lipoidal pathway in HMS are not exactly the same, and lipid-protein interactions are possibly involved in HMS. Especially because of these many differences in the SCLL and HMS systems studied, the good correlation seen between the enhancement effects of the different AP's on SCLL and the enhancement effects seen with the lipoidal pathway of HMS is particularly remarkable; this suggests the correlation is likely not accidental, i.e., the SCLL bilayer may be a useful model for the lipoidal pathway of the actual stratum corneum. Additional systematic research is required to fully understand the relationship between the iso-enhancement effects of the AP's on SCLL and the lipoidal pathway of HMS.

### Fluorescent probe studies of SCLL bilayers

The intercellular lipid domain is generally accepted as the lipoidal pathway of drug diffusion through the stratum corneum. It is also believed that transdermal enhancers have the ability to fluidize this lipid domain. Some specific regions such as the semi-polar interfacial regions of the intercellular lipid bilayers or the ordered hydrocarbon region near the interface may be viewed as the possible rate-limiting micro-environments of the lipoidal pathway. To test this hypothesis, SCLL have been used as a model to study the effects of the n-alkanols and the AP's on steady-state fluorescence anisotropy.

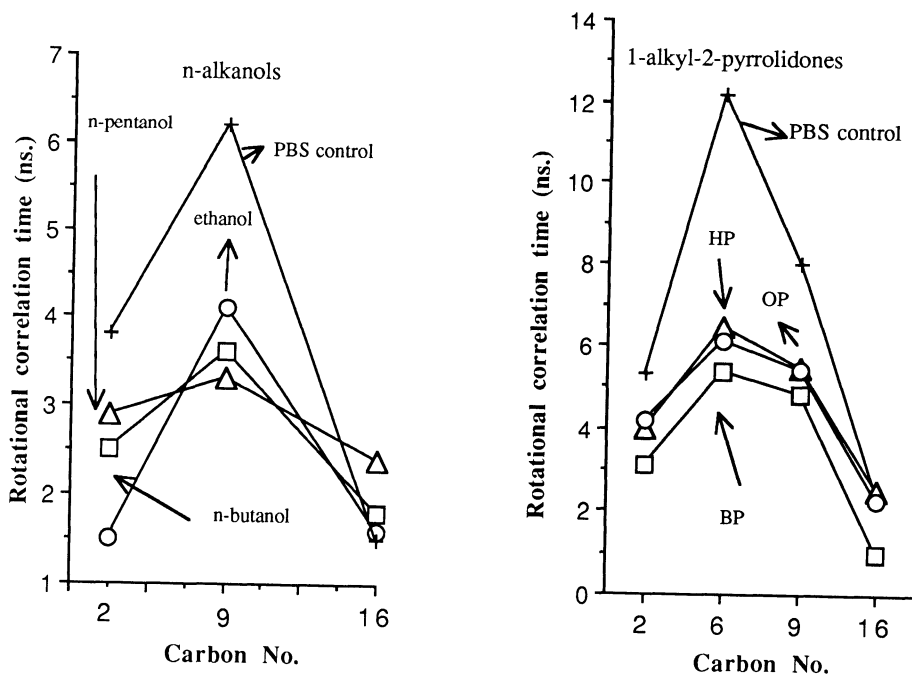


Fig. 4 Effects of n-alkanols and 1-alkyl-2-pyrrolidones under iso-enhancement ( $E_{HMS} = 10$ ) conditions on the average rotational correlation time obtained with fluorescent probes (C2 to C16) in stratum corneum lipid liposomes (SCLL).

As in the SCLL bilayer permeability studies (above), the strategy employed was to conduct experiments under the iso-enhancement concentration conditions (as defined above). Steady-state fluorescence and fluorescence lifetimes were determined for the fluorescent probes, the n-(9-anthroyloxy) fatty acids located at graded depths in the SCLL bilayer (at C2, C6, C9, and C16) in the absence of and in the presence of the n-alkanols or the AP's at their iso-enhancement concentrations corresponding to the enhancement factor,  $E_{HMS} = 10$ .

The data were used to calculate rotational correlation times and these are presented in Fig. 4. The results in Fig. 4 support the view that the appropriate microenvironment (primary action site) in the stratum corneum lipid bilayer for transport enhancement of lipophilic drugs induced by the short chain n-alkanols and AP's is the intermediate depth region (C2-C9), where the lipid alkyl chains are highly ordered and densely packed, rather than the deep hydrophobic interior. The n-alkanols and AP's at iso-enhancement ( $E_{HMS}=10$ ) concentrations induced increases in fluidity of around a factor of two in this intermediate depth region but caused only small changes in fluidity in the region near the bilayer center. Thus, the  $E_{HMS}$  values are not quantitatively proportional to these fluidity changes but the  $E_{SCLL}$  values are closer to these changes. Possible factors that need to be considered are the following: (a) it is not clear whether the rotational motion of the fluorophore should be a correlate of the translational diffusion of a permeant. The 'cavity volume' involved in the rotational motion of the fluorophore might be significantly smaller than the 'free volume' required for diffusion of large molecules; (b) the enhancement factor, E, may be dependent on the molecular size of the permeant; Liu [5] found that large steroids like  $\beta$ -estradiol, estrone, and hydrocortisone were enhanced 10-fold by 30% ethanol whereas ethanol as a permeant was enhanced only 2- to 3-fold; (c) the enhancement factor accounts for both the permeant's partitioning tendency and diffusivity; it is expected that lipid fluidization by the n-alkanols and AP's in the rate-limiting microenvironment would increase both the partitioning tendency and diffusivity for a permeant, yielding a possible squaring effect upon E. From the correlation found between these observed fluidity increases and the transport enhancement induced in the lipoidal pathway of HMS by the AP's and the n-alkanols, one may conclude that the SCLL may be a useful model mimicking the microenvironment and the barrier properties of the lipoidal pathway of the stratum corneum.

## ACKNOWLEDGMENTS

This research has been funded by NIH Grant GM43181. The authors wish to thank ISP Chemicals Inc., Wayne, NJ for supplying the 1-alkyl-2-pyrrolidones for this study.

## REFERENCES

1. Kim YH, Ghanem AH, Mahmond H, Higuchi WI (1992) Short chain alkanols as transport enhancers for lipophilic and polar/ionic permeants in hairless mouse skin: Mechanism(s) of actions. *Int. J. Pharm.* 80:17-31
2. Yoneto Y, Ghanem AH, Higuchi WI, Peck KD, Li SK (1995) Mechanistic studies of the 1-alkyl-2-pyrrolidones as skin permeation enhancers. *J. Pharm. Sci.* 84: 312-317
3. Abraham W, Downing DT (1989) Preparation of model membranes for skin permeability studies using stratum corneum lipids. *J. Invest. Dermatol.* 93:809-813
4. Elias PM (1981) Lipids and the epidermal permeability barrier. *Arch. Dermatol. Res.* 270:95-117
5. Liu P (1989) Ph.D. Dissertation, The University of Utah, Salt Lake City, Utah, USA

## TRANSBUCCAL DELIVERY OF POLAR COMPOUNDS

Bing Yang and Kristine Knutson

Department of Pharmaceutics and Pharmaceutical Chemistry/CCCD, College of Pharmacy,  
University of Utah, Salt Lake City, Utah 84112 USA

### ABSTRACT

Passive diffusion of polar solutes and weak electrolytes through canine buccal mucosa was investigated *in vitro* as a function of pH and solute molecular weight. The diffusion experiments were performed using modified Ussing chambers at constant temperature (37°C). Oxygen aeration and circulation of the Locke's solution maintained viability of the tissues throughout the experimental period. Transepithelial potential was monitored to assure tissue viability. Polar solutes (urea, glycerol, mannitol) exhibited molecular weight dependent permeation. The neutral species of a series of weak electrolytes (formic acid, benzoic acid, methyl amine and phenylethyl amine) permeated more rapidly than either charged species, reflecting contributions of both paracellular and transcellular pathways. However, the lower molecular weight, positively charged species (methyl amine) exhibited higher  $K_{\text{peff}}^{\pm}$  than the negatively charged weak electrolyte (formic acid), suggesting a molecular weight dependent selectivity of the paracellular pathway for positive species.

**KEYWORDS:** Buccal Delivery, Transport Mechanisms, Permeation, Transbuccal, Diffusion

### INTRODUCTION

Transbuccal delivery is an alternate delivery route for selected drugs such as peptides and proteins, which are unsuitable or less efficacious when delivered by other routes of administration. Human buccal epithelium is a highly vascularized, nonkeratinized squamous layer of cells composed of strata of varying cell types and maturity [1]. The major barrier strata include the compact differentiated nonkeratinized epithelial cells, a stratum of less flattened cells of varied differentiation including basal cells and the deeper porous basal lamina [2]. While the buccal membrane is perceived as an attractive alternate delivery route, permeation mechanisms and the influence of solute size and degree of ionization on permeation through buccal mucosa are not well defined [3]. Therefore, relative contributions of solute molecular size and ionization on permeation through transcellular and paracellular pathways of buccal mucosa are being investigated *in vitro*.

## EXPERIMENTAL MATERIALS AND METHODS

### Buccal Tissue Preparation

Fresh canine buccal membranes were obtained from animals immediately after being sacrificed. Epithelial tissues were removed and then placed in ice-cold and oxygen-rich Locke's solution. The underlying connective tissues were subsequently removed to isolate the buccal membranes, which were then mounted on Ussing chambers with the epithelial side facing the donor chamber.

### Permeability Measurements

Modified Ussing chambers were used for the permeability studies. The chambers consisted of two half-cells (7 ml/cell) and were surrounded by a water-jacket to maintain constant temperature (37°C). Oxygen aeration and circulation in the Locke's solution was accomplished by bubbling oxygen through the media. Transbuccal potential difference (PD) and short circuit current (Isc) were measured during the diffusion experiments. Transbuccal resistance (Rt) was calculated [ $Rt = PD(1000)(Area)/(ISC)$ ] from the open circuit potential difference and short circuit current. Selected model compounds (<sup>3</sup>H- or <sup>14</sup>C- labelled) were introduced into donor chambers, then aliquots were withdrawn from the receiver chambers as a function of time. Solute concentrations in donor and receiver chambers were determined by liquid scintillation counting on a Beckman LS-1800 scintillation counter. The effective permeability coefficients ( $K_{peff}$ ) were then calculated:

$$K_{peff} = \frac{V_{receiver} \cdot dC_{receiver}/dt}{A(C_{donor} - C_{receiver})} \quad \text{Equation 1}$$

where  $V_{receiver}$  is the receiver chamber volume,  $dC_{receiver}/dt$  is the change in receiver chamber concentration with time,  $A$  is the diffusional area of the cell and  $C_{donor} - C_{receiver}$  is the donor to receiver concentration gradient. Linear regression of receiver sample data collected after achieving constant flux across the membrane was used to calculate  $dC_{receiver}/dt$ . The dilution effect of sample replacement in the receiver chamber was normalized in the calculations.

## RESULTS AND DISCUSSION

### Electrophysiologic Parameters and Tissue Viability

Typical plots of buccal short-circuit current membrane potential and resistance as a function of time are shown in Figure 1. Representative membrane potential, short-circuit current and resistance values are  $-28(\pm 6)$  mV,  $21(\pm 7)$   $\mu$ A and  $1.7(\pm 0.4) \times 10^3$   $\Omega$ -cm<sup>2</sup>, respectively. Buccal epithelia exhibit electrical potential differences between the mucosal and serosal sides due to the ion transporting properties of the cells [4]. Thus, a change in potential difference signifies the breakdown of active "pump" mechanisms for ion transport or the development of "leaks" in the membrane. The magnitude of the transepithelial potential can be used to monitor the buccal epithelium viability. The membrane potential was maintained over the experimental time period.

### Molecular Size Effects on Permeability

Urea (60 MW), glycerol (92 MW) and mannitol (182 MW) were employed to study the effects of molecular size on permeability. The permeability coefficients decreased with

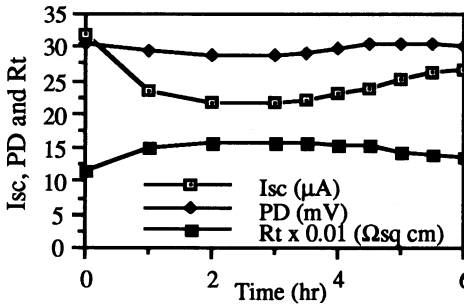


Fig. 1. Typical Isc, PD and Rt plots as a function of time.

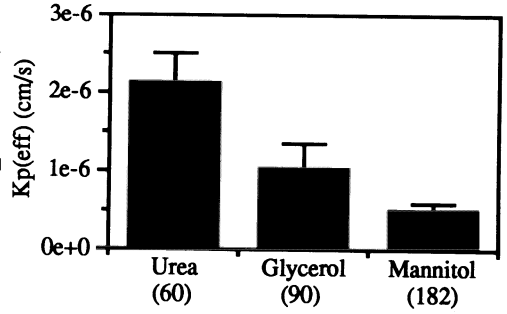


Fig. 2. Molecular size effects of nonionized polar solutes on permeability.

increasing molecular weight of the polar compounds as expected (Figure 2). The effective permeability of these polar compounds reflects diffusion via both the paracellular and transcellular pathways.

### Ionization Effects on Permeability

In order to determine the effects of ionization on transport mechanisms through the buccal mucosa, formic acid (46 MW; FA), benzoic acid (122 MW; BA), methyl amine (31 MW; MA) and phenylethyl amine (157 MW; PEA) were selected as model compounds. Diffusion experiments performed under controlled pH conditions provide insight into the role(s) of ionization on permeation along the selected permeation pathway(s). The effective permeability coefficients are strongly dependent on pH or solute ionization. Figures 3 and 4 illustrate the effects of pH on the percent of the solute ionized and the resultant effective permeability coefficients of the two higher molecular weight, weak electrolytes, benzoic acid and phenylethyl amine. Table 1 provides insight into the effect of pH and resultant ionization on the effective permeabilities of the lower molecular weight, weak electrolytes, formic acid and methyl amine. The effective permeability coefficients decrease with increasing ionization fractions.

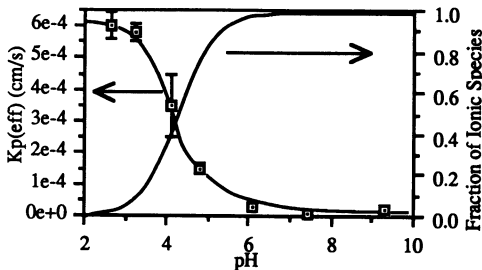


Fig. 3. pH dependent ionization fraction of benzoic acid and the effective permeability coefficient ( $K_{\text{peff}}$ ) of benzoic acid.

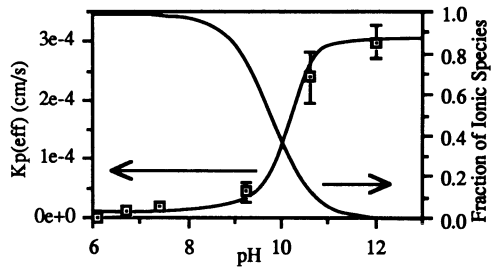


Fig. 4. pH dependent ionization fraction of phenylethyl amine and the effective permeability coefficient  $K_{\text{peff}}$  of phenylethyl amine.



Table 1. pH Dependent Ionization Fraction and Effective Permeability Coefficients ( $K_{peff}$ ) for Formic Acid and Methyl Amine.

Solute	pH	X	$K_{peff}$ (cm/sec)	pH	X	$K_{peff}$ (cm/sec)
Formic Acid	2.8	0.90	$1.3(\pm 0.3) \times 10^{-5}$	10.2	0	$4.5(\pm 0.4) \times 10^{-7}$
Methyl Amine	11.6	1.0	$12.4(\pm 2.4) \times 10^{-5}$	6.5	0	$25.0(\pm 4.3) \times 10^{-7}$

A mathematical model developed by Ho [5] models diffusion across the buccal membrane and separates the effective permeability coefficient into the contributions for the individual cellular layers:

$$\frac{1}{K_{peff}} = \frac{2}{K_{ABL}} + \frac{1}{(K_{cell} + K_p)X + K_p^{\pm}(1-X)} + \frac{1}{K_i} + \frac{1}{K_{BL}} \quad \text{Equation 2}$$

where  $K_{peff}$  is the effective permeability coefficient,  $K_{ABL}$  is the permeability coefficient of the aqueous boundary layer,  $K_i$  the permeability coefficient of the intermediate cell layer,  $K_{BL}$  is permeability coefficient of the basal lamina,  $K_{cell}$  the intrinsic permeability coefficient for neutral molecules through the transcellular pathway,  $K_p$  the intrinsic permeability coefficient for neutral molecules through the paracellular pathway,  $K_p^{\pm}$  is the intrinsic permeability coefficient for cationic/anionic species through the paracellular route, and X is the fraction of the nondissociated species of a weakly acidic or basic solute at the aqueous buffer solution/membrane interface. If the aqueous boundary layer, intermediate cell layer and basal lamina barriers to transport are considerable less than that of the compact cell layer, then Equation 2 may be simplified to Equation 3.

$$K_{peff} = (K_{cell} + K_p)X + K_p^{\pm}(1-X) \quad \text{Equation 3}$$

From Equation 3,  $K_p^{\pm}$  can be calculated from the plots of solute permeability versus fraction ionized. Both cationic and anionic solutes diffused through the buccal mucosa, although the neutral species permeated through the buccal mucosa more effectively than the ionized species. These data suggest that there are multiple pathways and barriers to transport. The neutral species have higher permeability coefficients through buccal mucosa than either negatively or positively charged solutes. Neutral species may permeate the buccal mucosa via either paracellular or transcellular pathways. However, charged solutes diffuse through the buccal mucosal primarily by paracellular pathways. For lower molecular weight weak electrolytes (formic acid and methyl amine), the positively charged species exhibited higher permeability coefficients as compared to the negatively charged species. This likely reflects selectivity of the more negatively charged paracellular pathway.

## CONCLUSIONS

Polar solutes may diffuse across buccal mucosa via either paracellular and or transcellular pathways. Passive diffusion of polar solutes through buccal mucosa was dependent on molecular size. For weak electrolytes, the effective permeability was dependent on ionization of the compounds. The neutral species exhibited higher permeability coefficients through the buccal mucosa than either the positively or negatively charged species. However, there was also a molecular weight dependence on the permeation of charged species. The lower molecular weight, positively charged species permeated the buccal mucosa with higher  $K_p^\pm$  than the negatively charged species. This suggests that the paracellular pathway is selective for low molecular weight, positively charged solutes.

## ACKNOWLEDGEMENTS

The authors express their appreciation to N.F.H. Ho for his insightful discussions, as well as C.C. Baird and J.H. Davis for their assistance in obtaining buccal membranes. These investigations were supported in part by the State of Utah Centers of Excellence Program.

## REFERENCES

1. Wertz, PW and Squier, CA. (1991) Cellular and molecular basis of barrier function in oral epithelium. *CRC Crit Rev Drug Carrier Syst* 8:237-269
2. Stablein, MJ and Meyer, J. The vascular system and blood supply. In, *The Structure and Function of Oral Mucosa*. Meyer, J, Squier, CA and Gerson, SJ (eds.) Pergamon Press, Elmsford, NY 1984; pp 237-256
3. Harris, D. and Robinson, JR. (1992) Drug delivery via the mucous membranes of the oral cavity. *J Pharm Sci* 81:1-10
4. Longer, MA, (1988) Characterization of buccal epithelia relevant to peptide drug delivery, Ph.D. Dissertation. University of Wisconsin, Madison, WI
5. Ho, NFH. (1993) Biophysical kinetic modeling of buccal absorption. *Advanced Drug Delivery Reviews* 12:61-97

# RECEPTOR-MEDIATED TARGETING OF PEPTIDES AND PROTEINS

Yuichi Sugiyama and Yukio Kato

*Faculty of Pharmaceutical Sciences, University of Tokyo, 7-3-1 Hongo, Bunkyo-ku, Tokyo 113, Japan*

## SUMMARY

Receptor-mediated endocytosis (RME) is important both as a clearance mechanism for biologically active polypeptide and as a target of drug delivery system (DDS). We have been kinetically analyzing the RME of epidermal growth factor (EGF) in hepatocytes and constructed a kinetic model describing RME. We examined the uptake kinetics of DDS for antisense oligonucleotide and demonstrated that the balance of the affinity of the DDS carrier for antisense and for the receptor is important to improve the targeting efficiency. The hepatic handling of hepatocyte growth factor (HGF) was analyzed using the liver perfusion system. HGF was found to be eliminated not only via RME, but also by the other nonspecific mechanism. Since the heparin-like substance on the cell-surface plays a role in such a clearance, we designed heparin-HGF complex as a DDS for the prevention of the nonspecific clearance.

**KEY WORDS :** receptor-mediated endocytosis, drug delivery system, epidermal growth factor, hepatocyte growth factor, antisense oligonucleotide

## INTRODUCTION

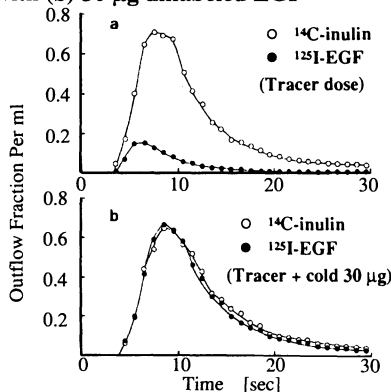
A remarkable feature of the disposition of polypeptides is the contribution of RME to their clearance in the body [1,2]. In addition, drug targeting utilizing RME is expected to have promise as a drug delivery system (DDS) to carry some drug specifically into the target cell expressing receptors on its plasma membrane [3,4]. Therefore, it is important to analyze the RME process kinetically, both to clarify the pharmacokinetics of polypeptide itself and to estimate the efficiency of drug targeting via polypeptide receptors. This study focuses on the kinetic analysis of RME of epidermal growth factor (EGF) and hepatocyte growth factor (HGF).

## RESULTS

### (1) Kinetic analysis of receptor-mediated disposition of EGF in liver

Multiple indicator dilution method in a single-pass perfusion system enables us to analyze the rapid interaction between EGF and liver cell-surfaces with a liver architecture maintained. In this technique we injected both  $^{125}\text{I}$ -EGF as a test compound and  $^{14}\text{C}$ -inulin as a reference compound into the portal vein and measured the time profile of the radioactivity in the hepatic vein outflow

**Fig.1 Representative dilution curves for  $^{14}\text{C}$ -inulin and  $^{125}\text{I}$ -EGF without (a) or with (b) 30  $\mu\text{g}$  unlabeled EGF**



(Dilution curve). The recovery of a tracer  $^{125}\text{I}$ -EGF in the outflow was only 20% of that of  $^{14}\text{C}$ -inulin (Fig. 1A). On the other hand, when the  $^{125}\text{I}$ -EGF was coinjected with 30  $\mu\text{g}$  of unlabeled EGF, this recovery was reduced almost to the comparable level with  $^{14}\text{C}$ -inulin (Fig. 1B), indicating the saturation of the binding and/or uptake by the liver [5]. We estimated association rate constant ( $k_{on}$ ), dissociation rate constant ( $k_{off}$ ), and sequestration rate constant of EGF, and the receptor density by fitting all the data obtained at any dosages to the kinetic model [5]. In the analysis of the internalization process, we measured the time profiles of both surface-bound and internalized  $^{125}\text{I}$ -EGF, separately [6]. A plot of an internalized amount of EGF against the integrated amount of the surface-bound EGF enables us to obtain the internalization rate constant ( $k_{int}$ ). The  $k_{int}$  value thus obtained was

0.33 min<sup>-1</sup> [6]. By the similar kinetic analysis, the degradation rate constant was found to be about 0.005-0.03 min<sup>-1</sup> in the isolated [7] and cultured [8] hepatocytes, which is much slower compared with the internalization process. We measured the recovery of the extraction ratio of a tracer <sup>125</sup>I-EGF after a perfusion of an excess unlabeled EGF (20 nM) [9] in the presence of cycloheximide to prevent the newly synthesis of the receptor. The externalization rate constant ( $k_{ext}$ ) of the receptor was estimated to be 0.015 min<sup>-1</sup> [9].

## (2) Consideration of the efficiency of drug targeting based on the kinetic model for RME

Based on the kinetic model describing RME, the preferable combination of ligand and receptor in view of the efficiency of drug targeting can be discussed. At steady state, the uptake rate of the ligand can be expressed by:

$$V_{uptake} = V_{max,app} C_p / (K_{m,app} + C_p) \quad \text{Eq. (1)}$$

where,

$$K_{m,app} = (k_t / k_{int}) \times \{(k_{off} + k_{int}) / k_{on}\} = \alpha \times \{(k_{off} + k_{int}) / k_{on}\} \quad \text{Eq. (2)}$$

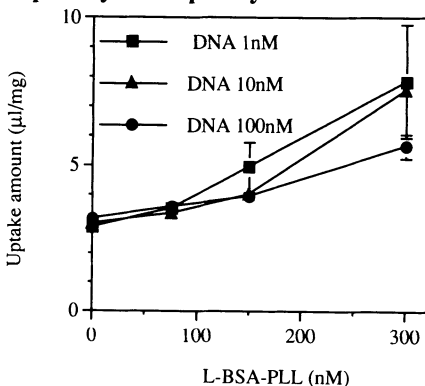
$$V_{max,app} = k_t R_s(0) = k_{ext} V_{syn} / k_{deg,R} \quad \text{Eq. (3)}$$

The  $k_t$ ,  $C_p$ ,  $V_{syn}$ , and  $R_s(0)$  are internalization rate constant for unoccupied receptors, plasma concentration, newly synthesis rate of receptors, and receptor density in the absence of the ligand, respectively. Based on Eq. (1), the uptake rate of the ligand cannot exceed  $V_{max,app}$  although the uptake rate increases as ligand concentration increases. The  $\alpha (= k_{int} / k_t)$  represents the acceleration of the internalization rate constant of the receptor induced by the binding to the ligand. When the ligand extensively induces receptor internalization, the  $\alpha$  value is high, resulting in the high efficiency of drug targeting. The  $V_{max,app}$  value is proportional to the  $R_s(0)$  value, indicating that the efficiency of drug targeting is high when we target densely expressed receptors on the cell-surface. Both the  $k_{ext}$  and  $k_t$  are positively correlated to the  $V_{uptake}$  value, indicating that the receptor which is transported rapidly between the cell-surface and cell-interior can be used as a preferential targeting site

## (3) DDS of antisense oligonucleotide utilizing asialoglycoprotein receptor

We attempted to develop DDS of antisense oligonucleotide targeted toward the asialoglycoprotein receptor. Based on the idea originally designed by Wu et al. [3,4] we prepared a mixture of the carrier (lactosylated BSA covalently bound to polylysine, L-BSA-PLL) and oligonucleotide, being composed of an antisense sequence against the transcriptional region of human ICAM-1. The advantage of this strategy is the minimal decrease in the biological activity of antisense oligonucleotide because of no covalent binding between the carrier and antisense. However, since the binding is reversible, it can be speculated that the affinity of the carrier to the antisense is important for the targeting efficiency. In fact, an equilibrium dissociation constant ( $K_d$ ) was 11 nM while the binding capacity was 1.6 oligonucleotides per 1 L-BSA molecule. Next, the kinetic analysis of the uptake of <sup>125</sup>I-L-BSA-PLL or <sup>32</sup>P-antisense alone by cultured rat hepatocytes was performed. Both the carrier and antisense uptake consist of saturable and non-saturable component ( $K_m=2.48$ ,

**Fig 2. Uptake of antisense DNA/L-BSA-PLL complex by rat hepatocytes**



$V_{max}=0.01$  pmol/min/mg protein,  $k$  (non-saturable uptake) = 1.4  $\mu$  l/min/mg protein for L-BSA-PLL and  $K_m=2.1$   $\mu$  M,  $V_{max}=0.093$  pmol/min/mg protein,  $k=0.023$  l/min/mg protein for antisense). Since the uptake clearance ( $v/c$ ) is much higher for L-BSA-PLL than antisense, the enhancement of the antisense uptake by the carrier was expected. However, such an enhancement was, in fact, minimal and at most twice the amount (Fig. 2). In addition, the increase in the uptake of oligonucleotide could be particularly observed at more than 100 nM of L-BSA-PLL (Fig. 2), which can occupy almost all of the cell-surface receptor considering that the  $K_m$  value for L-BSA-PLL is 2.5 nM. To clarify the reason for such a limited enhancement of oligonucleotide

**Fig 3. Kinetic model describing the uptake of the antisense, carrier, and complex**

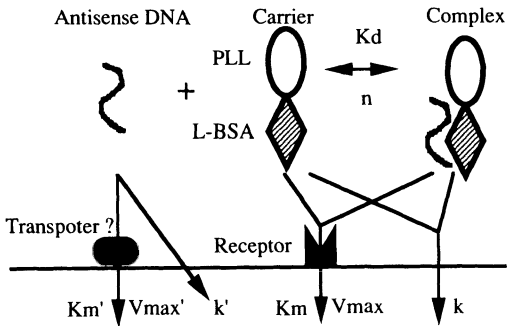
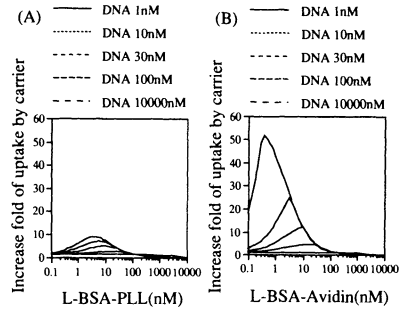


**Fig 4. Simulation of enhancement of antisense DNA uptake by carriers**



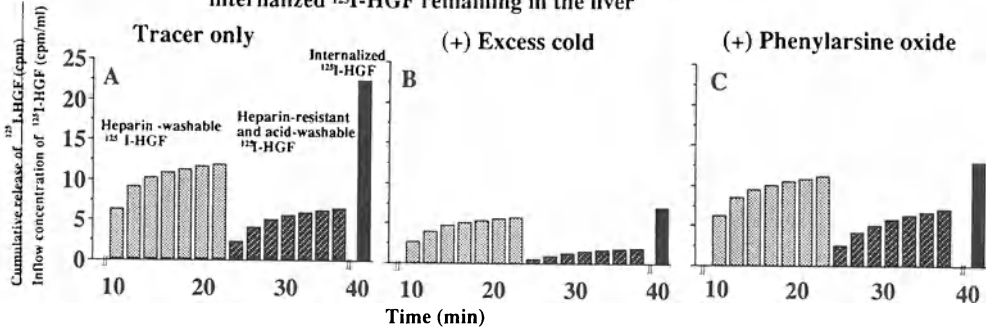
uptake, the uptake of oligonucleotide in the presence of L-BSA-PLL was simulated (Fig. 3, 4) based on the kinetic parameters representing the uptake of either oligonucleotide or L-BSA-PLL alone. In this study the Michaelis-Menten equations were used to describe the uptake of both antisense oligonucleotide and the carrier. The binding of the carrier and oligonucleotide was described by the Langmuir equation (Fig. 3). We assumed that the unbound carrier can competitively inhibit the uptake of the complex of the carrier and oligonucleotide and has a same affinity for the receptor as that of the complex (Fig. 3). Based on this model, we confirmed that the enhancement of the oligonucleotide uptake could be observed exclusively at a higher concentration of L-BSA-PLL than its  $K_m$  value, as in case of Fig. 2. This result can be explained when we consider that the nonsaturable uptake clearance ( $k$ ) of the carrier is much higher than that of oligonucleotide. When the uptake of oligonucleotide was simulated in assuming that the nonsaturable uptake of L-BSA-PLL is negligible ( $k = 0$ ) (Fig. 4A), an enhancement of the uptake could be especially observed at a L-BSA-PLL concentration around the  $K_m$  value while it was minimal at a higher concentration of the carrier where the saturation of receptor-mediated uptake occurs (Fig. 4A). Since the affinity of the L-BSA-PLL to the receptor is higher than its affinity to the oligonucleotide, we can intuitively speculate that a relatively higher concentration of L-BSA-PLL than the  $K_d$  value for the binding to antisense should exist to make almost all the oligonucleotide form a complex with L-BSA-PLL, resulting in the saturation of the binding and/or uptake via the asialoglycoprotein receptor induced by free L-BSA-PLL and a minimal enhancement of oligonucleotide uptake by the carrier. To overcome such a minimal enhancement we have to utilize the carrier with a much higher affinity for the antisense. To predict the case when the affinity between the carrier and oligonucleotide is much higher, the oligonucleotide uptake was also simulated in assuming that such an affinity is approximately  $10^7$  times higher ( $K_d = 1.0$  fM) where the nonspecific uptake of the carrier is also negligible (Fig. 4B). In this case, a dramatic enhancement of the uptake (approximately 50 times higher than oligonucleotide alone) can be observed (Fig. 4B). For example, avidin-biotin system is known to have such a high affinity and is now utilized as a DDS carrier for the polypeptide and antisense [10,11].

#### (4) Receptor-mediated and non-specific clearance of HGF

HGF is the most potent mitogen for hepatocytes [12]. HGF receptor expressed on hepatocytes has a strong affinity for HGF with an equilibrium dissociation constant of 20-40 pM [12]. In addition, the non-specific binding of HGF to cell-surface is very high. Such non-specific binding sites are considered to be heparin-like substances since HGF has an affinity for heparin [12]. Therefore, it seems to be likely, that not only the HGF receptor, but also other non-specific binding sites contribute to the elimination of HGF. After the liver perfusion of a tracer concentration of

$^{125}\text{I}$ -HGF, an ice-cold buffer containing heparin was perfused to remove relatively non-specific binding, which presumably represents the binding of HGF to cell-surface heparin-like substance [13,14]. A significant heparin-washable binding was detected (Fig. 5A). After the "heparin-washing," so-called "acid-washing" was done to remove the receptor-bound  $^{125}\text{I}$ -HGF. The

**Fig 5. Time profiles of heparin-washable, heparin-resistant and acid-washable  $^{125}\text{I}$ -HGF recovered in the outflow and internalized  $^{125}\text{I}$ -HGF remaining in the liver**

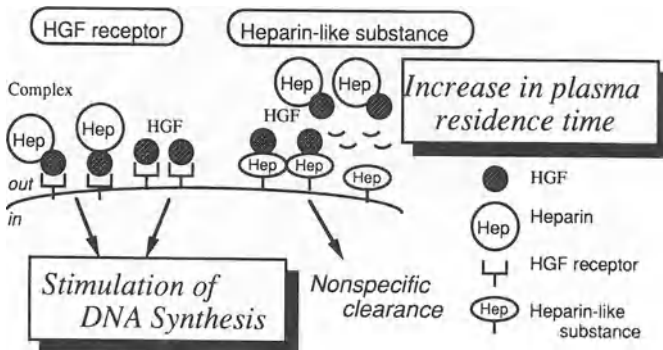


heparin-resistant and acid-washable binding was also observed in the outflow during the acid-washing (Fig. 5A). An excess unlabeled HGF (135 pM) can reduce especially the latter binding, suggesting that the latter binding mainly represents receptor binding (Fig. 5A, 5B). After both heparin- and acid-washing, the liver still contained radioactivity, presumably representing the internalized  $^{125}\text{I}$ -HGF (Fig. 5A). A clear saturation was observed also in the internalized fraction, suggesting that HGF is taken up via RME. In addition, the internalization of  $^{125}\text{I}$ -HGF was still observed even in the presence of either an excess unlabeled HGF (Fig. 5B) or phenylarsine oxide (Fig. 5C), an inhibitor of RME. These results suggest that HGF is taken up by not only RME, but also non-specific clearance mechanisms.

**(5) DDS of HGF for the decrease in nonspecific clearance**

To decrease the nonspecific binding and/or uptake HGF, we designed heparin-HGF complex as a DDS of HGF (Fig. 6)[15]. If the heparin-like substance on the cell-surface plays a role in the nonspecific clearance, the HGF molecule prebound to heparin cannot bind to such a binding site, resulting in the increase in the plasma residence time of HGF (Fig. 6). We have already demonstrated that the heparin-HGF complex shows lower plasma clearance than HGF alone. In addition, we found that the complex retains the proliferative activity of HGF, assessed as the incorporation of  $^{125}\text{I}$ -deoxyuridine in cultured rat hepatocytes [15].

**Fig.6 Hepatic Handling of HGF or Heparin-HGF Complex**



## CONCLUSION

It is demonstrated that the balance of (i) an affinity of the carrier to the receptor, (ii) an affinity of the carrier to the drug, and (iii) a concentration of the carrier is essential to improve the efficiency of DDS utilizing RME. It is suggested that heparin-HGF complex can be utilized as DDS for the increase in plasma residence time although the further studies such as the analysis of the mechanism for the decrease in the HGF clearance, examination of the biological activity in vivo, and the screening of the other heparin-like substance with a low activity of heparin have to be done.

## REFERENCES

1. Maack T, Suzuki M, Almeida FA, Nussenzweig D, Scarborough RM, Mckenroe GA, Lewicki JA (1987) Physiological role of silent receptors of atrial natriuretic factor. *Science* 238: 675-678
2. Sugiyama Y, Hanano M (1989) Receptor-mediated transport of peptide hormones and its importance in the overall hormone disposition in the body. *Pharm. Res.* 6: 192-204
3. Wu GY, Wilson JM, Shalaby F, Grossman M, Shafritz DA, Wu CH (1991) Receptor-mediated gene delivery in vivo. *J. Biol. Chem.* 266: 14338-14342
4. Wilson JM, Grossman M, Wu CH, Chowdhury NR, Wu GY, Chowdhury JR (1992) Hepatocyte-directed gene transfer in vivo leads to transient improvement of hypercholesterolemia in low density lipoprotein receptor-deficient rabbits. *J. Biol. Chem.* 267: 963-967
5. Sato H, Sugiyama Y, Sawada Y, Iga T, Sakamoto S, Fuwa T, Hanano M (1988) Dynamic determination of kinetic parameters for the interaction between polypeptide hormones and cell-surface receptors in the perfused rat liver by the multiple-indicator dilution method. *Proc. Natl. Acad. Sci. USA* 85: 8355-8359
6. Sato H, Sugiyama Y, Sawada Y, Iga T, Fuwa T, Hanano M (1990) Internalization of EGF in perfused rat liver is independent of the degree of receptor occupancy. *Am. J. Physiol.* 258: G682-G689
7. Yanai S, Sugiyama Y, Kim DC, Iga T, Fuwa T, Hanano M (1991) Kinetic analysis of receptor-mediated endocytosis of epidermal growth factor by isolated rat hepatocytes. *Am. J. Physiol.* 260: C457-C467
8. Kato Y, Sugiyama Y (1993) Binding, internalization, degradation, and mitogenic effect of epidermal growth factor in cultured rat hepatocytes. *STP Pharm. Sci.* 3: 75-82
9. Sugiyama Y, Sato H, Yanai S, Kim DC, Miyauchi S, Sawada Y, Iga T, Hanano M (1989) Receptor-mediated hepatic clearance of peptide hormones. In: *Topics in Pharmaceutical Sciences* 1989. Breimer DD, Crommelin DJA, Midha KK (eds). Amsterdam Medical Press B.V., Noordwijk, 1989, pp 429-443
10. Pardridge WM, Boado RJ (1991) Enhanced cellular uptake of biotinylated antisense oligonucleotide or peptide mediated by avidin, a cationic protein. *FEBS letters* 288: 30-32
11. Bickel U, Yoshikawa T, Pardridge WM (1993). Delivery of peptides and proteins through the blood-brain barrier. *Adv. Drug. Del. Rev.*, 10: 205-245.
12. Matsumoto K, and Nakamura T (1993) Roles of HGF as a pleiotropic factor in organ regeneration. In: *Hepatocyte growth factor-Scatter Factor(HGF-SF) and the C-Met Receptor*. I.D. Goldberg ID and Rosen EM (eds), Birkhauser Verlag, Basel, 1993; pp 225-249
13. Liu K, Kato Y, Narukawa M, Kim DC, Hanano M, Higuchi O, Nakamura T, Sugiyama Y (1992) The importance of the liver in the plasma clearance of hepatocyte growth factor in rats. *Am. J. Physiol.* 263: G642-G649
14. Liu K, Kato Y, Yamazaki M, Higuchi O, Nakamura T, Sugiyama Y (1993) Decrease in the hepatic uptake clearance of hepatocyte growth factor (HGF) in CCl<sub>4</sub>-intoxicated rats. *Hepatology* 17: 651-660
15. Kato Y, Liu K, Nakamura T, Sugiyama Y (1994) Heparin-hepatocyte growth factor complex with low plasma clearance and retained hepatocyte proliferating activity. *Hepatology* 20: 417-424

# TEMPERATURE SENSITIVE POLYMERS FOR DELIVERY OF MACROMOLECULAR DRUGS

SUNG WAN KIM

Department of Pharmaceutics and Pharmaceutical Chemistry/CCCD  
University of Utah, Salt Lake City, Utah 84112

## ABSTRACT

Significant progress has been made for the last decade in the research of drug delivery systems. For the sustained action, to maximize efficiency and minimize side effects of drugs, novel polymeric carriers or devices have been introduced. Intelligent drug delivery systems can be defined as a novel drug delivery which shows drug release based on metabolite concentration or regulated or modulated via external stimuli. In this paper, macromolecular drug delivery by using thermosensitive polymers is reviewed.

## KEY WORDS

Thermosensitive Hydrogels  
Macromolecular Drug Delivery  
Insulin Delivery  
Calcitonin Delivery

## INTRODUCTION

Recently, increased numbers of peptide and protein drugs have been in demand for the development of delivery systems. Conventional polymers are difficult to use in macromolecular drug delivery due to problems with fabrication and impermeable characteristics of macromolecular diffusion. Self regulated drug delivery (1) and modulated delivery systems (2) have been proposed using novel stimuli sensitive systems.

This manuscript includes the concept of macromolecular drug delivery by utilizing thermosensitive hydrogels. No product is currently available for the delivery of peptide drugs using stimuli sensitive polymers, though extensive research is currently underway for the synthesis, characterization and application of these polymers, and eventually basic research in this area will be utilized for therapeutic application. Peptide drugs and proteins cannot be delivered effectively in conventional dosage forms. For such therapeutic agents, new drug delivery carriers should be developed. It is important to construct a system where drug delivery occurs when it is required. The auto feedback concept is shown in Figure 1 (3).

When a stimuli is necessary, the delivery systems or carrier will respond to external stimuli (magnetic field, temperature, electric current, ultrasound, and photo-irradiation) or internal stimuli (pH, ionic strength, metabolites, enzyme substrate and biochemical bindings) to effect drug release. Stimuli responsive polymers, based on function, can be divided into open loop and closed loop systems. Table 1 and Table 2 list the mechanisms of hydrogels responding to the environmental stimuli (4).

It is known that pH-sensitive hydrogels contain pendant groups composed of weakly acidic or basic moieties, such as carboxylic acids and primary or substituted amines, or strong acids and bases, such as sulfonic acids and quaternary ammonium salts. The ionization state of these pendant groups change in response to pH changes, leading to water increase swelling properties. Recently Peppas and Klier (5) have studied the effect of pH and swelling on drug release behavior using graft copolymers of poly(ethylene glycol) (PEG) with poly(methacrylic acid) (PMAA). PMAA and PEG form complexes due to hydrogen bonding between the acidic protons of the carboxyl groups and the ether oxygens on PEG. Crosslinked poly(MAA-g-PEG) gels showed transition with pH change of external media.



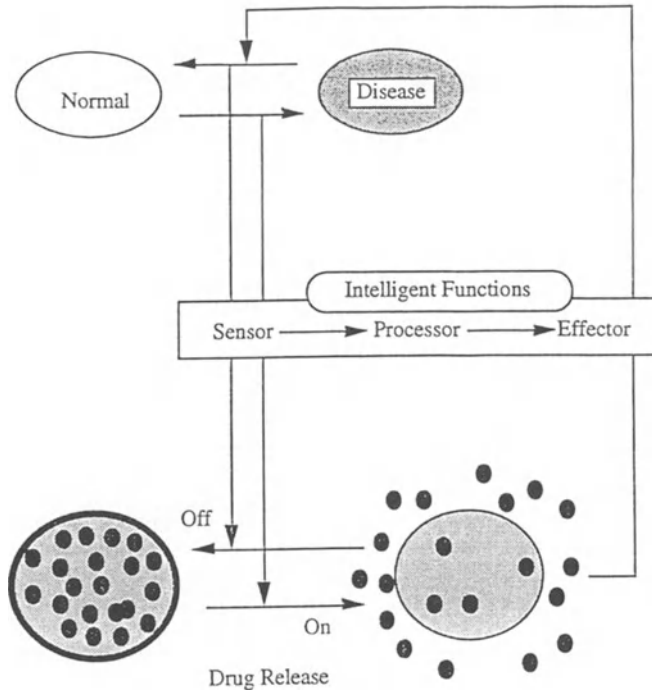


Fig. 1 Auto feed-back drug delivery

Dong and Hoffman (6) have prepared heterogeneous hydrogels possessing both pH- and temperature-sensitivity, by using *N*-isopropyl acrylamide (NiPAAm), acrylic acid and vinyl terminated polydimethylsiloxane loaded with indomethacin. At gastric conditions (pH 1-4 and 37°C), the gel did not swell because the lower critical solution temperature (LCST) of the gel is below 37°C. However, at pH 6.8-7.4, the gel's LCST shifts above 37°C and begins to swell due to ionization and repulsion of AAc groups. *In vitro* release studies of indomethacin showed that only a negligible amount of indomethacin was released at pH 1.4 within 24 hours. However, at pH 7.4 more than 90% of the total drug was released. The release profile resembled zero order kinetics for 5 hours, suggesting a swelling-controlled mechanism. The release rate of indomethacin from the gels at pH 7.4 changed, depending on the acrylic acid content. Siegel et al (7), prepared pH-sensitive hydrogels having ionizable groups from hydrophobic *n*-alkyl methacrylate (AMA) and *N,N*-dimethylaminoethyl methacrylate (DMA). These gels demonstrated sharp transitions in swelling, depending on the comonomer ratio and the length of the alkyl side chain. Factors influencing swelling properties of pH sensitive polymers were extensively discussed elsewhere (4).

The use of electro-sensitive polymers as drug delivery systems is based on the electro-kinetic phenomena of electrolyte gel or the electric properties of polymer surfaces. Eisenberg and Grodzinsky (8) reported permeability changes for neutral solutes or proteins across poly(methacrylic acid) or collagen membranes with an electric field. These changes were attributed to the variation of membrane hydration due to the intramembrane pH changes through electro-diffusion process. This hydration change and additional factors such as electro-osmotic or electrophoretic augmentation of solute transport are responsible for the control of solute permeability. Osada et al. (9) studied an electrically stimulated drug delivery system to deliver pilocarpine, glucose, and insulin using gels and microspheres of polyelectrolytes such as poly(acrylic acid), poly(methacrylic acid), and poly(*N,N*-dimethylaminopropyl acrylamide). The modulated release of solute from these polyelectrolyte gels was explained by gel shrinkage under electric current, resulting in the forced release of imbedded drug solution. Yuk et al (10)

Table 1 Responsive closed-loop systems (From Reference 4)

Stimulus	Hydrogel	Mechanism
pH	Acidic or Basic Hydrogel	Change in pH ==> change in swelling==> change in release of drug
Ionic strength	Ionic hydrogel	Change in ionic strength==> change in concentration of ions inside gel ==> change in swelling ==> change in release of drug
Chemical species	Hydrogel containing electron accepting groups	Electron donating compounds ==> formation of charge transfer complex ==> change in swelling ==> change in release of drug
Enzyme-substrate	Hydrogel containing immobilized enzyme	Substrate present ==> enzymatic conversion ==> product changes swelling of gel ==> change in release of drug
Competitive binding	Concanavalin A hydrogel containing	Increase in glucose concentration ==> displacement of glycosylated insulin by competitive binding sites ==> release of glycosylated insulin

Table 2 Responsive open-loop systems (From Reference 4)

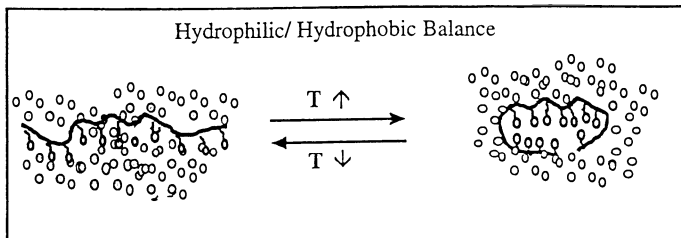
Stimulus	Hydrogel	Mechanism
Magnetic	Magnetic particles dispersed in alginate microspheres	Applied magnetic field ==> change in pores in gel ==> change in swelling ==> change in release of drug
Thermal	Thermo sensitive hydrogel, e.g. poly(N-isopropylacrylamide)	Change temperature ==> change in polymer-polymer and water-polymer interactions ==> change in swelling ==> change in release of drug
Electrical	Polyelectrolyte hydrogel	Applied electric field ==> change in membrane charging and electrophoresis of charged drug ==> change in swelling ==> change in release of drug
Ultrasound irradiation	Ethylene-vinyl alcohol hydrogel	Ultrasound irradiation ==> temperature increase ==> release of drug
Photochemical	2-Hydroxyethyl methacrylate hydrogel containing azobenzene in side chain	Photoirradiation ==> photosensitization of azobenzene moiety ==> change in swelling ==> change in release of drug

demonstrated the controlled release of hydrocortisone using calcium alginate/polyacrylic acid composite as a gel matrix for the electric current-sensitive drug delivery systems. In this system, the key factor for controlling the release rate was also the swelling changes of the matrix. Kwon et al (11) synthesized copolymer gels of AMPS with n-butylmethacrylate (BMA) loaded with a positively charged solute (edrophonium chloride) by an ion-exchange method. The drug was released only when an electric field was applied and "on-off" drug release was achieved. The mechanism was explained as an ion exchange between positive solute and hydroxy-onium ion produced at the anode by water hydrolysis. They also achieved "on-off" drug release utilizing the dissociation of the polymer complex in an electric field (12). Poly(ethylloxazoline) (PEOx) and poly(methacrylic acid) (PMAA) form solid complexes by hydrogen bonding below pH5, and the complex dissolves above pH 5.4. When an electric current was applied the matrix dissolved at the surface facing the cathode, because the local pH increased near the cathode and resultant hydrogen bonding was disrupted. Insulin was released from the matrix with dissolution in response to application of the electric current. The release rate at each "on" state was nearly constant because of the surface erosion mechanism of decomplexation. Furthermore, a polymeric ionic complex of polyallglamine and heparin was also designed by Kwon et al (13). The heparin release showed "on-off" profile by varying the local pH modulated with electric current.

### Thermo-Sensitive Hydrogels for Macromolecular Drug Delivery

Polymers demonstrating swelling-deswelling changes in response to temperature have been extensively studied. As shown in Figure 2 both negative or positive thermosensitive polymers can be designed, based on the concepts of hydrophobic interaction and hydrogen bond or ionic interaction respectively. Recently N-isopropyl acrylamide (NiPPAm) and its derivatives have been studied due to the unique properties of low solution critical temperature. Both laboratories (LCST) concurrently, of Hoffman and Kim have initiated innovative research in this area (14-21)

#### Driving Force to Precipitate Polymers at Low Temperature



#### Driving Force to Precipitate Polymers at Low and High Temperatures

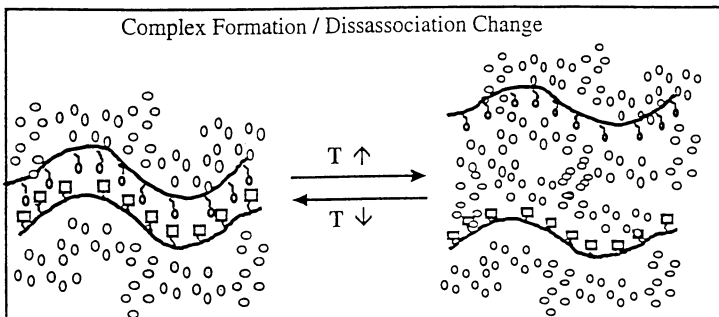


Fig. 2

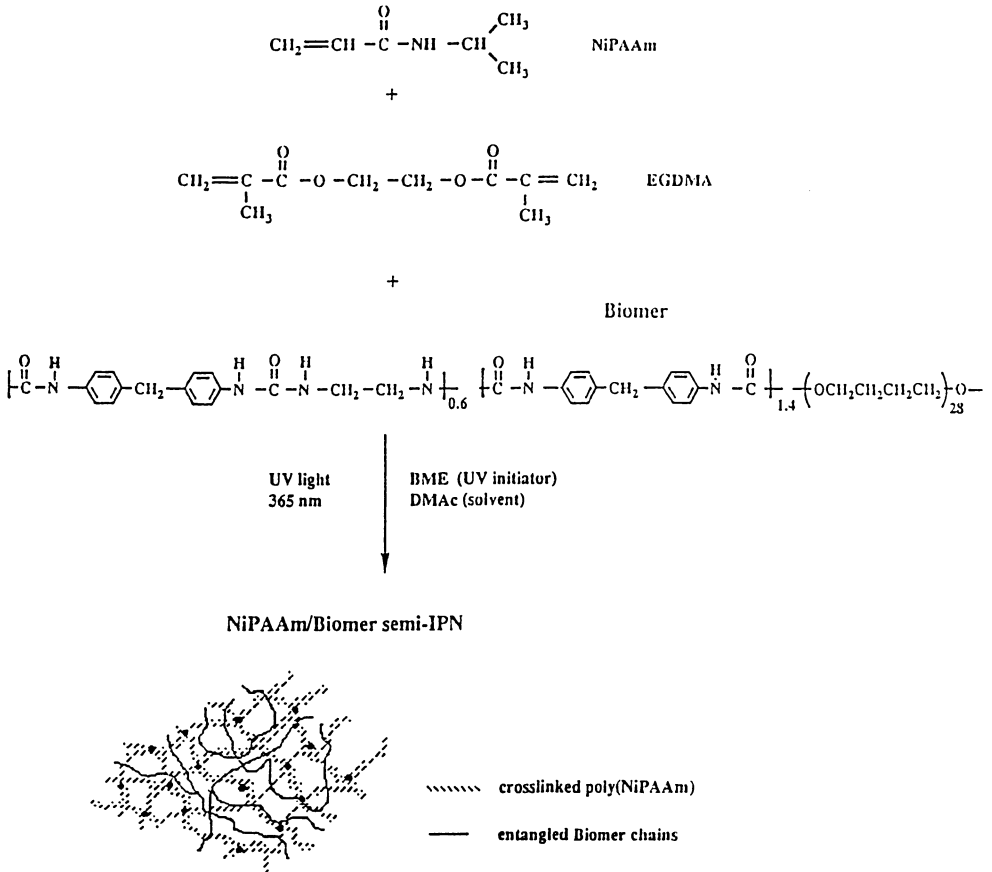


Fig. 3 Schematic diagram showing components and structure of NiPAAm/Biomer semi IPN's

Poly(acrylamide) gels normally swell with increasing temperature, while poly(N-alkyl substituted acrylamide) gels deswell. Under this influence, the thermosensitivity is attributed to the hydrophilic/hydrophobic balance of water-solubilized polymer chains and is readily affected by the size, configuration, and mobility of alkyl side groups, as an example, a sharp swelling transition occurs at 32°C for NiPAAm. These gels have been studied for applications in solute separations (22), concentrating dilute solutions (23), immobilization of enzymes (14) and for drug delivery, application and partition coefficients have been investigated in detail (24). Recently, thermally induced detachment of cultured cell has been attempted using grafted NiPPAAm (25). Hydrophobic butylmethacrylate (BMA) was introduced into gels to increase mechanical strength, and achieved complete "on-off" regulation of drug release in response to external temperature changes (26,27).

Recently, an IPN (interpenetrating polymer network) consisting of NiPAAm and polyurethane was studied for the delivery of the hydrophilic macromolecular drug, heparin (28). Both methods for the design of IPN and blended polymers are in Fig. 3 and Fig. 4. The NiPAAm polyurethane blend was coated onto a commercial polyurethane based catheter. The material was placed in a heparin solution at low temperature and extensive swells and drug loading occurred and the system will deswell in body temperature for the slow release heparin as shown in Fig. 5. The heparin loaded catheter was placed in a vein (canine) and demonstrated excellent blood biocompatibility (29).

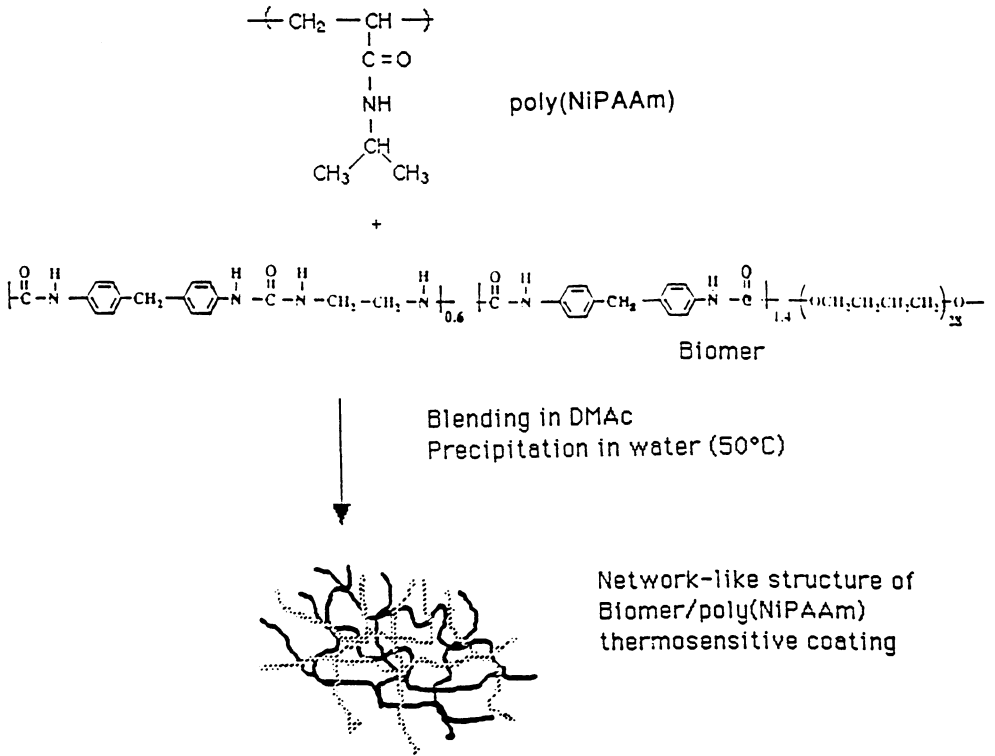


Fig. 4

Schematic diagram showing components used for the synthesis and the resulting network-like structure of Biomer/poly(NiPAAm) polymer blend.

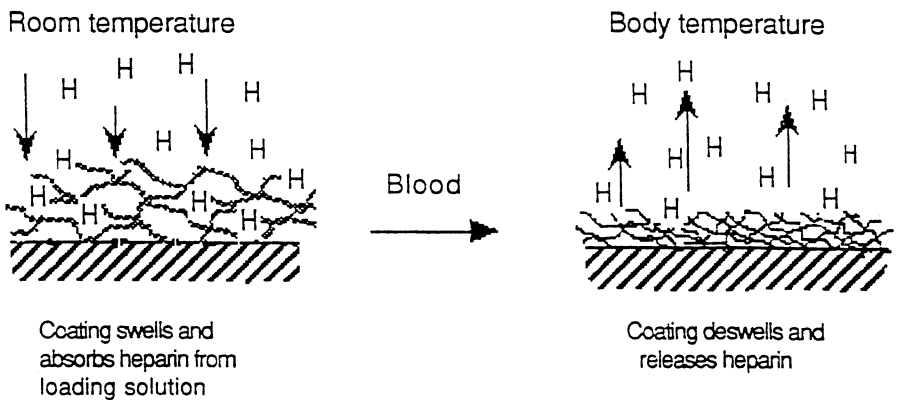


Fig. 5 Biomer/poly(NiPAAm)thermosensitive coatings as heparin releasing polymers

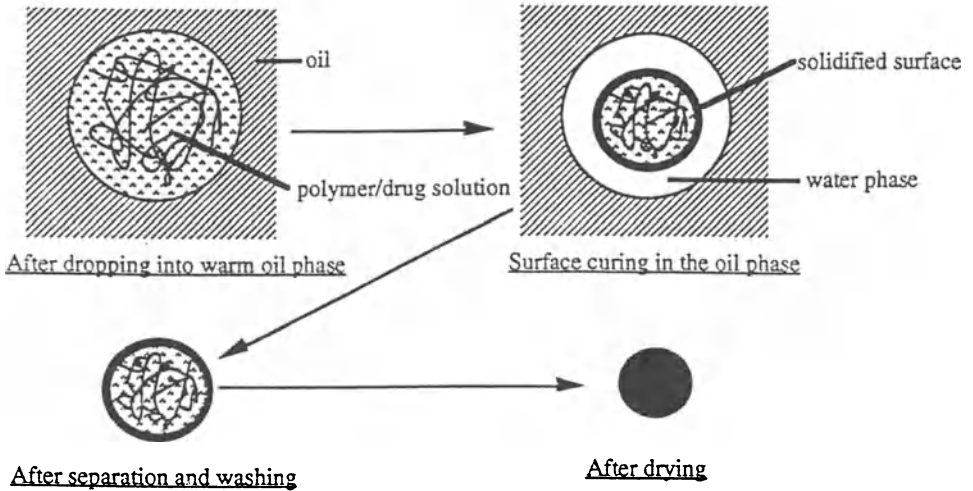


Fig. 6

A schematic presentation of bead formation from pH/temperature sensitive terpolymer

One advantage for the use of thermosensitive polymers is the possibility of peptide and protein loading in aqueous phase without organic solvent. The drug can be loaded in aqueous solution or less viscous gel at low temperature, and a gel or solid matrix can be formed spontaneously as the temperature increases. Based on this concept polymeric beads were made from linear pH/temperature-sensitive polymers, poly(N-isopropylacrylamide-co-butylmethacrylate-co-acrylic acid) and evaluated as a potential polypeptide drug carrier. The loading efficiency, pH-dependent release, and preservation of bioactivity of loaded drugs was studied. The beads were formed by precipitation of the polymers at the interface of a cold aqueous solution and warm oil phase, and subsequent drying process, as shown in Figure 6 (30).

The critical step in this bead formation and aqueous drug loading was found to be the initial formation of the skin layer, which was influenced by the oil bath temperature. The peptide drug loading efficiency was significantly increased by adjusting the ionic strength of the aqueous polymer/drug solution. As an example, the loading and release rate of insulin at pH 7.4 and 37°C was controlled by the acrylic acid content of the terpolymers, while minimal swelling and release were observed at pH 2.0 and 37°C, regardless of the acrylic acid content. The bioactivity of insulin released from the beads at pH 7.4 and recovered from the beads which were kept in rat stomach for 5 h was maintained. SEM of a bead obtained by this method showed smooth surface of bead with skin formation. Poly(NiPAAm)-co-butylmethacrylate-co-AA was also used to fabricate human calcitonin (hCT) delivery. By varying the percentage of AA, increased amounts of hCT were loaded into the polymer. The increased amounts of AA also helped to stabilize the protein. It was found that the hCT released from NiPAAm/BMA/AA was active, while hCT load in NiPAAm/BMA (noAA) lost activity. This was verified by CD studies which demonstrates hCT activity in acid polymers (31).

## REFERENCES

- [1] Sminoff LA, and Kim SW in *Pulsed and Self-Regulated Drug Delivery*, ed. by J. Kost CRC Press, Boca Raton, FL 1990 p.187.
- [2] Okano T, Bae YH, and Kim SW, *Ibid*, p.17.
- [3] Okano T, Yui N, Yokoyama M, and Yoshida R. Advance in Polymeric Systems for Drug Delivery, Japanese Technology Reviews Gordon and Breach Science, publisher, Vol. 4 (1) (1994).

- [4] Bronsted H, Ph.D. Thesis, University of Utah, (1991)
- [5] Peppas NA, and Klier J, J. Control. Rel., 16:203 (1991).
- [6] Dong LC, and Hoffman AS, J. Control. Rel., 15:141 (1991).
- [7] Siegel RA, Falamarzian M, Firestone BA, and Moxley BC, J. Control., Rel., 8:179 (1988).
- [8] Eisenberg SR, and Grodzinsky AJ, J. Memb. Sci., 19:173 (1984).
- [9] Osada Y, Adv. Poly. Sci., 82:1 (1987).
- [10] Yuk SH, Cho SH, and Lee HB, Pharm. Res. 9:955 (1992).
- [11] Kwon IC, Bae YH, and Kim SW, J. Control. Rel., 17:149 (1991).
- [12] Kwon IC, Bae YH, Kim SW, Nature, 354:291 (1991)
- [13] Kwon IC, Bae YH, and Kim SW, J. Contr. Rel. 30:155 (1994).
- [14] Hoffman AS, Afrassiaki A, and Dong LC, J. Control. Rel. 4:213 (1988).
- [15] Bae YH, Okano T, Hsu R, and Kim SW, Makromol. Chem. Rapid. Comm. 8:481 (1987).
- [16] Dong LC, and Hoffman AS, J. Control., Rel., 13:21 (1990).
- [17] Bae YH, Okano T, and Kim SW, J. Poly. Sci., Poly. Phys. 28:923 (1990).
- [18] Gutowska A, Bae YH, Feijen J, and Kim SW, J. Contr. Rel., 95 (1992).
- [19] Feil H, Bae YH, Fiejen J, Kim SW, Makromolekular Chemie, 14:465 (1993).
- [20] Feil H, Bae YH, Feijen J, and Kim SW, Macromolecules, 25:5528 (1992).
- [21] Feil H, Bae YH, Feijen J, Kim SW, Macromolecules, 26:2496 (1993).
- [22] Feil H, Bae YH, Feien J, and Kim SW, J. Membrane Sci., 64:283 (1991).
- [23] Gehrke SH, Andrews GP, and Cussler EL, Chem. Eng. Sci., 41:2153 (1986).
- [24] Palasis M, and Gehrke SH, J. Control. Rel., 18:1 (1992).
- [25] Yamada N, Okano T, Sakai H, Karikusa F, Sawasaki Y, and Sakurai Y, Makromol. Chem. Rapid. Comm., 11:571 (1990).
- [26] Okano T, Bae YH, Jacobs H, and Kim SW, J. Control. Rel., 11:255 (1990).
- [27] Bae YH, Okano T, and Kim SW, Pharmaceutical Research 8:624 (1991).
- [28] Gutowska A, Bae YH, Jacobs H, Feijen J, Kim SW, J. Biomed. Mater. Res. (in press)
- [29] Gutowska A, Bae YH, Jacobs H, Feijen J, Kim SW, J. Biomed. Mater. Res. (in press)
- [30] Kim YH, Bae YH, and Kim SW, J. Control. Rel. 28:143 (1994).
- [31] Serre A, Baudys M, and Kim SW, Pharm. Res., (submitted)

# **Biomedical Engineering**



# NOVEL BIOMATERIALS AS ARTIFICIAL CORNEA VIA PLASMA INDUCED GRAFTED POLYMERIZATION

Ging-Ho Hsiue<sup>1</sup>, Shyh-Dar Lee<sup>1</sup>, Chen-Yu Kao<sup>1</sup> and Patricia Chuen-Tsuei Chang<sup>2</sup>

1. Department of Chemical Engineering, National Tsing Hua University, Taiwan, R.O.C.

2. Department of Ophthalmology, Taichung Veterans General Hospital, Taiwan, R.O.C.

## SUMMARY

The primary objective of this study is to prepare a highly biocompatible polymer membrane by surface modification and to further develop an artificial cornea. Novel heterobifunctional membranes prepared by grafting different functional polymers onto silicone rubber membranes were achieved. In this work, we report preparation and surface characterization of the heterobifunctional membranes, and their biological analysis (*in vitro* and *in vivo* studies). Based on the biological analysis, the heterobifunctional membrane exhibits high potential to be used as artificial cornea.

**KEY WORDS:** plasma induced grafted polymerization, silicone rubber membrane, artificial cornea, epithelium, penetrating keratoplasty

## INTRODUCTION

When a progressive corneal ulceration or a penetrating corneal injury with tissue loss occurs, emergency penetrating keratoplasty (PK) or lamella keratoplasty (LK) is carried out to restore ocular integrity and to avoid further complications such as extensive chamber angle synechia, angle closure glaucoma and endophthalmitis (1-3). An artificial cornea is badly needed for PK or LK.

The preparation of artificial cornea has been under study in our laboratory (4). It is found that three important issues have to be dealt with if one is to obtain an artificial cornea. First, the implant is required to be completely covered with corneal epithelial cell (CEC). Secondly, downgrowth of CEC has to be suppressed when the implant is kept in the living cornea for a long period of time. Finally, the process of wound healing has to be considered because the implant need to be tightly fixed on the host cornea. Based on the above consideration, a heterobifunctional membrane is developed to be used as the artificial cornea (Figure 1). Upperside of the membrane is capable of improving the attachment and growth of cells, whereas lowerside of the membrane can suppress the adhesion strength of either cells or protein.

For the sake of comparison, a homobifunctional membrane is also developed. In this work, we report preparation, surface characterization and biological analysis on homobifunctional and heterobifunctional membrane. The grafting of 2-hydroxyethyl methacrylate (HEMA) or collagen serves the purpose of improving attachment and growth of CEC, whereas the grafting of 2-methacryloyloxyethyl phosphorylcholine (MPC) suppresses the downgrowth of CEC (5).

## MATERIALS AND METHODS

MPC is supplied by Prof. N. Nakabayashi (Tokyo, Japan). 1,1-diphenyl-2-picrylhydrazyl (DPPH)

was used to determine the amount of peroxides on surface of silicone rubber membrane (SR) by Ar-plasma treatment. Collagen type I (Sigma) was utilized to improve attachment of epithelium. Plasma Treatment: SR was activated by Ar plasma treatment. Moreover, the peroxide group was produced by exposing samples in oxygen gas.

## RESULTS

### Peroxide group analysis SIMS study

Negative spectra of SIMS for controlled SR and Ar-plasma treated SR are shown in Figure 2. For controlled SR (Figure 2(A)), the main peak appears at 15 D, which is  $-\text{CH}_3$  group. A 33 D peak is observed in Figure 2(B). This peak reflects the formation of peroxides on the surface of Ar-plasma treated SR.

### DPPH study

In Figure 3, the amount of peroxides is plotted as a function of plasma treatment time. Maximum amount of peroxides was reached at treatment times of 60 s, 60 s, 80 s at different treatment powers of 60 W, 30 W, and 5 W, respectively. However, the amount of peroxides started to decrease when plasma treatment time was more than that for reaching maximum amount of peroxides in each case. This is due to the fact that the peroxides are partially converted into an inactive species after prolonged plasma treatment. Furthermore, amount of active peroxides is studied as a function of storage time ( $30^\circ\text{C}$ , air). The peroxide concentration can be maintained constant within a time period of 2 h. However, it would quickly decay to 50 % of the original concentration at a storage time of 4 h, and would completely decompose at a storage time of 12 h. Therefore, graft polymerization must be carried out within the interval of 2 h after plasma treatment.

### Grafted polymerization ATR-FTIR study

The grafting of various polymers on the surface of SR was achieved as evidenced by ATR-FTIR study. The absorption peaks of hydroxyl group and carbonyl group appeared at  $3300\text{ cm}^{-1}$  and  $1720\text{ cm}^{-1}$ , respectively, when pHEMA, pAA, or pMPC was grafted onto SR.

### ESCA study

The high resolution C1s of ESCA spectra for various SR grafted with different polymers were obtained. The C1s spectra was deconvoluted by different functional peaks such as 285 eV ( $-\text{C}-\text{H}$ ), 286.4 eV ( $-\text{C}-\text{N}$ ), 287.7 eV ( $-\text{C}-\text{O}$ ), 289.1 eV ( $-\text{HN}-\text{C}=\text{O}$ ), and 290 eV ( $\text{O}=\text{C}-\text{O}$ ). The values of the deconvoluted peaks are listed in Table 1. Binding energies of  $-\text{OH}$  and  $-\text{C}=\text{O}$  group were found for the spectra of both SR-g-HEMA and SR-g-AA. Binding energies of  $-\text{C}-\text{N}$  and  $-\text{NH}-\text{C}=\text{O}$  were also found for the spectra of SR-g-MPC and SR-g-AA-collagen, respectively. SR grafted with pHEMA, pAA, pAA-collagen, and pMPC by plasma modification was achieved as confirmed by ESCA study.

### Biological analysis *In vitro* study

The cellular biocompatibility was considered according to four aspects (6): 1. the basal cellular function related to cell proliferation and cell protein content; 2. the specific related to its

morphology and synthesis of functional protein; 3. the bioactivation of the cell phenotype expression; 4. the integration of cell based on the attachment to foreign matrix. As a result of the above consideration, the ability of migration, attachment and proliferation of CEC were investigated to define the reaction of cellular entity with the various modified SRs in our study. Migration and proliferation of CEC to controlled SR were negligible (Figure 4(A), Figure 5). The morphology of CEC attaching onto the surface of controlled SR was poor as evidenced by the presence of CEC pseudopodium (Figure 6(A)). Moreover, migration of CEC from cornea to the surface of SR-g-MPC did not occur (Figure 4(B)). In CEC attachment study, a few suspended cells were found for SR-g-MPC, which did not adhere and grow onto the surface. This indicated that the morphology of CEC onto the surface of SR-g-MPC was abnormal (Figure 6(B)). The proliferation of CEC onto SR-g-MPC was also suppressed completely (Figure 5). Evidently, the surface of SR-g-MPC was incapable of CEC migration, attachment and growth. This is due to the fact that MPC contains polar head group of phospholipid (7). Additionally, CEC migration from cornea to respective SR-g-HEMA and SR-g-AA-collagen was observed and CEC spread fully over the surfaces within 96 h (Figure 4(C), 4(D)). Moreover, CEC attaching onto these surfaces was confluent within 72 h (Figure 7), and morphology of CEC on these surfaces was similar to that of normal CEC (Figure 6(C), 6(D)). In the proliferation study, SR-g-HEMA and SR-g-AA-collagen were found to be capable of providing a suitable environment for CEC growth (Figure 5). A layer of pHEMA grafted onto SR serving as a water content surface is responsible for SR-g-HEMA's excellent proliferation behavior. The satisfactory results of *in vitro* evaluation for the biocompatibility of SR-g-HEMA, SR-g-AA-collagen and SR-g-MPC allowed us to further proceed to *in vivo* study.

### ***In vivo* study**

PK technique was used and rabbits were served as animal model. Anterior chamber (AC) depth was measured by slit lamp microscope to evaluate the occurrence of CEC downgrowth. For homobifunctional SRs study, AC depth was lost for controlled SR at post-operative week one (Figure 8(A)). This implied that iris was adhered to the SR surface, and subsequently downgrowth of CEC occurred (3). At post-operative week three, the AC depth for SR-g-HEMA and SR-g-AA-collagen were less deeper than that of normal AC. Additionally, a depth of AC for SR-g-MPC was similar to that of normal AC (Figure 8(B)). The iris was not adhered to the surface of SR-g-MPC. Therefore, the downgrowth of CEC was not occurred. Some of complications also have been observed. The peripheral opacity of eye for controlled SR and SR-g-AA-collagen was observed. The peripheral neovascularization of eye for SR-g-AA-collagen was also revealed. Furthermore, the modified SRs were stained by immunofluorescence to evaluate the migration of CEC. In Figure 9, The immunofluorescence views of photographs for controlled SR and SR-g-MPC were shown to be white color. This indicated that the migration of CEC was not occurred in these samples. On the other hand, the CEC covered completely over the surface of SR-g-HEMA or SR-g-AA-collagen at post-operative week three.

For the heterobifunctional membrane, upperside and lowerside surfaces were grafted with collagen and MPC, respectively. It was found that a depth of AC was kept (Figure 10(A)). CEC covered completely over the SR upperside surface as shown in Figure 10(B). The upperside surface grafted with collagen was capable of improving the CEC migration from the host cornea, whereas the iris was not observed on the lowerside surface grafted with MPC. This indicated that no adverse reaction of inflammation such as vascular invasion for heterobifunctional membrane occurred. The heterobifunctional membrane is indeed promising for clinic application as judged by *in vivo* study.

### **CONCLUSION**

Alterations in the physicochemical properties of the modified SR surfaces prepared by plasma

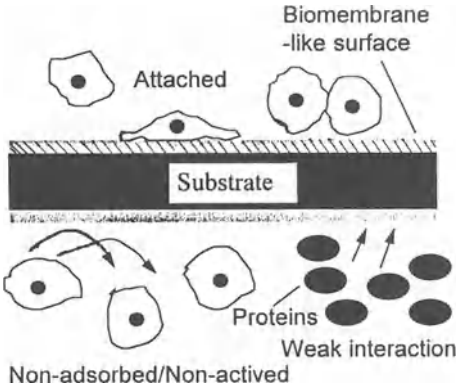


Figure 1. Schematic for biofunction of heterobifunctional membrane

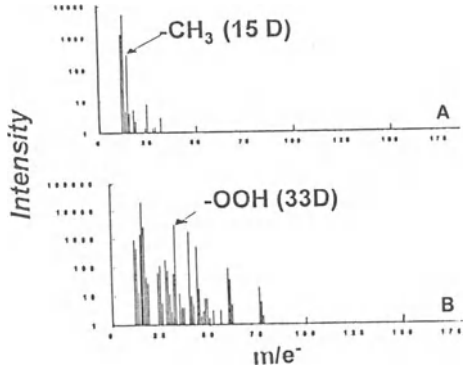


Figure 2. Negative spectra of SIMS for A. controlled SR, B. Ar-plasma treated SR (60 W, 60 s, 200 mtorr)

Table 1. The ratio of functional group on various surface of silicone rubber membrane by ESCA

Sample	C-H (285)	C-N (286.4)	C-O (287.7)	-HN-C=O (289.1)	O-C=O (290)
Control	100.00	-----	-----	-----	-----
Ar-plasma*	77.81	-----	15.21	-----	6.98
pHEMA(75)	53.01	-----	33.37	-----	13.63
pAA(420)	35.02	-----	42.27	-----	22.71
Collagen(100)	43.37	-----	16.73	27.15	12.75
pMPC(175)	40.61	21.10	10.14	-----	28.15

$\mu$  g/cm<sup>2</sup> is unit, \* 60W, 200 mtorr, 60 sec

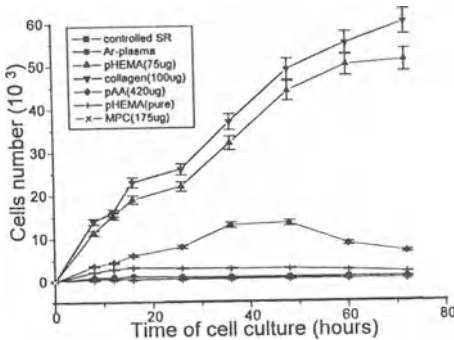


Figure 5. Proliferation of epithelium onto various modified SR

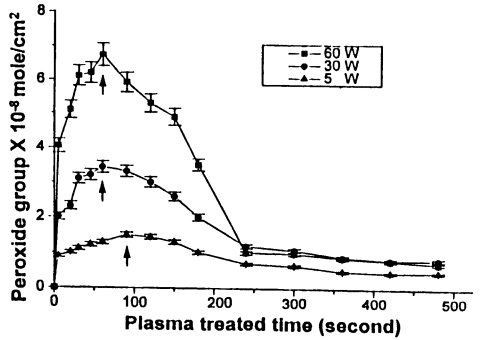


Figure 3. Formation of peroxide group on SR using Ar-plasma treatment

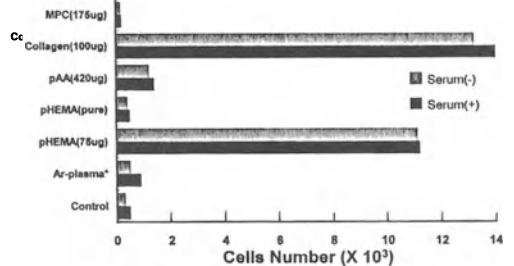


Figure 7. Attachment of epithelium onto various modified SR

induced graft polymerization were achieved and assessed by a combination of SIMS, ATR-FTIR and ESCA. A novel type of heterobifunctional membrane with upperside favoring cells attachment and growth, and lowerside suppressing cells adhesion is successfully developed. The excellent affinity of CEC for SR-g-HEMA and SR-g-AA-collagen are evaluated by three methods of in vitro study, whereas SR-g-MPC exhibits the poor capacity of CEC. This heterobifunctional membrane is found to be potentially applicable for artificial cornea based on *in vitro* and *in vivo* studies. Long term evaluation of an animal model and pathology study will be carried out to further application of artificial cornea in the near future.

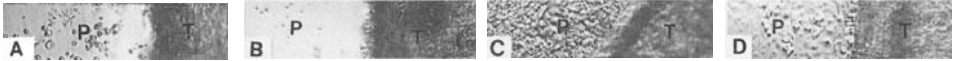


Figure 4. Migration of epithelium for A. controlled SR, B. SR-g-MPC, C. SR-g-HEMA, and D. SR-g-AA-collagen

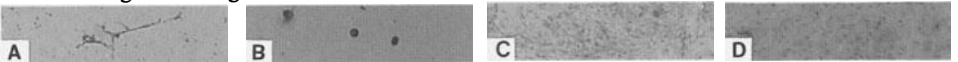


Figure 6. Morphology of epithelium onto A. controlled SR, B. SR-g-MPC, C. SR-g-HEMA, and D. SR-g-AA-collagen

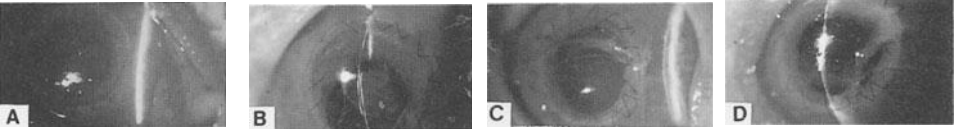


Figure 8. Slit lamp photographs for A. controlled SR, B. SR-g-MPC, C. SR-g-HEMA, and D. SR-g-AA-collagen

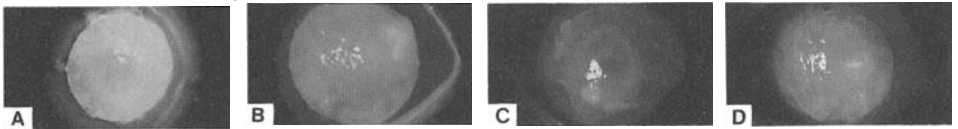


Figure 9. Immunofluorescence photographs for A. controlled SR, B. SR-g-MPC, C. SR-g-HEMA, and D. SR-g-AA-collagen

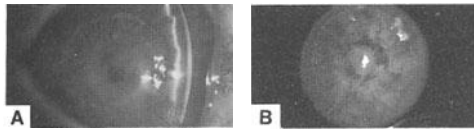


Figure 10. A. slit lamp photographs, B. immunofluorescence photographs for heterobifunctional membrane

This work is supported by the National Science Council of Republic of China (NSC83-0420-B075A-018M018) and VGH-NTHU Joint Research Program (VGHTH 83-021-2).

## REFERENCES

1. Cardona H, M.D. (1967), Keratoprothesis with a plastic fiber meshwork supporting plate, *Keratoprothesis*, 64(2), 228-233
2. Girard LJ, M.D. (1977), Keratoprothesis: a 12-year follow-up, *Symposium on Keratoprothesis*, 83, 252-267
3. Kobayashi H, Ikada Y, Moritera T, Ogura Y (1991), Collagen-immobilized hydrogel as a material for lamellar keratoplasty, *J. Applied Biomaterials*, 2, 261-267
4. Hsiue GH, Lee SD, Wang CC (1993), The effect of plasma induced grafted copolymerization of HEMA on silicone rubber towards improving corneal epithelial cells attachment and growth, *J. Biomater. Sci.; Polym. Edn.*, 5(3), 205-220
5. Ueda D, Oshida H, Ishihara K, and Nakabayashi N (1992), Preparation of 2-methacryloyloxyethyl phosphorylcholine copolymers with alkyl methacrylates and their blood compatibility, *Polymer J.*, 24(11), 1259-1269.
6. Harmand MF, Bordenave L, Duphil R, Jeandot R, Ducassou D (1985), Human differentiated cell cultures: in vitro models for characterization of cell/biomaterial interface, *Advances in Biomaterials*, 6, 361-366.
7. Watanabe A, Kojima M, Ishihara K, and Nakabayashi N (1989), Interaction of platelets and cultured cells with polymers containing phospholipid polar groups, *Reports of the Institute for Medical & Dental Engineering*, 23, 31-39.

## Ultrathin Polymeric Films as Biomedical Interfaces of Controlled Chemical Architecture

David W. Grainger, Guogiang Mao, David G. Castner\*

Department of Chemistry, Colorado State University, Fort Collins, CO 80523-1872

\*Department of Chemical Engineering, University of Washington, Seattle, WA 98195

### ABSTRACT

Polysiloxanes derivatized with alkyldisulfide anchors have been grafted with hydrophobic perfluoroalkyl or hydrophilic poly(ethyleneoxide) side chains. These terpolymers chemisorb spontaneously from dilute solution to metal substrates (gold, silver, copper), forming adherent monolayer polymer films expressing the surface chemistry of the grafted chain. High-resolution XPS, SIMS and ToF-SIMS have shown that those polymer films: (1) are stratified monolayers, having distinct regions enriched in each component, (2) are enriched in their outer atomic surface levels by the grafted side chain and (3) can be lithographed and patterned to form spatially tailored films of distinct chemistry. The robust character of these films has several advantages over conventional self-assembled monolayers, particularly for many applications where film oxidation/removal is a problem (e.g., biological environments, sensing, mechanics, friction).

### KEY WORDS

Self assembly, surface modification, ultrathin films, gold, poly(siloxanes)

### INTRODUCTION

We have pursued a new strategy for controlling the interfacial chemistry and architecture of polymer surfaces. This method combines principles of organization adapted from both Langmuir-Blodgett and self-assembled organic arrays(1,2). Polymer films, one molecular layer in thickness (30Å), bind spontaneously to solid surfaces, mediated by chemisorption. Multipoint polymer anchoring stabilizes these arrays from conditions that destroy monomeric self-assembled films. Micro-patterned chemistry can be fabricated using lithographic methods, coating pre-lithographed gold lines or directly milling structures from films. More importantly, grafting of these polymers with pendant, non-anchoring functional side chains, the chemisorbed polymer films are enriched with this grafted chemistry in their outer surface. This provides a convenient route to tailoring polymer surface properties for a number of applications where thin stable organic films are required, including biomedical surfaces. Our work has investigated many features of these ultrathin polymer arrays on surfaces(3-7).

## MATERIALS AND METHODS

### Polymer synthesis

We have reported the synthesis and characterization of a number of polymers and their respective assemblies as bound monolayers on solid surfaces(3-7). Generally, our strategy follows a polymer analog reaction, where linear polymer chains are grafted with sulfur or silane terminated alkyl chains. In some cases, an additional side chain chemistry is grafted, creating a terpolymer with a specific chemical character. Perfluoroalkyl and poly(ethylene oxide) grafts have been a focus. Two basic families--poly(acrylates) and polysiloxanes--have been investigated. Figure 1 shows the architectures we have studied as thin films.

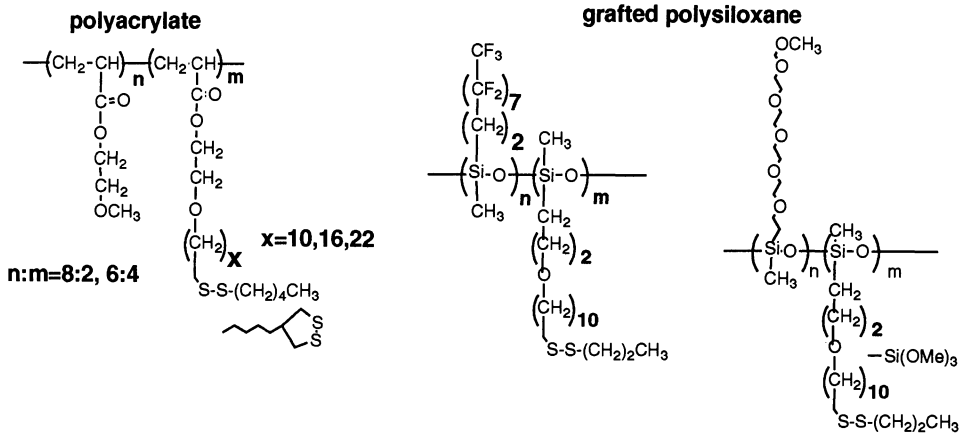


Figure 1: Chemical structures for polymeric ultrathin film-forming materials(3-7).

Polymer molecular weights are typically 40,000-60,000. However, we have investigated a cyclic siloxane oligomer with pendant mercaptopropyl chains(4). In addition, we have combined polymer films with monomeric alkyl or perfluoroalkyl thiols in composite thin films(4, unpublished work).

### Polymer Monolayer Films Assembly

Gold substrates for dithioalkyl-polysiloxane self-assembly were freshly prepared by evaporative deposition of a layer of 1500-2000Å gold (99.999%, Johnson-Mathey) onto Pd-coated (200 Å) silicon wafer surfaces in a diffusion-pumped thermal evaporator at a base pressure of  $6 \times 10^{-7}$  Torr. Immediately following deposition, the chamber was back-filled with purified  $\text{N}_2$ . These gold-coated substrates were immediately cut into 3 cm  $\times$  0.8 cm pieces and immersed into polymer- $\text{CHCl}_3$  solutions (0.1-1.5 mM) for up to 72 h, followed by thorough, sequential rinsing with  $\text{CHCl}_3$ , EtOH, and Millipore water, and drying under pure  $\text{N}_2$ . Monomeric self-assembled films of octadecane thiol and pentanethiol were fabricated for comparison from dilute ethanolic solutions on identical gold substrates.

### Polymer Ultrathin Film Characterization

Ellipsometry has been used to measure film thickness on gold(3). Contact angle analysis uses both water and hexadecane as probe liquids. Reflectance FTIR (polarized) has also been

used(3) to analyze polymer structure. Cyclic voltammetry using aqueous phase redox probes has been applied to characterize film microstructures on gold electrodes(4,6,7). Angular dependent x-ray photoelectron spectroscopy and static secondary ion mass spectrometry have proven critical for high-resolution chemical and structural information on assembled films. Instrumentation has been made available through NESAC/BIO, the Surface Analysis Center at University of Washington.

### **Patterning of Surface Chemistry**

We have applied lithographic processes to create two types of micropatterned organic thin films with the intent to grow cells within borders or directionally along surfaces. Conventional photolithographic methods were used to fabricate micron-scale gold lines on semiconductor-grade silicon oxide wafers in a commercial integrated circuit fabrication process in a Class 100 clean room. A second method was used to etch patterns into homogeneous thin films assembled on unpatterned gold surfaces using an automated commercial ion mill (610 Series focused ion beam workstation manufactured by FEI Company, Hillsboro, OR). Milled patterns were 20  $\mu\text{m}$  long lines with widths varying from 0.5 to 2.0  $\mu\text{m}$ . High resolution imaging of patterned film chemistry has been performed at PHI Electronics (Minnesota) using a state-of-the-art time-of-flight SIMS instrument.

## **RESULTS AND DISCUSSION**

### **Film Surface Chemistries**

A substantial amount is already known about SAM films on gold.[2] The interfaces of these films present an organized array of functional groups, depending on their chemistry. This interface can be analyzed by wet (contact angle) and dry (UHV surface analysis) techniques to investigate interfacial properties. For example,  $\text{CF}_3$ -terminated alkythiols have a layer thickness of 17 $\text{\AA}$  (monolayer) an aqueous contact angle of 111° (hydrophobic), and XPS and SIMS spectra consistent with dense-packed arrays of perfluoroalkyl chains packed nearly perpendicular to the gold surface. Octadecane thiol, by contrast, has a monolayer thickness of 25 $\text{\AA}$ , a contact angle of 100°, and XPS and SIMS spectra consistent with a dense hydrocarbon layer tilted 30° off normal on the gold surface. The higher-energy, shorter thioundecylalcohol has a layer thickness of 17 $\text{\AA}$ , a contact angle of 40° (hydrophilic) and XPS and SIMS spectra consistent with a dense-packed array of hydroxyl groups. Each system presents an organized chemical array at the interface.

Polymeric surfaces, while much more stable and durable, tend to have more defects and holes than monomeric SAM monolayers, presumably because large molecule anchoring precludes the required side chain close-packing. Nevertheless, we have shown that interesting polymer surface structures and surface chemistries, all in a monolayer arrangement on a solid support, are possible with such a strategy.[11-15] Bound monolayer polymeric arrays can present surfaces grafted with perfluoroalkyl chains or hydrophilic polyethylene oxide, both surfaces of biomedical interest. Each surface reacts uniquely to protein and cellular environments (unpublished data). Additionally, lithographed and patterned surfaces at the sub-micron level are readily formed from all of these monolayer assemblies, allow surface chemistry to be tailored spatially and permitting presentation of defined surface chemical patterns on surfaces at high resolution to biological systems.

### **Angular-dependent X-ray photoelectron spectroscopy (ADXPS)**

Figure 2 shows a typical high resolution XPS carbon 1s spectrum, detailing the four types of carbon in monolayer films of siloxane terpolymers on gold. The peak centered at 285 eV is characteristic of the hydrocarbon species (e.g.,  $\text{CH}_2$  present in the alkyl side chains while the



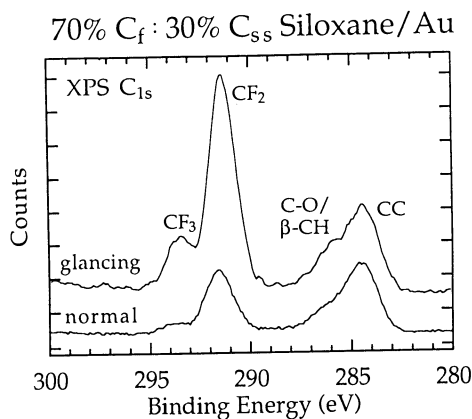


Figure 2: XPS C1s spectra for perfluoroalkyl-grafted polysiloxane monolayer surface.

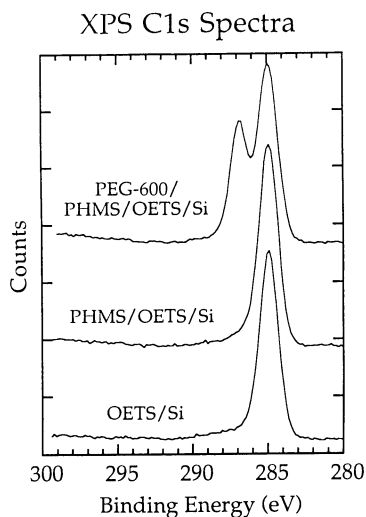


Figure 3: XPS C1s spectra for PEO-grafted polysiloxane monolayer surface.

peak at 287 eV results from C-O (ether) carbon present in the side chains. Fluorocarbon species present in the perfluoroalkyl side chains give rise to the peaks at 292 eV ( $\text{CF}_2$  groups) and 294 eV ( $\text{CF}_3$  groups). Quantitation of high-resolution spectra from the various chemical species in these systems can be compared as a function of depth to yield depth-dependent comparisons of film composition. The increasing F:C ratio with decreased sampling depth is consistent with the presence of a perfluorocarbon overlayer at the films' outermost surfaces attenuating the carbon signals from film layers underneath. Additionally, as a function of decreasing depth, fluorine signal increases beyond the stoichiometric bulk content, further supporting the presence of an enriched perfluorocarbon overlayer in these polymer monolayer films. This is paralleled by the predicted opposite trend in carbon signal with take-off angle; that is, a consistent decrease in carbon below its bulk content with increasing take-off angle (decreasing depth). Sulfur content steadily decreases with decreasing sampling depth, reaching concentrations significantly below the stoichiometric bulk content at the shallowest sampling depth. This observation is consistent with the sulfur anchor groups located under the films adjacent to the gold interface. Furthermore, because the silicon signal remains roughly constant despite the various changes in other species with sampling depth, the ratios of fluorine:silicon, carbon:silicon and sulfur:silicon are further evidence for a layered polymer monolayer structure: perfluoroalkyl-enriched outer surface layer, siloxane-enriched intermediate stratum, and an anchoring layer containing sulfur (disulfide) anchoring chains.

Therefore, the structural picture supported by FTIR, XPS and SIMS data on these monolayer films is one where perfluoroalkyl side chains extend away from the substrate-anchored siloxane backbone to enrich the outermost film region in an orientation more vertical than horizontal to the substrate plane. The only specific chemical interactions mediating this organization are the gold-thiolate bonds formed by anchoring side chains. This ensures that some fraction of the alkyldisulfide grafted chains are directly adjacent to the gold surface. Intrinsic immiscibility between this anchored alkyl component and more mobile siloxane and perfluoroalkyl substituents promotes formation of a stratified organic film, rich in perfluorinated groups near its surface.

Poly(ethylene oxide) (PEO) grafts can also be added to these films using several strategies(8). We have grafted PEO to siloxane backbones prior to film assembly, after film assembly or in a sequential manner: binding a self-assembling anchoring layer, then attaching the polymer backbone and then grafting PEO. Figure 3 shows a series of XPS spectra for PEO-grafted siloxanes as covalently assembled on surfaces sequentially. An olefin-terminated monomeric self-assembled film was first deposited and then derivatized with polysiloxane using hydrosilation chemistry. This is seen clearly in the differences between the lowest XPS curve (hydrocarbon only) and the middle XPS curve. PEO was then added covalently to the siloxane layer on the surface. The characteristic ether peak for C-O bonds is seen adjacent to the hydrocarbon signal from the siloxane backbone.

## CONCLUSIONS

Ultrathin polymer films with an array of biomedically relevant chemistries can be formed as stable, chemically bound monolayers on surfaces. These surfaces express the chemistry of their side chain grafts as an enriched side chain overlayer within a 30Å film architecture. Like their monomeric self-assembled organothiols analogs, these polymer films should exhibit interesting and useful properties as biomedical interfaces, yet without the stability/oxidation problems that the monomer films experience. Use of these polymers to mimic or immobilize heparin, attach proteins, act as sensor substrates and other surface modification applications is anticipated.

## ACKNOWLEDGEMENTS

We gratefully acknowledge continued assistance and collaboration from Professor D. G. Castner and Professor B. D. Ratner, NESAC/BIO, University of Washington, and Dr. P. McKeown (PHI Electronics) for surface analytical support. Support from the Whitaker Foundation and the National Science Foundation (Division of Materials Research) has been essential for pursuit of this work.

## REFERENCES

- Whitesides GM, Mathias JP, Seto CT (1991) Molecular self-assembly and nanochemistry. *Science* 254:1312-1319
- Ulman A (1991) An introduction to ultrathin organic films. Academic, Boston, MA
- Sun F, Castner DG, Grainger DW (1993) Ultrathin Self-Assembled Polymeric Films on Solid Surfaces. 2. Formation of 11-(n-Pentylidithio)undecanoate-Bearing Polyacrylate Monolayers on Gold. *Langmuir* 9:3200-3207
- Sun F, Grainger DW, Castner DG, Leach-Scampavia D (1994) Adsorption of Ultrathin Films of Sulfur-Containing Siloxane Oligomers on Gold Surfaces and Their In Situ Modification. *Macromolecules* 27: 3053-3062
- Sun F, Mao G, Grainger DW, Castner, DG (1994) Polymer Ultrathin Films by Self Assembly: Bound Perfluorinated Monolayers and Their Modification Using in Situ Derivatization Strategies. *Thin Solid Films* 242:106-111
- Sun F, Lei Y, Grainger DW (1994) Ultrathin Self-Assembled Polymer Films on Solid Surfaces. 4. Electrochemical Analysis of Film Microstructure on Gold Electrodes. *Colloids Surf A: Physicochem Eng Aspects* 93: 191-200
- Sun F, Castner DG, Mao G, McKeown P, Grainger DW (1995) Organization of Perfluorinated Polymeric Ultrathin Films on Solid Interfaces by Self-Assembly. *J Am Chem Soc*, in press
- Mao G, Castner DG, Grainger DW (1995) Ultrathin Polymer Films Fabricated by a Sequential Approach Based on Self-Assembly. *Chem Mater*. submitted

## RANDOMNESS AND BIOSPECIFICITY : RANDOM COPOLYMERS ARE ENDOWED WITH BIOSPECIFIC PROPERTIES

Marcel Jozefowicz and Jacqueline Jozefonvicz

L.R.M - CNRS - URA 502 - Inst. Galilée - U.P.N. - Av J.B. Clément - 93430 Villeteuse - France.

### SUMMARY

Biocompatible polymers should induce appropriate response from the host living bodies. Therefore they should be able to deliver appropriate messages. Biospecific random copolymers obtained by random substitution with suitable chemical groups of polymers like crosslinked polystyrene are biomaterials capable of mimicking the natural messenger molecules of a living system. The biospecific activities of the random copolymers depend on the overall chemical composition of the final product. Indeed, random copolymers endowed with antigen-like abilities have been synthesized. We recently developed a detailed analysis of the chemical structure of the specific sites responsible for the "factor VIII - like antigen" or "DNA-like antigen" properties of polystyrene derivatives synthesized by random derivatization. As a consequence, it appears that biospecificity is a continuous function of randomness from purely statistical distribution of chemical functional groups to the strictly defined chemical structure of ligand receptor molecules in living system.

**KEY WORDS :** Biospecificity Random Polystyrene derivatives - Factor VIII-like antigen - DNA-like antigen

### INTRODUCTION

Each constituent of any living system exchanges messages with its environment. These are essentially of electrical and chemical nature. As a consequence, each constituent of a living system behaves normally when it receives, from the environment, normal messages both qualitatively and quantitatively. As early as 1894, Emil Fischer showed that the basis of molecular recognition between a substrate and its binding site is the "key-lock system" implying geometrical complementarity and meaning that the recognition of chemical messengers is based on the formation of a specific complex between the messenger and its receptor. Polymeric messengers can be generated by grafting synthetic keys on a polymer backbone. Alternatively this goal has been reached in case of antigen-like polymers by random substitution of polystyrene with suitable chemical groups capable of mimicking the functional groups borne by the natural antigen. These random copolymers are endowed with either factor VIII - like or DNA-like antigen capacities.

### BIOACTIVE COPOLYMERS AND ANTIBODIES

Antibodies are proteins, immunoglobins (Ig), which are produced by B lymphocytes when they recognize a definite antigen. Antigens are toxins, proteins, DNA or may be molecules at the surface of a foreign biomaterial. The specificity of antibodies directed against an antigen such as factor VIII (FVIII) or DNA is correlated with the chemical nature of the variable regions present into the Fab fragment of these antibodies. Insoluble polystyrene derivatives with suitable chemical groups randomly grafted onto the macromolecule backbone possess sequences capable to have some similar structural aspects of the antigen. These constitute bioactive sites i.e. keys involved in the establishment of specific interaction with a given antibody. When anti-FVIII or anti-DNA antibodies

are under consideration, the above mentioned suitable groups are on the one hand sulfonate groups and on the other, either methylester tyrosylsulfamide groups [1] or phosphodiester groups respectively [2] (Fig. 1).

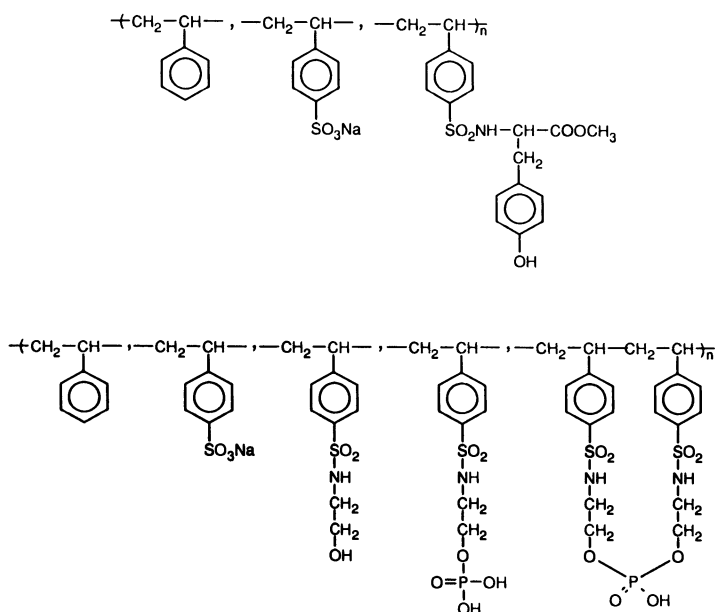


Fig.1 General chemical structures of derivatized polystyrene resins : Polystyrenes bearing sulfonate and methylester tyrosylsulfamide groups (TyrOMe) and polystyrene bearing sulfonate, hydroxyethyl sulfamide, hydroxyethyl sulfamide phosphomonoester (PME) and phosphodiester (PDE).

### Derivatized polystyrene and anti-FVIII antibodies

Factor VIII (FVIII) plays an important role in the maintenance of hemostasis. Its deficiency results in a severe bleeding disorder referred to as haemophilia A. Some severely affected haemophilic A patients (10%) develop antibodies against FVIII resulting in a rapid neutralization of FVIII in patients treated with FVIII concentrates. Various therapeutic approaches have been proposed to deplete plasma of these antibodies based on extensive plasma exchange but they remain non-specific methods and present some risks for the patients. It is therefore of interest to prepare synthetic immunoabsorbents able to interact specifically with anti-FVIII antibodies. Several studies have identified a specific sequence on the FVIII molecule as parts of the binding sites to the antibodies which neutralizes FVIII procoagulant activity. Indeed it was found that residues Asp<sup>1663</sup> - Ser<sup>1669</sup> neutralized FVIII activity [3]. We postulated that the methylester tyrosylsulfamide groups were able to mimic part of the FVIII epitopes recognized by anti-FVIII antibodies, taking into account that the binding regions of FVIII to these antibodies is often located at or near a tyrosyl residue. Based on this hypothesis, crosslinked polystyrene beads were randomly substituted with different overall ratio of sulfonate groups and methylester tyrosylsulfamide groups (TyrOMe). The adsorption of these antibodies in dynamic conditions using a chromatographic process was assessed. Haemophilic plasma containing anti-FVIII antibodies was loaded onto a column and kept under circulation. The residual concentration of anti-FVIII antibodies and total IgG was determined. Results show that the adsorption of anti-FVIII antibodies and total IgG onto the derivatized polystyrene beads which overall rates of substitution of TyrOMe groups were different, depends on the rate of these groups (Fig.2). It has to be emphasized that beads with a substitution ratio from 15 to 25% of TyrOMe are

those which show maximal adsorption of anti-FVIII antibodies while the same beads adsorb minimally the total IgG.

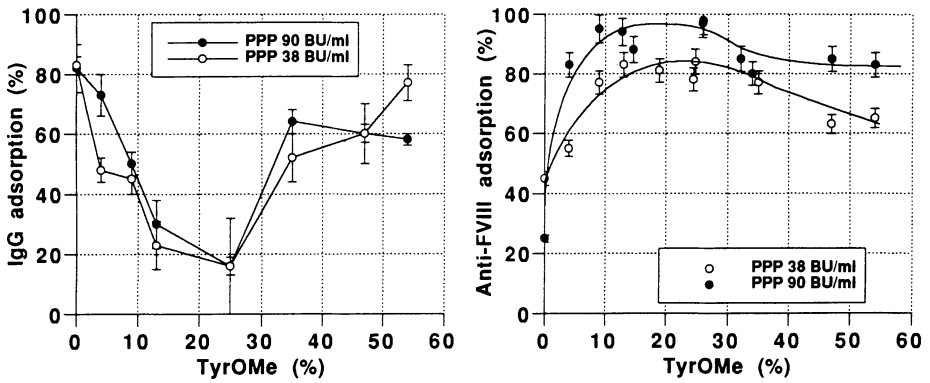


Fig. 2 Adsorption of anti-FVIII antibodies and total IgG to polystyrene beads derivatized with methylester tyrosylsulfamide groups from haemophilic plasma which anti-FVIII titer was 90 BU/ml and 38 BU/ml respectively (BU : Bethesda Unit).

Adsorption isotherms of anti-FVIII antibodies from haemophilic plasma and of total IgG from normal plasma, respectively, onto a number of derivatized styrene beads have been established using ELISA and clotting time procedures [4]. Results show that the adsorption obeys the Langmuir law. This allowed us, to calculate the apparent affinity constants ( $K_{aff}$ ). The  $K_{aff}$  values of anti-FVIII antibodies are relatively high ( $10^9 M^{-1}$ ) and a maximum is observed at about 15 to 25 % of TyrOMe groups while, those of total IgG are low (between  $10^4$  and  $10^5 M^{-1}$ ) (Fig 3).

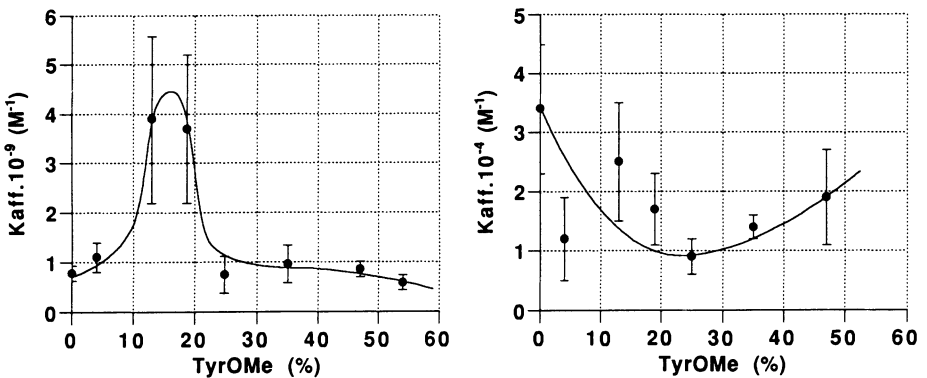


Fig 3 Apparent affinity constants ( $K_{aff}$ ) of anti-FVIII antibodies and total IgG, respectively, versus the percentage of units bearing TyrOMe groups for different derivatized polystyrene beads.

The results demonstrate that random substitution of polystyrene with sulfonate and methylester tyrosylsulfamide groups endows the resulting random copolymer with the ability to interact specifically with the anti-FVIII antibodies of haemophilic A patients. Moreover the above results

imply that specific sites are created onto the polymer as a result of the random substitution. These sites mimic the epitopes of the FVIII molecules involved in the interaction with the antibodies. They are constituted of a combination of sulfonate and methylester tyrosylsulfamide groups. The probability of occurrence of the specific sites reaches a maximum when the TyrOMe groups substitution rate is in between 15 and 25 %. Resins made of such polystyrene derivatives are promising candidates to perform the plasmatic epuration of haemophilic A patients by affinity chromatography resulting in a total depletion of the anti-FVIII antibodies and a small one of the total IgG.

### Phosphorylated polystyrene and anti DNA antibodies.

Systemic Lupus Erythematosus (SLE) is an auto immune disease. The diagnosis of SLE is based on the fact that the patients sera contain antibodies which were demonstrated "in vitro" to interact specifically with DNA and/or phospholipids. Considering the structure of native DNA it appears that phosphodiester of deoxyribose are probably at least part of the epitopes of the antigenic DNA sites involved in the biospecific interactions between DNA and SLE anti-DNA antibodies. We therefore postulated that randomly phosphorylated polystyrene could be endowed with DNA-like antigenic properties as far as SLE anti-DNA antibodies are under concern. Indeed, such polymers were demonstrated to interact specifically with DNA antibodies [2]. In order to investigate in more details the structure of the DNA-like antigenic site responsible for the above mentioned specific interactions, the synthesis and the characterization of crosslinked polystyrene substituted with PME and PDE groups (Fig 1) were performed and their interactions with anti DNA SLE antibodies assessed.

Based on the analytical data (elemental analysis and acidimetric titration) a Monte Carlo computation was achieved in order to determine the distribution of PDE and PME groups along the macromolecular chains. The results of both the chemical characterization and the computation are summarized in Fig (4) [5].

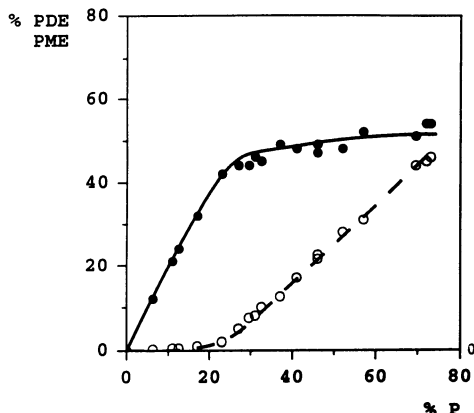


Fig 4 Dependence of the PDE (●) PME (○) content of phosphorylated crosslinked polystyrene versus the overall P content. Compositions are expressed in moles of either PDE, PME or P per mole of monomeric units. Curves are the results of the Monte Carlo computations.

These results show that the distribution of PDE and PME groups obeys a Markov statistics with a local effect distribution law, as described by AD. Litmanovich [6]. Indeed, this distribution is controlled by the fact that PDE formation results from a rapid two step reaction. The first step, formation of PME, is rapid if two vicinal OH groups are free, the second step, formation of PDE, occurs with a rate which depends on the availability of free OH groups adjacent to vicinal OH groups on PME. PME formation is a slower reaction when the vicinal OH groups are substituted and the reaction stops at the PME stage when the above requirements are not fulfilled [5].

Measurements of the adsorption of SLE anti-DNA antibodies to the phosphorylated polystyrene resins was carried out by use of  $^{125}\text{I}$  labelled anti bodies directed against the Fc fragment of human Immunoglobulins. Indeed the resins were first incubated with SLE patients sera diluted in buffer then with the labelled anti Fc antibodies solutions. Controls were obtained by the incubating the resins with normal immunoglobulins. Results, summarized in fig 5 show that recognition of adsorbed anti-DNA SLE antibodies present a maximum for resins which phosphorus (P) content is in between 18 and 22 % whereas no variation of the normal IgG recognition is observed [7].

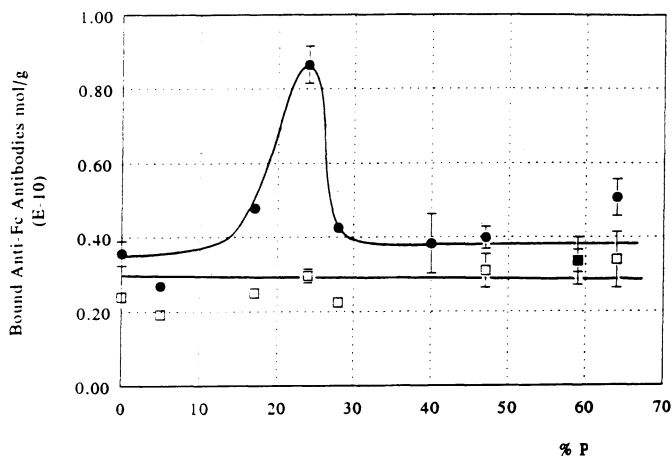


Fig 5 Adsorbed SLE anti DNA antibodies (●) and normal IgG (□) recognition by radiolabelled anti human Fc antibodies as a function of the phosphorus content of the resins.

Moreover these results confirm that the interaction between the phosphorylated polymers and the anti-DNA antibodies involve the antigen recognizing fragment of the antibodies and are therefore highly specific.

Based on the above data, computations were performed in order to determine the probability of occurrence of combinations of PME and PDE groups along the macromolecular chains as a function of the phosphorus content of the polymers. These probabilities vary and present maxima for P contents of the polymer which depend on the composition of the sequences. Results showed that the probability of occurrence of some sequences built of PDE groups reached a maximum for P contents in between 18 and 22 %. Considering that these sequences were most probably the biospecific DNA-like antigenic sites we computed the distances between the phosphodiester and found them similar to actual distances between phosphodiester in native DNA [5].

The above experimental study and computation data demonstrate that phosphorylated random polystyrene derivatives mimic DNA as far as the antigenic properties with regard to SLE patients anti-DNA antibodies are under consideration. The random phosphorylation of hydroxylated polystyrene creates on the macromolecular chains biospecific antigenic sites made of combination of PDE groups with a probability that depends on the phosphorus content of the resins. The distances between the PDE groups in the sites are similar to those of phosphodiester within the DNA double helix. It is likely that structure both the DNA-like antigenic sites and the natural antigenic sites in the DNA double helix have similar structures ie have at least two or three PDE groups which distances are the same.

## CONCLUSION

It is generally believed that biospecific molecular recognition is strictly associated with specific molecular structures. In contrast, our discovery that random copolymers are able to achieve biospecific molecular recognition in living systems establishes that biospecificity is a continuous function of randomness arising from a purely statistical distribution of functional groups to the precisely defined chemical structures of ligand- receptor molecules in the actual living systems [9].

## REFERENCES

1. Dahri L, Boisson-Vidal C, Muller D and Jozefonvicz J (1994) Tyrosyl sulfamide derivatives as ligand for affinity adsorption of anti FVIII antibodies. *J Biomater Sci Polymer Edn*, Vol. 6 N°8 : 695-705
2. Letourneur D, Douzon C and Jozefowicz M (1991) Synthesis and characterization of phosphorylated polystyrene derivatives for use in chromatography : DNA-like and phospholipid-like behavior. *J. Polym Sci. Part A : Polymer Chemistry* 29 : 1367-1377.
3. Shima M, Fulcher CA, de Graaf Mahaney, Houghten RA, Zimmerman TS (1988) Localization of a binding site for factor VIII activity neutralizing antibody to amino acid residues Asp<sup>1663</sup> - Ser<sup>1669</sup>. *J Biol Chem* 263 : 5230-5234.
4. Dahri L, Boisson-Vidal C, Regnault V., Muller D, Sultan Y, Stolz JF (1995) Synthetic sorbents for removal of factor VIII inhibitors from haemophilic A plasma. *J Chromatogr B* 664 : 47-54.
5. V. Migonney, A. Souirti, F. Pfluger, M. Jozefowicz. Biospecific polymers : Recognition of Anti DNA antibodies by phosphorylated polystyrene derivatives. *J Mater Sc, Materials in Medicine* (in press)
6. A.D. Litmanovich (1980) Change of Polymer reactivity in the course of macromolecular reaction *Eur Polym. J* 16, 269-275
7. E. Imbert, Paris North University PhD Thesis (1995).
8. J.D. Andrade (1992) Need, Problems and Opportunities in Biomaterials and Biocompatibility *Clinical Materials* 11, 19-23.



# STRATEGY AND BIONIC DESIGN OF VITAL FUNCTIONING VASCULAR WALL RECONSTRUCTION

Takehisa Matsuda

Department of Bioengineering, National Cardiovascular Center Research Institute  
5-7-1 Fujishirodai, Suita, Osaka 565, Japan

## Abstract

Several models of hybrid artificial grafts were developed, which were prepared from vascular cell types and collagen on artificial grafts. Tissue regeneration potentials of these models, including time-dependent cellular segregation, orientation and phenotypic alteration and production and self-assembling of extracellular matrix components such as collagen and elastin were thoroughly studied. Incorporation of three cell types markedly enhanced vascular wall reconstruction.

**Keyword:** hybrid graft, collagen, endothelial cell, extracellular matrix

## (1) Structure and Function of Vessel Wall

Living vascular wall is composed of three different cell types such as endothelial cell (EC), smooth muscle cell (SMC) and fibroblast (FC), each of which resides in a respective layer; the intima monolayerly lined with endothelial cells (ECs) which lie on a basement membrane, the media composed of SMCs embedded in extracellular matrices (ECMs) mainly composed of collagen, elastin and mucopolysaccharides, and the adventitia mainly composed of FCs and ECMs. An EC-incorporated artificial graft has been expected to provide nonthrombogenic potential similar to natural vessel at the blood-contacting surface. This is due to the inherent nonthrombogenic nature of ECs, which have built-in antiplatelet, anticoagulant and fibrinolytic functions. Beside nonthrombogenicity, a vital functional arterial replacement may require an appropriate tissue regeneration with highly organized fashions. At the blood-contacting intima, ECs align parallel to the direction of the blood flow, whereas SMCs in the media are highly oriented circumferentially. SMCs should be contractile-phenotype as same as those in healthy native tissues. As for ECMs, collagen and elastin, both of which are classified as structural proteins, are self-assembled or self-associated to form oriented fiber bundles or amorphous layers, respectively.

## (2) Strategy of Vascular Wall Reconstruction

Several types of preconstructed hybrid vessels, depending on vascular cell types incorporated, were prepared. Our interest has been focused on how a hybrid graft, in which a vascular tissue has preconstructed to some extent *in vitro*, undergoes to remodel and regenerate a vessel wall resembling natural ones *in vivo*, and which model restore vascular wall at an earliest implantation period. Cellular events of concern are cellular segregation, orientation and phenotypic alteration, and biomolecular events are regeneration of collagen and elastin and self-assembling to form fibers or layers.

## (3) Hierarchic Hybrid Artificial Graft : Step-by-Step Structuring

Prototypic models of novel hybrid vascular grafts prepared were based on organ reconstruction technology, an essential feature of which is a layer-by-layer construction. Irrespective of models, an EC monolayer was formed on an artificial basement membrane (ABM). **Model I** is an intimal model in which only ECs are incorporated, to cover monolayerly the entire luminal surface. In more biomimic models, SMCs and/or FCs were incorporated beneath the endothelium. **Figure 1** shows our preconstructed vessel wall models where **Model II** is a bilayered hybrid tissue into which intimal and medial layers were hierarchically incorporated. **Model III** is a three-layered hybrid tissue in which ECs, SMCs and FCs reside in respective layers. **Model IV** is a bilayered one which is composed of three cell types. Underneath endothelium, SMCs and FCs are homogeneously distributed. Regardless of models, ECM component used was type I collagen which spontaneously forms fibers upon thermal incubation at 37°C.

The step-by-step layering was schematically shown in **Figure 2**. Designed ABM is a complex gel of type I collagen and dermatan sulfate, which have been proven to impart enhanced EC adhesion and growth and reduced platelet adhesion. The hybrid media or adventitia was constructed *via* entrapping

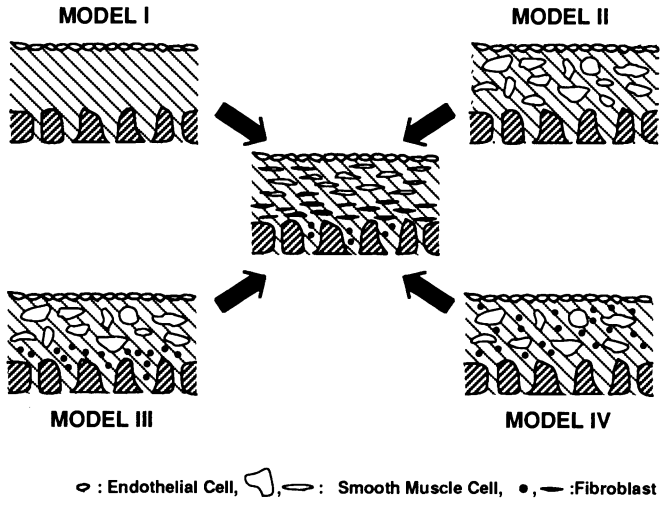
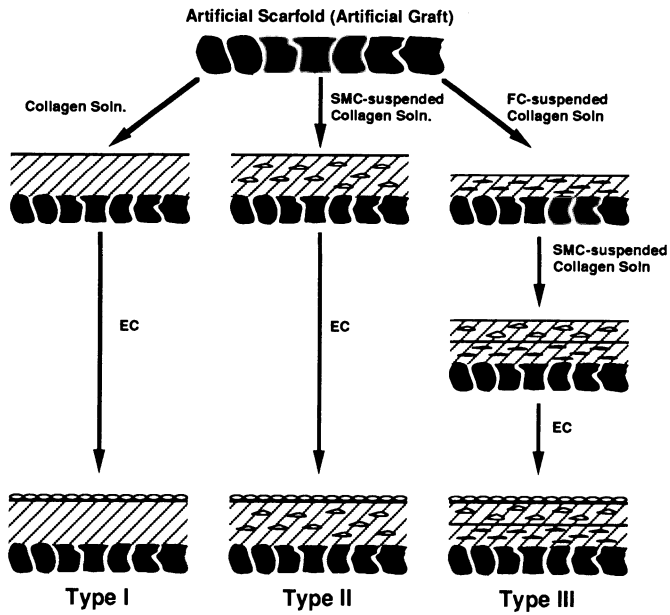


Figure 1: Four different types of hybrid artificial grafts



EC: Endothelial Cell, SMC: Smooth Muscle Cell, FC: Fibroblast

Figure 2: Preparation methods of hybrid artificial grafts.

Table 1: Summary of Morphogenesis Process of Hybrid Grafts with Different Degrees of Hierarchy

		<b>Model I</b> (EC)	<b>Model II</b> (EC/SMC)	<b>Model III</b> (EC/SMC/FC) <b>Model IV</b> (EC/SMC+FC)	<b>Model V</b> (EC/FC)
<b>Intima</b>	Hydrodynamic Stability (Early Phase)	Good	Very Good	Very Good	-
<b>Media</b>	SMC Orientation/Segregation	12-26 weeks	4-12 weeks	2-4 weeks	-
	Phenotypic Alteration (Contractile type %)	42% (12 weeks)	61% (12 weeks)	86% (12 weeks) 100% (23 weeks)	-
	Elastin Production	>26 weeks	12-26 weeks (regeneration)	4 weeks (regeneration) 26 weeks (layering)	-
<b>Adventitia</b>	Collagen Regeneration (Early Phase)	Very Small	Small	Medium	Very Large (occlusion due to excessive production)
	Orientation	12 weeks	4-12 weeks	2-4 weeks	-

EC: Endothelial Cell, SMC: Smooth Muscle Cell, FC: Fibroblast

of SMCs or FCs in a collagen gel, which was achieved by mixing of cells with a cold collagen solution and subsequent incubation at the physiological temperature.

#### (4) Morphogenesis: Remodeling & Regeneration

These hybrid tissues constructed on luminal surfaces of small-caliber artificial grafts (Dacron artificial grafts: inner diameter; 4 mm, length; 6 cm) were implanted in canine arteries for up to 12 months. The remodeling and regeneration processes were evaluated and discussed at cellular, biomolecular and whole tissue levels, respectively.

At the luminal surfaces, the integrity of ECs of **Model I** grafts in terms of EC coverage and orientation at 2 week's implantation were somewhat poor as compared with those of Model II and III grafts. However, at longer implantation period, complete endothelialization and cellular orientation parallel to the direction of blood flow were achieved, regardless of models used.

The cellular dynamics largely depended on models used. For **Model I**, the transmural invasion of SMCs occurred at 4 weeks, and its migration to and accumulation at the subendothelial layer and circumferential orientation occurred at 12 weeks. Phenotypic reversion from synthetic (as implanted) to contractile-phenotype needed one year of implantation. On the other hand, for **Model II** grafts, into which SMCs were pre-incorporated, SMC migration to the subendothelial layer and circumferential orientation were completed within 12 weeks of implantation and phenotypic alteration occurred within several months. For **Model III** grafts into which three vascular cell types are incorporated, these cellular events were markedly accelerated. The regeneration and subsequent macromolecular assembling of collagen and elastin occurred with time, which also depended on models used. The regeneration and subsequent circumferential orientation of collagen fiber bundles were enhanced with an incorporation with SMCs or FCs. When both cell types were incorporated at the same time, a markedly accelerated regeneration and remodeling was achieved. Especially, the incorporation of FCs in **Model III** grafts exhibited a remarkably enhanced elastin regeneration and remodeling potential. There was no difference in tissue regeneration potentials between **Model III** and **IV** grafts. At **Model IV** grafts, FCs (stained with fluorescent-labeled lipid) were migration into outer regions of vascular wall, whereas SMCs migrated to the subendothelial layer. Thus, cell segregation really occurred *in vivo*.

At the whole tissue level, a general tendency was that a vascular tissue is thickened as the implantation proceeds at an earlier period, but eventually thinned down at a later period. The period of wall thickening coincided with the period of invasion and proliferation of SMCs and FCs. The wall thinning seems to occur when collagen fiber bundles were circumferentially oriented and SMCs were also elongated to orient themselves circumferentially and segregated. Sooner or later, synthetic-

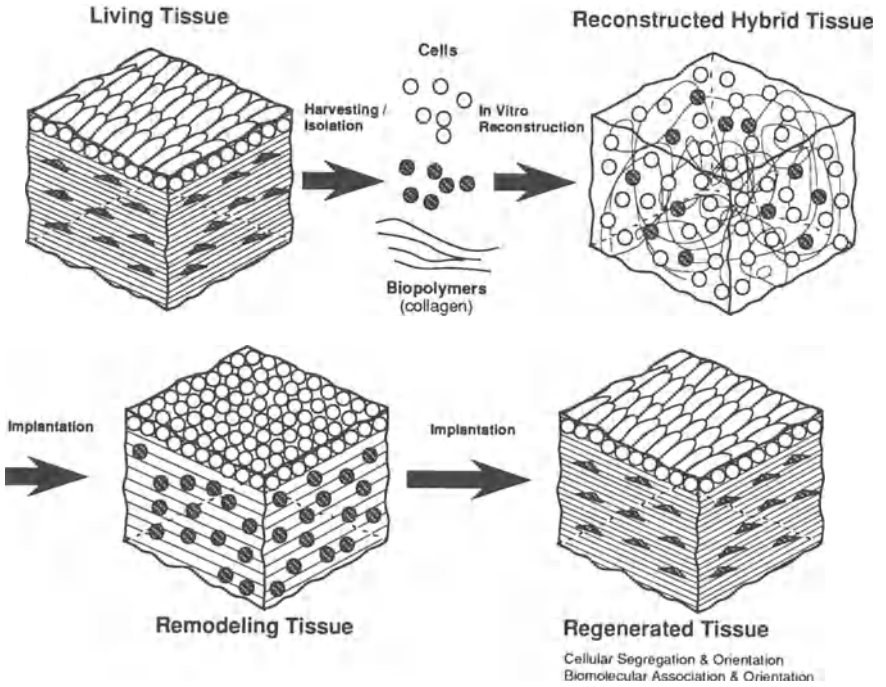


Figure 3: Vascular wall regeneration and remodeling process

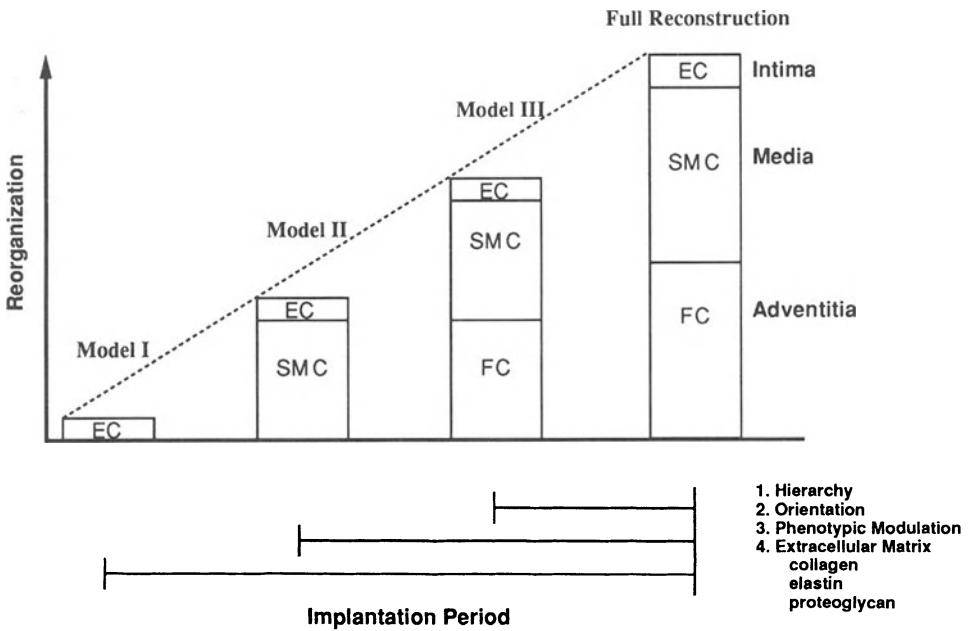


Figure 4: Regeneration potentials of three different types of hybrid artificial grafts.

phenotyped SMCs were reverted back to the contractile type. Thus, it is suggested that, once a suitable extracellular environment was formed around cells, normal wound healing process proceeds to remodel a regenerated tissue.

#### (4) Conclusion

**Table 1** summarizes time-dependent vascular wall regeneration and remodeling potentials for three different types of hybrid vascular grafts. The scenario of tissue remodeling is schematically shown in **Figure 3**. Our study showed that a preoriented, hierarchically structured hybrid vascular tissue undergoes to self-reorganize by responding to pulsatile stressing *in vivo*, resulting in the formation of vital vascular tissue with high degrees of structuring, segregation, orientation and phenotypic reversion. The resultant tissues were biomimic to those of natural vessels. As a structure of the tissue becomes closer to that of natural one, a more reliable and faster tissue regeneration occurred (**Figure 4**). Especially, the incorporation of three vascular cell types into hybrid grafts significantly enhanced the tissue regeneration. Thus, preconstructed vascular tissues effectively modulated by themselves as to provide structural assembling and functional adaptation *in vivo*.

#### References (limited to the authors' latest papers)

1. T.Matsuda, H.Iwata and T.Akutsu: Vascular Organ Reconstruction Technology for Hybrid Graft. Artificial Heart-2, Springer-Verlag, 65-81(1989)
2. T.Matsuda, T.Kitamura, H.Iwata and T.Akutsu: A Hybrid Artificial Vascular Graft Based on an Organ Reconstruction Model : Significance and Design Criteria of Artificial Basement Membrane. ASAIO Journal 35, 640-643(1989)
3. T.Matsuda, T.Akutsu, A.Kira and H.Matsumoto: Development of Hybrid Compliant Graft : Rapid Preparative Method for Reconstruction of a Vascular Wall. ASAIO Journal 35, 553-555(1989)
4. H.Miwa, T.Matsuda, K.Kondo, N.Tani, Y.Fukaya, M.Morimoto and F.Iida: Improved Patency of an Elastomeric Vascular Graft by Hybridization. ASAIO Journal 38, M512-M515 (1992)
5. K.Kanda, T.Matsuda and T.Oka: Two-dimensional Orientational Response of Smooth Muscle Cells to Cyclic Stretching. ASAIO Journal 38, M382-M385 (1992)
6. S. Niu and T. Matsuda: Endothelial Cell Senescence Inhibits Unidirectional Endothelialization In Vitro. Cell Transplantation Vol.1, 355-364 (1992)
7. H.Kito, T.Matsuda, J.Mathew, A.Kondo, N.Nakajima: Differentiated Biocompatible Design of Luminal and Outer Graft Surfaces: Photocurable Extracellular Matrices, Fabrication and Cellular Responses. ASAIO Journal Vol.39(3), M506-M511 (1993)
8. K.Kanda, T.Matsuda, H.Miwa, T.Oka: Phenotypic Modulation of Smooth Muscle Cells in Intima/Media-incorporated Hybrid Vascular Prostheses. ASAIO Journal Vol.39(3), M278-M282 (1993)
9. K.Kanda, T.Matsuda, T.Oka: In Vitro Reconstruction of a Hybrid Vascular Tissue: Hierarchical and Oriented Cell Layers. ASAIO Journal Vol.39(3), M561-M565 (1993)
10. K.Kanda, T.Matsuda, T.Oka: Mechanical Stress-induced Cellular Orientation and Phenotypic Modulation of 3D-cultured Smooth Muscle Cells. ASAIO Journal Vol.39(3), M686-M690 (1993)
11. H.Miwa, T.Matsuda, K.Kanda, F.Iida: Development of a Hierarchically Structured Hybrid Vascular Graft Biomimic to Natural Vessel. ASAIO Journal Vol.39(3), M273-M277 (1993)
12. H.Miwa, T.Matsuda, N.Tani, F.Iida: An In Vitro Endothelialized Compliant Vascular Graft Minimizes Anastomotic Hyperplasia. ASAIO Journal Vol.39(3), M501-M505 (1993)
13. K.Kanda and T.Matsuda: Behavior of Arterial Wall Cells Cultured on Periodically Stretched Substrates. Cell Transplantation 2(6), 475-484 (1993)
14. H.Miwa and T.Matsuda: An Integrated Approach to the Design and Engineering of Hybrid Arterial Prostheses. J. Vasc. Surg. 19(4), 658-667 (1994)
15. T.Matsuda and H.Miwa: Hybrid Vascular Model Biomimicking the Hierarchical Structure of Arterial Wall: Neointimal Stability and Neoarterial Regeneration Process under Arterial Circulation. J. Thor. Cardiovasc. Surg., in press
16. K.Kanda and T.Matsuda: In Vitro Reconstruction of Hybrid Arterial Media with Molecular and Cellular Orientation. Cell Transplantation 3(6), 537-545 (1994)
17. K.Kanda and T.Matsuda: Mechanical Stress-induced Orientation and Ultrastructural Change of Smooth Muscle Cells Cultured in Three-dimensional Collagen Lattices. Cell Transplantation 3(6), 481-492 (1994)
18. K.Kanda, H.Miwa and T.Matsuda: Phenotypic Reversion of Smooth Muscle Cells in Hybrid Vascular Prostheses. Cell Transplantation, in press
19. J.Hirai, K.Kanda, T.Oka and T.Matsuda: Highly-oriented, Tubular-shaped Hybrid Vascular Tissue for Low-pressure Circulatory System. ASAIO Journal 40(3), M383-388(1994)
20. K.Ishibashi, K.Kawazoe and T.Matsuda: Reconstruction of a Hybrid Vascular Graft Hierarchically Layered With Three Cell Types. ASAIO Journal 40(3), M284-290 (1994)

# **SURFACE MODIFICATION OF BIOMATERIALS BY TOPOGRAPHIC AND CHEMICAL PATTERNING**

Adam Curtis and Stephen Britland

*Laboratory of Cell Biology, Institute of Biomedical & Life Sciences, University of Glasgow, University Avenue, Glasgow, G12 8QQ, Scotland.*

## **SUMMARY**

The surface modification of polymers to form structures to aid tissue repair is described. The modification of polydioxanone, polyimides and polymethacrylates by forming topography on the 50nm to 10 $\mu$ m scale by photolithography, and by embossing is described and compared methods. with surface chemical modification with laminin. The effects of such treatments on cell orientation, morphology, adhesion and speed of movement are compared. The potential for use of these methods in prostheses is considered with inclusion of a practical example from tendon repair.

**KEY WORDS** microfabrication, nanofabrication, cell behaviour, cell activation, polymers

## **INTRODUCTION**

The use of biomaterials in medical prostheses introduces the possibility of interactions in both directions between the biomaterial and the cells of the organism. The aim in the use of prostheses is to achieve a perfect integration of cells and biomaterial. This perfection might be envisaged as an effective alliance between the two in which neither cells nor biomaterial is damaged. Though success in attaining this would be notable there is a still higher target to aim for. This is the development of biomaterials that encourage the correct rebuilding of the missing or damaged tissue and which then disappear as the cells develop the correct tissue structure. We term such materials 'templates for tissue repair'.

It is clear from work such as that of Aplin & Hughes [1] on the derivatisation of surface with immobilised proteins that specific surface chemistries can control cell attachment and cell shape. Similarly Curtis & Varde [2] showed that cells can react to the topography of the substrate. Since cells in tissues are exposed to the surrounding specific chemistry of nearby cells and intercellular materials and to the varied topographies offered by surrounding cells and intercellular materials it is clearly worth investigating these effects systematically examining the effects of specific surface chemistry or precise topography of biomaterials on cell functions in relation to tissue building and rebuilding.

The cell functions that contribute to tissue formation include adhesion, cell spreading, mechanical tension exerted by cells, cell orientation, cell movement, gene expression, secretion of extracellular materials and the maintenance of the correct water balance in those materials.

There have been many studies on the derivatisation of surfaces which affect cell adhesion eg [3,4,5], and on extracellular material production, quite a number on cell spreading and almost nothing on the other cell functions just listed. The same story is true for the effects of substratum topography.

The work I shall describe is an investigation of the effects of topography on cell behaviour, especially on polymers. However, the question of whether the cells respond to topography or chemistry or both arises frequently and needs resolution.

## **MATERIALS AND METHODS**

### **1. Topography**

Primary methods

There are two main methods for producing topography on a surface.. etching (erosion) and deposition. The topography can be patterned either by steering a beam over the surface or by using a mask.

### Summary of Fabrication Methods that may be used on polymers

Erosion	Laser Argon ion ablation Oxidative plasma Electron beam Chemical erosion (Etching)
Deposition	Photosensitisation Electron beam
Modification	Any of above Scanning near field optical methods

Erosion can be used to produce relief at least as great as 20 $\mu$ m or as little as a few nm. The lateral resolution depends on many factors but only in quite exceptional circumstances can structures with detail as narrow as 150nm be produced by photolithography and a usual limit for many fabricators is 2 $\mu$ m. Electron beam methods allow resolutions of a few nm.

## 2. Secondary replicative methods

Once a master, either positive or negative, has been formed they can be used to produce multiple copies of the topography. The techniques used are casting and embossing. Casting can be capable of very great precision and details of 2nm dimension have been replicated. Embossing is inherently less precise because the material being embossed flows into the mould but rarely reaches an equilibrium state before the embossing pressure is removed. There are two advantages in this method : first large areas can be prepared by repeated embossing, second, subsurface damage to the polymer by ion beam etc methods is avoided.

## 3. Surface chemical modification

It should be noted that two main types of method for attaining surface modification are available. In the first the polymer is exposed to a reagent that oxidises or hydrolyses the polymer. Methods include glow discharges or reactive plasmas usually with oxygen species as the reactive material but sometimes using nitrogen species instead. Because of the natural solubility of atmospheric gases in polymers it is very easy to obtain effects such as oxidation even when fairly thorough attempts have been made to exclude oxygen. On most polymers reagents such as these produce a wide spectrum of results including production of carboxyl, hydroxyl, peroxide and epoxide groups. Chain scission in the polymer may also take place. In the second type reagents are added that attach groupings to the surface, typically these are silane derivatives and these in themselves may confer desirable properties on the surface. Alternatively the silanes are intermediates in the addition of further groupings, for example azide silanes may be used for the photoactivated addition of proteins or amino-groups, as in aminosilanes, can be used for the addition of proteins or peptides.

## 4. Characterising the surface.

A wide range of methods can be used such as SEM, Surface plasmon resonance, interferometry, SPM (AFM), STM, ESCA, SIMMs, binding studies with suitably labelled reagents. In our studies we used SEM, binding studies, interferometry and have begun to use SPM. Interest has switched from methods that give overall averaged results such as groups per cm<sup>2</sup> to those that give microdetail. Quite often small areas of the surface will be defective either because of surface marks, dirt or because local variations in polymer composition or polymerisation will affect the extent to which the material reacts.

## 5. Establishing the cells on the material

In simple experiments cells of a wide variety of types ( endothelia B10D2.PCE, mouse and HGTHN human), fibroblast ( BHK21 C13 and human fibroblast (local stock)), P388D1 macrophage-like cells, and epithelial cells were trypsinised and then plated onto the surfaces of the fabricated polymers, glass coverslips or tissue culture polystyrene surfaces after these had been sterilised in 70% ethanol. Plating densities were 40,000 cm<sup>-2</sup>. Standard serum-containing culture medium were used. In further experiments cell behaviour in serum-free conditions was examined and the fast-adhesion procedure described by Wojciak-Stothard et al [6] was used which allows cells to establish viable adhesions in a few minutes. In general terms more complex methods of obtaining cells on the structures may include use of systems to permit migration of the cells into the area of interest, sequential attachment first of one cell type and then of the other, or attaching cells onto one surface and then allowing them to transfer to the other.

## 6. Interaction types

The effects of topography and of patterned chemical cues ( lines ) has been examined in terms of cell orientation, cell spreading and occasionally cell adhesion and cell movement speed. Standard methods described by Curtis and Lackie [ 7] by Wojciak-Stothard et al [ 6] and by Curtis [8] were used.

## RESULTS

### On topography

Cells orient to the lines of discontinuity on the structure, that is to the edges of grooves and ridges, see Fig. 1. Unless the grooves are very wide the cells normally contact the substratum only at the edges of the ridge and groove wall and along the ridge top. In other words they span the groove and may, if the cells are large enough, span across an intervening ridge. Most cell types show accelerated movement on this type of structure with speeds increasing up to 200% in extreme cases. Neurons show accelerated extension. Orientation increases with groove depth and decreases with groove width. Actin condensation occur in the cell directly over the discontinuity where groove wall and ridge top intersect. [6]. There is suggestive evidence [9] that cell adhesion may be activated by contact with groove/ridge topography.

Similar reactions occur on fibres [ 2,9]. More complex topographies [10,11] are also reacted to but there is no general theory yet which leads to an ability to predict how a cells will behave. Using 160nm wide grooves Clark and his colleagues [12] found that cells react in different ways to topography depending on whether they are isolated or in groups. We have made grooves in polymethylmethacrylates, polyimides and in polydioxanone and alignment and movement effects are very similar. on these surfaces and differ very little from those achieved on fused silica topographies.

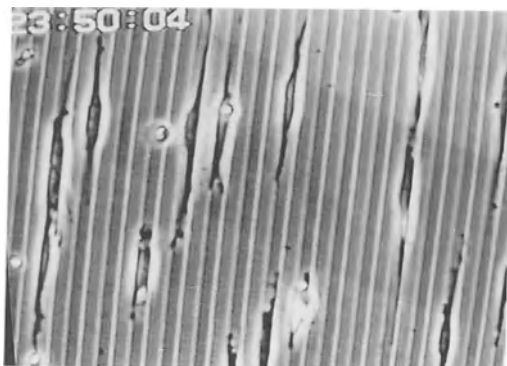
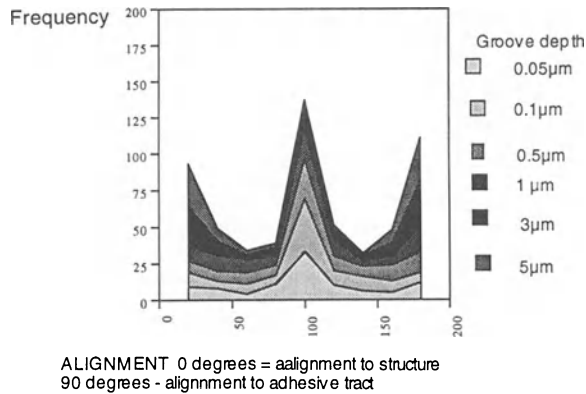


Fig. 1. Epithelial cells on 10  $\mu$ m grooves 3  $\mu$ m deep.



### Combining topographic and chemical patterning.

We made structures which contained both groove/ridge structure and bands of laminin patterned at a similar scale. The laminin bands were oriented either with the same orientation and register as the topography or at 90 degrees. We studied neuron guidance to discover which type of environmental clue had the greater effect on cell extension. Fig. 2.. For these cells types and structures both chemical patterning and topography have about equal effect on cells though the growth cones are much more extensive on laminin substrata than they are on bare fused quartz. Fig .2. Topographic and chemical clues affect orientation to similar extents.



### In organ culture and in vivo

An organ culture system [13] was set up using bisected tendon with a grooved surface to bridge between them. This encouraged the reformation of a nearly normal tendon tissue which rejoined the two fragments in several weeks. In vivo experiments are in progress using this approach to aid the production of correctly oriented tissue structure [13]

### DISCUSSION

#### Which types of cells react to topography.

Nearly all cell types so far studied show reactions to topography though it is important to appreciate that the degree of reaction to a given topography may vary considerably from cell to cell. For example DRG neurons are aligned by 2  $\mu\text{m}$  deep grooves but not by 1  $\mu\text{m}$  deep ones while endothelia and epitema may be aligned by grooves down to in depth. Complex relationships, not yet understood, exist between groove depth, width and pitch. Probably this range of behaviour provides us with the opportunity to produce structures which will select certain cell types for extensive movement and orientation.

#### The problem of surface chemical modification by fabrication.

Even the relatively unreactive treatments such as argon ion ablation may produce chemical alterations in polymers and there is the possibility that these alterations are different on surfaces which were parallel to the ion beam than those which were normal to it. To obviate this possibility polymers were given a brief blanket oxidative etch which is non-directional to remove any chemical differences. The argument that differences in this chemical modification produce the cell orientation seems unlikely for reasons set out in the next paragraph.

#### Do cells react to topography alone ?

Many of the methods of producing topography are open to the objection that they may either produce different chemistries on surfaces of different aspect or reveal any pre-existing

inhomogeneities in the substratum. To minimise such possibilities we have examined the reaction of cells to nanometric grooves where the groove walls are only a few protein molecules high. Perhaps the most convincing argument that the cells are not reacting to chemical variations between walls and horizontal surfaces is that when the cells are grown in the presence of various different protein molecules that can adsorb from the medium the reaction to topography remains the same. It is likely that different species of protein would show different adsorption reactions to differing substratum chemistry. Topographic reactions are the same in high or low serum media, or in the presence of laminin in serum-free media.

### **Competition or alliance between chemistry and topography.**

Obviously both types of clue may be fabricated onto a polymer surface and our results suggest that they can be used to reinforce the effects of each other. However, it should be noted that just as the discontinuities in the topography appear to control cell orientation and activation so the edges of the chemically patterned areas have most effect on cell position, and this suggests that discontinuity fabrication may be in itself a powerful tool for positioning cells.

Woven structures have been extensively used to aid tissue repair. Our investigations on the behaviour of cells on various types of topography suggests that this approach may be unwise. Though cells may migrate along the fibres and form an oriented structure they also align to the fibres crossing at 90 degrees and pools of immobile cells tend to accumulate at the intersections. The resulting tissue structure [14] is composed of cells arranged concentrically around the spaces in the fibres. This may perhaps be valuable for some types of tissue construction but is not typical of many.

### **REFERENCES**

1. Aplin J.D, Hughes, RC. (1981) Cell adhesion on model substrata: threshold effects and receptor modulation. *J. Cell Sci.* 50,: 89-103.
2. Curtis, ASG, Varde M. (1964) Control of cell behaviour.- topological factors. *J.Natl. Cancer Inst.* 33 : 15-26
3. Britland S, Clark P., Connolly P, Moores G. (1992) Micropatterned substratum adhesiveness: A model for morphogenetic cues controlling cell behavior. *Exp. Cell Res.* 198 : 124-129.
4. Brandley BK, Schnaar RL. (1988) Covalent attachment of an Arg-Gly-Asp sequence peptide to derivatizable polyacrylamide ssurfaces : support of fibroblast adhesion and long-term growth. *Anal. Biochem.* 172 :270-278.
5. Kleinfeld D, Kahler KH, Hockberger PE. (1988). Controlled outgrowth of dissociated neurons on patterned substrates. *J. Neurosci.* 8 : 4098-4120.
6. Wojciak-Stothard B, Curtis ASG, Monaghan W, McGrath M, Sommer I, Wilkinson CDW. (1995) The role of the cytoskeleton in the reaction of fibroblasts to multiple grooved substrata, *Cell Motil. Cytoskel.* ( in press)
7. Curtis, AS.G., Lackie, JM. (Ed.). (1991). *Measuring cell adhesion* (1st ed.). Chichester: John Wiley & Sons.
8. Curtis ASG ( in press) Accelerating cell movement. *Cell Eng.*
9. Dunn, GA, Heath, JP. (1976) A new hypothesis of contact guidance in tissue cells. *Exptl. Cell Res.*, 101 : 1-14.
10. Rovinsky YA., Bershinsky AD, Givargizov EI., Obolenskay LN, Vasiliev YM. (1991). Spreading of mouse fibroblasts on the substrate with multiple spikes. . *Exptl Cell Res.* 197: 107-112.
11. Dow, J.AT., Clark P., Connolly P., Curtis ASG.,Wilkinson CDW. (1987). Novel methods for the guidance and monitoring of single cells and simple networks in culture. *J. Cell Sci.,Suppl.* 8 : 55-79.
12. Clark P, Connolly P, Curtis, ASG, Dow J.AT., Wilkinson CW. (1991). Cell guidance by ultrafine topography in vitro. *J. Cell Sci.* 99,: 73-77.
13. Wojciak B, Crossan J, Curtis ASG, Wilkinson,CDW (1995) Grooved substrata facilitate in vitro healing of completely divided flexor tendons. *J.Materials Sci. Materials Med.* ( in press)
14. Curtis ASG, Seehar GM. (1978). The control of cell division by tension or diffusion. *Nature* 274: 52-53.

# Interleukin-4 Mediated Foreign Body Giant Cell Formation and Cytoskeletal Rearrangement on Poly(etherurethane Urea) *In Vivo* and *In Vitro*

James M. Anderson<sup>†‡</sup>, W. John Kao<sup>†</sup>, Kristin M. DeFife<sup>‡</sup>, Amy K. McNally<sup>‡</sup>, and Chris Jenney<sup>‡</sup>

Institute of Pathology<sup>‡</sup>, Department of Macromolecular Science<sup>†</sup>, and Department of Biomedical Engineering<sup>‡</sup>, Case Western Reserve University, Cleveland, OH, U.S.A.

## ABSTRACT

Interleukin-4 (IL-4) mediated foreign body giant cell (FBGC) formation on poly(etherurethane urea) (PEUU) *in vivo* was studied using the subcutaneous cage system in mice. Purified goat anti-mouse IL-4 neutralizing antibody (IL4Ab), normal goat nonspecific control IgG (gtIgG), recombinant murine IL-4 (muIL4), or PBS was injected into the implanted cages containing PEUU every two days for 7 days. The injection of IL4Ab significantly decreased the FBGC density on PEUU cage-implanted in mice, when compared with the nonspecific gtIgG or PBS injection controls. Conversely, the FBGC density was significantly increased by the injection of muIL4 when compared with nonspecific gtIgG and PBS injection controls. Confocal scanning laser microscopy (CSLM) was employed to visualize the spatial arrangement of the filamentous actin cytoskeleton of adherent macrophages and IL-4-induced FBGCs *in vitro*. Whereas the material surface-associated punctate actin structures occurred across the entire ventral cell surface in monocytes/macrophages cultured on PEUU, the structures became restricted to the periphery of the ventral cell surface upon addition of IL-4 as fused macrophages acquired FBGC phenotype. Our data suggest that IL-4 participates in FBGC formation on biomaterials *in vivo* and *in vitro* and that dramatic reorganization of the cytoskeleton occurs during FBGC formation.

**KEYWORDS:** interleukin-4, foreign body giant cell, polyurethane, actin, confocal microscopy

## INTRODUCTION

The presence of lymphocytes and monocyte-derived macrophages in the biomaterial-associated inflammatory milieu is well-documented [1]. IL-4, derived from T helper lymphocytes, modulates a variety of immune and inflammatory responses *in vivo*. Particularly relevant to long-term material biostability is the effect of IL-4 in inducing mouse or human macrophage fusion to form FBGCs *in vitro* in a surface property-dependent manner [2,3]. Monocyte-to-macrophage morphologic development is initiated by adhesion and is generally characterized by marked cytoplasmic spreading. This morphologic transformation is hypothesized to occur through the extensive reorganization of cytoskeletal elements and the establishment of intracellular adhesive structures. Reorganization of filamentous actin of monocytes cultured on coverslips has been reported [4,5]. Filamentous actin can be visualized fluorescently with CSLM which offers several notable advantages over conventional fluorescence microscopy. Out-of-focus light, which results in nonspecific signal and loss of resolution, is eliminated from the final image. Thin optical sections imaged through the specimen facilitate the localization of the fluorescent signal in three dimensions and can be projected into one high-resolution composite image.

## MATERIALS AND METHODS

PEUU was prepared from *p*-diphenyl-methanediisocyanate and poly(tetramethyleneoxide) in an approximately 1.6 to 1 capping ratio and chain extended with ethylenediamine [6]. For the *in vivo* FBGC formation study, PEUU film (1 x 2 cm<sup>2</sup>) was rolled and placed inside of cylindrical, stainless-steel wire mesh cages (1.5 cm in length and 0.8 cm in diameter) and gas-sterilized with ethylene oxide. A 1.5 cm clean incision was made on the skin at the posterior region of the backs of female, 8 weeks old, Balb/c mice. Each sample was implanted subcutaneously through and away from the incision site. Sterile, nonabsorbable silk surgical sutures were used to close the incision. To determine the applicability of the cage system in mice, total and differential leukocyte concentrations from cages containing PEUU and empty-cage controls were determined at 4, 7, and 14 days post-implantation. To determine the effects of the antibodies on FBGC formation, 100 to 500 µg of IL4Ab, 100 ng of muIL4, 100 to 500 µg of gIgG, or PBS were injected directly into each cage containing PEUU on days 0, 2, 4, and 6. All injections were made in volumes of 0.25 ml. Antibodies were obtained as lyophilized, affinity-purified IgG and reconstituted in sterile PBS. The mice were sacrificed after 7 days of implantation. PEUU specimens were stained with modified Wright's stain and the adherent cells were measured with a computerized video analyzer system.

For *in vitro* cytoskeletal CSLM analysis, PEUU was punched into 15 mm disks, inserted into 24 well tissue culture plates, and secured with silicone rubber rings. Human peripheral blood monocytes were isolated by a non-adherent method [3] and added at a concentration of 1 x 10<sup>6</sup> monocytes/well. Cultures were maintained for 10 days and were treated essentially as described [3]. Briefly, cultures were maintained until day 3 in RPMI-1640 culture medium containing 25% autologous serum. On days 3 and 7, medium was replaced with RPMI-1640 containing 25% heat-treated (56°C for 1 hour) autologous serum and 10 ng/ml IL-4 was added. Specimens were stained with May-Grunwald/Giemsa for light microscopy. For double label CSLM, rhodamine phalloidin and YOPRO-1 were used to stain filamentous actin and DNA, respectively.

## RESULTS AND DISCUSSION

Comparable total leukocyte, PMN, and lymphocyte concentrations were observed for cage-implanted PEUU without injections and empty cage controls indicating similar inflammatory response up to 14 days of implantation (data not shown). This data confirmed the applicability of the cage system in mice. At 7 days post-implantation, the FBGC density for the 100 to 500 µg of IL4Ab injection groups was significantly lower than both PBS and 100 to 500 µg/ml of gIgG controls (Table I). FBGC kinetic analysis was used [6] and the results further indicated that the number of macrophages participating in FBGC formation was decreased in the presence of IL4Ab. Conversely, the FBGC density for the muIL4 group was significantly higher than both nonspecific gIgG and PBS controls. FBGC kinetic analysis showed that the number of macrophages participating in FBGC formation was increased in the presence of muIL4. The adherent macrophage densities and average FBGC sizes were not significantly different among all injection groups.

Light microscopic analysis of PEUU showed similar FBGC morphology of extensive cytoplasmic spreading, pseudopodial extension, and randomly arranged nuclei between *in vitro* and *in vivo* specimens (data not shown). Fluorescent CSLM was used to image filamentous actin organization in adherent cells. After an initial 2 hour incubation, monocytes showed only a diffuse staining pattern (Fig. 1a). By day 3,

Table I. Adherent Cell Density on PEUU Cage-Implanted into Mice at 7 Days Post-Implantation with Direct Injection of muIL4, IL4Ab, gIlgG, or PBS Controls (mean  $\pm$  s.e.m.)

Treatment (n - value)	Adherent Macrophage (cells/cm <sup>2</sup> )	Adherent FBGC (cells/cm <sup>2</sup> )	Average FBGC Size (x 10 <sup>-3</sup> mm <sup>2</sup> )
100 ng muIL4 (3)	80200 $\pm$ 12960	6100 $\pm$ 460 ‡	2.90 $\pm$ 0.90
500 $\mu$ g IL4Ab (2)	83340 $\pm$ 15680	2320 $\pm$ 320 ‡	4.69 $\pm$ 0.62
250 $\mu$ g IL4Ab (4)	53040 $\pm$ 20170	1410 $\pm$ 260 ‡	2.09 $\pm$ 1.80
100 $\mu$ g IL4Ab (4)	52490 $\pm$ 14990	2380 $\pm$ 910 ‡	2.37 $\pm$ 0.90
500 $\mu$ g gIlgG (2)	77420 $\pm$ 4390	3770 $\pm$ 150	3.97 $\pm$ 0.57
400 $\mu$ g gIlgG (3)	75270 $\pm$ 14040	3720 $\pm$ 220	1.94 $\pm$ 0.75
250 $\mu$ g gIlgG (4)	63620 $\pm$ 13130	4430 $\pm$ 1010	2.80 $\pm$ 0.49
200 $\mu$ g gIlgG (3)	62650 $\pm$ 26510	3600 $\pm$ 1110	3.78 $\pm$ 1.21
100 $\mu$ g gIlgG (7)	62190 $\pm$ 20280	4320 $\pm$ 970	2.94 $\pm$ 0.87
PBS control (12)	73120 $\pm$ 21130	4280 $\pm$ 1050	3.58 $\pm$ 1.09

‡ indicates values which are significantly different at 99% confidence level ( $p < 0.01$ ) when compared with PBS and nonspecific gIlgG controls as determined by independent student's *t*-test. No differences were observed for respective values between gIlgG and PBS.

monocytes/macrophages began forming punctate adhesions across their entire ventral cell surfaces which remained through day 10 (Figs. 1b and 1c). However, the addition of IL-4 induced extensive cell fusion, increased cytoplasm irregularity, and promoted the reorganization of the actin cytoskeleton by day 10. Punctate fluorescence became restricted to the periphery of the ventral cell surfaces (Fig. 1d). Furthermore, F-actin was also generally absent from the cell cytoplasm except for a sphere encasing clusters of nuclei. Interference reflection microscopy and protein exclusion studies of adherent macrophages demonstrated the formation of closed compartments by the creation of tight seal along the periphery of the cell [7,8]. Our current data suggest that IL-4 mediated filamentous actin reorganization along the ventral cell surface may be a mechanism by which adherent macrophages/FBGCs form closed compartments. These closed microenvironments may allow the concentration of phagocytic activities, reactive oxygen intermediates, acid and enzymes at the cell-material interface.

## CONCLUSIONS

Our results demonstrate that the subcutaneous cage-implant system is applicable in mice to address the mechanisms of biomaterial-associated FBGC formation *in vivo*. We observed that FBGC density on PEUU cage-implanted into mice was significantly decreased by the direct injection of IL4Ab into the cages when compared to nonspecific IgG and PBS injection controls by 7 days post-implantation. Conversely, the injection of muIL4 significantly increased FBGC density when compared with the controls. *In vitro* FBGCs were morphologically similar to FBGCs observed *in vivo*. Significant reorganization of filamentous actin from a pattern of diffused cytoplasmic staining to ventral surface-associated punctate staining occurred over a 10 day culture period of human monocytes/macrophages. The addition of IL-4 induced FBGC formation and further restricted the punctate pattern to the periphery of the ventral cell surface and to a perinuclear sphere. Our data support a role for IL-4 in mediating FBGC formation on biomaterials *in vivo* and *in vitro* and suggest that a unique actin cytoskeleton organization characterizes the FBGC phenotype.

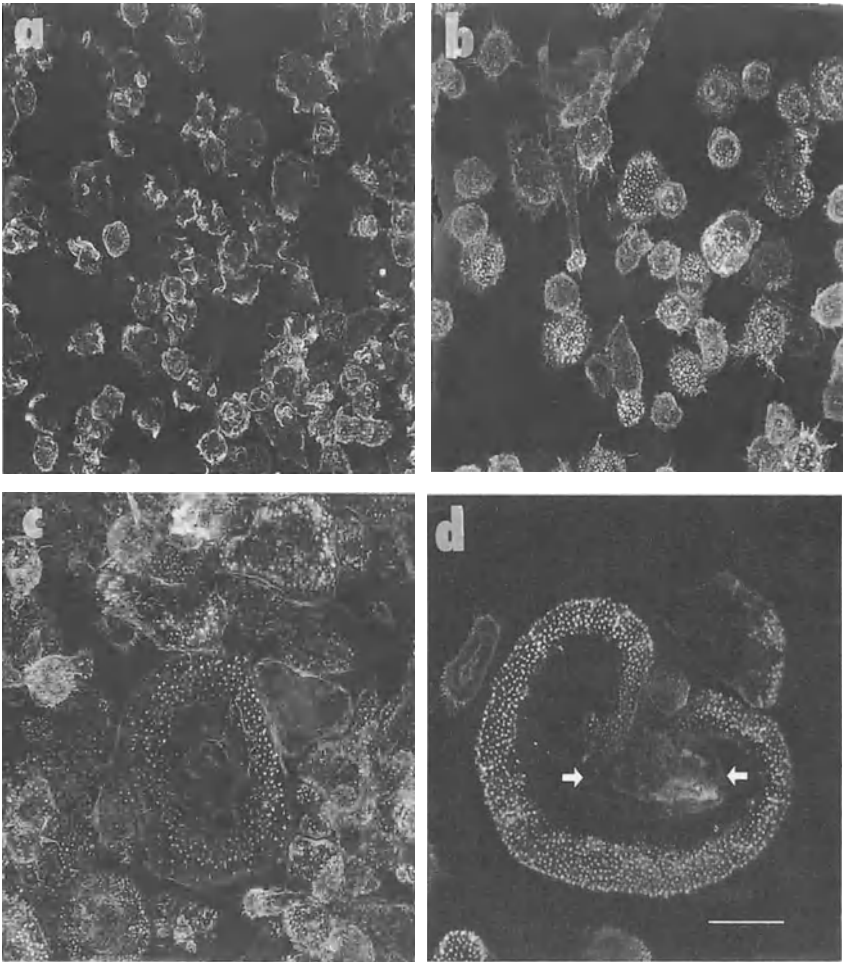


**Fig. 1.** Fluorescent CSLM visualization of filamentous actin of human monocytes, macrophages, and FBGCs cultured on PEUU *in vitro*. Adherent monocytes/macrophages not treated with IL-4 following incubations of (a) 2 hours, (b) 3 days, and (c) 10 days. (d) FBGC following 10 day incubation with 10 ng/ml IL-4 added on days 3 and 7; arrows indicate location of nuclei (not shown) visualized by double label CSLM. Scale bar represents 25  $\mu$ m.

#### ACKNOWLEDGMENT

These studies were supported in part by the National Institutes of Health, Grants HL-25239, HL-47300, and HL-33849.

**REFERENCES**

1. Remes A, Williams DF (1992) Immune response in biocompatibility. *Biomaterials* 13:731-743
2. McInnes A, Rennick DM (1988) Interleukin-4 induces cultured monocytes macrophages to form giant multinucleated cells. *J. Exp. Med.* 167:598-611.
3. McNally AK (1994) Mechanisms of monocyte/macrophage adhesion and macrophage fusion on different surfaces. Doctoral Thesis, Case Western Reserve University, Cleveland, Ohio, U.S.A.
4. Lehto VP, Hovi T, Vartio T, Badley RA, Virtanen I (1982) Reorganization of cytoskeletal and contractile elements during transition of human monocytes into adherent macrophages. *Lab. Invest.* 47:391-399.
5. Amato PA, Unanue ER, Taylor DL (1983) Distribution of actin in spreading macrophages: A comparative study on living and fixed cells. *J. Cell Biol.* 96:750-761.
6. Kao WJ, Hiltner A, Anderson JM, Lodoen GA (1994) Theoretical analysis of *in vivo* macrophage adhesion and foreign body giant cell formation on strained poly(etherurethane urea) elastomers. *J. Biomed. Mater. Res.* 28:819-829.
7. Wright SD, Silverstein SC (1983) Phagocytosing macrophages exclude proteins from the zones of contact with opsonized targets. *Nature* 309:359-361.
8. Heiple JM, Wright SD, Allen NS, Silverstein SC (1990) Macrophages form zones of close apposition to IgG-coated surfaces. *Cell Motil. Cytoskel.* 15:260-270.

# POLYMER-SUPPORTED TISSUE ENGINEERING

Yoshito Ikada

*Research Center for Biomedical Engineering, Kyoto University, 53 Kawahara-cho, Shogoin, Sakyo-ku, Kyoto 606, Japan*

## ABSTRACT

This paper overviews the current tissue engineering which makes the use of cells and polymers for tissue regeneration and tissue substitution. The tissue regeneration which, in a narrow sense, is the major purpose of the tissue engineering can be performed by seeding cells on a resorbable polymer scaffold or by using a polymer scaffold alone or with incorporated cell growth factors but without seeded cells. Implantation of polymer scaffolds with or without cells results in new tissue regeneration in vivo under simultaneous bioabsorption of the scaffold. On the contrary, the polymers used for tissue substitution are non-resorbable and function as the substrate for cell attachment and/or immunoisolation of cells. To date, the liver and pancreas have been most extensively studied for the temporary and permanent substitution, respectively.

**KEY WORDS:** tissue engineering, polymer scaffold, tissue regeneration, tissue substitution, cell seeding

## INTRODUCTION

Materials implanted in the body have been mostly used for permanent tissue or organ replacement up to now. However, the biomaterials would not need to be permanently implanted, once the damaged tissue or organ has been repaired. It should be noted that most of our tissues are known to be self-repairable if proper assistance is provided for the tissue repair. The assistance includes scaffolds for the tissue regeneration, cells, and growth factors. The scaffolds made from biomaterials should be resorbed in the body after completion of the tissue regeneration, because those foreign-bodies are no more necessary. This modern technology which aims at such tissue regeneration with the use of biomaterials is called tissue engineering. This is a new field in the biomaterials research, although regeneration of some tissues has already been clinically applied using this new technology. The well-known example is skin regeneration using artificial skins which function as scaffold for cell proliferation and disappear when skin is regenerated. This article will describe the basic concept and fundamentals of the tissue engineering performed with the use of polymeric biomaterials and some examples of the tissue engineering under investigation. Here tissue or organ substitution using cells and polymers, often called bioartificial organs or hybrid-type artificial organs, is included in the category of tissue engineering, since cells play an important role in these artificial organs, similar to the tissue regeneration.

## TISSUE REGENERATION

The major role of polymers used in the tissue engineering is either to provide scaffold (or template) to cells which produce the tissue or to keep a space for cell proliferation.

### Scaffold providing

Most of the polymer-supported tissue engineering makes the use of scaffold provided by bioabsorbable polymers. This tissue engineering involving scaffolds sometimes needs cell seeding to the scaffold prior to the implantation, but in some cases does not.



### 1. Without seeded cells

Recently Brittberg et al.[1] have shown that cultured autologous chondrocytes can be used to repair deep cartilage defects in the femorotibial articular surface of the knee joint. As full-thickness defects of articular cartilage in the knee have a poor capacity for repair, they performed autologous chondrocyte transplantation in patients, but without use of any scaffold. In this case the defective cartilage in the patient knee must have functioned as the scaffold for the new cartilage regeneration. However, if the tissue to be repaired is like a large hole, scaffold will be required which should work as a substrate for the cells to attach and proliferate. The cells come from the adjacent healthy tissue and the bioabsorbable scaffold disappears after regeneration of the tissue. We have revealed that a porous collagen sheet works very well as the scaffold of dermis regeneration[2]. A thin silicone sheet was covered on the collagen layer to prevent the body water loss and infection, but an addition of glycosaminoglycan to the collagen layer was not necessary[3]. This idea was extended to regeneration of esophagus and it was found that a bilayered tube composed of a silicone layer inside and a porous collagen tube outside could construct a new esophagus tissue covered with a mucous membrane. The silicone tube fell down into the stomach of dogs when the new tissue was constructed from the bilayered tube anastomosed to the dog esophagus[4]. A tracheal tissue could be also regenerated from a collagen sponge when implanted in the dog trachea[5]. Regeneration of broken anterior cruciate ligament(ACL) was attempted with the use of poly(L-lactide) fibers. The result on goats and sheep were as good as those of a non-resorbable ligament assist device[6].

### 2. With growth factors

It has been reported that bone is formed at the ectopic site where a carrier with incorporated bone morphogenic protein(BMP) is implanted[7]. The carrier may function not only as a base for the sustained release of BMP but also as a scaffold for bone formation from osteoprogenitor cells. Recently we have found that basic fibroblast growth factor (bFGF) can trigger bone formation when a gelatin hydrogel is implanted in a cavity formed in the rabbit mandibula after being impregnated with bFGF[8]. In this case osteoblasts present in the adjacent bone may be responsible for the bone regeneration.

### 3. With seeded cells

The dermis of skin can be regenerated from a polymer scaffold as mentioned above, whereas epidermal regeneration requires seeding of epidermal cells to the resorbable scaffold prior to its implantation. Similar to the dermis, some tissues need cell seeding for the regeneration. The well-known example is cartilage regeneration. Indeed, a large number of investigations have been reported on the cartilage regeneration from chondrocytes alone or chondrocyte-scaffold constructs. Langer et al. revealed that a cartilaginous tissue could be formed when a polyglycolide mesh was subcutaneously implanted in nude mice after seeding with chondrocytes harvested from hyaline cartilage on the articular surface of newborn calf shoulder[9]. In this connection we found that an addition of bFGF to a collagenous scaffold seeded with the rib cartilage of rat greatly accelerated the cartilaginous tissue regeneration in nude mice[10]. Joint resurfacing by the regeneration of articular cartilage was also reported by Freed et al.[11]. They used rabbit articular chondrocytes and synthetic, biodegradable polymer scaffolds, and then implanted them as allografts into full-thickness defects in the knee joints of adult rabbits. We have shown that repair of lost mandibula is possible when a poly(L-lactide) tray containing autologous cancellous bone marrow is implanted into the lost site[12]. This tissue engineering is at present under clinical trial. Vacanti et al. extensively studied cell transplantation using bioabsorbable polymers as cell scaffold[13]. They seeded single cells and clusters of fetal and adult rat and mouse hepatocytes, pancreatic islet cells, and small intestinal cells onto biodegradable polymers of polyglycolide, polyanhydrides, and polyorthoester. The polymer-cell constructs were implanted into host animals. In some cases the hepatocyte implantation was successfully engrafted, but no pancreatic islets could survive implantation. Arterial tissue regeneration has been also studied by several research groups using biodegradable tubes or conduits with seeded endothelial cells, but promising results have not yet been reported. One of the major reasons is the difficulty in balance between the new tissue formation and the material resorption. Burst will take place if the tube material is resorbed before strong tissue is constructed, because the tube is always under high blood pressure.

### Space keeping

The scaffolds described above are implanted into patients, since the patient living body which needs new tissue regeneration is lacking the scaffold required for cell attachment and

proliferation. On the contrary, there are such cases that have a scaffold for tissue regeneration in own living body but are not able to regenerate tissues. One reason for that is that there is no space available for new tissue generation, because a fibrous tissue present in direct contact with the damaged tissue to be repaired is occupying the space required for the tissue regeneration. In such a case the space which allows tissue regeneration should be secured by means of biomaterial. The membrane used for therapeutic treatments of periodontal disease is an example. This is called *Guided Tissue Regeneration (GTR)* in the periodontal surgery. Fig.1 shows implantation of a membrane to keep a space[14]. To date, polytetrafluoro-ethylene (PTFE) has been used for patients as the membrane. As this PTFE membrane requires surgical reoperation for the removal because of its non-bioabsorbability, we have developed a porous, bioabsorbable membrane from a glycolide-lactide copolymer which is more slowly bioabsorbed than collagen but more quickly than polylactide membrane[15].

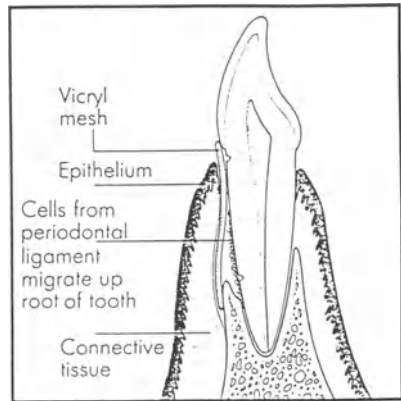


**Fig. 1 Space keeping for regeneration of lost attachment apparatus in periodontal disease**

Nerve guides which allow repair of broken peripheral nerves also aim primarily at keeping space for generation of a new nervous tissue. In addition, the nerve guides should maintain nerve growth factors released from the nerve in repair and allow nutrient supply from the outside. In the beginning of this kind of investigation silicone and collagen tubings had been used as a nerve guide, but recently glycolide-lactide copolymers are widely used for the nerve guide preparation. We have used a crosslinked gelatin tubing as a nerve guide because this material satisfies all the requirements as the guide[16].

## TISSUE SUBSTITUTION

When tissues or organs have undergone severe damage, they have been often replaced or substituted with non-resorbable biomaterials. However, some of tissues and organs are too difficult to be replaced by non-biological, man-made materials because of their very poor biofunctionalities compared with natural ones. The tissue engineering with polymer scaffolds has also failed in producing their new tissues or organs. Among such organs are the pancreas and liver that biosynthesize proteins. Thus, an alternative is to hybridize metabolic cells with polymers. They are called hybridized artificial organs, in which the polymer component functions primarily to isolate the heterologous cells from the attack by the host immune system. Therefore, the purpose of the tissue engineering using hybridized artificial organs is not to regenerate new tissues *in vivo*, but to substitute the lost biofunction of organs with the cell-polymer constructs. Such tissue substitution is performed either temporarily or permanently.

### Temporary substitution

Temporary substitution of the liver has been attempted both by implantation of polymer-hepatocyte constructs and by extracorporeal circulation. From the clinical point of view, the liver substitution by extracorporeal circulation seems to be much more practical. Indeed, Demetriou et al.[17] and Sussman et al.[18] have clinically applied cell-seeded hollow fiber devices to patients in an extracorporeal circulation system with good results. Demetriou et al. used microcarriers for attaching porcine hepatocytes and placed the cell-seeded microcarriers in the outside of the hollow fibers, while Sussman et al. attached C3A cells directly on the outer surface of hollow fibers. We keep hepatocytes inside hollow fibers with agarose gel which prevents the cell migration inside the fibers[19].

**Permanent substitution**

Langerhans islets of the pancreas are mostly used for permanent substitution of devastated pancreas. For this purpose Langerhans islets are encapsulated in microbeads, hollow fibers, or small bags. The encapsulating polymers function as an immunoisolation membrane. The currently used polymers here are hydrogels from alginate-poly(L-lysine) ion complex, agarose, and poly(vinyl alcohol). Recently we have found that immunoisolation of these hydrogels can be achieved not by preventing the permeation of immunoglobulin through the hydrogels but by consuming complement proteins until arriving at the encapsulated Langerhans islets[20]. The complement consumption will result from deactivation, trapping, or destruction of complement molecules during traveling through the hydrogel matrix. It was also revealed that aggregation of Langerhans islets in the hydrogel matrix had to be avoided[21]. Otherwise, the Langerhans islets would undergo reduction in their activity. Langerhans islets obtained from human cadavers and encapsulated in alginate-poly(L-lysine) ion complex microbeads have been clinically applied by Soon-Shiong et al.[22].

**CONCLUSION**

In summary it may be concluded that the tissue engineering which makes the use of cells and polymers seems very promising for tissue regeneration and substitution. This is because any foreign-body polymers do not remain any more in the body in the case of tissue regeneration when autologous tissues are formed, while in the case of tissue substitution the cells seeded on a polymer surface or encapsulated in a polymer container will synthesize and secrete required proteins. The cell-polymer constructs work temporarily for the period of extracorporeal blood circulation only or permanently if implanted into the body. Schematic illustration of the tissue

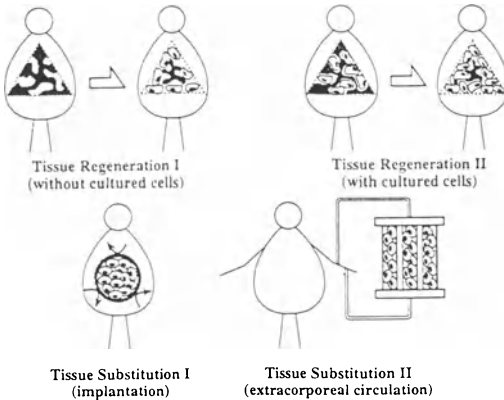


Fig. 2 Illustrative Representation of Tissue Engineering

Tab. I Materials and Technologies Required for Tissue Engineering

Materials for	Technologies for
Scaffold or template	Isolation of cells and tissues
Keeping space	Large-scale cell culture
Immuno-Isolation	Gene, protein, and cell manipulation
Antithrombolization	Control of material resorption
Cell proliferation	Sustained drug delivery
Cell differentiation	

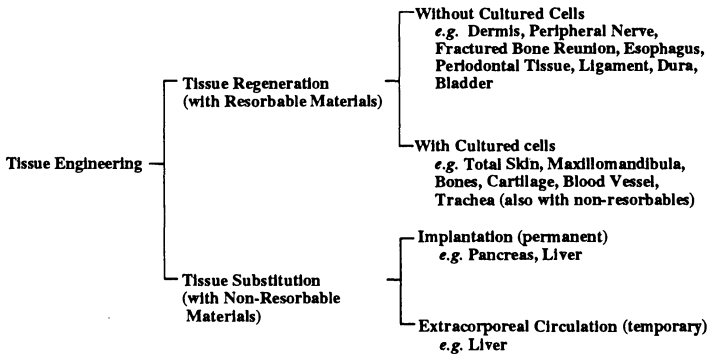


Fig.3 Tissues and Organs under Investigation by Means of Tissue Engineering

engineering is given in Fig.2. It is not yet established which tissue needs cell seeding and which tissue does not require the cells. The materials and basic technologies needed for the tissue engineering are presented in Tab.1. The problems to be solved for the success of the tissue engineering include the source of cells, the large-scale cell culture technology, and the material biodegradation rate balanced with that of tissue generation rate. Fig.3 represents the tissues which have been the target of current tissue engineering studies.

## REFERENCES

1. Brittberg M, Lindahl A, Nilsson A, Ohlsson C, Isaksson O, Peterson L. (1994) Treatment of deep cartilage defects in the knee with autologous chondrocyte transplantation. *N. Engl. J. Med.* 331: 889-895
2. Matsuda K, Suzuki S, Isshiki N, Ikada Y. (1993) Re-freeze dried bilayer artificial skin. *Biomaterials* 14: 1030-1035
3. Suzuki S, Matsuda K, Isshiki N, Ikada Y. (1992) GAG addition effects for bilayer artificial skin. *Japanese J. Plast. Surg.* 12: 137-148
4. Natsume T, Ike O, Okada T, Shimizu Y, Ikada Y, Tamura K. (1990) Experimental studies of a hybrid artificial esophagus combined with autologous mucosal cells. *Trans. Am. Soc. Artif. Organs* 36: 435-437
5. Okumra N, Teramachi M, Takimoto Y, Nakamura T, Ikada Y, Shimizu, Y. (1994) Experimental reconstruction of the intrathoracic trachea using a new prosthesis made from collagen grafted mesh. *ASAIJ* 40:M834-M839
6. Kobayashi H, Kawamoto Y, Gibbons DF, van Kampen CL, Mendenhall HV, Hara S, Tomizawa N, Ikada Y. (1994) Goat study of bioabsorbable poly(lactic acid) augmentation device of bone-tendon-bone ACL reconstructions. *Proc. 16th Ann. Meet. Japanese Soc. Biomater.* (Nov.4-5, 1994, Kohfu, Japan) p.155
7. Urist MR. (1965) Bone:formation by autoinduction. *Science* 150: 893-899
8. Unpublished result
9. Cima LG, Vacanti JP, Vacanti C, Ingber D, Mooney D, Langer R. (1991) Tissue engineering by cell transplantation using degradable polymer substrates. *J. Biomech. Eng.* 113:143-151
10. Fujisato T, Sajiki T, Liu Q, Ikada Y. Effect of basic fibroblast growth factor on cartilage regeneration in chondrocyte-seeded collagen sponge scaffold. *Biomaterials*, submitted
11. Freed LE, Grande DA, Lingham Z, Emmanuel J, Marquis JL, Langer R. (1994) Joint resurfacing using allograft chondrocytes and synthetic biodegradable polymer scaffolds. *J. Biomed. Mater. Res.* 28:891-899
12. Unpublished result
13. Vacanti JP, Morse MA, Salzman WM, Domb AJ, Perez-Atayde A, Langer R. (1988) Selective cell transplantation using bioabsorbable artificial polymer as matrices. *J. Pediatric Surg.* 23:3-9
14. Fleisher N, de Waal H, Bloom A. (1988) Regeneration of lost attachment apparatus in the dog using Vicryl absorbable mesh (Polyglactin 910). *Intnl J. Period. Restor. Dent.* 2:45-55
15. Yamada R, Matsumoto Y, Takahashi K, Yamanouchi K, Aoki E, Sato T, Ishikawa T, S.-H. Hyon, Ikada Y. (1991) Pathohistological study on the guided regeneration of periodontal tissue using a membrane from lactide-glycolide copolymer. *Japanese J. Period. Disease* 33:396-405
16. Li G, Nakamura T, Shimizu Y, Tomihata K, Ikada Y, Endo K. (1993) Study on artificial nerve-development of reconstruction guide for peripheral nerve using gelatin tube. *Japanese J. Artif. Organs* 22:364-369
17. J. Roza, Podesta L, Lepage E, Morsiani E, Moscioni AD, Hoffman A, Sher L, Villanil F, Woolf G, McGrath M, Kong L, Rosen H, Lanman T, Vierling J, Makowka L, Demetriou AA. (1994) A bioartificial liver to treat severe acute liver failure. *Ann. Surg.* 219:538-546
18. Sussman NL, Gilason GT, Conlin CA, Kelly JH. (1994) The Hepatix extracorporeal liver assist device: initial clinical experience. *Artificial Organs* 18:390-396
19. Unpublished result
20. Iwata H, Morikawa N, Fujii T, Takagi T, Samejima T, Ikada Y. Transplantation, submitted
21. Mitsuo M, Inoue K, Nakai I, Oda T, Gu Y, Shimohara S, Kogire M, Fujisato T, Maetani, Ikada Y, Tobe T, Oka T. (1992) Efficacy of mesh reinforced polyvinyl alcohol as a novel device for bioartificial pancreas. *Transp. Proc.* 24:2939-2940
22. Soon-Shiong P, Heintz RE, Merideth N, Yao QX, Yao Z, Zheng T, Murphy M, Moloney M, Schmehl M, Harris M. (1994) Insulin independence in a type 1 diabetic patient after encapsulated islet transplantation. *Lancet* 343:950-951

## New Frontier of Biomimetic Glycotechnology for Cellular and Tissue Engineering

Toshihiro Akaike<sup>\*</sup>, Mitsuaki Goto<sup>\*\*</sup>, Hirofumi Yura<sup>\*\*</sup>, Akira Kobayashi<sup>\*\*</sup>, Chong-su Cho<sup>\*,\*\*</sup>,  
Atsushi Maruyama<sup>\*</sup> and Kazukiyo Kobayashi<sup>#</sup>

<sup>\*</sup>Faculty of Bioscience and Biotechnology, Tokyo Institute of Technology, Midoriku, Yokohama, 226, Japan,

<sup>#</sup>School of Agricultural Science, Nagoya, University, Furou-cho, Chikusaku, Nagoya 464, Japan,

<sup>\*\*</sup>Kanagawa Academy of Science and Technology, Sakado,3-2-1, Takatsu-ku, Kawasaki, kanagawa 213, Japan

### Abstract

Biomimetic glycopolymers recognized by cell surface receptors, transporter and the like were synthesized and cell-polymer interactions were evaluated. Galactose- or glucose-carrying polystyrene derivatives were shown to be highly recognized by hepatocytes or erythrocytes via specific receptors or transporters and were applied to cell and tissue engineering.

### Key Words

Biomimetic Glycopolymers, Asialoglycoprotein, Galactose-carrying polystyrene, Hepatocytes, Glucose transporter

### Introduction

Glycoconjugates such as glycoproteins, glycolipids, and proteoglycans are important in cell-cell or cell-matrix interactions in living systems. Glycoconjugates usually have very complicated structures and the structure-function relationships of such molecules remain to be solved. Polymer chemistry can be used to mimic natural glycoconjugates in a simplified synthetic manner to clarify the biological phenomena mediated by sugar recognizing receptors and transporters. As compared with protein chemistry based on gene engineering, glycotechnology based on synthetic chemistry has lots of advantages, such as simplification of preparations and variation of modifications (Fig. 1).

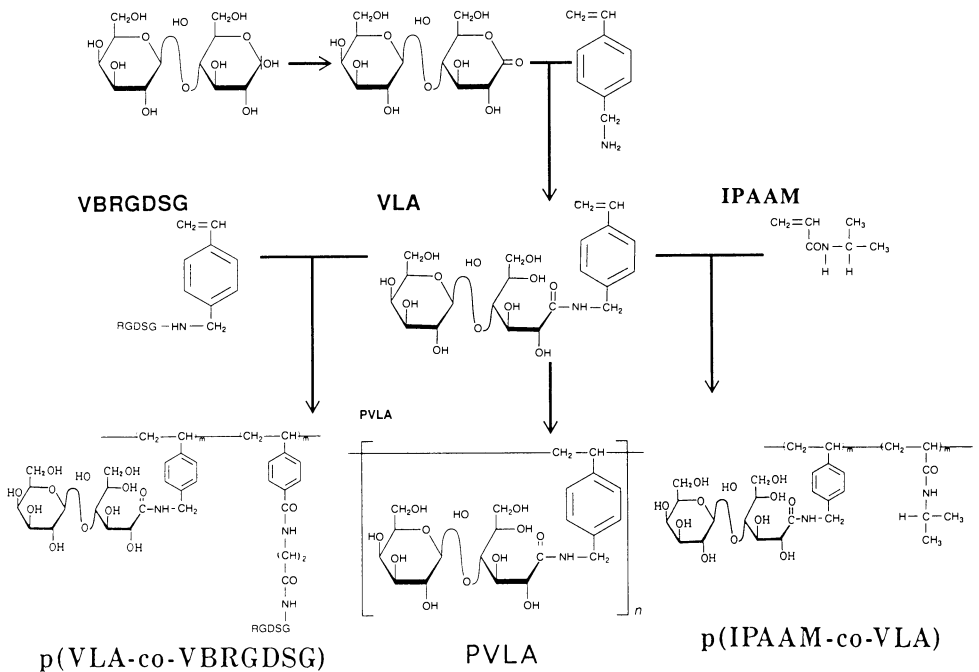


Fig. 1: Synthetic Schemes of Asialoglycoprotein Model Polymer and Applications to Super Glycopolymers

Molecular recognitions of sugar moieties involve many receptors specific to various growth factors and cytokines as well as glucose-transporters and galactose-transferase on cell surfaces (Fig.2). The synthesis of sugar-carrying polymers mimicking some glycoconjugates recognized by receptors may allow control of cell attachment and cell functions. Some polymers carrying various sugars may specifically make multiple and multivalent interactions with cells as if the recognition of the cell surface topology were made plainer(Fig.2). The interaction may enhance the accuracy of cell recognition, which will facilitate gene and drug targeting as well as selective isolation and culture of cells. In this paper, we reviews our recent works relating to the biomimetic design of cell specific glycopolymers and their applications to cell labeling, cell culture, cell targeting for diagnosis, artificial organs and drug(gene) delivery systems(DDS, GDS)

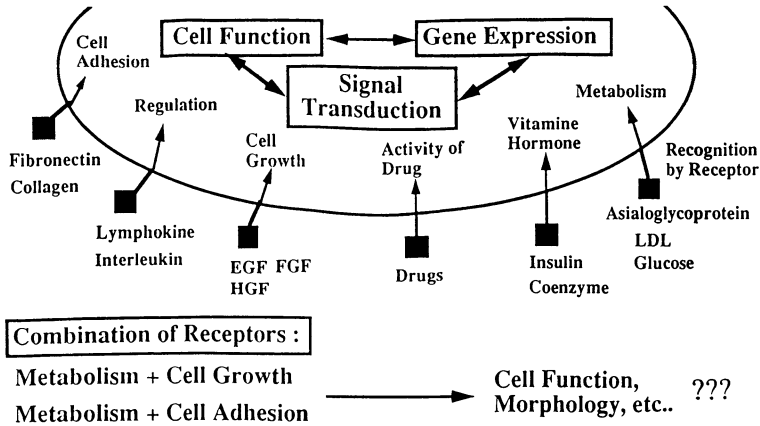


Fig.2: Design of Multiligands Polymers recognizing Cell Surface Topology

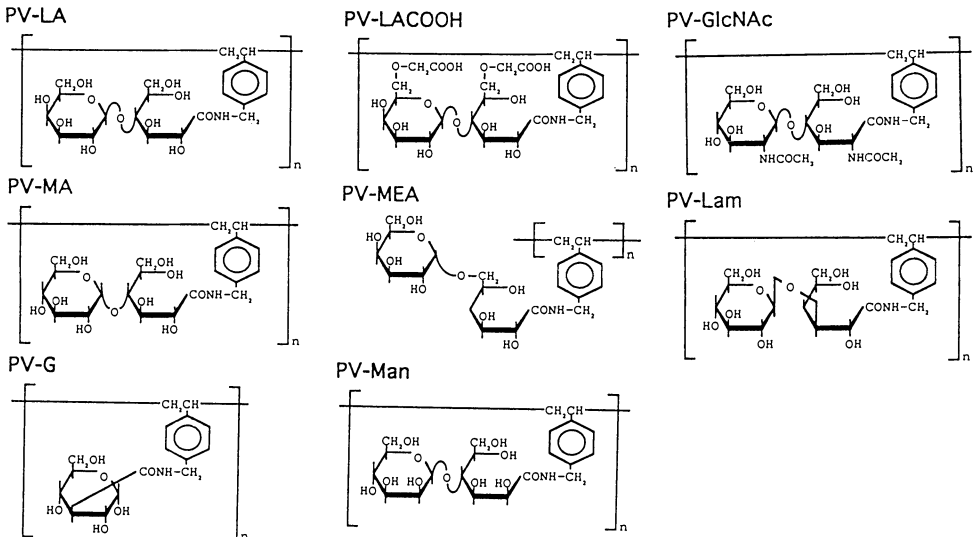


Fig.3: Design of Sugar-carrying Amphiphilic Polymers

## Materials and Methods

The syntheses of various sugar-carrying homopolystyrene derivatives and other biomimetic glycopolymers in Fig. 1 and Fig. 3 were made according to reported method<sup>1)4)</sup>. The physicochemical evaluations of these polymers and cell-polymer interactions were also made as reported<sup>2)3)</sup>.

## Results and Discussion

### *Asialoglycoprotein-mimicking Polymers for Hepatocytes Culture*<sup>3)4)5)</sup>

We reported that a lactose-carrying polystyrene, poly N-p-vinylbenzyl-[O- $\beta$ -D-galactopyranosyl-(1-4)-D-gluconamide] (PVLA, Fig. 1), is a useful substratum for hepatocytes on PVLA which were distinct from those on naturally occurring substrata such as collagen, fibronectin, laminin, and proteoglycan. It was reported that hepatocytes on PVLA showed a round morphology and expressed highly differentiated functions. They could be detached easily by treating the culture dish with EDTA to remove  $\text{Ca}^{2+}$  ions from the medium. It was demonstrated that the adhesion is mediated by the galactose-specific interactions between hepatocytes and PVLA which carries highly concentrated  $\beta$ -galactose residues along the polymer chain. Proliferation and differentiation of hepatocytes are regulated not only by soluble factors but also extracellular matrices. For example, DNA synthesis in cultured hepatocytes is induced by several soluble proteins such as insulin, epidermal growth factor (EGF), and hepatocyte growth factor (HGF), and inhibited by transforming growth factor- $\beta$  (TGF- $\beta$ ). Extracellular matrices such as collagen, laminin, and fibronectin have been recently revealed to control spreading, migration, adhesion, and proliferation of hepatocytes since they have several globular domains which are specialized for binding to a particular molecule or cell. Cell-cell contact is also important in controlling proliferation and differentiation of hepatocytes. In these interactions, cell-matrix interactions are especially important. The surroundings of cells are arranged through these interactions which may determine to control functions and cell-shapes.

We are interested in the regulation of the proliferation, differentiation, and shapes of hepatocytes using an artificial cellular matrix, PVLA, as a substratum (containing an ideal ligand to asialoglycoprotein receptors on hepatocytes).

Morphology and responses of hepatocytes are investigated using PVLA as a culture substratum, especially in focusing on the effect of the surface density of the PVLA substratum. The surface density of PVLA on polystyrene dishes was determined using fluorescein-labeled PVLA as a probe under a fluorescence laser microscope. PVLA-coated surfaces were observed by scanning electron microscope and atomic force microscopies (AFM) under air and water,

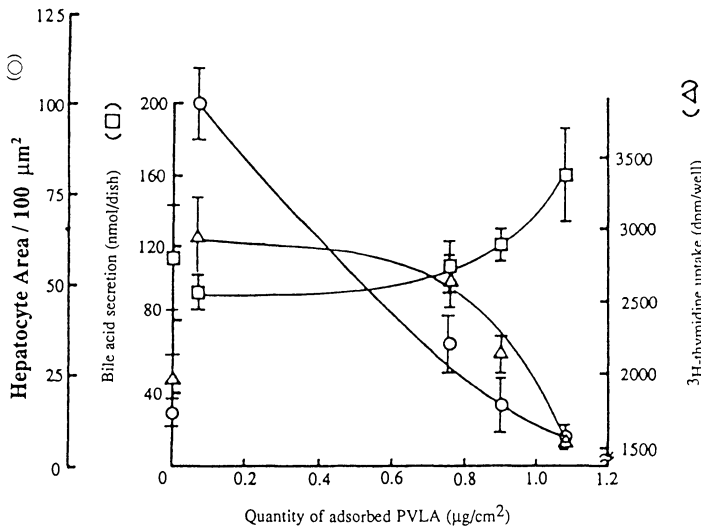


Fig. 4: The relation between hepatocyte shape (○), Bile acid release (□) and <sup>3</sup>H-thymidine uptake of hepatocytes cultured on various amounts of PVLA on polystyrene culture dishes.

which showed that PVLA molecules were adsorbed patchily on low density surfaces and uniformly concentrated all over the dish on high density surfaces. It was suggested from the requirement of the  $\text{Ca}^{2+}$  ion, inhibition of galactosyl substances, and localization of receptors that the adhesion of hepatocytes to both low and high PVLA-density surfaces is mediated by galactose-specific interactions between PVLA and asialoglycoprotein receptors. At low PVLA densities ( $0.07 \mu\text{g}/\text{cm}^2$ ), the hepatocytes were flat and expressed high levels of  $^3\text{H}$ -thymidine uptake and low levels of bile acid secretion. Contrastingly, at high PVLA densities ( $1.08 \mu\text{g}/\text{cm}^2$ ), they were round and expressed a low level of  $^3\text{H}$ -thymidine uptake and a high level of bile acid secretion. The shapes, proliferation, and differentiation of hepatocytes could be regulated by varying the densities of PVLA absorbed to polystyrene dishes (Fig4). We assume that there are two recognition mechanisms operating between PVLA and hepatocytes: (1) adhesion through highly concentrated or clustered galactose-specific interaction; and (2) responses in shapes, proliferation, and differentiation by PVLA-coating densities.

*Supra-molecular assembly of Amphiphilic Glycopolymers for drug and Gene Delivery System* <sup>2)</sup>

We also demonstrated that, owing to the hydrophilic-hydrophobic structures, a PVLA molecule can form a tightly coiled conformation in water. In addition, several polymer molecules are inclined to aggregate mutually to form a kind of supra molecular assemblies. Several hydrophobic drugs could be included in PVLA micelles. We also found that the hepatocyte cells recognized the galactose moiety of PVLA, mediated by asialoglycoprotein receptor which existed onto hepatocyte cells.

Directed toward pharmacological applications of lactose-carrying polystyrene, its body distribution, clearance from blood, and specific binding to receptors have been investigated using radiolabeled PVLA. When  $^{125}\text{I}$ -labeled PVLA was injected into rats through their tail veins, the radioactivity was distributed highly to liver, less to thyroid gland, cecum-large intestine, urine, feces, and blood, and much less to lung, heart, kidney, spleen, pancreas, small intestine, and urinary bladder (Table1). Its concentration to the liver was visible by the whole-body autoradiography. It was clarified that about 97% of PVLA was distributed to parenchymal liver cells and only the rest to nonparenchymal liver cells. The radioactivity in blood was decreased with time according to a biexponential curve. Two open compartment models are proposed on the basis of the pharmacokinetic analysis of the equation, which elucidated that PVLA migrated rapidly from blood to parenchymal liver cells. Specific binding between  $^{125}\text{I}$ -labeled PVLA and asialoglycoprotein receptors on parenchymal liver cells was demonstrated by its inhibition with asialofetuin.

Dissociation constant of the bond estimated by Scatchard analysis was  $K_d = 1.4 \times 10^{-9}\text{M}$ . The binding was as strong as those of several naturally occurring asialoglycoproteins. These properties of PVLA, as liver-specific targeting materials using galactose ligands as recognition signals to asialoglycoprotein receptors, are speculated to be closely related with the conformational structures of PVLA which can carry drugs in their hydrophobic regions.

Table 1. Percentage radioactivity distribution of  $^{125}\text{I}$ -labeled PVLA per total weight of tissue

Tissue	Radioactivity (% of dose)		
	15 min	1 h	24 h
Blood	$3.08 \pm 0.08$	$1.99 \pm 0.12$	$0.44 \pm 0.07$
Thyroid Gland	$0.13 \pm 0.02$	$0.33 \pm 0.03$	$2.48 \pm 0.41$
Heart	$0.08 \pm 0.01$	$0.06 \pm 0.01$	$0.03 \pm 0.00$
Lung	$0.20 \pm 0.02$	$0.11 \pm 0.01$	$0.05 \pm 0.01$
Liver	$61.31 \pm 0.07$	$58.81 \pm 0.99$	$53.48 \pm 1.71$
Kidney	$1.00 \pm 0.01$	$0.36 \pm 0.02$	$0.13 \pm 0.02$
Spleen	$0.12 \pm 0.01$	$0.09 \pm 0.01$	$0.06 \pm 0.00$
Pancreas	$0.07 \pm 0.00$	$0.05 \pm 0.00$	$0.02 \pm 0.00$
Stomach	$1.91 \pm 0.18$	$2.76 \pm 0.41$	$0.80 \pm 0.17$
Small intestine	$3.35 \pm 0.07$	$2.92 \pm 0.13$	$0.19 \pm 0.32$
Cecum large intestine	$0.38 \pm 0.01$	$0.27 \pm 0.01$	$4.13 \pm 0.29$
Urinary bladder	$0.35 \pm 0.13$	$0.52 \pm 0.40$	$0.01 \pm 0.01$
Urine	$12.66 \pm 2.11$ (3.14) <sup>b</sup> (9.25) <sup>c</sup>	$19.37 \pm 0.46$	$35.23 \pm 0.52$ (3.21) <sup>b</sup> (31.71) <sup>c</sup>
Feces	-	-	$1.97 \pm 0.62$
Total	$84.64 \pm 1.76$	$87.63 \pm 0.65$	$99.91 \pm 1.49$



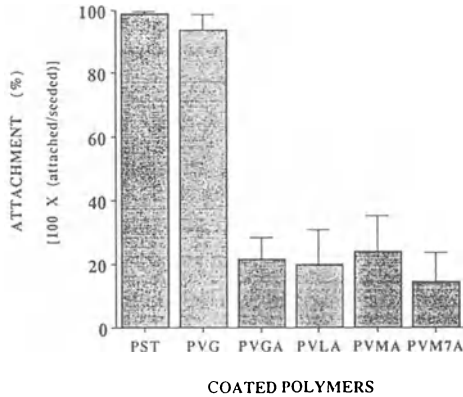


Fig. 5: The highest attachment of erythrocytes occurred on PVG-coated dishes and uncoated hydrophobic polystyrene dish (PST)

Table 2. The patterns of various ligands binding to liver cells.

Ligands with FITC	Rat hepatocytes	Hep G2 cells	Chang Liver cells
PVLA	++	+	-
Asialofetuin	+	-	-
LDL	++	+	+

"+" and "++", The degree of increase in ligand bound.

#### *Glucose Transporter-mediated Dynamic Attachment of Erythrocytes onto a Reducing Glucose-carrying Polymers* <sup>6)</sup>

In this part we focus on a novel ligand-receptor combination of a reducing glucose derivative and glucose transporter. A polystyrene derivative (PVG in Fig. 3) substituted with a reducing glucose moiety on each repeating unit has been applied as a substratum for the attachment of erythrocytes which carry the erythrocyte-type glucose transporter (GLUT-1). The structure, ligand specificity, molecular mechanism and regulation of glucose transporters have been well investigated, but no attempt had been reported to construct a cell-substratum complex mediated through glucose transporters. It is also worth to note that reducing carbohydrates are employed here as cell-recognition signals, while glyco-signals composed of nonreducing carbohydrate moieties are well-documented to play important roles in the specific interactions with antibodies and cell-surface lectins. Erythrocytes, which carry type-1 glucose transporters (GLUT-1) in their plasma membrane, were found to be attached specifically and strongly to dishes which had been coated with (PVG) substituted with reducing glucose moieties (Fig.5). The concave erythrocytes took teardrop shapes, stood on the rim, and swayed with gentle disturbance in the medium. The attachment to PVG substratum was suppressed by (1) GLUT-1 inhibitors such as phloretin, phoridzin, and cytochalasin B, and (2) PVG molecules in solution, and (3) at 4°C, suggesting that the specific recognition of high density of glucose on PVG and the dynamic movement of GLUT-1 are essential for the attachment. This novel combination of glucose transporter-carrying cells and reducing glucose-carrying polymer may lead to biomaterials with a wide range of applications. Therefore we could propose the application of glucose-carrying polystyrene (PVG) to substratum of cellular engineering as that of asialoglycoprotein model polymer (PVLA etc.) to hepatocytes engineering.

#### *Application of glycopolymers to cell labeling and cell recognition of surface topology*

Specific interaction between endocytic receptor such as asialoglycoprotein receptor or low-density lipoprotein (LDL) receptor and its ligand was estimated by flow cytometry with fluorescent PVLA and LDL. Rat hepatocyte, and human hepatomas (HepG2 and Chang Liver) were classified by binding profiles of FITC-labeled ligands depending on the difference of receptor expression as shown in Table2. Flow cytometry using fluorescent ligands suggested a

promising application to clinical diagnosis based on phenotypic assay indicating distinctly hepatocellular disorder or carcinogenesis.

Moreover, we examined the recognition mechanism of expressing several receptors on the cell surface. These receptors recognize several saccharides, hormones, and proteins as ligands which transduce various external signals in different manners even at the same time as shown in Fig. 2.

The interaction between hepatocyte and double ligands (lactose and RGDS)-carrying polystyrene, resulted in very effective cell attachment. The study demonstrated that the specific attachment is based on the combination of the interaction mediated by cell surface asialoglycoprotein receptors which can recognize  $\beta$ -galactose moiety and also the interaction mediated by integrin families (RGDS recognizable receptor). The results suggested that the design of polymers carrying multiple and multivalent ligands is very effective to the enhancement of cell recognizability. Biotin-carrying PVLA, sulfonyleurea-carrying PVLA and the like were also synthesized and evaluated. As above mentioned, PVLA, amphiphilic glycopolymer has been found out to be super-asialoglycoprotein analogs and had a number of biomedical applications in cellular and tissue engineering as well as DDS and GDS. The concept of biomimetic glycopolymer design will open the new frontier in bioscience as well as biotechnology.

### References

- 1) K.Kobayashi, et al, Polym. J. 17, 567-575 (1985)
- 2) M.Goto, T.Akaike, K.Kobayashi, et al, J. Controlled Release, (28), 223-233 (1994)
- 3) A.Kobayashi, K.Kobayashi, T.Akaike, et al, J. Biomater. Sci. Polymer Edn, (6), 325-342 (1994)
- 4) K.Kobayashi, T.Akaike et al, Neoglycoconjugates, (ed. by Y.C.Lee and R.T.Lee) Academic Press 261-284 (1994)
- 5) A.Kobayashi, T.Akaike, K.Kobayashi, et al, Makromol. Chem. Rapid Commun., 7, 645-650 (1986)
- 6) A.Kobayashi, A.Koyama, K.Kobayashi, T.Akaike, et al, Proc. Japan Acad., 69, Ser. B 89-94 (1993)

# CONTROL OF HEALING WITH PHOTOPOLYMERIZABLE BIODEGRADABLE HYDROGELS

Jeffrey A. Hubbell, Jennifer L. West, Sanghamitra M. Chowdhury

Division of Chemistry and Chemical Engineering, Mail Code 210-41, California Institute of Technology, Pasadena, CA 91125, Tel: (818) 395-4675, Fax: (818) 568-8743

## ABSTRACT

Post-surgical wound healing has been modified by the use of biodegradable hydrogel barriers to block cell adhesion to tissue surfaces, e.g. to the mesothelium in abdominopelvic surgery or to the subendothelium in angioplasty. These materials were formed in situ by photopolymerization of an aqueous precursor to obtain barriers that were conformal and adherent to the tissue. The precursor was comprised of a central chain of polyethylene glycol, with peripheral blocks of lactic acid oligomer, and with acrylate termini, the polyethylene glycol chain providing water solubility and biocompatibility, the lactic acid oligomer providing water lability, and the acrylate termini providing polymerizability to form a crosslinked hydrogel. Using these materials, it was possible to dramatically improve abdominal healing with less postoperative adhesions in rats and arterial healing with no thrombosis and less intimal thickening in rats. The hydrogel barriers were also employed as controlled release depots for protein drugs, the proteins being contained by entanglement. It was possible to further reduce postoperative abdominal adhesion formation in rats by releasing tissue plasminogen activator or urokinase plasminogen activator from the tissue-adherent barrier.

**KEY WORDS:** Healing, polyethylene glycol, biodegradable polymer, fibrinolytic

## INTRODUCTION

Cell adhesion to tissues is frequently involved in an undesired healing response. One example is the formation of postoperative adhesions, where a fibrin bridge initially forms between two traumatized peritoneal surfaces and fibroblasts migrate from the tissue surfaces into the fibrin bridge. Another example is post-percutaneous transluminal coronary angioplasty (post-PTCA) thrombosis, where the vascular endothelium is damaged by therapeutic intervention. Platelets may play a role in post-PTCA restenosis, since they produce thrombin, a smooth muscle cell mitogen, and release platelet-derived growth factor, also a smooth muscle cell mitogen. In the present investigations, we have sought to interrupt these cell-tissue interactions using tissue-adherent hydrogels as both mechanical barriers and as drug-release depots.

## METHODS

Water-soluble copolymers of polyethylene glycol (PEG) and lactic acid were formed, with degrees of polymerization approx. 5 on each end of a 8000 or a 10 000 Da PEG chain [1], as noted. The hydroxyl termini of this ABA (A, lactic acid; B, PEG) copolymer were acrylated, to yield a diacrylated, water-labile, water-soluble prepolymer. Solutions of this prepolymer (5 - 23%) in physiological saline were readily photopolymerizable with a variety of photoinitiation systems, two of which are described below.

One model of interest was the prevention of post-operative pelvic adhesions. Uterine tissue was treated in such a post-operative adhesion model in the rat, consisting of an electrocautery devascularization of the mesenteric arcade feeding both uterine horns, in addition to an electrocautery injury to the serosa of the horns at two regions along each horn [2]. A PEG chain of

8000 Da was used in the prepolymer, synthesized as described above. 2,2-dimethoxy, 2-phenyl acetophenone was dissolved in N-vinyl pyrrolidinone (NVP), and this was used as the photoinitiation and cocatalyst system, at 900 ppm initiator and 1500 ppm NVP in the final aqueous prepolymer solution. This was photopolymerized in situ with a Xe arc lamp filtered to emit mainly 360-365 nm light, approx. 10 mW/cm<sup>2</sup>, 20 s.

A series of proteins of increasing molecular weight was employed to characterize the release characteristics of the hydrogel system described above. Insulin (6000 Da), lysozyme (14,300 Da), lactate dehydrogenase (36,500 Da), ovalbumin (45,000 Da), bovine serum albumin (66,000 Da) or immunoglobulin G (150,000 Da) were dissolved at 1 mg/mL into a precursor solution of PEG molecular weight 10000 Da with a lactic acid oligoester region of degree of polymerization of 5 at each end, with acrylate termini. Gel disks of 0.25 mL were formed using the initiation conditions described above at 23% precursor w/v, and the release of the probe proteins was measured with a total protein assay in vitro at 37C, pH 7.4, under sterile conditions.

Fibrin formation is considered to be an initial step in the formation of permanent postoperative adhesions. To explore a combined barrier and pharmacological approach to prevention of post-operative adhesions, fibrinolytic agents were incorporated within the hydrogel prepolymer solution, simply by dissolving the protein in the solution immediately prior to application of the prepolymer solution and formation of the hydrogel [3]. Tissue plasminogen activator, urokinase plasminogen activator, and streptokinase were investigated, at therapeutically similar doses (tPA, 3 mg/mL; uPA, 1.8 mg/mL; SK, 1.2 mg/mL; each at 1.5 mL/animal). Additional experiments were performed with these same total doses, divided into four equal daily injections, to test the effect of semi-sustained (daily) but non-local delivery.

A second model of interest is the prevention of post-PTCA thickening of the arterial intima. Carotid arteries in rabbits were treated after a balloon treatment that causes both stretch and denudation injury [4]. Eosin Y (1 mM) was dissolved in saline and was used to stain the vessel segments to be treated; excess initiator was rinsed away. The remainder of the photopolymerization system was subsequently injected into the vessel segment, namely the prepolymer (23%; from PEG 10 000 Da in the prepolymer, synthesized as described above) with triethanolamine (100 mM) and NVP (1500 ppm) in buffered saline. Illumination, through the vessel wall, was performed with an Ar ion laser, 514 nm, 70 mW/cm<sup>2</sup>, 2 s.

## RESULTS AND DISCUSSION

### Protein Release

Proteins were released from the degradable hydrogel at a rate that depended upon the protein molecular weight, as shown in Fig. 1. Insulin was released at an initial rate of approximately 48%/day, lysozyme at 40 %/day, lactate dehydrogenase at 32 %/day, ovalbumin at 25 %/day, and bovine serum albumin at 19 %/day, while immunoglobulin G was released at < 1 %/day over the first 6 days in vitro. The gel mass did not change significantly over this short period in vitro, indicating that there exist two regimes of release, that occurring by diffusion prior to degradation, and that occurring only after degradation and loosening of the gel network structure. For a PEG molecular weight of 10000 Da, this transition occurred at a protein molecular weight somewhere between 66,000 Da and 150,000 Da. Presumably this transition can be shifted by employing shorter or longer PEG molecular weights in the precursor.

### Postoperative Abdominal Adhesions Model

In the post-operative pelvic adhesion model, the hydrogel (from 10% prepolymer solution) was microscopically observed to reduce in thickness and disappear over a approx. 5 day period. Results on efficacy in adhesion prevention are shown in Table 1. An optimum in precursor concentration in the hydrogel barrier was observed. This optimum may relate to the rate of degradation of the gels and their post-curing swelling. The gel from 5% precursor was observed to degrade more quickly than gels from 10% precursor. The gel from 10% precursor is cured nearer to its equilibrium swelling (approx. 95% water) than the higher concentration gels, and this may impact the swelling-induced stress imposed on the tissue by the gel.

Daily injection of tPA reduced the extent of postoperative adhesion formation, as previously observed [6], while by contrast injection of uPA did not, also as previously observed [7]. When tPA was incorporated in the hydrogel barrier the extent of adhesion formation was reduced relative to treatment with the gel alone and to treatment with daily injections of the same amount of tPA. uPA incorporated in the hydrogel barrier was equally effective as tPA, thus demonstrating that the site-localizing ability of tPA can be conferred to uPA by local delivery.

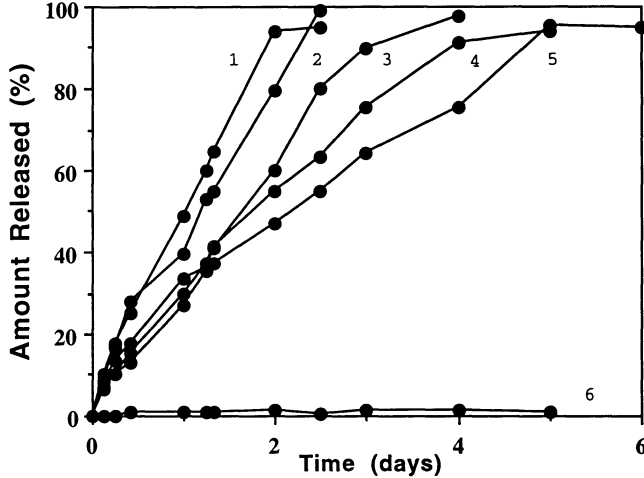


Figure 1. Release of Proteins from PEG-based Hydrogel.

Proteins of different molecular weight were used to determine the release characteristics of a hydrogel formed from a 23 % solution of a prepolymer from PEG of molecular weight 10 000 Da with an average of 5 lactic acid residues per end. Proteins are as follows: 1, insulin (6000 Da); 2, lysozyme (14 300 Da); 3, lactate dehydrogenase (36 500 Da); 4, ovalbumin (45 000 Da); 5, bovine serum albumin (66 000 Da); and 6, immunoglobulin G (150 000 Da). Reprinted from [5], with permission.

Table 1. Prevention of Post-operative Pelvic Adhesions in the Rat

Treatment	n	Extent of Adhesions	Significance, Rel. to Marked (*) Control
No treatment	7	76%	*
Gel, from 5% solution	7	22%	P<0.001
Gel, from 10%	7	10%	P<0.001
Gel, from 15%	7	18%	P<0.001
Gel, from 20%	7	26%	P<0.001
No treatment	7	77%	*
Injected tPA	7	49%	P<0.05
Injected uPA	7	78%	P>0.5
Injected SK	6	83%	P>0.5
No treatment	7	72%	P<0.01
Gel, from 15% solution	7	22%	*
Gel, with tPA	7	4%	P<0.01
Gel, with uPA	7	6%	P<0.01
Gel, with SK	7	45%	P<0.05

#### Post-Angioplasty Intimal Thickening Model

In the post-PTCA intimal thickening model, the thickness of the hydrogel formed was readily controlled via the illumination duration (e.g., 7  $\mu\text{m}$  at 5 s, 13  $\mu\text{m}$  at 10 s, 24  $\mu\text{m}$  at 20 s). The hydrogel thickness was observed to reduce to zero over a 24 hr period. Results on efficacy of prevention of thrombosis and intimal thickening in the rabbit model are presented in Table 2.

Blockade of thrombosis was essentially complete. Platelets were not observed to be adherent to the hydrogel surface; where platelets were observed, they were in direct contact with the subendothelium, indicating incomplete coverage.

The short term presence of the hydrogel barrier impacted the long term healing outcome. The amount of intimal thickening, assessed by the ratio of the intimal to medial cross-sectional area, was reduced by 80% relative to control. This is consistent with an important role for the platelet in inducing smooth muscle cell migration, proliferation, and/or matrix secretion [8].

Table 2. Prevention of Post-PTCA Thrombosis and Intimal Thickening

Treatment	% Lumen Occluded with Thrombus, 2hr; n	Ratio of Intima to Media Area, 14d; n
No treatment	87%; 4	1.56; 7
Gel	3%; 4	0.32; 7

## REFERENCES

1. Sawhney AS, Pathak CP, Hubbell JA. (1993) Bioerodible Hydrogels Based on Photopolymerized Poly(ethylene glycol)-co-Poly( $\alpha$ -hydroxy acid)-Diacrylate Macromers. *Macromolecules* 26:581-587.
2. Hill-West JL, Chowdhury SM, Sawhney AS, Pathak CP, Dunn RC, Hubbell JA. (1994) Prevention of Postoperative Adhesions in the Rat by In Situ Photopolymerization of Bioresorbable Hydrogel Barriers. *Obstet. Gynecol.* 83:59-64.
3. Hill-West JL, Dunn RC, Hubbell JA. (1995) Local Release of Fibrinolytic Agents for Adhesion Prevention. *J. Surg. Res.*, In Press.
4. Hill-West JL, Chowdhury SM, Slepian MJ, Hubbell JA. (1994) Inhibition of Thrombosis and Intimal Thickening by In Situ Photopolymerization of Thin Hydrogel Barriers. *Proc. Nat. Acad. Sci. USA* 91:5967-5971.
5. West JL, Hubbell JA. (1995) Photopolymerized Hydrogel Materials for Drug Delivery Applications. *React. Polym.*, In Press.
6. Doody KJ, Dunn RC, Buttram VC. (1989) Recombinant Tissue Plasminogen Activator Reduces Adhesion Formation in a Rabbit Uterine Horn Model. *Fertil. Steril.* 51:509.
7. Rivkind AI, Lieberman N, Durst AL. (1985) Urokinase Does Not Prevent Abdominal Adhesion Formation in Rats. *Eur. Surg. Res.* 17:254.
8. Fuster V, Badimon L, Badimon JJ, Chesbro JH. The Pathogenesis of Coronary Artery Disease and the Acute Coronary Syndromes. *N. Engl. J. Med.* 326:242:250; 326:310-318.

# A NOVEL BIOMATERIAL: ARAMID-SILICONE RESIN

Mitsuru Akashi,<sup>1</sup> Tsutomu Furuzono,<sup>1</sup> Takeo Matsumoto,<sup>1,2</sup> Akio Kishida and Ikuro Maruyama<sup>3</sup>

<sup>1</sup>Department of Applied Chemistry and Chemical Engineering, Faculty of Engineering, Kagoshima University, 1-21-40 Korimoto, Kagoshima 890, Japan

<sup>2</sup>NOF Corp., Ltd., 4-20-3, Ebisu, Shibuya-ku, Tokyo 150, Japan.

<sup>3</sup>Faculty of Medicine, Kagoshima University, 8-35-1 Sakuragaoka, Kagoshima 890, Japan.

## SUMMARY

Aramid-silicone resins (PASs) consisting of aromatic polyamide (aramid) and poly (dimethylsiloxane) (PDMS) segments were synthesized by low temperature solution polycondensation. Using 3-bis(3-aminopropyl)-1,1,3,3-tetramethyl-disiloxane (BATS) instead of PDMS, disiloxane-aramid multiblock copolymers (2SiPASs) were obtained. PAS and 2SiPAS films were prepared by casting from 10 wt% N,N'-dimethylacetamide solution. Ultrathin films of PAS were afforded by the methods of water casting and spin coating. The surface properties of the films were investigated in detail by means of contact angle measurements, electron probe micro analysis (EPMA), and X-ray photoelectron spectroscopy (XPS). The results suggested that PDMS segments were condensed at the outermost surface of PAS films, though this phenomenon was affected by the molding method especially the solvent evaporation conditions. For the evaluation of blood compatibility *in vitro*, the thromboxane B<sub>2</sub>(TXB<sub>2</sub>) release test from platelets attaching to PAS and Biomer®, and the observation of the platelet adhesion or the surface of PAS by scanning electron microscopy (SEM) were carried out. PAS was found to be bio-inert *in vitro*. The gas permeation properties and dynamic thermomechanical properties of the PAS films were also investigated. PAS containing ≥ 53 wt% of PDMS showed high enough oxygen permeability compared with conventional silicone rubbers.

**KEY WORDS** : poly(dimethylsiloxane), multiblock copolymer, blood compatibility, surface analysis, oxygen permeability

## INTRODUCTION

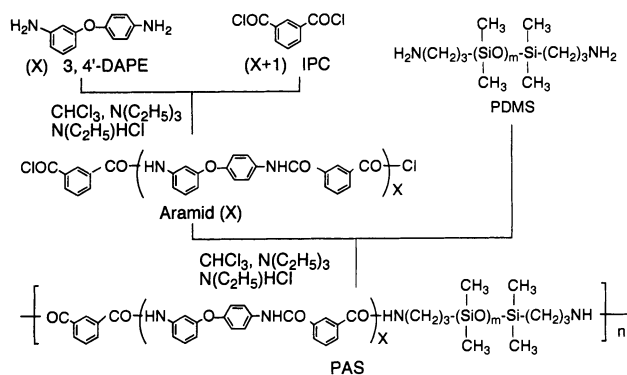
Silicone rubber is widely used in medical fields, in many forms, such as blocks, tubes, sutures and films. Generally, the desirable properties of the silicone are high thermal stability, oxidative stability, low surface energy, water repellency, good dielectric properties, high gas permeability and good biocompatibility. Especially in the medical field, the last two characteristics were important. On the other hand, the mechanical properties of silicone rubber, especially low tensile strength, sometimes limit their medical application. To improve the mechanical properties of silicone rubber, many researchers have reported the syntheses of high-modulus resin including silicone unit which possess both good mechanical properties and the characteristics of silicone. For instance, poly(dimethylsiloxane-co-carbonate) and poly(dimethylsiloxane-co-hydroxystyrene), of which both mechanical properties and oxygen permeability were excellent, were synthesized and applied to the membrane for preparing the oxygen-enriched air in the industrial field.

In 1989, Y. Imai *et al.*, first reported the synthesis of PDMS and aromatic polyamide (aramid) copolymer (PAS) [1]. PAS is multiblock copolymer consisting of hard segment (aramid) and soft segment (PDMS). The aramid is known to have very high-mechanical properties, such as high-thermal stability and high modulus of elasticity. It is expected that the incorporation of PDMS domain into an aramid matrix allows the system to exhibit many of the often desirable properties of both polymers. However, there has so far been only a few studies reported on characteristics of PAS [1]. First, we traced Imai's synthetic procedure and polished up it with a little modification to attain a considerably large amount of PAS. Then, the study on the functionalities of PAS was started. In this review, from the point view of novel biomaterial having silicone, we report on the synthesis, the preparation of films, characteristics of the surfaces, evaluation of *in vitro* blood compatibility and oxygen permeation properties of PAS[2-6].

## RESULTS

## Surface Properties

As shown Scheme 1, PAS was synthesized by low temperature solution polycondensation through a two step procedure according to the method developed by Imai *et al.* [1] with a little modification [2]. Using BATS instead of PDMS, 2SiPAS was prepared [5]. Table 1 summarized the typical results. PAS films are cast from N,N'-dimethylacetamide solution in stainless steel petri dishes. First, mechanical property of PASs was studied, and the stress-strain curves are shown in Fig. 1 [2]. It is obvious that the tensile properties of the PAS films are dependent on the PDMS content in the copolymers. A comparison of the curves shows a significant decrease in tensile strength and an increase in elongation at break with increasing PDMS content. Over the whole composition range, PAS can afford films between a rubber-toughened plastic and an elastomer. On the contrary, the tensile strength for 2SiPAS has been found to be drastically improved (40 to 80 MPa) [5].



Scheme 1 Synthesis of PAS

Table 1. Preparation of PAS

No.	Aramid oligomer(x)		PDMS <sup>a</sup> content(wt%)		yield (%)
	in feed	in polymer <sup>b</sup>	Calcd <sup>c</sup>	Found <sup>b</sup>	
1	-	-	0	0	100
2	7	14.9	41	25	83
3	3	4.1	60	53	77
4	1	1.3	78	75	56

<sup>a</sup>Mn (PDMS)=1680<sup>b</sup>Calculated from the SiCH<sub>3</sub>/aromatic ratio in the <sup>1</sup>H NMR spectrum.<sup>c</sup>Weight (PDMS)/[weight (PDMS) + weight (aramid)] in feed.

Ultrathin films (35-70 nm) of PASs can be obtained by the methods of water casting and spin coating. The surface properties of the films were investigated using contact angle measurements, X-ray (XPS) and (EPMA). Si/C stoichiometries of the PAS films measured by XPS show that the Si/C ratio of the cast films and the spin-coated films increases logarithmically with increasing the PDMS content, whereas the Si/C ratio of water-cast films increased almost linearly and was very low throughout all PDMS contents (Fig. 2). From this results it is clear that the silicone block was condensed at the surface compared to the bulk phase for the cast films and spin-coated films, while such condensation of PDMS units was not observed for the water-cast films. The relationship



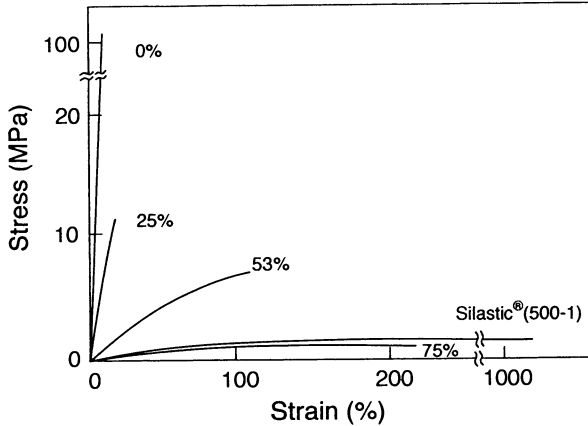


Fig. 1 Stress-Stain Curves for PAS(PDMS: Mn=1680) and Silastic® 500-1. PDMS contents are shown.

between the water contact angles and PDMS content of PAS also indicates that the outermost surfaces of both cast and spin-coated films in all ranges of PDMS content are almost fully covered with silicone units. These results are acceptable because PDMS has a low surface energy [4]. From the result on Si/C stoichiometries of the 2SiPAS films by XPS, it is apparent that the Si/C ratio increases with increasing BATS content in the 2SiPAS films. The surface Si/C ratio calculated from XPS spectra increased logarithmically with increasing BATS content, whereas the bulk Si/C ratio calculated from  $^1\text{H}$  NMR spectra increased exponentially. It can be assumed that a significant amount of excess of BATS units in the near surface region was observed for all the 2SiPASs.

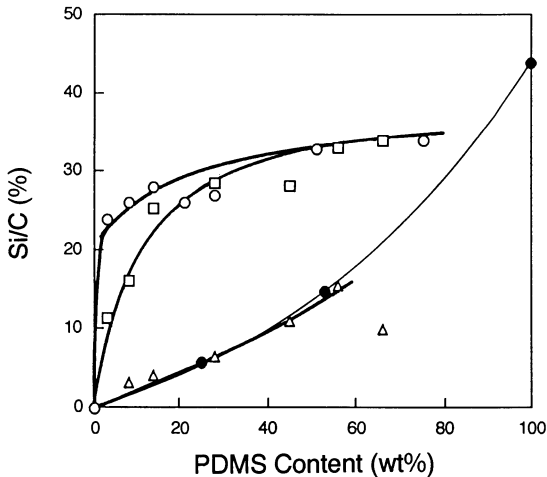


Fig. 2 Si/C Stoichiometries of PAS Surfaces by XPS with PDMS Contents. (O) Prepared by casting, (□) prepared by spin coating, (Δ) prepared by water casting, (●) Si/C in bulk, calculated from PDMS content.

## Blood Compatibility

For the evaluation of blood compatibility *in vitro*, the thromboxane B<sub>2</sub>(TXB<sub>2</sub>) release test from platelets attaching to PAS was first carried out, compared with aramid and Biomer<sup>®</sup> (Fig. 3) [2]. It was apparent that the aramid homopolymer surface induced severe release of TXB<sub>2</sub> from the attached platelets. The TXB<sub>2</sub> release from them attached to PASs was significantly lower regardless of the PDMS content. Biomer<sup>®</sup> induced slightly higher release of TXB<sub>2</sub> than PAS. Platelets adhering to the surfaces of PASs, Biomer<sup>®</sup>, Silastic<sup>®</sup> and glass plate was observed using a scanning electron microscope(SEM). On the surface of the aramid homopolymer and glass, many platelets adhered, deployed pseudopods and aggregated. On the other hand, on the surfaces of PAS films, only a few platelets were found without any aggregation and morphological deformation.

It is thought that the surface of 26 wt% of BATS content of 2SiPAS may possess blood compatibility similar to PAS, from the fact that the surface free energy is a very low value. On the surface of 2SiPAS, actually, platelets were scarcely adhered. It might be concluded that the surfaces of 2SiPASs whose BATS content was more than 26 wt% in bulk had *in vitro* bio-inertness.

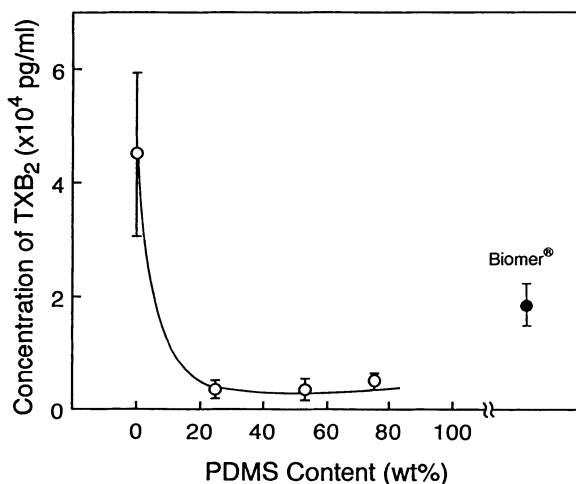


Fig. 3 *In Vitro* Thromboxane B<sub>2</sub> Released from Platelets on PAS and Biomer<sup>®</sup>. Standard errors are shown (n=4), (O) PAS, (●) Biomer<sup>®</sup>.

Table 2. The Oxygen and Nitrogen Permeability of PAS Films

No.	PDMS Content (wt%) <sup>a</sup>	PO <sub>2</sub> <sup>b</sup>	PN <sub>2</sub> <sup>b</sup>	PO <sub>2</sub> /PN <sub>2</sub>
1	26	-	-	-
2	35	40	18	2.2
3	46	41	17	2.4
4	53	171	76	2.3
5	75	224	97	2.3

<sup>a</sup>Calculated from the Si-CH<sub>3</sub>/aromatic H ratio in the NMR spectrum.

<sup>b</sup>[cm<sup>3</sup>(STP)cm/cm<sup>2</sup>·sec·cmHg] x 10<sup>10</sup>.

## Gas Permeability

It is known that PDMS is highly permeable to common gases such as oxygen and nitrogen. This is due to the flexibility of the Si-O linkage which results in high diffusion coefficients as compared to the C-C backbone of many organic polymers. From the tensile properties of PAS films which are dependent on the PDMS content, PAS can afford films between a rubber-toughened plastic and an elastomer. Hollow fibers can be prepared from PAS [3]. When PAS has enough oxygen permeability, therefore, it can be used as a membrane for an artificial lung. The oxygen and nitrogen permeabilities of the PAS films were determined by means of high-vacuum method [6]. The result was summarized in Table 2. It was found that the oxygen permeability of the PAS films increased with increasing PDMS content, while the oxygen/nitrogen separation factors of them were independent of PDMS content and almost the same as that of silicone rubber. The oxygen permeability of the PAS films containing greater than 53 wt% PDMS was high enough compared with conventional silicone rubber. As to clarify the reason why PAS has high oxygen permeability, the thermal behavior was evaluated by dynamic mechanical measurements. The result suggests that PAS has microphase-separation structures consisting of soft PDMS and hard aramid segments [6].

In conclusion, PAS can be a novel biomaterial owing to its unique properties.

## REFERENCES

1. Kajiyama M, Kakimoto M, Imai Y (1989) Synthesis and characterization of new multiblock copolymers based on poly(dimethylsiloxane) and aromatic polyamides. *Macromolecules* 22: 4143-4147
2. Furuzono T, Yashima E, Kishida A, Maruyama I, Matsumoto T, Akashi M (1993) A novel biomaterial: Poly(dimethylsiloxane)-polyamide multiblock copolymer I. Synthesis and evaluation of blood compatibility. *J Biomater Sci Polym Ed* 5: 89-98
3. Furuzono T, Kishida A, Akashi M, Maruyama I, Miyazaki T, Koinuma Y, Matsumoto T (1993) Development of a novel biomaterial aramid-silicone resin: Studies of gas-permeability and blood-compatibility. *Jpn Artif Organs* 22: 370-375
4. Kishida A, Furuzono T, Ohshige T, Maruyama I, Matsumoto T, Itoh H, Murakami M, Akashi M (1994) Novel functional polymers: Poly(dimethylsiloxane)-polyamide multiblock copolymer II. Study of the surface properties of ultrathin films of poly(dimethylsiloxane)-polyamide multiblock copolymers. *Angew Makromol Chem* 220: 89-97
5. Furuzono T, Seki K, Kishida A, Ohshige T, Waki K, Maruyama I, Akashi M, Novel functional polymers: Poly(dimethylsiloxane)-polyamide multiblock copolymer III. Synthesis and surface properties of disiloxane-aromatic polyamide multiblock copolymer. *J Appl Polym Sci.* in contribution
6. Matsumoto T, Koinuma Y, Waki K, Kishida A, Furuzono T, Maruyama I, Akashi M, Novel functional polymers: Poly(dimethylsiloxane)-polyamide multiblock copolymer IV. Gas permeability and thermomechanical properties of aramid-silicone resins. *J Appl Polym Sci.* in contribution

# GRADIENT SURFACES AS TOOLS TO STUDY BIOCOMPATIBILITY

Hai Bang Lee, Bong Jin Jeong, and Jin Ho Lee\*

*Biomaterials Laboratory, Korea Research Institute of Chemical Technology, P.O.Box 9, Daedeog Danji, Taejeon 305-606, Korea; Phone, 82-42-860-7220; Fax, 82-42-861-4151*

*\*Department of Macromolecular Science, Han Nam University, 133 Ojeong Dong, Daedeog Ku, Taejeon 300-791, Korea; Phone, 82-42-629-7391; Fax, 82-42-625-5874*

**ABSTRACT** : It is recognized that the behavior of the adsorption and desorption of blood proteins or the adhesion and proliferation of different types of mammalian cells on polymeric materials depend on the surface characteristics such as wettability, chemistry, charge, dynamics, roughness, and rigidity. In this study, we prepared wettability gradients, chargeable functional group gradients, and comb-like polyethylene oxide (PEO) gradients on low density polyethylene (PE) surfaces. Gradient surfaces whose properties are changed gradually along the material length are of particular interest for basic studies of the interaction between biological species and surfaces since the effect of a selected property can be examined in a single experiment on one surface. We used the gradient surfaces prepared as tools investigate protein or cell interactions continuously related to the surface wettability, chemistry and charge, or dynamics of polymeric materials.

**KEY WORDS** : corona discharge, gradient surfaces, protein adsorption, cell adhesion, polyethylene oxide (PEO)

## INTRODUCTION

Systematic study of the effect of one parameter on the surface properties of materials requires many different samples, each with a different values of the surface parameter of interest. Such a study is often tedious, laborious, and time-consuming because a large number of samples must be prepared to characterize the complete range of the desired surface property. It may also involve the strong possibility of methodological error because each sample is prepared separately.

Many studies have recently been focused on the preparation of surfaces whose properties are changed gradually along the material length. Such gradient surfaces are of particular interest for basic studies of the interaction between biological species and surfaces since the effect of a selected property can be examined in a single experiment on one surface.

The concept of a gradient surface was first introduced by Elwing et al. [1]. They prepared a wettability gradient on a flat hydrophilic silicon plate by diffusing dimethyl dichloro silane through xylene onto the plate surface. Many research groups [1-4] have used the wettability gradient surfaces to investigate surface hydrophilicity-induced changes of adsorbed proteins. The wettability gradient surfaces prepared by the above methods seem to be useful as basic research tools, but have a limitation; they can be applied to only hydrophilic inorganic substrates such as silicon, silica, quartz, or glass.

A method for preparing wettability gradients on various polymer surfaces was developed by our group [5] and Pitt et al. [6,7]. The wettability gradients were produced via radio-frequency (RF) plasma discharge treatment by exposing the polymer sheets continuously to plasma. The polymer surfaces oxidized gradually along the sample length with increasing plasma exposure time and thus the wettability gradients were created.

Recently, we developed a new method for preparing wettability gradients on polymer surfaces by treating the polymer sheets with corona from a knife-type electrode whose power is changed gradually along the sample length [8]. This method of preparing wettability gradients on polymer surfaces is simpler and more practical than the plasma treatment method because the samples are

discharged in air at atmospheric pressure in this method, whereas they are discharged under vacuum in the plasma treatment method.

We have also prepared chargeable functional group gradient surfaces by the corona discharge treatment with gradually increasing power, followed by the graft copolymerization and subsequent substitution reactions [9]. Comb-like polyethylene oxide (PEO) gradient surfaces were also prepared by the above corona discharge treatment and the following graft copolymerization of poly (ethylene glycol) mono-methacrylates.

Those gradient surfaces prepared were used as tools investigate protein or cell interactions continuously related to the surface wettability, chemistry and charge, or dynamics of polymeric materials, as described in this article.

## WETTABILITY GRADIENT SURFACES

For the preparation of wettability gradient surfaces, cleaned PE sheets, 250-300  $\mu\text{m}$  thick, were treated with RF corona discharge apparatus made by our laboratory for the preparation of gradient surfaces (Fig. 1) [8]. The PE sheet was placed on the sample bed and dry air was purged through the apparatus at a flow rate of 20 l/min. The knife-type electrode was 1.5 mm away from the sample surface. At the same time that the sample bed was translated at a constant speed of 1.0 cm/sec, the corona was discharged from the knife-type electrode onto the sample with gradually increasing power (from 10 to 35 watt at 100 kHz). The sample sheet (5 x 5 cm) was treated for 5 sec. By this treatment, the sample surface was continuously exposed to the corona with increasing power.

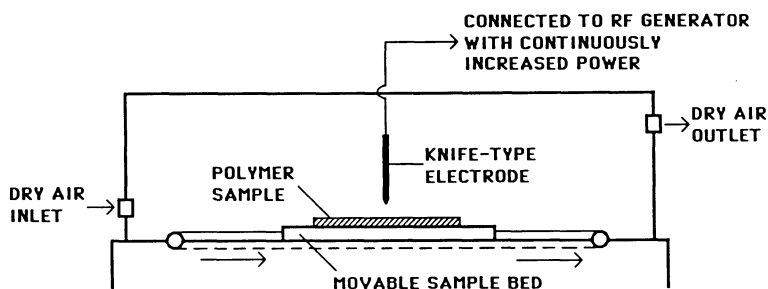


Fig. 1. Schematic diagram showing corona discharge apparatus for the preparation of wettability gradient surfaces [8].

The water contact angles of the corona-treated surfaces gradually decreased along the sample length with increasing corona power (from about 95 deg. to about 45 deg.). The decrease in the contact angles (and thus the increase in wettability) along the sample length was due to the oxygen-based polar functionalities (hydroxyl group, ether, ketone, aldehyde, carboxylic acid, carboxylic ester, etc.) incorporated on the surface by the corona treatment, as evidenced by Fourier-transform infrared spectroscopy in the attenuated total reflectance mode (FTIR-ATR) and electron spectroscopy for chemical analysis (ESCA). The oxygen-based functional groups produced on the PE surfaces increased with the increase in corona power and this contributed to the formation of the wettability gradient.

Chinese hamster ovary (CHO) cells as a model system were cultured for 2, 24, and 48 hrs on the PE gradient surfaces and the number of cells adhered onto each section of the gradient surfaces was determined by a electronic cell counter [10]. As the results, the cells were adhered and grown more onto the sections with moderate hydrophilicity of the wettability gradient surface (Fig. 2). The maximum adhesion and growth of the cells appeared at around a water contact angle of 50-55 degree. The observation of scanning electron microscopy (SEM) also

verified that the cells are more adhered, spread, and grown onto the sections with moderate hydrophilicity. Cells attached on surfaces are spread only when they are compatible on the surfaces. It seems that surface wettability plays an important role for cell adhesion and spreading.

Human albumin as a model protein was adsorbed onto the PE gradient surfaces and the relative amount of protein adsorbed onto the gradient surfaces was analyzed by ESCA. The nitrogen signal from the surface was used as an indicator of the protein adsorption. It is mainly derived from peptide bonds in the structure of the albumin. From Fig. 3, we can see that the albumin adsorption increased gradually with the increasing hydrophobicity of the gradient surface. This is probably due to the increased hydrophobic interactions of the protein molecules with the hydrophobic sections of the gradient surface. For the desorption study, the albumin-adsorbed gradient surfaces were exposed to a non-ionic polymeric surfactant, Tetricon 1504 [11]. The exposure of the albumin-adsorbed gradient surface to Tetricon 1504 solution resulted in partial displacement of the protein (Fig. 3). This displacement was much greater on the hydrophobic sections of the gradient surface than the hydrophilic ones.

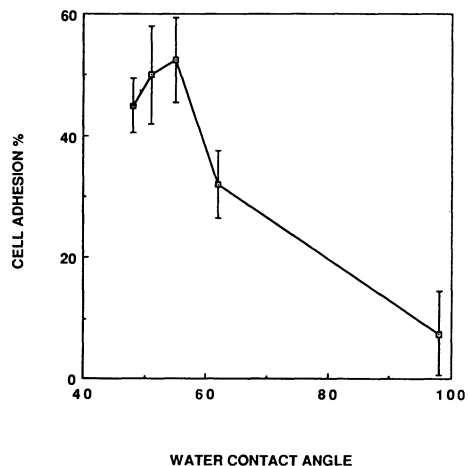


Fig. 2. CHO cell adhesion on corona-treated PE surface (Number of seeded cells,  $4 \times 10^4/\text{cm}^2$ ; culture time, 2 hr). Sample numbers,  $n = 3$  [10].

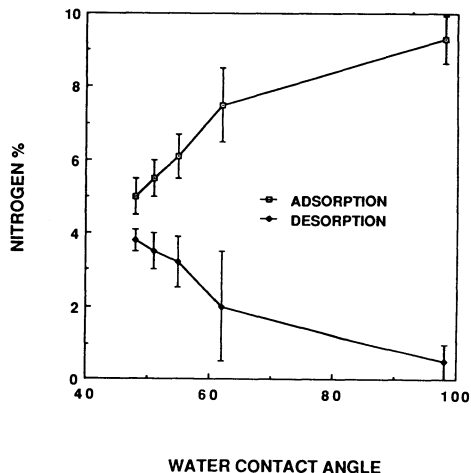


Fig. 3. Albumin adsorption and desorption on corona-treated PE surface (Adsorption, 1 hr in 1 mg/ml albumin solution; Desorption, 30 min in 1 mg/ml Tetricon 1504 solution after 1 hr adsorption in albumin solution).  $n = 3$  [10].

## FUNCTIONAL GROUP GRADIENT SURFACES

For the preparation of chargeable functional group gradient surfaces, directly after the PE sheet was treated by the corona with gradually increasing power, it was immersed in aqueous acrylic acid solution. The graft copolymerization of acrylic acid (-COOH, negatively chargeable at physiological pH) onto the corona-treated PE surface was performed at 70 °C for 1 hr in nitrogen gas atmosphere. The acrylic acid-grafted sheet was agitated in water at 70 °C overnight to eliminate the homopolymer probably formed on the surface. Some of acrylic acid-grafted PE sheets were further treated with 10 wt%  $\text{PCl}_5$  in dry ether for 1 hr at room temperature to substitute -COOH groups on the surfaces with -COCl groups. Then the surfaces were treated with saturated  $\text{NH}_4\text{OH}$  aqueous solution for 1 hr to produce amide group (-CONH<sub>2</sub>, neutral)-grafted surface or with 0.5 wt%  $\text{LiAlH}_4$  in dry ether for 24 hr to produce hydroxyl group (-CH<sub>2</sub>OH, neutral)-grafted surface. Some of amide-group grafted sheets were also treated with  $\text{LiAlH}_4$  solution to produce amine group (-CH<sub>2</sub>NH<sub>2</sub>, positively

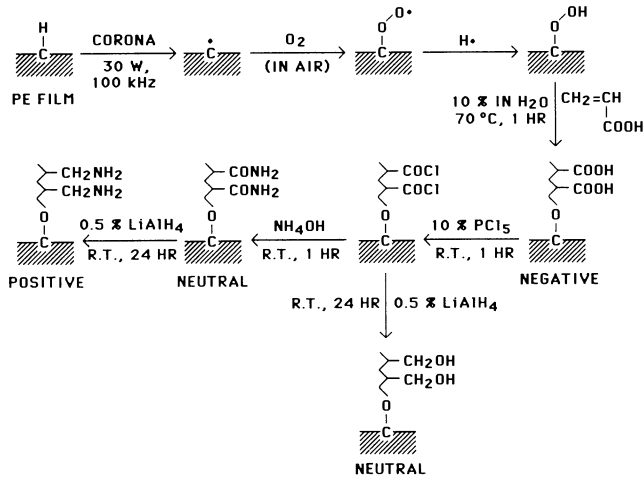


Fig. 4. Schematic diagram showing the formation of functional group-grafted PE surfaces by corona discharge treatment followed by graft copolymerization and subsequent reactions [9].

chargeable)-grafted surface (Fig. 4). The changes in chemical structure on the PE surfaces after the grafting of acrylic acid and the substitution of carboxylic acid groups to hydroxyl, amide, or amine groups were identified by ESCA and FTIR-ATR [9].

The CHO cells were cultured on the functional group-grafted PE surfaces. The amine group-grafted PE surface showed the best cell adhesion and growth of the surfaces used. It is probably due to the positive charge character of the amine groups in the cell culture medium (pH, about 7.4); the large portion of cell or serum protein surface is recognized as charged negatively. The acrylic acid-grafted surface which is charged negatively showed poor cell adhesion and growth. For the surfaces with neutral functional groups, amide and hydroxyl groups, the hydroxyl group-grafted surface showed better cell adhesion and growth, probably due to the specific hydrogen bondings between the surface hydroxyl groups of the polymer and the polar groups of the cell surfaces. The amine group-grafted surface also showed best cell spreading. It seems that the amine group-grafted surface is most compatible with the cells among the functional group-grafted surfaces used [12].

The positive charge gradient surface was also prepared by the treatment of PE sheet using corona with gradually increasing power and the following graft copolymerization of allyl amine. The interaction of model cells, CHO and baby hamster kidney (BHK) cells, with the allyl amine-grafted gradient surface was investigated to see the effect of surface positive charge density on the cell adhesion and the growth behavior. As the result, it was observed that the allyl amine-grafted surface shows effective adhesion and spreading of both CHO and BHK cells on the sections of higher allyl amine density probably due to the positive charge character.

## COMB-LIKE PEO GRADIENT SURFACES

Comb-like PEO gradient surfaces were prepared onto PE sheets by corona discharge treatment with gradually increasing power and the following graft copolymerization of poly (ethylene glycol) monomethacrylates (PEG-MA). The poly (ethylene glycol) monomethacrylates with different PEO chain lengths (1, 5, and 10) were used for this purpose. The prepared comb-like PEO gradient surfaces were characterized by the measurement of water contact angle, FTIR-ATR, and ESCA. All these measurements indicated that the PEO chains are immobilized on the PE surface with gradually increasing surface density of PEO (Fig. 5) [13].

The behaviors of plasma protein adsorption and platelet adhesion on the PEO-grafted surfaces were

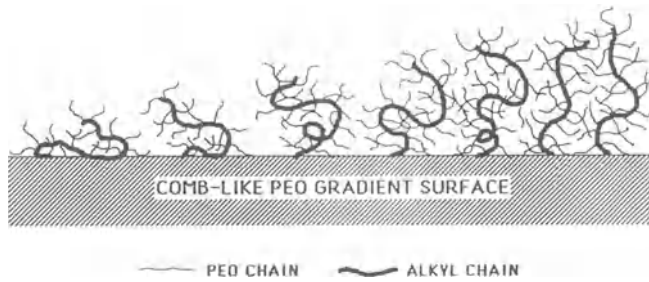


Fig. 5. Schematic diagram showing a comb-like PEO gradient surfaces [13].

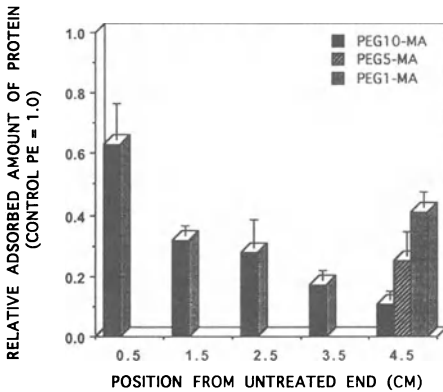


Fig. 6. Plasma protein adsorption on PEG-MA grafted PE gradient surfaces with different PEO chain length (Adsorption, 1 hr in 1 % plasma solution).  $n = 3$ .

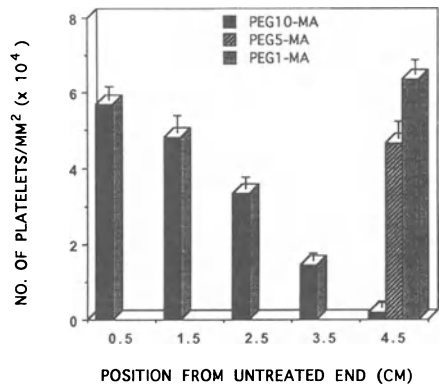


Fig. 7. Platelet adhesion on PEG-MA grafted PE surfaces with different PEO chain length (Adhesion, 30 min in platelet-rich plasma separated from citrated canine blood).  $n = 3$ .

investigated in terms of comb-like PEO chain length and surface density. It was observed that the plasma protein adsorption and platelet adhesion on the PEO gradient surfaces are gradually reduced by increasing PEO chain length and surface density (Fig. 6 & 7). This is probably due to PEO's low interfacial free energy with water, unique solution properties and molecular conformation in aqueous solution, hydrophilicity, high surface mobility, and steric stabilization effects [11,14].

## REFERENCES

- [1] Elwing H, Welin S, Askendal A, Nilsson U, Lundstrom I (1987) *J. Colloid Interface Sci.* 119: 203
- [2] Elwing H, Golander CG (1990) *Adv. Colloid Interface Sci.* 32: 317
- [3] Hlady V, Golander C, Andrade JD (1988) *Colloids Surf.* 33: 185
- [4] Golander CG, Lin YS, Hlady V, Andrade JD (1990) *Colloids Surf.* 49: 289
- [5] Lee JH, Park JW, Lee HB (1990) *Polymer (Korea)* 14: 646
- [6] Pitt WG (1989) *J. Colloid Interface Sci.* 133: 223
- [7] Golander CG, Pitt WG (1990) *Biomaterials* 11: 32
- [8] Lee JH, Kim HG, Khang GS, Lee HB, Jhon MS (1992) *J. Colloid Interface Sci.* 151: 563
- [9] Lee JH, Kim HW, Pak PK, Lee HB (1994) *J. Polymer Sci., Polymer Chem.* 32: 1569
- [10] Lee JH, Lee HB (1993) *J. Biomater. Sci., Polymer Edn.* 4: 467
- [11] Lee JH, Kopecek J, Andrade JD (1989) *J. Biomed. Mater. Res.* 23: 351
- [12] Lee JH, Jung HW, Kang IK, Lee HB (1994) *Biomaterials* 15: 705
- [13] Lee JH, Jeong BJ, Khang GS, Lee HB (1995) *Trans. Soc. Biomaterials* 18: 146
- [14] Jeon SI, Lee JH, Andrade JD, de Gennes PG (1991) *J. Colloid Interface Sci.* 142: 149



# PREPARATION OF SELF-ASSEMBLED BIOMIMETIC MEMBRANES AND THEIR FUNCTIONS

Nobuo NAKABAYASHI

Institute for Medical and Dental Engineering, Tokyo Medical and Dental University  
2-3-10, Kanda-surugadai, Chiyoda-ku, Tokyo 101, Japan

## ABSTRACT

New hypothesis to prepare nonthrombogenic materials was proposed and the supporting evidence is going to be discussed. That was a surface which could adsorb phospholipids, would be biocompatible and a methacrylate having affinity with phospholipids was designed. 2-Methacryloyloxyethyl phosphorylcholine (MPC) was prepared, copolymerized with several monomers and their evaluation was carried out. It was found that polymers having phosphorylcholine groups, phospholipid polymers, have good affinity with phospholipids and could adsorb them on the surface. Liposomal structure was kept when the phospholipid polymers were soaked in liposomal solution. The structure were identified by X-ray photoelectron spectroscopy, comparison of the gel-liquid crystalline transition temperature of phospholipid liposome with differential scanning calorimeter, desorption amount of phospholipids. These data suggested that self-assembled biomimetic membrane was prepared on the MPC copolymers. Their unusual but interesting property was inhibition of protein adsorption even they were soaked in plasma solution and blood. They could not adsorb platelets and activate them which induce thrombus. Preparation of dialysis membranes which do not require anticoagulants is also possible. So it was concluded that MPC copolymers are promising basic biocompatible biomaterials.

**KEY WORDS :** Phospholipid, 2-Methacryloyloxyethyl phosphorylcholine, Nonthrombogenicity, Self-assembled biomimetic membrane, Protein adsorption, Hydrogel, Biocompatibility, Biomedical material

## INTRODUCTION

Many attempts to prepare blood compatible polymers have been carried out[1]. But we do not have such good surface like blood vessel yet. Albumin adsorbed surface, hydrophilic surfaces and phase-separated microdomain surfaces were proposed to resolve it. Surfaces of cells and vessels are covered with biomembranes. The biomembranes are composed of phospholipids, cholesterol, peptides, saccharide and supported by basement membranes. They are not simple. Ringsdorf et al.[2] and Regen et al.[3] tried to stabilize liposome by linking the alkyl chain which has unsaturated group by  $\gamma$ -irradiation. Interaction of linked liposomal suspension and blood cells were studied. The idea is very interesting but this technology was very difficult to apply in development of biomedical materials. Introduction of phosphorylcholine groups on several substrates by chemical reaction was proposed and their evaluation was reported [4-6]. Our interest was to prepare such surface which could adsorb phospholipids molecule in site and examine their biocompatibility. We expected that this kind efforts could give us good information to make biocompatible materials. So a methacrylate with phosphorylcholine group, 2-methacryloyloxyethyl phosphorylcholine(MPC), was tried to synthesize and copolymerized with methyl methacrylate[7-9]. And hemolysis test and the cell culture were carried out to evaluate the biocompatibility. The results were promising but there was limitation in

the preparation of the monomer at that time. We did not choose the polymer reaction to introduce phosphorylcholine groups as polymer reaction does create rather complicated surfaces, not so suitable for biocompatible study. We had hypothesized that phospholipid molecules which contact with blood must move dynamically like biomembranes, not bind to the substrates. So preparation of such polymer surfaces that have good affinity with phospholipids to accumulate them on the surface. Fortunately we could improve the preparation method in 1989 and it increased the possibility to develop biomedical materials[10]. Through our evaluation of MPC copolymers, phospholipids accumulated on the surface which have affinity with them could form liposome-like surface by themselves. It could be self-assembled biomimetic membranes.

### PREPARATION OF POLYMERS WITH PHOSPHORYLCHOLINE GROUP

As a methacrylate with phosphorylcholine group, MPC (Fig. 1) was synthesized[10]. The MPC was copolymerized with hydrophobic alkyl methacrylates such as *n*-butyl methacrylate(BMA)[10,11].

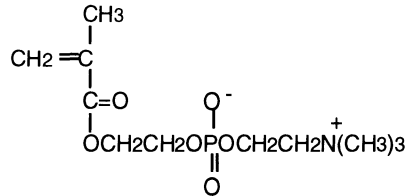


Fig.1. Structure of MPC

### INTERACTION OF MPC POLYMER WITH PHOSPHOLIPID LIPOSOME

The interesting property of the MPC copolymers is its affinity for phospholipids. The amount of phospholipids, dipalmitoylphosphatidylcholine (DPPC), adsorbed on MPC copolymers was larger than that on polystyrene, poly(BMA) and poly(HEMA) and increased with increasing MPC moiety when the MPC copolymers contacted with a liposomal solution of DPPC[12]. This tendency was the same as that of the adsorption of phospholipids from human plasma which is indicated in Fig. 2[13]. Thus, the affinity of poly(MPC-co-BMA) for the phospholipids could be observed even in the plasma. The DPPC molecules adsorbed on the poly(MPC-co-BMA) surface assumed an organized structure like that for a bilayer membrane, which was confirmed by differential scanning calorimetry(DSC) and X-ray photoelectron spectroscopy(XPS) when the poly(MPC-co-BMA) membrane was immersed in the solution containing DPPC[14]. It is therefore concluded that the MPC copolymers stabilized the adsorption layer of phospholipids on the surface. Little albumin and  $\gamma$ -globulins were adsorbed on the MPC copolymer surface treated with DPPC, which is in sharp contrast to the fact that on a poly(BMA) surface, pretreatment of DPPC was not effective for suppression of protein adsorption. The difference in protein adsorption on these polymer surface reflects the difference in the orientation of the DPPC which covered the polymer surfaces.

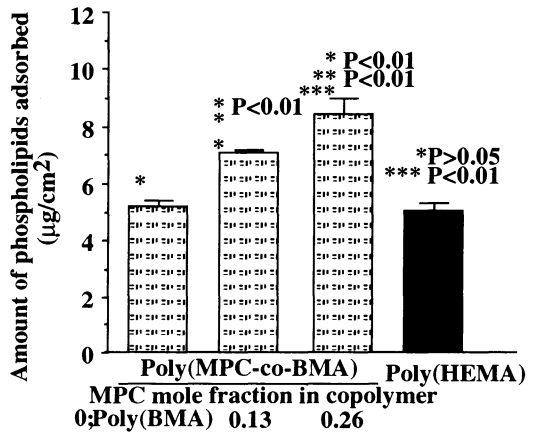


Fig. 2 Amount of PC adsorbed on poly(MPC-co-BMA) and poly(HEMA) from human plasma after 60min-contact.

The interesting property of the MPC copolymers is its affinity for phospholipids. The amount of phospholipids, dipalmitoylphosphatidylcholine (DPPC), adsorbed on MPC copolymers was larger than that on polystyrene, poly(BMA) and poly(HEMA) and increased with increasing MPC moiety when the MPC copolymers contacted with a liposomal solution of DPPC[12]. This tendency was the same as that of the adsorption of phospholipids from human plasma which is indicated in Fig. 2[13]. Thus, the affinity of poly(MPC-co-BMA) for the phospholipids could be observed even in the plasma. The DPPC molecules adsorbed on the poly(MPC-co-BMA) surface assumed an organized structure like that for a bilayer membrane, which was confirmed by differential scanning calorimetry(DSC) and X-ray photoelectron spectroscopy(XPS) when the poly(MPC-co-BMA) membrane was immersed in the solution containing DPPC[14]. It is therefore concluded that the MPC copolymers stabilized the adsorption layer of phospholipids on the surface. Little albumin and  $\gamma$ -globulins were adsorbed on the MPC copolymer surface treated with DPPC, which is in sharp contrast to the fact that on a poly(BMA) surface, pretreatment of DPPC was not effective for suppression of protein adsorption. The difference in protein adsorption on these polymer surface reflects the difference in the orientation of the DPPC which covered the polymer surfaces.

### INTERACTION WITH PLASMA PROTEINS ON THE MPC POLYMER

The amount of total proteins adsorbed on poly(HEMA) from human plasma was significantly smaller than that on poly(BMA) ( $P<0.01$ ), and it was at the same level as on poly(MPC-co-BMA) with a 0.13

MPC mole fraction as shown in Fig. 3[13]. However, that on poly(MPC-co-BMA) with a 0.26 MPC mole fraction was quite small compared with that on other polymers tested. It is clearly demonstrated that there are weak interactions between the surface and proteins. If nonthrombogenic materials are to be designed, it may be necessary to decrease protein adsorption, particularly proteins such as coagulation factors and complement components on the blood contacting surface. The surface concentration of all proteins including fibrinogen, coagulation factors and complement component decreased with an increase in the MPC moiety and appeared to absorb on the surfaces in a uniform and evenly distributed manner[15]. The potential use of phospholipid polymers for biocompatibility and reduced thrombogenicity may be useful for these applications.

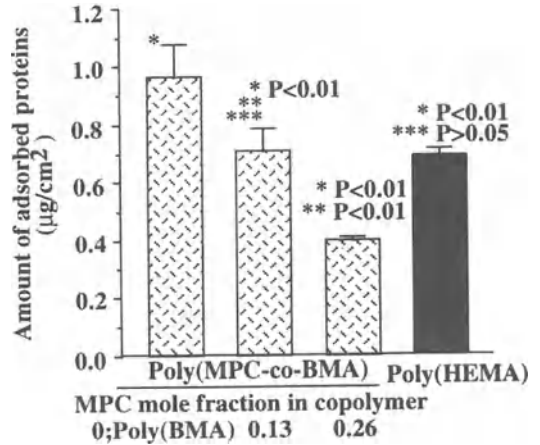
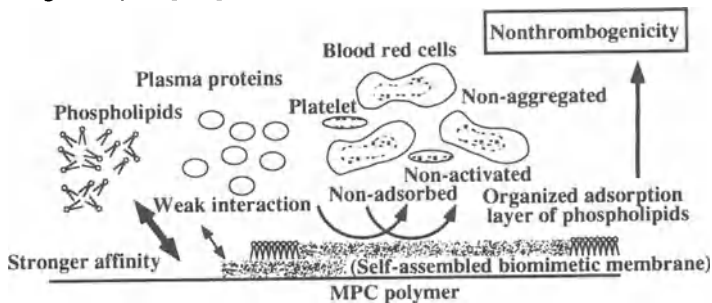


Fig. 3 Amount of plasma proteins adsorbed on poly(MPC-co-BMA) and poly(HEMA) from human plasma after 60min-contact.

### MECHANISM OF NONTHROMBOGENICITY OBSERVED ON THE MPC POLYMER

By comparison of the adsorption behavior of phospholipids on MPC copolymers with that of proteins, a mechanism of nonthrombogenicity observed on MPC copolymers is considered as shown in Fig. 4[13]. Since the molecular size of phospholipids is smaller than that of proteins and the molar concentration of phospholipids is larger than that of proteins, the diffusion of phospholipid molecules from plasma to the polymer surface occurs more easily than proteins. (1) Adsorption of phospholipid molecules, (2) their accumulation, (3) their rearrangement by themselves could be taken place before (4) adsorption of proteins. And protein molecules are very large comparing with the lipids it takes time to stabilize on the surface. Before the stabilized adsorption, lipids molecules could make off with the place where the proteins are going to be adsorbed. The MPC copolymers have both a strong affinity for phospholipids and protein adsorption-resistant properties in buffered



**Phospholipids on MPC polymer surface**  
**1. Adsorption, 2. Accumulation, 3. Rearrangement,**  
**4. Formation of self-assembled biomimetic membrane**

Fig. 4 Schematic representation of interaction between MPC polymer and blood components. Formation of self-assembled biomimetic membrane by phospholipids adsorbed on the MPC polymer is important to obtain nonthrombogenicity.

aqueous protein solution. From these findings, it is concluded that the phospholipids in plasma are adsorbed immediately on the surface and form a stable adsorbed layer with a biomembrane-like surface by their self-organizing properties.

## FUTURE OF MPC POLYMERS AS BIOMEDICAL MATERIALS

By use of the MPC polymers, the improvements of blood compatibility on biomedical membranes such as cellulose hemodialysis membrane, polyolefin membrane for oxygenator, permeation controlled membrane for drug delivery, and covering membrane for implantable biosensor were investigated [16-18]. Because the MPC copolymers have nonthrombogenicity, protein adsorption resistant property, and good permeability of solutes. Water-soluble MPC polymers are prepared easily therefore, they can apply as a blood compatible stabilizer of phospholipid liposome which will be used as an injectable drug carrier due to their strong affinity to phospholipids. Very recently blood compatible polymeric additives could be prepared from MPC polymers for improvement of blood/biocompatibility of segmented polyurethanes. This polymeric additive did not leach out from matrix polyurethane under continuous stress and modified polyurethane suppressed platelet adhesion drastically compared with that on the non-treated polyurethane. We confirm that the MPC is key compound to create new type blood/biocompatible polymeric materials and wide applications of MPC polymers in biomedical fields will be expected strongly.

## REFERENCES

- [1] Ishihara K(1993) Blood compatible polymers. In: Tsuruta T, Hayashi T, Kataoka K, Ishihara K, Kimura Y(eds) *Polymeric Materials for Biomedical Applications*. CRC, Boca Raton, FL, pp90-115
- [2] Hupfer B, Ringsdorf H, Schupp H(1981) Polymeric phospholipid monolayers. *Makromol Chem* 182: 247-253
- [3] Bonte F, Hsu MJ, Papp A, Wu K, Regen SL, Juliano RL(1987) Interactions of polymerizable phosphatidylcholine vesicles with blood components: relevance to biocompatibility. *Biochim Biophys Acta* 900: 1-9
- [4] Durrani AA, Hayward JA, Chapman D (1986) Biomembranes as models for polymer surfaces II. The syntheses of reactive species for covalent coupling of phosphorylcholine to polymer surfaces. *Biomaterials* 7: 121-125
- [5] Hayward JA, Durrani AA, Shelton CJ, Lee DC, Chapman D(1986) Biomembranes as models for polymer surfaces III. Characterization of a phosphorylcholine surface covalently bound to glass. *Biomaterials* 7: 126-131
- [6] Hayward JA, Durrani AA, Ju Y, Clayton CR, Chapman D (1986) Biomembranes as models for polymer surfaces. *Biomaterials* 7: 252-258
- [7] Kadoma Y, Nakabayashi N, Masuhara E, Yamauchi J (1978) Synthesis and hemolysis test of the polymer containing phosphorylcholine groups. *Kobunshi Ronbunshu* 35: 423-427
- [8] Nakabayashi N, Masuhara E (1980) Preparation of hard tissue compatible materials: Dental polymers. In: *Biomedical polymers, Polymeric materials and pharmaceuticals for biomedical use*. Goldberg EP, Nakajima A (eds). Academic Press, New York, NY, pp 85-111
- [9] Fukushima S, Kadoma Y, Nakabayashi N(1983) Interaction between the polymer containing phosphorylcholine group and cells. *Kobunshi Ronbunshu* 40: 785-793
- [10] Ishihara K, Ueda T, Nakabayashi N (1990) Preparation of phospholipid polymers and their properties as polymer hydrogel membranes. *Polym J* 22: 355-360
- [11] Ueda T, Oshida H, Kurita K, Ishihara K, Nakabayashi N (1992) Preparation of 2-methacryloyloxyethyl phosphorylcholine copolymers with alkyl methacrylates and their blood compatibility. *Polym J* 24: 1259-1269

- [12] Ishihara K, Oshida H, Endo Y, Watanabe A, Ueda T, Nakabayashi N (1993) Effect of phospholipid adsorption on nonthrombogenicity of polymer with phospholipid polar group. *J Biomed Mater Res* 27: 1309-1314
- [13] Ishihara K, Oshida H, Endo Y, Ueda T, Watanabe A, Nakabayashi N (1992) Hemocompatibility of human whole blood on polymers with a phospholipid polar group and its mechanism. *J Biomed Mater Res* 26: 1543-1552
- [14] Ueda T, Watanabe A, Ishihara K, Nakabayashi N (1991) Protein adsorption on biomedical polymers with a phosphorylcholine moiety adsorbed with phospholipids. *J Biomat Sci Polymer Edn* 3:185-194
- [15] Ishihara K, Ziats NP, Tierney BP, Nakabayashi N, Anderson JM (1991) Protein adsorption from human plasma is reduced on phospholipid polymers. *J Biomed Mater Res* 25:1397-1407
- [16] Ishihara K, Ohta S, Yoshikawa T, Nakabayashi N (1992) Protein adsorption resistible membranes for biosensor composed of polymer with phospholipid polar group. *J Polym Sci Part A Polym Chem* 30: 929-932
- [17] Ueda T, Ishihara K, Nakabayashi N (1992) Temperature effect on drug release from poly(2-methacryloyloxyethyl phosphorylcholine-co-n-butyl methacrylate) membrane. *Membrane* 17: 101-106
- [18] Ishihara K, Fukumoto K, Miyazaki Nakabayashi N (1994) Improvement of the hemocompatibility on a cellulose hollow fibers with a novel biomedical polymer phospholipid polar group. *Artificial Organs* 18: 559-564

# SYNTHESIS AND CELL-ADHESION PROPERTIES OF POLYURETHANES CONTAINING COVALENTLY GRAFTED RGD-PEPTIDES

Horng-Ban Lin\* and Stuart L. Cooper\*\*

\*Meadox Medicals, Inc., 112 Bauer Drive, Oakland, NJ 07436

\*\*University of Delaware, College of Engineering, Newark, DE 19716

## ABSTRACT

In an attempt to improve endothelial cell adhesion and growth on a polyurethane copolymer, cell adhesive RGD-containing peptides were grafted to the polymer backbone. Two peptide grafting reaction schemes, including one-step and two-step approaches, were developed. Amino acid analysis confirmed that the two-step approach had a higher peptide coupling efficiency. The two-step reaction scheme was utilized to prepare GRGDSY, GRGDVY and GRGESY (inactive control) peptide grafted polyurethanes with two different peptide densities (100 and 250  $\mu\text{mol/g}$  polymer). In-vitro endothelial cell adhesion experiments showed that, without the presence of serum in culture medium, the GRGDSY- and GRGDVY-grafted polyurethanes dramatically enhanced cell attachment and spreading. Increasing the peptide density from 100 to 250  $\mu\text{mol/g}$  polymer for the GRGDSY- and GRGDVY-grafted polyurethanes resulted in an increase in cell attachment. Similar trends were observed in endothelial cell growth studies using culture medium containing serum and growth supplement.

**KEY WORDS:** polyurethanes, RGD binding, peptides, endothelial cells

## INTRODUCTION

Polyurethane block copolymers have been widely used for blood-contacting devices due to their excellent mechanical properties and relatively good blood compatibility [1,2]. To date, surface-induced thrombosis remains a major drawback which hinders the successful utilization of polyurethanes and other polymers in many clinical applications. In-vitro endothelialization has been proposed as a way to further improve the blood compatibility of polyurethanes [2]. Several studies [3,4] have suggested that conventional polyurethanes are poor substrates in supporting endothelial cell adhesion and growth. Immobilization of RGD-containing peptides onto polymer surfaces has been shown to support cell attachment and spreading [5,6]. In this study, an alternative approach was undertaken in that cell adhesive RGD-containing peptides were grafted to a polyurethane backbone. The main challenge was to develop a reaction scheme which has a good peptide coupling efficiency and preserves the cell binding activity of the peptide after it is coupled to the polyurethane. Two peptide-grafting reaction schemes including one-step and two-step methods were explored. The reaction scheme which had a higher peptide coupling efficiency was then utilized to prepare the GRGDSY (containing the cell adhesive sequence of fibronectin, RGDS), GRGDVY (containing the cell adhesive sequence of vitronectin, RGDV), and GRGESY (containing a non-cell adhesive sequence, RGES) grafted polyurethanes. The effect that the peptide sequence and density has on endothelial cell adhesion and growth was investigated.

## EXPERIMENTAL

**Polymer and Peptide synthesis:** The syntheses of a poly(tetramethylene oxide) (PTMO) based polyurethane, and its derivatized carboxylated polymer have been reported previously in detail [7]. A PTMO-based polyurethane based on a 3:2:1 molar ratio of methylene diphenylene diisocyanate (MDI), 1,4-butanediol (BD), and poly(tetramethylene oxide) (PTMO, MW=1000) was synthesized. Carboxylated polyurethanes with approximately 4% and 10% substitution of urethane hydrogen by

ethyl carboxylate groups were used in this study. Three fully protected hexapeptides, including Fmoc-Gly-Arg(Pmc)-Gly-Asp(OtBu)-Ser(OtBu)-Tyr(OtBu)-OtBu(Fmoc-GRGDSY\*), Fmoc-Gly-Arg(Pmc)-Gly-Asp(OtBu)-Val-Tyr(OtBu)-OtBu (Fmoc-GRGDVY\*), and Fmoc-Gly-Arg(Pmc)-Gly-Glu(OtBu)-Ser(OtBu)-Tyr(OtBu)-OtBu (Fmoc-GRGESY\*), were synthesized by a standard solution phase method. The amine-terminated protected peptides were prepared by removing the Fmoc protecting group of each fully protected hexapeptide. A free hexapeptide was prepared from the amine-terminated peptide GRGDSY\* by removing the side-chain protecting groups (Pmc and OtBu) [8].

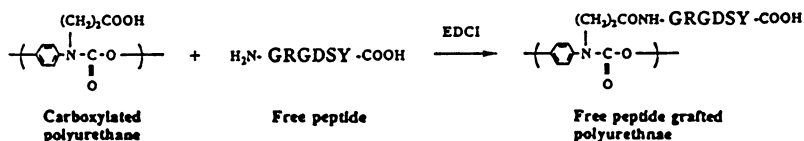
**Synthesis of peptide grafted polyurethanes:** A carboxylated polyurethane, which had 4% of its urethane hydrogens substituted by ethyl carboxyl groups, was used for the synthesis of GRGDSY peptide grafted polymers using the one-step and two-step reaction schemes illustrated in Figure 1.

In the one-step reaction, the free hexapeptide GRGDSY was directly coupled onto the carboxylated polyurethane via amide linkage formation. The coupling reaction was performed under dry nitrogen at room temperature in a 25% (w/v) carboxylated polyurethane/dimethyl formamide (DMF) solution using the coupling reagent 1-(3-dimethylaminopropyl)3-ethylcarbodiimide hydrochloride (EDCI) [7]. The two-step reaction approach has been reported in detail [7]. Briefly, the first step included coupling of the amine-terminated peptide GRGDSY\* to the carboxylated polyurethane via the formation of amide linkages between the carboxyl groups on the polymer backbone and the N-terminus amine group of the protected peptide. The second step involved-cleavage of the protecting groups of the grafted peptide using Reagent K [9].

**Peptide grafted polyurethanes: various peptide sequences and densities:** The reaction scheme which had a higher peptide coupling efficiency (i.e. two-step scheme, see results and discussion) was utilized to prepare two series of peptide grafted polyurethanes. The hexapeptides were separately coupled onto the carboxylated polyurethanes (i.e. PEU-COOH and PEU-HD-COOH), which had 4% and 10% of the urethane hydrogen substituted.

**Sample Nomenclature:** The starting polymer and the carboxylated polyurethanes are denoted as PEU, PEU-COOH, and PEU-HD-COOH. The free peptide grafted polymers are designated as PEU-GRGDSY(I), PEU-GRGDSY(II), PEU-GRGESY(II), PEU-GRGDVY(II), PEU-HD-GRGDSY(II), PEU-HD-GRGESY(II), and PEU-HD-GRGDVY(II). The notations (I) and (II) are used to distinguish the polymers prepared from the one-step and two-step schemes, respectively. The notation -HD- is used to represent samples with a higher carboxyl or grafted peptide density.

(a) ONE-STEP SCHEME



(b) TWO-STEP SCHEME

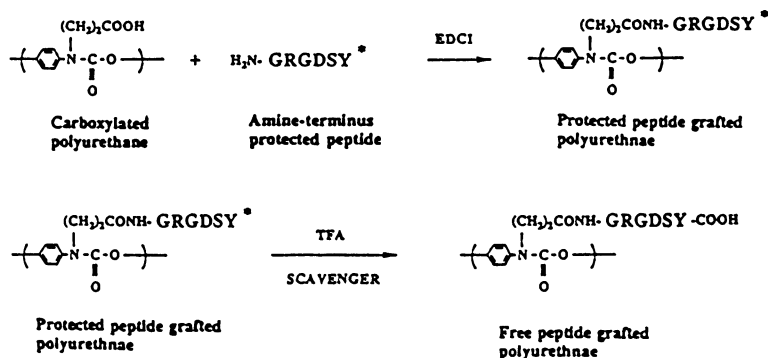


Fig. 1: Reaction schemes for the synthesis of RGD-containing peptide grafted polyurethanes: (a) one-step and (b) two-step methods.

**Amino Acid Analysis:** Amino acid analyses were performed on a Beckman 6300 Amino Acid Analyzer (Department of Chemistry, University of Minnesota). Samples were hydrolyzed in 6N HCl at 110°C for 48 hours.

**Cell adhesion:** Human umbilical vein endothelial cells were used for the in-vitro cell attachment studies. Cell suspension ( $5 \times 10^5$  cells/ml) was prepared using DMEM with 0.1% heat inactivated bovine serum albumin (BSA). Polymer coated coverslips were placed in 24-well tissue culture plates (Corning) and equilibrated in Tris buffered saline (TBS, pH = 7.4) overnight prior to the experiment.  $1 \times 10^4$  cells/cm<sup>2</sup> were seeded on each polymer substrate and allowed to attach for the desired time. The wells were subsequently rinsed with TBS to remove non-adherent cells, and the adherent cells were fixed with a solution of 3% paraformaldehyde for 2 hours. The number of attached cells was determined visually using 100x magnification on a microscope equipped with phase contrast objectives (Nikon, Japan). Adherent cells were counted in 5 or 6 areas randomly chosen in the central and peripheral regions of each polymer substrate. The morphology of attached cells was examined using a JOEL JSM-35C scanning electron microscope.

**Cell Growth:** Porcine pulmonary aortic endothelial cells were used in the in-vitro cell growth studies. Polymer coated coverslips were rinsed with sterile PBS (pH = 7.4; Gibco) and then sterilized for 15 minutes under a ultraviolet light. The polymer-coated coverslips were placed into 24-well tissue culture plates. In each experiment,  $1 \times 10^4$  cells were separately seeded onto each of the polymer-coated coverslips and the tissue culture polystyrene wells (i.e. controls) and incubated at 37°C and 5% CO<sub>2</sub>/95% air. After 72 hours, the cell growth was assayed using the MTT assay [10]. All experiments were performed at least three times for each independent assay.

## RESULTS AND DISCUSSION

**Amino Acid Analysis and Cell Adhesion:** Amino acid analysis showed that the peptide incorporation in PEU-GRGDSY(I) and PEU-GRGDSY(II) were approximately 25 and 100 μmol/g polymer, respectively. Since the same molar ratios of peptide:EDCI:carboxylated polymer were used in the one-step and two-step methods, the larger amount of peptide incorporated in PEU-GRGDSY(II) indicates that a higher peptide coupling efficiency was achieved by the two-step reaction scheme. The lower peptide coupling efficiency for the one-step reaction scheme can be attributed to side reactions such as polypeptide formation. Additionally, the one-step GRGDSY peptide may be coupled to the carboxylated polymer via the guanidino functionality of arginine, which would result in the grafted peptide losing its cell binding activity. Since the two-step reaction method had a higher peptide coupling efficiency and produced the more cell-adhesive polyurethane [7], it was utilized to prepare two series of peptide grafted polyurethanes which had different peptide sequences and densities.

**Amino Acid Analysis:** Amino acid analyses showed that the amount of peptide incorporated in PEU-GRGESY(II), PEU-GRGDSY(II), and PEU-GRGDVY(II) was approximately 80, 100, 100 μmol/g polymer, respectively. The amount of grafted peptide in PEU-HD-GRGESY(II), PEU-HD-

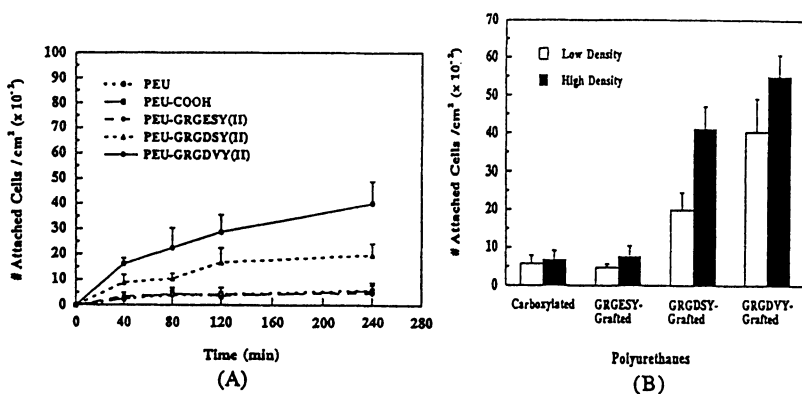


Fig. 2: A) Human umbilical vein endothelial cell (HUVEC) attachment in serum-free DMEM containing 0.1% BSA. (B) Effect of peptide density on the HUVEC attachment after 240 minutes incubation in serum-free DMEM containing 0.1% BSA.



GRGDSY(II), and PEU-HD-GRGDVY(II) was approximately 200, 250, and 250  $\mu\text{mol/g}$  polymer, respectively.

**Cell adhesion:** Figure 2A shows the cell attachment profiles for the polyurethane substrates in serum-free medium. After 4 hours of incubation, approximately 4-5% of seeded cells attached to PEU, PEU-COOH, and PEU-GRGESY(II). The number of attached cells on PEU-GRGDSY(II) and PEU-GRGDVY(II) both increased with time, and PEU-GRGDVY(II) supported more attached cells than PEU-GRGDSY(II). The differences in cell attachment between the two series of polyurethanes after 4 hours incubation are shown in Figure 2B. Increases in the degree of carboxylation and non-cell adhesive GRGESY peptide density did not improve cell adhesion. Enhanced cell attachment was observed on PEU-HD-GRGDSY(II) compared to PEU-GRGDSY(II), and on PEU-HD-GRGDVY(II) compared to PEU-GRGDVY(II).

At each peptide density (100 or 250  $\mu\text{mol/g}$  polymer), the GRGDVY-grafted polyurethanes supported more attached cells than the GRGDSY-grafted polyurethanes. This may be attributed to the affinity of the peptides for the endothelial cell receptors, the availability of the grafted peptide at the substrate surface (i.e. peptide surface density), or a combination of these effects. Hirano et al. [11] showed that the RGDV tetrapeptide immobilized ethylene-acrylic acid copolymer film supported more cell attachment than the RGDS tetrapeptide immobilized film, in agreement with this study. Hubbell and coworkers [12] showed that the affinity and specificity of short peptides (e.g., GRGDY pentapeptide) may change after immobilization on the glycophasic glass surface. Studies have shown that endothelial cells contain both vitronectin and fibronectin receptors, and these receptors are highly specific to their ligands [13, 14]

**Cell Growth:** Cell adhesion studies have shown that cells adhere preferentially to the GRGDSY- and GRGDVY-grafted polyurethanes. The long-term cell growth studies confirmed these findings as shown in Figure 3, however, with some marked differences. After 72 hours, no organized endothelial cell monolayer growing on the PEU substrate was observed. Endothelial cells grew comparatively well on the carboxylated and GRGESY peptide grafted polyurethanes. In line with the findings of adhesion studies, optimal endothelial cell growth was observed on the GRGDSY and GRGDVY peptide grafted polyurethanes. The effect of increasing the grafted GRGDSY and GRGDVY peptide densities on the cell growth was not as marked as that seen in the cell adhesion studies. The discrepancy between the short-term adhesion and long-term growth studies is believed to be due to the media used to assess cell attachment versus cell growth. In the cell attachment experiments, the medium used only contained bovine serum albumin which does not promote endothelial cell adhesion. In the cell growth studies, the medium contained 10% fetal calf serum. The serum adhesive proteins, such as fibronectin and vitronectin, and the growth factors, including endothelial cell and basic fibroblast growth factors, are known to promote cell adhesion and growth [15, 16]. During the 72 hour incubation period, the presence of these proteins and growth factors may interfere or mask the selective interactions of the GRGDSY and GRGDVY peptides with the endothelial cell receptors.

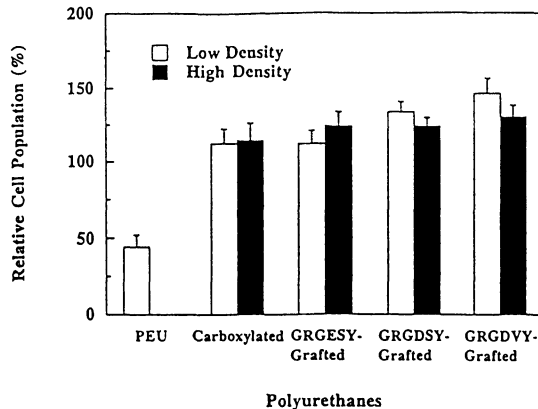


Fig. 3: Relative porcine pulmonary aortic endothelial cell growth on polyurethanes after 72 hours in medium contained 10% fetal calf serum and endothelial cell supplement. (Cell population on tissue culture polystyrene = 100%).

## CONCLUSIONS

Two different peptide grafting reactions, including one-step and two-step schemes, were developed to couple RGD-containing peptides to a polyurethane backbone. Amino acid analysis confirmed that coupling of the peptide was achieved by both methods. However, the two-step approach showed a higher peptide coupling efficiency and resulted in better control of the orientation of the grafted peptide. In-vitro endothelial cell adhesion showed that, without adhesive plasma proteins in the culture medium, the GRGDSY-grafted polyurethane prepared using the two-step method supported more attached cells than the one prepared using the one-step method. In the absence of adhesive plasma proteins in the culture medium, the starting, carboxylated versions, and GRGESY-grafted polyurethanes did not support endothelial cell adhesion and spreading, whereas the GRGDSY- and GRGDVY-grafted polyurethanes greatly enhanced cell adhesion and spreading. Increasing the peptide density from 100 to 250  $\mu\text{mol/g}$  polymer for the GRGDSY- and GRGDVY-grafted polymers resulted in an increase in cell attachment. The results suggest that RGD-containing peptide incorporation onto the polyurethane is a promising approach to promote in-vitro endothelialization.

## ACKNOWLEDGMENTS

The authors wish to acknowledge Drs. William Ershler, Daniel H. Rich (University of Wisconsin-Madison) and Peter I. Lelkes (Sinai Samaritan Medical Center) for helpful suggestions and kind collaboration. This work was supported by the National Institutes of Health through grants HL-24046, HL-29684 and HL-47179.

## REFERENCES

1. Lelah MD and Cooper SL (1986) *Polyurethanes in Medicine*. CRC Press, Boca Raton, FL, pp. 57-71
2. Ito Y and Imanishi Y (1989) *Crit. Rev. Biocompat.* 5:45
3. Gospodarowicz D and Ill C (1980) *J. Clin. Invest.* 65:1351
4. Nichols NK, Gospodarowicz D, Kessler TR, and Oslen DB (1981) *Trans. Am. Soc. Artif. Intern. Organs* 27:208
5. Massia SP and Hubbell JA (1991) *J. Biomed. Mater. Res.* 25:223
6. Matsuda T, Kondo A, Makino K, and Akutsu T (1989) *Trans. Am. Soc. Artif. Intern. Organs* 35:677
7. Lin H-B, Zhao Z-C, García-Echeverría C, Rich DH, and Cooper SL (1992) *J. Biomater. Sci., Polymer Ed.* 3:217
8. Beck-Sickinger AG, Schnorrenberg G, Metzger J, and Jung G (1991) *Int. J. Peptide Protein Res.* 38:25
9. King DS, Fields CG, and Fields GB (1990) *Int. J. Peptide Protein Res.* 36:25
10. Ohno M and Abe T (1991) *J. Immunol. Methods* 145:199
11. Hirano Y, Kando Y, Hoyashi T, Goto K, and Nakajima A (1991) *J. Biomed. Mater. Res.* 25:1523
12. Massia SP and Hubbell JA (1991) *J. Cell Biol.* 114:1089
13. Dejana E, Colella S, Conforti C, Abbadini M, Gobili M, and Marchisio PC (1988) *J. Cell Biol.* 107:1215
14. Fath K, Edgell C-J S, and Burrige K (1989) *J. Cell Sci.* 92:67
15. van Wachem PB, Hogt AH, Beugeling T, Feigen J, Bantjes A, Detmers JP, van Aken V (1987) *Biomaterials* 8:323
16. Steele JG, Johnson G, Norris WD, and Underwood PA (1991) *Biomaterials* 12:531

# **Biomaterials and Biomedical Engineering**

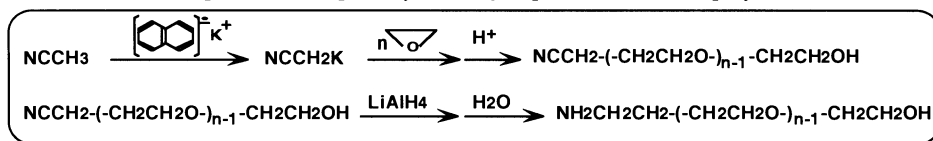
# ONE POT SYNTHESIS OF POLY(ETHYLENE OXIDE) WITH A CYANO GROUP AT ONE END AND A HYDROXYL GROUP AT THE OTHER END

Michihiro Iijima, Yukio Nagasaki, Masao Kato, Kazunori Kataoka

Department of Materials Science and Technology, Science University of Tokyo,  
Yamazaki 2641, Noda 278, Japan, 0471-24-1501

## SUMMARY

Well-defined poly(ethylene oxide) with a cyano group at one end and a hydroxyl group at the other terminus was quantitatively synthesized by anionic polymerization of ethylene oxide using cyanomethylpotassium as an initiator in the presence of 18-crown-6. The molecular weight of the polymers determined from GPC results agreed well with expected values calculated from the monomer/initiator molar ratios. From  $^{13}\text{C}$ -NMR analysis, the polymer shows several signals derived from terminal groups together with methylene protons of PEO main chain. The chemical shifts of these signals were in good accordance with those of cyano hydroxyl terminals calculated. In addition, in  $^1\text{H}$ -NMR spectrum, the peak intensity ratio of OH signal vs.  $\text{CH}_2\text{CH}_2\text{CN}$  were 1/2. And heterotelechelic PEO with a primary amino group at one end and a hydroxyl group at the other end was quantitatively synthesized by reduction of the cyano-ended hetero PEO. In the  $^{13}\text{C}$ -NMR spectrum of the polymer, all peaks originated from cyano-ended PEO disappeared completely and several signals derived from a primary amino terminal were appeared. The measurement of the TOF-MS revealed the presence of a primary amino group at the end of the polymer.



**Scheme 1** Synthesis of heterotelechelic poly(ethylene oxide)

**KEY WORDS** : poly(ethylene oxide), anionic polymerization, acetonitrile, potassium naphthalene, cyanomethylpotassium

## METHODS

### Synthesis of heterotelechelic PEO with a cyano group at one end and a hydroxyl group at the other end

All of anionic polymerizations of EO were carried out under argon atmosphere in a glass reactors equipped with a 3way stopcock. One of the representative procedures of anionic polymerizations is described. THF solution of potassium naphthalene(1.0mmol, 2.17ml) was added to a stirred THF solution(15ml) of acetonitrile(3.0mmol, 0.16ml). After stirring for 30 minutes to form cyanomethylpotassium, EO(80mmol, 4.0ml) was added to the mixture using a syringe. After the mixture was allowed to react for 2days at room temperature, few drops of acetic acid was added to stop reaction. The mixture was poured into a 20 fold volume of diethyl ether to precipitate. The polymer sample collected was subjected to freeze drying with benzene to remove the solvents employed.

### Reduction of a terminal cyano group

One of the procedures of reductions of a terminal cyano group is described. The polymer sample obtained by above-mentioned experiments(0.2mmol) was dissolved in THF(15ml) under atmosphere. A 15 fold molar quantity of Lithium Aluminium Hydride was added to the polymer solution. After stirring for 2 hours at room temperature, a excess amount of water was added to deactivate excess amount of  $\text{LiAlH}_4$ , and then, pH of the mixture was adjusted to pH 7 by 0.1N HCl. The procedures of purification was similar to that described above.

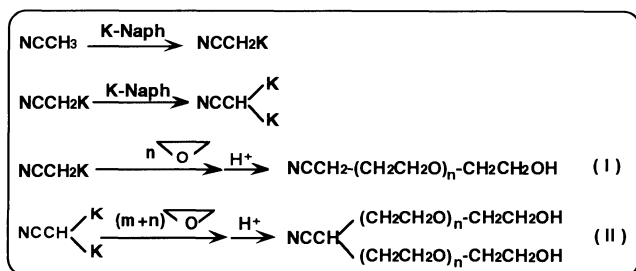
## RESULTS AND DISCUSSION

The polymerizations proceeded smoothly and gave the polymer almost quantitative yield. Table 1 shows the results of anionic polymerizations of EO. The molecular weight of the polymers determined from GPC results agreed well with expected values calculated from the monomer/initiator molar

ratios. In addition, the molecular weight distributions of the polymers obtained were narrow. From these results, it is indicated that the initiation efficiency of potassium acetonitrile was almost one and the polymerization proceeded without any side reactions. Fig.1 shows MALDI-TOF-MS spectrum of the polymer after the polymer was treated with LiAlH<sub>4</sub>. The molecular mass of the each molecule can be determined as follows:

$$MW_{\text{mass}} = 44.053n + 89.14 \quad (1)$$

where, 44.053 means molecular weights of EO. 89.14 in Eq.(1) agreed exactly with a summation of molecular mass of both terminal moieties, viz. HOCH<sub>2</sub>CH<sub>2</sub> (45.06) + CH<sub>2</sub>CH<sub>2</sub>NH<sub>2</sub> (44.08)=89.14. The peaks of the cyano-ended PEO was not detected at all. From these results, since reduction of the terminal group from a cyano group to a primary amino group quantitatively proceeded, there is possibility that hetero PEO with a primary amino group at one end and a hydroxyl group at the other end was quantitatively synthesized. In the <sup>13</sup>C NMR spectra, however, there were more peaks than those expected. This may be due to the side reaction in the initiation step. If dianion(NCCHK<sub>2</sub>) was prepared by the reaction between acetonitrile and potassium naphthalene, PEO possessing one cyano group and two hydroxyl groups can be obtained (In this case, mass number of each PEO molecule should be the same as that of the hetero PEO.)(Scheme.2). If this side reaction was assumed, the signals in the <sup>13</sup>C NMR spectrum can be reasonably assigned. This assignments agreed well with the calculated values[1].



Scheme 2 The formation of the dianion

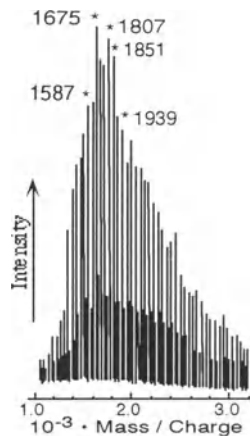


Fig.1 MALDI-TOF-MS spectrum of the polymers obtained by reduction

To suppress the formation of the dianion, we carried out the EO polymerization in the presence of 18-crown-6. Our idea was to avoid the dianion formation by a steric hindrance between K<sup>+</sup>-crown complexes. The molecular weight of the polymers determined from GPC results agreed well with expected values calculated from the monomer/initiator molar ratios. And the molecular weight distributions of the polymers formed were narrow. In the <sup>13</sup>C NMR spectrum of the polymers, all peaks originated from II disappeared completely. In addition, in <sup>1</sup>H NMR spectrum, the peak intensity ratio of OH signal(at 4.5ppm) vs. CH<sub>2</sub>CH<sub>2</sub>CN(at 1.8ppm) were 1/2.

On the basis of above all results, it is indicated that the polymers thus obtained have one hydroxyl group and one cyano group terminuses stoichiometrically. By the reduction of PEO,I, using LiAlH<sub>4</sub>, PEO possessing a primary amino group and a hydroxyl group quantitatively without any contamination.

## REFERENCES

- 1.Clerc P.,Simmon S.,(1983) "Tables of Spectral Data for Structure Determination of Organic Compounds", Springer-Verlag.

# Creation of New Si-containing Block Copolymer Membrane with Both High Gas Permeability and Blood compatibility

Hotaka Ito<sup>1</sup>, Atsusi Taenaka<sup>1</sup>, Yukio Nagasaki<sup>1</sup>, Kazunori Kataoka<sup>1,2</sup>, Masao Kato<sup>1</sup>, Teiji Tsuruta<sup>2</sup>, Ken Suzuki<sup>3</sup>, Teruo Okano<sup>3</sup>, Y. Sakurai<sup>3</sup>

1.Department of Materials Science and Technology, Science University of Tokyo, Noda, 278

2.Research Institute for Biosciences, Science University of Tokyo, Noda 278

3.Tokyo Women's Medical College, Shinjuku-ku Tokyo 162

## Summary

Multiphase separated polymers are of great interest owing to unique characteristics such as high mechanical strengths, surface functionality and blood compatibility. It was well known that surface consisting of poly(styrene-*b*-HEMA) showed an excellent blood compatibility [1]. While, it was found that poly[4-{bis(trimethylsilyl)methyl}styrene](BSMS) membrane had fairly high oxygen permeability among vinyl polymers owing to its high Si-content and fairly high free space in the membrane [2]. So, we synthesized new silicon-containing block copolymer based on BSMS with HEMA, possessing the hydrophobic and hydrophilic segments. The block copolymer membranes were prepared by the different two methods. Thus obtained block copolymer surface showed microphase separated structures in spite of membrane preparation methods. However, the membranes obtained by the deprotection in matrix was found numerous pores. On the other hand, no pore was shown in the membrane prepared by another method. Moreover, even in the membrane having pores on the surface, a significant degree of platelets adhesion and deformation was suppressed. In this paper, we report on synthesis of poly(BSMS-*b*-HEMA) and their properties.

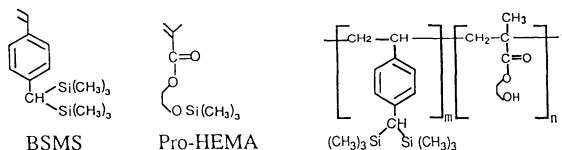


Fig.1 Chemical structures of monomers used and block copolymer obtained

**Key words** 4-{bis(trimethylsilyl)methyl}styrene, membrane lung, deprotection, block copolymer

## Results and Discussion

1) Synthesis of block copolymer : To a living poly(BSMS) solution, which is prepared by the anionic polymerization using butyllithium as initiator in THF at -74°C , ProHEMA was injected through dropping funnel. The block efficiency in this method attained 77%. By GPC and NMR analyses, the resulting polymers thus obtained was confirmed as poly(BSMS-*b*-ProHEMA) but not mixture of both components [3].

2) Membrane preparation : poly(**BSMS-b-HEMA**) membranes were prepared by the two different methods as follows.

2-1) Method A : After poly(**BSMS-b-ProHEMA**) membrane was prepared by casting from toluene solution, the membrane was soaked into 0.1N-HCl/THF(15/1(v/v)) solution for 72h for deprotection of the trimethylsilyl groups. From CP/MAS  $^{29}\text{Si}$ -NMR analysis, it was confirmed that the deprotection of trimethylsilyl groups proceeded completely.

2-2) Method B : To a THF solution of poly(**BSMS-b-ProHEMA**), few drops of 1.0N HCl was added to deprotect the trimethylsilyl groups. The resulting poly(**BSMS-b-HEMA**) was used for preparation of the membrane by casting from suitable solvent (toluene and t-BuOH).

3) Morphology (SEM and TEM analysis) :

From the SEM analysis of Poly(**BSMS-b-HEMA**) membrane (Method A), it was found that these were numerous pores not only on surface but in the bulk. This may be due to the voids after the exclusion of the protective groups from the membrane. On the other hand, no pore was shown in the membrane prepared by method B. From the TEM analysis of Poly(**BSMS-b-HEMA**) (Method B; BSMS 30mol%), it was confirmed that the spherical domain was formed both on the surface and in the bulk.

4) Deposition of platelets : Deposition of platelets on the polymer surface were investigated to estimate blood compatibility. From SEM view of the adhered platelets on the polymer, a significant degree of platelets adhesion and deformation was suppressed on poly(**BSMS-b-HEMA**) (Method A), which shows sharp contrast to poly(**BSMS**) homopolymer. Such poly(**BSMS-b-HEMA**) membrane with unique structural properties can be anticipated as high performance functional materials.

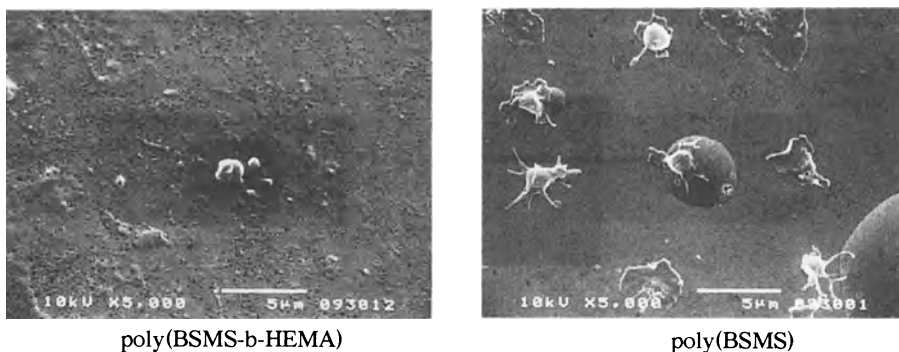


Fig.2 SEM picture of block polymer and poly(BSMS) surface after contacting platelets for 10min.

#### Reference

- 1) Okano T., Nishiyama S., Shinohara I., Akaike T., Sakurai Y., Kataoka K., Tsuruta T., *J. Biomed. Mater. Res.* **15**, 393, 1981.
- 2) Nagasaki Y., Suda M., Tsuruta T., and Ishihara K., Nagase Y., *Makromol.Chem., Rapid Commun.*, **10**, 255, 1989
- 3) Ito H., Taenaka A., Nagasaki Y., Kato M., Kataoka K., Tsuruta T., *Polymer*, to be submitted.

Tetsuji Yamaoka, Yoshiyuki Takebe, and Yoshiharu Kimura

*Department of Polymer Science and Engineering,  
Kyoto Institute of Technology, Matsugasaki, Kyoto 606, Japan*

## ABSTRACT

Good cell-attachment property was imparted to poly(L-lactic acid) (PLLA) by an easy reaction process in a mild condition. By immersing PLLA films in the alkaline solution for a given period of time, many carboxyl groups were produced on the film surface based on an alkaline degradation but no molecular weight change was observed. The number of carboxyl groups, which was quantified using a fluorescent reagent with high reactivity against carboxyl groups, greatly depended on the hydrolysis time. The mechanical property and the rate of degradation of PLLA matrices did not change because only the film surface was hydrolyzed. As an example of surface modifications of PLLA, cell attachment factor RGD peptides was immobilized through the carboxyl groups and the high cell attachment property of RGD-PLLA film was confirmed using 3T3 cells in vitro. The RGD-PLLA was found to be useful implantable matrix because it has high affinity against cells, excellent mechanical property, and biodegradability.

**KEYWORDS** : poly(lactic acid) (PLLA), RGD, cell attachment, guided tissue regeneration, biodegradation

## INTRODUCTION

In treating patients with damaged cartilage due to congenital abnormalities or trauma or with periodontal diseases, the guided tissue regeneration (GTR) technique using bioabsorbable scaffolds is an attractive therapy <sup>1)</sup>. Recently, it has been reported that poly(L-lactic acid) (PLLA) is a useful scaffold because of its degradability, low toxicity, and good mechanical property <sup>2)</sup>. However, PLLA has poor cell adhesion property, and the growth of cells or tissue is rather retarded. Therefore, its surface modification should be needed although it may be quite difficult because of the absence of reactive functional group. The present report discloses a new technique in modifying the PLLA surface with bioactive peptides, RGD <sup>3)</sup>, without its mechanical properties lost.

## MATERIALS AND METHODS

A PLLA film with a thickness of 0.2 mm was prepared by hot-pressing of PLLA with a molecular weight of  $2 \times 10^5$  or  $3 \times 10^5$  at 220 °C. PLLA film was immersing in a 3.75 M NaOH at r.t. for a given period of time. The treated film was then dipped in a 0.01 M HCl for neutralization and thoroughly washed with a flushed water. The amount of carboxyl groups in the PLLA film surface was measured by the capping method using fluorescent reagent, 9-anthryl diazomethane (ADAM). A PLLA film (1 x 1 cm) was reacted with a large excess of ADAM in 30 ml of isopropanol with gentle stirring for 1 hr. The film was then washed, dried and dissolved into 4 ml of chloroform. The fluorescence of the solution was measured at ex. of 369 and em. of 416 nm to calculate the amount of carboxyl groups based on a calibration curve.

A PLLA film (1 x 4 cm) was immersed into an isopropanol solution of a given amount of dicyclohexyl carbodiimide for 5 h at r.t. The film, washed thoroughly with a isopropanol solution containing 2 mg of RGD at r.t. for 2 days. It was then washed with a distilled water and dried in vacuo. The amount of immobilized RGD was measured by a ninhydrin test after hydrolysis of the film under acidic conditions at 124 °C in an autoclave. A piece of the PLLA film was placed in a well of a 24-well multi-dish, and 1 ml of the cell suspension ( $1 \times 10^5$ ) was added to it. After incubation for a given period of time, the film was taken out from the well, washed with PBS to remove non-adherent cells, and stained with a Giemsa's dye solution. The number of adhered cells on the PLLA film was counted on a microscope.



## RESULTS

The GPC chromatograms of the PLLA films treated in an alkaline solution for different times indicated that the molecular weight and its distribution did not change during the treatment. As shown in Table 1, the mechanical properties of these films did not show big change. These results indicate that the hydrolysis occurred only at the top surface of the PLLA films without changing their bulk properties.

Table 2 shows the changes in water contact angle of the alkali-treated and RGD-immobilized PLLA films with increasing hydrolysis time. The contact angle of the alkali-treated films was slightly decreased with increasing hydrolysis time due to an increased production of carboxyl groups in the surface. Their surface concentration determined by the fluorescence of the immobilized ADAM was found to increase by the hydrolysis, but to reach a plateau after 60 min. The cell attachment of these hydrolyzed films was almost the same (data not shown). The amount of immobilized RGD on these films greatly depended on the hydrolysis time, and the water contact angle was slightly lowered after immobilization of RGD. The changes in the cell attachment properties of the RGD-immobilized films are shown in Figure 1. As is seen, the cell adhesion increased with increasing surface concentration of RGD which should be correlated with the alkali treatment time. This feature was irrespective of the molecular weight of PLLA.

In conclusion, the alkali treatment of PLLA film could increase the surface concentration of carboxyl groups without deterioration of the mechanical properties of the films. The carboxyl groups could be utilized for surface modification. It was demonstrated that the RGD-immobilized PLLA films have excellent cell adhesion properties, and they can be applied to the GTR technique as a biodegradable scaffold.

## REFERENCES

1. van Wachem PB, van Luyn MJA, Olde Damink LHH, Dijkstra, J. Feijen PJ, Nieuwenhuis P, (1994) Biocompatibility and tissue regenerating capacity of cross linked dermal sheep collagen. *J Biomedical Material Res* 28:353-363
2. Freed LE, Marquis JC, Nohria A, Emmanuel J, Mikos AG, Langer R, (1993) Neocartilage formation *in vitro* and *in vivo* using cells cultured on synthetic biodegradable polymers. *J. Biomedical Material Res.*, 27:11-23
3. Lin H-B, Sun W, Mosher DF, Echeverria CG, Schaufelberger K, Lelkes PI, Cooper SL, (1994) Synthesis, surface, and cell-adhesion properties of polyurethanes containing covalently grafted RGD-peptides. *J. Biomedical Material Res.*, 28:329-342

**Table 1.** Mechanical properties of the alkaline-hydrolyzed PLLA films.

Hydrolysis time (min)	Elongation at break (%)	Tensile strength (x10 MPa)	Elastic modulus (GPa)
control	5.3	5.2	1.2
20	7.0	5.5	1.2
60	6.0	5.4	1.2
120	5.9	5.7	1.3

**Table 2.** Water contact angles of the alkaline-hydrolyzed and RGD-immobilized PLLA films with a molecular weight of  $2 \times 10^5$ .

Films	Hydrolysis time (min)	Immobilized RGD ( $\text{mg}/\text{cm}^2$ )	Water contact angle (degree)
Alkali-treated	0	-	73.6
	5	-	69.4
	10	-	65.4
	60	-	63.9
	120	-	63.3
RGD immobilized	0	0.01	69.2
	5	0.02	66.1
	20	0.13	66.6
	60	0.28	64.9
	120	0.31	62.4

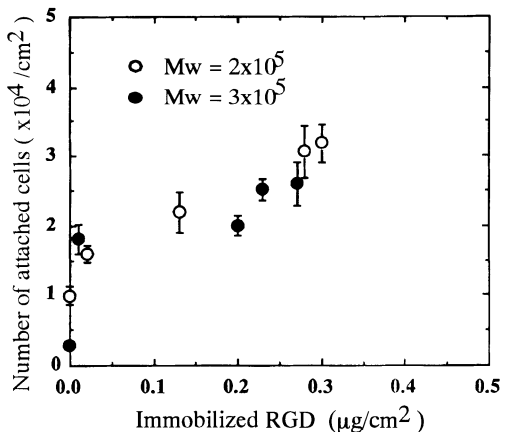


**Figure 1.** Relationship between the amount of immobilized RGD and the number of adhered cells.

# ADSORPTION OF BIOMOLECULES ONTO MULTIBLOCK COPOLYMER CONSISTING OF AROMATIC POLYAMIDE AND POLY(DIMETHYLSILOXANE)

Tsutomu Furuzono<sup>1</sup>, Akio Kishida<sup>1</sup>, Takeo Matsumoto<sup>2</sup>, Ikuro Maruyama<sup>3</sup>, Takao Nakamura<sup>4</sup> and Mitsuru Akashi<sup>1</sup>

<sup>1</sup>Department of Applied Chemistry and Chemical Engineering, Faculty of Engineering, Kagoshima University, 1-21-40 Korimoto, Kagoshima 890, Japan

<sup>2</sup>Tsukuba Research Laboratory, NOF Corp., Ltd., 5-10 Tokodai, Tsukuba 300-26, Japan

<sup>3</sup>Faculty of Medicine, Kagoshima University, 8-35-1 Sakuragaoka, Kagoshima 890, Japan

<sup>4</sup>Kagoshima Institute of Preventive Medicine, 1-72-8 Myoenji Ijyuin, Kagoshima 899-25, Japan

## SUMMARY

Multiblock copolymer(Aramid-Silicone Resin; PAS) consisting of aromatic polyamide(aramid) and poly(dimethylsiloxane)(PDMS) has desirable properties of both components. In this study, we investigated the protein adsorption, cell adhesion and tissue reaction for PAS surface in order to clarify the interaction between PAS and biomolecules. It was found that biomolecules adsorption onto PAS was scarcely occurred compared with aramid and nylon films, comparable to Silastic<sup>®</sup> film. These prevention of biomolecules onto PAS seemed to be due to low surface free energy of PAS surface due to the condensation of PDMS block to outermost surface of PAS. Because of its unique properties, PAS is expected to be useful as a novel biomaterial.

**KEY WORDS:** poly(dimethylsiloxane), aramid, multiblock copolymer, protein adsorption, cell adhesion

## INTRODUCTION

In previous reports[1-5], we have studied about synthesis, blood compatibility and gas permeability for aramid-silicone resin(PAS) consisting of aromatic polyamide(aramid) and poly(dimethylsiloxane)(PDMS) from the point of view of a novel biomaterial. In these results, it was recognized that PAS didn't interact strongly with platelet, and possessed good gas-permeability and superior mechanical properties which were widely variable from tough plastic to rubber-like elastomer. However, the interactions between PAS and biomolecules in living body are still unclear. In this study, we investigated the protein adsorption, cell adhesion and tissue reaction for PAS surface in order to clarify the interaction between PAS and living body.

## METHODS

PAS was synthesized by low temperature solution polycondensation using a PDMS whose molecular weight was 1680 through two step procedure according to the method developed by Imai et al.[6] with a little modification[1]. PAS, aramid, Silastic<sup>®</sup>(DOW CORNING Co.), nylon(ICN BIOMEDICALS Co.) and regenerated cellulose films were used for these experiments. In the experiment of Bovine serum albumin(BSA) adsorption onto PAS, BSA solution(4.0 mg/ml) was poured into a plastic tube containing sample films and then incubated at 37°C for 3h. The absorbed BSA was eluted by 1.0% sodium laurylsulfate(SDS) solution. Amount of BSA was detected by use of Micro BCA Protein Assay Reagent Kit (Pierce Chemical Co.). In cell adhesion experiment, L929 cells were plated onto the polymer films in 24 well multiplate(10 mm diameter) at density of  $5 \times 10^5$  cells/well, and incubated at 37°C for 24h. The adhered cells were observed by phase transmission microscope, and counted by use of Cell Counting Kit(DOJINDO Co.). For further study, ethylene oxide gas sterilized PAS films were implanted in the back of Wister rats in one month. The films containing tissue were explained, and the specimens with hematoxylin-eosin stain were observed by use of optical microscope.

## RESULTS AND DISCUSSION

Three types of PAS were prepared, that are 8, 41 and 71 wt% of PDMS content in PAS. In the following, these PASs were indicated as PAS-8, PAS-41 and PAS-71, respectively. In the BSA adsorption test, it was found that BSA adsorption onto PAS was scarcely occurred compared with aramid and nylon films, and comparable to Silastic<sup>®</sup> film. In previous works[1-3], it was found that PDMS blocks were condensed at outermost surface of PAS by means of contact angle measurement and X-ray photoelectron spectroscopy. This prevention of protein adsorption of PAS seemed to be due to low surface free energy of the surface caused by the condensation of PDMS block to outermost surface of PAS. Next, the L929 cell adhesion test onto the polymer surfaces was done. The cells could not adhere onto all the PAS surfaces compared with aramid and nylon films. Moreover, the amount of cell adhesion of PAS surfaces were decreased with increasing PDMS content in PAS, and the amount of cell adhesion of PAS-41 and 71 surfaces were lower than that of Silastic<sup>®</sup> film which was fully covered with PDMS. It is thought that this effect may have been caused for the presence of microphase-separation-like structure in PDMS enriched surface. Now, we are investigating the surfaces of PAS by means of staining method. In histological observation in one month, there were no severe reactions around the PASs and their surfaces were in contact with a thin fibrous tissue. Similar reactions were also observed in aramid and Silastic<sup>®</sup> films.

In previous paper, we already reported that PAS surface interacted slightly with platelet[1-2]. From the results in this report, it is thought that platelet and cell adhesion are depressed in order to reduce protein adsorption onto PAS surface. This result was due to the condensation of PDMS blocks on PAS surface. Because of its unique properties, PAS is expected to be useful as a novel biomaterial.

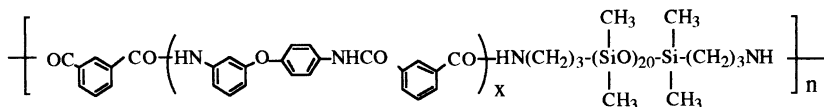


Fig. 1 Aramid-Silicone Resin (PAS)

## REFERENCES

1. Furuzono T, Yashima E, Kishida A, Maruyama I, Matsumoto T and Akashi M. (1993) A novel biomaterial: Poly(dimethylsiloxane)-polyamide multiblock copolymer I. Synthesis and evaluation of blood compatibility. *J Biomater Sci Polym Ed* 5: 89-98
2. Furuzono T, Kishida A, Akashi M, Maruyama I, Miyazaki T, Koinuma Y and Matsumoto T. (1993) Development of a novel biomaterial aramid-silicone resin: Studies of gas-permeability and blood-compatibility. *Jpn J Artif Organs* 22: 370-375
3. Kishida A, Furuzono T, Ohshige T, Maruyama I, Matsumoto T, Itoh H, Murakami M and Akashi M (1994) Study of the surface properties of ultrathin films of poly(dimethylsiloxane)-polyamide multiblock copolymers. *Angew Makromol Chem* 220: 89-97
4. Furuzono T, Seki K, Kishida A, Ohshige T, Waki K, Maruyama I and Akashi M. (in contribution) Novel functional polymers: Poly(dimethylsiloxane)-polyamide multiblock copolymer III. Synthesis and surface properties of disiloxane-aromatic polyamide multiblock copolymer. *J Appl Polym Sci*
5. Matsumoto T, Koinuma Y, Waki K, Kishida A, Furuzono T, Maruyama I and Akashi M. (in contribution) Novel functional polymers: poly(dimethylsiloxane)-polyamide multiblock copolymer IV. Gas permeability and thermomechanical properties of aramid-silicone resins. *J Appl Polym Sci*
6. Kajiyama M, Kakimoto M and Imai Y (1989) Synthesis and characterization of new multiblock copolymers based on poly(dimethylsiloxane) and aromatic polyamides. *Macromolecules* 22: 4143-4147

# HEMOCOMPATIBLE CELLULOSE DIALYSIS MEMBRANE MODIFIED WITH PHOSPHOLIPID POLYMER

Kazuhiko ISHIHARA and Nobuo NAKABAYASHI

Institute for Medical and Dental Engineering, Tokyo Medical and Dental University  
2-3-10, Kanda-surugadai, Chiyoda-ku, Tokyo 101, Japan

## ABSTRACT

Surface modification of cellulose hemodialysis membrane with phospholipid polymer was investigated to reduce protein adsorption, platelet adhesion and complement activation. The mechanical properties and permeation for solutes were did not change even after the modification. Both protein adsorption and complement activation after contact with plasma were significantly suppressed by the modification compared with these of the original membrane. Moreover, platelet adhesion was completely inhibited on the phospholipid polymer-modified cellulose membrane.

**KEY WORDS :** Hemodialysis membrane, Cellulose membrane, Phospholipid polymer, Surface modification, Protein adsorption, Complement activation, Platelet adhesion

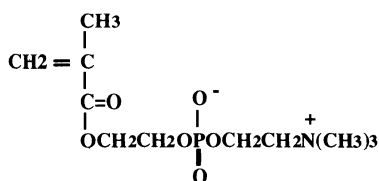


Fig. 1. Structure of MPC

## INTRODUCTION

The properties required for a hemodialysis membrane are excellent ultrafiltration rate, permeability for solutes, mechanical strength and blood compatibility. Though the cellulose membrane has both good permeability and mechanical strength, its blood compatibility must be improved for hemodialysis. Moreover, the cellulose membrane induces the activation of a complement system because the membrane surface interacts strongly with the complement proteins. We have found that polymers containing a phospholipid polar group, 2-methacryloyloxyethyl phosphorylcholine(MPC) polymers, show excellent blood compatibility[1,2]. Therefore, if the surface of the cellulose membrane can be modified with an MPC polymer, improvement of the blood compatibility can be achieved. In this article, the surface modification of cellulose hemodialysis membrane by the various techniques using MPC polymers is described.

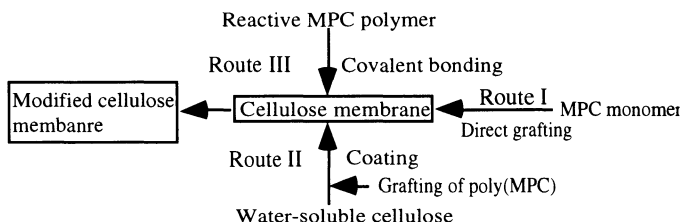


Fig. 2 Surface modification of cellulose membrane with MPC polymer

## MATERIALS AND METHOD

MPC(Fig. 1) was synthesized by the method described previously[1]. Three different routes of modification of the cellulose membrane(Cuprophane) with MPC polymers were investigated. These were direct grafting of MPC onto the cellulose membrane(Route I)[3], coating with water-soluble cellulose grafted with poly(MPC)(Route II)[4], and chemical reaction between reactive MPC polymer and cellulose(Route III). The routes of these modifications are represented in Fig. 2.

## RESULTS AND DISCUSSION

### Modification of cellulose membrane with MPC polymers

From the IR and X-ray photoelectron spectra confirmed that the surface of the cellulose membrane modified with MPC polymers by every method. The permeability and mechanical properties of the membrane did not change after the modification.

### Protein adsorption and complement activation on MPC polymer-modified cellulose membrane

The amount of adsorbed protein from human plasma after 60-min contact on the original cellulose membrane was decreased significantly when the membrane was modified with the MPC polymers. The percentage of complement consumption after contact with the cellulose membrane was high, but the value was lowered by the modification with the MPC polymers. The reduction of the value became greater with an increase in the surface MPC mole fraction. These results clearly indicated that immobilized chains of MPC polymer on the cellulose membrane suppressed activation of the complement system.

Table 1. Blood compatibility of cellulose membrane modified with MPC polymers

Abb.	Modification method	Surface mole fraction of MPC unit	Amount of adsorbed protein on the surface ( $\mu\text{g}/\text{cm}^2$ )	Complement consumption (%)
Original	none	0	$1.3 \pm 0.1$	$47 \pm 6$
I-1	Route I	0.27	$0.81 \pm 0.1$ *	$21 \pm 5$ *
I-2		0.36	$0.41 \pm 0.02$	$12 \pm 7$
II-1	Route II	0.14	—	$23 \pm 5$
II-2		0.27	$0.55 \pm 0.07$	$12 \pm 3$
III-1	Route III	0.15	$0.86 \pm 0.1$	$17 \pm 3$
III-2		0.28	$0.66 \pm 0.1$	$14 \pm 4$

The values are mean  $\pm$  S.D. (n=5)

\* Significant difference vs the value of the original membrane ( $p < 0.01$ ).

### Platelet adhesion on cellulose membrane modified with MPC polymers

When platelet-rich plasma of rabbit was in contact with the original cellulose membrane, deformation and aggregation of platelets adhered on the surface occurred and severe fibrin net formation was observed. On the other hand, platelet adhesion was reduced due to the modification with MPC polymers. We found that a surface which can inhibit protein adsorption is very important for a blood compatible hemodialysis membrane. This modification technique can be easily applied to cellulose hollow fibers and the modified hollow fibers show excellent hemocompatibility even in *ex vivo* test[5].

## REFERENCE

- [1] Ishihara K, Ueda T, Nakabayashi N (1990) *Preparation of Phospholipid Polymers and Their Properties as Hydrogel Membrane. Polym J* **22**: 355
- [2] Ishihara K, Oshida H, Ueda T, Endo Y, Watanabe A, Nakabayashi N (1992) *Hemocompatibility of Human Whole Blood on Polymers with a Phospholipid Polar Group and Its Mechanism, J Biomed Mater Res* **26**: 1543
- [3] Ishihara K, Fukumoto K, Aoki J, Nakabayashi N (1992) Improvement of Blood Compatibility on Cellulose Dialysis Membrane. 1. Grafting of 2-Methacryloyloxyethyl Phosphorylcholine onto a Cellulose Membrane Surface. *Biomaterials* **13**: 145
- [4] Ishihara K, Miyazaki H, Kurosaki T, Nakabayashi N (1995) Improvement of Blood Compatibility of Cellulose Dialysis Membrane. 3. Synthesis and Performance of Water-soluble Cellulose Grafted with Phospholipid Polymer as Coating Materials on Cellulose Dialysis Membrane. *J Biomed Mater Res* **29**: 181
- [5] Ishihara K, Fukumoto K, Miyazaki H, Nakabayashi N (1994) Improvement of the Hemocompatibility on a Cellulose Hollow Fibers with a Novel Biomedical Polymer Having a Phospholipid Polar Group. *Artif. Organs* **18**: 559

ARTIFICIAL GLYCOCONJUGATE POLYMERS: CELL-SPECIFIC BIOMEDICAL MATERIALS USING CARBOHYDRATES AS RECOGNITION SIGNALS

Kazukiyo Kobayashi,\* Taichi Usui,\*\* and Toshihiro Akaike#

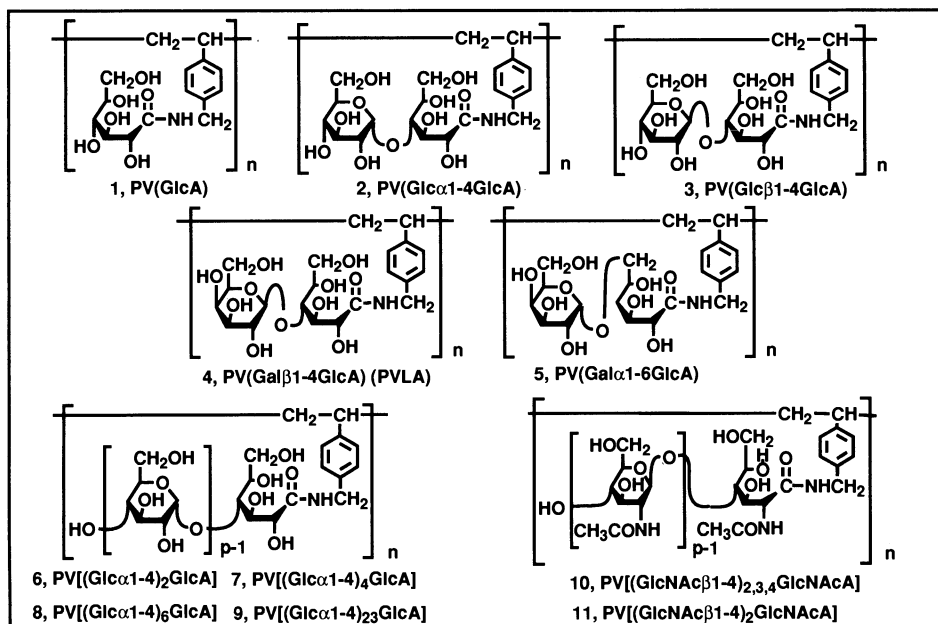
\* Faculty of Agricultural Sciences, Nagoya University, Chikusa, Nagoya 464-01, Japan,

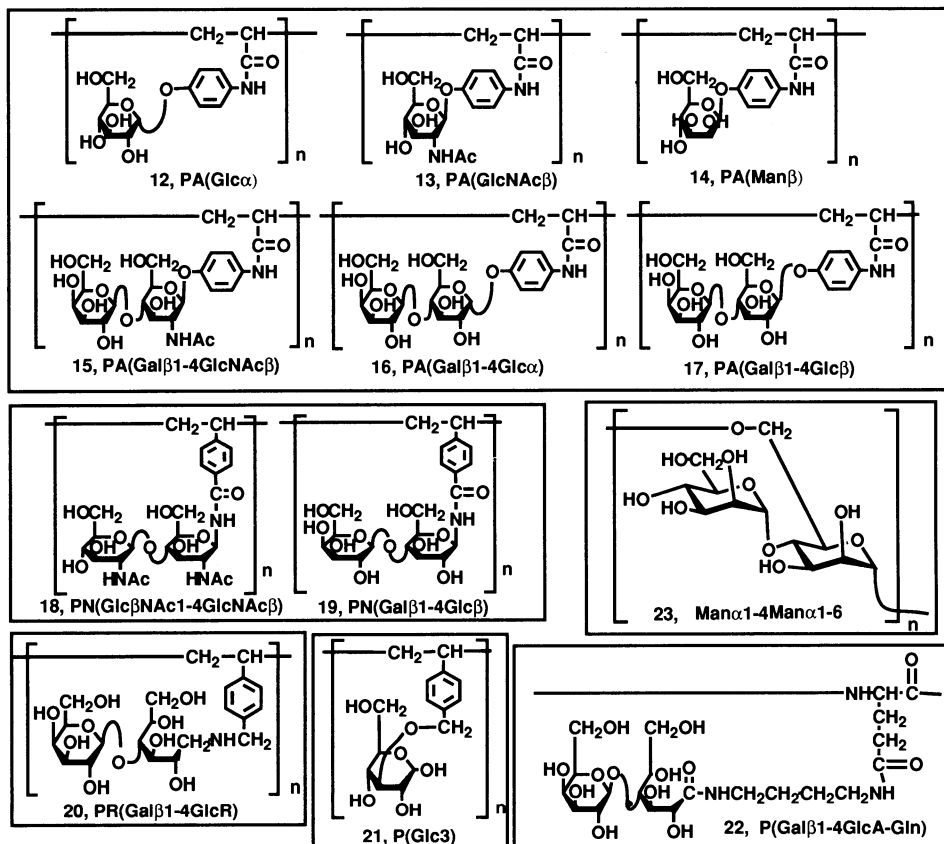
\*\*Faculty of Agriculture, Shizuoka University, Shizuoka 836, Japan, and # Faculty of Bioscience and Technology, Tokyo Institute of Technology, Midori, Yokohama, 226, Japan.

**ABSTRACT.** Well-defined polymers having mono- and oligosaccharide chains are of interest as biological probes and cell-specific biomedical materials. We prepared several oligosaccharide-substituted polymers of which chemical structures are shown in the next page. The main chains of the polymers are the derivatives of polystyrene (1-11, 18-21), polyacrylamide (12-17), polypeptide (22), and polysaccharide (23). The starting mono- and oligosaccharides include glucose (1,12,21), mannose (14,23), *N*-acetylglucosamine (13), cellobiose (3), maltose (2), maltotriose (6), maltopentaose (7), maltoheptaose (8), amylose (9), lactose (4,16,17,19,20,22), melibiose (5), *N*-acetyllactosamine (15), *N,N'*-diacetylchitobiose(18), *N,N',N''*-triacetylchitotriose(11), and so on.

**INTRODUCTION** Much attention has been given to oligosaccharide chains as the key participants in cell-cell recognition events. The synthetic polymers substituted with pendant carbohydrate moieties have been applied for biomedical materials such as cell-specific culture substrata, artificial antigens, and targeted drug delivery systems. They are also useful as tools for investigating biological recognition phenomena using lectins and anti-carbohydrate monoclonal antibodies. This paper attempts to design more simple synthetic routes in order to introduce more biologically important, complex oligosaccharides.

**SIMPLE SYNTHETIC METHODOLOGY** Carbohydrate-substituted vinyl-monomers were prepared by the following reactions without any protection and deprotection steps of oligosaccharides. Water-soluble polymers of high-molecular weight were prepared by the homo- and copolymerizations using radical initiators in dimethyl sulfoxide and in water at 60 °C.





- a) Polymers **1-11**. Oxidation of the reducing terminals of oligosaccharides followed by amidation with *p*-vinylbenzylamine.
- b) Polymers **12-17**. Reduction of *p*-nitrophenyl glycosides followed by amidation with acrylic acid.
- c) Polymers **18-19**.  $\beta$ -*N*-Glycosidation of *p*-vinylbenzoyl chloride with glycosylamine having an amino function in the reducing terminal.
- d) Polymer **20**. Reductive amination in the presence of *p*-vinylbenzylamine.

#### FEATURES OF THESE ARTIFICIAL GLYCOCONJUGATE POLYMERS

- a) Several bioactive oligosaccharides obtained by chemo-enzymatic synthesis, by selective hydrolysis of polysaccharide, and extraction of natural products were used as the starting substances.
- b) Numerous high-density glyco-signals protruded from the polymer molecules.
- c) The clustered glyco-signals were interacted strongly with lectins.
- d) The strong interaction is promising as cell culture substrata for hybrid-type artificial organs and as probes for biochemical researches.

REFERENCES (1) Kobayashi K, Kobayashi A, Tobe S, Akaike T, In: *Neoglycoconjugates: Preparation and Application*. Lee YC, Lee RT (eds). Academic Press: San Diego, California 1994; pp 261-284. (2) Kobayashi K, Kakishita N, Okada M, Akaike T, Usui T (1994) *J. Carbohydr. Chem.*, **13**: 753-766. (3) Kobayashi K, Akaike T, Usui T, In: *Methods in Enzymology, Vol. 242, Neoglycoconjugates Part A Synthesis*, Lee YC, Lee RT (eds). Academic Press, San Diego, California 1994; pp 226-235. (4) Kobayashi K, Kobayashi A, Akaike T, In: *Methods in Enzymology, Vol. 247 Neoglycoconjugates Part B Biomedical Applications*, Lee YC, Lee RT (eds). Academic Press, San Diego, California 1994; pp 409-418. (5) Kobayashi K, Tuchida A, Okada M, Akaike T, Usui T (1994) *Polym. Jpn.*, **43**: 2857-2858.

# PREPARATION OF ACRYLAMIDE COATED PVC TUBE BY APG TREATMENT AND ITS CHARACTERIZATION

Y. Babukutty, M. Kodama, H. Nomiya<sup>\*</sup>, M. Kogoma<sup>\*\*</sup> and S. Okazaki<sup>\*\*</sup>

Bionic Design Research Group, National Institute for Advanced Interdisciplinary Research, Tsukuba, Ibaraki 305, JAPAN, <sup>\*</sup>Kawasumi Lab. Inc., Kanagawa, <sup>\*\*</sup> Dept. of Chemistry, Sophia University, Tokyo.

## SUMMARY

Atmospheric plasma glow (APG) discharge method is an efficient method recently developed to modify material surfaces. Here, we modified the inner surface of a commercial PVC tube with a hydrophilic functional group, acrylamide. A thin uniform layer of the polymerized monomer was obtained on the surface and was characterized by FTIR/ATR, ESCA, contact angle measurement and platelet adhesion studies. Presence of peaks corresponding to amide functional group in FTIR/ATR spectra and N1s peak in the ESCA spectra showed the surface modification due to acrylamide on the surface. Contact angle values also decreased considerably, indicating increase in surface hydrophilicity. Antithrombogenicity of the surface was evaluated by platelet adhesion studies using platelet rich plasma (PRP) from rabbit blood and found less number of platelets and less deformation to the platelets as compared with the non-treated PVC samples.

**KEY WORDS:** Atmospheric plasma glow (APG) discharge, acrylamide, antithrombogenicity, hydrophilicity,

## INTRODUCTION

Among the various surface modification techniques Atmospheric pressure glow (APG) plasma discharge method ranks as an effective one to modify materials of versatile structures and properties. Since atmospheric pressure and temperature are maintained in this technique, structural damage due to high temperature which may occur to soft materials in conventional plasma treatment technique can be overcome. Yokoyama *et al* (1990) has reported certain conditions necessary to obtain stable glow discharge at atmospheric pressure. They include (i) use of He as the dilute gas, (ii) use of a high frequency source and (iii) introduction of insulating plate in between the electrodes. Here, we used the APG treatment method to introduce a hydrophilic functional group, acrylamide, to the inner surface of a soft PVC tube to make it a biocompatible material.

## METHODS

PVC tube having inner and outer diameters of 6.5mm and 8.4 mm respectively is incubated with acrylamide dissolved in ethyl alcohol for the preadsorption of acrylamide onto the surface. It is dried and placed inside the cylindrical electrode and helium gas is passed continuously (flow rate 1500 ml/min) under atmospheric pressure. Plasma glow discharge was effected for 20 min using high frequency source of 20 kHz.

Surface characterizations were done by VG Scientific X-ray photoelectron spectrometer ESCALAB MKII and Jasco Janssen Micro FT/IR - 200 with ATR attachment. Contact angles were measured with a FACE Contact Angle Meter (Kyowa). In vitro experiments were conducted by exposing the samples to rabbit platelet rich plasma (PRP) for 1hr at 37°C and fixed with 2.5% glutaraldehyde (in saline). Samples were dried, coated with gold and Scanning Electron Micrographs were taken using Hitachi S - 4500 Scanning Electron Microscope.



## RESULTS AND DISCUSSION

Contact angle values are given in Table 1 and change in hydrophilicity can be observed from the difference in contact angle values of the modified and unmodified surfaces. Contact angle value of pure PVC ( $91.5 \pm 1.4$ ) was decreased to less than  $50^\circ$  depending on the concentration of acrylamide used for preadsorption. Figure 1. represents the ESCA spectra of pure PVC tube, acrylamide coated PVC tube and polyacrylamide.

Table 1. Contact angle values of modified and unmodified PVC samples

Surface	Unmodified PVC	Acrylamide Treatment Conc.		
		10%	20%	30%
Contact angle ( $^\circ$ )	$91.5 \pm 1.4$	$49.4 \pm 2.8$	$45.2 \pm 2.7$	$43.3 \pm 2.3$

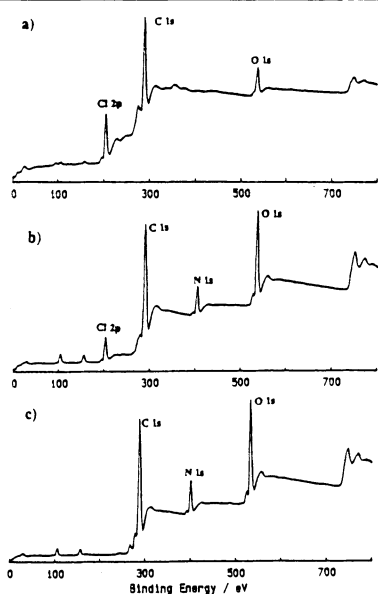


Fig. 1. ESCA spectra of **a)** PVC sample (commercial)  
**b)** Acrylamide treated PVC sample **c)** Polyacrylamide

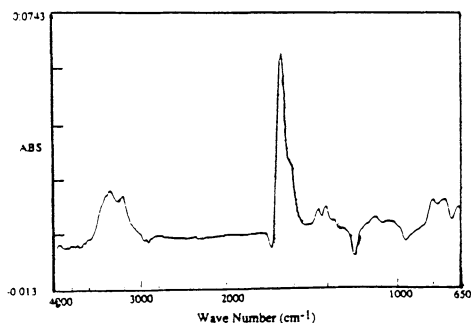


Fig.2. FTIR/ATR spectrum of the surface coating of acrylamide

Presence of N1s peak at 400 eV corresponding to that of pure polyacrylamide is obtained on the treated PVC surface. N atom has appeared on the PVC surface due to the modification of the surface by acrylamide. Figure 2. is the FTIR/ATR spectrum of the surface coating obtained by the subtraction of pure PVC spectrum from the acrylamide treated PVC spectrum. Presence of prominent peaks around  $1670 \text{ cm}^{-1}$  and between  $3000 \text{ cm}^{-1} - 3500 \text{ cm}^{-1}$  are characteristics of amide ( $-\text{CONH}_2$ ) group. All these factors indicate the successful incorporation of a hydrophilic functional group onto the PVC tube surface. These samples were further evaluated for their antithrombogenic property using platelet rich plasma adhesion (PRP) studies. Adhesion and deformation of platelets were comparatively less on the modified surface relative to the unmodified surface. Detailed studies in this regard are under progress. Evidently, APG treatment method is a useful technique for modifying materials, especially inner side of tubular structures and other specially shaped structures.

## REFERENCE

T. Yokoyama, M. Kogoma, T. Moriwaki and S. Okazaki (1990). The mechanism of the stabilisation of glow plasma at atmospheric pressure *J. Phys. D: Appl. Phys.*, **23**: 1125-1128

# ANTICOAGULANT PROPERTIES OF SULFONATED GLUCOSIDE-BEARING POLYMER

Nobuyuki Sakamoto, Kazuya Suzuki, Akio Kishida, and Mitsuru Akashi

Department of Applied Chemistry and Chemical Engineering, Faculty of Engineering,  
Kagoshima University, 1-21-40, Korimoto, Kagoshima 890, JAPAN.

## ABSTRACT

Previously, we found that the sulfonated poly(glucosyloxyethyl methacrylate) (poly(GEMA)-sulfate), which bears sulfonated D-(+)-glucose, had anticoagulant activity. In this study, we tried to clarify the mechanism of anticoagulant activity of poly(GEMA)-sulfate. So we carried out activated partial thromboplastin time (APTT), prothrombin time (PT) and thrombin time (TT) tests to recognize the mechanism of anticoagulant activity for poly(GEMA)-sulfate. The results of these *in vitro* clotting tests showed that poly(GEMA)-sulfate had anticoagulant activity of which mechanism was different from that of heparin. It seems that inhibiting fibrin network formation of anticoagulant may be occurred by the entrapment of fibrinogen by poly(GEMA)-sulfate or inhibiting thrombin activity by the activation of heparin cofactor II.

**KEY WORDS:** Anticoagulant activity, Heparinoid, Polysaccharide Analogue, Glucoside Polymer

## INTRODUCTION

Heparin, which is sulfonated dextro-rotatory mucopolysaccharide, is known to act as an anticoagulant by increasing the rate of formation of the irreversible complex between thrombin (T) and antithrombin III (ATIII). Many studies of heparin have been interest in order to develop the anticoagulant biomaterials using heparin, though there are some difficulties for usage of heparin. For instance, physiological activity of heparin has not been clarified completely, and the immobilization of heparin is not so easy. To solve these problems, various synthetic heparinoids have been synthesized and their anticoagulant properties were evaluated. In our previous study, we have found that sulfonated poly(glucosyloxyethyl methacrylate) (poly(GEMA)-sulfate)[1], which bears sulfonated D-(+)-glucose, had anticoagulant activity. In the evaluation of its activity by the method of Lee-White, both the degree of sulfonation and the concentration of poly(GEMA)-sulfate influenced on the coagulation time. It became also apparent that poly(styrene sulfuric acid), and poly(vinyl sulfone) exert slightly their effects, however, dextran sulfate showed higher anticoagulant activity than that of poly(GEMA)-sulfate in the same condition. This result suggests that sulfonated saccharide residue play an important role for acquisition of anticoagulant activity. However, the mechanism of anticoagulant activity of poly(GEMA)-sulfate has not been cleared. The aim of this work is to clarify the mechanism of anticoagulant activity of poly(GEMA)-sulfate and to understand whether saccharide moieties are necessary for anticoagulant activity.

## EXPERIMENTAL

Poly(GEMA)-sulfate was synthesized as follows. Poly(GEMA)[2] and SO<sub>3</sub> were dissolved in N,N-dimethyl formamide(DMF) in ratio of 1:11. The mixture was stirred under nitrogen atmosphere at

25 °C for 24 hours. Then, after cooling to 0 °C, the reaction product was neutralized with NaOH in methanol-water mixture solution and purified by dialysis with water for three days. Then, polymer solution was freeze-dried for four days. Sulfonation was confirmed by IR spectroscopy. Absorption at 1240-1250 cm<sup>-1</sup> and 800 cm<sup>-1</sup> of poly(GEMA)-sulfate was assigned to S=O and C-O-S stretch, respectively. Degree of sulfonation was estimated by elemental analysis as 3.8.

The anticoagulant activity of poly(GEMA)-sulfate was measured by activated partial thromboplastin time (APTT), prothrombin time (PT), and thrombin time (TT) tests. Each experimental procedure was conventional ones. Fresh human blood which contained sodium citrate was centrifuged at 3000 rpm for 10 min at 4 °C and platelet-poor plasma(PPP) was obtained. PPP, poly(GEMA)-sulfate, and other reagent were placed in a test tube kept at 37 °C and the time of the formation of a fibrin network by addition of each clotting reagent was measured.

## RESULT AND DISCUSSION

At first, we investigated whether poly(GEMA)-sulfate could interact with ATIII using the SDS-polyacrylamide gel electrophoresis (SDS-PAGE). There occurred no increasing of the rate formation of the T-ATIII complex in the presence of poly(GEMA)-sulfate. From this result, we found that poly(GEMA)-sulfate did not bind to ATIII. Secondary, we examined whether poly(GEMA)-sulfate could form ion complex with calcium ion in serum. In spite of increasing the added poly(GEMA)-sulfate, however it was not observed that concentration of calcium ion in serum was decreased (Table 1). Then we carried out APTT, PT and TT tests to recognize the mechanism of anticoagulant activity for poly(GEMA)-sulfate. In APTT and PT tests, clotting time was prolonged when intrinsic and extrinsic coagulant factors were inhibited. In TT test, clotting time was prolonged when the inactivation of fibrinogen occurred. In the case of poly(GEMA)-sulfate, APTT and PT were prolonged and there was no fibrin network formation over 100 mg/ml of poly(GEMA)-sulfate. This phenomenon was also observed in the TT test. The results of these *in vitro* clotting tests showed that poly(GEMA)-sulfate had anticoagulant activity of which mechanism was different from heparin. It is concluded that inhibiting fibrin network formation of anticoagulant may be occurred by the entrapment of fibrinogen by poly(GEMA)-sulfate or the inhibition of thrombin activity by the activation of heparin cofactor II.

Table 1. Effect of poly(GEMA)-sulfate on the concentration of Ca<sup>++</sup> in the serum.

Poly(GEMA)-sulfate concentration(μg/ml)	500	100	50	10	1	none
Serum calcium ion concentration(mmol)	2.7	2.6	2.6	2.6	2.6	2.6

## REFERENCES

- 1.Sakamoto N, Suzuki K, Kishida A, Akashi M (1993) Physical activity of sulfonated glucoside polymer. *Polym.Prepr.Jpn.* 42: E1060
- 2.Fukudome N, Suzuki K, Yahshima E, Akashi M (1994) Synthesis of nonionic and anionic hydrogels bearing a monosaccharide residues and their properties. *J.Appl.Polym.Sci.*, 52, 1759-1763.

# HISTOLOGICAL AND MORPHOLOGICAL COMPARISON OF EXPLANTED SMALL DIAMETER PU AND ePTFE VASCULAR PROSTHESES: A PRELIMINARY STUDY

Zhaoxu Wang, Ze Zhang, and Makoto Kodama

National Institute for Advanced Interdisciplinary Research, Tsukuba, Ibaraki, Japan. Tel: (0298)54-6263; Fax: (0298)54-6382

## SUMMARY

In order to evaluate tissue and cell infiltration and endothelialization behaviors of small diameter polyurethane (PU) vascular prosthesis, PU grafts (1.5 mm ID, 1 cm in length) prepared by using a low temperature technique were implanted into the abdominal aorta of rats for about two weeks. SEM and histological analyses were performed after harvesting. Polytetrafluoroethylene grafts (ePTFE) of the same size were used as control. Endothelial-like cells were observed on 5 out of 6 PU and 2 out of 4 ePTFE grafts. Azan and Victoria blue staining revealed higher collagen and elastin content in PU grafts. Both grafts had similar inflammatory reaction.

**KEY WORDS:** Vascular grafts, Polyurethane, ePTFE, in vivo, Microporous

## INTRODUCTION

In the previous work from this laboratory, a new small diameter polyurethane (PU) vascular prosthesis prepared by using a low temperature technique has demonstrated novel microporous structure, high processing flexibility and excellent compliance (1). The present work is to report the primary results of in vivo experiment, especially in terms of tissue infiltration and endothelialization.

## MATERIALS AND METHODS

PU grafts were prepared from 10% Tecoflex® PU solution by using a low temperature technique (1). Briefly, PU solution was filled into a mould that was constructed by a glass tube and a glass rod that was longitudinally fixed at the center of the tube. The mould was then frozen at low temperature and freeze-dried. Then PU tube was released from glass mould and sterilized for animal implantation. Six PU grafts of 1.5 mm ID and 1 cm in length were implanted into the abdominal aorta of rats for about two weeks. After harvesting, those grafts were rinsed in heparinized saline. Then the specimens for SEM analysis were fixed in 2% glutaraldehyde, critical point dried and coated with gold. Specimens for histological analysis were fixed in 10% formaldehyde, critical point dried and stained with HE, Azan and Victoria blue. As control, four ePTFE grafts of 30 µm in microfibre length, 1.5 mm internal diameter and 1 cm in length were implanted, harvested and prepared in the same fashion as PU grafts.

## RESULTS AND DISCUSSION

The results of SEM and light microscope observations were summarized in Table 1. In the total six PU grafts, PU6 was occluded and significant thrombus was found at the distal side of PU5 (33%). Small thrombus was found in the middle part of ePTFE4 (25%). Other PU and ePTFE grafts had smooth and glistening luminal surface at the time of harvesting. Endothelial-like cells (ECs) were observed at proximal and/or distal sites of five out of six (83%) PU and two out of four (50%) ePTFE grafts. No ECs presented at middle part and at the site where thrombosis occurred. Apparently PU grafts showed better endothelialization as compared with ePTFE controls in the aspects of earlier occurrence and better development. In the case of PU10, ECs developed about 1.8 mm from distal anastomosis into the luminal of graft. Based on Azan and Victoria blue staining, much higher content of collagenous tissue and some elastin fibres presented in the PU prostheses. Since the presence of collagenous substrate in the luminal side of the graft is very important to the endothelialization process, the higher collagen synthesis activity within the microporous structure of the PU grafts

Table 1. Summarized data of explanted PU and ePTFE grafts

	ePTFE1	ePTFE2	ePTFE3	ePTFE4	PU5	PU6	PU7	PU8	PU9	PU10
Throm	-	-	-	+	++++	OCL	-	-	-	-
EC Pro	-	-	-	+	+	-	-	-	+	++
Mid	-	-	-	-	-	-	-	-	-	-
Dis	-	-	+	+	-	-	++	+	+	++
Collag.	+	+	+	+	++++	++++	++++	++++	++++	++++
Elastin	-	-	-	-	+	-	+	-	-	-
Inflam.	++	+++	++	+++	+++	++	++	++	++	+++
ImpDay	13	16	22	22	14	14	14	13	15	14

Throm: thrombus (OCL: occluded); EC: endothelial-like cells (Prox, proximal site; Mid, middle site; Dis, distal site); Collag.: collagen; Inflam.: inflammatory reaction; ImpDay: days of implantation; -: not observed; +: observed; ++: light; +++: moderate; ++++: significant.

could be a key factor that had contributed to the better endothelialization of the PU grafts. From material point of view, PU is relatively more hydrophilic than PTFE and the PU grafts prepared in this particular manner is even more hydrophilic. Among other factors, the higher hydrophilicity and the suitable microporous structure of the PU grafts provided a good access for the surrounding cellulosic components and extra cellular fluid to get into the prosthetic wall and then might have promoted higher cellular activity including collagen synthesis by fibroblasts. ePTFE grafts also possess microporous structure and permit the infiltration of cells. However, perhaps because of the extremely high hydrophobic nature and the particular microfibre configuration, the cellular infiltration process in the ePTFE grafts was apparently slower. It took 13 days for ECs to grow into PU grafts but 22 days into ePTFE. The thickness of the internal capsule of the ePTFE grafts was very thin or there was no well organized internal capsule, which again slowed down the endothelialization. The higher occurrence of thrombosis among PU grafts was believed due to technique error during operation. In conclusion, PU grafts showed better endothelialization and tissue infiltration than ePTFE controls, which addressed the importance of hydrophilicity and the microporous structure of the testing grafts.

## REFERENCES

1. Liu SQ and Kodama M (1992) Porous polyurethane vascular prostheses with variable compliances. *J. Biomed. Mater. Res.* 26: 1489-1502.

# POLY (ACRYLAMIDES) CONTAINING SUGAR RESIDUES :SYNTHESIS, CHARACTERIZATION AND CELL COMPATIBILITY STUDIES.

Raman Bahulekar, Junko Kano and Makoto Kodama\*

National Institute for Advanced Interdisciplinary Research, Bionic Design Group, 1-1-4 Higashi, Tsukuba-shi, Ibaraki 305.

## ABSTRACT

Hydrophilic poly (acrylamide) compounds having simple mono saccharides (such as glucose and galactose) as pendent groups were synthesized. Cell culture polystyrene plates were coated with these polymers. A distinct transition for water contact angle from higher to a lower value was noted for coated plates. FTIR-ATR of coated plates showed a characteristic band at  $1653\text{ cm}^{-1}$ ,  $1706\text{ cm}^{-1}$  and  $1611\text{ cm}^{-1}$  due to amide carbonyl for native, glucose and galactose poly (acrylamides) respectively. The XPS spectra of cell culture plates coated with native and sugar derivatives of poly (acrylamides) showed peaks around 277, 287 eV(C 1s), 401 eV(N 1s) and 525, 534 eV(O 1s). The growth rate of mouse fibroblast L929 cells was found to be higher on poly (acrylamide) having galactose residues than that of glucose. A high degree of cell aggregation was also observed in case of galactose poly (acrylamides).

**KEYWORDS :** Poly (acrylamides), Sugar residues, Cell attachment, Artificial substrates.

## INTRODUCTION

Recently there has been a lot of activity in glycotechnology field for biomedical applications. One of the major obstacles in understanding the biological recognition processes is the complicated structure of sugars, glycolipids and glycoproteins. It has been realized that the synthetic polymers bearing sugar residues recognize cells through the marker molecules present on cell surface. Such polymers also offer good surface for cell attachment and proliferation.

The synthetic approach to fabricate the polymers having simple sugar residues may provide an easy solution to understand the complicated phenomena of biological recognition processes. we report here the synthesis, characterization and cell adhesion abilities of poly (acrylamides) having simple sugar residues such as glucose and galactose.

## METHODS

The polymers were generated by first polymerizing acryloyl chloride to form poly (acryloyl chloride) in dry 1,4-dioxane. The amino sugars in alkaline medium are then reacted with poly (acryloyl chloride) solution (Scheme 1). The resulting solution is diluted with ethanol and poured into acetonitrile to precipitate the polymers. The polymers were purified by repeated dissolution and precipitation (3 times) and finally freeze-dried from aqueous solution.

Aqueous solution of these polymers was contacted with cell culture polystyrene plates. The plates were thoroughly dried under vacuum at room temperature. The polymer coating was confirmed by surface characterization techniques such as FTIR-ATR, ESCA and contact angle measurements.

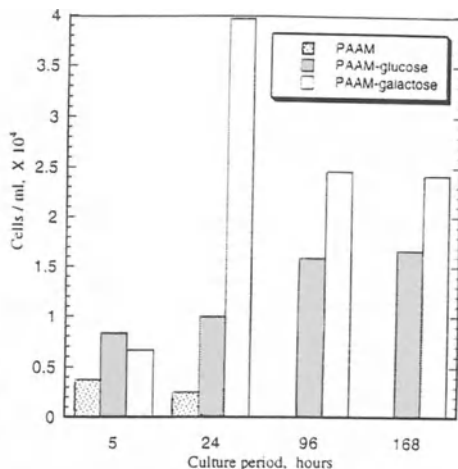
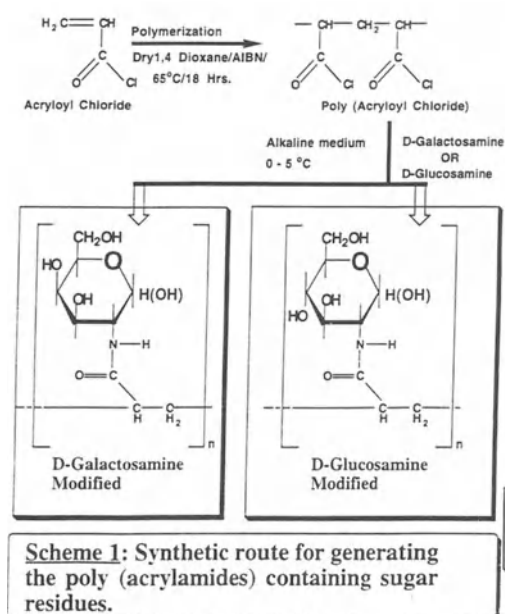


**Figure 1:** L929 cell growth pattern on poly (acrylamide) and its sugar derivatives.

Standard procedures were followed in cell culture experiment with pure mouse fibroblast L929 cell line (RIKEN cell bank). Poly (acryl amide) was used as control.

## RESULTS AND DISCUSSION

Two poly (acryl amide) derivatives bearing glucose and galactose sugar moieties were synthesized. The two sugar residues chosen are isomers of each other. These poly (acryl amide)-sugar derivatives are hydrophilic and miscible with water in all proportion. The aqueous 1 % (w/v) solution was used to coat the cell culture polystyrene plates. Polymer layer was adsorbed strongly on to cell culture polystyrene plates. The polymer coating was found to be quite stable under surface characterization and cell culture experimental condition. The water contact angle was remarkably decreased after coating. Polystyrene plate has contact angle of  $71.8^\circ$ . Poly (acryl amide) coated plate showed contact angle of  $24.3^\circ$ . In case of polymers containing sugar residues the contact angle was observed to be too low (below  $20^\circ$ ). FTIR-ATR of coated plates showed band at  $1653\text{ cm}^{-1}$ ,  $1706\text{ cm}^{-1}$  and  $1611\text{ cm}^{-1}$  due to amide carbonyl for native, glucose and galactose poly (acryl amides) respectively. XPS spectra of coated polystyrene plates showed N 1s peak in 401- 403 eV region, besides C 1s and O 1s peaks. These results indicate the firm coating of poly (acryl amide) and its sugar derivatives.

Cell proliferation results (Figure 1) shows that there is remarkable cell attachment in case of poly (acryl amide) having glucose and galactose residues. A marginal difference in cell growth rate was noted for initial period of 5 hours for two PAAm-sugar derivatives. The overall rate of cell growth was found to be highest in case of PAAm-galactose and a high degree of cell aggregation & cell deformation was observed in case of poly (acryl amide) bearing galactose residue. PAAm-galactose seems to favor the L929 attachment and growth as compared to PAAm- glucose.

# Molecular Design of Artificial Lectin; Recognition and Killer Cell Induction of Lymphocytes by a Novel Water Soluble Polymer Having Phenylboronic Acid Moiety

Hiroaki Miyazaki<sup>1</sup>, Kazunori Kataoka<sup>1</sup>, Teruo Okano<sup>2</sup>, Yasuhisa Sakurai<sup>2</sup>,

1.Department of Materials Science, and Research Institute for Biosciences, Science University of Tokyo, 2641 Yamazaki, Noda-shi, Chiba 278, Japan

2.Institute of Biomedical Engineering, Tokyo Women's Medical College, 8-1 Kawadacho, Shinjuku-ku, Tokyo 162, Japan

## SUMMARY

To design of synthetic polymer with mitogenic property, a novel water-soluble polymer was synthesized by radical copolymerization of 3-acrylamidophenylboronic acid with dimethylacrylamide (poly(DMAA-co-PBA)). Since boronic acid moiety has an affinity for vicinal diol compounds, boronic acid was introduced as recognition site of sugar residues existing on the plasma membrane surface of lymphocyte. Interaction of phenylboronic acid with cell was confirmed through <sup>11</sup>B-NMR. Then, proliferative response of mouse lymphocytes was evaluated by the incorporation of <sup>3</sup>H-thymidine. Boronate-containing polymer with higher molecular weight induced higher proliferation of lymphocytes, and significant proliferation was achieved in the presence of polymers with Mw 300,000(DB30). Moreover, Killer cell activity was estimated by Cr<sup>51</sup>-release assay. In the presence of boronate-containing polymer, Cytolysis of YAC-1 was increased similar to, typical killer cell inducer, PHA lectin. Further, significant acceleration in lymphocyte proliferation was found in the presence of both IL-2 and boronate-containing polymer.

**KEYWORD:** phenylboronic acid, mitogen, adoptive immunotherapy, lymphocyte proliferation, killer cell, IL-2

## INTRODUCTION

Lymphocytes with tumoricidal activity have received special impetus for adoptive immunotherapy of several cancers. Activation and proliferation of tumoricidal lymphocytes can be achieved by treating with so-called mitogens. Most well-known mitogen is lectin. However, lectin has serious immunogenic properties, and its stability is not always adequate for various applications. These problems might be solved through the development of a synthetic polymer with lectin-like function. It is known that lectins contain at least two recognition sites toward sugar chains and lectins need the multivalent binding per molecule for lymphocyte activation. This binding of lectin induce the crosslinking of glycoproteins, inducing the change in the intracellular metabolism. To prepare artificial lectin, we designed a synthetic polymer having multiple binding site for sugar residues along a polymer chain. We focused on phenylboronic acids as binding sites to the sugar residues. It is known that boronic acids can easily form reversible covalent bonds with polyol compounds. In this study, we synthesized a novel water-soluble polymer having phenylboronic acid moiety. This boron-containing polymer exhibited to induce proliferative response of lymphocytes as well as induction of killer cells.

## METHODS

Polymer synthesis: Radical copolymerization of dimethylacrylamide with AAPBA (3-acrylamidophenylboronic acid) was carried out to obtain polymer samples with varying content of AAPBA by changing feed ratio of AAPBA content or solvent. Molecular weight of the polymer



samples was determined by static light scattering. The structure of the obtained polymers was confirmed by  $^1\text{H-NMR}$  and UV spectroscopy. Evaluation of lymphocyte proliferation: Mouse lymphocytes were suspended in 25mM HEPES-buffered-RPMI1640 medium supplemented with 10 % of FCS (pH 7.4) at  $2 \times 10^6$  cells/ml. Lymphocytes were incubated at 37 °C for 48 h in a humidified atmosphere of 5 %  $\text{CO}_2$  in air.  $^3\text{H-thymidine}$  was added to the culture dish at 45 h cultivation. After 3 h, incorporated radioactivity was measured using a Liquid Scintillation Counter.

Evaluation of induction of killer cell: Cytotoxic activity was determined by  $^{51}\text{Cr}$  release assay. YAC-1 was used as target cell.

## RESULTS AND DISCUSSION

To estimate interaction between phenylboronic acid and carbohydrate on the cell membrane, binding constant between propionamidophenylboronic acid and several carbohydrate compounds was estimated by  $^{11}\text{B-NMR}$ . Phenylboronic acid showed binding with sugars including glucose and galactose, sialic acid in phosphate buffered saline at pH 7.4. Especially, The peak of boronate / polyol complex in the propionamidophenylboronic acid with lymphocytes was confirmed through  $^{11}\text{B-NMR}$ . These results indicated that phenylboronic acid moiety in the boronate-containing polymer preferably binds sugar residues in the cell surface and induces proliferative signal in lymphocytes.

Then, proliferative response of lymphocytes by the addition of boronate-containing polymer(DB) was evaluated. Proliferation of lymphocytes was determined by the uptake of  $^3\text{H-thymidine}$  after 48 h cultivation. Dose dependent increase of  $^3\text{H-thymidine}$  uptake was observed in the presence of DB copolymer, while little proliferative response of lymphocytes was observed in the presence of homopolymer. It is considered that the binding of boronic acid residues in the polymer to glycoproteins on the plasma membrane of lymphocytes induced the proliferative response of lymphocytes. The effects of molecular weight and PBA content on the proliferation of murine lymphocytes were thoroughly investigated. Polymer with higher molecular weight induced higher proliferation of lymphocytes, allowing to achieve significant proliferation in the presence of copolymers with Mw 300,000(DB30).

Worthy to mention is the induction of killer cells by DB copolymers. Higher cytotoxicity of target cell was observed when lymphocytes were cocultured with DB copolymer than with polydimethylacrylamide for 120 h. These results suggest that DB copolymer provides an inductive signal to the cytotoxic cells inducing killer cell activity.

In conclusion, polymer containing phenylboronic acid portions were confirmed to work as an artificial lectin. This thoroughly synthetic polymer having sugar recognition sites like lectin successfully induces the proliferative response of lymphocytes, suggesting the promising future to apply to artificial Biological Response Modifier (BRM).

## REFERENCES

- 1)H.Miyazaki, A.Kikuchi, S.Kitano, Y.Koyama, T.Okano, Y.Sakurai, K.Kataoka, Molecular design of artificial lectin: Recognition and proliferation of lymphocytes by a novel water soluble polymer having phenylboronic acid moiety, Proceedings of the First International Conference on Intelligent Materials Eds., T. Takagi, K. Takahashi, M. Aizawa, S. Miyata, Technomic Lancaster, 1993, 481-484, 108
- 2)H.Miyazaki, A.Kikuchi, S.Kitano, K.Kataoka, Y.Koyama, T.Okano, Y.Sakurai, Boronate containing polymer as novel mitogen for lymphocytes, Biochem. Biophys. Res. Comm., 1993, 195, 829-836
- 3)H.Miyazaki, K.Kataoka, Y.Koyama, T.Okano, Y.Sakurai, Water soluble polymer having phenylboronic acid moieties as synthetic mitogen, Jap. J. Artif. Organs, 1994, 23, 3, 978-981

# SELECTIVE ADHESION AND SPONTANEOUS FUSION OF PLATELETS ON POLYION COMPLEX COMPOSED OF PHOSPHOLIPID POLYMERS

Kazuhiro Ishihara, Hikaru Inoue\*, Kimio Kurita\*, Nobuo Nakabayashi

Institute for Medical and Dental Engineering, Tokyo Medical and Dental University, 2-3-10, Kanda-surugadai, Chiyoda-ku, Tokyo 101, Japan

\*Department of Industrial Chemistry, School of Science and Technology, Nihon University, 1-8-14, Kanda, Chiyoda-ku, Tokyo 101, Japan.

## ABSTRACT

To investigate the effect of electrical charges in polymer with phospholipid polar group on the interactions between blood cell and polymer, cell adhesion on 2-methacryloyloxyethyl phosphorylcholine(MPC) polymer having various charges was examined. Blood cells did not adhere on the MPC polymers even they have charges. However, polyion complex(PIC) composed of anionic and cationic MPC polymers could adhere platelet selectively by contact with whole blood. This phenomenon was due to specific composition of albumin and fibrinogen adsorbed on the PIC. Moreover, adherent platelets on the PIC fused each other spontaneously.

**KEY WORDS** : Phospholipid polymer, Blood cell, Protein adsorption, Polyion complex, Platelet adhesion, Cell fusion, Nonthrombogenicity

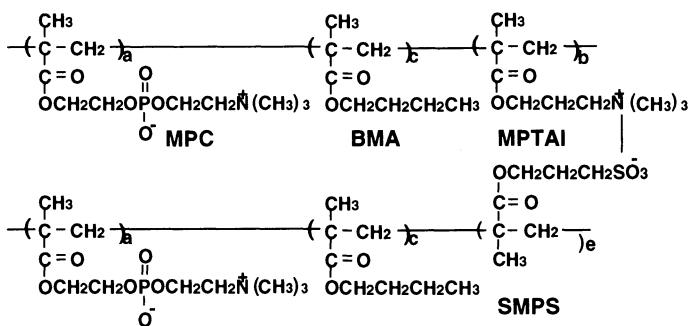
## INTRODUCTION

We have synthesized phospholipid polymers as a novel biocompatible polymer and examined its blood compatibility[1]. The copolymers of 2-methacryloyloxyethyl phosphorylcholine(MPC) and hydrophobic monomers, particularly *n*-butyl methacrylate(BMA) showed nonthrombogenicity, that is, suppression of platelet adhesion, activation, and aggregation when the copolymers contacted human whole blood, even in the absence of an anticoagulant[2]. Moreover, adsorption of plasma proteins was reduced on the MPC polymer surface from human plasma[3]. We became interested in the electrically charged MPC polymers and attempted to prepare new types of functional polymers which show selective adhesion of the cell. In this report, the interactions between blood components and the MPC copolymer with various electrical charges and the polyion complex(PIC)s prepared from anionic and cationic MPC copolymers were investigated[4].

## MATERIALS AND METHOD

MPC and BMA, one of the charged monomers, that is, sodium 3-methacryloyloxypropyl sulfonate (SMPS) or 3-(methacryloyloxypropyl)trimethyl ammonium iodide (MPTAI) were

polymerized in ethanol[4]. The poly(BMA) membrane was immersed in the 1.0 wt% ethanol solutions containing these polymers and dried to coat PIC on the surface. Citrated platelet-rich plasma(PRP) was obtained from rabbit. The poly(BMA) membrane coated with the MPC polymer or the PIC in a disk shape were placed in the 24-well tissue culture plate. A phosphate-buffered



solution (PBS, pH 7.4) was allowed to stand in the wells for a day to equilibrate the surface. Whole blood or PRP were poured into each well for a given period. The membrane was rinsed three times with PBS and the blood components adherent to the membrane were fixed with glutaraldehyde. The surface of the membrane was observed using a scanning electron microscope (SEM).

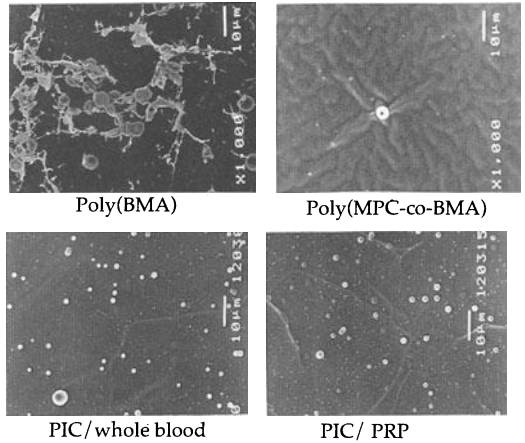


Fig. 1 SEMs of polymer surfaces after contact with blood

## RESULTS AND DISCUSSION

### Cell adhesion from whole blood or PRP

Fig.1 shows SEMs of the membrane surface after contact with rabbit whole blood for 60 min. Cells adhered and a fibrin network formed on the surface of the original poly(BMA) membrane. However, less cell adhesion and no fibrin deposition could be

observed on the membrane coated with any of the MPC copolymers. In the case of the PIC, few red blood cells adhered but many platelets were found on the surface. The adherent platelets on the PIC maintained a discoid shape, that is, their original shape. On the poly(BMA) membrane, a large amount of adsorbed protein and some aggregates were observed which was determined by a gold-colloid labeled immunoassay. A few proteins were adsorbed on the MPC polymers. On the other hand, greater amount of albumin were adsorbed on the surface but less  $\gamma$ -globulin and fibrinogen could be found on the PIC surface. To estimate the activity of platelets attached to a polymer surface, the amount of remaining adenosin triphosphate (ATP) in the platelet was determined. Although the amounts of ATP in platelets adhered to poly(BMA) were quite low, though on both poly(MPC-co-BMA) and PIC were maintained at a higher level than in PRP. Thus, platelets adhered to the PIC did not induce drastic changes in their shape and activity.

### Spontaneous fusion of adherent platelets on PIC

It could found dramatically phenomena of the platelets adhered on the PIC surface, that is, spontaneous fusion. Fig. 2 demonstrates that phenomena. The PRP was contact with PIC for more than 60 min. The fused platelets did not change in the their shape. Though the reason of this phenomena is not known yet, it is first report to show the fusion of platelets without deformation and activation.

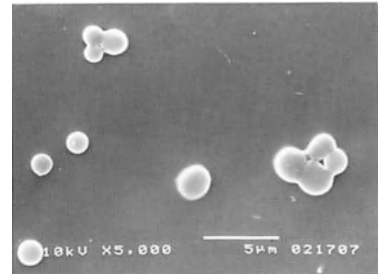


Fig. 2. SEM of fused platelets adhered on PIC.

## REFERENCES

- [1] Ishihara K, Ueda T, Nakabayashi N (1990) *Preparation of Phospholipid Polymers and Their Properties as Hydrogel Membrane. Polym J* **22** : 355
- [2] Ishihara K, Oshida H, Ueda T, Endo Y, Watanabe A, Nakabayashi N (1992) *Hemocompatibility of Human Whole Blood on Polymers with a Phospholipid Polar Group and Its Mechanism, J Biomed Mater Res* **26** : 1543
- [3] Ishihara K, Ziats N P, Tierney B P, Nakabayashi N, Anderson J M (1991) *Protein Adsorption from Human Plasma is Reduced on Phospholipid Polymer. J Biomed Mater Res* **25** : 397
- [4] Ishihara K, Inoue H, Kurita K, Nakabayashi N (1994) *Selective Adhesion of Platelet on a Polyion Complex Composed of the Phospholipid Polymers with Sulfonate Group and Quarternary Ammonium Group. J Biomed Mater Res* **28** :1345

# THERMO-RESPONSIVE POLYMER SURFACES FOR CELL CULTURE: ANALYSIS OF THE SURFACES AND CONTROL OF THE CELL ATTACHMENT / DETACHMENT

HIDEAKI SAKAI, YASUHIRO DOI, TERUO OKANO<sup>a)</sup>, NORIKO YAMADA<sup>a)</sup> and YASUHISA SAKURAI<sup>a)</sup>

Wakayama Research Laboratories, KAO Corporation, 1334 Minato, Wakayama-shi, Wakayama 640, Japan. <sup>a)</sup> Institute of Biomedical Engineering, Tokyo Women's Medical College, 8-1 Kawada-cho, Shinjuku-ku, Tokyo 162, Japan.

## SUMMARY

Poly(N-isopropylacrylamide)(PIPAAM) has been applied to thermal on-off switching polymers for drug release[1]. We have reported that, when PIPAAm is grafted on the surface of a cell culture dish, the cells cultured on the dish can easily be detached at a temperature lower than the LCST of PIPAAm without any help of trypsin *etc.*[2]. In this study, the grafted surface was characterized and the cell attachment / detachment behavior of the grafted dishes was discussed. The grafted surface changed from hydrophobic(37°C) to hydrophilic(15°C) and the degree of these changes was able to be controlled by the amount of grafted PIPAAm. Bovine endothelial cells could adhere on the grafted surfaces whose PIPAAm graft level were below  $2.2 \mu\text{g}/\text{cm}^2$  at 37°C and could detach from the grafted dishes whose graft level were over  $0.8 \mu\text{g}/\text{cm}^2$  at 15°C. It was concluded that the PIPAAm grafted dishes whose graft level were  $0.8 \sim 2.2 \mu\text{g}/\text{cm}^2$  were good for cell attachment / detachment behavior. **KEYWORDS:** poly(N-isopropylacrylamide), grafted substrate, cell culture, cell attachment, non-enzymatic cell detachment

## METHODS

Preparation of PIPAAm grafted dishes: A 0.07 ml of IPAAm solution (20-60 wt%) in isopropyl alcohol (IPA) was added to a tissue culture polystyrene dish (Falcon 3002: referred to as control dish), followed by the irradiation by 0.25 MGy electron beam (190 kV) using an Area Beam Electron Processing System (Nissin-High Voltage, Japan) (DISH (IPAAm 20 - 60)). The PIPAAm grafted dishes were rinsed with cold water to remove nongrafted PIPAAm, dried under nitrogen gas and gas-sterilized by ethylene oxide before use in cell culture experiments.

Analyses of PIPAAm grafted surfaces: The amount of the grafted PIPAAm on the each surface was estimated by FT-IR-ATR method using a JIR-RFX3002 (JEOL, Japan). And contact angle of the each surface was determined by a drop method using a Face Contact Angle Meter CA-D (Kyowa Surface Chemistry, Japan) at 15°C and 37°C.

Cell culture / detachment: Bovine aorta endothelial cells were cultured at 37°C in 5% CO<sub>2</sub>, using a DMEM containing 10% FCS on the PIPAAm grafted and control dishes. After cultivation the dishes were cooled to 10°C for 30 min. without changes of medium to detach the cells.

## RESULTS AND DISCUSSION

PIPAAM could be grafted uniformly onto tissue culture polystyrene dishes by irradiation using an

electron beam. Table 1 shows the amounts of the grafted PIPAAm on these dishes determined by FT-IR-ATR method and the contact angles at 37°C and at 15°C. Each amount of grafted PIPAAm was below 3.0  $\mu\text{g}/\text{cm}^2$  and was increased with increasing monomer concentration.  $\cos \theta$  ( $\theta$ : contact angle) of the PIPAAm grafted dishes was increased with increasing the amount of the grafted PIPAAm and was increased with decreasing the temperature from 37°C to 15°C. On the other hand, contact angle of the control dish was not changed, even if it was cooled. These results reveal that the surface of the PIPAAm grafted dishes changes from hydrophobic(37°C) to hydrophilic(15°C) and the degree of these changes is able to be controlled by the amount of grafted PIPAAm.

Bovine endothelial cells were cultured both in the grafted dishes and a control dish (Table 2). As for the grafted dishes whose  $\cos \theta$  were below 0.72 (DISH(IPAAm-40)), the degree of adhesion of the endothelial cells (37°C) was almost the same as that of the control dish. In the DISH(IPAAm-60) whose  $\cos \theta$  was 0.75, however, endothelial cells did not adhere. The detachment of the cultured cells from the PIPAAm grafted dishes whose  $\cos \theta$  were over 0.77 was observed at 15°C. On the other hand, grafted dishes whose  $\cos \theta$  was below 0.62 or a control dish, the cultured cells did not detach by low temperature treatment.

Table 1 Amount of grafted PIPAAm and contact angle of the surface of grafted dishes at 37°C and at 15°C

code	graft level ( $\mu\text{g}/\text{cm}^2$ )	$\cos \theta$ ( $\theta$ : contact angle)		
		37°C	15°C	$\Delta(15^\circ\text{C}-37^\circ\text{C})$
control	0	0.56	0.56	0
DISH(IPAAm-20)	0.5	0.56	0.62	+0.06
DISH(IPAAm-30)	0.8	0.67	0.77	+0.10
DISH(IPAAm-40)	1.4	0.72	0.83	+0.11
DISH(IPAAm-50)	2.2	0.73	0.87	+0.14
DISH(IPAAm-60)	3.0	0.75	0.93	+0.18

Table 2 Cell adhesion and growth on PIPAAm grafted dishes, and cell detachment by low temperature treatment (BAE cells)

code	cell attachment growth detachment		
	(37°C)		(15°C)
control	±	±	no detachment
DISH(IPAAm-20)	±	±	no detachment
DISH(IPAAm-30)	±	±	+
DISH(IPAAm-40)	±	±	++
DISH(IPAAm-50)	-	-	++
DISH(IPAAm-60)	no adhesion	ND	ND

In conclusion, an even infinitesimal amount of grafted PIPAAm can cause the hydrophobic surface to change the hydrophilic one, and the switching of this changes is effective to control the cell attachment / detachment behavior. On the other hand, the detachment of cultured cells was partially inhibited by sodium azide treatment, suggesting that cell metabolism directly affects cell detachment[3]. Therefore mechanism of cell detachment from the PIPAAm grafted surface should be studied in connection with not only the remarkable hydration of PIPAAm grafted surface but also the active cell morphological changes.

## REFERENCES

- [1] Okano T, Bae YH, Jacobs H, Kim SW (1990) Thermally on-off switching polymers for drug permeation and release. *J. Controlled Release* 11:255-265
- [2] Okano T, Yamada N, Sakai H, Sakurai Y (1993) A novel recovery system for cultured cells using plasma-treated polystyrene dishes grafted with poly(N-isopropylacrylamide). *J. Biomedical Materials Research* 27:1243-1251
- [3] Okano T, Yamada N, Okuhara M, Sakai H, Sakurai Y (1993) Alternately of Detachment from Temperature Modulated, Hydrophilic-Hydrophobic Polymer Surfaces. *Biomaterials*, submitted

# RGDS-CARRYING LATEX PARTICLES FOR CELL ACTIVATION AND INTEGRIN SEPARATION

Yuji Kasuya, Yukio Inomata, Hideki Gakumazawa, Keiji Fujimoto and Haruma Kawaguchi

Department of Applied Chemistry, Faculty of Science & Technology, Keio University  
3-14-1 Hiyoshi, Kohoku-ku, Yokohama 223 Japan

## ABSTRACT

RGDS-carrying affinity latex particles were used for cell activation through RGD-integrin interaction and for integrin separation/purification from platelet membrane extract. The effects of particle composing material, spacers and reaction conditions on the activation and purification were studied in detail.

**KEY WORDS :** affinity latex, RGDS, integrin, bioseparation, spacer

## Introduction

Cell adhesive tetra-peptide RGDS was immobilized on latex particles. They were used for two purposes. One is for cell activation via integrin / RGDS binding. The other is for integrin purification from cell membrane extracts. The effects of the mode of RGDS immobilization and of the surface chemistry of particles on cell activation and integrin purification were studied.

## Methods

### Preparation of RGDS-carrying particles

Styrene-acrylamide (SA) and styrene-glycidyl methacrylate (SG) copolymer latex particles were prepared soap-free emulsion polymerization. Acrylamide-methacrylic acid (AM) copolymer hydrogel particles were prepared by precipitation polymerization. Carboxyl or amino groups were introduced on the surface of SA particles. To these particles, cell adhesive peptide RGDS was immobilized directly or via spacer (ethyleneglycol diglycidyl ether, EGDE, or oligoglycine). The amount and composition of immobilized RGDS were determined by amino acid analysis.

### Activation of leukocytes by RGDS-carrying particles

The extent of activation of leukocytes or neutrophil-like HL60 by RGDS-carrying particles was determined by the amount of oxygen consumption or active oxygen production by the cells on contact with RGDS-carrying particles. The oxygen and active oxygen were measured

with an oxygen electrode and by chemiluminescence, respectively.

#### Purification of receptor

RGDS-carrying particles were mixed with octylglucoside extracts of human platelet at 4°C for 60 min. The particles were separated from the supernatant and soaked in a buffer containing 1 mg/ml GRGDS for 1 hr to desorb the receptor from the particle surface. The molecular weight of the purified proteins was determined by SDS-PAGE. The proteins were identified by Western blotting.

### Results and Discussion

#### Activation of cells

The extent of cell activation by RGDS-carrying particles significantly depended on the kind of the carrier particles (Fig.1). Cationic SA particles carrying RGDS forced the neutrophil-like cells to produce the largest amount of active oxygen, that is, gave the strongest stimulus to the cells. Similar results were obtained when the amount of oxygen consumption was measured in different particles systems<sup>1)</sup>. The cell-activation efficiency of immobilized RGDS itself is assessed from the length of the solid bar relative to those of the open or slashed bars in each system in Fig. 1. The difference in the activation efficiency between RGDSs on cationic and anionic SA particles was attributed to the electrostatic interaction between the particle and cell, and RGDS immobilization mode. When RGDS<sub>n</sub> (n=2 or 4) was immobilized on cationic SA particles, a spacer effect contributed to the more effective expression of the RGD function.

#### Purification of receptor

RGDS-carrying SA particles and SG particles were used for the purification of receptor proteins from octylglucoside extracts of human platelet. The purified protein was identified to be the receptor GP IIb / IIIa. The molecular weights of proteins purified under reducing or nonreducing conditions were 116 / 118 kD or 90 / 133 kD, respectively. The affinity between RGDS on particles and receptor molecules depended on the divalent cations and temperature. Between two kinds of particles mentioned above, GRGDS-carrying SG particles were better at purifying the receptor with less contamination. Spacer EGDE was a necessary component in this separator system.

(1) Kasuya, Y., et al. *Biomaterials*, 15, 570 (1994)

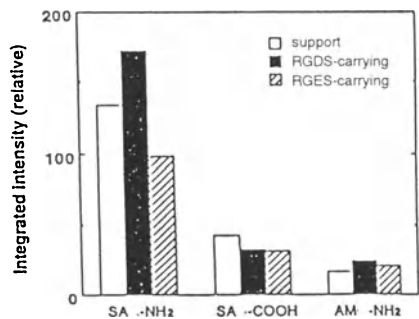


Fig.1 Comparison of production of reactive oxygen by neutrophil-like cells among three kinds of microsphere systems. Data are indicated by relative values to that in the non-coated PST dish system after 30 min.

# ESTIMATION OF THE SECONDARY STRUCTURE OF FIBRONECTIN ADSORBED TO POLYSTYRENE AND DEPROTECTED POLY( $\epsilon$ -N-BENZYLOXYCARBONYL-L-LYSINE) BY FTIR ATR SPECTROSCOPY

Kohei Kugo, Ken Matsutani, and Jun Nishino

Department of Applied Chemistry, Faculty of Science, Konan University, Okamoto 8-9-1, Higashinada-ku, Kobe 658, JAPAN

## ABSTRACT

The secondary structure of fibronectin (FN) adsorbed to polymer surfaces were investigated in a quantitative manner using Fourier transform infrared attenuated total reflectance (FTIR ATR) techniques. Polystyrene (PSt), poly( $\epsilon$ -N-benzyloxycarbonyl-L-lysine) (PBCL), and 10 mol% deprotected PBCL (CL10) were used as polymer substrates. The conformation of adsorbed FN was substrate dependent even though the comparable amount of FN adsorbed. The contents of the  $\beta$ -structure,  $\alpha$ -helix, and random coil structure of FN on PSt at 10 min after the injection were 61%, 22%, and 17%, respectively. The  $\beta$ -structure content increased gradually and reached ca.70% after 180 min. In the case of CL10, the content of the  $\beta$ -structure,  $\alpha$ -helix, and random coil structure at 10 min were 47%, 43%, and 10%, respectively. The  $\beta$ -structure content increased as well as PSt and reached 65% after 180 min, while the  $\alpha$ -helical content decreased to 26%. Deconvolved infrared spectra in the amide II region showed that the  $\beta$ -structure content in FN increased upon adsorption to PSt and CL10, but the secondary structure content changed depending on polymers.

**KEY WORDS** : secondary structure, fibronectin, FTIR ATR, polystyrene, poly( $\epsilon$ -N-benzyloxycarbonyl-L-lysine)

## INTRODUCTION

Fibronectin (FN) is a multifunctional glycoprotein with a molecular weight of 440,000 Da consisting of two subunits linked by disulfide bond. It binds to collagen, glycosaminoglycans, cells, platelets, fibrin, and bacterial cell walls. However, several reports suggest that cellular behavior is substrate dependent even in the surface saturating level of adsorbed FN[1,2]. It can be assumed that surface characteristics of the substrate influence the secondary structure of adsorbed FN molecules, and limiting the specific receptor-ligand interaction and the organization of extra cellular matrix. In this study, FN adsorbed to polymer surfaces was monitored *in situ* by Fourier transform infrared attenuated total reflectance (FTIR ATR) spectroscopy. Curve analysis was carried out to examine the conformational change of adsorbed FN.

## MATERIALS AND METHODS

Polystyrene (PSt), poly( $\epsilon$ -N-benzyloxycarbonyl-L-lysine) (PBCL), and 10 mol% deprotected PBCL (CL10) which was kindly supplied by Dr. Maruyama A. of Tokyo Institute of Technology were used. FTIR spectra of FN adsorbed to thin polymer films were obtained on a Nicolet 20DXB and Magna 750 FTIR spectrometer equipped with the Contact Sampler (Spectra Tech Inc.) using a horizontal flat ZnSe (45° facecut angle) ATR crystal. The horizontal ATR cell, specially designed to monitor protein adsorption spectrally *in situ*, was thermostated using circulating water at 37 °C. PSt, PBCL, and CL10 films were spin cast onto the ZnSe 45° crystal, and dried *in vacuo* at 60 °C for at least 90 min. All spectra were collected by co-adding 200 scans at 4 cm<sup>-1</sup> resolution with Happ-Genzel apodization with a broad band pass HgCdTe



(MCT) detector. Curve analysis including Fourier self-deconvolution and the band fitting was carried out in the amide II region by the program FOCAS (Nicolet Analytical Instruments)[3].

## RESULTS AND DISCUSSION

FTIR ATR spectra of FN adsorbed to PSt and a ZnSe ATR crystal surfaces were obtained at 0, 10, 20, 60, 120, 180 min after the initial injection of a FN solution into the horizontal ATR cell. The amide I and amide II bands were observed in each spectrum around  $1650\text{ cm}^{-1}$  and  $1550\text{ cm}^{-1}$ , respectively. Curve analysis was applied to the amide II band of FN, because the intensity of the amide I band is more subjected to the water subtraction process. From the results on the curve analysis, the individual calculated components were assigned to parallel-chain pleated sheet ( $1551\text{ cm}^{-1}$ ),  $\alpha$ -helix ( $1545\text{ cm}^{-1}$ ), random coil ( $1536\text{ cm}^{-1}$ ), parallel- and antiparallel-chain pleated sheet ( $1530\text{ cm}^{-1}$ ), and  $\alpha$ -helix ( $1517\text{ cm}^{-1}$ )[3]. For each spectra, the areas of the resolved components associated with  $\alpha$ -helix,  $\beta$ -structure, and random coil structure were obtained as fraction of the total amide II area. Fig.1 shows the changes of the fraction for each structure, that is, the secondary structure content of FN adsorbed to (a) PSt and (b) CL10 surfaces. As shown in Fig.1 (a), the contents of the  $\beta$ -structure,  $\alpha$ -helix, and random coil structure at 10 min after the injection were 61%, 22%, and 17%, respectively. The  $\beta$ -structure content increased slowly and reached ca.70% after 180 min. The random coil structure content, on the contrary, decreased gradually to 8%. In the case of CL10, the content of the  $\beta$ -structure,  $\alpha$ -helix, and random coil structure at 10 min after the injection were 47%, 43%, and 10%, respectively. The  $\beta$ -structure content increased as well as PSt and reached 65% after 180 min. The  $\alpha$ -helical content decreased to 26%, while the content of random coil structure was almost constant at ca.10%. Cooper *et al.* [4] in their investigation on adsorption of FN to polyurethane surfaces using FTIR showed qualitatively that the amount of  $\beta$ -structure in FN increased upon adsorption to all polymers, based on the changes in the amide I and the amide III region of adsorbed FN.[4] We have shown in a quantitative manner by means of deconvolved ir spectra in the amide II region that the  $\beta$ -structure content in FN increased upon adsorption to PSt and CL10, but the secondary structure content changed depending on polymers.

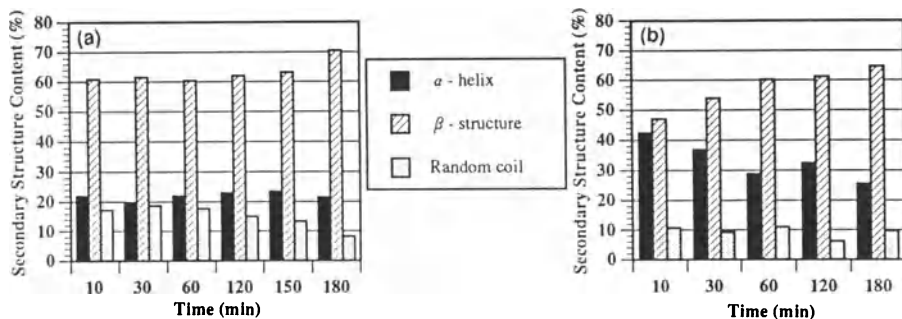


Fig.1 Variation of secondary structure content of FN adsorbed to (a) PSt and (b) CL10 surfaces.

## References

- Lewandowska K, Balachander N, Sukenik CN, Culp LA. (1989) Modulation of fibronectin adhesive functions for fibroblasts and neural cells by chemically derivatized substrata. *J Cell Physiol* 141: 334-345
- Schakenraad JM, Arends J, Busscher HJ, Dijk F, Van Wachem PB, Wildevuur CRH. (1989) Kinetics of cell spreading on protein precoated substrata. *Biomaterials* 10: 43-50
- Kugo K, Okuno M, Kitayama K, Kitaura T, Nishino J, Ikuta N, Nishio E, Iwatsuki M. (1992) Fourier transform ir attenuated total reflectance study on the secondary structure of poly( $\gamma$ -methyl L-glutamate) surfaces treated with formic acid. *Biopolymers* 32: 197-207
- Pitt WG, Spiegelberg SH, Cooper SL. (1987) Adsorption of fibronectin to polyurethane surfaces: Fourier transform infrared spectroscopic studies. In: Brash JL, Horbett TA (eds) *ACS Symposium Series No.343*. Amer Chem Soc, pp 324-338

# HYBRID BIOMATERIALS COMPRISING DOUBLE-HELICAL DNA. COVALENT COUPLING BETWEEN $\lambda$ PHAGE DNA AND POLY(N-ISOPROPYLACRYLAMIDE)

Mizuo Maeda, Daisuke Umeno, and Makoto Takagi

*Department of Chemical Science and Technology, Kyushu University, Fukuoka 812-81, Japan*

**SUMMARY:** We describe a bioconjugate consisting of DNA and poly(N-isopropylacrylamide). The conjugation relies on a vinyl monomer (**1**) having a psoralen moiety, which is bound covalently to double-helical DNA upon UV-irradiation. The vinyl-derivative of DNA was copolymerized with N-isopropylacrylamide to give the temperature-responsive conjugate, which would be useful for affinity separation of DNA-binding proteins, molecules and ions.

**KEY WORDS:** bioconjugate,  $\lambda$  phage DNA, poly(N-isopropylacrylamide), affinity separation

## INTRODUCTION

Poly(N-isopropylacrylamide) (NIPAAM) is known to show the transition between the coil (soluble) and globule (insoluble) conformations reversibly around 31 °C [1]. Chen *et al.* took advantage of this property for the thermally-induced separation of biomolecules by using a polyNIPAAM-protein conjugate [2]. Takei *et al.* also reported the temperature-responsive bioconjugate from proteins and polyNIPAAM [3]. In contrast, there have been few reports on a polyNIPAAM-conjugate comprising DNA which play important roles as a 'host' in biological affinity reactions. We reported a reversible complex of DNA with polyNIPAAM having DNA-intercalative groups [4]. We also conducted a covalent coupling of polyNIPAAM with DNA by virtue of a vinyl monomer having a psoralen moiety, which can form a photoadduct with DNA double helix [5]. However, in both cases, the efficiency of thermally-induced precipitation was not satisfactory. In the present study, we developed an improved psoralen monomer (**1**) by the use of N,N-bis(3-aminopropyl)methylamine as a spacer between psoralen and vinyl group so that the efficient precipitation was attained.

## MATERIALS AND METHODS

**1** was prepared according to the literature [5], but with using N,N-bis(3-aminopropyl)methylamine instead of ethylenediamine. Photo-reaction of **1** with  $\lambda$  DNA was made by irradiating UV light (ca. 60 mW/cm<sup>2</sup>) on an ice bath for 10 min. The reaction mixture was extracted twice by chloroform-isoamyl alcohol (24:1, v/v) in order to remove **1** which was not covalently bound to DNA. Then NIPAAM, N,N,N',N'-tetramethylethylenediamine, and ammonium peroxydisulfate were successively added into the mixture under nitrogen atmosphere. Polymerization was carried out at 24 °C for 1 h. The mixture was then analyzed by gel electrophoresis (0.5 %-agarose gel at 10 °C and 7 V/cm for 1 h). After electrophoresis, DNA in the gel was stained by ethidium bromide. On the other hand, the mixture just after the polymerization was centrifuged (15000 rpm, 30 min) at 37 °C in order to precipitate the DNA-polyNIPAAM conjugates. The supernatant was collected and subjected to gel electrophoresis. The band due to unprecipitated DNA was evaluated by scanning densitometry. Concentration conditions for the reactions were the same as those described in the literature [5].

## RESULTS AND DISCUSSION

$\lambda$  DNA which had been reacted photochemically with **1** was co-incubated in the polymerization system of NIPAAM. The gel electrophoresis of the product showed retarded migration as well as

broadening of the DNA band (see Fig. 1(a), lanes 3-5). The degree of retardation increased with increasing concentration of **1**. In contrast, as seen in lanes 6-8, the light-induced binding of **1** to  $\lambda$  DNA did not affect the migration in the concentration range examined here. Since the mobility in gel electrophoresis is dependent on size and charge of migrating species, the retardation is ascribed to the increase in size brought about by the modification of DNA with nonionic polyNIPAAM chains. On the other hand, lane 2 where DNA was not reacted with **1** showed no retardation after the polymerization. The vinyl-derivatized DNA incubated in the polymerization system of NIPAAM is thus concluded to be conjugated with polyNIPAAM by means of **1** residues, which had been previously introduced in DNA and then took part in copolymerization with NIPAAM.

Temperature-responsiveness of the present conjugate was evaluated by the centrifugation of the post-polymerization mixture at 37 °C. As seen in Fig. 1(b), almost 100 % of DNA acquired the temperature-responsive property when a comparable molar amount of **1** was used for DNA at the antecedent photo-reaction. Thus the efficiency of themally-induced precipitation was strikingly improved as compared with those values (ca. 50 % max.) in our previous studies [4,5]. This should be ascribed to the longer and more hydrophilic spacer chain of **1**. The present DNA-polyNIPAAM conjugate should be a useful tool for separating DNA-binding proteins, molecules and ions.

This work was supported in part by The Naito Foundation. Financial support by a Grant-in-Aid for Scientific Research from Ministry of Education, Science and Culture of Japan is also acknowledged.

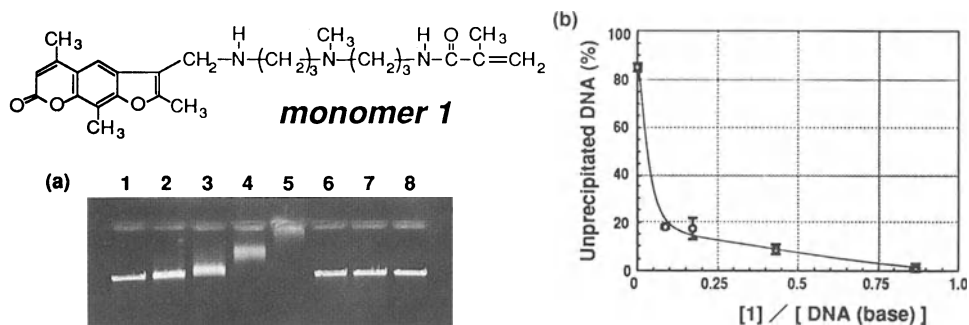


Fig. 1 (a) Gel electrophoresis of DNA-polyNIPAAM conjugates (0.5 % agarose).  $\lambda$  DNA (115  $\mu$  M) was irradiated by UV in the presence of **1** (lanes 3-8). After removing unbound **1**, samples at lanes 2-5 were co-incubated in the polymerization mixture of NIPAAM. Lane 1, DNA alone; lane 2,  $[1] = 0$ ; lane 3 and 6,  $[1] = 0.5 \mu$  M; lane 4 and 7,  $[1] = 2 \mu$  M; lane 5 and 8,  $[1] = 5 \mu$  M. The concentrations of **1** ( $[1]$ ) represent those at the antecedent photochemical reaction. (b) Amount of unprecipitated DNA when centrifuged at 37 °C in percent to the DNA originally added vs. the molar ratio of **1** to DNA (base) at the antecedent photochemical reaction; Average  $\pm$  SEM (n = 3).

## REFERENCES

- [1] Schild HG, Tirrell DA (1990) Microcalorimetric detection of lower critical solution temperatures in aqueous polymer solutions. *J. Phys. Chem.* 30:4352-4356
- [2] Chen JP, Hoffman AS (1990) Polymer-protein conjugate II. Affinity precipitation separation of human immunoglobulin by a poly(N-isopropylacrylamide)-protein A conjugates. *Biomaterials* 11:631-634
- [3] Takei YG, Aoki T, Sanui K, Ogata N, Okano T, Sakurai Y (1993) Temperature-responsive bioconjugates 2. Molecular design for temperature-modulated bioseparations. *Bioconjugate Chem.* 4:341-346
- [4] Maeda M, Nishimura C, Inenaga A, Takagi M (1993) Modification of DNA with poly(N-isopropylacrylamide) for thermally induced affinity separation. *Reactive Polym.* 21:27-35
- [5] Maeda M, Nishimura C, Umeno D, Takagi M (1994) Psoralen-containing vinyl monomer for conjugation of double-helical DNA with vinyl polymers. *Bioconjugate Chem.* 5:527-531

# PREPARATION OF GLUCOSE-SENSITIVE HYDROGELS BY ENTRAPMENT OR COPOLYMERIZATION OF CONCAVALIN A IN A GLUCOSYLOXYETHYL METHACRYLATE HYDROGEL.

Takashi Miyata\*, Atsushi Jikihara, Katsuhiko Nakamae, Tadashi Uragami\*, Allan S. Hoffman\*\*, Keisuke Kinomura\*\*\* and Masakazu Okumura\*\*\*

Faculty of Engineering, Kobe University, Rokko, Nada, Kobe 657 JAPAN, \*Faculty of Engineering, Kansai University, Suita, Osaka 564 JAPAN, \*\*Center for Bioengineering, University of Washington, Seattle, WA 98195 USA, \*\*\*Nippon Fine Chemical Co., Ltd., Takasago 676 JAPAN

## SUMMARY

Two type of glucose-sensitive hydrogels were prepared by entrapment of Concanavalin A (Con.A) in a glucosyloxyethyl methacrylate (GEMA) hydrogel and copolymerization of GEMA and modified Con.A in which double bonds were introduced. The swelling ratio of their hydrogels depended on the glucose concentration. This is due to the fact that glucose results in the dissociation of the complex between pendant glucose of GEMA and Con.A and the crosslinking density in the hydrogels decreases. Con.A leaked from the Con.A-entrapment GEMA hydrogel but didn't from the Con.A-copolymerized GEMA hydrogel. The Con.A-copolymerized GEMA hydrogel showed the reversible swelling changes in response to a step-wise change in glucose concentration.

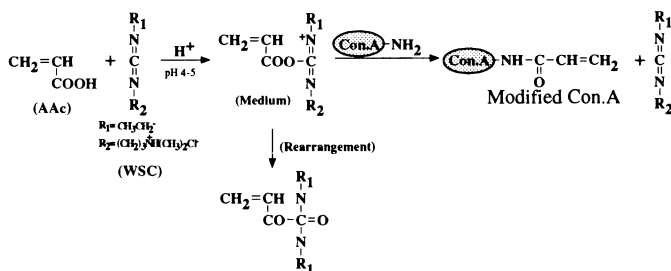
**KEY WORDS:** Hydrogel, Glucose-sensitivity, Polymer with pendant glucose groups, Concanavalin A

## INTRODUCTION

Several investigations have been undertaken for the development of glucose-stimulated, feed-back insulin delivery systems [1-4]. We previously studied the complex formation between Concanavalin A (Con.A) and a polymer with pendant glucose groups (Poly(glucosyloxyethyl methacrylate), poly(GEMA)) in order to design a glucose-sensitive polymer [5]. The previous study revealed that poly(GEMA) forms a complex with Con.A in a buffer solution and the addition of free glucose results in dissociation of the complex. This indicates that the complex between poly(GEMA) and Con.A is a kind of glucose-sensitive material. Such an intelligent material can be used for insulin release stimulated by blood glucose. In the present work, we focus on the binding of Con.A to pendant glucose in GEMA and prepared two type of glucose-sensitive hydrogels by the application of their complex formation and dissociation in response to glucose.

## METHODS

Con.A-entrapment GEMA hydrogel was prepared by the copolymerization of GEMA and *N, N'*-methylene bisacrylamide in the presence of Con.A with ultraviolet light. Con.A-copolymerized GEMA hydrogel was prepared in a similar manner as above, using Con.A in which double bonds were introduced by the carbodiimide technique



Scheme 1 Introduction of double bond into Con.A.

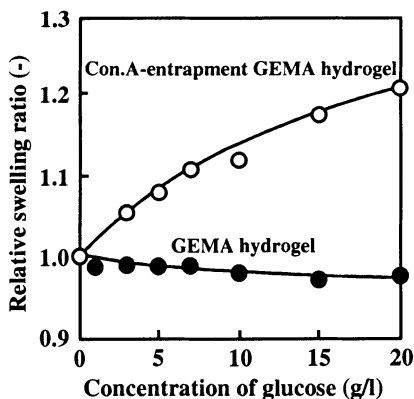


Fig.1 Effect of the glucose concentration in 0.1 M tris HCl buffer solution (pH 7.5) on relative swelling ratio of the Con.A-entrapment GEMA hydrogel (○) and the GEMA hydrogel (●). The concentration of Con.A entrapped in the former hydrogel is 18.8 wt%.

(Scheme 1). Swelling ratio of the hydrogel was determined from the weight of the swollen hydrogel ( $W_s$ ) and dried gel ( $W_d$ ) as follows;

$$\text{Swelling ratio (g/g)} = (W_s - W_d) / W_d$$

## RESULTS AND DISCUSSION

Fig. 1 shows the relationship between the glucose concentration and the relative swelling ratio of the hydrogel in an aqueous glucose solution. Though the swelling ratio of the GEMA hydrogel was constant, the swelling ratio of the Con.A-entrapment GEMA hydrogel increased with the glucose concentration. Such a glucose-sensitive swelling of the Con.A-entrapment GEMA hydrogel is attributed to the dissociation of the complex between poly(GEMA) and Con.A in the presence of glucose (Fig. 2). Furthermore, the swelling ratio of Con.A-entrapment GEMA hydrogel changed by the presence of mannose as well as glucose, but didn't by galactose (Fig.3). This demonstrates that the Con.A-entrapment GEMA hydrogels can recognize the kind of monosaccharide. Therefore, this hydrogel may also be useful to sense different sugars in a solution.

The Con.A-entrapment GEMA hydrogels have a problem that Con.A may leak out of them when they swell in an aqueous solution containing free glucose. The leak of Con.A prevents the hydrogel from reversible swelling changes in response to glucose. Therefore, Con.A must be covalently immobilized within the GEMA hydrogel for the development of a reversibly glucose-sensitive hydrogel. The amount of Con.A leaking out of the Con.A-entrapment GEMA hydrogel and Con.A-copolymerized GEMA hydrogel were measured in an aqueous solution containing glucose. When the Con.A-entrapment GEMA hydrogel swelled in the presence of free glucose, the amount of Con.A leaking out of the hydrogel increased gradually. To the contrary, Con.A did not leak out of the Con.A-copolymerized GEMA hydrogel in spite of the swelling in the presence of free glucose. Consequently, the Con.A-copolymerized GEMA hydrogel shows reversible swelling change in response to the glucose concentration.

## REFERENCES

- 1) Ishihara K, Kobayashi M, Ishimaru N, Shinohara I. (1984) Glucose induced permeation control of insulin through a complex membrane consisting of immobilized glucose oxidase and a poly(amine). *Polym J* 16: 625-631
- 2) Albin G, Horbett TA, Ratner BD. (1985) Glucose sensitive membranes for controlled delivery of insulin: insulin transport studies. *J Controlled Release* 2: 153-164
- 3) Kim SW, Pai CM, Makino K, Seminoff LA, Holmberg DL, Gleeson JM, Wilson DE, Mack EJ. (1990) Self-regulated glycosylated insulin delivery. *J Controlled Release* 11: 193-201
- 4) Kitano S, Koyama Y, Kataoka K, Okano T, Sakurai Y. (1992) A novel drug delivery system utilizing a glucose responsive polymer complex between poly(vinyl alcohol) and poly(N-vinyl-2-pyrrolidone) with a phenylboronic acid moiety. *J Controlled Release* 19: 162-170
- 5) Nakamae K, Miyata T, Jikihara A, Hoffman AS. (1994) Formation of poly(glucosyloxyethyl methacrylate)-Concanavalin A complex and its glucose-sensitivity. *J Biomater Sci Polym Edn* 6: 79-90

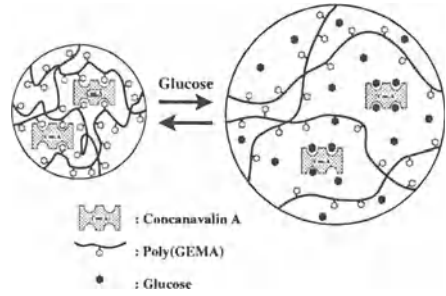


Fig.2 Schematic of glucose-sensitivity of the Con.A-entrapment GEMA hydrogel.

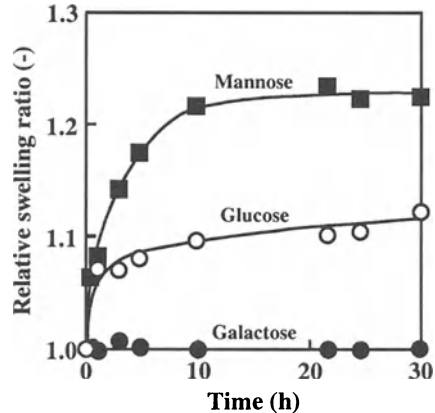


Fig.3. Swelling ratio changes of Con.A-entrapment GEMA hydrogel as a function of time, when the hydrogels were immersed in 0.1 M tris HCl buffer solution (pH 7.5) containing 10g/l of monosaccharide: (○) glucose; (■) mannose; (●) galactose. The concentration of Con.A entrapped in the hydrogel is 18.8 wt%.

# COMPLEXATION OF NEOCARZINOSTATIN CHROMOPHORE WITH A HYDROPHOBIZED POLYSACCHARIDE AS AN APOPROTEIN MODEL

Makiko Kuboyama<sup>†</sup>, Takehiko Ueda<sup>†</sup>, Kazunari Akiyoshi<sup>‡</sup>, and Junzo Sunamoto<sup>†,‡</sup>

<sup>†</sup>Surface Recognition Group, Supermolecules Project, Research Development Corporation of Japan SuperLab.1F-3, Keihanna Plaza, 1-7 Hikaridai, Seikacho, Sourakugun, Kyoto 619-02, Japan

<sup>‡</sup>Division of Synthetic Chemistry & Biological Chemistry, Graduate School of Engineering, Kyoto University, Yoshida-Hommachi, Sakyo-ku, Kyoto 606, Japan

## SUMMARY

Interaction between neocarzinostatin chromophore (NCS-chr) and a self-aggregate of cholesterol-bearing pullulan (CHP) was investigated. NCS-chr was isolated by gel chromatography (solvent: dimethylsulfoxide (DMSO)) after NCS-chr was released from neocarzinostatin (NCS) in DMSO. The amphiphilic CHP nanoparticle bound NCS-chr in the hydrophobic binding site. The chemical stability of the chromophore in water increased upon the complexation.

## KEY WORDS

neocarzinostatin, chromophore, hydrophobized polysaccharide, complexation, dimethylsulfoxide

## INTRODUCTION

Neocarzinostatin (NCS, MW=11,750) is an anticancer drug extracted from *Streptomyces carzinosticus* var. F-41 [1]. NCS is consisted of two components, protein component (apo-NCS, MW=11,090) and non-protein component (NCS-chr, MW=660). X-ray crystallographic studies suggested the NCS-chr should be stabilized through hydrophobic interaction with apo-NCS [2]. The active center of NCS is thought to be NCS-chr, but it is so easily degraded by heat, by UV irradiation, or in higher pH [3]. Therefore, the isolated NCS-chr is hardly applicable as an active reagent. Recently, we have reported that hydrophobized polysaccharides such as cholesterol-bearing pullulan (CHP) form monodisperse nanoparticle by self-assembly in water. The amphiphilic nanoparticle complexed with various hydrophobic compounds and also soluble proteins [4]. In this study, we describe the function of CHP nanoparticle as an artificial apo-NCS.

## MATERIALS AND METHODS

NCS was supplied from Kayaku Antibiotic Res. Corp., Tokyo. Sephadex G-75 gel was purchased from Bio-Rad Laboratory, U.S.A. Other compounds and solvents were reagent grade and were used without further purification. NCS-chr was isolated from NCS by two methods using different solvents for dissociation of NCS-chr from NCS, A) AcOH-MeOH [5], B) DMSO. Crude NCS-chr was purified by gel chromatography. All the procedures were performed in the dark. NCS-chr was detected by UV absorption at 340 nm and by a characteristic fluorescence emission (a broad band at 410 nm on excitation at 340 nm). CHP nanoparticle solution was prepared by the same method previously reported [4].

## RESULTS AND DISCUSSION

### *Isolation of NCS-chr*

In method A, the isolated yield of NCS-chr was less than 5%. Because apo-NCS is consisted of a stable  $\beta$ -barrel structures and tightly complexes the chromophore, it could not be easy to dissociate from the protein in AcOH-MeOH solution. Therefore, we changed the solvent from AcOH-MeOH to DMSO for the effective release of NCS-chr from the protein. Fig. 1 shows the typical gel chromatogram of NCS in DMSO. Finally, NCS-chr was isolated in 42% yields in method B.

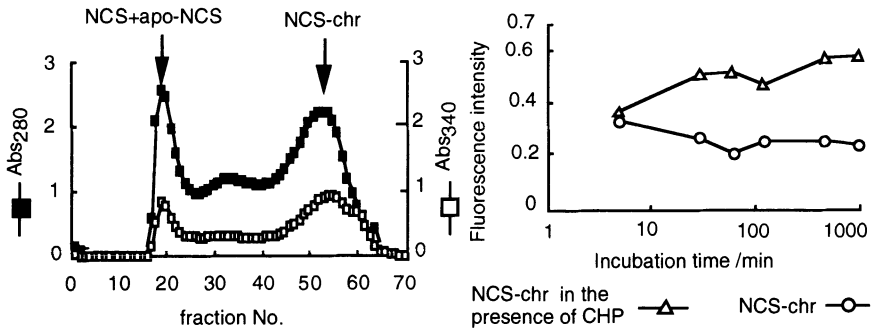


Fig.1 GPC profile of NCS dissolved in DMSO. 42.1 % of NCS-chr was recovered.

Fig.2 The time course of complex formation in water. Fluorescence intensity at emission peak (excited at 340 nm [6]) was plotted for NCS-chr in the absence of CHP.

### Interaction of NCS-chr with CHP self-aggregate

NCS-chr was incubated with CHP self-aggregate aqueous solution at 37 °C. Free NCS-chr was gradually decomposed in water with decrease in its fluorescence intensity (Fig.2). In the presence of CHP self-aggregate, however, the fluorescence intensity increased with time. This could be due to the binding of NCS-chr to the hydrophobic binding site of CHP self-aggregate. The chemical stability of NCS-chr would increase upon the complexation.

In the case of NCS-chr extracted by method B, the complex with CHP self-aggregate was isolated as follows. NCS-chr and CHP were dissolved in DMSO and mixture incubated for 30 min at 24 °C in the dark. Subsequently, the mixture was dialyzed against water at 4 °C. The complex was further purified by ultrafiltration. About 90% of NCS-chr employed bound to the CHP self-aggregate. Approximately six NCS-chr molecules were complexed by one CHP self-aggregate (diameter: 20 nm).

In conclusion, CHP self-aggregate effectively bound NCS-chr in the hydrophobic binding site. The chemical stability of the chromophore in water increased upon the complexation.

### REFERENCES

- Otsuki K, Ishida N(1981) The inhibitory mechanism of in vitro protein phosphorylation by a nonprotein chromophore removed from neocarzinostatin. *Protein Nucleic Acid&Enzyme* 26:937-949
- Teplyakov A, Obmolova G, Wilson K, Kuromizu K(1993) Crystal structure of apo-neocarzinostatin at 0.15-nm resolution. *Eur. J. Biochem.* 213:737-741
- Saito I(1989) New DNA cleaving molecules. Neocarzinostatin and photochemically cleaving molecules. *Kagaku* 44:726-731
- Akiyoshi K, Deguchi S, Moriguchi N, Yamaguchi S, Sunamoto J (1993) Self-aggregates of hydrophobized polysaccharides in water. Formation and characterization of nanoparticle. *Macromolecules* 26:3062-3068.
- Myers AG, Proteau PJ, Handel TM (1988) Stereochemical assignment of neocarzinostatin chromophore. Structures of neocarzinostatin chromophore-methyl thioglycolate adducts. *J. Am. Chem. Soc.* 110:7212-7214
- Edo K, Saito K, Akiyama-Murai Y, Mizugaki M, Koide Y, Ishida N (1988) An antitumor polypeptide antibiotic neocarzinostatin: The mode of apo-protein- chromophore interaction. *J. Antibiotics* 16:254-562

Atsuyoshi NAKAYAMA, Ioannis Arvanitoyannis, Norioki Kawasaki, Kazuko Hayashi,  
and Noboru Yamamoto

*Dept. of Organic Materials, Osaka National Research Institute, AIST,  
1-8-31 Midorigaoka, Ikeda, Osaka, 563 Japan*

## SUMMARY

Poly(ε-caprolactone-co-L-lactide)s were synthesized at various feed ratios by ring-opening polymerization using tin(II) octanoate as an initiator. The biodegradability of these copolymers was evaluated with both enzymatic and non-enzymatic hydrolyses. The enzymes used were *Rhizopus arrhizus*, *Rhizopus delemar*, and *Candida cylindracea* lipases and hog liver esterase. The hydrolyzability of these copolymers depends on the polymer composition, and is higher than that of both homopolymers. The hydrolysis products are 6-hydroxycaproic acid, lactic acid, and oligomers.

## KEY WORDS

biodegradable polymer, lactide, ε-caprolactone, hydrolysis, polyester

## INTRODUCTION

Poly(L-lactide) (polyLA) is a well-known biodegradable and biocompatible polymer which can be used for biomedical and environmental applications. However, semicrystalline polyLA is a relatively stiff and brittle material and has rather low degradation rate in vivo. Copolymerizations of LA with other cyclic esters as lactones have been studied from the viewpoint of the improvement of mechanical properties of polyLA and their control of degradation rates in contact with various biological and environmental media. Poly(ε-caprolactone-co-L-lactide)(poly(CL-co-LA)) has in particular attracted attention due to its excellent processability and its good biodegradability[1-5]. This paper describes the enzymatic and non-enzymatic hydrolyses of the statistical poly(CL-co-LA)s.

## EXPERIMENTAL

Poly(CL-co-LA)s were synthesized in bulk at 120°C for 4 days using tin(II) octanoate as an initiator. The biodegradability of these copolymers was examined with both enzymatic and non-enzymatic hydrolyses for the polymers coated inside of test tubes. Enzymatic hydrolyses were carried out in phosphate buffer (pH7.0) at 37°C for 24h and the enzymes used were lipases from *Rhizopus arrhizus*, *Rhizopus delemar*, and *Candida cylindracea* and hog liver esterase. The hydrolyzability of these polymers was evaluated by total organic carbon concentration (TOC) measurement which show the amount of the hydrolyzed water-soluble products[6].

## RESULTS AND DISCUSSION

Figure 1 shows the results of enzymatic hydrolysis with hog liver esterase. It is found that degradability depends on the copolymer composition. The copolymer containing 82mol% CL units



shows the highest susceptibility to hydrolysis. The esterase degrades polyLA and polyCL only to a limited extent and degrades CL rich copolymers more than LA rich copolymers and both homopolymers. In the case of lipases, the same tendency is found, however they proved to be rather more effective than the esterase. On the other hand, the degradability of the copolymers at 37°C without enzyme was much lower. The results of hydrolysis in distilled water (37°C, 8 weeks) shows that the LA rich copolymers are, in turn, much susceptible to hydrolysis, especially the one with 20mol% CL content (Fig.2). CL-rich oligomers, 6-hydroxycaproic acid, and lactic acid are identified by NMR as the main products of enzymatic hydrolysis. These hydrolysis results are discussed in terms of the chemical structure, hydrophilic-hydrophobic balance, crystallinity of the polymers and the substrate specificity of enzyme compared with those of poly( $\delta$ -valerolactone-*co*-LA)s and poly( $\beta$ -methyl- $\delta$ -valerolactone-*co*-LA)s[7].

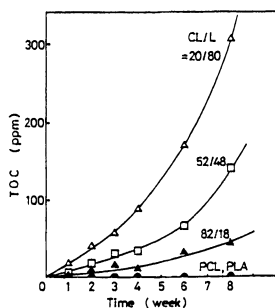


Fig.1 Non-enzymatic hydrolysis of poly( $\epsilon$ -caprolactone-*co*-L-lactide)s in distilled water at 37°C; (●) poly( $\epsilon$ -caprolactone) and poly(L-lactide); ( $\Delta$ ) CL/L=20/80; ( $\square$ ) CL/L=52/48; ( $\blacktriangle$ ) CL/L=82/18.

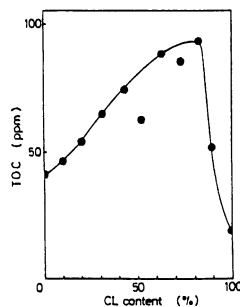


Fig.2 Relationships between enzymatic hydrolysis of poly(CL-*co*-LA)s and polymer composition. Conditions: enzyme: hog liver esterase 200U, temp.:37°C, time: 24h.

## CONCLUSION

Poly(CL-*co*-LA)s are hydrolyzed with both lipases and hog liver esterase. Further, they are non-enzymatically gradually hydrolyzed at 37°C and 70°C. The hydrolyzability of these copolymers depends on the polymer composition, and is higher than that of both homopolymers. In all enzymatic hydrolyses, the copolymer of 82mol% CL units shows the highest susceptibility. On the other hand, LA rich copolymers are much susceptible to non-enzymatic hydrolysis.

## REFERENCES

- 1) Reed AM, Gilding DK (1981) Biodegradable polymers for use in surgery-poly(glycolic)/poly(lactic acid) homo and copolymers:2. In vitro degradation. *Polymer* 22:494-498
- 2) Grijpma DW, Pennings J (1994) (Co)polymers of L-lactide.1. Synthesis, thermal properties and hydrolytic degradation. *Makromol Chem Phys* 195:1633-1647
- 3) Zhang X, Wyss UP, Pichora D, Goosen MFA (1993) Biodegradable polymers for orthopedic applications: synthesis and processability of poly(L-lactide) and poly(lactide-*co*- $\epsilon$ -caprolactone). *JMS-Pure Appl Chem* A30:933-947
- 4) Kricheldorf HR, Kreiser I (1987) Poly lactones.13. Transesterification of poly(L-lactide) with poly(glycolide), poly( $\beta$ -propiolactone), and poly( $\epsilon$ -caprolactone). *J Macromol Sci-Chem* A24:1345-1356
- 5) Feng XD, Song CX, Chen WY (1983) Synthesis and evaluation of biodegradable block copolymers of  $\epsilon$ -caprolactone and DL-lactide. *J Polym Sci:Polym Lett* 21:593-600
- 6) Tokiwa Y, Suzuki T, Ando T (1979) Synthesis of copolyamide-esters and some aspects involved in their hydrolysis by lipase. *J Appl Polym Sci* 24:1701-1711
- 7) Nakayama A, Kawasaki N, Arvanitoyannis I, Iyoda J, Yamamoto N, Synthesis and degradability of a novel aliphatic polyester: poly( $\beta$ -methyl- $\delta$ -valerolactone-*co*-L-lactide) *Polymer* in press.

# SELECTIVE ADSORPTION OF PLASMA PROTEIN ONTO PHASE-SEPARATED DOMAIN OF IMMOBILIZED ORGANOSILANE MONOLAYER SURFACES

Atsushi TAKAHARA, Ken KOJIO, Shouren GE, and Tisato KAJIYAMA

Faculty of Engineering, Kyushu University, Hakozaki 6-10-1,  
Higashi-ku, Fukuoka 812, JAPAN

## ABSTRACT

The phase-separated surfaces of mixed organosilane monolayers on silicon wafer are excellent model system with which to study the interaction of proteins with organic surfaces. The phase-separated structures of the immobilized mixed monolayers were confirmed by atomic force microscopic (AFM) observation. The patterning of adsorption of plasma protein onto surface was achieved by using the phase-separated organosilane monolayers.

**KEY WORDS:** organosilane monolayer, phase-separated structure, atomic force microscopy (AFM), surface structure control, protein adsorption

## INTRODUCTION

An organosilane monolayer is a novel monolayer system which can be polymerized and immobilized on a substrate surface with hydroxyl groups. The authors proposed the novel drawing method for preparation of the structurally controlled organosilane monolayers by an upward drawing method [1,2]. In this study, the organosilane mixed monolayers were prepared and an attempt has been made on the two-dimensional surface structure control and the patterning of protein adsorption by utilizing the mixed monolayer composed of reactive and non-reactive components.

## METHOD

Octadecyltrichlorosilane (OTS,  $\text{CH}_3(\text{CH}_2)_{17}\text{SiCl}_3$ ), [2-(perfluorooctyl) ethyl]trichlorosilane (FOETS,  $\text{CF}_3(\text{CF}_2)_7\text{CH}_2\text{CH}_2\text{SiCl}_3$ ) and lignoceric acid (LA) were used to prepare the OTS, the FOETS, the (OTS/FOETS)(50/50 molar), and the (LA/FOETS) (50/50 molar) mixed monolayers. These organosilane mixture solutions were spread on the pure water surface at the subphase temperature of 293 K. The monolayer on the water surface was transferred onto a clean silicon wafer surface by the upward drawing method[1,2]. Topographic images of the monolayer surfaces were observed with AFM (SPA300, Seiko Instruments Industry, Co., JAPAN). The protein adsorption behavior onto the monolayers was investigated on the basis of the ATR FT-IR flow cell method and the AFM observation. The two-dimensional surface structure control and the patterned adsorption of plasma protein were investigated by using AFM.

## RESULTS AND DISCUSSION

### Phase-separated structure of the (OTS/FOETS) mixed monolayers

Figure 1(a) shows the AFM image of the (OTS/FOETS)(50/50) mixed monolayer. The (OTS/FOETS) mixed monolayer was in a phase-separated state with circular flat-topped domains of ca.  $1\mu\text{m}$  diameter. These domains were higher by 1.1-1.3 nm than the surrounding flat region. Since the difference in molecular lengths between OTS and FOETS is ca. 1.3 nm, it is apparent that the higher, circular domains and the surrounding flat region are composed of OTS and FOETS molecules, respectively. The difference in the spreading coefficients between OTS and FOETS

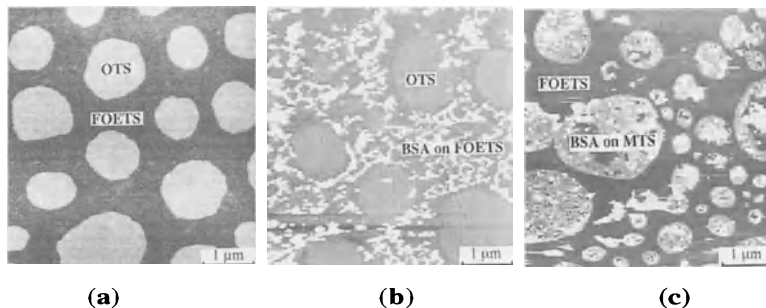


Figure 1 AFM images of the (OTS/FOETS)(50/50) mixed monolayers before (a) and after exposure to a BSA solution (b) and the (MTS/FOETS) mixed monolayer adsorbed BSA (c).

molecules makes OTS dispersed in the amorphous FOETS matrix and then, the domains of OTS are formed. Since the OTS component formed the circular domain which was in a crystalline state even if the molar percent of OTS was 75%, the crystallization of OTS molecules may be an important factor for the formation of phase-separated structure. Therefore, it can be concluded that the crystallization of OTS and the faster spreading rate of FOETS are important factors for the phase separation of (OTS/FOETS) mixed monolayers.

### Interaction between plasma protein and immobilized organosilane monolayer

The interaction between bovine serum albumin (BSA) and the organosilane monolayer surface was studied on the basis of the ATR FT-IR flow cell method. The monolayer was transferred onto a silicon ATR crystal. The initial adsorption rate of BSA to the organosilane monolayer was very fast. The amount of equilibrium adsorption onto the OTS and the FOETS monolayers indicates the side-on monolayer adsorption of BSA. The (OTS/FOETS) mixed monolayer showed a remarkable decrease in the magnitude of equilibrium adsorption. Fig.1(b) shows the AFM image of the (OTS/FOETS)(50/50) mixed monolayers after exposure to a BSA solution. It is apparent from the AFM observation that BSA selectively adsorbs onto the hydrophobic FOETS phase of the (OTS/FOETS) mixed monolayer in order to minimize the interfacial free energy between monolayer and water.

### Two-dimensional surface structure control and patterning of adsorbed protein

The phase-separated monolayer can be prepared from both FOETS and the non-polymerizable and crystallizable amphiphile such as LA. The (LA/FOETS) mixed monolayer was in a phase-separated state in a similar fashion to the (OTS/FOETS) monolayer. The circular LA domains were preferentially extracted with hexane. Then, the patterned surface with high surface free energy (bare Si wafer) and low surface free energy (FOETS) can be obtained after the removal of LA. The holes in the extracted (LA/FOETS) mixed monolayer were modified by the chemisorption of (3-mercaptopropyl) trimethoxysilane (MTS) with thiol groups (SH), and then, the (MTS/FOETS) mixed monolayer with SH groups was obtained. BSA was adsorbed onto (MTS/FOETS) mixed monolayer. Fig.1(c) shows the (MTS/FOETS) mixed monolayer adsorbed with BSA. The BSA adsorbed region was observed as the bright region, which was higher by 4nm than MTS adsorbed region. BSA was adsorbed onto the MTS part selectively due to a specific reaction between (-S-S-) groups in BSA and SH groups in MTS. The above mentioned results showed that two-dimensional surface structure control and patterning of adsorbed protein can be realized by utilizing the mixed monolayer composed of reactive and non-reactive components. The surface with patterned protein can be utilized as biomaterials or biological devices with various novel functionalities.

### REFERENCES

- [1] Ge SR, Takahara A, Kajiyama T(1994) Aggregation structure and surface properties of immobilized organosilane monolayers prepared by the upward drawing method. *J. Vac. Sci. Technol.* **A12**: 2530
- [2] Ge SR, Takahara A, Kajiyama T(1995) Phase separated morphology of an immobilized organosilane monolayer studied by a scanning probe microscope. *Langmuir* **11**

# The Possibility of the Constitution of an Artificial Thymus by Utilizing Keratinocytes

NEGISHI, Naoki<sup>1</sup>, NIZAKI, Motohiro<sup>1</sup>, CHINO Jun<sup>2</sup>, TODA, Toshifusa<sup>3</sup>, and MATSUSHITA, Hiroshi<sup>4</sup>

<sup>1</sup>Dept. of Plastic & Reconstructive Surgery, Tokyo Women's Medical College, 8-1, Kawadacho, Shinjuku-ku, Tokyo, 162, JAPAN, <sup>2</sup>Dept. of Oral Pathology, Meikai University, <sup>3</sup>Dept. of Molecular Biology, Tokyo Metropolitan Institute of Gerontology, <sup>4</sup>Institute for Advanced Skin Research

The production-ability of thymopoietin (TP) II was investigated by immunohistochemical detection in normal human skin besides cultured human keratinocytes (KC3). In interferon  $\gamma$  (IFN- $\gamma$ ) treated skin, the distinct staining of anti-TP was noted in the KC3 from basal to the middle of the spinous layers. No epithelial staining of anti-TP was observed in skin without treatment of IFN- $\gamma$ . It can therefore be presumed that KC3 play an important role for function of skin-specific T-cells. If so, we may be able to use a hybrid artificial skin as an artificial thymus.

**KEY WORDS:** Artificial skin / Skin immunology / Thymopoietin II / Artificial thymus / Keratinocytes

## INTRODUCTION

Skin appears to be an immunological tissue similarly to thymus<sup>1</sup>. Epidermal keratinocytes (KC3) resemble thymic epithelial cells (TECs)<sup>2</sup>, and it is deduced that KC3 play an important role for functional action of intracutaneous T-cells<sup>3-5</sup>. It has been also suggested that some thymic hormone like substances such as thymulin<sup>6</sup> or thymopoietin (TP)<sup>7</sup> exist in epidermis. Figure 1 shows our working hypothesis concerning the mechanism of TEC and KC as a stromal cell for T-cell development. It is interesting to see whether KCs actually produce T-cell developing factors or not and to explore under what kind of condition such factors are induced. In this research, we investigated by immunohistochemical staining in normal human skin whether it is possible for KCs similarly to TECs to elaborate T-cell developing factors such as TP II by stimulating with interferon  $\gamma$  (IFN- $\gamma$ ). We would like to discuss the possibility of ectopic application of a hybrid artificial skin to an artificial thymus, including a philological study.

## METHODS

The tetradecapeptide fragment TP14(aa29-42) which contains immunological active site TP5(aa32-36) of TP II was used as an antigen moiety. The anti-TP serum was prepared using TP14-myoglobin conjugate in rabbit. The anti-TP polyclonal antibody (rabbit Ig) was obtained from the anti-TP serum by affinity column purification. As normal human skins, the remainders (ca. 0.5-1cm by 1cm section) of skins obtained from skin grafting and so on were used. The thickness of normal skin taken from scalp or thigh for skin grafting was 8/1000 inch (0.203mm). Obtained skins were allowed to remove bacteria for 30min at 310K in medium RPMI 1640 (Gibco) containing 300 $\mu$ g/ml ampicillin, 10mg/ml amikacin as antibiotics, and 2.5 $\mu$ g/ml amphotericin B as antimycotics, and divided into quarters. Interferon  $\gamma$  was used human recombinant IFN- $\gamma$  (Boehringer Mannheim). IFN- $\gamma$  was solved in KC growth medium (modified K100 containing 0.5 $\mu$ g/ml hydrocortison, Kyokuto Pharm. Co.) and the treatment of skin with IFN- $\gamma$  was carried out as follows; 1) A divided skin was frozen in OCT compound (Miles Inc.) as it is, or was frozen following incubation in KC growth medium (modified K100) for 24h at 310K under 5%CO<sub>2</sub> (Control 1). 2) A divided skin in modified K100 was treated to penetrate the medium under the condition from reduced pressure (ca. 110mmHg) to atmospheric pressure and then frozen in OCT compound (Control 2). 3) A divided skin was frozen in OCT compound after incubation in modified K100 containing 1,000U/ml IFN- $\gamma$  for 24h at 310K under 5%CO<sub>2</sub> (Sample 1). 4) A divided skin in modified K100 with 1,000U/ml IFN- $\gamma$  was treated under reduced pressure (ca. 110mmHg), and then allowed to penetrate IFN- $\gamma$  solution by pressure injection under atmospheric pressure (ca. 760mmHg) according to the method of reduced pressure-penetration<sup>8</sup>. After treatment of reduced pressure-penetration, the sample skin was incubated in modified K100 with 1,000U/ml IFN- $\gamma$  for 24h at 310K under 5%CO<sub>2</sub>, and then frozen in OCT compound (Sample 2). These skins were explored by immunohistochemical staining with anti-TP, anti-ICAM 1 (Br. Bio-tech.), anti-HLA-DR (Becton D), anti-IL-7 (Genzyme), and anti-B7 (Becton D) antibodies using in direct alkaline phosphatase method.

## RESULTS & DISCUSSION

It is important to elucidate whether the induction of T-cell maturation/differentiation factors such as TP II or interleukin 7 is observed by interferon  $\gamma$  (IFN- $\gamma$ ) stimulation in KCs similarly to TECs or not. Thus, the production-ability of TP II was investigated by immunohistochemical detection in normal human skin. In the case of normal human skin (Control 1), neither the skin frozen as it is nor the skin incubated in modified K100 for 24h was observed TP elaboration by immunostaining using anti-TP antibody. And in normal human skin treated with reduced pressure alone (Control 2), no staining of anti-TP was observed, that is, physical stimulation of pressure *per se* was not a factor to induce TP production. While, in IFN- $\gamma$  treated skin (Sample 1, 2),

the distinct staining of an anti-TP was noted in the epidermis (Fig. 2). The distinct staining of anti-ICAM-1 was also observed in IFN- $\gamma$  treated skin (Sample 1,2). No epithelial staining of an anti-ICAM-1 was observed in skin without treatment of IFN- $\gamma$  (Fig. 3). It is known that IL-7 is a growth and maintenance factor for mature and immature pre-T-cells<sup>9</sup>. Recently, it is reported that TBCs produce IL-7<sup>10</sup>. Thus, it is an interesting subject to explore the distribution of IL-7 in skin. The distinct staining of anti-IL-7 was noted in the basal layer. However, the distinct staining of anti-IL-7 was also observed in the absence of IFN- $\gamma$  or the mock controls. Further investigation in mRNA level of IL-7 is needed to answer whether KCs constitutively produce IL-7 or not. It is also known that antigen-specific T cell activation depends on T cell receptor-ligand interaction and costimulatory signals<sup>11</sup>. That is, the maximal T-cell response to its antigen requires presentation of the antigen by a major histocompatibility complex (MHC) class II (human immune response gene HLA-DR) molecule as well as the delivery of one or more costimulatory signals provided by the antigen-presenting cell (APC). Recent research suggests that one such critical costimulatory pathway involves the interaction of the T-cell surface antigen CD28 with its ligand B7 on the APC. Human T-cell clonal energy is induced by antigen presentation in the absence of B7 costimulation<sup>12</sup>. When the B7 molecule on the surface of antigen-presenting cells binds to the T cell surface molecule CD28, a costimulatory signal for T cell activation is generated<sup>12</sup>. Epidermal Langerhans cells (LC), bone marrow-derived cells, are known to express B7<sup>13</sup>. Dendritic cell seemed to LC expressed a strong staining of anti-B7, while no staining of anti-B7 was noted in KCs. It is reported that the class II MHC-bearing, non-bone marrow-derived cells such as IFN- $\gamma$  treated TBCs<sup>14</sup> or KCs<sup>15</sup> induce an antigen-specific unresponsiveness. It can therefore be presumed that KCs play a key role for function of T-cells. If so, we may be able to use a hybrid artificial skin as an artificial thymus by utilizing IFN- $\gamma$  treated KCs.

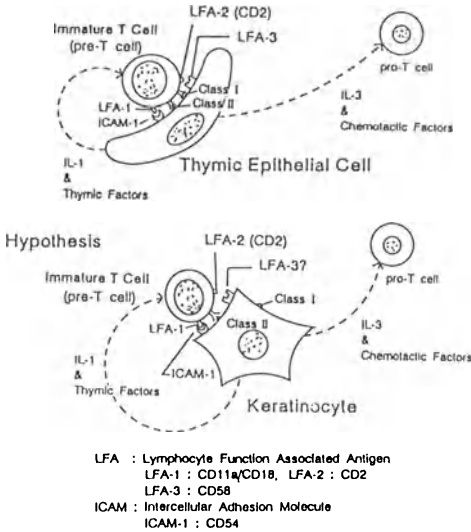


Fig.1 The Deduced Mechanism of Thymic Epithelial Cell and Keratinocyte as a Stromal Cell for T-cell Development

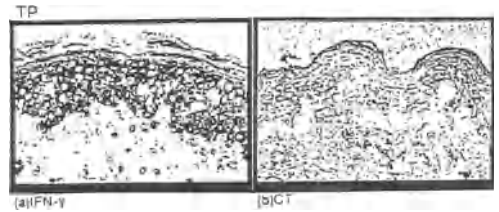


Fig.2 Immunohistochemical detection of TP in normal skin with (a) or without (b) IFN- $\gamma$ .

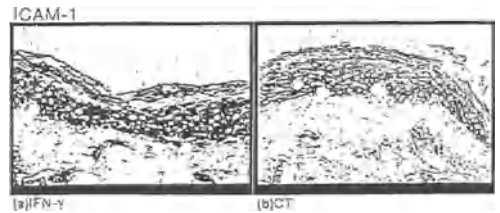


Fig.3 Immunohistochemical detection of ICAM-1 in normal skin with (a) or without (b) IFN- $\gamma$ .

## REFERENCES

1. R.L. Edelson, J.M. Finck, *Sci Am.*, 252(6), 34-41 (1985).
2. K.H. Singer, E.A. Harden, A.L. Robertson, et al., *J Invest. Dermatol.*, 85, 67s-71s (1985).
3. M.R. Rubenfeld, A.E. Silverstone, D.M. Knowles, et al., *J Invest. Dermatol.*, 77, 221-224 (1981).
4. K.H. Singer, P.T. Le, S.M. Denning, et al., *J Invest. Dermatol.*, 94, 85s-90s (1990).
5. A. Ebe, O. Kilgus, R. Strohal, et al., *J Immunol.*, 149, 1694-1701 (1992).
6. K. Kato, S. Ikeyama, M. Takaoki, et al., *Cell*, 24, 885-895 (1981).
7. A. C. Chu, J. A. K. Patterson, G. Goldstein, et al., *J Invest. Dermatol.*, 81, 194-197 (1983).
8. S. Wakamatsu, N. Negishi, M. Takeuchi, et al., *Nishinippon Hihyu*, 53, 1190-1197 (1991).
9. D.I. Godfrey, A. Zlotnik, *Immunol. Today*, 14, 547-553 (1993).
10. R. Murray, T. Suda, N. Wrighton, et al., *Int. Immunol.*, 1, 526-531 (1990).
11. R.H. Schwartz, *Cell*, 71, 1065-1068 (1992).
12. C.D. Gimmi, G.J. Freeman, J.G. Gibben, et al., *Proc. Natl. Acad. Sci. USA*, 90, 6586-6590 (1993).
13. C.P. Larsen, S. Ritchie, T.C. Pearson, et al., *J Exp. Med.*, 176, 1215-1220 (1992).
14. R.G. Lorenz, P.M. Allen, *Nature*, 340, 557-559 (1989).
15. V. Bal, A. McIndoe, G. Denton, et al., *Eur. J. Immunol.*, 20, 1893-1897 (1990).

# IMPROVED NONTHROMBOGENICITY OF HEPARIN IMMOBILIZED AND SULFONATED POLYURETHANE: *IN VITRO* EVALUATION USING EPIFLUORESCENT VIDEO MICROSCOPY

Chisato Nojiri, Shigeru Kuroda\*, Takayuki Kido, Kazuhiko Hagiwara, Kazuhisa Senshu, Ki Dong Park\*\*, Young Ha Kim\*\*, Kiyotaka Sakai\*, Tetsuzo Akutsu

Institute of Biomedical Science, TERUMO Corp. 1500 Inokuchi, Nakai-machi, Ashigarakami-gun, Kanagawa 259-01, Japan

## SUMMARY

We have developed novel surface modification techniques to improve the blood compatibility of polyurethane (PU). One was heparin immobilization using a polyethylene imine spacer and the other was a sulfonated polyallylamine grafting onto a PU surface. Both techniques utilized ozone-induced graft copolymerization, thereby having an advantage to be applied to medical devices even with a complex design. *In vitro* blood compatibility of modified PUs were evaluated using an epifluorescent video microscopy (EVM) combined with a parallel plate flow cell. Both modified PUs showed significantly less platelet coverage on the surfaces with less  $\beta$ -TG and C3a production compared to the control. These results suggest that both PU-PEI-HEP and PU-PAA-SO<sub>3</sub> surfaces are promising for the application to a variety of medical devices.

**KEY WORDS:** surface modification, heparin, sulfonated polyurethane, ozone-induced graft copolymerization, epifluorescent video microscopy

## INTRODUCTION

Polyurethane (PU) has been widely used in various biomedical applications, such as artificial hearts, vascular grafts and pacemaker leads due to its superior physical and mechanical properties. However, the inherent blood compatibility of PU remains as a problem for long-term *in vivo* application. We have recently developed novel surface modification techniques to improve the blood compatibility of PU. One was heparin immobilization using a polyethylene imine (PEI) spacer (PU-PEI-HEP) and the other was a sulfonated polyallylamine (PAA) grafting (PU-PAA-SO<sub>3</sub>) onto a PU surface. The modified PUs were evaluated *in vitro* using an epifluorescent video microscopy (EVM) system.

## MATERIALS & METHODS

**Heparin Immobilization onto PU Surfaces Using PEI Spacer (PU-PEI-HEP):** The PU surfaces were first treated with ozone gas, and PEI was graft copolymerized onto the surfaces through a coupling reaction between peroxide of the PU surfaces and -NH<sub>2</sub> groups of PEI. Heparin was covalently bound to PEI spacer by glutaraldehyde, then the reduction of Schiff's base was carried out.

### Surface Grafting of Sulfonated PAA on PU Surfaces

**Synthesis of sulfonated polyallylamine (PAA-SO<sub>3</sub>):** PAA-HCl was first treated with KOH solution, followed by dialysis to obtain free form of PAA. 1,3-propane sultone (PST) was then added to PAA solution in DMSO and reacted at 60°C for 24hrs. The reactant was fully precipitated in acetone and vacuum dried at room temperature.

**Surface grafting of PAA-SO<sub>3</sub> (PU-PAA-SO<sub>3</sub>):** The surface grafting of PAA-SO<sub>3</sub> on PU surfaces was performed using ozone oxidation as utilized in PU-PEI-HEP.

**Characterization of modified PUs:** These modified PUs were analyzed by ESCA and FXa bioactivity was measured on these surfaces.

**In Vitro Blood Compatibility:** The modified PUs were evaluated using an epifluorescent video microscopy (EVM) combined with a parallel plate flow cell [1]. The EVM system measured real-time platelet adhesion onto the surfaces from whole human blood containing Mepacrine labeled platelets

perfused at a wall shear rate of  $100\text{sec}^{-1}$  for 20 min. Blood which had passed through the flow cell was collected and centrifuged, then supernatant  $\beta$ -TG and C3a were measured. Non-treated PU was used as a control.

RESULTS & DISCUSSION

Table 1 summarizes the results of ESCA analyses and FXa assay.

Table 1.

SURFACE	C	O	N	S	FXa assay (IU/cm <sup>2</sup> )
PU-PEI-HEP	80.6	12.9	5.8	0.63	0.21
PU-PAA-SO3	85.7	8.7	5.3	0.25	0.011

PU-PEI-HEP showed high FXa bioactivity on the surfaces. In *in vitro* EVM experiments, these modified surfaces demonstrated minimal platelet coverage on the surfaces with less  $\beta$ -TG and C3a levels, while untreated PU showed considerable amount of platelet coverage with higher  $\beta$ -TG and C3a levels (Fig. 1-3).

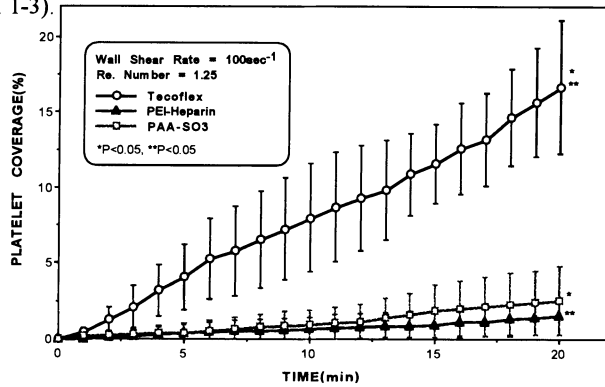


Fig. 1. The plots for time vs. platelet coverage on PU surfaces

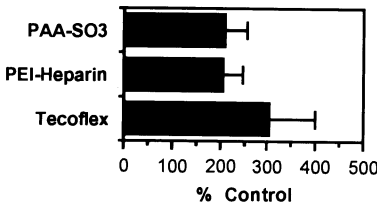


Fig. 2.  $\beta$ -TG release from platelet

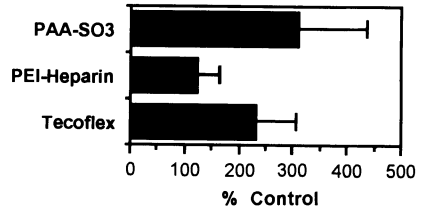


Fig. 3. C3 activation

In the present study, we utilized polyfunctional polymer (PFP), PEI and PAA as a spacer for surface modification to increase the amount of heparin and sulfonation. PFP has been proven to amplify the surface concentration of bioactive molecules by increasing the amount of available coupling sites[2]. The high FXa bioactivity and excellent *in vitro* blood compatibility of PU-PEI-HEP and PU-PAA-SO3 are attributable to this mechanism. The *in situ* ozone oxidation utilized for surface grafting in this study has also advantages to be able to uniformly introduce peroxides onto a variety of substrates of the medical devices even with a complex design, such as artificial heart and membrane oxygenator.

REFERENCES

1. Kawagoishi N, Nojiri C, et al: In vitro evaluation of platelet/biomaterial interactions in a epifluorescent video microscopy(EVM) combined with a parallel plate flow cell. Artificial Organs 18:588-595, 1994.
2. Piao AZ, et al: Heparin immobilization by surface amplification. ASAIO J 38:638- 643, 1992.

## EVALUATION OF A NEWLY DEVELOPED BIOLOGICAL PATCH

Hsing-Wen Sung, Yen Chang<sup>#</sup>, Yung-Tang Chiu<sup>\*</sup>, Jen-Her Lu<sup>#</sup>, Hung-Liang Hsu, Chin-Chin Shih

Department of Chemical Engineering, National Central University, Chung-Li, Taiwan, R.O.C.

<sup>#</sup>Department of Cardiovascular Surgery, Veterans General Hospital, Taipei, Taiwan, R.O.C.

<sup>\*</sup>Department of Veterinarian Pathology, Pig Research Institute, Taiwan, R.O.C.

### ABSTRACT

This study was intended to evaluate a newly developed biological patch fixed with an epoxy compound (EC) ionically bonded with heparin (H). In the study, it was observed that the EC-fixed patch appeared more natural and was more pliable than the glutaraldehyde-fixed (GA) one. Additionally, both the GA- and EC-fixed pericardia had significant increases in denaturation temperature ( $T_d$ ) and fixation index (F.I.) as compared to the fresh one. In a canine study, it was noted that the biological patches ionically bonded with heparin had lighter inflammatory response, fibrosis, and tissue adhesion than the synthetic ones. The results of this study suggests that the EC-fixed patch with ionically bonded heparin might have a better performance than those currently used in clinical practice.

**Key Words:** biological patch, epoxy compound, cross-linking characteristics, biological reaction

### INTRODUCTION

Many problems encountered with the currently available prosthetic pericardial patches have been reported clinically [1]. To overcome these problems, we undertook the development of an EC-fixed biological patch ionically bonded with heparin. This EC fixation technique has been recently used in developing various bioprosthetic devices [2]. The study was intended to compare the cross-linking characteristics of this newly developed EC-fixed patch with those of its GA-fixed counterpart. In addition, a composite pericardial patch—which consisted of (1) EC-fixed patch with ionically bonded H, (2) GA-fixed patch with ionically bonded H, (3) PTFE patch, (4) Dacron patch, (5) EC-fixed patch without ionically bonded H, (6) GA-fixed patch without ionically bonded H—was evaluated in a canine model.

### MATERIALS AND METHODS

Fresh porcine pericardia procured from a slaughter house were used to fabricate various biological patches. A 4% EC (ethylene glycol diglycidyl ether) solution or a 0.625% GA solution was employed to fix the porcine pericardia. The cross-linking characteristics— $T_d$ , moisture content (M.C.), and F.I.—of each sample were then determined. In the animal study, mongrel dogs (ca. 10 kg) were used to evaluate the composite pericardial patch implanted orthotopically. The implanted patches were retrieved at 1-week, 2-weeks, 4-weeks, or 12-weeks post implantation, respectively. The retrieved patches were then analyzed as per their biological reactions: inflammatory response, fibrosis, and adhesion. The severity of each biological reaction was classified as: 0 (no reaction), 1 (light reaction), 2 (mild reaction), 3 (moderate reaction), 4 (severe reaction), and 5 (very severe reaction).

### RESULTS AND DISCUSSION

The results of the cross-linking characteristics of various biological patches tested in the study are shown in Table 1.



Table 1. Cross-Linking Characteristics of Various Biological Patches Tested in the Study

n=3	Fresh	EC w/ H	GA w/ H	EC w/o H	GA w/o H
T <sub>d</sub> (C)	58.7±0.2	82.7±0.6	87.6±0.6	80.1±0.7	88.1±0.7
F.I. (%)	0.0±0.0	90.1±1.2	92.6±0.5	92.8±0.4	94.8±0.4
M.C. (%)	86.1±1.4	83.2±1.7	74.2±2.3	84.8±0.5	75.1±1.4

It was noted that the EC-fixed patch appeared more natural and was more pliable than the GA-fixed patch. This may be due to the higher moisture content of the EC-fixed patch than its GA-fixed counterpart (see Table 1). Both the EC- and GA-fixed pericardia had significant increases in T<sub>d</sub> and F.I. as compared to the fresh one (see Table 1).

The results obtained in the animal study are presented in Table 2.

Table 2. Animal Study Results

Patch	Time (Weeks)	Inflammatory Response		Fibrosis		Adhesion
		A	B	A	B	A
EC with Heparin	1	0	1	0	0	0
	2	1	2	1	2	0
	4	0	1	1	1	0
	12					3
GA with Heparin	1	2	3	0	0	0
	2	2	4	0	3	0
	4	1	2	0	2	2
	12					4
PTFE	1	3	4	0	0	0
	2	3	4	1	3	2
	4	1	2	1	4	3
	12					5
Dacron	1	3	4	0	0	0
	2	4	4	3	4	3
	4	4	5	5	5	4
	12					5
EC without Heparin	1	2	2	0	0	0
	2	3	3	2	3	3
	4	2	4	0	3	3
	12					5
GA without Heparin	1	2	2	0	0	0
	2	3	3	1	2	3
	4	1	4	0	3	2
	12					4

A: near the heart's side; B: near the lung's side

As shown in the table, the biological patches ionically bonded with heparin had lighter inflammatory response, fibrosis, and tissue adhesion than the synthetic ones. The results of this study suggests that the EC-fixed patch with ionically bonded heparin might have a better performance than those currently used in clinical practice.

## REFERENCES

- [1] Araujo JD, Braile DM, Azenha Filho JO (1987) The use of bovine pericardium as an arterial graft—A five year follow-up. *J Cardiovasc Surg* 28:434-439.
- [2] Noishiki Y, Kodaira K, Furuse M, Miyata T. Method of preparing antithrombogenic medical materials. *U.S. Patent* 4,806,599, 21, Feb. 1989.

# APPLICATION OF HEMA-ST BLOCK COPOLYMER COATED SMALL CALIBER VASCULAR GRAFT FOR VEINS

Ken Suzuki, Teruo Okano, Yasuhisa Sakurai, Shin-ichi Terada\*, Mikihiro Nozaki\*, Naoto Takemura\*\*

Institute of Biomedical Engineering, Tokyo Women's Medical College, 8-1 Kawada-cho, Shinjuku-ku, Tokyo 162, Japan. \*Department of Plastic and Reconstructive Surgery, Tokyo Women's Medical College. \*\*R & D Center, Terumo Co, 1500 Inokuchi, Nakai-machi, Ashigarakami-gun, Kanagawa 259-01.

## SUMMARY

We were already reported that the amphiphilic block copolymer composed from 2-hydroxyethylmethacrylate and styrene(HSB) which formed micro-domain structure show excellent nonthombogenicity. In this study, we applied HSB coated small vascular graft for vein. The grafts were implanted into the rabbits inferior vena cave. After 1 week implantation, the round shape HSB coated graft tube shows 100% patency after 1 week implantation. No thrombus was observed on the anastomotic site and the grafts surfaces. When the edges were rounded, the damage of natural blood tube and turbulent flow were perverted, the HSB coat graft tubes keep patency more than 1 week in low flow rabbit vein. The cross-section of graft was observer with TEM. After staining with OsO<sub>4</sub>, only monolayer-like protein layer(about 200Å) were observed on surface. The monolayre-like absorbed protein layer improved blood compatibility without persudointima formation. Thus the HSB coated graft could be a promising small vessel prosthesis even in vaines.

**KEY WORDS** : block copolymer, micro-domain structure, small vascular graft, absorbed protein layer

## INTRODUCTION

Materials with improved surface properties are required to keep pace with the increasing demand for blood contacting devices. We were already reported that the amphiphilic block copolymer composed from 2-hydroxyethylmethacrylate(HEMA) and styrene(St) which formed micro-domain structure show excellent nonthombogenicity in vitro and in vivo experimental [1]. From in vitro study, the possibility of enhanced adherent platelet metabolic activity preventing cytoplasmic Ca<sup>2+</sup> increase on HEMA-St block copolymer(HSB) surface was demonstrated [2]. In vivo application, the HSB coated graft tubes(ID:3mm) were implanted in abdominal aortic of dog. The proteins monlayer covered surface and keep patency more than one year [3]. The mechanism of nonthrobogenicity was completely different from other materials.

In this study, we applied HSB coated small vascular graft for vein that demanded severe nonthrobogenicity compare with the artery because of low flow rat and no pulsation. The development of the small vascular graft applicable for vein expand graft tubes application and could change the surgical operation technique in many fields.

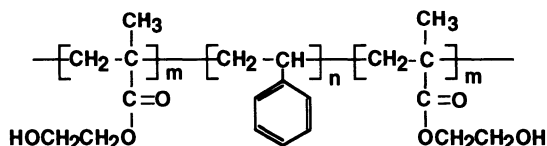


Fig.1 Chemical Structure of HEMA-St Block Copolymer

## METHODS

The polyurethane tube(OD:4mm, ID:3mm, length:25mm) was prepared as vascular graft with

two different end shapes. One was the angled shape with just cutting( edged). the other was round edges of tubes after cutting(round). The surfaces of these tubes were coated with HSB(Mn=38,000, HEMA:67mol%) from DMF solution by dipping method. The grafts were implanted into the inferior vena cave of rabbit(2.5-3.5kg) by only insertion without stitches. After 1 week, patency was checked with flow meter.

## RESULTS AND DISCUSSION

To use this HSB coated grafts material in large field, the grafts were implanted into the rabbits blood tubes by insertion without stitches. So the micro-sugary technique was not necessary for this experimental model. The blood flow rat of inferior vena cave of rabbit after implantation was 20 ml/min. This flow rat was about 1/20 of that of dog's abdominal aortic that we used former study. After 1 week, flow rat of grafts was measured and check the patency of implanted tubes. The results were show in table 1. In the case of no coated tubes, no tube kept patency. The shapes of end of graft tubes show no difference. The nonthorombogenicity of polyurethane was no enough for vein. The graft tube was occluded in earlier period after implantation. The patency of HSB coated angle shaped graft tubes were 5/9, about 50%. The thrombus was formed from anastomotic site of natural blood tube, not from the graft tubes. On the other hand, the round shape HSB coated graft tube shows 100% patency after 1 week implantation. No thrombus was observed on the anastomotic site and the grafts surfaces. The occlusion of angled HSB coat tube was caused by the injuring of surface of natural blood tube at insertion or turbulent flow by edge of the graft tubes. When the edges were rounded, the damage of natural blood tube and turbulent flow were perverted, the HSB coat graft tubes keep patency more than 1 week in low flow rabbit vain.

The surface of HSB coated graft tubes after 1 week implantation were observed with SEM. Almost no blood cell was observed on surface. The cross-section of graft was observer with TEM. After staining with OsO<sub>4</sub>, only monolayer-like protein layer(about 200Å) were observed on surface. As mentioned in dog artery experimental, the monolayre-like absorbed protein layer improved blood compatibility without persudointima formation. Thus the HSB coated graft could be a promising small vessel prosthesis even in low flow rate vaines.

**Table 1 The patency of small caliber vascular grafts after 1 week implantation in inferior vena cava**

Surface coating	Shape	Patency after 1week
non	angled	0/5
non	round	0/4
HSB	angled	5/9
HSB	round	3/3

3mm-ID, 4mm-OD, 2.5cm-long, Flow rate 20ml/min

## References

1. Okano T, Nishiyama S, Shinohara I, Akaike T, Sakurai Y, Kataoka K, Tsuruta T (1981) Effect of hydrophilic and hydrophobic microdomains on mode of interaction between block copolymers and blood platelet. *J. Biomed. Mater. Res.* 15: 393-402
2. Okano T, Suzuki K, Yui N, Sakurai Y, Nakahama S (1993) Prevetion of changes in platelet cytoplasmic free calcium levels by interaction with 2-hydroxyethyl methacrylate/styrene block copolymer surfaces. *J. Biomed. Mater. Res.* 27: 1519-1525
3. Nojiri C, Okano T, Koyanagi H, Nakahama S, Park KD, Kim SW (1992) In vivo protein absorption on polymers: visualization of abaorbed proteins on vascular implants in dog. *J. Polym. Sci. Polym. Ed.* 4: 75-88

# TRANSFER AND SURFACE FIXATION OF GELS BY AN EXCIMER LASER ABLATION

Yasuhide Nakayama and Takehisa Matsuda

*Department of Bioengineering, National Cardiovascular Center Research Institute  
Fujishiro-dai 5-7-1, Suita, Osaka 565, Japan*

## SUMMARY

This paper presents a new method to provide a durable layering of gels on a polymer film by an excimer laser ablation. The procedure is as follows. At first, three-layered (**A-B-A** type) polymer films were prepared, where **A** is polyethylene or poly(vinyl alcohol), both of which have extremely small absorption coefficients at the laser wavelength (193nm) and **B** is poly(*N,N*-dimethyl acrylamide) or polystyrene, both of which have large ones. The layered film was subjected to irradiation of ArF excimer laser pulses. The irradiated surface portion of **A** film exhibited a gel-like nature. No delamination occurred even upon vigorous washing with water or organic solvents. XPS and FT-IR spectral analyses showed that the **A** surface was completely layered with a polymer resembled to **B**. The thickness of the fixed gel increased with an increase in fluence and the number of pulses. Significant inhibition of platelets adhesion on hydrogelated surface was observed *in vitro*. When heparin was mixed with the polymer **B**, heparin was immobilized in a hydrogelated surface.

**KEY WORDS:** surface gelation, excimer laser, ablation, biocompatibility, microprocessing

## INTRODUCTION

The surface modification on functional biomedical devices such as advanced artificial organs, micromachines and microbiosensors needs precisely dimensional control at the microscopic level. We have been developing surface photo-microprocessing technologies to provide biocompatibility and functioning for these devices.<sup>(1,2)</sup>

Excimer lasers are powerful sources of pulsed, monochromatic ultraviolet light. When the laser pulses whose fluence is above a well-defined threshold value fall on a polymer, photolyzed reactive materials including monomer and oligomer are spontaneously ejected away from the polymer surface, leading to three-dimensional (3-D) surface structuring.<sup>(3)</sup> In this paper, using this phenomenon, called ablation, a novel durable layering of gels on a substrate surface was demonstrated.

## MATERIALS AND METHODS

Polyethylene (PE), poly(vinyl alcohol) (PVA) and polystyrene (PSt) were obtained commercially. Poly(*N,N*-dimethyl acrylamide) (PDAA) was prepared by radical polymerization. An ArF excimer laser (Hamamatsu L4500, Shizuoka) was used as the light source (wavelength: 193nm, fluence: 20 to 70mJ/cm<sup>2</sup>pulse). Surface chemical composition at the outermost layers was determined by x-ray photoelectron spectroscopy (Shimadzu ESCA-750, Kyoto). The gel thickness was measured with a real-time scanning laser microscope (ILM21, Lasertech, Kanagawa).

## RESULTS AND DISCUSSION

The surface fixation of a hydrogel on PE film and an organogel on PVA film was attempted, respectively. The procedure is as follows. At first, three-layered (**A-B-A** type) polymer films were prepared by solvent-casting of polymer **B** between two **A** films, where **A** is PE or PVA, both of which have extremely small absorption coefficients ( $\alpha$ ) at the laser excitation wavelength and **B** (thickness: 8 $\mu$ m) is PDAA or PSt, both of which have large  $\alpha$ . The layered films were subjected to irradiation of ArF excimer laser pulses as schematically shown in **Figure 1**.

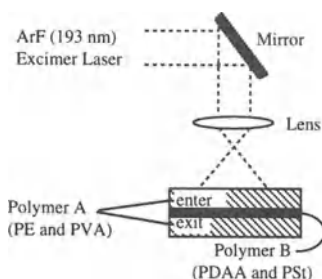


**Figure 1.** A schematic diagram showing an optical equipment used for this study and laser irradiation.

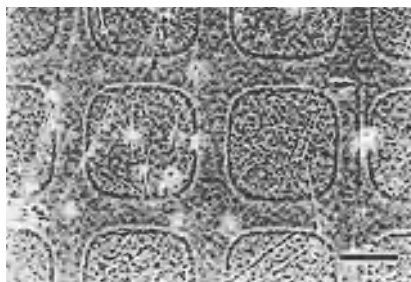


**Figure 2.** A hydrophilic/hydrophobic surface obtained by laser irradiation through a photomask. Scale bar=100 $\mu$ m.

A layered PE-PDAA-PE film was irradiated with laser pulses. The PE surface at the side of laser incidence (enter side) (Figure 1) exhibited a water-wettable, hydrogel-like nature upon immersion into water. No appreciable surface modification at the exit side was observed. XPS and FT-IR spectral analyses showed that the PE surface at the enter side was completely layered with a polymer resembling PDAA. Little appreciable spectral changes in XPS measurements were observed for samples that were subjected to further vigorous washing with water, indicating that once a hydrogel is chemically fixed on a surface, it is quite durable. Irradiation to a layered PVA-PSt-PVA film created a hydrophobic organogel on the hydrophilic PVA surface.

We speculate that these surface gelation is due to complex photochemical reactions: ejection of highly reactive fragments with radical and ion species from PDAA or PSt, which are generated by absorption of laser photons which pass through the A layer with a small  $\alpha$ , such as PE or PVA film, and subsequently chemical reactions such as radical recombination reactions between fragment radicals and between a fragment radical and a substrate radical generated by a chain transfer reaction.

The thickness of the gel was determined by a real-time scanning laser microscopy. Above a fluence at 30mJ/cm<sup>2</sup>pulse, a gel with a measurable thickness was formed. The thickness of the fixed gel increased with an increase in fluence and the accumulation of pulses. The maximum thickness of the gel obtained in this experiment was approximately 0.7 $\mu$ m which was achieved with the fluence of 70mJ/cm<sup>2</sup>pulse and pulses of 100shots.

To determine how this method provides two-dimensional (2-D) accuracy, the PE-PDAA-PE film was irradiated through a photomask placed on the layered film and was subsequently washed with water. A fine structured 2-D pattern with hydrophilic and hydrophobic domains was successfully formed, where the irradiated regions were converted to a hydrogel, and the non-irradiated portions remained hydrophobic (**Figure 2**).

The effect of the hydrogelled surface on platelet adhesion was assessed *in vitro* by means of a scanning electron microscope. A non treated PE surface caused a marked platelet adhesion and deformation upon incubation with platelet-rich plasma for 1hr, whereas a significant inhibition of platelets adhesion was observed on hydrogelled surfaces. When heparin was premixed in a PDAA layer, immobilized heparin was released from a fixed hydrogel upon immersion into saline solution.

A new surface processing method enabling gel transfer and its surface fixation by an excimer laser ablation was developed. The photoprocessing technique developed here is based on a combination of UV-absorbing and non-absorbing substrates.

## REFERENCES

1. Nakayama Y, Matsuda T (1993) Photo induced surface heparin immobilization, *ASAIO J* 39: M754-M75
2. Nakayama Y, Matsuda T (1993) A novel surface photo-graft polymerization method for fabricated devices, *ASAIO J* 39: M542-M544
3. Srinivasan R, Braren B (1989) Ultraviolet laser ablation of organic polymers, *Chem Rev* 89: 1303-1316

## PVA HYDROGEL AS AN ARTIFICIAL VITREOUS BODY

Makoto.Kodama, Benlian Wang, Guoying Mu\*, Aizo Yamauchi\*\*,Toyoaki Matsuura\*\*\*, Yoshiaki Hara\*\*\*,Mototsugu Saishin\*\*\*

National Institute for Advanced Interdisciplinary Research, Tsukuba, Ibaraki 305, Japan, \*Jinan Municipal Center Hospital, \*\*HOYA Co. Ltd, \*\*\*Nara Medical University

### SUMMARY

This research goal is to explore biocompatible and extremely transparent artificial vitreous body, using poly (vinyl alcohol) (PVA) hydrogel. PVA of degree of polymerization (DP) 2,000 and DP 8,000 in aqueous solution were irradiated by gamma-ray to form hydrogels. These hydrogels were characterized by viscosity and dynamic light scattering to check about degradation and polymerization process. In vitro, the activity of chemotaxis of PVA hydrogel is almost same as that of silicone. PVA hydrogels were implanted into vitreous bodies of rabbits. No abnormality was histologically observed in cornea, lens and vitreous body, except some damage to injection areas in a few cases. No inflammatory reaction was observed between PVA hydrogels and native vitreous body. The postoperative intraocular pressure (IOP) was maintained within 8 mmHg higher than before operation. PVA hydrogel seems to have good biocompatibility for clinical usage.

KEY WORDS: PVA,  $\gamma$ -irradiation, hydrogel, artificial vitreous body, biocompatibility

### INTRODUCTION

A turbid, bleeding vitreous body will affect the sight, and the drainage of vitreous body can lead to serious damage of the retina and loss of vision. In the search for a substitute for the vitreous body, many materials have been tried, such as SF<sub>6</sub>, C<sub>3</sub>F<sub>8</sub> gases, hyaluronic acid, silicon oil and glycerol methacrylate etc. Each of them has shown some disadvantages, especially for long term usage. PVA can be changed into highly viscous and transparent hydrogel by  $\gamma$ -rays irradiation.<sup>1</sup> The biocompatibility and physical properties of this hydrogel are studied for clinical usage.

### MATERIALS AND METHODS

Poly (vinyl alcohol) (Kurare Inc.Ltd., Japan) of PVA 120 (DP 2,000) and PVA180 (DP 8,000) were used. PVA powders dispersed in water were put in an autoclave at 120°C for 60 min and then centrifuged at 10,000 rpm for 90 min, the supernatant solutions were transferred for  $\gamma$ -irradiation and PVA hydrogels were obtained. After being twice diluted with 0.3M NaCl and then centrifuged at 14,000 rpm for 60 min, the sample solutions for in vivo experiments were obtained. Here, the samples used in vivo are PVA 120. A sol: 3.5% in saline, no irradiation; B gel: 1.75% in saline, 0.48 MRad; C gel: 3.5% in saline, 0.17 MRad; D gel: 1.75% in saline, 0.17 MRad.

### EXPERIMENT

Rotating viscometer (Model, Tokyo Keiki Co.,Ltd.) and dynamic light scattering spectrophotometer (Model, DLS-700, Otsuka Electronics Co.,Ltd.) were used for characterization of PVA hydrogel. Male rabbits (Japanese white rabbit) were used for in vivo experiments. After extracting 0.4-0.6 ml of vitreous body, the same amounts of PVA substances were injected.

### RESULTS AND DISCUSSION

After  $\gamma$ -irradiation, the viscosity of gel, at first, slightly decreased within 0.1MRad and then increased beyond 0.3MRad as shown in Table 1 and the diameter determined by dynamic light scattering showed also same manners as listed in Table 1. This phenomenon seems to be

independent on molecular weight as shown in Table 1. These results suggest that it is necessary to take degradation and polymerization process in  $\gamma$ -irradiation into account to prepare PVA hydrogels. As Fig.1 shows, the activity of chemotaxis of PVA hydrogels was low and very close to that of medical silicon oil. Compared with the control saline, the intraocular pressure (IOP) of the implanted PVA hydrogel did not change so much and returned to the initial level after 3 weeks as shown in Fig.2.

Tab.1 Dependence of Viscosity and Radius Gyration of PVA Hydrogels on Dose of  $\gamma$ -irradiation

Sample	Concentration	Dose of Irradiation (MRad)	Viscosity (cp)	Radius Gyration (nm)
PVA120	3.80%	0	16.59	39.1
		0.08	13.20	26.2
		0.32	23.42	47.8
PVA180	0.46%	0	2.21	79.0
		0.08	1.32	61.0
		0.16	2.14	62.7
		0.32	31.20	377.0

## CONCLUSION

PVA hydrogel has good biocompatibility for clinical usage as substitute of vitreous body. Tissue growth process into network of PVA hydrogel and the biological interaction difference between PVA hydrogel and PVA sol will be further investigated.

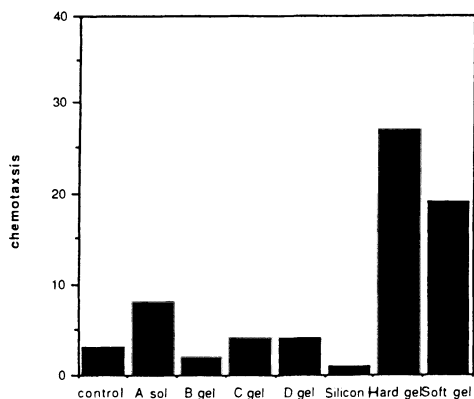


Fig. 1 Activity of Chemotaxis

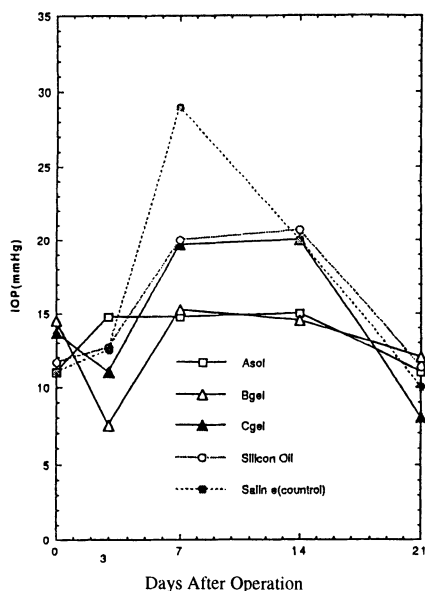


Fig. 2 IOP Changes After Implantation

## REFERENCE

1. Aizo Yamauchi (1981) Application of PVA-Gel for Optical Bio-medical Materials. J. Organic Synthesis Chemistry 39:238-242

# ANALYSIS OF PLASMA MEMBRANE GLYCOCALYX AND/OR OF QUANTITATIVE COMPUTERIZED CYTOLOGICAL IMAGE OF PLATELETS ADHERED TO HEMA-St ABA TYPE BLOCK COPOLYMER SURFACES WITH GOOD ANTITHROMBOGENICITY

Kazuhiko Abe, Motoaki Sugawara, Toshinobu Horie \* , Ken Suzuki \*\* , Teruo Okano \*\* and Yasuhisa Sakurai \*\*

Department of Cardiovascular Science, \* Department of Cardiology, The Heart Institute of Japan, and \*\* Institute of Biomedical Engineering, Tokyo Women's Medical College, 8-1 Kawada-cho, Shinjuku-ku, Tokyo 162, Japan.

**Keywords:** HEMA-St ABA type block copolymer, antithrombogenic material, platelet plasma membrane glycocalyx, platelet ultrastructure, computerized transmission electron microscopic image analysis

## Introduction

In the present study, for the purpose of making clearer the antithrombogenicity of HEMA-St ABA type block copolymer(HSB) surfaces<sup>1-9)</sup>, the preservation of the plasma membrane glycocalyx(GC) of the platelets adhered to the HSB surfaces was analyzed by transmission electron microscopy(TEM) because the GC plays an important role as an antenna for an informational recognition of a foreign surface. And then, the cytological changes observed by the TEM of the ultrathin vertical sections of the adhered platelets to the HSB surfaces were evaluated quantitatively using a high-speed image processor-analyzer(IA). PST and HEMA-St random copolymer surfaces were prepared as controls.

## Methods

All the polymer beads ( $\phi$  150  $\mu$ m) were closely packed in PVC columns(length: 10cm, inner diameter: 3mm) equipped with three-way cocks. The rat platelet suspension(density: nearly  $3 \times 10^{11}$  cells/ $\ell$ ) was prepared from the platelet pellet using  $\text{Ca}^{2+}$ ,  $\text{Mg}^{2+}$  free Hanks' balanced salt solution. The platelets flowed out of the columns at flow rate 0.5 ml/min for 3 minutes by the microsphere column method. And then, the columns were kept at room temperature for 5 hours. The polymer beads taken from the columns were fixed in buffered 1% glutaraldehyde solution with ruthenium red(R.R) and/or in buffered 1%OsO<sub>4</sub> solution with R.R. The preservation of the GC was analyzed by the TEM after carrying out the routine procedures such as EtOH dehydration, epoxy resin embedding etc. The cytological changes of the adhered platelets were evaluated by the IA on the strength of the TEM negative films. The four parameters (area, breadth, roundness and number of the storage granules per 1  $\mu$ m<sup>2</sup>) were measured by it. Comparison of the 3 groups and/or the 2 groups was made with statistics taken using the machintosh StatView.

## Results and Conclusions

Preservation of the adhered platelet GC: The platelets adhered to the HSB surfaces were observed to be round, holding the storage granules and the microtubules at both poles. The platelets were supported by the narrow spaces which formed scaffolding, keeping good preservation of the GC, the same as the intact platelet GC(Fig.1-A). On the other hand, the platelets adhered to the control polymer surfaces were observed to be spreading without the storage granules. The platelets didn't observe the narrow spaces in the GC, indicating strong adhesion. Their external GC was observed to be lacking in some places(Fig.1-B,C).

Quantitative evaluation of the adhered platelets' cytological changes: As shown in Figs. 2-4, the area, breadth and roundness of the platelets adhered to the HSB surfaces indicated significant difference compared to those of the control polymer surfaces. And then, as presented in Fig.5, the number of the storage granules per 1  $\mu$ m<sup>2</sup> of the platelets adhered to the HSB surfaces didn't indicate any significant difference compared to that of intact platelets.

It was found that the HSB surfaces inhibited remarkably the cytological and GC changes of the adhered platelets compared to those of the control polymer surfaces throughout 5 hours. These results suggest that remarkable inhibition of the platelets' cytological changes on the HSB surfaces is due to good preservation of the ultrastructure of the platelet GC and the continued soft landing of the platelets for 5 hours.

## References

- 1)Okano T. et al.: J Biomed Mater Res, 15: 393, 1981.
- 2)Okano T. et al.: Prg Artif Organs 7: 863, 1983.
- 3)Okano T. et al.: J Biomed Mater Res, 20: 919, 1986.
- 4)Nojiri C. et al.: Trans Am Soc Artif Intern Organs 33: 596, 1987.
- 5)Abe K. et al.: Jpn J Artif Organs, 21: 162, 1992.
- 6)Okano T. et al.: J Biomed Mater Res, 27: 1519, 1993.
- 7)Abe K. et al.: Jpn J Artif Organs, 22: 380, 1993.
- 8)Abe K. et al.: Jpn J Artif Organs, 23: 740, 1994.
- 9)Abe K. et al.: Jpn J Artif Organs, 24: 79, 1995.



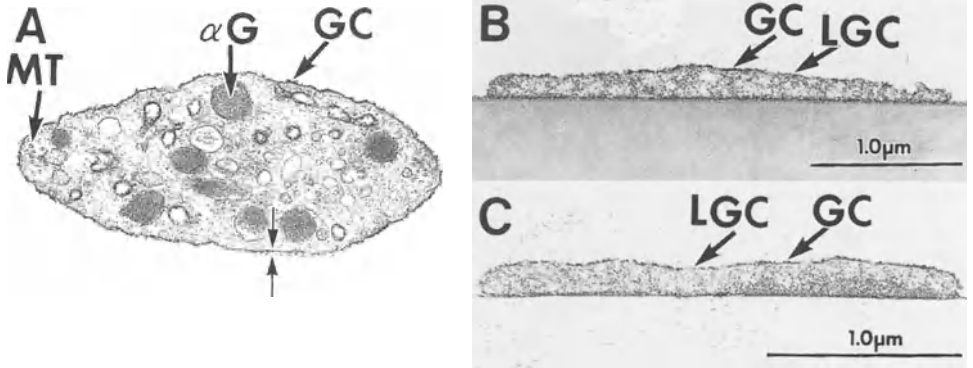
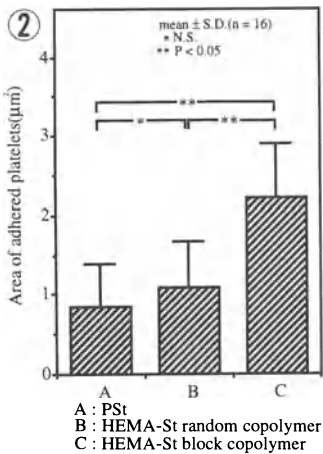
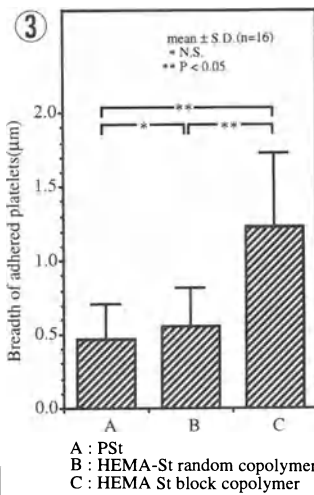


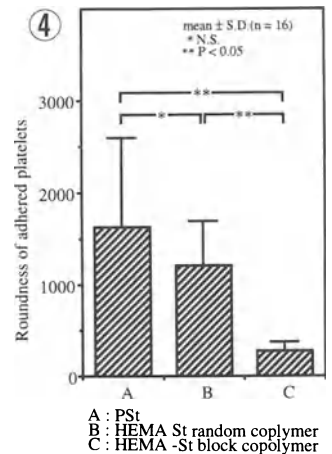
Fig.1 Transmission electron micrographs of platelet membrane glycocalyx adhered to the polymer surfaces for 5 hours. A, HEMA-St ABA type block copolymer ; B, PSt; C, HEMA-St random copolymer:  $\alpha$ G, alpha granule; MT, microtubule; GC, glycocalyx; LGC, lack of glycocalyx. The narrow space between the arrows is the platelet plasma membrane glycocalyx.



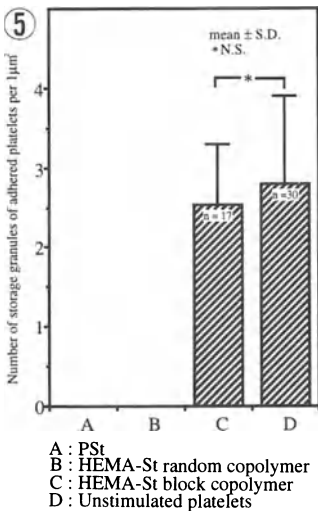
A : PSt  
B : HEMA-St random copolymer  
C : HEMA-St block copolymer



A : PSt  
B : HEMA-St random copolymer  
C : HEMA-St block copolymer



A : PSt  
B : HEMA-St random copolymer  
C : HEMA-St block copolymer



A : PSt  
B : HEMA-St random copolymer  
C : HEMA-St block copolymer  
D : Unstimulated platelets

Fig.2 Area of platelets adhered to the polymer surfaces for 5 hours, quantified by computer analysis of transmission electron microscopic images.

Fig.3 Breadth of platelets adhered to the polymer surfaces for 5 hours, quantified by computer analysis of transmission electron microscopic images.

Fig.4 Roundness of platelets adhered to the polymer surfaces for 5 hours, quantified by computer analysis of transmission electron microscopic images. "Roundness" indicates a coefficient of shape which is the maximum length squared, divided by the area. That is, the shape of cell indicates a value close to 100 as nearer to a circle, and greater value as more slender.

Fig.5 Number of storage granules per 1 μm² of platelets adhered to the polymer surfaces for 5 hours, quantified by computer analysis of transmission electron microscopic images

# IMMOBILIZATION OF HUMAN THROMBOMODULIN ONTO BIOMATERIALS: EVALUATION OF ANTITHROMBOGENICITY USING SMALL DIALYZER

Akio Kishida<sup>1</sup>, Yu-ki Akatsuka<sup>1</sup>, Yasuhiro Ueno<sup>1</sup>, Ikuro Maruyama<sup>2</sup>, Mitsuru Akashi<sup>1</sup>

1) *Department of Applied Chemistry and Chemical Engineering, Faculty of Engineering, Kagoshima University, 1-21-40 Korimoto, Kagoshima 890, Japan*

2) *Clinical Laboratory of Medicine, School of Medicine, Kagoshima University, 8-35-1 Sakuragaoka, Kagoshima 890, Japan*

## SUMMARY

Thrombomodulin (TM) is a newly described endothelial cell associated protein. In this study, focusing on the establishment of the practical evaluation of the hTM-immobilized materials, a novel testing systems for the immobilized-hTM activity were developed and studied. As the basis of immobilization, regenerated cellulose films and hollow fibers were used. Using hTM-immobilized cellulose hollow fiber, the small scale dialyzer was assembled and the its antithrombogenic effect on the human blood were studied using human blood circulation experiment. In conclusion, the immobilized hTM still has co-enzymatic activity for activation of protein C and anti-coagulant activity. We expect that hTM-immobilized biomaterials should be complement for conventional antithrombogenic biomaterials.

**KEY WORDS:** Human Thrombomodulin, Cellulose, Dialyzer, Immobilization,

## INTRODUCTION

Thrombomodulin (TM) is a newly described endothelial cell associated protein that functions as a potent natural anticoagulant by converting thrombin from a procoagulant protease to an anticoagulant.<sup>1)</sup> For fundamental study of usage of hTM, we have reported the immobilization of hTM onto various substrates<sup>3)</sup>. In those studies, we have defined that hTM-immobilized polymers were excellent for inhibiting both coagulation and platelet aggregation of human blood and that hTM was one of the most valuable biologically active substances to endow antithrombogenicity on polymer surface. However, it was difficult to determine the practical antithrombogenic activity of hTM-immobilized polymers because of the complex activation mechanism of hTM. As hTM needs frequent contact with thrombin for exhibiting high activity, the immobilized hTM shows relatively low activity by the conventional testing method. In this study, focusing on the establishment of the practical evaluation of the hTM-immobilized materials, a novel measuring method of immobilized-hTM were studied. As the basis of immobilization, regenerated cellulose films and hollow fibers were used. Using hTM-immobilized cellulose hollow fiber, the small scale dialyzer was assembled and the its antithrombogenic effect on the human blood were studied using human blood circulation experiment.

## MATERIALS AND METHODS

hTM, protein C and regenerated cellulose films and hollow fibers were donated by Asahi Chemical Industry Co., Ltd.(Tokyo, Japan). Fibrinogen was purchased from Baxter Healthcare Corporation(Miami, FL, U.S.A.). Other chemicals were purchased from WAKO Pure Chemicals(Osaka, Japan). The immobilization of hTM onto cellulose films and hollow fibers surfaces were carried out using cyanogen bromide method. The immobilized amount of hTM was quantified by the ninhydrin method which was reported in the former study. hTM activity was estimated by two kinds of methods, that is protein C activation test and fibrinogen clotting time test. Each experimental procedure was modified from that for the soluble hTM in order to measure the activity of immobilized hTM. The small scale dialyzer were assembled using 50 pieces of hTM-immobilized cellulose hollow fiber. The blood circulation experiment was designed using this small dialyzer(Fig.1). The clotting time of the eluted human blood through the hTM-immobilized dialyzer and original cellulose dialyzer were measured and compared, respectively.

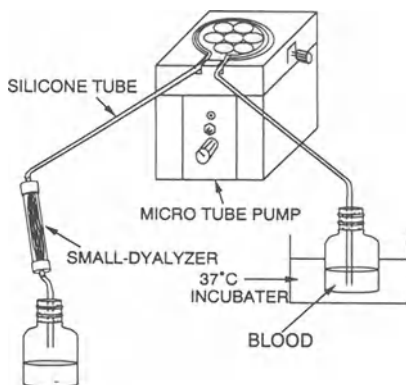


Fig.1 Human blood circulating test using small-dialyzer consisted of hTM-immobilized cellulose hollow fibers.

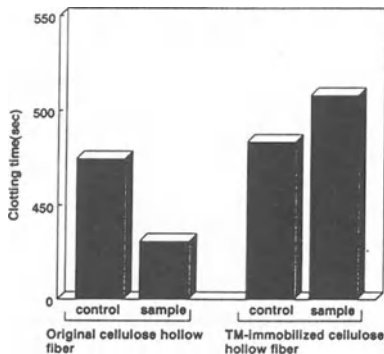


Fig.2 Anticoagulant activity of hTM-immobilized cellulose hollow fiber. Blood coagulation time was evaluated by the method of Lee-White.

## RESULTS

The almost same immobilized amount of hTM were obtained irrespective of substrate. The amount of immobilized hTM (ca.  $0.2 \mu\text{g}/\text{cm}^2$ ) in this case is approximately the 1/4 value as the value immobilized onto PAAc-grafted polymer surface. However, in protein C activation test, it was apparent that immobilized hTM onto cellulose film possessed enough protein C activation activity (data are not shown). On the other hand, the effect of the immobilized hTM on the thrombin-induced fibrinogen clotting time were very low. By simple calculation, the activity of the immobilized hTM seems to be 1/10 less than that of free hTM, but it is not correct that comparing those activities with each other so simply. Because, in the case of the free hTM, the hTM was dissolved homogeneously in the testing solution and could bind to thrombin everywhere in the solution, whereas the immobilized hTM could only bind to the thrombin which existed around the substrate. Thinking about these difference of local concentration of hTM, the activity of immobilized hTM was not so low. It needs other evaluation methods to determine the relative activity of immobilized hTM.

Consequently, the small dialyzer method were developed. In this system, the hTM/blood ratio could make much larger than that of conventional system. The result are shown in Figure 2. In the case of original cellulose dialyzer, the clotting time were shortening after passing the circuit. On the other hand, the clotting time of eluted blood through hTM-immobilized small dialyzer were markedly elongated. From this result, it become clear that immobilized hTM could exhibit superior antithrombogenicity under the adequate condition and this small dialyzer system was suitable for evaluation of hTM activity.

It is concluded that immobilized hTM still has co-enzymatic activity for activation of protein C and anti-coagulant activity. The relative activities of immobilized hTM were not determined accurately, however, it became clear that the immobilized hTM possessed the practically enough antithrombogenic activity. We expect that hTM-immobilized biomaterials should be complement for conventional antithrombogenic biomaterials.

## REFERENCES

1. Shirai T, Shiojiri S, Ito H, Yamamoto S, Kusumoto H, Deyashiki Y, Maruyama I, Suzuki K (1986) Gene structure of human thrombomodulin, a cofactor for thrombin-catalyzed activation of protein C. *J Biochem* 103: 281-285
2. Kishida A, Ueno Y, Maruyama I, Akashi M (1994) Immobilization of human thrombomodulin on biomaterials: evaluation of the activity of immobilized human thrombomodulin. *Biomaterials* 15: 1170-1174
3. Suzuki M, Kishida A, Iwata H, Ikada Y (1986) Graft copolymerization of acrylamide onto a polyethylene surface pretreated with glow discharge. *Macromolecules* 19: 1804-1808

# SURFACE CHARACTERIZATION OF HEMA-STYRENE BLOCK COPOLYMER USING TRANSMISSION ELECTRON MICROSCOPY

Kazuhiisa Senshu, Chisato Nojiri, Takayuki Kido, Shuzo Yamashita, Akira Hirao<sup>§</sup>, Seiichi Nakahama<sup>§</sup>

*R&D Center, Terumo Corp., 1500 Inokuchi, Nakai-machi, Ashigarakami-gun, Kanagawa, 259-01, Japan Phone #81-465-81-4121, Fax #81-465-81-4114*

*§ Dep. Polym. Chem., Tokyo Institute of Technology, 2-12-1 Ohokayama, Meguro-ku, Tokyo, 152, Japan Phone #81-3-5734-2138, Fax #81-3-5734-2888*

**ABSTRACT :** We have already demonstrated that an amphiphilic block copolymer composed of 2-hydroxyethyl methacrylate(HEMA) and styrene, HS, showed excellent blood compatibility. The present study was carried out to characterize the surface structure of HS under dry and wet conditions, and after 372 days implantation as a vascular graft, using transmission electron microscopy (TEM). The HS which contains 63 wt% of polyHEMA segment was synthesized by the coupling reaction between semitelechelic polyHEMA and telechelic polystyrene. Under dry condition, the top surface of HS film was almost completely covered with polystyrene segment. On the other hand, at the surface after hydration, the polystyrene microdomains wrapped with PHEMA segments stretched toward the water side, which indicated surface restructuring in response to environmental changes. Protein layer thickness on the graft surface after implantation measured by TEM indicated to be less than 200 Å, and in the microdomain structure beneath the protein layer with an alternate arrangement of polystyrene and PHEMA segments, stretched domains could not be recognized. These differences in the surface structures might be attributable to differences of the ambient environment. Moreover, such surface dynamics might influence the blood compatibility of HS.

**KEY WORDS :** HEMA/styrene block copolymer, vascular graft, transmission electron microscopy, adsorbed protein layer, surface restructuring

## INTRODUCTION

Hydrophilic-hydrophobic block copolymer composed of poly(2-hydroxyethyl methacrylate) (PHEMA) and polystyrene(PSt), HS, has been well-known as an excellent blood compatible material [1]. It is said that the nonthrombogenicity of HS surfaces is attributable to the organized protein layer adsorbed on HS corresponding to the morphology and size of its microdomain structure [2]. In order to investigate the mechanism of nonthrombogenicity of HS, surface structure was characterized by transmission electron microscopy(TEM) observation under dry and wet conditions, and compared with that of after implantation as a small vascular graft.

## METHODS

### Graft Preparation, Implantation, and Harvesting

The HS was prepared by the addition reaction of telechelic polystyrene with isocyanate terminals and semitelechelic PHEMA with amino group at one chain end [3]. Commercialized Dacron vascular graft (3 mm ID, 7 cm in length) was first coated on its luminal surface with polyurethane(PU) to obtain a smooth surface, then coated with HS. HS coated grafts were implanted in bilateral carotid arteries of dogs. After implantation at 372 days, the grafts were surgically removed with adjacent arteries intact at the proximal and distal anastomosis [4].

### TEM Observation

The harvested grafts were stained and fixed with a 1% OsO<sub>4</sub> aqueous solution. After freeze-dried, it was provided for TEM observation. To obtain the cross sectional TEM views of HS before implantation under dry and wet conditions, the sample preparation was carried out as follows; HS coated PU sheets were prepared by dipping method, and dried *in vacuo* for 24 h. Then, the dry sample was fixed with OsO<sub>4</sub> crystal vapor, and the wet ones (immersed in water or saline for 1 h.) were fixed with 4% OsO<sub>4</sub> aqueous solution. After dried, the samples (dry, wet in water, wet in saline, and after implantation for 372 days) were embedded in epoxy resin, and sectioned with an ultramicrotome. TEM views were observed with a JEOL 1200EX at an accelerated voltage of 80 kV [5].

## RESULTS AND DISCUSSION

The cross sectional TEM views of the HS coated PU under dry and wet conditions are shown in Figure 1. Black area indicates the PHEMA domains stained with OsO<sub>4</sub>. Both dry and wet HSs showed the sea-island like microdomain structures in bulk. However, there was significant difference at the outermost surface between under dry and wet conditions. At the top surface under dry condition, both PSt island and PHEMA matrix were partly observed intact, and several PSt islands were combined with each other to form the larger domains (Fig.1a). It is indicated that PSt segment was concentrated at the surface, yet not completely. These results well corresponded to those of angle-dependent XPS and static-SIMS measurement performed by Ratner *et al* [6]. At the top surface after soaking in water for 1 h, the PSt layer almost disappeared and the PSt islands at the top surface were stretched toward water side (Fig 1b). Such distorted PSt domains observed all over the surface was ambiguous, PHEMA chains linked with PSt segment on the stretched domain might diffuse into water resulting in the wettable surface. It should be noticed that the morphological change by soaking in water occurs only at the top surface region. The similar TEM view was obtained from the sample by soaking in saline for 1h. Before implantation, the HS coated graft was immersed in saline overnight. Figure 1b shows the surface structure of HS coated graft before implantation.

Figure 2 shows the cross sectional TEM view of HS surface 372 days after carotid replacement. At the top surface, the thin protein layer on the HS surface stained with OsO<sub>4</sub> was observed (thickness: less than 200 Å), and the microdomain structure of HS was also observed. When the surface structure of HS after implantation was compared with the original surface (Fig. 1b), the domains stretched toward the water side at the top surface were not recognized. The difference of the surface structures might be attributable to the difference of the immersion medium, *i.e.*, saline or blood. It is indicated that the HS showed the dynamic surface structural changes in response to the environmental change. Though it can not explain well in this study why these phenomena occur, such a strange surface dynamics of HS might be attributed to its blood compatible behavior *in vivo*.

## REFERENCES

- Okano T, Suzuki K, Yui N, Sakurai Y, Nakahama S (1993) Prevention of changes in platelet cytoplasmic free calcium levels by interaction with 2-hydroxyethyl methacrylate/styrene block copolymer surfaces. *J. Biomed. Mater. Res.* 27:1519-1525
- Nojiri C, Okano T, Grainger D, Park KD, Nakahama S, Suzuki K, Kim SW (1987) Evaluation of nonthrombogenic polymers in a new rabbit A-A shunt model. *Trans ASAIO*, 33:596-601
- Okano T, Katayama M, Shinohara I (1978) The influence of hydrophilic and hydrophobic domains on water wettability of 2-hydroxyethyl methacrylate-styrene copolymers. *J. Appl. Polym. Sci.* 22:369-377
- Nojiri C, Okano T, Takemura N, Senshu K, Kido T, Koyanagi H, Kim SW, Akutsu T (1993) Improved Patency of HEMA/styrene block copolymer-coated small vessel prosthesis without neointima formation. In: Akutsu T, Koyanagi H (eds) *Artificial Heart 4*. Springer-Verlag, Tokyo, pp53-60
- Senshu K, Yamashita S, Ito M, Hirao A, Nakahama S (1995) Surface characterization of 2-hydroxyethyl methacrylate/styrene block copolymers by TEM observation and contact angle measurement. *Langmuir* in press
- Castner DG, Ratner BD, Grainger DW, Kim SW, Okano T, Suzuki K, Nakahama S (1992) Surface characterization of 2-hydroxyethyl methacrylate/styrene copolymers by angle-dependent X-ray photoelectron spectroscopy and static secondary ion mass spectrometry. *J. Biomater. Sci. Polym. Edn.* 3:463-480

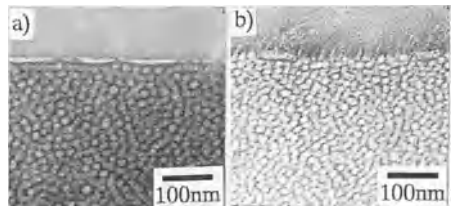


Fig.1 Cross sectional TEM pictures of HS a) under dry condition , b) after soaking in water for 1h (from [5] copyright, reprinted by permission of ACS)



Fig. 2 Cross sectional TEM picture of HS surface 372 days after carotid replacement (from [4] copyright, reprinted by permission of Springer-Verlag)

# INDUCTION OF ENDOTHELIAL CELL DIFFERENTIATION ON COPOLYMER SURFACES HAVING PHENYLBORONIC ACID GROUPS

Takashi Aoki\*, Yayoi Nagao\*, Etsuko Terada\*, Kohei Sanui\*, Naoya Ogata\*, Noriko Yamada\*\*, Akihiko Kikuchi\*\*, Teruo Okano\*\*, Yasuhisa Sakurai\*\* and Kazunori Kataoka\*\*\*

\*Department of Chemistry, Faculty of Science and Technology, Sophia University, 7-1 Kioi-cho, Chiyoda, Tokyo 102, Japan,

\*\*Institute of Biomedical Engineering, Tokyo Women's Medical College, 8-1 Kawada-cho, Shinjuku, Tokyo 162, Japan,

\*\*\*Department of Materials Science and Research Institute for Biosciences, Science University of Tokyo, 2641 Yamazaki, Noda, Chiba 278, Japan,

## ABSTRACT

The ternary copolymers composed of *m*-acrylamidophenylboronic acid, N,N-dimethylaminopropylmethacrylamide and N-isopropylacrylamide were synthesized. Bovine aortic endothelial cells (BAECs) on the copolymer substrata demonstrated adhesion and spontaneously developed into capillary networks. The interactions between phenylboronic acid groups in copolymer and glycoconjugates on endothelial cell plasma membranes are proposed to regulate the induction of tissue formation, since phenylboronic acid groups are known to specifically form reversible complexes with *cis*-diol compounds such as glucose. The copolymers having phenylboronic acid moieties are novel materials capable of mediating specific signals analogous to extracellular matrix to induce endothelial cells into capillary structures.

**KEYWORDS:** Phenylboronic acid, Endothelial cell, Cell culture, Capillary formation, Glycoconjugates

## INTRODUCTION

The boronate compounds strongly bind to 1,2 *cis*-diol compounds such as glucose<sup>1,2</sup>). Recently, glucose-sensitive polymer complexes based on boronate/diol interactions have been reported<sup>3,4</sup>). It is understood that phenylboronic acid groups bind the *cis*-diol compounds in aqueous media at above pH8.5<sup>3</sup>) and that incorporation of amino groups into the copolymer promotes the formation of these complexes under physiological pH conditions<sup>4</sup>). Furthermore, proliferation of lymphocytes in culture has been induced via binding of cell membrane components with phenylboronic acid groups within a copolymer molecule<sup>5</sup>). It is hypothesized that boronate moieties interact with glycoconjugates existed on cell membranes and send specific signals to the cells. From this perspective, BAECs have been cultured on a synthetic ternary copolymer (IAB) substrate composed of *m*-acrylamidophenylboronic acid (B), N,N-dimethylaminopropylmethacrylamide (A) and N-isopropylacrylamide (I), and tissue formation of the cells have been observed<sup>6</sup>). It is found that the ternary copolymer induces BAECs into capillary structures. This paper describes that the related copolymers with various compositions of both boron and amine units are synthesized and the shape changes to network formation of the BACEs on the copolymer substrates are investigated.

## MATERIALS AND METHODS

The ternary copolymers (IAB/X, X denotes the mole percentage of boron unit in the copolymer) were each synthesized in 100cm<sup>3</sup> of DMF at 70°C for 2h using 0.13mM of 2,2'-azobis(isobutyronitrile) as a free-radical initiator. Bacteriological dishes (Falcon #3001) were precoated by casting aqueous solutions of the copolymers. BAECs were plated at an initial cell density of approximately 2x10<sup>4</sup>cells/cm<sup>2</sup> on each polymer-coated dish. Dulbecco's modified essential medium (DMEM) with supplements was used as a culture medium. The cultured cells were observed by a phase-contrast microscope.

## RESULTS AND DISCUSSION

The BAECs plated onto IAB/2-coated dishes showed lower adhesion efficiencies than those on tissue culture (TC) dishes. The cell adhesion % on IAB-coated and TC dishes after 1day in culture were approximately 24% and 87%, respectively. Furthermore, there were different mechanisms of the cell adhesions between on the both dishes. The treatment of the cultured cells with a trypsin-EDTA solution occurred to easily detach from TC dish surfaces and to remain of attachment to the IAB substrate surface. Then, the cells stabilized on IAB-coated dishes were readily removed from this copolymer surfaces by addition of buffer solution containing 4.5mg/ml of glucose into the copolymer-coated wells. It was considered that the cell adhesion onto the IAB substrate surfaces is mediated through interactions between carbohydrates on cell membranes and phenylboronic acid groups exposed at the surface of the IAB copolymer coating. Moreover, long-term culture of the BAECs on both IAB/2 copolymer and TC culture dishes was carried out. In the confluent state, while cell monolayers on TC dishes did not show any further changes, formation of capillary cell structures was clearly observed after 26days in culture. It is confirmed that the TEM observation proves that a tube seems to be a true vacuole surrounded by four cells. As network formation of BAECs cultured on IAB-coated dishes is observed under normal culture conditions, it is considered that interactions between IAB copolymer surfaces and cell membrane components govern these morphological changes<sup>6</sup>).

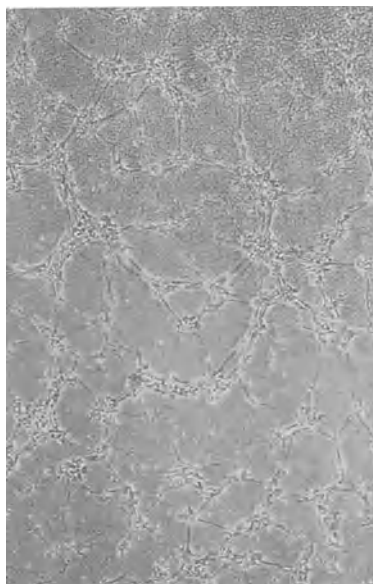


Figure1 Phase-contrast photograph of BAECs cultured on IAB/12-coated dishes for 1day. Magnification: 100X.

The BAECs were cultured on the other copolymer (IAB/12) with different compositions of boron and amine units. The IAB/12 copolymer contained higher composition of both units than IAB/2. As shown in Figure1, the cells plated on IAB/12-coated dishes showed adhesion of network formation after 1day in culture. It was observed that the network formation of the cells on the IAB/12 substrate exhibited high efficiency compared with that of the IAB/2 substrate. It is considered that the IAB/12 surfaces enhance the interactions between the cell membrane components and phenylboronic acid moieties, showing the network formation after 1day in culture.

In conclusion, these results indicate that IAB copolymer surfaces spontaneously induce differentiation of BAECs into capillary structures resembling angiogenesis and that phenylboronic acid groups in the IAB polymer are responsible in part for inducing the attachment, alignment and organization of BAECs into angiogenic-like tubes.

## REFERENCES

- 1) S. A. Barker, A. K. Chopra, B. W. Hatt and P. J. Somers (1973) The interaction of areneboronic acids with monosaccharides. *Carbohydr. Res.* 26: 33-40.
- 2) S. A. Barker, B. W. Hatt, P. J. Somers and R. R. Woodbury (1973) The use of poly(4-vinylbenzeneboronic acid) resins in the fractionation and interconversion of carbohydrates. *Carbohydr. Res.* 26: 55-64.
- 3) S. Kitano, K. Kataoka, Y. Koyama, T. Okano and Y. Sakurai (1991) Glucose-responsive complex formation between poly(vinylalcohol) and poly(N-vinyl-2-pyrrolidone) with pendant phenylboronic acid moieties. *Makromol. Chem., Rapid Commun.* 12: 227-233.
- 4) S. Kitano, I. Hisamitsu, Y. Koyama, K. Kataoka, T. Okano and Y. Sakurai (1991) Effect of the incorporation of amino groups in a glucose-responsive polymer complex having phenylboronic acid moieties. *Polymers for Advanced Technologies* 2: 261-264.
- 5) H. Miyazaki, A. Kikuchi, Y. Koyama, T. Okano, Y. Sakurai and K. Kataoka (1993) Boronate-containing polymer as novel mitogen for lymphocytes. *Biochem. Biophys. Res. Commun.* 195: 829-836.
- 6) T. Aoki, Y. Nagao, E. Terada, K. Sanui, N. Ogata, N. Yamada, Y. Sakurai, K. Kataoka and T. Okano, Endothelial cells differentiation into capillary structures by copolymer surfaces with phenylboronic acid groups. Accepted to *J. Biomaterials Sci., Polym. Ed.*

# IMMOBILIZATION OF BIOSIGNAL PROTEINS TO CONTROL CELLULAR FUNCTIONS

Yoshihiro Ito\*, Ji Zheng, and Yukio Imanishi

*Division of Material Chemistry, Faculty of Engineering, Kyoto University, Kyoto, 606-01, Japan*

## ABSTRACT

Insulin was immobilized on surface-hydrolyzed poly(methyl methacrylate) membrane anchorage-dependent and anchorage-independent cells were cultured on the insulin-immobilized membrane. The growth of anchorage-dependent cell was efficiently enhanced by the very small amount of immobilized insulin (1/10 to 1/100 of free insulin) and coimmobilization of cell adhesion factors promoted the effect. Although anchorage-independent cell was not affected by the immobilized insulin, coimmobilization accelerated the cell growth by enhancing the adhesion. In addition by using a cell overexpressing insulin receptor it was revealed that the cellular receptors was autophosphorylated by the immobilized insulin after time lag needed for the adhesion.

**KEY WORDS:** Immobilization, Insulin, Growth Factor, Adhesion factor, Cell Culture

## INTRODUCTION

Cellular functions, such as proliferation and differentiation, are generally regulated by communications between the cell and biosignals including those from cells, extracellular matrices, and soluble molecules. The soluble biosignal molecules are classified into two types. One is that of low molecular weight, which permeates cell membrane and directly interacts with nucleus. The other is that of high molecular weight such as polypeptide growth factors. They interact their receptor on the cell membrane and form complexes. The complexes are internalized into the target cell to be decomposed in lysosomes. Some of the liberated receptors are transported back to the cell surface.

We covalently immobilized insulin, one of the representative growth factor, on various materials and found that the materials significantly accelerated cell growth. In addition, the immobilized insulin was more active than soluble one (1,2).

This paper shows the biochemical analysis of signal transduction of immobilized insulin and the coimmobilization of different types of biosignal protein to enhance the biosignal effect of immobilized insulin.

## MATERIALS AND METHODS

Poly(methyl methacrylate) (PMMA) film was prepared as previously reported (3,4). After the hydrolysis of the film insulin or adhesion factor polypeptides, polylysine and collagen was immobilized on the treated film by water-soluble carbodiimide. Covalent immobilization of insulin was confirmed using <sup>125</sup>I-labelled insulin.

Chinese hamster ovary (CHO) cell overexpressing insulin receptor (5) for biochemical analysis, mouse fibroblast cell STO as an anchorage-dependent cell, human chronic myelogenous leukemia K562 cell as an anchorage-independent cell were cultured and the growth rates (DNA syntheses) were measured as previously reported (3,4).



Autophosphorylation of insulin receptor (IR) and insulin receptor substrate-1 (IRS-1), and activation of phosphatidylinositol-3 (PI-3) kinase of the transfected CHO cell were analyzed as previously reported (5).

## RESULTS AND DISCUSSION

CHO cells were cultured on the insulin-immobilized PMMA film. The cell growth was significantly accelerated on the film, and the growth rate was higher than that in the presence of soluble insulin. Very small amount of immobilized insulin (1/10 to 1/100 of free insulin) was enough for the acceleration of cell growth.

Autophosphorylation of IR and IRS-1 and activation of IP-3 kinase was observed in CHO cells cultured on the insulin-immobilized film as in the presence of soluble insulin. In addition, although a straightforward comparison of the effects of soluble and immobilized insulin is difficult because of the different numbers of interacting cells and the lag time for cell adhesion in the case of immobilized insulin, the time course of phosphorylation and activation of signal proteins is apparently different between the two states. In the case of immobilized insulin, the receptor phosphorylation and enzyme activation increased with increasing interaction time, whereas in the case of soluble insulin both reactions reached maximum after several ten of minutes and ceased. These results indicate that specific interactions occur between the immobilized insulin and the receptor, and that the higher acceleration of cell growth by immobilized insulin is attributed to the overphosphorylation and overactivation as a result of the inhibition of internalization. Phosphorylation of integrin or neighboring proteins without internalization of extracellular matrices and growth of cells having noninternalizing EGF receptors have recently reported. Taking these results into consideration, it is feasible to say that the immobilized insulin stimulates IR without down-regulation of the insulin.

STO (anchorage-dependent) and K562 (anchorage-independent) cells were cultured on the insulin-immobilized, and insulin- and adhesion-factor (polylysine or gelatin)-coimmobilized PMMA films. The growth of STO was accelerated on the insulin-immobilized film, and the acceleration effect was enhanced by coimmobilization of adhesion factors. No significant difference between polylysine, physicochemical adhesion factor, and gelatin, biological adhesion factor, was observed in the acceleration effect.

In the case of K562 cell, the growth rate was not accelerated on the insulin-immobilized film. However, by coimmobilization of adhesion factors, the cell adhesion was enhanced, resulting in growth enhancement. There is also no significant difference among the adhesion factors. Coimmobilization of adhesion factors should increase the frequency of interaction between the target cell and the immobilized insulin.

## REFERENCES

1. Ito Y (1992) Cell-growth-factor-immobilized materials. In: Imanishi Y (ed) *Synthesis of Biocomposite Materials*, CRC Press, Boca Raton, 285-305
2. Ito Y, Zheng J, Liu SQ, Imanishi Y (1994) Novel biomaterials immobilized with biosignal molecules. *Materials Science & Engineering C2*:67-72
3. Zheng J, Ito Y, Imanishi Y (1994) Cell growth on immobilized cell-growth factor. Insulin and polyallylamine coimmobilized materials. *Biomaterials* 15:963-968
4. Zheng J, Ito Y, Imanishi Y (1995) Growth enhancement of anchorage-dependent and anchorage-independent cells by coimmobilization of insulin with polyallylamine and gelatin. *Biotechnol. Prog.* in press
5. Endemann G, Yonezawa K, Roth R (1990) Phosphatidylinositol kinase or an associated protein is a substrate for the insulin receptor tyrosine kinase. *J. Biol. Chem.* 265:396-400

# TEMPERATURE-MODULATED SURFACE HYDROPHILIC / HYDROPHOBIC ALTERATIONS FOR NOVEL RECOVERY OF CULTURED CELLS

Akihiko Kikuchi, Minako Okuhara, Fumiko Ogura, Yasuhisa Sakurai and Teruo Okano

Institute of Biomedical Engineering, Tokyo Women's Medical College  
8-1 Kawadacho, Shinjuku, Tokyo 162, JAPAN

## SUMMARY

Poly(*N*-isopropylacrylamide) (PIPAAM)-grafted surfaces show hydrophilic/hydrophobic surface property alteration upon temperature changes. Utilizing this property changes, we can cultivate cells on its surface at 37°C and detach cultured cells by lowering temperature. Cellular metabolisms are revealed to be involved in cell detachment from PIPAAm-grafted surfaces by temperature changes. We have also succeeded to recover viable confluent culture of hepatocytes as well as endothelial cells from PIPAAm grafted surfaces by temperature treatment.

**KEYWORDS:** Poly(*N*-isopropylacrylamide) (PIPAAM), temperature-responsive surfaces, hydrophilic/hydrophobic surface property changes, cell detachment, cell metabolism

## INTRODUCTION

PIPAAM shows reversible soluble-insoluble changes in aqueous milieu upon temperature changes. Due to this unique property, PIPAAm and its derivatives have been utilized for thermo-responsive bioseparation as well as drug delivery systems [1-4]. We have been studying PIPAAm-grafted surfaces for novel recovery system of cultured cells [5-7]. Hydrophilic/hydrophobic property changes of PIPAAm-grafted surface can easily be controlled by temperature changes, being hydrophobic above its LCST. Cultured cells on PIPAAm-grafted surfaces have found to be recovered by lowering temperature. This is quite interesting, because trypsin treatment for cell recovery is not necessary by using PIPAAm-grafted dishes. In the present study, mechanism of cell detachment from the surface of PIPAAm-grafted dishes are investigated. Furthermore, successful recovery of confluent culture was achieved using PIPAAm-grafted dish.

## MATERIALS AND METHODS [5-7]

PIPAAM molecules were introduced to polystyrene surface by electron beam irradiation. Briefly, IPAAm in isopropyl alcohol was added to polystyrene dishes, and these dishes were allowed to irradiate electron beam. After washing with cold water to remove non-grafted IPAAm and drying, PIPAAm-grafted dishes were gas-sterilized by ethylene oxide. Cells used in culture experiments were bovine aortic endothelial cells and rat hepatocytes. These cells were cultured in DMEM and William's E with supplements, respectively, in a humidified atmosphere of 5% CO<sub>2</sub> at 37 °C. Lower temperature treatment was carried out as follows: Cells were plated on PIPAAm-grafted dishes at 4 x 10<sup>4</sup> cells/cm<sup>2</sup> and inoculated for 2 days. Temperature was then lowered to a predetermined degree for 30 min without changing medium. The detached cells were collected with minimal pipetting and counted to determine %-recovery.

## RESULTS AND DISCUSSION

On the surfaces of PIPAAm-grafted dish, both endothelial cells and hepatocytes attached and proliferated. Growth rate of these cells were comparable to that on conventional tissue culture dishes. The detachment of cultured cells are investigated in terms of temperature and cellular metabolism. Changes in cell morphologies at 25 °C after 30 min incubation at 10 °C was observed by SEM. By 30 min incubation at 10 °C, attached hepatocytes were in spread shape and they did not detach from the surface. However, following incubation at 25 °C greatly affected the cell morphology, cells become in round shape and finally detached from the surface. Figure 1 shows the temperature dependence of hepatocyte detachment from PIPAAm-grafted surfaces. Cells remained on the surface by 30 min and/or 35 min incubation at constant temperature, T °C (curves B and C).

As temperature decreases, PIPAAm chains are assumed to be hydrated and be in expanded conformation, resulting in reduced cell-materials interaction. From Figure 1, hydration of PIPAAm at cell-materials interface is not considered to be only a factor for cell detachment. An additional 5 min incubation at 25 °C after 30 min at T °C drastically enhanced cell detachment as shown in Figure 1 (curve A). As cellular metabolism is suppressed at lower temperature, the results suggest that the cellular metabolic process as well as hydration of PIPAAm grafts might be involved in the cell detachment process. The effect of NaN<sub>3</sub> was then investigated to elucidate the role of cell metabolism in cell detachment. Cultured hepatocytes were treated with 2 mM NaN<sub>3</sub> to partially inhibit cell metabolism and examined cell detachment by lowering temperature. The percentage of detached cells by lowering temperature (30 min at 10 °C and additional 5 min at 25 °C) was decreased from 90% to approximately 50% by the treatment of cells with 2 mM NaN<sub>3</sub>. This result strongly suggests that cell metabolism enables morphological changes of attached cells and, as a consequent, detachment of cells from hydrated surfaces is observed. Similar results were obtained for endothelial cells.

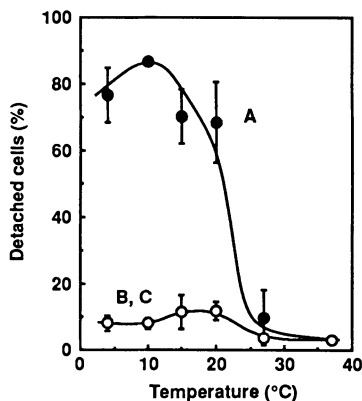
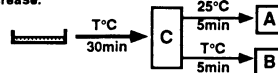


Figure 1 Hepatocytes detachment by temperature decrease.



There are two distinct stages involved in cell adhesion; 1) passive adhesion by contact cells with surfaces, and 2) active adhesion where cells dynamically change their morphologies to optimize and stabilize cell-material interaction. For detachment of cells in active adhesion, energy consuming cell shape change might be necessary. By lowering temperature, hydration of grafted PIPAAm initiates cell detachment. Adhered cells are required to change their shape consuming metabolic energy for further detachment. Therefore, optimum temperature is observed for cell detachment from PIPAAm-grafted surfaces. It is revealed that cells recovered by temperature treatment retained their high functionality as judged by secretion of 6-keto-PGF<sub>1</sub>α for endothelial cells and albumin for hepatocytes, respectively. These results strongly suggest the feasibility of novel cell recovery system using temperature-responsive hydrophilic/hydrophobic alterations of PIPAAm-grafted surfaces.

## REFERENCES

- Chen JP, Hoffman AS (1990) Polymer-protein conjugates II: Affinity precipitation separation of human immunoglobulin by a poly(N-isopropylacrylamide)-protein A conjugates. *Biomaterials* 11:631-634
- Takei YG, Aoki T, Sanui K, Ogata N, Okano T, Sakurai Y (1993) Temperature-responsive bioconjugates 2: Molecular design for temperature-modulated bioseparations. *Bioconjugate Chem* 4:341-346
- Matsukata M, Takei Y, Aoki T, Sanui K, Ogata N, Sakurai Y, Okano T (1994) Temperature modulated solubility-activity alterations for poly(N-isopropylacrylamide)-lipase conjugates. *J Biochem* 116:682-686
- Okano T, Bae YH, Jacobs H, Kim SW (1990) Thermally on-off switching polymers for drug permeation and release. *J Controlled Release* 11:255-265
- Yamada N, Okano T, Sakai H, Karikusa F, Sawasaki Y, Sakurai Y (1990) Thermo-responsive polymer surfaces; control of attachment and detachment of cultured cells. *Makromol Chem Rapid Commun* 11:571-576
- Okano T, Yamada N, Sakai H, Sakurai Y (1993) A novel recovery system for culture cells using plasma-treated polystyrene dishes grafted with poly(N-isopropylacrylamide). *J Biomed Mater Res* 27:1243-1251
- Okano T, Yamada N, Okuhara M, Sakai H, Sakurai Y (1995) Mechanism of cell detachment from temperature-modulated, hydrophilic-hydrophobic polymer surfaces. *Biomaterials* 16:297-303

# CELL CULTURES ON PLASMA-MODIFIED NYLON MESHES AND COLLAGEN/NYLON COMPOSITE BIOMATRIX

S.M. Kuo, S. W. Tsai and Y. J. Wang

Institute of Biomedical Engineering, National Yang Ming University, Shih Pai, Pei Tou, Taipei, Taiwan, Fax No (02)8210847

## SUMMARY

Commercial nylon meshes were aminated with plasma in the presence of ammonia gas and then used for culturing of 3T3 cells. The cell densities of 3T3 cells are about the same on these films in spite of their differences of pore size. A higher cell density can be further attained by the inclusion of reconstituted collagen matrices within the pores of nylon mesh. This collagen/nylon composite biomatrix provides a good environment for cell growth.

Key words: plasma, nylon, collagen, biomatrix.

## INTRODUCTION

Low temperature plasmas have been used quite often in modifying the surfaces of polymeric materials. One modification method involves the amination of the membrane with the plasma-activated ammonia gas. We have previously aminated the surface of the poly(propylene) membrane and reported its application in the urea sensor construction [1]. In this study, we aminate porous nylon meshes with plasma and investigate their applications as matrices for cell culture. In addition, collagen/nylon composite biomatrices were fabricated by reconstituting collagen fibrils in the presence of nylon mesh. The growth characteristics of the 3T3 fibroblast cells cultured in these matrices are discussed.

## MATERIALS AND METHODS

Nylon membranes with three different pore sizes ( $5\ \mu\text{m}$ ,  $10\ \mu\text{m}$  and  $20\ \mu\text{m}$  in diameter) were treated with the anhydrous ammonia gas activated in the chamber of a bell-jar type plasma reactor (model PD-2, Samco) under the ammonia pressure of 0.01 Torr and 30 W power for 10 min. The plasma-activated nylon was then exposed to the ammonia gas for another 30 min. Type I collagen was prepared from rat tail tendon according to the method described by Grinnell *et al* [2]. The prepared collagen was dissolved in acetic acid and stored at  $4^{\circ}\text{C}$ . The collagen solution was dialyzed against PBS overnight at  $4^{\circ}\text{C}$  before use. The pores of nylon membrane were then filled with ice cold collagen solution which was reconstituted by raising temperature to  $37^{\circ}\text{C}$ . 3T3 fibroblast cells were cultured in the matrices of nylon membranes or collagen/nylon composites. The petri dishes of bacterial grade were used as the containers to minimize the attachment of cells to the culture dishes. The 3T3 fibroblast cells were harvested by detachment of cells from the matrices with trypsin digest. The number of the viable cells were counted by using the trypan blue exclusion method.

Table 1 Proliferation of cells on nylon membranes

Days after inoculation	Cells density, $\times 10^4$ cells/cm <sup>2</sup>	
	Plasma-activated membrane	Unmodified membrane
1	1.3	0.4
2	2.0	1.0
3	4.6	1.6

## RESULTS AND DISCUSSION

The polymeric surfaces of three commercial nylon films with mesh openings of  $5 \mu$ ,  $10 \mu$  and  $20 \mu$  were treated with anhydrous ammonia gaseous plasma. Cells cultured on the plasma-treated nylon films have higher proliferation rates than the unmodified nylon membranes (Table 1). Furthermore, cells grew on the plasma-aminated membrane exhibited rougher surface than that of the cells grew on the untreated nylon membrane. The cells wrapped around smoothly on the curved surfaces of the nylon fibers. These cells displayed bipolar shape with their long axis coincide with the fiber direction. The same phenomena were also reported by Ricci et al [3] by culturing tendon cell on carbon fiber. The cell density of the plasma-modified nylon mesh reached  $4.6 \times 10^4$  cells/cm<sup>2</sup> in three days as compared to  $1.6 \times 10^4$  cells/cm<sup>2</sup> proliferated on the plain nylon membrane.

Of the three plasma-modified membranes, cells proliferated to the largest population on the membrane with mesh openings of  $5 \mu$  m. This is mainly due to the effect of surface area since the cell densities of the cultures on all three plasma-modified membranes are  $3.8 \times 10^4$ ,  $4.2 \times 10^4$ , and  $3.4 \times 10^4$  cells/cm<sup>2</sup>, respectively.

The reconstitution of collagen inside the pores of Nylon meshes was observed continuously under inverted microscope. According to the observation under inverted microscope, the collagen fiber matrix started to form in about 2.5 min and completed in about 15 min after the temperature was raised. The proliferation rate of cells in the collagen/nylon mesh composite biomatrix is much higher than the plasma-modified nylon without the reconstituted collagen. The collagen/nylon composite biomatrix has stronger mechanical property than the conventional collagen matrix, yet still provides an excellent environment for cell growth.

## REFERENCES

1. Wang YJ, Chen CH, Yeh ML, Hsiue GH and Yu BC (1990), A one-side hydrophilic polypropylene membrane prepared by plasma treatment, *J. of Mem. Sci.*, 53: 275-285.
2. Grinnell F and Bennett MH (1982), Ultrastructural studies of cells-collagen interaction, *Methods in Enzymology*, 82: 535-551.
3. J. L. Ricci et al, *J. Biomed. Mat. Res.*, 25, 651-666, 1991

# DIRECT EXTRACTION OF TASTE RECEPTOR PROTEINS BY LIPOSOME FROM INTACT EPITHELIUM OF BULLFROG TONGUE

Mikihiko Nakamura\*, Kaoru Tsujii\* and Junzo Sunamoto\*\*

\*Kao Institute for Fundamental Research, Kao Corporation, 2606, Akabane, Ichikaimachi, Hagan, Tochigi, 321-34, Japan, \*\*Laboratories of Artificial Cell Technology, Division of Synthetic Chemistry, Graduate School of Engineering, Kyoto University, Kyoto 606, Japan

## SUMMARY

Membrane proteins being in tongue epithelium are of special interest relating with the taste transduction. Despite many years of research, molecular biological attempts to purify taste receptors have been unsuccessful<sup>1)</sup>. Because, their small quantity in the membrane and weak binding constant with the taste substances make the isolation, purification, and characterization for precise investigation rather difficult. For an extraction of membrane proteins, one of the present authors (J.S.) and his coworkers have recently developed a new methodology by using an artificial boundary lipid, 1,2-dimyristoylamido-1,2-deoxyphosphatidylcholine(DDPC)<sup>2)</sup>. This method has been successfully applied to several intact cells, such as human erythrocyte<sup>3)</sup>, B16 melanoma cell<sup>4)</sup>, and BALBRVD tumor cells<sup>5),6)</sup>. Hence, in order to obtain taste receptor proteins, we studied an application of this method for extracting taste receptor proteins from bullfrog tongue.

## KEY WORDS

Artificial boundary lipid, Liosome, Membrane protein, Taste receptor, Affinity chromatography

## METHODS

Figure 1 shows a flow chart of nerve response measurements and the liposome treatment. A given concentration of an aqueous solution of taste stimulus (100mM NH<sub>4</sub>Cl as a standard, 250mM L-Alanine, 1.0 M sucrose, 100mM L-Leucine and 0.1mM quinine hydrochloride)was used in this experiment. Before taste stimulus was applied, the tongue was washed with deionized water to stabilize taste nerve response (W1-8 in Figure 2). After washing the tongue, taste nerve response was measured against all taste stimuli (S1-2 and T1-2 in Fig. 1). The cycle between W1 and W4( before liposome treatment) and the cycle between W5 and W9 ( after liposome treatment) were repeated to obtain taste nerve response against all taste stimuli. Liposome treatment was carried out by liposome suspension(10 ml) with 5.0 mM as the lipid concentration at room temperature.

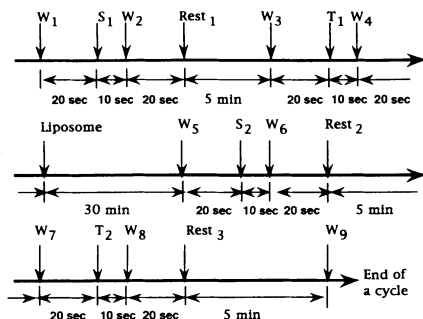


Fig. 1 Flow chart of the liposomal treatment of the frog tongue and the measurement of nerve response of the tongue against taste stimuli; W stands for washing with pure water; S for stimulation with an aqueous NH<sub>4</sub>Cl solution as the standard; and T for stimulation with an aqueous solution of a taste stimulus such as L-Alanine, sucrose, L-Leucine, or quinine hydrochloride.

The proteins obtained were separated into soluble proteins and membrane proteins trapped inside the liposome, and followed by analyzing with SDS-PAGE and affinity chromatography.

## RESULTS AND DISCUSSION

### 1, Neurophysiological measurement

The nerve response before and after liposomal treatment were compared. Taste nerve response of bullfrog to L-Alanine, sucrose and L-Leucine clearly decreased and did not recover within 90 minutes after the liposomal treatment. On the other hand, change of the nerve response to  $\text{NH}_4\text{Cl}$  was scarcely observed and it to quinine hydrochloride recovered within 60 minutes (shown in Fig. 2). Most of amino acids and sugars bind to specific receptors coupled to activation of G-proteins.  $\text{NH}_4\text{Cl}$  and quinine hydrochloride show another transduction mechanism, which block certain ion channel.<sup>7)</sup> Judging from the above results, the present liposome could extract the receptors of L-Alanine, L-Leucine and sucrose.

### 2, Electrophoretic analysis and affinity chromatography

Gel electrophoretic analysis of proteins transferred to the liposome from the tongue was done. Major bands of water soluble proteins on SDS-PAGE were 150 kd(8.5%), 73 kd(38.2%), 27 kd(6.8%), 15 kd(8.7%) and 14 kd(5.8%). Major proteins found in the liposomal membrane were 147 kd(12.8%), 95 kd(6.5%), 79 kd(4.5%), 57 kd(2.3%), 28 kd(3.4%) and 15 kd(10.4%). Plausible candidates for taste receptor proteins were 147, 95, 79 and 57 kd taking the difference in SDS-PAGE between the two parts of water soluble and membrane proteins into consideration.

L-Alanine affinity proteins were shown to be present in the membrane protein portions by affinity chromatography technique.

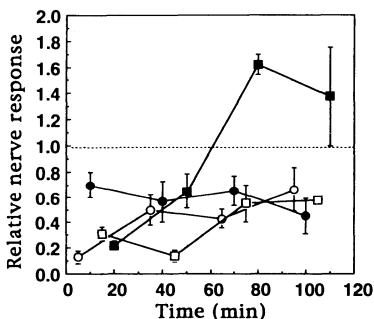


Fig. 2 Relative nerve response of bullfrog tongue for four major taste stimuli as a function of time after the liposomal treatment. The horizontal broken line refers to the value without the liposomal treatment; ○, L-Alanine; ●, sucrose; □, L-Leucine; and ■, quinine hydrochloride. Plotted Relative nerve response was calculated relative to magnitude of response to 100mM  $\text{NH}_4\text{Cl}$ .

## REFERENCES

- [1] Margolskee RF (1993) The biochemistry and molecular biology of taste transduction. *Current Opinion in Neurobiology*. 3: 526-531
- [2] Sunamoto J, Nagai K, Goto M, Lindoman B (1990) Synthesis and characterization of 1,2-dimyristoylamido-1,2-deoxyphosphatidylcholine as an artificial boundary lipid. *Biochim. Biophys. Acta*. 1024: 209-219
- [3] Sunamoto J, Goto M, Akiyoshi K (1990) Effective transfer of membrane proteins from human erythrocytes to artificial boundary lipid-containing liposome. *Chem. Lett.*: 1249-1252
- [4] Sunamoto J, Mori Y, Sato T (1992) Direct transfer of membrane proteins from B16 melanoma cell to artificial cell liposome. *Proc. Japan Acad. Sci.* 68B: 69-74
- [5] Shibata R, Noguti T, Sato T, Akiyoshi K, Sunamoto J, Shiku H, Nakayama E (1991) Induction of in vitro and in vivo anti-tumor responses by sensitization of mice with liposomes containing a crude butanol extract of leukemia cells and transferred inter-membranously with cell-surface proteins. *Int. J. Cancer*. 48:434-442
- [6] Sunamoto J, Noguti T, Sato T, Akiyoshi K, Shibata R, Nakayama E, Shiku H (1992) Direct transfer of tumor surface antigenic protein (TSAP) from tumor cell to liposome for making liposome vaccine. *J. Control. Release*. 20: 143-154
- [7] Gilbertson TA (1993) The physiology of vertebrate taste reception. *Current Opinion in Neurobiology*. 3: 532-539

# The Influence of Serum on The Spreading of Tumor Cells on Synthetic Glycolipid Films

Toshinori Sato, Masanori Endo, and Yoshio Okahata

Department of Biomolecular Engineering, Tokyo Institute of Technology,  
Nagatsuda, Midori-ku, Yokohama 226, Japan

## SUMMARY

Adhesion and spreading of HeLa cells to a synthetic glycolipid film was studied. Human adenocarcinoma cells (HeLa), mouse melanoma cells (B16) and human hepatoma cells (HuH7) selectively adhered and spread on a glycolipid carrying galactose moiety in serum medium, but not in serum-free medium. Cell spreading also occurred on galactose-bearing glycolipid film pre-coated with serum. Cell spreading in serum medium was inhibited in the presence of lactose, but not in the presence of maltose. Adsorption of the components of serum medium was quantitatively detected by use of a quartz-crystal microbalance (QCM). The surfaces of the glycolipid membranes were entirely covered with serum components. Adsorption of the components of serum medium to the galactose-bearing glycolipid was suppressed compared with that to glucose-bearing glycolipid and a phosphatidylcholine.

**KEY WORDS:** glycolipid, phospholipid, cell spreading, quartz-crystal microbalance, adhesion of tumor cells

## INTRODUCTION

Investigations for the interaction between cells and sugar-conjugated materials give a very important information for the development of biocompatible materials or artificial organs, because recognition at cell surface is intimately related to the basic process involving saccharide recognition [1-4]. Rat hepatocytes adhered specifically to culture dishes whose surface was coated with a lactose-carrying polystyrene (PVL A) [5]. That adhesion of hepatocytes was explained as galactose specific interaction between hepatocytes and PVL A. In this paper, we investigate adhesion and spreading of tumor cells on a phosphatidylcholine, a galactose-bearing glycolipid (2C<sub>18</sub>-gal), and a glucose-bearing glycolipid (2C<sub>18</sub>-glc).

## RESULTS AND DISCUSSION

### Spreading of HeLa Cells on Lipid Films in Serum-free Medium and Serum Medium

Figure 1 show the chemical structures of the glycolipids used in this study. In serum-free medium, no obvious differences in cell spreading between the 2C<sub>18</sub>-gal/DSPC and the 2C<sub>18</sub>-glc/DSPC membranes were observed, though the number of spreading cells increased with glycolipid content. On the 100 % DSPC membranes cell morphology was almost spherical. On the other hand, in the presence of fetal bovine serum (FBS), spreading of HeLa cells was greatly promoted on the 2C<sub>18</sub>-gal/ DSPC films, whereas cell spreadings on the 2C<sub>18</sub>-glc/DSPC films were less than that on the 2C<sub>18</sub>-gal/DSPC films at every content of glycolipid (Figure 2). More than 80 % of cells were spread on the 2C<sub>18</sub>-gal/DSPC-coated plate at each content of 2C<sub>18</sub>-gal. The cell spreading on the DSPC film was near-completely inhibited.



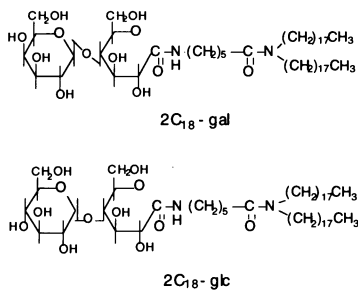


Fig. 1 Chemical structures of glycolipids

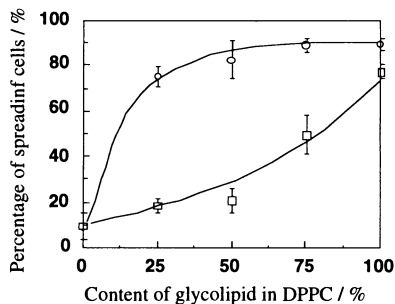


Fig. 2 Percentage of the spreading of Hela cells on 2C<sub>18</sub>-gal (○) and 2C<sub>18</sub>-glc (□) in serum medium

To know the specificity of cell spreading on the 2C<sub>18</sub>-gal membranes in the serum medium, inhibition experiments in the presence of lactose or maltose were carried out. The addition of the given amount of lactose or maltose (0 - 5 mg/ml) did not inhibit cell spreadings on non-coated plastic plates. In the serum-free medium, cell spreadings were not inhibited by the addition of lactose or maltose. This result indicated that adhesion of Hela cells on glycolipid membranes in the serum-free medium nonspecifically occurred. On the other hand, in the serum medium, cell spreadings on 2C<sub>18</sub>-gal/DSPC membranes were inhibited by the presence of lactose, but not by maltose. The percentage of the spreading cells on the 2C<sub>18</sub>-gal/DSPC membrane in the presence of lactose was nearly equal to that on the 2C<sub>18</sub>-glc/DSPC membrane. These results suggest that the cell spreadings on the 2C<sub>18</sub>-gal membranes may be mediated by lactose-specific recognition.

When 2C<sub>18</sub>-gal/DSPC membranes were pre-treated with FBS for 1 h at 37 °C, spreading of Hela cells were observed. These results suggest that the serum layer adsorbed to the surface of 2C<sub>18</sub>-gal/DSPC membrane contributes to the enhanced spreading of Hela cells.

### Quantification of Serum Components Adsorbed to Lipid Membranes by A QCM

Adsorption amount of the components of serum medium to the lipid membranes was measured by a QCM method [6] at 37 °C. Adsorption amount of the components of serum medium was ca. 1200 ng for DSPC membrane, and ca. 300 ng for the 2C<sub>18</sub>-gal(50%)/ DSPC(50%) membrane. From SDS-PAGE, major serum components adsorbed to the lipid membranes were indicated to be a protein of about 60 kD, which may involve albumin or alpha-globulin. When bovine serum albumin (BSA) adsorbed as a Langmuir-type monolayer, the adsorption amount is calculated to be 150 ng on the QCM. Considering that experimental values obtained were larger than 150 ng, we could imagine that multilayer adsorption of protein on lipid membranes or penetration of hydrophobic molecules into lipid membranes occurred.

### CONCLUSION

In this paper, we investigate the influence of serum on cell spreading on DSPC, glucose- and galactose-bearing lipid membranes. Morphological changes of Hela cells on galactose-bearing lipid were found to be mediated by the adsorption of serum components to the glycolipid membrane.

### REFERENCES

- 1) R. L. Schnaar, *Glycobiology* **1**, 477 (1991).
- 2) N. Kojima, *Trends in Glycoscience and Glycotechnology* **4**, 491 (1992).
- 3) T. Sato and J. Sunamoto, *J. Prog. Lipid Res.* **31**, 345 (1992).
- 4) T. Sato and J. Sunamoto, in: *Liposome Technology Vol. III, 2nd Edition*, p180, G. Gregoriadis (Ed.), CRC press, London (1993).
- 5) A. Kobayashi, K. Kobayashi and T. Akaike, *J. Biomater. Sci. Polymer Edn.* **3**, 499 (1991).
- 6) Y. Okahata and H. Ebato, *Anal. Chem.* **63**, 203 (1991).

# TRANSFER OF MEMBRANE PROTEINS FROM HUMAN ERYTHROCYTES TO LIPOSOMES

Yukihisa Okumura, Ken-ichi Suzuki, Masamitsu Goto and Junzo Sunamoto

*Division of Synthetic Chemistry and Biological Chemistry, Graduate School of Engineering, Kyoto University, Yoshida-Hommachi, Sakyo, Kyoto 606-01, Japan*

## SUMMARY

Transfer of a membrane bound enzyme acetylcholinesterase (AChE) from human erythrocyte to liposome was carefully examined. An artificial lipid 1,2-dimyristoylamido-1,2-deoxyphosphatidylcholine (D14DPC) showed predominant control over the transfer. The transfer was induced by a certain change of erythrocyte membrane during incubation with liposome, which is probably due to transfer of lipids from the liposome to the erythrocyte. The shorter induction period observed with D14DPC containing liposome can be attributed to both the faster transfer of D14DPC and the higher ability of D14DPC to induce the AChE transfer.

**KEYWORDS:** membrane protein transfer, erythrocyte, acetylcholinesterase, Band 3, liposome

## INTRODUCTION

Membrane proteins play key roles in various cell functions as a channel or a receptor, and their use as a molecular device will open a wide range of possibility in designing highly sophisticated artificial supramolecular systems. In order to avoid exposure of membrane proteins to non-bilayer environment during extraction and reconstitution of the proteins, which may cause denaturation of the proteins, we have been studying spontaneous transfer of membrane proteins from cell to liposome and its utilization in the protein reconstitution. The low transfer efficiency of Huestis' original condition [1,2] was remedied by Sunamoto's finding that the transfer of membrane proteins from various cells was enhanced by incorporation of an artificial boundary lipid 1,2-dimyristoylamido-1,2-deoxyphosphatidylcholine (D14DPC) in the liposome [3,4]. However, the exact mechanism of the transfer, including the role of D14DPC, is not clear yet. To obtain insight into the mechanism, we carefully examined the transfer of a membrane bound enzyme acetylcholinesterase (AChE) from human erythrocyte to liposome.

## METHODS

Liposome was prepared by the extrusion method and incubated with human erythrocyte. The liposomal fraction was separated from the cell by centrifugation. Enzymatic activity of acetylcholinesterase (AChE) was determined by using hydrolysis of acetylthiocholine.

## RESULTS AND DISCUSSION

With any lipid compositions of liposome examined, the transfer started after an induction period and reached a plateau after a while (Fig. 1), suggesting that the incorporation of D14DPC in the liposome does not change the mechanism of the transfer. Without D14DPC, the transfer profiles were significantly different among DMPC, DPPC [2] and EggPC. Incorporation of D14DPC in the liposome had a definite effect on the transfer of AChE from human erythrocyte. With 40 mol% of D14DPC incorporated, the transfer of AChE was enhanced both in speed and amount. And the

transfer profiles became almost identical regardless of the kinds of the lipid coexisting in the liposome, clearly indicating predominant control of D<sub>14</sub>DPC over the transfer.

#### AChE ACTIVITY (Arbitrary unit)

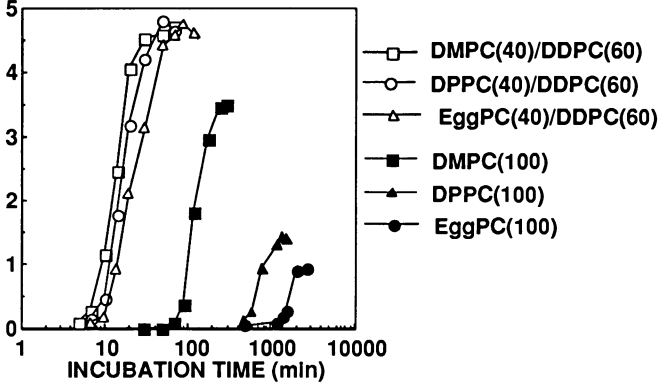


Fig. 1 Transfer of acetylcholinesterase from human erythrocyte to liposomes at 37°C.

Preincubation of erythrocyte with liposome reduced the length of the induction period in following incubation with fresh liposome. On the other hand, preincubation of liposome with erythrocyte made no difference on the induction period in following incubation with fresh erythrocyte. This result indicates that incubation of erythrocyte with liposome causes a certain change in the erythrocyte, which induces the transfer of AChE from the erythrocyte.

The most plausible cause of the change is transfer of lipids from the liposome to the erythrocyte. Initial rate of the transfer of D<sub>14</sub>DPC from liposome to intact erythrocytes measured by using radio-labeled lipids was approximately 12 times higher than that of DMPC. Also, the dipalmitoyl analog, D<sub>16</sub>DPC, which is expected to transfer slower than D<sub>14</sub>DPC, was much less effective for the induction of the protein transfer from human erythrocyte than D<sub>14</sub>DPC. These results strongly support the idea that the lipid transfer precedes the AChE transfer and that the predominant control and the shorter induction period observed with D<sub>14</sub>DPC containing liposome at least partly comes from the faster transfer of D<sub>14</sub>DPC to erythrocyte.

Furthermore, the amount of the total phospholipids transferred during the induction period from pure DMPC liposome was approximately twice as much as that from D<sub>14</sub>DPC/DMPC(60/40) liposome; the amount of D<sub>14</sub>DPC which is necessary to induce the AChE transfer is smaller than that of DMPC. This result indicates that the higher ability of D<sub>14</sub>DPC to induce the AChE transfer may also contribute to the shorter induction period.

#### REFERENCES

- [1] Bouma SR, Drislane W, Huestis WH (1977) Selective Extraction of Membrane-bound Proteins by Phospholipid Vesicles. *J Biol Chem* 252: 6759-6763
- [2] Cook SL, Bouma SR, Huestis WH (1980) Cell to Vesicle Transfer of Intrinsic Membrane Proteins: Effect of Membrane Fluidity. *Biochemistry* 19: 4601-4607
- [3] Sunamoto J, Mori, Y (1992) Direct Transfer of Membrane Proteins from B16 Melanoma Cell to Artificial Cell Liposome. *Proc Japan Acad* 68(B):69-74
- [4] Okumura Y, Ishitobi M, Sobel M, Akiyoshi K, Sunamoto J (1994) Transfer of Membrane Proteins from Human Platelets to Liposomal Fraction by Interaction with Liposomes Containing an Artificial Boundary Lipid. *Biochim Biophys Acta* 1194:335-340

# RECONSTITUTION OF BOVINE PLACENTAL INSULIN RECEPTOR ON ARTIFICIAL VESICLES BY USING DIRECT PROTEIN TRANSFER TECHNIQUES

Takehiko Ueda<sup>†</sup>, and Junzo Sunamoto<sup>†,‡</sup>

<sup>†</sup>Surface Recognition Group, Supermolecules Project, Research Development Corporation of Japan; Keihanna Plaza Superlab. Wing 1F-3, 1-7 Hikaridai Seikacho Sourakugun, Kyoto 619-02, Japan.

<sup>‡</sup>Department of Synthetic Chemistry and Biological Chemistry, Graduate School of Engineering, Kyoto University, Yoshida-Hommachi, Sakyo-ku, Kyoto 606, Japan

## ABSTRACT

Direct protein transfer with artificial boundary lipid, DDPC, has been used as a powerful isolation procedure for membrane proteins. In contrast to other methods using detergents as protein solubilizer, the target membrane proteins can be transferred directly from biomembrane to liposomes by this direct protein transfer method, without severe denaturation in the course of isolation. We have investigated the transfer of insulin receptor proteins from bovine placental plasma membrane into liposomes. All the subunits of insulin receptor was found reconstituted in liposomes. The reconstituted insulin receptor retained almost full activity to bind to insulin, leading to autophosphorylation as a result of signal transduction activity. It is quite important that the reconstituted insulin receptor can be isolated in liposomes, which can be served to further investigation of insulin receptor without any interferences from other enzymes in cells. Then we focused on the insulin binding activity. The reconstituted insulin receptor showed much higher binding affinity than that on plasma membrane or that solubilized in micelles, suggesting that insulin receptor protein isolated by a conventional method might catch a significant denaturation. A fully active and complete insulin receptor was isolated by this direct protein transfer method. This method is applicable extensively to other membrane proteins.

## KEY WORDS

protein transfer, insulin receptor, boundary lipid, binding activity, QCM

## INTRODUCTION

It has been reported that membrane proteins on living cells are transferred to artificial liposomes under a mild condition for culturing the cells. The protein transfer technique, which was reported by Bouma et al., is one of the procedures for extraction by which integral proteins could be directly transferred from erythrocytes to small unilamellar vesicles (SUV) during sufficient coincubation. Sunamoto et al. reported that protein transfer was accelerated by using liposomes containing DDPC. So far many integral proteins have been isolated generally by means of solubilization techniques by detergents such as Triton X-100 or by organic solvents, resulting in severe denaturation or inactivation of the proteins. This problem can be overcome by the direct protein transfer method. Since the direct protein transfer method does not require such solubilization treatments, it is believed that there is only little denaturation effects on the membrane proteins. Especially, it is believed that vesicles with an artificial boundary lipid of DDPC, which can contribute to stabilization of proteins on membrane, promise high transfer efficiency.

The objective of this project is the establishment of direct purification method of human insulin receptors, which are locating in the lipid bilayer membrane. To obtain completely intact insulin receptor proteins, a novel extraction procedure for integral proteins on biological membrane without any denaturation and deactivation has been examined.

Table 1 Ligand binding constants of insulin receptor proteins on biomembrane, in micelle, or on liposomes.

	$R_{all}^{(nM)}$	K (nM)	
		$K^H$	$K^L$
IR on biomembrane	334	58.8	2.49
Solubilized IR	386	54.6	2.33
IR on liposomes	242	339.0	1.75

## METHODS

Multilamellar liposomes were made from an appropriate mixture of DMPC as the matrix lipid and DDPC as the boundary lipid. A mixture of DMPC (24.4 mg, 60.0 mol%) and DDPC (16.2 mg, 40.0 mol%) was dissolved in dry chloroform and a lipid thin film was prepared at the bottom of a round-bottomed flask by gentle evaporation at r.t. and subsequently dried under reduced pressure for 16 h. This thin film was swelled in 10.0 ml of 10 mM hepes buffer containing 150 mM NaCl (pH 7.4) on a vortex mixer for 5 min. A liposomal suspension so obtained was extruded (by the Extruder, Lipex Biomembrane Inc.) several times by passing through a polycarbonate membrane filter (Nucleopore Corp.), with different pore size, 10 times through for 1.0  $\mu\text{m}$  pore, 10 times for 0.2  $\mu\text{m}$  pore, and 10 time for 0.1  $\mu\text{m}$  pore. The final concentration of the liposomal suspension (10.0 ml) was adjusted to 4.00 mg/ml as determined by the phospholipid determination procedure.

Coincubation was performed by just mixing liposomes for 2 hours at 37°C with placental plasma membrane and subjected to the density gradient ultra centrifugation to obtain a liposome solution as a supernatant.

## RESULTS AND DISCUSSION

Bovine plasma membranes purified from placenta organ and liposomes containing DDPC were mixed and coincubated at 37°C for 5 min to 240 min. The liposomes were isolated from the mixture by applying a discontinuous density gradient ultracentrifuge. Insulin receptor proteins and the subunits were detected in the fraction of the isolated liposomes, which was confirmed by Western-blotting techniques using biotin-labelled wheat germ agglutinin or biotin-labeled insulin .

Time course of protein transfer was followed and analyzed by nonlinear least square fitting method. Total amount of protein transfer to the liposomes was highest when liposomes containing 30% of DDPC were applied, while the kinetic constant was highest when liposomes containing 40% of DDPC were applied.

Competitive binding assay showed the insulin receptor protein transferred on the liposome retained full insulin binding activity, and was analyzed as a bi-binding site model. The binding property was compared with that of the conventionally purified insulin receptor protein in a micelle. The binding constants were significantly increased in case of transferred receptors (Table 1), indicating the directly transferred insulin receptors retained the same biochemical properties as the native receptors much more than that of conventionally purified insulin receptors.

# PROTEIN RECONSTITUTION FROM CELL MEMBRANE TO MONOLAYER USING DIRECT TRANSFER TECHNIQUE

Guiscard Glück, Yukihsa Okumura, and Junzo Sunamoto

Division of Synthetic Chemistry and Biological Chemistry, Graduate School of Engineering  
Kyoto University, Yoshida-Hommachi, Sakyo-ku, Kyoto 606-01, Japan

## SUMMARY

Membrane proteins from human erythrocyte ghosts have been reconstituted into monolayers at the air/water interface using direct transfer technique. Proteins were at first transferred from natural cell membrane to liposomes containing the artificial boundary lipid 1,2-dimyristoylamido-1,2-deoxyphosphatidylcholine (D<sub>14</sub>DPC). These liposomes transformed spontaneously at the air/water interface to result in a protein-containing lipid monolayer. Liposomes with different protein/lipid ratios could be transformed. The surface pressure of such monolayers was stable even after hours if kept below the collapse pressure of the monolayer and well above zero surface pressure conditions. Acetylcholinesterase activity was found in the monolayer by cleaving acetylthiocholine as a substrate that was injected into the subphase. Preliminary experiments indicate a relationship between the surface pressure and the enzymatic activity reconstituted into the monolayer.

**KEY WORDS** membrane protein, protein transfer, liposome, artificial boundary lipid, monolayer

## INTRODUCTION

Monomolecular films at the air/water interface supply precise information about the molecular packing and orientation of amphiphiles that can not be gained from other model membranes. Furthermore the properties of membrane proteins incorporated into a physically and chemically defined surrounding can be studied. During the reconstitution of the membrane proteins from natural membrane to model membrane it is crucial to avoid any denaturation or deactivation. For this purpose, Sunamoto et al.[1] have recently proposed an improved method that involves *in vitro* and *in vivo* direct transfer of membrane proteins from intact cell to a liposome that contains an artificial boundary lipid, 1,2-dimyristoylamido-1,2-deoxyphosphatidylcholine (D<sub>14</sub>DPC). Liposomes so obtained can be immediately transformed at the air/water interface to result in a protein-containing lipid monolayer. Since monolayers represent only one half of the natural membrane bilayer we have concentrated on acetylcholinesterase (AChE) from human erythrocytes. This amphiphatic enzyme is anchored through a phosphatidylinositol moiety in only one layer of the biomembrane that the enzymatically active part of the protein does not penetrate.

## MATERIALS AND METHODS

Membrane proteins from ghosts of human erythrocytes were transferred to large unilamellar vesicles with a diameter of 100 nm which contained 40 mol % dimyristoylphosphatidylcholine (DMPC) and 60 mol % D<sub>14</sub>DPC according to previously published results[2]. The preparation of monolayers from vesicle suspensions was performed according to the "wet-bridge" method[3]. This rather unusual way of spreading a monolayer was necessary because organic solvents usually denature the proteins. The setup consists of a miniature film balance and a self-made trough that was manufactured from a block of teflon. The trough includes also a small spreading well for the liposomal solution. A thin film of buffer on a strip of filter paper bridges the two compartments. The lipid in the vesicle solution of the spreading well is in an equilibrium with the air/water interface resulting in a monolayer. Due to the lateral pressure gradient the monolayer expands and moves over the buffer bridge onto the surface of the trough, while the vesicles are retained in the spreading well. We could

use as small as 0.5 ml of vesicle solution for the formation of several monolayers. The whole film balance was fixed inside a temperature controlled box. The activity of acetylcholinesterase reconstituted into the monolayer was determined by adding 0.3 mM acetylthiocholine to the subphase that was stirred with a magnetic mini-stirrer. The amount of thiocholine produced was measured by using a microfluorescence method[4].

## RESULTS AND DISCUSSION

After DMPC/D<sub>14</sub>DPC mixed vesicles were added to the subphase, an increase in the surface pressure at the air/water interface was observed indicating the transformation of vesicles to a monolayer. A lipid monolayer so formed exhibited essentially the same pressure area diagram as a monolayer obtained by spreading from a chloroform solution indicating that no vesicles were partly fused or attached to the monolayer. The increase in surface pressure was nearly proportional to the concentration of vesicles in the subphase whereas a sharp increase in transformation speed was observed above the phase transition temperature of the lipids. The surface pressure did not increase above the collapse pressure (45 mN/m) of the monolayer film at any time.

Vesicles that contained proteins reconstituted from erythrocyte ghosts showed the same concentration and temperature behavior. Compared with vesicles that contained no proteins the transformation in the case of proteovesicles was largely facilitated. A nearly exponential relationship between protein concentration and transformation speed was found in the range of 0.4 to 4 mg/ml protein concentration. The pressure area diagrams of such obtained monolayers showed the same collapse point like the corresponding one without proteins. Significantly, protein containing monolayers showed a spontaneous increase in surface pressure when they were kept at surface pressures below 10-15 mN/m. In these cases the surface pressure increased up to 10-15 mN/m. This phenomenon is largely attributed due to the unfolding of proteins at the air/water interface. Above 15 mN/m the surface pressure kept constant even over hours. The area covered by the monolayer decreased to some extent when the surface pressure was kept constant at 40 mN/m. However the halt of this process might indicate that a rearrangement inside the monolayer or a release of monolayer material into the subphase took place rather than the collapse of the whole monolayer.

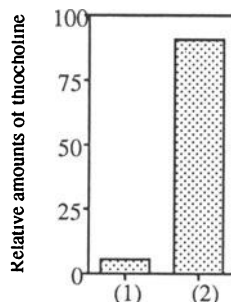


Fig. 1: Relative amounts of produced thiocholine without (1) and with (2) proteins reconstituted into the monolayer (observation time: 2 hrs.)

Acetylthiocholine in the subphase was cleaved to thiocholine and acetic acid as it could be determined by the microfluorometric assay for thiocholine. Only when proteins were present in the monolayer a large increase in thiocholine concentration was observed. This confirmed that the increase in thiocholine concentration is due to enzymatic activity reconstituted into the monolayer. Preliminary experiments indicate a relationship between surface pressure and the enzymatic activity of the monolayer. Currently we are further investigating the structural and functional properties of the protein containing monolayer.

## REFERENCES

- [1] Sunamoto J, Nagai K, Goto M, Lindman B (1990) Synthesis and characterization of 1,2-dimyristoylamido-1,2-deoxyphosphatidylcholine as a boundary lipid model. *Biochim. Biophys. Acta* 1024:209-219
- [2] Sunamoto J, Goto M, Akiyoshi K (1990) Effective transfer of membrane proteins from human erythrocytes to artificial boundary lipid containing liposomes. *Chem. Lett.* 1990:1249-1252
- [3] Kolomytkin OV (1987) Structure of planar membrane formed from liposomes. *Biochim. Biophys. Acta* 900:145-156
- [4] Parvari R, Pecht I, Soreq H (1983) A microfluorometric assay for cholinesterases, suitable for multiple kinetic determinations of picomoles of released thiocholine. *Anal. Biochem.* 133:450-456

**Acknowledgment.** G.G. gratefully acknowledges the support by the Supermolecules Project, the Research Development Corporation of Japan (JRDC).

# GLUCOSE RESPONSIVE INTER-POLYMER COMPLEX GEL BASED ON THE COMPLEXATION BETWEEN BORONIC ACID AND POLYOLS -MECHANISM OF GELATION AND GLUCOSE EXCHANGE-

<sup>1</sup>Issei. Hisamitsu, <sup>1</sup>Kazunori. Kataoka, <sup>2</sup>Teruo. Okano, and <sup>2</sup>Yasuhisa. Sakurai

<sup>1</sup>Dept. of Materials Science, Science University of Tokyo, 2641 Yamazaki, Nodashi, Chiba 278

## SUMMARY

We have synthesized poly (*m*-acrylamidophenylboronic acid-co-N,N-dimethylaminopropyl acrylamide-co-N,N-dimethylacryl amide ); DBA and investigated use for insulin delivery. And polymer complex formation between DBA and poly (vinyl alcohol) (PVA) as well as its dissociation responding to glucose concentration were studied. It was found that amino groups of DMAPAA were important to improve the response to glucose at pH 7.4. It is considered that amino groups may coordinate to boronic acid group. This coordination was observed with <sup>11</sup>B-NMR.

**KEY WORDS:** boronic acid / amino group / insulin delivery / gel / <sup>11</sup>B-NMR

## INTRODUCTION

The inter-polymer complex system responding to the change in the concentration of glucose is studied for insulin delivery system. We have designed copolymers having a boronic acid group as a sensor moiety for glucose by a radical copolymerization of *m*-acrylamidophenylboronic acid (AAPBA), N,N-dimethylaminopropylacrylamide (DMAPAA) and N,N-dimethylacrylamide (DMAA). The structure of DBA is as follows (Fig. 1.). And the polymer complex formation

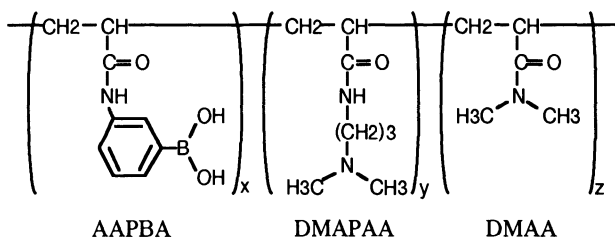


Fig. 1. The structure of DBA copolymer

between poly(AAPBA-co-DMAPAA-co-DMAA); DBA poly(vinyl alcohol) (PVA) as well as its dissociation responding to glucose concentration were studied. The complex between PVA and the copolymer without DMAPAA is usually formed at only alkaline state where the boronic acid groups are in ionized form. DBA having DMAPAA can make the complex with PVA even under physiological conditions (pH 7.4), because the amino groups of DMAPAA allow boronic acid groups to be in the ionized form by coordination to vacant orbital of boron atom.

Ionization of the boronic acid group in the polymer (DBA) by coordination with amino group was investigated with <sup>11</sup>B-nmr measurement.

## METHOD

When PVA solution is added to DBA solution, the viscosity of the mixed solution increases due to the formation of inter-polymer complex. Blood-coagulometer was used to measure the viscosity



change to evaluate the formation of polymer complex. The effect of composition of the copolymer (DBA) with several pH was examined. In this study, the abbreviation of DBA x/y was used to express the composition. The x stands for the mol% composition of AAPBA, and y stands for the mol% of DMAPAA in DBA respectively.

$^{11}\text{B}$ -NMR measurements of DBAs having various composition were carried out in phosphate buffer solution (pH 7.4) to observe the coordination between boronic acid group and amino group.

## RESULTS AND DISCUSSION

Increasing pH led an increase in the complexation rate of DBA with any composition by increasing ionized boronic acid. Compared to copolymers without DMAPAA, DBA copolymers showed the higher complexation rate. Since the complexation rate should increase by increasing boronic acid group in tetrahedral-form, the coordination of amino group to boronic acid group seems to take place to increase the fraction of boronic acid in tetrahedral-form resulting in an increase in the complexation rate. Further, optimal DMAPAA composition to induce prompt complex formation has found for DBA. The excess amino group ratio to boronic acid group may cause electrostatic repulsion to decrease the complexation rate.

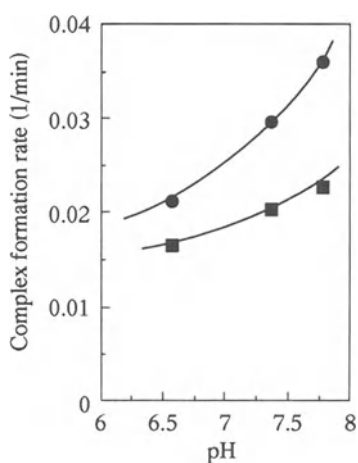


Fig. 2. Change in the complexation rate with the pH. The copolymer containing DMAPAA showed the higher complexation rate at every pH.

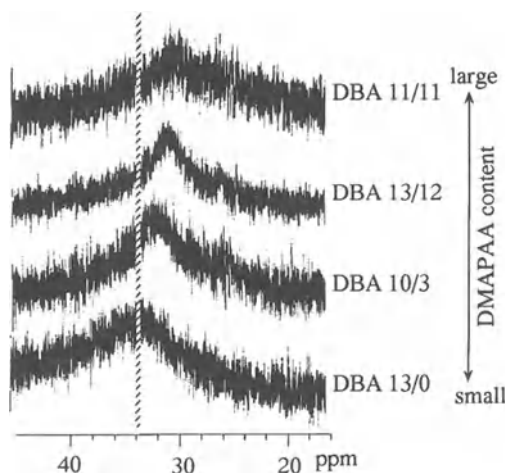


Fig. 3.  $^{11}\text{B}$ -NMR spectra of DBAs at pH 7.4. Boron atom in DBA having amino group has higher electron density, confirming that the amino group of DBA coordinates to boronic acid group.

Through the  $^{11}\text{B}$ -NMR measurement at pH 7.4, the peak of DBA having amino group was found at higher magnetic field than that with no amino group (Fig. 3). This indicates that boron atom in DBA has higher electron density at pH 7.4, confirming that the amino group of DBA coordinates to boronic acid group. The peak of boron in DBA with optimal amino group ratio to boronic acid was found at highest magnetic field. This result is consistent with the results of the complexation rate.

## CONCLUSION

These results indicate that amino group in DBA surely contributes to improve the rate of gelation by coordination, which is quite essential for the formulation of device used for glucose-responsive insulin delivery system.

# SYNTHESIS OF IONIC POLYURETHANE ELASTOMERS AS CHEMOMECHANICAL MATERIALS

Tetsuro Shiiba and Mutsuhisa Furukawa

Department of Materials Science and Engineering, Faculty of Engineering, Nagasaki University, 1-14, Bunkyo-machi, Nagasaki 852, Japan. TEL 0958-47-1111, FAX 0958-48-7547.

## ABSTRACT

Anionic and cationic polyurethane elastomers were synthesized and applied to chemomechanical materials. Various ionic polyurethane elastomers were synthesized and their mechanical properties were measured. When ionic polyurethane elastomer was set in the electrolyte solution under electric field, the specimen showed bending behavior.

**KEY WORDS :** polyurethane / ionic gel / chemomechanical

## INTRODUCTION

Polyurethane elastomers are well known to have excellent mechanical properties and many methods for polyurethane ionomer synthesis. Recently significant interest has been focused onto the electrically activated chemomechanical system consisting of ionic hydrogels<sup>1</sup>). These gels exhibit shrinking, swelling, or bending in electrolyte solutions under the influence of electric fields. The deformation of the gel shows the possibility of chemomechanical system, which converts electrochemical energy to mechanical energy. In order to obtain the mechanical energy effectively, it is important to improve the mechanical properties of the polyelectrolyte gel<sup>2</sup>). Polyurethane elastomer is well known to have excellent mechanical properties and many methods for polyurethane ionomer synthesis were reported<sup>3,4</sup>). In this study we prepared polyurethane elastomers with carboxyl or quaternary ammonium groups and measured their chemomechanical behaviors.

## EXPERIMENTAL

Anionic polyurethane elastomers having carboxyl groups were prepared as depicted in Fig. 1. Dimethylolpropionic acid(DMPA) and lysine diisocyanate(LDI) were reacted at 60 °C for 60

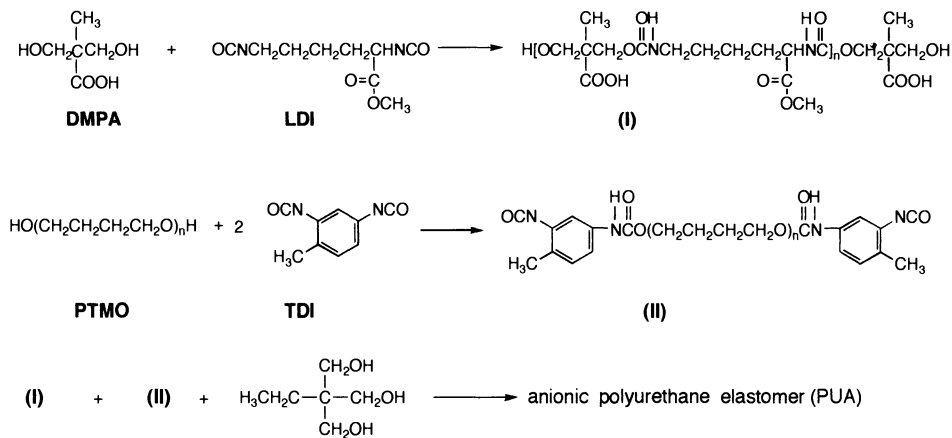


Fig. 1 Synthesis of the anionic polyurethane elastomer

min to obtain hydroxy-terminated anionic hard segment components(I). (I), isocyanate-terminated poly(oxytetramethylene) (PTMO) prepolymer(II), and trimethylolpropane(TMP) were reacted at 90°C.

## RESULTS AND DISCUSSION

It is well known that the mechanical properties of the polyurethane elastomers strongly depend on their components. Table 1 shows the structural parameters and mechanical properties of PUAs obtained by various reaction ratios. The strain at break, tensile strength, and other properties of the PUAs could be controlled by changes in structural parameters. This result is important to give excellent properties such as large strain and tensile strength to elastomeric chemomechanical materials.

The carboxyl group concentration was increased by immersing PUA in NaOH solution for the hydrolysis of the ester groups of the LDI residues. The Young's modulus of the hydrolyzed polyurethane elastomers (PUN) was much higher than that of PUA.

Table 1 Structural Parameters and Mechanical properties of PUA

No.	Mn	K	M	[TMP]	[COOH]	[COOCH <sub>3</sub> ]	E	ε b	σ b
					x 10 <sup>4</sup> (mol /g)		(MPa)		(MPa)
PUA-1	1000	0.80	0.5	0.93	14.0	11.2	10.9	2.8	8.9
PUA-2	1000	0.80	1.0	1.56	11.9	9.4	1.4	8.4	4.3
PUA-3	1000	0.80	1.5	2.00	10.0	8.0	3.5	7.7	8.1
PUA-4	1000	0.80	2.0	2.34	8.8	7.0	2.3	9.1	7.2
PUA-5	816	0.66	0.6	1.42	10.3	6.9	1.2	7.6	3.2
PUA-6	816	0.66	0.9	1.84	8.9	5.9	0.6	11.3	1.4
PUA-7	1300	0.85	0.8	0.99	13.2	11.2	9.4	4.3	7.4
PUA-8	1300	0.85	1.7	2.02	10.0	8.5	5.0	5.5	5.8

Mn : Mn of PTMO ; K = [DMPA] / [LDI] ; M = [OH]<sub>TMP</sub> / [OH]<sub>DMPA-LDI</sub>

E : Young's modulus ; ε b : strain at break ; σ b : tensile strength

The bending behaviors of PUAs and PUNs under electric fields (3.3 V/cm) were observed in various electrolyte solutions. PUAs and PUNs were immersed to the electrolyte solutions and cut into pieces(20 mm long x 3 mm wide x 1 mm thick), and then set in the electric fields. All PUAs and PUNs bent to the negative electrodes.

Cationic polyurethane elastomers having quaternary ammonium groups were also prepared. Polyurethane cationomers bent to the positive electrodes and had strength enough to be used as chemomechanical materials.

In conclusion, ionic polyurethane elastomers bent in electrolyte solutions under electric fields. These results indicate high potentialities of the ionic polyurethane elastomers as chemomechanical materials.

## REFERENCES

- 1)Y. Osada, H. Okuzaki and H. Hori, Nature, 242, 353(1992)
- 2)T. Shiga et. al., J. Appl. Polym. Sci., 44, 249(1992)
- 3)R. J. Goddard and S. L. Cooper, J. Polym. Sci., Polym. Phys. Ed., 32, 1557(1994)
- 4)H. A.. AL-Salah et.al., J. Polym. Sci., Polym. Chem. Ed., 26, 1609(1988)

# A SYNTHETIC POLYANION POLYMER AS A GROWTH PROMOTER FOR L929 MOUSE FIBROBLAST

Tomohiro Sawa<sup>1</sup>, Yukihisa Okumura<sup>1</sup>, Jian-L. Ding<sup>2</sup>, Raphael M. Ottenbrite<sup>2</sup>, and Junzo Sunamoto<sup>1</sup>

<sup>1</sup>Division of Synthetic Chemistry and Biological Chemistry, Graduate School of Engineering, Kyoto University, Yoshida-hommachi, Sakyo-ku, Kyoto 606-01, Japan.

<sup>2</sup>Department of Chemistry, Virginia Commonwealth University, Richmond, VA 23284, U.S.A.

## SUMMARY

A synthetic polyanion polymer, poly(maleic acid-alt-7,12-dioxaspiro[5,6]dodec-9-ene) (MACDA), enhanced the growth of L929 mouse fibroblasts in a serum- and protein-free condition. The highest promotion efficiency was obtained at 10 µg/ml of MACDA, resulting 2.1-fold increase in the cell number against a control experiment without MACDA. At that time, no significant morphological change of L929 was observed. The unnecessary of external growth factors distinguishes MACDA from other synthetic polymers those have been known to show such a cell growth promotion.

**KEY WORDS:** polyanion polymer, fibroblast, MACDA, serum-free culture, growth promotion

## INTRODUCTION

Generally, cultured cells required a serum for their proliferation. However the presence of unidentified compounds in serum complicates a study of cellular functions at molecular level [1]. A chemically well-defined medium is essential for a controlled biological study using cultured cells [1][2]. One of the method to culture cells in a serum-free medium is the modification of culture substrata because their functions and proliferation strongly depend on the characteristics of the surface of culture substrata [3]. Most cell lines, however, fail to grow in that condition and require further protein growth factors for their complete proliferation. For well defined synthetic media, synthesis of artificial growth promoter could be indispensable.

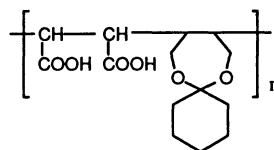


Fig. 1 MACDA

We have investigated a large number of polyanion polymers with different pendant structures, chain rigidity, hydrophobicity and surface charge density for their tumoricidal activity. From these studies, it was found that poly(maleic acid-alt-7,12-dioxaspiro[5,6]dodec-9-ene)(MACDA, Fig. 1) had *in vivo* antitumor [4] and *in vitro* macrophage stimulation activities [5]. Activation of macrophages is accompanied by a number of molecular events such as an activation of phosphoinositide turnover, an increase in the intracellular concentration of Ca<sup>2+</sup>, and a protein kinase C translocation from cytosol to membrane [6]. These events are thought to be associated with signal transduction processes, and also occur in cell proliferation and differentiation [7]. These findings led us to investigate the effect of MACDA on cells other than macrophages, particularly on their growth responses. In this study, the effect of MACDA on the growth of L929 mouse fibroblasts is discussed.

## METHODS

MACDA was synthesized by radical copolymerization of maleic anhydride and 7, 12-dioxaspiro[5,6]dodec-9-ene using  $\alpha, \alpha'$ -azobisisobutyronitrile as an initiator. The polymer so obtained was fractionated and characterized by <sup>1</sup>H-NMR and gel permeation chromatography.

L929 mouse fibroblasts in their growth phase were trypsinized and resuspended in Eagle's minimal essential medium (MEM) supplemented with 10 % FBS and seeded at a density of 2.5 × 10<sup>4</sup> cells/cm<sup>2</sup> on a 24-well micro plate. After incubation at 37 °C under 5 % CO<sub>2</sub> for 8 hours, the medium

was removed, and the cells were incubated for another 16 hours in a serum-free MEM. Then the medium was changed to one containing MACDA or heparin. A serum-free MEM was used for a control experiment. After 3 days incubation, cell proliferation was evaluated by counting living cells.

## RESULTS AND DISCUSSION

The addition of MACDA to a serum- and protein-free MEM promoted the growth of L929 cells (Fig. 2). The growth promotion activity of MACDA depended on the concentration of the polymer. The highest promotion was obtained at 10  $\mu\text{g/ml}$  of MACDA, resulting 2.1-fold increase of cell number against a control experiment without MACDA. Heparin, which was a naturally occurring polyanion polymer, showed no growth promotion under the comparable condition. It is known that heparin promotes the growth of several types of cells *via* enhancement of the activity of fibroblast growth factors [8]. The result obtained here indicates that the mechanism of the cell growth promotion by MACDA is different from that of heparin.

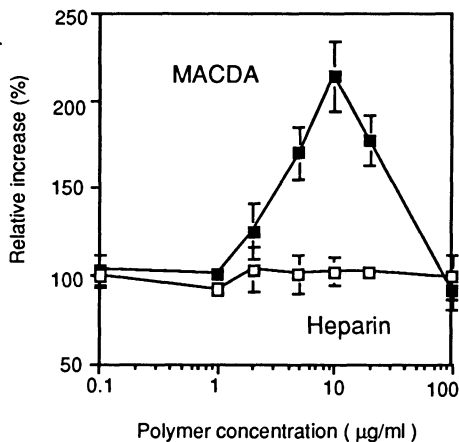


Fig. 2 Effect of MACDA and heparin on the growth of L929 mouse fibroblasts. All runs were triplicated.

Several synthetic and semi-synthetic polymers, other than polymers used for the modification of substrata, have been reported their growth promotion activities [2]. Among them, polyvinylpyrrolidone and methylcellulose showed the activity in a serum-free medium. However, the effect of these polymers seems to work simply as protective agents of cytoplasm membrane against mechanical and enzymatic damages, because these polymers were effective only at subculturing procedure and above the concentration of 0.1 wt %. In this study, MACDA showed significant growth promotion at 100-times lower concentration compared to polyvinylpyrrolidone and methylcellulose without subculturing steps. This suggests that the action of MACDA must be direct to proliferation of cells and unique. The clarification of the action of MACDA will give us considerable information to design of an artificial growth promoter. A further study on the action of MACDA is currently ongoing.

## REFERENCES

- [1] Barnes D and Sato G (1980) Methods for growth of cultured cells in serum-free medium. *Anal. Biochem.* 102:255-270
- [2] Mizrahi A, and Lazar A (1991) *Animal Cell Culture and Production of Biologicals*. Kluwer Academic Publishers, Netherlands, pp159
- [2] Folkman J and Moscona A (1978) Role of cell shape in growth control. *Nature*, 273: 345-349
- [3] Turk TM, Webb SR, Ottenbrite RM (1991) Antitumor effects of macrophages activated by polyanionic polymers. *J. Bioact. Compat. Polym.*, 6:358-376
- [4] Sato T, Kojima K, Ihda T, Sunamoto J, Ottenbrite RM (1986) Macrophage activation by poly(maleic acid-alt-2-cyclohexyl-1,3-dioxap-5-ene) encapsulated in polysaccharide-coated liposomes. *J. Bioact. Compat. Polym.*, 1:448-460
- [5] F. Rossi (1986) The  $\text{O}_2^-$ -forming NADPH oxidase of the phagocytes: nature, mechanisms of activation and function. *Biochim. Biophys. Acta*, 853:65-89
- [6] Y. Nishizuka (1992) Intracellular signaling by hydrolysis of phospholipids and activation of protein kinase C. *Science*, 253:607-614
- [7] Belford DA, Hendry IA, Parish CR (1992) Ability of different chemically modified heparins to potentiate the biological activity of heparin-binding growth factor 1: lack of correlation with growth factor binding. *Biochemistry*, 31:6498-6503

# ADHESION OF FIBROBLAST ONTO POLY( $\gamma$ -BENZYL L-GLUTAMATE)/POLY(ETHYLENE OXIDE) DIBLOCK COPOLYMER LANGMUIR-BLODGETT FILMS

Chong-Su Cho<sup>1</sup>, Akira Kobayashi<sup>2</sup>, Mitsuaki Goto<sup>2</sup>, Keun-Hong Park<sup>3</sup>, and Toshihiro Akaike<sup>2,3</sup>

<sup>1</sup>Department of Polymer Engineering, Chonnam National University, Kwangju 500-757, Korea,

<sup>2</sup>The 3rd Laboratory, Kanagawa Academy of Science and Technology, Kawasaki 213, Japan

<sup>3</sup>Department of Biomolecular Engineering, Tokyo Institute of Technology, Yokohama 227, Japan

**ABSTRACT:** Block copolymers consisting of poly( $\gamma$ -benzyl L-glutamate)(PBLG) as the hydrophobic part and poly(ethylene oxide)(PEO) as the hydrophilic part were prepared and their structural studies were performed. Cell attachment onto the surfaces of block copolymers fabricated either as well-defined ordered Langmuir-Blodgett(LB) films, or solvent cast microphase-separated structure consisting of bilayers. Monolayers of the block copolymers could be formed. The monolayer behavior of the block copolymer was affected by the content of PEO. The block copolymer LB films were formed as oriented state of the polymer chains. More fibroblasts adhered onto the LB surface than onto microphase-separated cast surfaces. Adhered fibroblast showed extensive morphological changes associated with the LB surface as compared to cast film surfaces. The number of cells grown on the LB surfaces is larger than that on the cast film.

**KEY WORDS:** Langmuir-Blodgett(LB) film, micro-separated structure, fibroblast

## INTRODUCTION

Cellular behaviors, such as adhesion, morphological change, functional alteration, and proliferation, are greatly affected by the surface properties, such as hydrophilicity, roughness, charge, free energy, and morphology[1].

In previous studies[2, 3], it was found that the surface microstructure of block copolymers fabricated through solvent casting and Langmuir - Blodgett(LB) methods influenced cellular interactions.

In this study, the attachment of fibroblast onto poly( $\gamma$ -benzyl L-glutamate)(PBLG)/poly(ethylene oxide)(PEO) block copolymers will be evaluated. The surfaces are fabricated either as LB films, presenting a well-defined, ordered surface structure, or as solvent cast surfaces, presenting a microphase-separated surface.

## EXPERIMENTAL

### Synthesis of PBLG/PEO diblock copolymer

It was prepared by polymerization of  $\gamma$ -benzyl L-glutamate N-carboxyanhydride(BLG-NCA) initiated with H<sub>2</sub>N-PEO(M.W.=2,000) in methylene chloride by the same method as that described previously[4].

### Preparation of block copolymer films

Monolayers were formed using a procedure described previously[5]. The block copolymer monolayers were transferred onto silane-treated glass plates by a horizontal lifting method. To

form solvent cast films, the block copolymer chloroform solutions were deposited onto silane-treated glass plates.

### Cell adhesion

Copolymers prepared by the LB films and solvent cast onto glass plates were immersed in separate cell suspensions and placed in an incubator with 5 wt.-% CO<sub>2</sub> at 37° C. The non-adhering cells were collected and counted by a hemocytometer.

## RESULTS AND DISCUSSION

The copolymer was prepared by polymerization of BLG-NCA initiated by the amine-terminated PEO in methylene chloride. The copolymer composition and molecular weights were estimated by NMR measurements. In Table 1 are listed the amount of PEO and the molecular weight of the copolymers.

**Table 1. Characteristics of PBLG/PEO diblock copolymers prepared.**

Sample	Content of monomeric units in mol %		Mn
	PBLG	PEO	
GE1	87.1	12.9	68,500
GE2	76.6	23.4	34,300
GE3	61.0	39.0	17,400
GE4	27.9	72.1	5,800

From the surface pressure-area isotherms of PBLG homopolymer and PBLG/PEO diblock copolymers, PBLG monolayer has the compressed type whereas diblock copolymers have the expanded types due to the incorporation of PEO in the diblock copolymers.

From the fibroblast adhesion onto the block surfaces, more fibroblasts adhered onto the LB surface than onto cast surfaces for the block copolymers. Also, more morphological changes of fibroblast adhered onto the LB surfaces were observed than surface of the cast film. From the fibroblast growth, the number of cells grown on the LB surfaces is larger than on the cast film.

## REFERENCES

- [1] Kataoka K, in *Biomaterials Science*, Vol. 1, T.Tsuruta et al.(eds.), Nankodo, Tokyo, 1982, p93.
- [2] Cho CS, Takayama T, Kunou M, Akaike T(1990) Platelet adhesion onto the Langmuir-Blodgett film of poly( $\gamma$ -benzyl L-glutamate)-poly(ethylene oxide)-poly( $\gamma$ -benzyl L-glutamate) copolymer. *J.Biomed.Mater.Res.* 24: 1369-1375
- [3] Cho CS, Kotaka T, Akaike T(1993) Cell adhesion onto block copolymer Langmuir-Blodgett films. *J.Biomed.Mater.Res.* 27: 199-206
- [4] Cho CS, Kim SW, Komoto T(1990) Synthesis and structural study of an ABA block copolymer consisting of poly( $\gamma$ -benzyl L-glutamate) as the A block and poly(ethylene oxide) as the B block. *Makromol.Chem.* 191: 981-991
- [5] Cho CS, Nagata R, Yagawa S, Takahashi S, Kunou M, Akaike T(1990) Monolayers of poly( $\gamma$ -benzyl L-glutamate)/polyether block copolymers on the air/water interface.*J.Polymer.Sci:Part C:Polymer Letters* 28: 89-93

# NEW BIOACTIVE MACROMOLECULAR GLYCOLIPIDS FROM BACTERIAL CELL SURFACE

Yasuo Suda\*, Haruhiko Takada†, Tomoko Hayashi‡, Toshihide Tamura§, Shozo Kotani¶ and Shoichi Kusumoto\*

\*Department of Chemistry, Faculty of Science, Osaka University, Toyonaka, Osaka 560, Japan,

†Department of Microbiology and Immunity, Kagoshima University Dental School, Kagoshima 890, Japan,

‡Department of Bacteriology, Hyogo College of Medicine, Nishinomiya, Hyogo 663, Japan,

¶Osaka College of Medical Technology, Osaka 530, Japan.

## SUMMARY

New bioactive glycolipids were effectively isolated and purified from cells of *Mycobacterium bovis* Ravenel and Gram-positive *Enterococcus hirae* ATCC 9790. These glycolipids had macromolecular features and showed high cytokine-inducing activity as evaluated with an assay using human peripheral whole blood cells. These natural macromolecules may be good references for developing a new synthetic polymer drug having an immuno-stimulating activity.

**KEY WORDS:** Natural polymer, glycolipid, interleukin-6, tumor necrosis factor- $\alpha$ , bacterial cell

## INTRODUCTION

A variety of glycolipids capable of modulating the host defence function (biological response modifier, BRMs) are located in the surface layer of bacterial cells [1]. Representatives are endotoxic lipopolysaccharide (LPS) from Gram-negative bacteria and muramyl peptide which constitutes a structural unit of the cell wall peptidoglycan of most bacteria irrespective of Gram-stainability. Recently other glycolipids having immuno-stimulating activity were reported from cells of Mycobacteria [2,3] as well as Gram-positive bacteria [4]. These bioactive components proved to have macromolecular features, but their structure responsible for the activity have not been fully characterized. We report here the isolation and purification of the new bioactive glycolipids from cells of *Mycobacterium bovis* Ravenel and Gram-positive *Enterococcus hirae* ATCC 9790, and their chemical composition and cytokine inducing activity are also discussed.

## MATERIALS AND METHODS

**Bacterial cells:** *M. bovis* Ravenel was grown in Sauton media at 37 °C for 4 weeks and killed at 100 °C for 15 min. The cells were collected by filtration and washed with distilled water, then dehydrated with acetone. *E. hirae* ATCC 9790 was grown aerobically at 37 °C for 6 h in trypticase-tryptose-yeast extract medium. Cells were harvested by centrifugation and washed with phosphate buffered saline.

**Immuno-stimulating activity (Cytokine-inducing activity):** Test samples dissolved in saline was incubated with heparinized human peripheral whole blood cells and a culture medium at 37 °C in 5% CO<sub>2</sub> for 24 h. After the centrifugation at 1,800 rpm for 2 min, the interleukin-6 (IL-6) and tumor necrosis factor- $\alpha$  (TNF- $\alpha$ ) in the obtained supernatant were measured by ELISA.

## RESULTS AND DISCUSSION

***M. bovis* Ravenel:** The cells delipidated with chloroform/methanol (1/2, v/v) were suspended in a buffer solution and treated with 80 % phenol at 65 °C for 45 min. After cooling in an ice bath, the mixture was centrifuged at 15,000 g for 20 min to separate aqueous phase, in which the active



fractions were extracted. The extract was subjected to hydrophobic chromatography (Octyl-sepharose CL-4B, Pharmacia LKB) with linear gradient of 1-propanol to give an active fraction. Then, further purification was performed by the ion-exchange chromatography (DEAE-Sephacel, Pharmacia LKB) using Tris-buffer (pH 7.4) containing 0.1 % (w/v) Triton X-100. The detergent was removed by the repeated precipitation using ethanol to give a bioactive glycolipid, a single but broad band being observed at about 40K dalton in SDS-PAGE stained with periodate and silver. The glycolipid, thus designated 40 kDaGL, which possessed remarkable cytokine-inducing activity (Table 1), contained mannose (32 wt%), arabinose (26 wt%), and inositol (2 wt%); 3 wt% fatty acids (C16:0, 10MeC18:0) and <1 wt% phosphorus were also found among its constituents.

***E. hirae* ATCC9790:** Delipidation, phenol-extraction and the subsequent hydrophobic chromatography were performed in a manner similar to those described above. The obtained fraction was subjected to ion-exchange membrane chromatography (QM-Mem Sep 1000, Japan Milipore Co.) in the presence of 35% (v/v) 1-propanol to remove the contaminating biologically inactive components. Finally, the bioactive fraction was purified by the hydrophobic interaction chromatography (Octyl-sepharose) to give five distinct glycolipids (FOS-1, -2, -3R, -4R and -5R). Their molecular weights were estimated by SDS-PAGE stained with Alcian blue as summarized in Table 1. All these five glycolipids also exhibit high cytokine-inducing activity (Table 1) and have chemical composition including glucose, glycerol, phosphorus, fatty acids (mainly C16:0, C18:1) and amino acid (mainly alanine) but in distinct relative ratios.

The structural characterization of these macromolecular glycolipids from both bacteria is currently being performed toward the goal of understanding the structure-activity relationship.

Table 1. Cytokine-inducing activity of macromolecular glycolipids from bacterial cells

Glycolipid	Bacteria	MW*1	IL-6 (pg/ml)		TNF- $\alpha$ (pg/ml)	
			100 $\mu$ g/ml*2	10 $\mu$ g/ml*2	100 $\mu$ g/ml*2	10 $\mu$ g/ml*2
40 kDaGL	<i>M. bovis</i> Ravenel	40 kDa	22100 $\pm$ 1700	650 $\pm$ 188	97.0 $\pm$ 32.5	79.5 $\pm$ 4.5
FOS-1*3	<i>E. hirae</i> ATCC 9790	> 100 kDa	14400 $\pm$ 180	3780 $\pm$ 98.5	695 $\pm$ 18.2	95.6 $\pm$ 10.2
FOS-2	<i>E. hirae</i> ATCC 9790	12-18 kDa	17200 $\pm$ 571	2770 $\pm$ 423	676 $\pm$ 17.2	54.8 $\pm$ 3.0
FOS-3R	<i>E. hirae</i> ATCC 9790	12-18 kDa	4360 $\pm$ 1120	1990 $\pm$ 786	114 $\pm$ 12.6	9.8 $\pm$ 3.2
FOS-4R	<i>E. hirae</i> ATCC 9790	12-18 kDa	10100 $\pm$ 489	4730 $\pm$ 472	303 $\pm$ 16.8	57.8 $\pm$ 15.8
FOS-5R	<i>E. hirae</i> ATCC 9790	12-18 kDa	9010 $\pm$ 148	1790 $\pm$ 64.5	201 $\pm$ 6.0	57.8 $\pm$ 5.6

\*1 Estimated from SDS-PAGE.

\*2 Final concentration of the tested glycolipid in the peripheral whole blood cell culture (125  $\mu$ l).

\*3 Rhamnose was detected in addition to glucose.

## REFERENCES

- [1] Kotani S, Tsujimoto M, Takada, H, Ogawa T, Takahashi L, Ikeda T, Shiba T, Kusumoto S, Kato K, Koikeguchi S, Yano I (1986) Immunomodulation activities of bacterial cell-surface components. In: Bacteria and the Host, Ryč M and Franěk J (eds) Avicenum, Czechoslovak Medical Press, Prague, pp.157-169.
- [2] Ikeda-Fujita T, Kotani S, Tsujimoto M, Ogawa T, Takada H, Takahashi I, Shimauchi H, Koikeguchi S, Kato K, Okamura H, Tamura T, Yano I, Tanaka S, Kato Y (1987) A novel immunomodulator derived from *Mycobacterium bovis* BCG which holds many bioactivities in common with endotoxins. Jpn. J. Bacteriol. 42: 597-602.
- [3] Chatterjee D, Roberts AD, Lowell K, Brennan PJ, Orme IM (1992) Structural basis of capacity of lipoarabinomannan to induce secretion of tumor necrosis factor. Infect. Immun. 60: 1249-1253.
- [4] Yamamoto A, Usami H, Nagamuta M, Sugawara Y, Hamada S, Yamamoto T, kato K, Koikeguchi S, Kotani S (1985) The use of lipoteichoic acid (LTA) from *Streptococcus pyogenes* to induce a serum factor causing tumor necrosis. Br. J. Cancer 51: 739-742.

# **<sup>13</sup>C-LABELING IN METHIONINE METHYL GROUPS OF GLYCOPHORIN A<sup>M</sup> AND ITS EFFECT ON THE SECONDARY STRUCTURE**

**Zhe Zhou<sup>1</sup>, Yukihisa Okumura<sup>2</sup> and Junzo Sunamoto\*<sup>1,2</sup>**

<sup>1</sup> Supermolecules Project, Research Development Corporation of Japan, Keihanna Plaza, Seika-cho 1-7, Soraku-gun, Kyoto 619-02, JAPAN; <sup>2</sup> Division of Synthetic Chemistry & Biological Chemistry, Graduate School of Engineering, Kyoto University, Kyoto 606-01, JAPAN

## **SUMMARY**

On the way of dynamic study of human glycophorin A<sup>M</sup> in lipid bilayer, we tried [<sup>13</sup>C]-methylation of its two methionines, Met-8 and -81, in the presence of 8 M urea. <sup>1</sup>H, <sup>13</sup>C and CD spectra revealed that the A, D and E helical domains of the protein were partly affected upon the methylation, while B and C domains were not disturbed. <sup>13</sup>C signals of methyl groups for both Met-8 and -81 appeared at the same position, at 15.7 ppm. The corresponding <sup>1</sup>H chemical shifts were assigned as 2.11 ppm by using HMQC. These results indicate that previously reported <sup>13</sup>C chemical shift of Met-81 methyl group may be wrong, and 8 M urea which was used during the methylation procedure certainly and irreversibly affect the secondary structure of the protein.

## **KEY WORDS**

<sup>13</sup>C-Labeling, methyl group, glycophorin A, secondary structure, NMR

## **INTRODUCTION**

Glycophorins comprise the predominant transmembrane sialoglycoproteins found in human erythrocyte membrane. Because of the immense interest in the structure-function relationship of biomacromolecules such as GP-A, characterization of molecular motion is crucial for understanding of their biological functions. We are now studying dynamics of the two methionines, Met-8 and -81, of GP-A<sup>M</sup> in an aqueous medium by using new proton-detected <sup>13</sup>C NMR technique.[1] During the investigation, we found that the previous result reported by Hardy and Dill[2] was wrong. In their study, they employed 8 M urea in the <sup>13</sup>C-methylation of Met-8 and -81 of GP-A<sup>N</sup> as if the method did not cause any change of the secondary structure of the protein. In this paper, we would like also to report about new assignment to the chemical shifts of methyl groups for Met-8 and -81 of GP-A.

## **METHODS**

Glycophorins were isolated using LIS-phenol method from homozygous MM-type human blood. GP-A<sup>M</sup> was obtained by gel filtration in the presence of lauryldimethylamine oxide. The methyl groups of Met-8 and -81 were labeled with [<sup>13</sup>C]-methyl iodide.[2] CD spectra were measured on a Jasco J-720 spectropolarimeter. NMR was run on a JEOL a-500 NMR spectrometer at 28°C.

## **RESULTS AND DISCUSSION**

For GP-A<sup>M</sup> all the NMR and CD spectra were in good agreement with those previously reported. However, after the <sup>13</sup>C-labeling, CD spectrum showed a decrease in the intensity. After further treatment with 8 M urea at pH 4.0 for 6 h and, then, with 5 M urea at pH 6.0 for 15 h at 4°C, CD intensity more decreased. Byers et al.[3] reported that the decrease in the ellipticity at 220 nm (θ<sub>220</sub>)

after treatment with 5-8 M guanidine-HCl was due to partial, but irreversible, loss of the secondary structure of glycophorin, even complete removal of the denaturant by dialysis resulted in only 85% recovery of  $\theta_{220}$ . Also in our case, even complete removal of urea by dialysis resulted in only 83-88% recovery of ellipticity .

Human GP-A contains five His, four Tyr and two Phe residues. With  $^1\text{H}$  NMR, resonances at 7.34, 7.15 and 6.84 ppm are respectively assigned to His (ring H-4), Tyr (ring H-2,6) and Tyr (ring H-3,5). In native GP-A, the resonances of ring protons for the two Phe residues cannot be detected because they are located in highly ordered helices which are near or in the hydrophobic domains. This agrees with a model of human GP-A; Phe-68 locates in helix B and Phe-78 is in helix C. These two helical domains are responsible for the dimerization of GP-A and are very tolerant to pH, temperature and ionic strength even in 6 M guanidine/4 M urea. If the helices B and C were disrupted, the ring proton signal of the Phe groups would appear at 7.3 ppm and the integral would significantly increase. Integrals of the peaks in  $^1\text{H}$  NMR spectrum of GP-A<sup>M</sup> at 7.34, 7.15 and 6.84 ppm corresponded to 5, 8 and 8 protons, and they could be assigned to ring protons of five His and four Tyr residues. Even labeling of methionine methyl groups in the presence of 8 M urea or further treatment of the  $^{13}\text{C}$ -labeled protein with urea did not show the Phe signal. This means that the labeling and additional urea treatment do not change the helical structure B and C domains and leave the dimerization unaffected. This well explains the unchanged electrophoretic pattern reported by Hardy.[2]

Resolution of the proton and carbon spectra increased, especially, for the bulk carbohydrate region. This means that several regions of the protein were denatured leading to an increase in the mobility of these regions. Combining both results of NMR and CD measurements, we concluded that the helices A, D and E were certainly affected during the labeling procedures. Hardy and Dill failed to get this result because they investigated this point only from electrophoresis. In addition, their  $^{13}\text{C}$  NMR spectra showed an apparent increase in the resolution over the range of 60 to 80 ppm upon the labeling.

For two new peaks that appeared after the labeling, they assigned the peak at 15.7 ppm to the  $\epsilon$ -carbon of Met-8 and the other at 2.0 ppm to that of Met-81. They attributed the unusual chemical shift of the  $\epsilon$ -carbon of Met-81 to its microenvironment in the hydrophobic domain of GP-A. Although Met-8 is in hydrophilic domain and Met-81 is in hydrophobic portion, both are exposed to bulk solvent phase in water, and the  $^{13}\text{C}$ -chemical shifts should not show any dramatic difference. Jones et al. specifically enriched the methionine methyl groups of whale sperm myoglobin with  $^{13}\text{C}$ -labeling and carried out detailed NMR studies under various conditions.[4] Through the investigation, they found that the  $^{13}\text{C}$  chemical shifts of the methionine methyl groups were within the region from 14.2 to 16.7 ppm. Therefore, the peak at 2.0 ppm as reported by Hardy and Dill is most likely from an impurity. Comparing the  $^{13}\text{C}$  NMR spectra between native and labeled GP-A<sup>M</sup>, we recognized a new intense peak at 15.7 ppm only for the labeled protein. It could be assigned to the overlap of two Met-8 and -81 methyl groups. From the proton-detected spectrum HMQC, we could assign the  $^1\text{H}$  chemical shift of Met-8 and -81 methyl groups to 2.11 ppm, while the  $^{13}\text{C}$  chemical shift of the 50 N-acetylmethyl groups in the 16 oligosaccharides to 23.4 ppm. The  $^{13}\text{C}$ -chemical shifts for bulk of the carbohydrates are found over a region from 60 to 80 ppm.

## REFERENCES

- [1] Palmer AG, Wright PE, Rance M (1991) Measurement of relaxation time constants for methyl groups by proton-detected heteronuclear NMR spectroscopy. *Chemical Physics Letters* 185: 41-46.
- [2] Hardy RE, Dill K (1982) Magnetic resonance study of glycophorin A-containing  $^{13}\text{C}$ -enriched methionines. *FEBS letters* 143:327-331.
- [3] Byers DM, Verpoorte JA (1978) Structural stability of glycophorin effects of heat and guanidine-HCl. *Biochim. Biophys. Acta* 533 :478-486.
- [4] Jones WC, Rothgeb TM, Gurd FRN (1976) Nuclear magnetic resonance studies of sperm whale myoglobin specifically enriched with  $^{13}\text{C}$  in the methionine methyl groups. *J. Biol. Chem.* 251:7452-7460.

# STABILIZATION OF ENZYME BY POLYMER WITH PENDANT MONOSACCHARIDE

Katsuhiko Nakamae, Takashi Nishino, Yuji Saiki, Yoshio Yoshida, Masakazu Okumura\*, Keisuke Kinomura\* and Allan.S.Hoffman\*\*

*Faculty of Engineering, Kobe University, Rokko, Nada, Kobe 657, Japan; \*Nippon Fine Chemical Co., Ltd., Takasago 676, Japan; \*\*Center for Bioengineering Univ. of Washington, Seattle, WA, USA*

## SUMMARY

Stability of enzymes, lactate dehydrogenase (LDH) and trypsin, was evaluated in the presence of polymer with pendant monosaccharide. Enzyme was incubated in aqueous solutions of poly(glucosyloxyethyl methacrylate)(PGEMA), poly(ethylene glycol)(PEG), glucose, and saccharose.

The relative activity of LDH increased to 140% in the presence of 0.05 mol unit of monomer/l of PGEMA. The apparent Michaelis-Menten constant ( $K_m$ ) was determined at 30°C for LDH in the presence of PGEMA by using pyruvate as substrate. The  $K_m$  value of LDH with PGEMA was lower than that of pure LDH. The retained activity of LDH and trypsin increased in the presence of PGEMA.

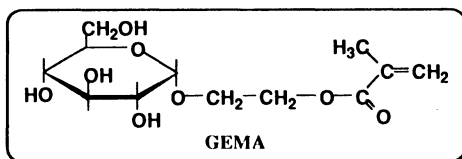
**KEY WORDS:** stability of enzyme , retained activity,lactate dehydrogenase, trypsin, glucosyloxyethyl metacrylate

## INTRODUCTION

Enzymes are intrinsically unstable, and if they are to be employed in applications such as pharmaceuticals, diagnostics, vaccines and various bioreactor processes, they must be stabilized against the myriad chemical and physical changes that can cause them to lose their desired functionality.

Various substances are used to stabilize enzyme in solution. These include salts, amino acids, polyhydroxy compounds, and nonionic detergents[1]. However, in most cases, they enhance stability only at low temperature, including freezing[2].

In this study, the effect of PGEMA on the stability of LDH and trypsin were evaluated in solution at various temperatures.



## METHODS

GEMA was polymerized in aqueous solution at 70°C with 2,2'-azobis(2-amidinopropane) dihydrochloride as an initiator for 4hours under nitrogen atmosphere. LDH and trypsin were chosen as the model enzyme, because it has potential use as a therapeutic agent. LDH from Rabbit muscle (Sigma) and trypsin from porcine pancreas (Sigma) was used without further purification. The activity of LDH was measured using pyruvate and b-Nicotinamide adenine dinucleotide (NADH) as substrate in 0.01M sodium phosphate buffer (pH 7.5) at 30°C. The activity of trypsin

was measured using  $\alpha$ -N-benzoyl-DL-arginine-p-nitroanilide hydrochloride (BAPNA) as substrate in 0.01M Tris-HCl buffer (pH 7.5) at 30°C.

## RESULTS AND DISCUSSION

Figure 1 shows the retained relative activity of LDH. The relative activity of LDH increased to 140% in the presence of 0.05 mol unit of monomer/l of PGEMA. It is suggested that the affinity between enzyme and substrate increased with adding PGEMA, possibly leading to the changes in the enzyme kinetics for LDH. Therefore, the apparent Michaelis-Menten constant ( $K_m$ ) was determined at 30°C for LDH in the presence of PGEMA by using pyruvate as substrate. The  $K_m$  value of LDH with PGEMA was lower than that of pure LDH. This may mean that the addition of PGEMA has somewhat higher affinity for the substrate than the pure LDH. This indicates that there is interaction between enzyme and PGEMA. The retained activity of pure LDH after incubation at 30°C for 48 hours is ca. 70% of its initial activity. In contrast, the LDH in the presence of PGEMA retained ca. 90% of initial activity of pure LDH. It is clear that PGEMA stabilized LDH in buffer solution. Fig. 2 shows the effect of incubation time on the retained activity of trypsin at 60°C. The pure trypsin and the trypsin in the presence of PEG retained little percent of its initial activity by incubation at 60°C for 90 min. In contrast, trypsin in the presence of PGEMA retained 20% of initial activity of pure trypsin. It is clear that the storage stability of trypsin increased in the presence of PGEMA more than the presence of PEG. This indicates that the addition of PGEMA provides protection against thermal inactivation of enzyme.

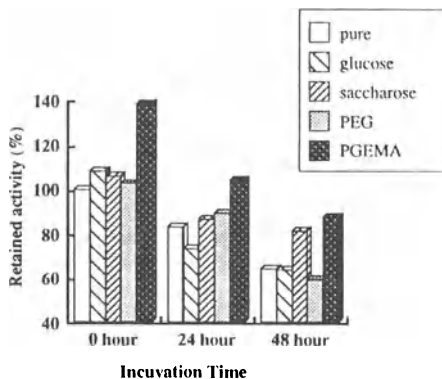


Fig. 1 Effects of the additives on the retained activity of LDH at 30°C, in 0.01M phosphate buffer, pH 7.5. The additives concentration was 0.05 mol/l. The retained activity of pure LDH without incubation is taken as 100%

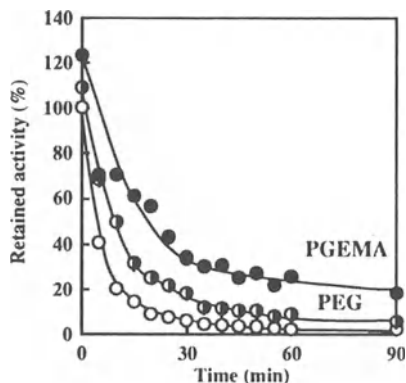


Fig. 2 Effects of incubation time on the retained activity of trypsin at 60°C, in 0.01M tris-HCl buffer, pH 7.5, in the presence of PGEMA (●), PEG (○). The retained activity of pure trypsin without incubation at 60°C is taken as 100%.

## REFERENCES

1. K. P. Antonsen, W. R. Gombotz and A. S. Hoffman. (1994) Attempts to stabilize a monoclonal antibody with water soluble synthetic polymer of varying hydrophobicity. *J. Biomater. Sci. Polym. Edn.* 6: 55-65.
2. J. F. Carpenter and J. H. Crowe. (1988) The mechanism of cryoprotection of proteins by solutes. *Cryobiology* 25: 244-255.

## Molecular Architecture of Temperature-Responsive Bioconjugates

Miki Matsukata, Takashi Aoki, Kohei Sanui, Naoya Ogata, Akihiko Kikuchi\*, Yasuhisa Sakurai\*, and Teruo Okano\*

Department of Chemistry, Faculty of Science & Technology, Sophia University 7-1, Kioi-cho, Chiyoda-ku Tokyo 102 Japan

\*Institute of Biomedical Engineering, Tokyo Women's Medical College, 8-1, Kawada-cho, Shinjuku-ku Tokyo 162 Japan

### SUMMARY

Chemical modification of biomolecules with synthetic and natural polymers has developed new applications of proteins in the fields of medicine, bio-engineering and bioreactor. We have been investigating polymer-protein hybrid modified by a temperature-responsive polymer, poly(N-isopropylacrylamide) (PIPAAM) and reported the possibility of regulation and recycling system of PIPAAM-enzyme by changing temperature with PIPAAM-lipase. We have also discussed that the molecular architecture of PIPAAM-enzyme conjugate affects their response towards temperature and stability in solution and demonstrated the necessity of molecular designing in protein modification by functional polymers. In this study, we prepared PIPAAM-conjugated BSA with semitelechelic oligomer containing carboxyl group(IDc) and amino group(IDa), in which different number of polymer chains attach to BSA by single-end. Their response towards temperature change was reversible and dependent on concentration and number of polymer chains, which indicated phase separation of conjugates was enhanced by hydrophobic interaction of dehydrated PIPAAM chains.

### KEYWORDS

Temperature-responsive bioconjugate / poly(N-isopropylacrylamide) / BSA / semitelechelic oligomer

### INTRODUCTION

In polymer-protein conjugation, poly(ethylene glycol)-modified proteins decreased the immunoreactivity and/or immunogenicity of antigenic proteins and increased their *in vivo* stability. Using these techniques functional polymers are capable of integrating new functions to the biomolecules. A water-soluble polymer, poly(N-isopropylacrylamide) (PIPAAM) shows unique, reversible hydration-dehydration changes in aqueous solution in response to small temperature changes[1]. We have been studying PIPAAM-biomolecule conjugates constructed by PIPAAM chain with a single end attachment[2,3,4], comparing multi-point attachment system[5]. Single-end attachment system was capable of temperature-induced separation and recycling without denaturation, whereas in multi-point attachment system, the conjugate was irresistible towards temperature changes[6]. In this paper, we modified bovine serum albumin(BSA) with two kinds of semitelechelic oligomers to prepare conjugates having different number of polymer chains and discussed their solution behavior as a new temperature induced biosystem.

### MATERIALS AND METHODS

Semitelechelic oligo(IPAAM-co-N,N-dimethylacrylamide)(Oligo(IPAAM-co-DMAAM)) with carboxyl end group (IDc) and amino group (IDa) were synthesized by telomerization reactions of IPAAM with DMAAM using 3-mercaptopropionic acid and 2-aminoethanethiol as a chain transfer agent, respectively in DMF at 70°C for 5 hr. Bovine serum albumin was used without purification. IDc-BSA was prepared by condensation reactions of amino groups located at the protein surface with activated carboxyl groups of IDc. IDa-BSA was prepared via sulfhydryl group by reaction with maleimide-activated IDa. Their LCSTs were measured spectrophotometrically by determining optical transmittance at 500nm using a spectrophotometer.

## RESULTS AND DISCUSSION

### Response towards temperature change

Both IDc and IDa exhibited LCST at 37°C as a result of introducing 10 mol% of DMAAm. BSA is known to have fifty nine lysine residues and one sulfhydryl group. IDc-BSA had five IDc chains in average per molecule which was measured by fluorescamine assay and IDa-BSA had one IDa chain per molecule. Both IDc-BSA and IDa-BSA conjugates were soluble in water at room temperature as well as organic solvent, and exhibited a temperature-induced phase separation according to the LCST of the polymer. Response toward temperature change of 1wt% aqueous solution of both conjugate was rapid and reversible due to the highly mobile free end groups of the grafted oligomers. This indicated that the solubility of BSA did not affect the solubility of IDc-BSA and IDa-BSA and their LCSTs could be regulated precisely by the LCST of oligomers.

### Effect of concentration on LCSTs

Concentration of conjugate was normalized by BSA concentration and transmittance change of dilute conjugate solution was measured as shown in Figure 1. In dilute solution their LCSTs shifted to higher temperature and their transmittance change became broader. LCSTs of IDc-BSA were lower than IDa-BSA when comparing at the same BSA concentration. These results indicates that the phase separation of polymer occur intramolecularly and hydrophobic interaction of dehydrated polymer chains enhance the precipitation of conjugates. The reason that their LCSTs of 1wt% solution was same as that of oligomers can be interpreted that at high concentration aggregates were formed fast due to the short distance between conjugates.

### Conclusion

Temperature-responsive BSA conjugates having different number of PIPAAm chains were prepared. Their LCSTs were dependent on concentration; in condensed aqueous solution intermolecular aggregation occurred as a result of hydrophobic interaction of dehydrated polymer chains which enhanced conjugates precipitation. Response toward temperature change was rapid and reversible due to the highly mobile free end groups of the grafted oligomers. This temperature-responsive BSA conjugate demonstrated that when changing temperature, the conjugate precipitate was formed firstly by the intramolecular dehydration of the polymer chains and secondly by the intermolecular aggregation between dehydrated polymers.

### REFERENCES

- [1]Heskins M, Guillet JE, James E (1968) Solution properties of poly(N-isopropylacrylamide). *J. Macromol. Sci. Chem.* A2:1441-1455
- [2]Takei YG, Aoki T, Sanui K, Ogata N, Okano T, Sakurai Y (1993) Temperature-responsive bioconjugates I. Synthesis of temperature responsive oligomers with reactive end groups and their coupling to biomolecules. *Bioconjugate Chem.* 4:42-46
- [3]Takei YG, Aoki T, Sanui K, Ogata N, Okano T, Sakurai Y (1993) Temperature-responsive bioconjugates 2. Molecular design for temperature-modulated bioseparations. *Bioconjugate Chem.* 4:341-346
- [4]Matsukata M, Takei Y, Aoki T, Sanui K, Ogata N, Sakurai Y, Okano T (1994) Temperature Modulated Solubility-Activity Alterations for Poly(N-Isopropylacrylamide)-Lipase Conjugates. *Journal of Biochemistry* 116:682-686
- [5]Park GT, Hoffman AS (1993) Synthesis and characterization of a soluble temperature-sensitive polymer-conjugated enzyme. *J. Biomater. Sci. Polymer Edn.* 4:493-504
- [6]Matsukata, M, Aoki T, Sanui K, Ogata N, Kikuchi A, Sakurai Y, Okano T (1994) Properties of Temperature-responsive PIPAAm-trypsin Conjugate. *Polymer preprints* 43:2479-2480

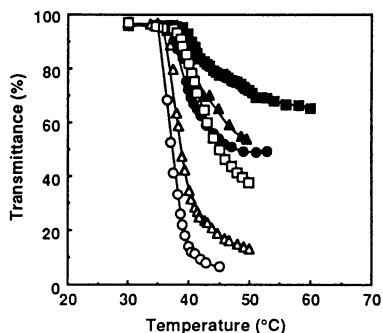


Figure 1. Temperature dependence of optical transmittance for aqueous solutions of PIPAAm-BSA conjugates at various BSA concentration (○; IDc-BSA, 0.5%, △; IDc-BSA, 0.3%, □; IDc-BSA, 0.1%, ●; IDa-BSA, 0.5%, ▲; IDa-BSA, 0.3%, ■; IDa-BSA, 0.2%).

# STABILIZATION OF L-ASPARAGINASE BY CHEMICAL MODIFICATION WITH POLY(ETHYLENE GLYCOL) DERIVATIVES

Misao Hiroto, Ayako Matsushima, Hiroyuki Nishimura, Yoh Kodera, and Yuji Inada

Toin Human Science and Technology Center, Department of Materials Science and Technology, Toin University of Yokohama, 1614 Kurogane-cho, Aoba-ku, Yokohama 225, Japan

## SUMMARY

L-Asparaginase modified with comb-shaped polyethylene glycol derivative, activated PM, markedly prolonged the clearance time *in vivo* and enhanced the stability against heat (65°C), urea (4.0 M) and acidity (pH 4.0).

**KEY WORDS:** comb-shaped copolymer, polyethylene glycol, stabilization of enzyme, chemical modification, L-asparaginase.

## INTRODUCTION

L-Asparaginase from *Escherichia coli* has been used clinically for the therapy of acute lymphocytic leukemia and lymphosarcoma. The disadvantage of this therapy lies in short circulation time in blood and in immunological side effects ranging in severity from mild allergic reaction to anaphylactic shock, as the enzyme is a protein foreign to humans. We had been trying to overcome these disadvantages of asparaginase by modifying with poly(ethylene glycol) (PEG) derivatives. Asparaginase modified with the chain-shaped PEG (activated PEG<sub>2</sub>, Fig. 1a) reduced its immunoreactivity while only 11% of the original activity was retained.

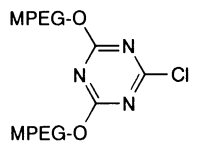
Recently, we developed a comb-shaped copolymer of PEG and maleic anhydride (Fig. 1b) with the molecular weight of 13,000 (activated PM<sub>13</sub>) and 100,000 (activated PM<sub>100</sub>) as a protein modifier. The PM<sub>13</sub>- and PM<sub>100</sub>-modified asparaginases with undetectable immunoreactivity by the quantitative precipitin reaction retained 46% and 85% of the original activity, respectively[1].

## MATERIALS AND METHODS

To an L-asparaginase solution in 0.5 M borate buffer (pH 8.5) was added activated PM<sub>13</sub> or PM<sub>100</sub>. After 1-h reaction at 4°C, uncoupled modifier was removed by ultrafiltration. Lipase from *Pseudomonas fluorescens* and trypsin from bovine pancreas were modified with activated PMs in the same manner.

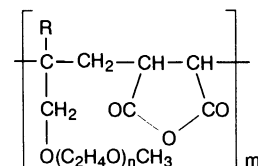
The *in vivo* clearance of the asparaginase preparations were measured after intravenous injection into rats. The asparaginase activity and L-asparagine (Asn) concentration in the serum were measured by the GOT method and with an amino acid analyzer, respectively. In the case of *in vitro* stability, the residual activity of asparaginase was determined by the Nessler's method after the incubation for a given time. The activities of lipase and trypsin were measured by using polyvinyl alcohol-emulsified olive oil and benzoyl-L-arginine ethyl ester as substrates, respectively.

### a. chain-shaped PEG



Activated PEG<sub>2</sub> 10 kD

### b. comb-shaped PEG



Activated PM<sub>13</sub>

m=8, n=33, R=H, 13 kD

Activated PM<sub>100</sub>

m=50, n=40, R=CH<sub>3</sub>, 100 kD

**Fig. 1**  
**Structure of modifiers**



## RESULTS AND DISCUSSION

After the *i.v.* injection of PM<sub>100</sub>-asparaginase, the enzymic activity was retained at least 11 days in blood circulation and the Asn concentration in serum remained undetectable for 27 days. After 27 days, the concentration of Asn in serum was increased with time. In the case of nonmodified asparaginase, Asn was eliminated from serum for less than 1 day. The clearance time of asparaginase *in vivo* was prolonged by the modification with activated PM<sub>100</sub>; the half-lives of modified and nonmodified asparaginases were 50 and 1.5 h, respectively.

The effect of the modification with activated PM<sub>13</sub> and PM<sub>100</sub> on the stability of asparaginase *in vitro* was tested towards heat, urea and acidity (Fig. 2). In the heat-stability at 65°C, the enzymic activity of nonmodified asparaginase was completely lost after a 30-min incubation. On the other hand, PM<sub>13</sub>- and PM<sub>100</sub>-asparaginases retained 35% and 90% of their enzymic activities, respectively, at the same incubation time. In the case of urea-denaturation, nonmodified asparaginase lost almost the enzymic activity with 4.0 M urea in 10 min, while PM<sub>13</sub>- and PM<sub>100</sub>-asparaginases retained 70% and 85% of the initial activities, respectively. The stabilization test was also performed with acidity. At pH 4.0, the enzymic activity of nonmodified asparaginase decreased markedly to 10% of the original activity by the 60-min incubation. The PM<sub>13</sub>- and PM<sub>100</sub>-asparaginases retained approximately 80% of their enzymic activities, respectively. On the contrary, the stabilities of PEG<sub>2</sub>-asparaginase towards heat and acidity were quite similar to those of nonmodified enzyme[2], probably because activated PEG<sub>2</sub> has a chain-shaped form with a monovalent reactive site.

These results indicate that the stabilization of asparaginase is caused by the modification with activated PM. This may be due to the interaction with covalent bonds and noncovalent bonds between PM and the protein molecule. In fact, lipase and trypsin were also stabilized toward heat (55–60°C) and urea (4.0 M) by the same modification with activated PM[3, 4]. In order to generalize the stabilization of various enzymes, experiments are now in progress. We believe that this novel technique may open a new avenue to biomedical and biotechnological fields.

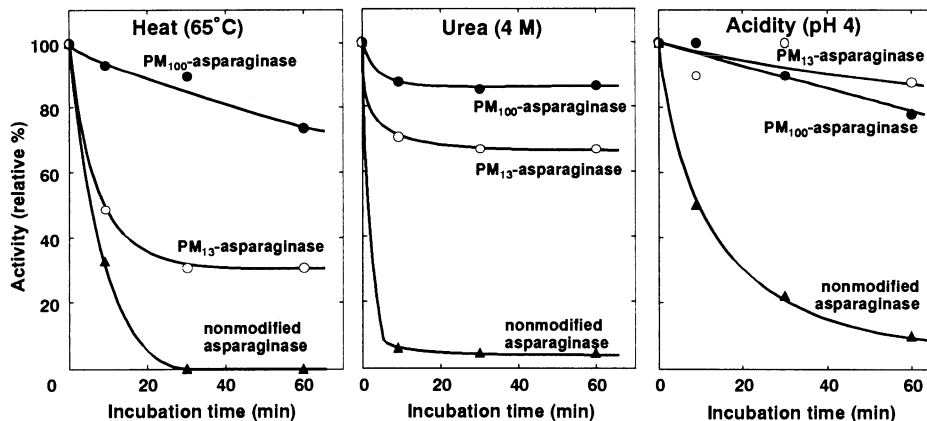


Fig. 2 Stabilization of L-asparaginase modified with activated PMs

## REFERENCES

1. Koderu Y, Tanaka H, Matsushima A, Inada Y (1992) *Biochem Biophys Res Commun* 5:283–286
2. Yoshimoto T, Nishimura H, Saito Y, Sakurai K, Kamisaki Y, Wada H, Sako M, Tsujino G, Inada Y (1986) *Jpn J Cancer Res* 77:1264–1270
3. Hiroto M, Matsushima A, Koderu Y, Shibata Y, Inada Y (1992) *Biotechnol Lett* 14:559–564
4. Hiroto M, Yamada M, Ueno T, Yasukochi T, Matsushima A, Koderu Y, Inada Y (1995) *Biotechnol Tech* 9:105–115

# NEW POLYMERIC HYDROGELS FOR THE REMOVAL OF URAEMIC TOXINS

G. Barsotti<sup>1</sup>, E. Chiellini<sup>2</sup>, E. Dossi<sup>2</sup>, D. Giannasi<sup>2</sup>, S. Giovannetti<sup>1</sup>, G. Mazzanti<sup>3</sup>, R. Solaro<sup>2</sup>

<sup>1</sup> II Medical Clinic, University of Pisa, 56126 Pisa, Italy

<sup>2</sup> Dept. of Chemistry and Industrial Chemistry, University of Pisa, via Risorgimento 35, 56126 Pisa, Italy

<sup>3</sup> I.S.I. SpA, Castelvechio Pascoli-Lucca, Italy

## SUMMARY

New polymeric hydrogels were prepared by radical copolymerization of methacrylic acid with acrylamides and oligo(oxyethylene)glycol mono- and dimethacrylates. Semisynthetic polymers containing a large number of aldehyde groups and in some case acid groups were also prepared by chemical modification of natural polysaccharides. "In vitro" tests have shown that the prepared matrices are characterized by a large capacity of water uptake, tunable by pH modulation, accompanied by a parallel ability to uptake urea, ammonia, sodium and potassium, matching the requirements for their utilization as adjuvants in the therapy of uraemic patients.

**KEY WORDS:** hydrogels, oxidized polysaccharides, chronic uraemia therapy, urea up-take

## INTRODUCTION

Chronic uraemia is a pathology characterized by a complex symptomatology due to accumulation of toxic metabolites and inability of kidneys to maintain constant pH and hydro-electrolytic balance in body fluids. Chronic uraemia therapy can be either *conservative*, implying the reduction of catabolites by ipoproteic diets, or *substitutive*, in which toxic metabolites are removed by extracorporeal dialysis. The possibility of reducing accumulation of water and toxic metabolites could greatly help to increase the time between dialyses and to improve the life quality of uraemic patients.

Within the framework of an investigation aimed at the preparation of new polymeric materials to be used for biomedical and pharmaceutical applications<sup>1-6</sup>, in the present paper we report on the synthesis of new macromolecular systems able to absorb water and other toxic metabolites from body fluids in the gastrointestinal tract and hence potentially valuable in uraemia therapy.

## RESULTS AND DISCUSSION

Polymeric hydrogels containing carboxylic and hydrophilic groups were prepared by polymerization of methacrylic acid (MAA), acrylamides [acrylamide (AAm), N-isopropylacrylamide (NIPA), N-terbutylacrylamide (NTBA)], oligo(oxyethylene)glycol monomethacrylates (OEGMA, degree of oligomerization 2, 4, 8) and tetra(oxyethylene)glycol dimethacrylate (TOEDMA) mixtures, in dioxane at 70 °C in the presence of AIBN as radical initiator (Table 1). In all cases polymeric products containing 5 meq/g of carboxylic groups were obtained with conversions generally higher than 75%. In order to evaluate the potentiality of these systems in removing body fluids from uraemic patients, the swelling in physiological solutions buffered at pH values of 4, 7 and 9 was evaluated for all polymer samples. The swelling power at pH 4, measured as weight of absorbed water per weight of dry polymer, resulted included between 2 and 13, the larger values being observed for samples having a larger content of amide units. Degrees of swelling not lower than 20 and in some cases larger than 100 were observed both at pH 7 and 9. All hydrogels were characterized by a significant ability to remove cations (1-8 meq/g) and urea (25-200 mg/g) from pH 7 buffered solutions containing 200 mg urea, 13 meq Na<sup>+</sup> and 0.5 meq K<sup>+</sup> in 100 ml.

Table 1. Preparation of methacrylic hydrogels.

Run	Polymerization feed <sup>a)</sup>					Conv. (%)	Polymeric product			
	AMA (mol %)	Amide type	Amide (mol %)	OEGMA n	OEGMA (mol %)		IEC <sup>b)</sup> (meq/g)	Swelling <sup>c)</sup>		
							pH 4	pH 7	pH 9	
PAA2R	47.0	AAM	39.0	2	13.0	97	5.2	2.1	21	19
PAA4R	52.0	AAM	35.0	4	12.0	98	5.3	2.3	32	36
PAA8R	59.0	AAM	30.0	8	10.0	78	5.0	2.3	23	24
PAAR	40.0	AAM	59.0	-	-	73	5.0	8.0	21	28
PAPAR	51.0	NIPA	48.0	-	-	35	5.1	13.0	121	90
PABAR	54.0	NTBA	45.0	-	-	36	5.0	3.0	61	73

<sup>a)</sup> Containing 1% of TOEDMA. <sup>b)</sup> Ion-exchange capacity. <sup>c)</sup> In physiological solution at 25°C, evaluated as weight of swelled polymer/weight of dry polymer.

Parallel to the strategy based on synthetic matrices, a second line focused on the preparation of semisynthetic polymers containing a large number of aldehyde groups and in some cases acid groups was developed. Accordingly, chemical modification of polysaccharides such as dextran, cellulose, starch, glucuronic acids and  $\beta$ -cyclodextrin was performed by  $\text{NaIO}_4$  oxidation either followed or not by crosslinking reaction.

It is well known that the presence of acid moieties kinetically favors the reaction between carbonyl groups and  $\text{NH}_2$  groups by imide or imine formation. Accordingly, some of the oxidized polysaccharides were further modified by phosphorylation, carboxylation, and carboxymethylation reactions.

Polymeric materials containing carboxylic and/or aldehydic groups were utilized in preliminary "in vitro" tests for the uptake of urea and ammonia from physiological solutions containing 200 mg urea and 50 mg ammonia in 100 ml, at 37°C. Under the adopted conditions the investigated samples resulted capable of uptaking 10–50 mg/g urea and 1–9 mg ammonia in 24 h. Nevertheless, in all cases the recorded uptake is at least one order of magnitude lower than that expected on the basis of the chemical constitution of the samples. Moreover the influence of degree of oxidation and of acidic groups content on extent and rate of uptake of urea and ammonia is not yet fully understood and further experimentation is needed.

The characteristics of some of the prepared matrices, that is a large capacity of water uptake, tunable by pH modulation, accompanied by a parallel ability to remove urea, ammonia, sodium and potassium, seem to positively match "in vitro" the requirements for their utilization in the therapy of uraemic patients. At present, an investigation of their "in vivo" activity is being carried out. Preliminary results obtained on healthy rats seem to confirm the results obtained in "in vitro" tests.

## ACKNOWLEDGMENTS

Financial support by I.S.I. SpA, MURST-40% and CNR is gratefully acknowledged. Oligo(oxyethylene)glycol monomethacrylates were kindly supplied by Nippon Oil & Fats Co. (Japan).

## REFERENCES

1. E. Chiellini, S. Faggioni, R. Solaro, *J. Bioact. Compat. Polym.*, **5**, 16 (1990)
2. R. Solaro, E. Chiellini, in *Synthetic Polymers as Drug Carriers. Interactions with Blood*, A. Baszkin, P. Ferruti, M.A. Marchisio, M.C. Tanzi, Eds., ALFA, Brescia, p. 71 (1991)
3. E. Chiellini, G. Leonardi, D. Giannasi, R. Solaro, *J. Bioact. Compat. Polym.*, **7**, 161 (1992)
4. E. Chiellini, R. Solaro, G. Leonardi, D. Giannasi, R. Lisciani, G. Mazzanti, *J. Controlled Release*, **22**, 273 (1992)
5. E. Chiellini, R. Solaro, *Makromol. Chem., Macromol. Symp.*, **54/55**, 483 (1992)
6. E. Chiellini, R. Solaro, *ChemTech.*, 29 (1993)

# ESTIMATION OF BIOCOMPATIBILITY OF POLYMERIC MATERIALS USING RT-PCR METHOD

Shinya Kato, Kaori Ohmura, Akio Kishida, Kazuhisa Sugimura and Mitsuru Akashi

Department of Applied Chemistry and Chemical Engineering, Faculty of Engineering, Kagoshima University, 1-21-40, Korimoto, Kagoshima 890, JAPAN

## SUMMARY

One of the most important factors in determining biocompatibility is the cellular response at the tissue-biomaterial interface. In this study, we would introduce a novel research method for the estimation of biocompatibility of polymeric materials, which is the evaluation of mRNA expression of the cells contacting with polymer surfaces using reverse transcription-polymerase chain reaction(RT-PCR) method. Interleukin-1 $\beta$ (IL-1 $\beta$ ) were selected to estimation of the extent of inflammation. The various polymer films were put into the 6well tissue culture plate. Human premyelocytic leukemia cell line(HL-60) were added to each well in containing 10% serum and with or without lipopolysaccharide(LPS) stimulation, or without serum, and were differentiated to macrophage-like cells by phorbol 12-myristate 13-acetate. After predetermined time, the total RNA were isolated from HL-60 cells and mRNA expression were quantitated by RT-PCR method. As a result, in the presence of serum and LPS stimulation, the expression of IL-1 $\beta$  mRNA increased with increasing the contact angle of films and reached to maximum at 70-80°. In the case of without LPS stimulation, IL-1 $\beta$  mRNA expression was decreased compared to the condition of presence of serum and LPS stimulation. From other results, IL-1 $\beta$  mRNA expression was influenced by the kind of substrate, LPS stimulation, serum presence and their combination. We assumed that RT-PCR method is one of the powerful methods to study the biocompatibility of materials.

**KEY WORDS** : RT-PCR, mRNA Expression, Cell-Polymer Interaction, Macrophage, Cytokine

## Introduction

One of the most important factors in determining the biocompatibility of implanted material is the cellular response to the material at the tissue-material interface. The cell-polymer interaction has been mainly investigated in vitro using various kinds of cells and various technic, such as cell adhesion counting, morphology observation, proliferation quantification and evaluation of cell functions. In this study, we would introduce a novel research methodology, the evaluation of mRNA expression of the cells contacting with polymeric materials. As the mRNA expression is the initial cellular response to the material, it seems possible to know how cells recognize the material by studying what kind of mRNA are transcribed. For this purpose, macrophage like cell, HL-60, was selected as the typical functional cell. Macrophage is known to play an important role in determining the immunological response to the material. Thus, it is useful to study the macrophage response to the material for evaluation of the biocompatibility of the material[1]. In this study, expression of IL-1 $\beta$  mRNA, which is the well known cytokine secreted by macrophage and was selected to estimation of the extent of inflammation, in the HL-60 cells contacting with various substrates were reported.

## Methods

The testing polymers selected as the culture substrate were as follows : tissue-culture-polystyrene(TCPS), polyethylene(PE), Silastic®(silicone), Nylon, tetrafluoroethylene-hexafluoropropylene copolymer(6F), Cellulose, acrylamide surface-grafted PE(AAm-g-PE) which has hydrophilic nonionic surface, N,N-dimethylaminopropylacrylamide surface-grafted PE(DMAPAA-g-PE) which has hydrophilic cationic surface, and p-styrenesulfonic acid sodium salt

surface-grafted PE(NaSS-g-PE) which has hydrophilic anionic surface. The polymer film were cut into 33mm diameter discs and set in the 6well tissue culture plate. Human premyelocytic leukemia cell line (HL-60) were added to each well at a concentration of  $3 \times 10^5$  cells/well in RPMI1640 containing 10%FCS. HL-60 cells were differentiated to macrophage like cell by phorbol 12-myristate 13-acetate and cultured with  $10 \mu\text{g/ml}$  lipopolysaccharide(LPS) stimulation. After predetermined time, the RNA was isolated from HL-60 cells by acid guanidine method[2] and reverse transcribed to cDNA. For the quantitation of mRNA, the method developed by Nakajima et al. was used[3]. 10-fold titrated cDNA( $10 \mu\text{l}$  -  $100 \text{pl}$ ) were amplified by PCR and the amplified cDNA by PCR were fractionated by electrophoresis in agarose gel. Relative expression were evaluated by detection of 821bp band (IL-1 $\beta$  mRNA) visualized by ethidium bromide staining.

## Results and Discussion

In this study, the reverse transcription-polymerase chain reaction (RT-PCR) was used to determine and quantify the expression of mRNA expression. This method is known to be applicable for detecting the mRNA expression with high sensitivity without using radio-isotope. We determined the experimental condition of detecting and quantifying mRNA expression by RT-PCR as shown in experimental section. Using the method of Nakajima, the quantification of expressed mRNA was carried out successfully. Fig.1 shows the expression of IL-1 $\beta$  mRNA in the presence of serum and LPS stimulation. The expression of mRNA increased with increasing the contact angle of films and reached to maximum at 70-80°, then slightly decreased. In the case of Cellulose, IL-1 $\beta$  mRNA expression was not observed. These profile with contact angle is same as the cell adhesion phenomena reported by Ikada et al[4]. From other results, IL-1 $\beta$  mRNA expression was influenced by the kind of substrate, LPS stimulation, serum presence and their combination. We would emphasize that RT-PCR method is one of the novel powerful research methods for studying biocompatibility of polymeric materials.

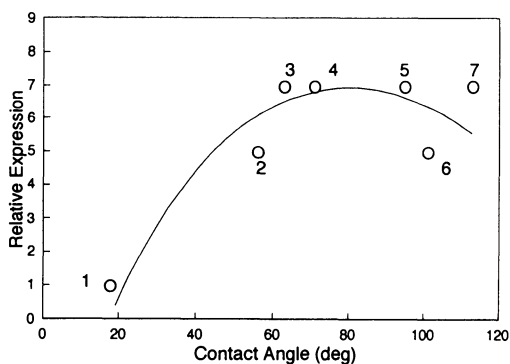


Fig. 1 Evaluation of mRNA Expression by RT-PCR method in Serum(+), LPS(+).  
1:Cellulose, 2:EVAL, 3:Nylon, 4:TCPS, 5:PE,6:Silastic, 7:F

## References

1. Bonfield TL, Colton E, Marchant RE, Anderson JM (1992) Cytokine and growth factor production by monocytes/macrophages on protein preadsorbed polymers. *J Biomed Mater Res* 26: 837-850
2. Chomozyski P, Sacchi N (1987) Single-step method of RNA isolation by acid guanidinium thiocyanate-phenol-chloroform extraction. *Anal Biochem* 162: 156-159
3. Nakajima T, Aono H, Hasunuma T, Yamamoto K, Maruyama I, Nosaka T, Hatanaka M, Nishioka K (1993) Overgrowth of Human Synovial Cells Driven by the Human T Cell Leukemia Type I tax Gene. *J Clin Invest.* 92: 186-193
4. Ikada Y, Tamada Y : *Polymer in Medicine 2* : Plenum Publishing, 1986; pp101

# TEMPERATURE RESPONSIVE SWELLING-DESWELLING KINETICS OF POLY(*N*-ISOPROPYLACRYLAMIDE) GRAFTED HYDROGELS

Yuzo Kaneko, Kiyotaka Sakai, Ryo Yoshida\*, Akihiko Kikuchi\*, Yasuhisa Sakurai\*, Teruo Okano\*

*Department of Chemical Engineering, Waseda University, 3-4-1 Ohkubo, Shinjuku-ku, Tokyo 169, JAPAN ; \*Institute of Biomedical Engineering, Tokyo Women's Medical College, 8-1 Kawada-cho, Shinjuku-ku, Tokyo 162, JAPAN*

## SUMMARY

A new approach is proposed to speeding up a deswelling response to temperature in a polymer hydrogel by tailoring the gel architecture at the molecular level. This novel structural design allows rapid conformational changes of grafted poly(*N*-isopropylacrylamide) (PIPAAM) chains within similar thermo-sensitive backbone network. Owing to easier expulsion of water from the network induced by the strong dehydration of side chains, the shrinking rate of this comb-type grafted hydrogel becomes much faster. A new deswelling mechanism rather than polymer network diffusion is introduced, and the intrinsic size-independent control of gel dynamics is achieved.

**KEY WORDS:** poly(*N*-isopropylacrylamide), comb-type grafted hydrogel, thermosensitivity, rapid conformational changes, faster deswelling

## INTRODUCTION

Recently, the swelling and deswelling volume changes of hydrogels in response to external stimuli, such as electric field [1] and heat [2] are utilized for the several potential applications, such as smart actuators [3] and drug delivery system [2]. For these applications of the stimuli responsive hydrogels, a fast response is needed. The kinetics of swelling and deswelling in these gels are typically governed by diffusion-limited transport of the polymeric components of the network in water, the rate of which is inversely proportional to the square of the smallest dimension of the gel [4]. Several strategies have been explored for increasing the responsive dynamics, such as introducing porosity [5,6]. In contrast to these previous works, we have attempted a novel deswelling mechanism rather than diffusion [7]. We prepare the hydrogel having side polymer chains grafted onto the main polymer network (Fig.1). This comb-type grafted hydrogel is improved its molecular mobility due to the existence of the free mobile chains. In our gel, a fast deswelling is achieved due to the immediate dehydration of grafted polymers which might aid the expulsion of water from the network during collapse and enhance the hydrophobic aggregation forces between polymer network. With this novel comb-type grafted hydrogel, more rapid stimuli responsive swelling dynamics of gel is attained.

## EXPERIMENTAL METHODS

The details of method for preparation of comb-type grafted hydrogel is described in elsewhere [7]. The solution containing IPAAm monomer (70wt%), PIPAAm macromer (30wt%) was polymerized by redox initiator, and crosslinked with methylenebisacrylamide at 15°C for 1 day. After washing, the swollen gel membranes were cut into disks using a cork borer (2mm thick, 15mm diameter). To determine the swelling-deswelling kinetics of gels, the weight change of gels in response to temperature change was measured. The kinetics of conventional gel (100wt% of monomer) was also measured as a reference.

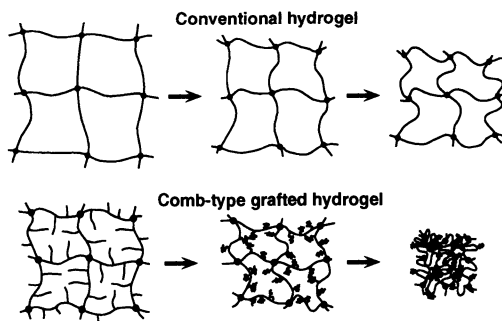


Fig.1 Structure and deswelling mechanisms for conventional PIPAAm and comb-type grafted PIPAAm hydrogels undergoing temperature induced collapse in water.

## RESULTS AND DISCUSSION

Figure 2 clearly shows the difference between deswelling behaviors of hydrogels undergoing shrinking at 40°C. The conventional PIPAAm hydrogel containing same amount of IPAAm shrinks slowly, need for more than a month to reach its equilibrium deswelling. On the other hand, the comb-type grafted hydrogel shrinks rapidly on the minute time scale, the quick response is demonstrated. The conventional gel formed the skin layer on the surface which have high impermeability to water [2,4]. Due to this surface skin formation, the slow release of entrapped water is observed. In contrast, the grafted gel shows mechanical buckling, indicative of the strong aggregation forces operating within the gel. Water is strongly squeezed out of the gel.

This strong repulsion of entrapped water was readily observed by DSC measurements of water content inside the hydrogel networks [7]. The amount of freezable water decreased dramatically within 20 min after an increase of temperature to 40°C, although non-freezable water content was maintained almost constant and low. Therefore, drastic swelling change observed for the grafted hydrogel is attributed to the significant change in freezable water content in the gel. In contrast to comb-type grafted hydrogel, slight change in freezable water content was observed for conventional gel. With increasing temperature, grafted polymers exposed to water rapidly dehydrate, and almost freezable water is released. The rapid deswelling of grafted gel is caused by this immediate dehydration of graft chains which is followed by the strong hydrophobic interaction between dehydrated graft chains. The dehydrated chains create hydrophobized portion in the network which enhance hydrophobic aggregation of the crosslinked network. The rapid shrinking kinetics of the comb-type grafted hydrogel also results from the lack of collapsed polymer skin on the gel surface, and an increase in void volume within the polymer network subsequent to the dehydration of grafted chains may also contribute to facilitate the release of entrapped water to the gel exterior.

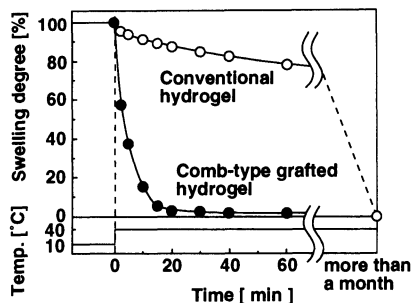


Fig.2 Deswelling kinetics for hydrogels undergoing shrinking at 40°C in response to stepwise temperature increase from 10°C.

## CONCLUSIONS

In this research, we have achieved a dramatic new deswelling changes in PIPAAm gels in response to temperature by introducing rapid conformational changes of mobile, grafted polymers. In contrast to the dynamic properties dominated by the diffusion-limited transport (collective diffusion), we demonstrate the other concept for controlling the gel swelling behaviors with this comb-type grafted hydrogel structure. We believe that by using such a fast responsive gels, we can eliminate the current limitations to realize the rapid acting actuators composed of the smart hydrogels.

## REFERENCES

1. Tanaka T, Nishio I, Sun ST, Ueno-Nishio S (1981) Collapse of gels in an electric field. *Science* 218: 467-469.
2. Okano T, Yui N, Yokoyama M, Yoshida R (1993) Temperature-responsive polymers and drug delivery. In: Ikoma T, Karube I, Kuroda, R (eds) *Advances in polymeric systems for drug delivery*. Gordon and Breach Science Publishers: Yverdon, pp 67-105
3. Osada Y (1977) Hydrothermal contraction-dilation of polymer networks by reversible complexation with a complementary macromolecules. *J. Polym. Sci. Polym. Chem. Edn.* 15: 255-267
4. Sato Matsuo E, Tanaka T (1988) Kinetics of discontinuous phase transition of gels. *J. Chem. Phys.* 89: 1695-1703
5. Kabra BG, Gehrke SH (1992) Synthesis of fast response, temperature-sensitive poly(*N*-isopropylacrylamide) gel. *Polymer commun.* 32: 322-323
6. Wu HS, Hoffman AS, Yager P (1992) Synthesis and characterization of thermally reversible macroporous poly(*N*-isopropylacrylamide) hydrogels. *J. Polym. Sci., A. Polym. Chem.* 30: 2121-2129
7. Yoshida R, Uchida K, Kaneko Y, Sakai K, Kikuchi A, Sakurai Y, Okano T (1995) Comb-type grafted hydrogels with rapid de-swelling response to temperature changes. *Nature* 374: 240-242

# TEMPERATURE-SENSITIVE CHANGES IN SURFACE PROPERTIES OF A POLY(N-ISOPROPYLACRYLAMIDE) HYDROGEL LAYER

Kimiko Makino<sup>a</sup>, Ken Suzuki<sup>b</sup>, Yasuhisa Sakurai<sup>b</sup>, Teruo Okano<sup>b</sup>, and Hiroyuki Ohshima<sup>a</sup>

<sup>a</sup>*Faculty of Pharmaceutical Sciences and Institute of Colloid and Interface Science, Science University of Tokyo, 12 Ichigaya Funagawara-machi, Shinjuku-ku, Tokyo 162, Japan.*

<sup>b</sup>*Institute of Biomedical Engineering, Tokyo Women's Medical College, 8-1 Kawadacho, Shinjuku-ku, Tokyo 162, Japan.*

## SUMMARY

A poly(N-isopropylacrylamide)-coated glass was prepared and its interfacial electrokinetic properties were studied with a special emphasis on the phase transition behavior of the hydrogel. The electro-osmotic flow velocity was measured on the hydrogel surface immersed in an electrolyte solution at pH 7.4 as a function of temperature and ionic strength. The data were analyzed with an electrokinetic theory for "soft" surfaces to determine the charge density ( $zN$ ) and the softness parameter ( $1/\lambda$ ) of the hydrogel layer. The charge density ( $zN$ ) and the softness parameter ( $1/\lambda$ ) obtained have been well explained the volume change of the hydrogel.

KEY WORDS : Poly(N-isopropylacrylamide), Electro-osmosis, Soft surfaces

## INTRODUCTION

Poly (N-isopropylacrylamide) hydrogel, which has a phase transition temperature at 33 °C, is in a swollen state below 33 °C and is in a shrunken state above it. In previous papers [1,2], we have shown results of the measurements and the analysis of the electrophoretic mobility of a latex particle composed of poly(styrene) and poly(N-isopropylacrylamide). The dependence of the electrophoretic mobility of a latex particle covered with a poly(N-isopropylacrylamide) hydrogel layer upon temperature and ionic strength of the dispersing medium was well explained via an electrophoretic mobility formula for "soft particles" [3]. In the present paper, we have prepared poly(N-isopropylacrylamide) hydrogel plates, measured the electro-osmotic flow on its surface and have analyzed the experimental data via a formula for the electro-osmotic velocity on a charged "soft surface" [4]. The number of fixed charges in the hydrogel was also determined by potentiometric titration and the swelling ratio at equilibrium was measured as a function of ionic strength and temperature. Also the wettability of the hydrogel was measured as a function of temperature.

## METHODS

### Preparation of poly(N-isopropylacrylamide) hydrogel

Poly(N-isopropylacrylamide) hydrogel was prepared in the same way as reported before[4].

### Measurement of anionic charges in the hydrogel

The hydrogel was immersed in a sodium hydroxide solution to produce complete dissociation of all sulfonic groups at the terminal of each polymer chain and the residual sodium hydroxide concentration was measured potentiometrically with a hydrochloride solution at 25 °C.

### Equilibrium swelling measurements

The swelling ratio of the hydrogel at equilibrium was measured as a function of temperature and the ionic strength of phosphate buffer solutions at pH 7.4. The swelling ratio,  $W_s/W_p$ , is defined as the weight of adsorbed water ( $W_s$ ) per unit weight of the sample in a dry state ( $W_p$ ).

### Measurement of eletro-osmotic flow on the hydrogel surface

The electro-osmotic flow of electrolyte solution with various ionic strengths was measured on the hydrogel surface at various temperatures with an Otsuka ELS800 electrophoretic light scattering apparatus.

### Measurement of wettability of the hydrogel

The dynamic contact angle of the hydrogel in distilled water was measured at various temperatures with the Wilhelmy plate technique using an Orientec DCA-20 apparatus.



## RESULTS AND DISCUSSION

Figure 1 shows the electro-osmotic velocity per unit electric field (mobility,  $-U_{EO} / E = \mu$ ) on the hydrogel surface at various temperatures and the theoretical curves obtained by analyzing the experimental data with eq. (1)[3] to determine the softness,  $1/\lambda$  (nm), and the charge density,  $zN$  (M), of the hydrogel surface.

$$\mu = \frac{\epsilon_r \epsilon_0}{\eta} \frac{\Psi_0 / \kappa_m + \Psi_{DON} / \lambda}{1 / \kappa_m + 1 / \lambda} + \frac{z e N}{\eta \lambda^2}, \quad (1)$$

where  $\eta$  is the viscosity,  $\epsilon_r$  is the relative permittivity of the solution,  $\epsilon_0$  is the permittivity of a vacuum,  $\Psi_{DON}$  is the Donnan potential of the hydrogel layer,  $\Psi_0$  is the potential at the boundary between the hydrogel layer and the surrounding solution, and  $\kappa_m$  is the Debye-Hückel parameter in the hydrogel layer. The negative charge density in the hydrogel layer ( $zN$ ) decreases and the surface of the hydrogel becomes harder ( $1/\lambda$  increases) as the temperature rises, as shown in Table 1. This change, which is seen most appreciable around the phase transition temperature (33 °C), is consistent with the prediction from the number of sulfonic acid determined by titration (-0.008 M at 25 °C) and the gel volume at various temperatures. Also, the dynamic contact angle drastically increases around the phase transition temperature (33 °C) as shown in Fig. 2, exhibiting that the hydrogel surface becomes more hydrophobic as the temperature rises.

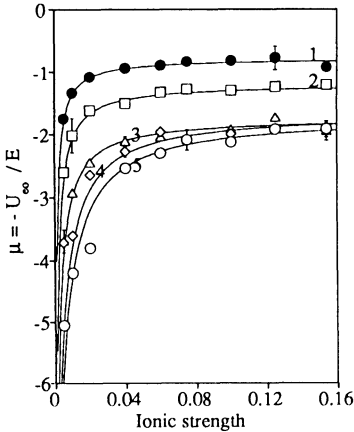


Fig. 1. Electro-osmotic mobility ( $\mu$ ) against the ionic strength of the bulk solution at several values of temperature. Symbols represent experimental data : ●, 25°C; □, 30°C; △, 33°C; ◇, 35°C; ○, 40°C. Solid curves are theoretical results calculated with the values shown in Table 1.

Table 1. Charge density,  $zN$  [M], and softness parameter,  $1/\lambda$  [nm], of poly(IPAAm) surface at various temperatures.

Temperature (°C)	$zN$	$1/\lambda$
25	-0.008	3.0
30	-0.011	3.0
33	-0.015	3.0
35	-0.028	2.1
40	-0.032	1.9

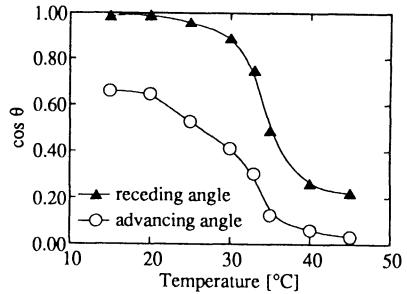


Fig. 2. Dynamic contact angle ( $\theta$ ) against temperature.

## ACKNOWLEDGMENT

K.M. gratefully acknowledges the SUT Grant for Research Promotion 1994.

## REFERENCES

- [1] H. Ohshima, K. Makino, T. Kato, K. Fujimoto, H. Kawaguchi (1993) Electrophoretic mobility of latex particles covered with temperature-sensitive hydrogel layers. *J. Colloid Interface Sci.* 159: 512-514.
- [2] K. Makino, S. Yamamoto, K. Fujimoto, H. Kawaguchi, H. Ohshima (1994) Surface structure of latex particles covered with temperature-sensitive hydrogel layers. *J. Colloid Interface Sci.* 166: 251-258.
- [3] H. Ohshima (1994) Electrophoretic mobility of soft particles. *J. Colloid Interface Sci.* 163:474-483.
- [4] K. Makino, K. Suzuki, Y. Sakurai, T. Okano, H. Ohshima, Electro-osmosis on a thermosensitive-hydrogel surface. *J. Colloid Interface Sci.*, in press.

# EFFECT OF ANION-EXCHANGE CAPACITY AND POROSITY OF POLYETHYLENEIMINE-IMMOBILIZED CELLULOSE FIBERS ON SELECTIVE REMOVAL OF ENDOTOXIN

Sunao Morimoto, Toru Iwata, Akihiko Esaki, Masayo Sakata, Hiroataka Ihara and Chuichi Hirayama

Department of Applied Chemistry, Faculty of Engineering, Kumamoto University, Kumamoto 860, Japan

## SUMMARY

Endotoxin is a component of cell-wall of gram-negative bacteria. Removal of endotoxin from cell products used as drugs is very important. Its potent biological activity causes pyrogenic and shock reactions in man and mammals on intravenous injection even in nanogram amounts. To remove it from protein solutions, the adsorption method has proven to be the most effective.

We developed novel cellulosic adsorbents (Cell-PEI) having polyethyleneimine (PEI) as a ligand. The Cell-PEI with anion-exchange capacity of 1.1 - 3.0 meq/g and  $M_{lim}$  2000 - 43000 satisfactorily removed endotoxin, but the adsorption ratio of the BSA was increased with increase in the anion-exchange capacity of more than 1.1, and with increase in the  $M_{lim}$  of more than 5000. The Cell-PEI ( $M_{lim}$ : 2000, anion-exchange capacity: 1.1 meq/g) selectively reduced endotoxin from various proteins, even at a low ionic strength of  $\mu = 0.05$  without affecting protein recovery.

## KEY WORD

endotoxin, selective removal, anion-exchange capacity, porosity, ionic strength

## MATERIALS AND METHODS

Cellulose fibers were prepared by means of mixing viscose (containing 9.5 % of cellulose) and polyethyleneimine. This was span into the coagulation bath containing sulfuric acid, sodium sulfate, zinc sulfate and water. The coagulation was effected through a nozzle of 10000 holes, each of diameter 0.07 mm. The obtained regenerated fibers

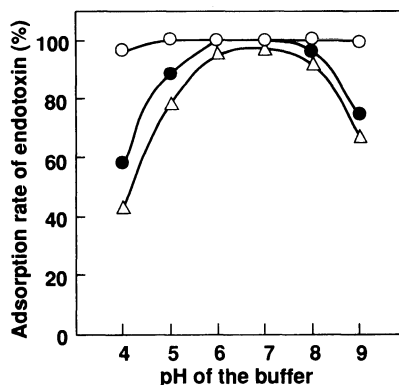


Fig. 1 Effects of pH on adsorption of endotoxin by Cell-PEI adsorbents.

Adsorbent: 100 mg of Cell-PEI-1 (anion-exchange capacity 1.1 meq/g,  $M_{lim}$  2000), BSA solution: 2 ml (500  $\mu$ g/ml), Ionic strength of the buffer: (○)  $\mu = 0.05$ ; (●)  $\mu = 0.2$ ; (△)  $\mu = 0.4$ .

were fixed with glutaraldehyde. The cellulose fibers were used as adsorbents.

The endotoxin concentration of the solution was assayed by a Limulus test method. The protein concentration was determined spectrophotometrically.

## RESULTS

The pore size and the amino-group content of the Cell-PEI adsorbent can be readily adjusted by changing the ratio of sodium carbonate and that of polyethyleneimine to cellulose. The endotoxin-adsorbing activity increased with the increase in the anion exchange capacity of the adsorbent. Figure 1 showed the adsorbents had a high endotoxin-adsorbing capacity at pH from 5 to 8 even at high ionic strengths ( $\mu = 0.2, 0.4$ ). As shown in Figure 2, the adsorption rate of BSA increased from 1 to 60 % with increase in  $M_{lim}$  of the adsorbents from  $M_{lim}$  5000 to 43,000 at a low ionic strength ( $\mu=0.05$ ).

The Cell-PEI adsorbents with anion-exchange capacity of 1.1-3.0 meq/g and  $M_{lim}$  2000 satisfactorily removed endotoxin, but the adsorption ratio of BSA was increased with an increase in the anion-exchange capacity, as shown in Figure 3.

We also observed that Cell-PEI ( $M_{lim}$  2000, amino-group content 1.1 meq/g) adsorbent was an efficient agent for removal of natural endotoxin from various protein-containing solutions without affecting the recovery of the protein (Table 1). This good selectivity can be explained by the fact that the adsorbent ( $M_{lim}$  2000) has smaller pores than the histidine immobilized polysaccharides ( $M_{lim}$  100,000).

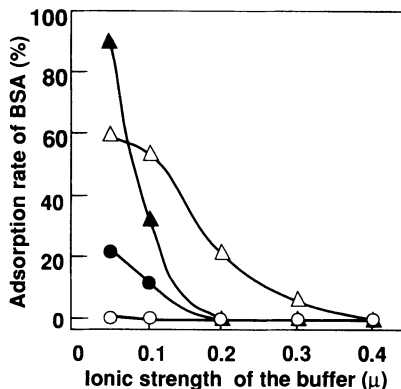


Fig. 2 Effects of  $M_{lim}$  and ionic strength on adsorption of BSA by various adsorbents.

Adsorbent: 100 mg, BSA solution: 2 ml (500  $\mu$ g/ml, pH 7.0,  $\mu = 0.05 - 0.4$ ),  $M_{lim}$  of Cell-PEI: (○), 5000; (●), 10,000; (△), 43,000,  $M_{lim}$  of histidine-immobilized cellulose spheres; (▲) 100,000, Anion-exchange capacity of the adsorbent: 0.3 meq/g.

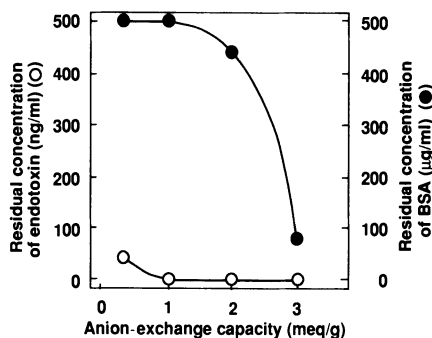


Fig. 3 Effect of anion-exchange capacity on removal of endotoxin from a BSA solution containing endotoxin by the Cell-PEI fibers ( $M_{lim}$  2000, anion-exchange capacity 0.3 - 3.0 meq/g).

Adsorbent: 100 mg, Sample solution: 2 ml (BSA 500  $\mu$ g/ml, *E.coli* O111:B4 LPS 500 ng/ml, pH 7,  $\mu = 0.05$ ).

Table 1 Removal of endotoxin from various protein solutions with Cell-PEI-1 adsorbent

Compound (500 $\mu$ g/ml)	Concentration of endotoxin (ng/ml)		Recovery of protein (%)
	Before treatment	After treatment	
BSA	22	0.07	98
Myoglobin	0.9	0.02	99
$\gamma$ -Globulin	8.6	0.05	99
Cytochrome c	1.2	<0.01	100

Adsorbent: 0.25 g ( $M_{lim}$  2000, amino-group content 1.1 meq/g),  
Sample solution: 5 ml (pH 7.0,  $\mu = 0.05$ ).

# Cellular communication with conducting electroactive polymers

Anthony J. Hodgson, Melinda J. John, Michael Kelso, and Gordon G. Wallace

*Intelligent Biomaterials Research Unit, IPRL, Dept. Chemistry, University of Wollongong, and Dept. Haematology, The Wollongong Hospital, Crown St, Wollongong, NSW Australia, 2500.*

## ABSTRACT

New biomaterials with dynamically active properties were constructed as composites containing the conducting electroactive polymer, polypyrrole, dextran sulphate and the protein human serum albumin. This material is an excellent surface for the culture of mammalian cells. It is a hydrophilic matrix with a high water content and here we report the ability to control the release of protein by reducing the polypyrrole backbone.

Keywords: conducting polymers, polypyrrole, albumin, controlled release, hydrogel composite

## INTRODUCTION

Developing new biomedical devices (for example vascular grafts) depends on the successful long term integration of new biomaterials with tissues and cells of the body. The interaction of these materials, usually polymers, with cells depends to a major extent on the chemistry of the surface of the polymer. Older concepts that inertness was required for biocompatibility are rapidly being re-placed by concepts of biospecific interaction. Successful integration of a new material is more likely by tailoring an appropriate reaction between cells and the interface. This concept inevitably requires a re-positioning of the notion of biocompatibility itself. Biocompatibility can no longer be used as a global term to describe the favorable integration of a material with tissues and organs in general. Its definition will need to include specification at a much more localised level. What may be 'compatible' at one site may be incompatible at another. This argument has been capably put by Ratner who used the example of the different requirements for compatibility with veins versus arteries [1]. We prefer to use the term "bio-integration" to describe more accurately the process that we strive to engineer.

A careful consideration of the many chemical, mechanical and biological processes occurring at the polymer-tissue interface leads to the conclusion that design of a surface capable of bio-integration will have to take into account the immediate micro-environment of this interface. It must also be designed with consideration of the time domain. The ability to change the properties of the material as interaction with the tissues and cells occurs can lead to significant advantages in engineering a favorable biological response. Biodegradable polymers and the many drug delivery devices are examples of use of materials whose properties change as a function of time. However, the materials used have limited capability. In our view to create effective integration with cells and tissues of the body re-quires a material or surface that is able to mimic many of the properties of the site. This mimicry may take place at the level of the organ, tissue, cell or molecule. This of course demands, among many other things, a high degree of multifunctionality in the material. This rapidly leads to the realisation that composite materials are required to deliver such complex requirements. Not only this but as our powers of cellular and molecular engineering improve the possibilities of tailoring surfaces to selectively interact with targeted molecules at any one particular site become more realistic.

We have studied a new class of materials that have many properties useful in development of materials for molecular-cellular communication. Cells inter-communicate by using a variety of dynamic membrane events. Thus cells (particularly nerve cells, the communications experts) receive and transmit information by using electrochemical potentials at the cell membrane, ion fluxes and release of a variety of chemical substances including proteins. Their membranes contain bio-active macromolecules capable of dynamic changes (modulation) in binding properties. Conducting electroactive polymers share many of these properties. They are electronic conductors and are electro-active. This enables the design of materials that are dynamically active and able to change surface properties rapidly and reversibly. Bioactive proteins can be incorporated into them and the activity of the protein changed simply by application of small electrical potentials [2]. We have previously reported the synthesis of composite materials suitable for supporting the growth and differentiation of a variety of mammalian cells [3]. More recently we have been able to control the release of protein from them.

## EXPERIMENTAL

Polypyrrole composites were synthesised galvanostatically on gold coated mylar films (20cm<sup>2</sup>) at a current density of 1 mAcm<sup>-2</sup> for 30 to 240 sec. Synthesis solution contained 0.2M pyrrole, 5gL<sup>-1</sup> dextran sulphate (Mr 50,000) and I<sup>125</sup> labelled human serum albumin (HSA).

Polymers contained an amount of protein that was a function of the amount of HSA in the synthesis

RELATIONSHIP BETWEEN THE AMOUNT OF HUMAN SERUM ALBUMIN PRESENT IN A 15 ml. ELECTROCHEMICAL CELL & THE AMOUNT THAT IS SUBSEQUENTLY INCORPORATED INTO A POLYPYRROLE DEXTRAN POLYMER UPON SYNTHESIS.

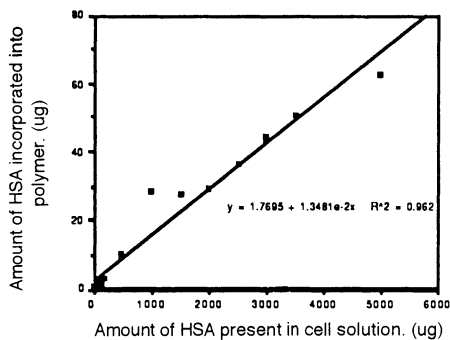


Figure 1

GRAPH SHOWING THE % HSA RELEASED FROM A POLYMER Vs THE AMOUNT OF TIME THE POLYMER WAS HELD AT -900mV. (w.r.t. Ag/AgCl)

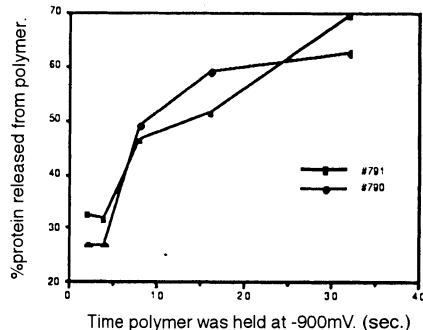


Figure 2

solution, (fig 1). The HSA was retained within the polymer and did not diffuse from it when incubated in saline solution, 0.15M NaCl; after 7 hours 98 ( $\pm 3$ )% remained and even after 3 days 95 ( $\pm 10$ ) % remained. When the polymer was reduced by applying a cyclic voltage ramp from +0.5 V to -0.7, -0.8 or -0.9 V appreciable HSA was released into the saline electrolyte solution. The amount of HSA released was greater for more negative potentials. The time course of release was investigated by applying a fixed negative potential for times ranging from 2 to 32 seconds. Figure 2 shows the protein was released rapidly from the polymer. Within 2 seconds 20 to 30 percent of the protein contained within the polymer had been released. After only 32 seconds most of the contents of the polymer had been re-released. When oxidising potentials (+0.5 V) were applied or potentials close to the rest potential of polypyrrole (+0.17 V) no protein was released. The polymer was electroactive and showed a cyclic voltammogram similar to polypyrrole/dextran sulphate, (fig 3).

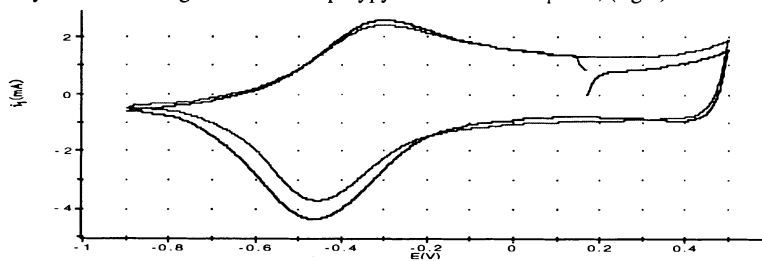


Figure 3

We are currently investigating the fine control of protein by using small pulses (10-100 msec) of reduction as well as studying the influence of potential cycling on other proteins such as growth factors. In previous work we have shown release of basic proteins on oxidation [3]. The rapid release of protein from these polymers is facilitated by several factors. At the pH studied, pH 6.5, the protein released, HSA, is an anion. When polypyrrole is reduced it is well known that anions are expelled to maintain charge balance. Large macro-anions are sterically trapped within the polymer. However we have designed our polymers to be hydrophilic by the incorporation of the highly hydrated polyanion, dextran sulphate. The polymers have water contents of 60 to 80%. The open, porous, hydrophilic matrix is responsible for the facile expulsion of the negatively charged protein. Even though the protein is expelled as an anion it must be retained within the polymer by more than ion exchange. Simple anions like chloride diffuse from the polymer by ion exchange. There was no such tendency for albumin to diffuse despite the high water content. Therefore there must be other forces retaining the protein within the polymer matrix. This could include hydrophobic effects as well as ion pairing, hydrogen bonding and steric restriction.

## REFERENCES

- [1] Ratner, BD (1993) *J.Biomed Mater. Res.* 27 283-287
- [2] Hodgson AJ, Lewis, TL, Maxwell, K, Spencer, MJ, and Wallace GG. (1990) *J.Liquid Chromatog* 13, 3091.
- [3] Hodgson AJ, Gilmore K, Small, C, MacKenzie, IL, Wallace GG, Aoki, T, Ogata, N, (1995) *Supramol Struct* In Press

# **Drug Delivery Systems**

# STIMULI-SENSITIVE RELEASE OF LYSOZYME FROM HYDROGEL CONTAINING PHOSPHATE GROUPS

Katsuhiko Nakamae, Takeshi Nizuka, Takashi Miyata\*, Tadashi Uragami\*, Allan S. Hoffman\*\* and Yoshio Kanzaki\*\*\*

*Faculty of Engineering, Kobe University, Rokko, Nada, Kobe 657 JAPAN; \*Faculty of Engineering, Kansai University, Suita, Osaka 564 JAPAN; \*\*Center for Bioengineering, University of Washington, Seattle, WA 98195 USA; \*\*\*Unichemical Co., Ltd., Ikoma, Nara 636 JAPAN*

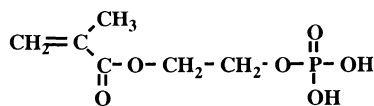
## SUMMARY

Large amount of lysozyme could be loaded in hydrogels containing phosphate groups by ionic binding between negatively-charged phosphate groups and positively-charged lysozyme. Lysozyme release from the hydrogels was influenced by the conditions such as ionic strength and pH. The rate of lysozyme release at pH 7.4 was much faster than that at pH 1.4. The lysozyme release at pH 7.4 is based on the ion exchange mechanism due to the ionization of the phosphate groups. The pH-sensitive dissociation of ionic binding resulted in the lysozyme release in response to a step-wise pH change.

**KEY WORDS:** Hydrogel containing phosphate groups, Lysozyme release, Stimuli-sensitivity, Ion exchange mechanism

## INTRODUCTION

Stimuli-sensitive hydrogels attract our attention in the development of intelligent drug release systems. We previously prepared pH- and temperature-sensitive hydrogels containing phosphate groups by copolymerizing various monomers with a monomer containing a phosphate group (phosmer) [1, 2]. In previous works, amylase and lysozyme which are anionic and cationic proteins, respectively, were loaded into lightly crosslinked anionic copolymer hydrogels by ionic binding [3]. In the present work, we focus on stimuli-sensitivity of ionic binding between phosphate groups and lysozyme, and studied the release of lysozyme from the hydrogels containing phosphate groups under various conditions.



**Phosmer**

## METHODS

The hydrogels containing phosphate groups and carboxyl groups were prepared by the copolymerizations of *N*-isopropyl acrylamide (NIPAAm) with phosmer and methacrylic acid (MAAc), respectively, using *N,N'*-methylene bisacrylamide as a crosslinker. Lysozyme was loaded into the hydrogels by swelling the dried gel samples in 10mg/ml solutions of lysozyme in distilled water (pH 3.2). After the hydrogels were then rinsed in water and dried under reduced pressure, they were used for lysozyme release experiments. Lysozyme release from the dried gels during swelling was carried out in KCl solutions or buffer solutions (pH 1.4 or 7.4) at 37°C, and was monitored with a UV spectrophotometer.

## RESULTS AND DISCUSSION

An approximately linear relationship existed between the phosphate group content and the amount

of lysozyme loaded into the hydrogels containing phosphate groups and carboxyl groups. The amount of lysozyme loaded into the hydrogel containing phosphate groups was twice larger than that into the hydrogel containing carboxyl groups. Especially, 50wt% of lysozyme could be loaded into the hydrogel with the phosphate group content of 20 mol%. This is probably due to the fact that the phosphate group is a stronger acidic group at pH 3.2 than the carboxyl group. Carboxyl groups of MAAC are not ionized at pH 3.2, but the phosphate groups are a little ionized. Therefore, lysozyme is mainly loaded in the MAAC-NIPAAm gel by the entrapment, but in the phosmer-NIPAAm gel by ionic binding between negatively-charged phosphate group and positively charged lysozyme (pI 11) as well as the entrapment.

Release profiles of lysozyme from the hydrogel containing phosphate groups and its swelling ratio in 0.05 and 0.5M KCl solutions (pH 7.4, 37°C) were investigated. The swelling ratio of the hydrogel in 0.5M KCl was much lower than that in 0.05M KCl. In spite of less swelling, lysozyme was more effectively released from the hydrogel in the former solution than in the latter. These imply that the lysozyme release is driven by the ion exchange mechanism. This result leads us to the speculation that lysozyme release can be controlled by using dissociation of ionic binding between lysozyme and phosphate groups in response to various stimuli.

Release profiles of lysozyme from the hydrogel into 0.1M KCl solution at pH 1.4 and 7.4 (37°C) were examined. The rate of lysozyme release at pH 7.4 was much faster than that at pH 1.4 (Fig.1). Furthermore, lysozyme was completely released at pH 7.4, but the lysozyme release was suppressed at pH 1.4. Since the phosphate groups are negatively ionized at pH 7.4, lysozyme is released by the ion exchange mechanism. At pH 1.4, however, the ion exchange mechanism cannot operate due to the low content of ionized phosphate groups. Lysozyme could be released from the hydrogel in response to a step-wise pH change between 1.4 and 7.4 at 37°C. A pulsatile release pattern indicates that lysozyme was released at pH 7.4 (enteric conditions) and resisted release at pH 1.4 (gastric conditions). This demonstrates that pH-sensitive dissociation of ionic binding enable us to deliver drugs to the small intestines with avoiding release in the stomach.

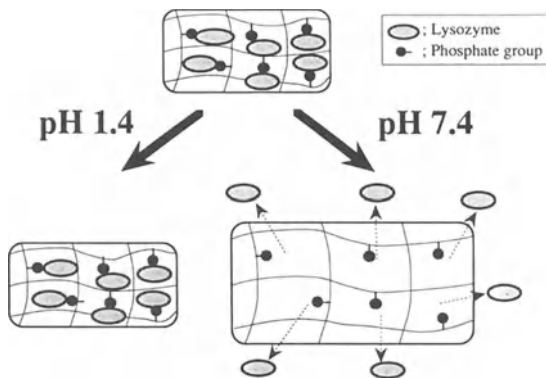


Fig. 1 Schematic of pH-sensitive release of lysozyme from the hydrogel containing phosphate groups.

## REFERENCES

1. Nakamae K, Miyata T, Hoffman AS. (1992) Swelling behavior of hydrogels containing phosphate groups. *Makromol Chem* 193: 983-990
2. Miyata T, Nakamae K, Hoffman AS, Kanzaki Y. (1994) Stimuli-sensitivities of hydrogels containing phosphate groups. *Macromol Chem Phys* 195: 111-112
3. Nagamatsu S, Nabeshima Y, Hoffman AS. (1992) Ion exchange drug delivery system; loading of lysozyme into poly(acrylic acid) hydrogels. *ACS Polym Preprints* 33(2): 478-479



# SLOW RELEASE OF HEPARIN FROM A HYDROGEL MADE FROM POLYAMINE CHAINS GRAFTED TO A TEMPERATURE-SENSITIVE POLYMER BACKBONE

Y. Nabeshima<sup>1</sup>, Z. L. Ding<sup>1</sup>, G. H. Chen<sup>1</sup>, A. S. Hoffman<sup>1</sup>,  
H. Taira<sup>2</sup>, K. Kataoka<sup>2</sup>, and T. Tsuruta<sup>3</sup>

<sup>1</sup>Center for Bioengineering, FL-20, University of Washington, Seattle, WA 98195, USA;

<sup>2</sup>Department of Materials Science & Technology, Science University of Tokyo, Yamazaki 2641;

<sup>3</sup>Research Institute for Biosciences, Science University of Tokyo, Yamazaki 2669, Noda-shi, Chiba 278, Japan

## SUMMARY

We have recently reported a dual-sensitivity graft copolymer which has a temperature-sensitive polymer (poly(N-isopropylacrylamide) (PNIPAAm)) grafted onto a pH-sensitive backbone (polyacrylic acid) (PAAc)<sup>1</sup>. This unusual graft copolymer exhibits temperature-induced phase transitions over a wide range of pHs, even at high PAAc contents. In this paper, we report on another unique dual-sensitivity graft copolymer (and its hydrogel), which has a pH-sensitive polyamine grafted onto a temperature-sensitive PNIPAAm backbone. This gel is suitable for heparin delivery. Others have studied heparin release from temperature-sensitive IPNs or polyamine-coated polyurethanes<sup>2,3</sup>. In this study, we have studied delivery of heparin from these novel, dual-sensitivity graft copolymer gels.

**KEY WORDS** Temperature-sensitive; pH-sensitive; graft copolymers; heparin delivery

## METHODS

Copolymers of a polyamine grafted onto a PNIPAAm backbone were synthesized by radical copolymerization of the polyamine macromer ( $M_n = 3,000$ ,  $M_w/M_n = 1.3$ ) and NIPAAm. Details of the synthesis have been published elsewhere<sup>4</sup> (Figure 1). The phase transition behavior of the graft copolymers was measured by determination of the turbidity (absorbance) at 600 nm. Hydrogels were synthesized by the same copolymerization method, with addition of a crosslinker (methylene-bis-acrylamide). To load heparin, the pre-swollen gels were immersed in 5 mg/ml heparin-NaAc buffer (20 mM, pH = 4.0), at 23 °C for 48 hours. The loaded gels were dried in air and then in vacuum at room temperature. Heparin was released in 50 mM of PBS (containing 150 mM of NaCl, pH=7.4), at 37 °C. Heparin concentration was determined using Azure A dye.

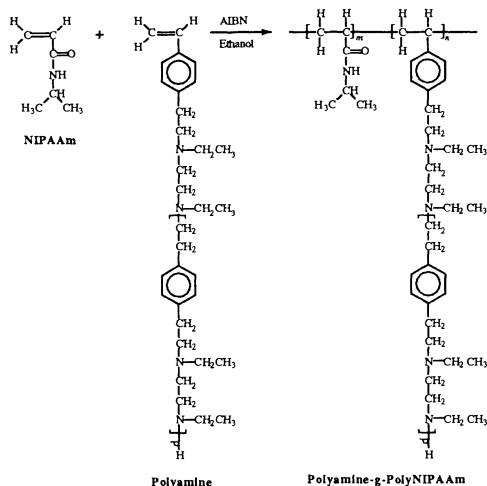


Figure 1 Synthesis of the graft copolymer of polyamine-g-PNIPAAm.

## RESULTS AND DISCUSSION

We synthesized three graft copolymers and hydrogels with 5, 10 and 15% graft contents. The graft copolymers are soluble at temperature below their LCSTs at both pH 4.0 and 7.4, which indicates that these copolymers have enough hydrophilicity to be soluble below their LCSTs despite the lack of protonation of the relatively hydrophobic amine groups of polyamine, especially at pH 7.4. (The macromer exhibits a conformational change around pH 7.0, from an expanded chain to a compact

chain, which continues to compact with increasing pH due to continuing deprotonation of the amino groups<sup>4</sup>.) The graft copolymers exhibit temperature-induced phase transitions at both pH 7.4 and 4.0 (Figure 2). The amount of heparin loaded into the grafted hydrogel increases significantly with increase of polyamine content due to the ionic bonding at pH 4.0 and room temperature. At pH 7.4 and 37°C, significant amounts of heparin are gradually released over a period of days from the 15% polyamine grafted hydrogel (Figure 3). Gels with lower polyamine contents trap most of the loaded heparin inside the gel at those conditions. These heparin-containing, graft hydrogels may be useful as slow-releasing coatings on devices contacting blood for several hours to several days, such as catheters and components of dialysers.

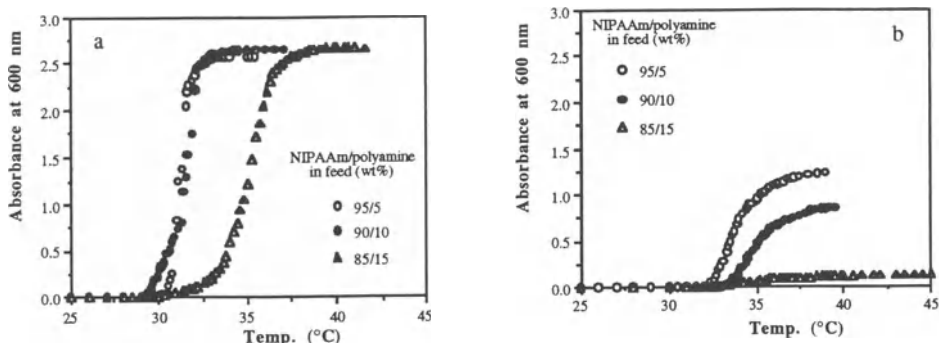


Figure 2 Phase-transition temperatures of graft copolymers of polyamine-g-PNIPAAm. a) at pH 7.4 and b) at pH 4.0.

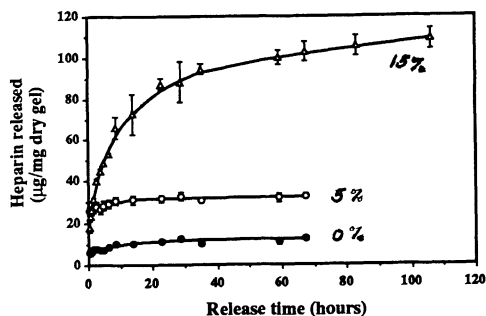


Figure 3. Heparin release kinetics from the polyamine-g-PNIPAAm hydrogels.

## REFERENCES

1. Chen GH, and Hoffman AS (1995), *Nature* 373: 49-52
2. Kim SW et.al. (1994), *Proceed. Intern. Symp. Control. Rel. of Bioact. Mater.* 21Control. Rel. Soc. Inc.: 40-41.
3. Piao AZ, Jacobs HA, Park KD, and Kim SW (1994), *Wuhan Intern. Symp. on Biomater. and Fine Polymers*, 147-148.
4. Kikuchi A, Tsuruta T and Kataoka K (1994), *J. Biomater. Sci. Polym. Ed.* 5: 569.

# Formation of core-shell type nano-associates through electrostatic interaction between peptide and block copolymer with poly(ethylene glycol) segment

Atsushi Harada and Kazunori Kataoka

Department of Materials Science, and Research Institute for Bioscience, Science University of Tokyo, 2641 Yamazaki, Noda-shi, Chiba 278, Japan.  
Phone : 81-471-24-1501 Ext.(4330), Fax : 81-471-23-9362

## SUMMARY

In this study, it was investigated the preparation of core-shell type nano-associates as a carrier in order to improve the bioavailability of biologically active compounds *in vivo*. poly(L-lysine) (P(Lys)) and lysozyme were used as model peptides, and nano-associates were formed by mixing with poly(ethylene glycol)-poly(aspartic acid) block copolymer (PEG-P(Asp)). For P(Lys)/PEG-P(Asp) associates, it was confirmed that nano-associates were spherical particles and electrically neutral. We consider that this nano-associates may have core-shell structure. For lysozyme/PEG-P(Asp) associates, nano-associates formation was evidenced for the block copolymer with higher molecular weight of poly(ethylene glycol). Secondary structure of lysozyme did not change even after the formation of nano-associates, suggesting that lysozyme entrapped in the core of nano-associates may retain its original activity.

**KEY WORDS** : lysozyme, block copolymer, poly(ethylene glycol), nano-associates, electrostatic interaction

## INTRODUCTION

In the field of pharmacology, biologically active compounds, e.g. peptide hormone and growth factor, have recently received a considerable attention. In such studies, the search and the development of new biologically active compounds are required. Further, the design of carriers which are stable and improve the bioavailability of biologically active compounds *in vivo* are also required, because of the instability of these substances in the body compartment. We have focused on the design of a carrier which is similar to natural carriers such as viruses [1]. A virus is a natural ingenious macromolecular association which is characterized by a small size and a core-shell structure. We have investigated the preparation of nano-associates through electrostatic interaction between a pair of poly(ethylene glycol)-polycation block copolymer and a poly(ethylene glycol)-polyanion block copolymer [2]. Nano-associates are characterized by their small size (ca 30nm) and core-shell structure. This kinds of nano-associates should be a useful carrier for peptides; charged peptides entrap in the core of nano-associates through electrostatic interaction.

In this study, we select poly(ethylene glycol)-poly(aspartic acid) block copolymer (PEG-P(Asp)) as a charged block copolymer, poly(L-lysine) (P(Lys)) and chicken egg white lysozyme as model peptides. Successful entrapment of these model compounds in the core of nano-associates was confirmed

## EXPERIMENTAL

### Preparation of P(Lys) / PEG-P(Asp) associates

The P(Lys) (polymerization degree = 5, 20, 45) and the PEG-P(Asp) (PEG Mw = 5000, polymerization degree of aspartic acid = 20, 40 and 80) were dissolved separately in a phosphate buffer solution (10mM, pH 7.4). The P(Lys) / PEG-P(Asp) associates were prepared by mixing

these solutions in an equal unit ratio of lysine and aspartic acid residues. The mixed solutions were analyzed by dynamic light scattering (DLS).

### Preparation of lysozyme / PEG-P(Asp) associates

Chicken egg white lysozyme ( $M_w = 14300$ ,  $pI = 11$ ) and the PEG-P(Asp) (PEG  $M_w = 5000$  and  $12000$ , polymerization degree of aspartic acid = 20, 40 and 80) were dissolved in phosphate buffer solution. Lysozyme / PEG-P(Asp) associates were prepared by mixing these solutions in various unit ratios (charge ratio) of lysine and arginine residues in lysozyme and aspartic acid residues in PEG-P(Asp). The mixed solutions were analyzed by DLS in order to determine the diameter. Circular dichroism measurements were carried out for the aqueous solutions of the nano-associates to follow the conformation change of the lysozyme in the associates.

## RESULTS AND DISCUSSION

### Preparation of P(Lys) / PEG-P(Asp) associates

In the case of mixture of lysine pentamer and PEG-P(Asp), nano-associates were not observed by DLS. However, by increasing the length of lysine units to 20 and 45, the formation of nano-associates of these oligo-lysine with PEG-P(Asp) was confirmed by DLS. These results show that the chain length of P(Lys) is important for the formation of stable associates. The formation of nano-associates need a chain length of P(Lys) to be longer than the value required to form a bridge between the PEG-P(Asp) block copolymers. Angular dependence of diffusion coefficient ( $D$ ) was studied and it was confirmed that the  $D$  values of P(Lys)/PEG-P(Asp) associates were independent on detection angles. This indicated this nano-associates were spherical particles. Further, laser-doppler electrophoresis measurement was carried out to determine zeta-potential of P(Lys) ( $n=20$ ) / PEG-P(Asp) associates. The average zeta-potential thus calculated has an extremely small absolute value ( $0.643 \pm 0.569$  mV). These results support that the P(Lys) / PEG-P(Asp) associates may have a core-shell structure with a polyion complex core surrounded by a PEG corona.

### Preparation of lysozyme / PEG-P(Asp) associates

In the case of mixture of lysozyme and PEG-P(Asp) (5-20,40 and 80), large aggregates or precipitates were observed and nano-associates with diameter of less than 100nm were not formed. On the other hand, in the case of lysozyme mixture with PEG-P(Asp) having longer PEG chain (12-40 and 80), nano-associates formation were evidenced with diameter of ca.30nm (Figure 1). This shows the solubility of polyion complexes with lysozyme and P(Asp) segments was improved by the increment of molecular weight of PEG. Further, circular dichroism spectra of native lysozyme and lysozyme / PEG-P(Asp) associates were completely identical, indicating that secondary structure of lysozyme did not change by the formation of associates. From these results, we assume that the activity of lysozyme may retain even after the formation of nano-associates.

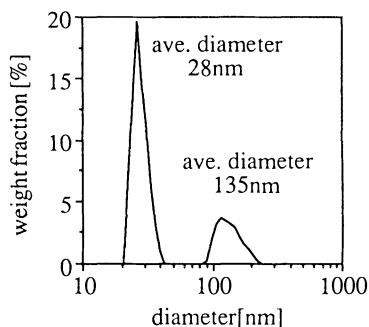


Figure 1 Size distribution of lysozyme/PEG-P(Asp) associates (mixing in an equal charge ratio of lysozyme and PEG-P(Asp)(12-80))

## REFERENCES

- [1]Kataoka K, Kwon GS, Yokoyama M, Okano T, Sakurai Y (1993) *Jornal of Controlled Release* 24: 119-132
- [2]Harada A, Kataoka K, Yokoyama M, Okano T, Sakurai Y (1994) *Polymer preprints, Japan* 43: 2589-2590

# PEG-Poly(lysine) block copolymer as a novel type of synthetic gene vector with supramolecular structure

Satoshi Katayose,  
Kazunori Kataoka

Department of Materials Science and Technology & Research Institute for Bioscience,  
Science University of Tokyo, Yamazaki 2641, Noda-shi Chiba 278  
Phone:81-471-24-1501 Ext.4330, Fax:81-471-23-9362

## ABSTRACT

As a novel system of DNA vector, soluble complexes of DNA with Poly(ethyleneglycol)-Poly(lysine) AB type block copolymer was synthesized. And the thermal denaturation behavior of the complexes were studied. As a result, soluble nano-associates were obtained even at the electrostatically neutralized point, and stabilization of DNA structure were confirmed by measuring melting curves of complexes. Furthermore, PEG-Poly(lysine)/DNA complex was reversibly dissociated by addition of poly-L-aspartic acid. Poly-L-aspartic acid replaced DNA in the complex with PEG-Poly(lysine) and resulted in the formation of free DNA. This feature suggests that complexed DNA can be released from nano-associate in appropriate condition to achieve effective transfection.

**KEYWORDS:** gene vector, melting curve, polyion complex, polylysine

## INTRODUCTION

Engineered viruses are widely used for gene vector *in vitro* condition. However, *in vivo* method is required in future gene therapy which has a great advantage from practical point of view. To achieve *in vivo* gene therapy, traditional gene vector has to overcome some problems related to cellular toxicity, inconvenience, and inefficiency of DNA delivery. Polycations, e.g. Poly(L-lysine) were widely used as modifier of DNA through an electrostatic interaction. But increasing the peptide cation/DNA phosphate ratio ( $=r$ ), up to electrostatic equivalence, yielded insoluble precipitation. In this study, Poly(lysine) was modified with PEG to get soluble complex with DNA through nano-associate formation surrounding by palisade of PEG segments.

## MATERIALS & METHODS

### Synthesis of PEG-Poly(lysine) block copolymer

At first PEG-Poly(lysine(Z)) block copolymer was synthesized using an amino terminated PEG to initiate the polymerization of lysine(Z)-NCA. Then PEG-Poly(lysine) (M.W. of PEG chain = 4300, number of Lys units = 20) was obtained by deprotection of Z group in Trifluoroacetic Acid-Methanesulfonic Acid-Anisole system.

### Preparation of PEG-Poly(lysine)/DNA complex

PEG-Poly(lysine) and DNA (Sodium salt from Salmon Testes, Sigma) were dissolved each other in 1mM phosphate buffer (pH 7.40) then mixed immediately. Then same volume of methanol were added to each sample before measuring of melting curves. Melting curves were monitored by measuring UV absorptions at 260nm.

Reversibility of complex formation of PEG-Poly(lysine) and DNA was studied by using the

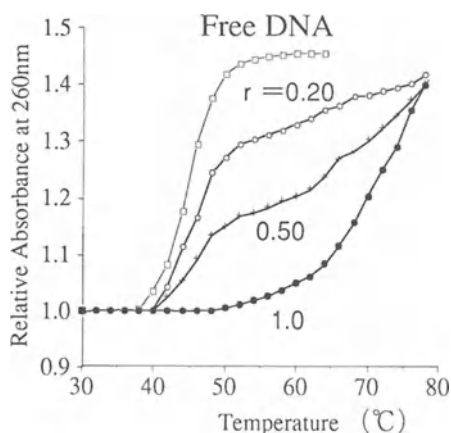


**Fig.1** Melting curves of PEG-Poly(lysine)/DNA complexes in 50% (v/v) methanol-1mM phosphate buffer (pH7.40)  $r=[NH_2]/[Nucleotide]$

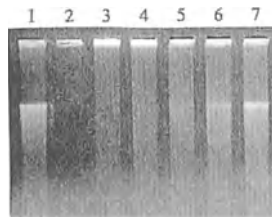


**Fig.2** The effect of increasing proportions of poly-L-aspartic acid on PEG-Poly(lysine)/DNA complex electrophoretic migration through a 0.9% agarose gel.

Increasing amount of poly-L-aspartic acid were added to PEG-Poly(lysine)/DNA(1:1) complex. After incubation at room temperature for 20 h, samples were electrophoresed through an 0.9% agarose gel using a Howly buffer system and stained with ethidium bromide to visualize DNA. Lane 1, DNA alone; Lane 2, PEG-Poly(lysine)/DNA complex; Lane 3-7, PEG-Poly(lysine)/DNA complexes with progressively increasing proportions of poly-L-aspartic acid (1.0, 2.0, 4.0, 10, 20 equivalent of poly-L-aspartic acid to DNA).

electrostatic complex prepared in 10mM phosphate buffer (pH7.4). Increasing amount of poly-L-aspartic acid, anionic polymer, were added to PEG-Poly(lysine) / DNA complexes to estimate the reversibility of complexes. Then, the DNA which dissociated from complexes were quantified through a 0.9% agarose gel electrophoresis.

## RESULTS & DISCUSSIONS

By addition of PEG-Poly(lysine) to DNA, no precipitate formation was observed even at the electrostatic equivalence at low DNA concentration as 25 mg/ml. On the other hand, mixture of Poly(lysine) (number of Lys units = 20) and DNA caused precipitate in the same condition. Agarose gel electrophoretic measurement revealed that stoichiometric soluble and stable complex was formed between PEG-Poly(lysine) and DNA.

Addition of PEG-Poly(lysine) block copolymers to DNA resulted in a stabilization of the double-stranded helix of DNA against thermal denaturation as in the case of Poly(lysine). Thermal denaturation monitored at 260 nm revealed a biphasic transition profile in 50% (v/v) methanol-1mM phosphate buffer (pH7.40) (Figure 1). DNA fraction showing lower transition temperature based on melting of DNA was decreased with addition of the PEG-Poly(lysine) while the fraction having higher temperature transition based on denaturation of complex was increased. At the electrostatic equivalence the lower transition was disappeared, and only transition due to the complex was observed. These results also indicate that stoichiometric complex was formed between DNA and PEG-Poly(lysine) to associate into supramolecular assembly. This result is quite promising from the standpoint of using the complex for *in vivo* gene delivery, because the complex may have enough stability during circulating in the body compartment.

Furthermore, DNA in the PEG-Poly(lysine)/DNA complex was dissociated by addition of 20eq. excess of poly-L-aspartic acid. Poly-L-aspartic acid replaced DNA in the complex with PEG-Poly(lysine) and resulted in the formation of free DNA (Figure 2). This feature suggests that complexed DNA can be released from nano-associate in appropriate condition to achieve effective transfection.

# DEVELOPMENT OF POLYMERIC MICELLES FOR DRUG DELIVERY OF INDOMETHACIN

Sung Bum La<sup>1</sup>, Kazunori Kataoka<sup>1,2</sup>, Teruo Okano<sup>1,3</sup>, and Yasuhisa Sakurai<sup>1,3</sup>

<sup>1</sup> International Center for Biomaterials Science, Research Institute for Biosciences, Science University of Tokyo, Yamazaki 2669, Chiba 278, Japan, <sup>2</sup> Department of Materials Science and Technology, Science University of Tokyo, Yamazaki 2641, Chiba 278, Japan, and <sup>3</sup> Institute of Biomedical Engineering, Tokyo Women's Medical College, Kawada-cho, Tokyo 162, Japan

## SUMMARY

To estimate a feasibility of novel containers for drugs, poly(ethylene oxide)-poly( $\beta$ -benzyl L-aspartate) (PEO-PBLA) micelles were prepared by dialysis into water from different solvents (e.g., DMF, acetonitrile, THF, DMSO, DMAc, and ethyl alcohol), determining the critical micelle concentration (cmc) of the prepared micelles in distilled water by a fluorescence probe technique using pyrene. Then, indomethacin (IMC) as a model drug was incorporated into the micelles by dialysis and O/W emulsion method. Characteristics of PEO-PBLA micelle without and with the physically trapped IMC in the inner core of the micelles (IMC/PEO-PBLA) were studied by dynamic light scattering and GPC/HPLC as well as *in vitro* release test of IMC from the micelle was conducted.

**KEY WORDS:** AB amphiphilic block copolymer, polymeric micelles, indomethacin, dissolution rate, drug delivery system

## INTRODUCTION

An amphiphilic AB type block copolymer is made of two segments of different chemical structure with hydrophilic and hydrophobic components. This system has been the focus of numerous investigations, because of the intrinsic interest in self-assembling systems [1]. This type of diblock copolymer can form a spherical micelle structure in aqueous milieu. The hydrophobic segment forms the hydrophobic core of the micelle, while the hydrophilic segment surrounds this core as a hydrated outer shell. This core-shell structure provides a potential utility of polymer micelle as vehicles for drug delivery, since the hydrophobic core may serve as a micro-container of drugs which is segregated from the outer environment by a palisade of the hydrophilic segment. In this paper, IMC-incorporated micelles were prepared based on AB block copolymers of poly(ethylene oxide) (PEO) and poly( $\beta$ -benzyl L-aspartate) (PBLA) as alternative approach to decrease the side effects of IMC. The objective of this research is to develop IMC-loaded polymeric micelles for oral delivery that may be capable of delivering therapeutic concentrations of IMC into the body with decreasing side effects.

## METHODS

### Preparation of PEO-PBLA micelles

PEO-PBLA block copolymers were obtained by ring-opening polymerization of  $\beta$ -benzyl L-aspartate N-carboxy anhydride (BLA-NCA) using the amino-end group of  $\alpha$ -methoxy- $\omega$ -amino-poly(ethylene oxide) as an initiator [2]. The number of BLA units of PEO-PBLA was determined to be 21 by <sup>1</sup>H NMR. To form micelles, the PEO-PBLA block copolymer was dissolved in DMF, acetonitrile, THF, DMSO, DMAc, and ethyl alcohol, respectively, and stirred overnight at room temperature. Then, the reaction mixture was dialyzed against distilled water using a Spectra/por 2 dialysis membrane (MWCO; 12,000-14,000), followed by lyophilization.

The prepared micelle was investigated to determine the critical micelle concentration (cmc) in distilled water by fluorescence probe techniques using pyrene.

### Preparation of IMC incorporated micelles

The physical entrapment of IMC in PEO-PBLA block copolymer micelles was carried out by the methods based on dialysis [3] and O/W emulsion. After lyophilization, the loading amount of physically trapped IMC in the inner core of the micelles (IMC/PEO-PBLA) using dialysis and O/W emulsion methods was determined by measuring the absorbance at 319 nm. The PEO-PBLA and IMC/PEO-PBLA were studied by dynamic light scattering in order to determine their diameter and by GPC/HPLC in PBS (0.10M, pH 7.4). The release study of IMC from the micelle in various pH range from 1.2 to 7.4 was investigated.

## RESULTS AND DISCUSSION

For the PEO-PBLA block copolymer, DMAc was found to be the best solvent to form a micelle in the solvents tested, and the cmc of PEO-PBLA micelle thus prepared was determined to be ca. 18 mg/L in distilled water. The size distributions of the PEO-PBLA micelles were determined to be ca. 19 nm by DLS in distilled water and the gel exclusion volume of the micelles were observed at 6.1 mL by absorption at 254 nm.

In order to decrease of side effect of IMC and to deliver by oral route, IMC/PEO-PBLA micelles were prepared using DMAc by dialysis and using chloroform by O/W emulsion method. In GPC/HPLC analysis of the micelles in PBS (0.10 M, pH 7.4), a sharp peak at the gel exclusion volume (6.1 ml) was observed. The peak was detected at 319 nm because IMC was free of any influence of PEO-PBLA at this wavelength. This peak indicates that IMC was incorporated in PEO-PBLA micelles. In order to know the micellization behavior in aqueous solution of the IMC/PEO-PBLA micelles, DLS measurement was also performed. After incorporating IMC into PEO-PBLA micelle, these micelles had a narrow size distribution, and the average diameter based on number distribution of the micelles (dialysis method: 29 nm, O/W emulsion method: 25 nm) were slightly higher than that of PEO-PBLA micelles (19 nm).

The release study of IMC from IMC/PEO-PBLA into various buffer solutions in the pH range from 1.2 to 7.4 at 37 °C revealed that the more basic the release medium, the higher the rate of release of IMC (Fig. 1). This result indicated, that the release rate of IMC from IMC/PEO-PBLA micelles is considerably influenced by the pH of the medium. The results of this study suggest the maintenance of IMC within the micelle for a long time at pH 1.2 which corresponds to the pH of the stomach and a rapid release at pH 6.5 as it corresponds to the small intestine and indicate, that our formulations, IMC/PEO-PBLA micelles, will be effective for oral delivery of IMC as a novel drug carrier.

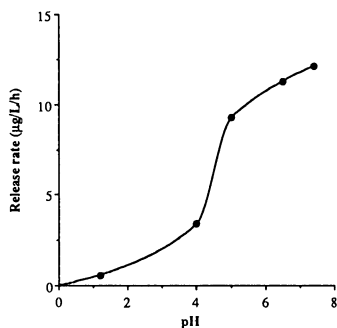


Fig. 1 Release rate profile of IMC from IMC/PEO-PBLA micelles in different pH solutions at 37 °C.

## REFERENCES

- [1] Kataoka K (1994) Design of nanoscopic vehicles for drug targeting based on micellization of amphiphilic block copolymers. *JMS Pure Appl Chem A31* (11): 1759-1769
- [2] Yokoyama M, Kwon GS, Okano T, Sakurai Y, Seto T, Kataoka K. (1992) Preparation of micelle-forming polymer-drug conjugates. *Bioconjugate Chem* 3: 295-301
- [3] Yokoyama M, Okano T, Sakurai Y, Kataoka K (1994) Improved synthesis of adriamycin-conjugated poly(ethylene oxide)-poly(aspartic acid) block copolymer and formation of unimodal micellar structure with controlled amount of physically entrapped adriamycin. *J Controlled Rel* 32: 269-277



# Synthesis of heterobifunctional poly(ethylene glycol) with a reducing monosaccharide residue at one end for drug delivery

Teruo Nakamura, Yukio Nagasaki, Masao Kato, and Kazunori Kataoka

Department of Materials Science and Technology, Science University of Tokyo, Yamazaki 2641, Noda-shi 278 Japan  
Phone:81-471-24-1501 Ext(4330), Fax:81-471-23-9362

## SUMMARY

Install of pilot molecules on surface of the micelle-forming polymeric drug is considered to further enhance cellular uptake of the micelle at target tissue. In order to achieve this strategy, new heterobifunctional poly(ethylene glycol) with a reducing monosaccharide residue at one end were synthesized. Potassium alkoxides of carbohydrate derivatives reacted with ethylene oxide(EO) to yield a variety of sugar derivative bearing poly(ethylene glycol). Subsequently, protective groups on carbohydrate residue were removed to yield target compounds. Reducing monosaccharide residue was incorporated to one end of poly(ethylene glycol) chain regiospecifically and quantitatively without a spacer moiety.

**KEY WORDS** : heterobifunctional poly(ethylene glycol), reducing monosaccharide residue, Sugar-PEG, pilot molecule, receptor mediated endocytosis

## INTRODUCTION

A series of our previous studies have demonstrated the utility of polymeric micelle, composed of drug-conjugated poly(ethylene glycol)-polypeptide block copolymers, as a vehicle of antitumor agents[1]. The polymeric micelle circulated stably in blood compartment with a reduced non-specific uptake by reticuloendothelial systems. Consequently, there was observed a remarkable accumulation of the polymeric micelles in solid tumors by i.v. injection, leading to the effective antitumor activity.

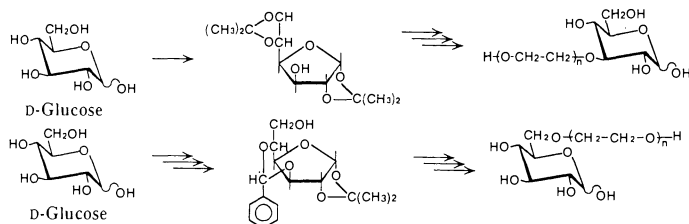
Install of pilot molecules on surface of the polymeric micelle is expected to further enhance cellular uptake of the micelle at target tissue via receptor mediated endocytosis. For this purpose, we have been carrying out to synthesize poly(ethylene glycol)(PEG) with heterobifunctional reactive-groups(HeteroPEG) which can be utilized as hydrophilic outer shell of functionalized polymeric micelle[2]. Polymeric micelle prepared from HeteroPEG should possess the ability to install an appropriate ligand for target sites.

Recent progress in glycobiology clarified remarkable functions of sugar residues in endogenous glycoconjugates and numerous carbohydrate recognition systems. These findings suggest potential usefulness of glycoconjugates as drug carriers for targeting. Incorporation of carbohydrate residues to polymeric drugs has been carried out to enhance their targeting function[3]. Here we report novel syntheses of new HeteroPEG with a reducing monosaccharide residue at one end designated Sugar-PEG.

## MATERIALS AND METHODS

Synthesis of Sugar-PEG was performed by following three steps: (a)introduction of protective groups to a monosaccharide, (b)polymerization of ethylene oxide(EO) with a sugar derivative as an initiator, (c)removal of protective groups from sugar residue. Monosaccharides with proper protective groups were synthesized as previously reported[4][5]. The initiator of polymerization, potassium alkoxide of sugar derivative, was prepared by adding equimolar amount of potassium naphthalene to sugar derivative in tetrahydrofuran. EO was added to the solution of initiator and

polymerization was carried out for 2days in a water bath. Protective groups attached to carbohydrate was cleaved in aqueous acid.



Scheme.1. Synthesis of heterobifunctional poly(ethylene glycol) with a reducing monosaccharide residue at one end.

## RESULTS AND DISCUSSION

Polymerization of EO with sugar derivative gave water soluble HeteroPEG in high yield. In the case of using 3,5-O-benzylidene-1,2-O-isopropylidene-D-glucopyranose (BIG) as an initiator, PEG with hydroxyl groups at both ends was produced as a byproduct owing to a trace amount of water in BIG. PEG with reducing glucose end and with OH ends were successfully separated by column chromatography. Analysis of Sugar-PEG and its derivatives by  $^1\text{H-NMR}$  revealed that the carbohydrate residue had a free reducing end and was linked with PEG at the optionally defined position. The potential utility of the Sugar-PEG would be a construction of targeting vehicle toward glucose transporters expressed on several tissues such as small intestine and brain. The procedure mentioned above can be expanded for the synthesis of a series of Sugar-PEG with a variety of carbohydrate units at the chain end. Application of Sugar-PEG to the polymeric micelle drug is favorable to construct a virus mimicking vehicle composed of drug-conjugated (Sugar-PEG)-polypeptide block copolymers. Furthermore, these Sugar-PEG may have a wide applicability to prepare biospecific biomaterials through surface modification technologies.

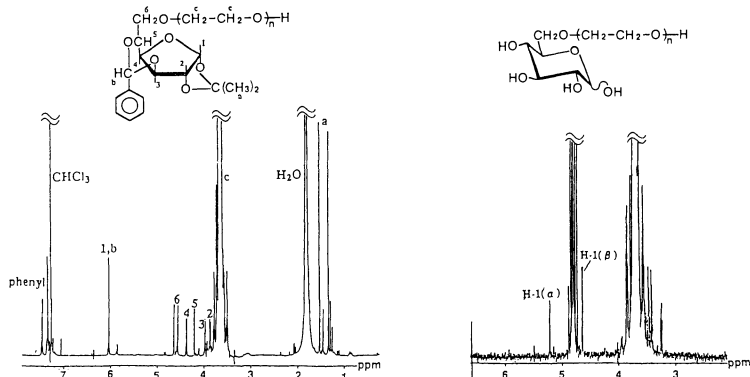


Fig.1. 500MHz  $^1\text{H-NMR}$  Spectrum of BIG-PEG in  $\text{CDCl}_3$  and Glc-PEG in  $\text{D}_2\text{O}$ .

## REFERENCES

- [1] Kataoka K, Kwon GS, Yokoyama M, Okano T, Sakurai Y (1993) *Journal of Controlled Release* 24:119
- [2] Cammas S, Kataoka K; *Macromolecular Chemistry and Physics* submitted
- [3] Kopecek J, Duncan R (1987) *Journal of Controlled Release* 6:315
- [4] Schmidt OT (1963) *Isopropylidene Derivatives*. In: Whister RL, Wolfrom ML (eds) *Methods in Carbohydrate Chemistry*. Academic Press, New York, pp318
- [5] Schmidt OT (1963) *6-Deoxy-D-glucose*. In: Whister RL, Wolfrom ML (eds) *Methods in Carbohydrate Chemistry*. Academic Press, New York, pp198

# FUNCTIONAL POLYMERIC MICELLES : SYNTHESIS AND CHARACTERIZATION

Sandrine Cammas, Yukio Nagasaki, Kazunori Kataoka, Teruo Okano and Yasuhisa Sakurai.

Tokyo Women's Medical College, Institute of Biomedical Engineering, 8-1 Kawada-Cho, Shinjuku-Ku, Tokyo 162, Japan and Science University of Tokyo, Department of Materials Science and Technology, Yamazaki 2641, Noda-Shi, Chiba 278.

## SUMMARY

Heterobifunctional poly(ethylene oxide-co- $\beta$ -benzyl-L-aspartate) -PEO/PBLA- block copolymers having methoxy groups or hydroxy functions at the free end of the PEO chains were synthesized and characterized. They show a stable left-handed  $\alpha$ -helix conformation in chloroform, whereas in dimethylsulfoxide (DMSO) and in dimethylacetamide (DMAc), their conformation is random-coil.  $\alpha$ -hydroxy and  $\alpha$ -methoxy PEO/PBLA polymeric micelles were obtained by dialysis against water of the corresponding block copolymers solution in DMAc. Both polymeric micelles have a similar diameter ( $< 50\text{nm}$ ), a very low critical micellar concentration ( $\text{cmc} \leq 10 \text{ mg/L}$  in water) and a good stability in PBS and in PBS/Serum. About 18% of Adriamycin (ADR) was loaded in the inner-core of both polymeric micelles. The diameter of the ADR-loaded micelles was similar to the diameter of the corresponding empty micelles, and they were found to be stable in PBS and in PBS/Serum. The first results on the cytotoxicity of entrapped ADR against P388D1 leukemia cells show quite high cytotoxicity level for both carriers.

**KEY WORDS :** heterobifunctional PEO/PBLA block copolymers, functional polymeric micelles, stability, drug loading, drug delivery systems.

## INTRODUCTION

Polymeric micelles made up by poly(ethylene oxide-co- $\beta$ -benzyl-L-aspartate) -PEO/PBLA- block copolymers have an important place in the field of drug delivery systems<sup>1</sup>. The polymeric micelles formed by  $\alpha$ -methoxy PEO/PBLA block copolymers already gave interesting results : small diameter, c.a. 20 nm, which allows the comparison with natural carriers such as viruses, good stability in aqueous media, low critical micellar concentration (cmc), c.a. 10 mg/L, which permits their use in diluted media such as body fluid, and possibility of anti-cancer drugs solubilization<sup>1</sup>. Besides the fact of decreasing the side effects of anti-cancer drugs by entrapment in a carrier, the preparation of intelligent materials which are able to recognize selectively their objective is of great interest. For this purpose, the obtention of PEO/PBLA polymeric micelles having functional groups on their outer shell is necessary in order to allow further introduction of a homing device (sugar or anti-body, for exemple). In this paper, we report first on the synthesis and characterization of heterobifunctional PEO/PBLA block copolymers. In a second part, the preparation and some physico-chemical properties of the corresponding polymeric micelles are described. At last, results on ADR-loaded micelles are given.

## METHODS

### Preparation of heterobifunctional PEO/PBLA block copolymers

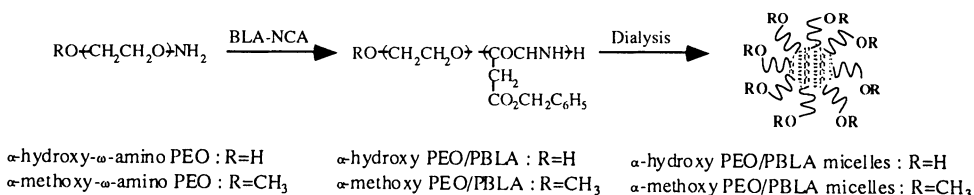
$\alpha$ -hydroxy and  $\alpha$ -methoxy PEO/PBLA block copolymers were synthesized by anionic polymerization of the  $\beta$ -benzyl-L-aspartate-N-carboxy anhydride (BLA-NCA) with the primary amino end-groups of  $\alpha$ -hydroxy- $\omega$ -amino and  $\alpha$ -methoxy- $\omega$ -amino PEOs as initiators, respectively, in the mixture DMF/ $\text{CHCl}_3$ . In both cases, the molecular weight of the PEO segments was determined to be 5000 (GPC and NMR)<sup>2</sup> and the number of BLA units was calculated to be 20 (NMR)<sup>3</sup>. Both block copolymers were purified by selective precipitation<sup>3</sup> and characterized by GPC,  $^1\text{H}$  and 2D  $^1\text{H}$ ,  $^1\text{H}$  NOESY NMR ( $\text{CDCl}_3$  and DMSO- $d_6$ ) as well as by specific rotation measurements ( $\text{CHCl}_3$  and DMSO).

## Preparation of the functional polymeric micelles

$\alpha$ -hydroxy and  $\alpha$ -methoxy PEO/PBLA polymeric micelles were obtained by the dialysis against water of a dimethylacetamide (DMAc) solution of the corresponding block copolymers ( $[c] = 6$  mg/ml). After lyophilization, both polymeric micelles were characterized by dynamic light scattering (DLS) in order to determine their diameter and by fluorescence spectroscopy using pyrene as a fluorescence probe (cmc). The stability of both micelles in PBS and in PBS/serum (9/1) was studied by HPLC (Asahipack column in phosphate buffer, pH=7.4).

## RESULTS AND DISCUSSION

The synthesis of  $\alpha$ -hydroxy and  $\alpha$ -methoxy PEO/PBLA block copolymers is based on the polymerization of the BLA-NCA by the primary amino end-groups of  $\alpha$ -hydroxy- $\omega$ -amino and  $\alpha$ -methoxy- $\omega$ -amino PEOs, respectively (scheme 1).



Scheme 1 Preparation of the PEO/PBLA block copolymers and polymeric micelles

For both copolymers, the PBLA segments adopt a particular conformation in chloroform : the poly(amino benzyl ester) blocks have a left-handed  $\alpha$ -helix conformation in chloroform (optical rotation measurement) which is stabilized by interactions with the PEO segments (<sup>1</sup>H and 2D NMR study). On the other hand, the conformation of the PBLA blocks in DMSO is random-coil, the same conformation is observed in DMAc.

The diameter of  $\alpha$ -hydroxy and  $\alpha$ -methoxy PEO/PBLA polymeric micelles was measured by DLS in water : 30 nm and 25 nm, respectively. The cmc of the  $\alpha$ -methoxy PEO/PBLA micelles was found to be similar in water (10 mg/L) and in PBS (20 mg/L) ; on the other hand, the cmc of the functional carrier depends on the solvent : 4 mg/L in water and 30 mg/L in PBS. However, the stability of both polymeric micelles in PBS and in PBS/serum is very similar :  $\alpha$ -hydroxy and  $\alpha$ -methoxy PEO/PBLA micelles showed a good stability in both solvent for, at least 72 hours.

About 18% of Adriamycin (ADR) were entrapped in the inner core of both polymeric micelles. The diameter of both ADR-loaded micelles was found to be similar to the diameter of the corresponding empty micelles. In addition, the  $\alpha$ -hydroxy and  $\alpha$ -methoxy ADR-loaded micelles were found to be stable in PBS and in PBS/Serum. The first results on the cytotoxicity of entrapped ADR against P388D1 leukemia cells show quite high level of cytotoxicity for both kind of carriers.

In conclusion, these results suggest that the new functional PEO/PBLA polymeric micelles have a promising future as drug delivery system. The interest of these functional micelles goes further than the synthesis of a new carrier. Indeed, because of the presence of functional groups, a homing device can be introduced on the outer-shell of the polymeric micelles thus allowing site specific drug delivery. The activation of the hydroxy groups is under investigation.

## REFERENCES

- 1-K. Kataoka (1994) J.M.S., Pure Appl. Chem. A31 (11) : 1759.
- 2-S. Cammas, Y. Nagasaki, K. Kataoka (1995) Bioconjugate Chem, in press.
- 3-S. Cammas, K. Kataoka (1995) Macromol. Chem. and Phys., in press.

# MICELLE FORMING POLYMERIC ANTICANCER DRUG CONTAINING CHEMICALLY BOUND AND PHYSICALLY INCORPORATED ADRIAMYCIN

Takashi Seto<sup>1</sup>, Shigeto Fukushima<sup>1</sup>, Hisao Ekimoto<sup>1</sup>, Masayuki Yokoyama<sup>2</sup>, Teruo Okano<sup>2</sup>, Yasuhisa Sakurai<sup>2</sup> and Kazunori Kataoka<sup>3</sup>

1. Takasaki Research Laboratories, Nippon Kayaku Co., Ltd. Iwahana-cho 219 Takasaki-shi Gunma 370 -12 Japan
2. Tokyo Women's Medical College, Kawada-cho 8-1 Shinjuku-ku Tokyo 162 Japan
3. Science University of Tokyo, Yamazaki 2641 Noda-shi Chiba 278 Japan

## SUMMARY

Micelle forming polymeric drug(MFPD) containing chemically bound and physically incorporated adriamycin(ADR) was designed. Three MFPD samples containing various contents of physically incorporated ADR were prepared and their antitumor activities were evaluated with murine tumor cell C26 *in vivo*. The activities seemed to depend on a dose of physically incorporated ADR rather than a dose of total ADR. Therefore, it is presumed that the major part of the activity of MFPD depends on physically incorporated ADR. This MFPD with both chemically bound and physically incorporated ADR is promising for a highly active antitumor agent against solid tumors.

**KEY WORDS:** micelle forming polymeric drug, adriamycin, chemical incorporation, physical incorporation, antitumor activity

## INTRODUCTION

We have been investigating micelle forming polymeric drug (MFPD): poly(ethylene oxide)poly-(aspartic acid) block copolymer-adriamycin conjugate(PEO-P(Asp.)ADR). In the course of investigation, it was found that a small amount of ADR physically entrapped in the micelle core has a considerable effect on antitumor activity. This result led us to prepare MFPD with both chemically and physically incorporated ADR to achieve higher anticancer activity(Fig.1).

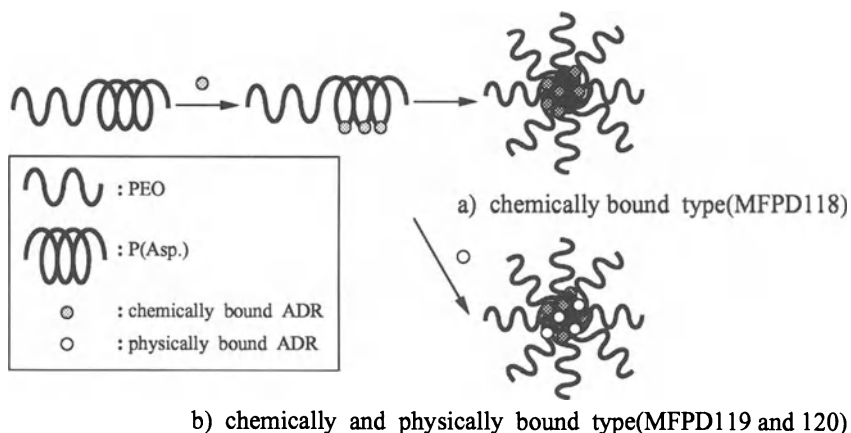


Fig.1 The chemical and physical incorporation of ADR

## MATERIALS and METHODS

The synthetic procedure of ADR-bound poly(ethylene oxide)-poly(aspartic acid) block copolymer was reported elsewhere[1]. The content of remained unreacted ADR was 0.59% of total ADR after purification and ultrafiltration. This water solution of PEO-P(Asp.)ADR was mixed with DMF

solution of ADR and triethyleamine and stirred for 2h. Then the resulting solution was dialyzed and further purified by ultrafiltration. The contents of total ADR were determined by measuring absorbance at 485nm, and the contents of physically incorporated ADR were determined by HPLC measurement. Antitumor activities were evaluated with murine tumor cell C26 *in vivo*.

## RESULTS

Three samples were prepared. MFPD118 was PEO-P(Asp.)ADR, the content of unreacted ADR in this sample was 0.59% of total ADR. MFPD119 and 120 contained increased amount of physically incorporated ADR, where the contents were 8.5% and 18.4% of total ADR respectively. The contents of physically incorporated ADR were controllable.

The antitumor activities of three samples and free ADR are shown in Fig. 2. The activities seemed to depend on a dose of physically incorporated ADR rather than a dose of total ADR, and MFPD with considerable amount of physically incorporated ADR(MFPD119 and 120) gave superior antitumor activity compared to free ADR.

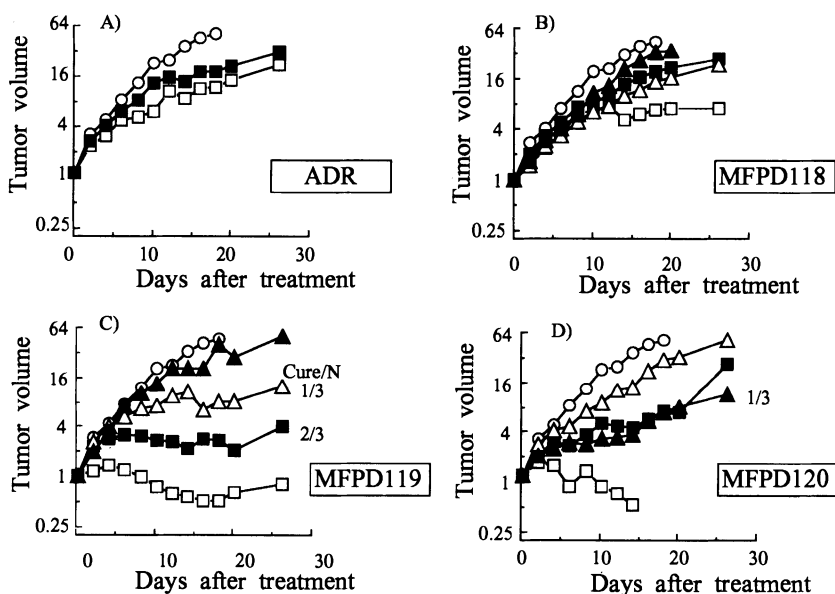


Fig. 2 *In vivo* antitumor activities against C26

Tumor cells were inoculated *s.c.* into the backs of mice, and drug injections were started the week after. Drugs were injected *i.v.* three times at intervals of four days, and tumor volumes and body weights were measured every few days. ○:control. A)ADR: □, 10; ■, 5mg/kg. B)MFPD118: □, 200[dose of total ADR](1.18)[dose of physically incorporated ADR]; ■, 100(0.59); △, 50(0.3); ▲, 25(0.15)mg/kg. C)MFPD119: □, 200(17.0); ■, 100(8.5); △, 50(4.2); ▲, 25(2.1)mg/kg. D)MFPD120: □, 100(18.4); ■, 50(9.2); △, 25(4.6); ▲, 12.5(2.3)mg/kg.

## CONCLUSION

The major part of the activity of MFPD depends on physically incorporated ADR. Chemically bound ADR is considered to contribute to micelle formation and stabilization.

## REFERENCE

1. M.Yokoyama, G.S.Kwon, T.Okano, Y.Sakurai, T.Seto, K.Kataoka (1992) Preparation of micelles as vehicles for drug delivery. *Bioconjugate Chem.* 3:295-301.

## PHARMACEUTICAL ASPECTS OF BLOCK COPOLYMER MICELLES

Glenn S. Kwon<sup>1</sup>, Mayumi Naito<sup>2</sup>, Masayuki Yokoyama<sup>3</sup>, Teruo Okano<sup>3</sup>, Yasuhisa Sakurai<sup>3</sup>, and Kazunori Kataoka<sup>2,4</sup>

<sup>1</sup> Faculty of Pharmacy and Pharmaceutical Sciences, University of Alberta, Edmonton, Alta., T6G 2N8, Canada,

<sup>2</sup> Department of Materials Science and Technology, Science University of Tokyo, 2641 Yamazaki, Noda, Japan

<sup>3</sup> Institute of Biomedical Engineering, Tokyo Women's Medical College, 8-1 Kawada-cho, Shinjuku-ku, Tokyo, Japan

<sup>4</sup> To whom to forward correspondence

### SUMMARY

We studied the stability of micelles of poly(ethylene oxide-*block*- $\beta$  benzyl L aspartate) (PEO-PBLA) containing doxorubicin (DOX), an anti-cancer drug. DOX entrapped in PEO-PBLA micelles had greater chemical stability in aqueous solution in comparison with free drug as assessed by UV and fluorescence spectroscopy. As well, gradual release of DOX from PEO-PBLA micelles was evidenced. Notably, it was revealed by dynamic light scattering (DLS) and by fluorescence quenching technique that PEO-PBLA micelles retained DOX in their cores after freeze-drying and reconstitution in water. Possible pharmaceutical advantages of PEO-PBLA micelles will be discussed.

**KEY WORDS:** ab block copolymer, poly(ethylene oxide), poly(L amino acid), block copolymer micelle, doxorubicin

### INTRODUCTION

Block copolymer micelles were recently developed as long-circulating, drug vehicles (1-3). Due to low uptake by the mononuclear phagocyte system and small size, they show promise as vehicles for the delivery of anti-cancer drugs to tumor sites. Their clinical use, however, depends on both chemical and physical stability after drug loading. A pharmaceutical study in this regard is given on PEO-PBLA micelles loaded with DOX (PEO-PBLA/DOX).

### METHODS

DOX (0.50-1.0 mg) was added to  $\text{CHCl}_3$  (1.0 ml) and solubilized by 2.0 equivalents of TEA with sonication. PEO-PBLA (5.0 mg), having PEO and PBLA molecular weights of 12,000 and 4000 g/mol, respectively, was dissolved in 10.0 ml of  $\text{H}_2\text{O}$  with sonication (30 sec). The  $\text{CHCl}_3$  solution was added to the stirred, aqueous solution, forming an o/w emulsion. The o/w emulsion was kept overnight in the dark at 25°C and in an open atmosphere, allowing evaporation of  $\text{CHCl}_3$ . Free DOX was removed from the micelles by ultrafiltration (Amicon YM-30). DOX in the micelles was quantitated by measuring its UV absorbance at 485 nm after addition of DMF (4-fold volume). Samples were diluted with 0.10 M PBS, pH 7.4, to 10  $\mu\text{g}/\text{ml}$  DOX and stored in a solution state at 25°C, in a frozen state or in a freeze-dried state (Eyela, FD-5N, Japan).

The UV absorbance of DOX at 485 nm was followed as a function of time (JASCO, Ubest 50, Japan). The level of DOX was 10  $\mu\text{g}/\text{ml}$ . The following samples were studied: (1) free DOX, (2) a solution of DOX and PEO-PBLA simply equilibrated in buffered solution, and (3) PEO-PBLA/DOX subjected to loading process. All samples were in 0.10 M PBS, pH 7.4, and were stored in the dark at 25°C.

Methods of DLS, fluorescence quenching study, and size exclusion chromatography (SEC) are given elsewhere (3).

### RESULTS AND DISCUSSION

The loading of DOX into PEO-PBLA micelles proceeded without precipitation. Yields were 65% based on the initial levels, and DOX contents of the micelles were invariably about 10% (w/w).

Entrapment of DOX inside PEO-PBLA micelles precludes the chemical degradation of the drug in solution (Figure 1). The absorbance of free DOX at 485 nm decreased due to the chemical degradation of the drug. The absorbance of DOX entrapped in PEO-PBLA micelles, in contrast, was nearly constant over the same period. Cores of the micelles are likely devoid of water, preventing hydrolytic reactions of DOX. The absorbance of DOX added to a micellar solution of PEO-PBLA decreased but more gradually than free DOX, perhaps as a result of interaction of DOX with PEO in the shell regions of the micelles.

UV spectroscopy also suggested that DOX was slowly released from PEO-PBLA micelles since a decrease in UV absorbance at 485 nm due to released DOX was not evident. Also, there was a slight increase in total fluorescence

**Table 1. Weight-Average, Diameters of PEO-PBLA/DOX and PEO-PBLA Micelles<sup>1</sup>**

Sample	non-treated sample (nm)	frozen sample (nm)	freeze-dried sample (nm)
PEO-PBLA	19 (83) <sup>2</sup>	19 (68)	16 (72)
PEO-PBLA/DOX	37 (139)	38 (147)	28 (116)

<sup>1</sup> samples at 25°C, freeze-dried samples reconstituted with distilled water

<sup>2</sup> values in parenthesis are the diameters of particles due to the secondary association of micelles

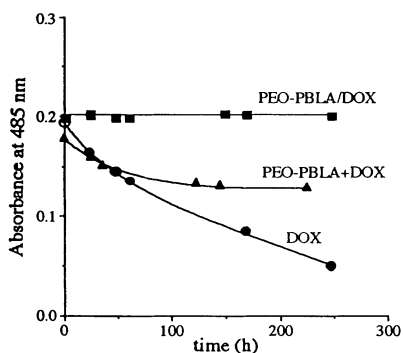


Figure 1. Absorbance of DOX, PEO-PBLA micelles + DOX, and PEO-PBLA/DOX in PBS (0.10 M, pH 7.4) over time. (10 µg/ml DOX).

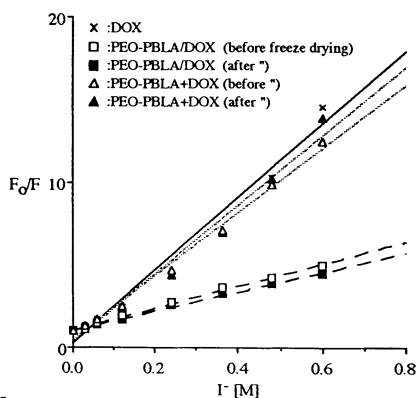


Figure 2. Stern-Volmer plots

intensity of PEO-PBLA/DOX over the same time period, whereas free DOX loses its ability for fluorescence (data not shown). Self-association of DOX in the micelles occurs (low total fluorescence intensity), slowing the release of the drug from PEO-PBLA micelles.

Table 1 summarizes the results of the DLS study. The mean diameter of PEO-PBLA/DOX is, ca., 37 nm, whereas the diameter of the unloaded micelles is ca., 19 nm. The mean sizes of the drug-loaded and nonloaded micelles are largely unchanged by freezing or by freeze-drying (Table 1). This is important since residual, toxic solvent such as  $\text{CHCl}_3$  is removable by freeze-drying, and for proper storage of the formulation. The results suggest that it is possible to reconstitute PEO-PBLA/DOX after freeze-drying and obtain a micellar solution.

We examined whether release of DOX occurred as a result of freeze-drying of PEO-PBLA/DOX and its reconstitution in distilled water. The results from SEC (data not shown) and fluorescence quenching technique suggested that DOX was retained in the micelles.

Collisional quenching constants,  $K_{SV}$ , were derived from Stern-Volmer plots (Figure 2). DOX had a  $K_{SV}$  of  $22 \text{ M}^{-1}$ , whereas PEO-PBLA/DOX had a  $K_{SV}$  of  $5.8 \text{ M}^{-1}$ . In the former case, DOX is in an aqueous milieu and is readily quenched by  $\text{I}^-$ . In the latter case, DOX is inside the micelles, is not readily accessible to  $\text{I}^-$ , and is only slightly quenched by  $\text{I}^-$ . Importantly,  $K_{SV}$  of PEO-PBLA/DOX was largely unaffected by freeze-drying and reconstitution, ca.,  $6.7 \text{ M}^{-1}$ ; this suggests that PEO-PBLA micelles were not disrupted and kept DOX in their cores. Simply equilibrating DOX and PEO-PBLA in an aqueous solution led to a  $K_{SV}$  of  $21 \text{ M}^{-1}$ .

In conclusion, DOX inside PEO-PBLA micelles has greater chemical stability than free drug in solution. PEO-PBLA micelles gradually release DOX, acting as a drug depot. It is possible to freeze-dry PEO-PBLA/DOX and obtain micelles containing drug upon reconstitution in water. PEO-PBLA/DOX are sterilizable by simple filtration due to their small size. Lastly, PEO-PBLA/DOX may be concentrated by ultrafiltration. It is expected that these pharmaceutical properties of PEO-PBLA micelles will contribute to their further development as vehicles for DOX and for other hydrophobic drugs in cancer chemotherapy.

## REFERENCES

- [1] Kataoka K, Kwon GS, Yokoyama M, Okano T, Sakurai, Y (1992) Block copolymer micelles as vehicles for drug delivery. *J. Controlled Release* 24:119-132
- [2] Kwon GS, Naito, M, Kataoka, K, Yokoyama, M, Sakurai, Y, Okano, T (1994) Block copolymer micelles as vehicles for hydrophobic drugs *Colloids and Surfaces B: Biointerfaces* 2:429-434
- [3] Kwon, GS, Naito, M, Yokoyama, M, Okano, T, Sakurai, Y, Kataoka, K (1995) Physical entrapment of adriamycin in ab block copolymer micelles. *Pharm Res.* 12:192-195.



# NANOSIZE HYDROGEL FORMED BY SELF-ASSEMBLY OF HYDROPHOBIZED POLYSACCHARIDES

K. Akiyoshi, S. Deguchi, I. Taniguchi, and J. Sunamoto

Division of Synthetic Chemistry & Biological Chemistry, Graduate School of Engineering, Kyoto University, Sakyo-ku Kyoto 606, Japan

## SUMMARY

The hydrophobized polysaccharides, which were partly substituted by hydrophobic moieties such as cholesterol, formed nanosize hydrogel by the self-assembly in water. We have additionally synthesized several functional polysaccharides that are cell-specific or thermosensitive. For this purpose, cell-specific saccharide determinants, pluronic or polyethylene oxide (PEO) was further conjugated to the hydrophobized polysaccharides. These functional amphiphilic polysaccharides also formed nanosize hydrogel in water. Their synthesis and characterization are described.

**KEY WORDS :** hydrogel, nanoparticle, amphiphilic polysaccharide, self-assembly, cholesterol

## INTRODUCTION

Hydrogel has attracted much interest with respect to various applications in biotechnology and medicine. A concept of supramolecular assembly has brought about a new methodology for the architecture of functional nanostructures. Recently, we have reported a new nanosize hydrogel that was formed in water by self-assembly of polymer amphiphile such as hydrophobized polysaccharide or hydrophobized polyamino acid. Especially, cholesterol-bearing pullulan (CHP) forms monodisperse nanoparticle in water (20-30 nm) [1-3]. The amphiphilic nanoparticle showed a unique binding behavior to various hydrophobic compounds such as antitumor drug (adriamycin) and even soluble proteins such as insulin [4,5]. The proteins were colloidal and thermally stabilized upon the complexation [5]. We have also synthesized other hydrophobized polysaccharides that were additionally introduced cell-specific saccharide determinants, thermosensitive polymer or polyethylene oxide (PEO). They were widely utilized in biotechnology and medicine. In this paper, the characteristics of these functional and nanosize hydrogels are described.

## RESULTS AND DISCUSSION

### Formation of hydrogel nanoparticle by self-assembly of CHP

Pullulan ( $M_w = 5.5 \times 10^4$ ) was partly substituted by 1.1, 1.7, 2.5, and 3.4 cholesterol moieties per 100 glucose units (CHP-55-1.1, -1.7, -2.5, and -3.4) [2]. The all self-aggregates were monodisperse and colloidally stable. No precipitation was observed even after a month. The particle size (hydrodynamic radius,  $R_H$ ) decreases with increase in the number of cholesterol moieties of CHP; 11.6 nm for CHP-55-1.1, 10.2 nm for CHP-55-1.7, 9.5 nm for CHP-55-2.5, and 8.4 nm for CHP-55-3.4. The aggregation number calculated from the molecular weight ( $M_w$ ) of the aggregate was approximately 10-12 for all CHPs. The polysaccharide chains are densely packed in the self-aggregate. An average polymer density in one nanoparticle was calculated from  $R_H$  and  $M_w$ . The CHP nanoparticle contains a large amount of water (50-90%) which is almost comparable to that of typical polysaccharide hydrogels such as agarose. Therefore, the CHP self-aggregate would be regarded as a nanosize hydrogel in which the associating cholesterol forms non-covalent cross-link site [3]. The CHP nanosize hydrogel complexed with various hydrophobic substances [3] such as fluorescent probes, porphyrin, bilirubin, adriamycin, and even soluble proteins [4,5].

### Functional hydrogel nanoparticles

#### CHP modified by cell-specific saccharides

In order to endow cell specificity to the CHP, a saccharide determinant such as galactose and lactose was introduced to CHP. Twenty or twenty three aminosaccharide moieties per 100 glucose units were conjugated to CHP by the reaction with the activated CHP. These CHPs so obtained also formed nanosize hydrogel with similarly to the parent CHP self-aggregate. The nanoparticle

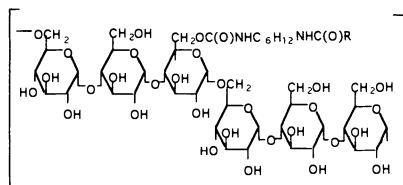
complexed with hydrophobic substances such as adriamycin or soluble protein. The galactose-bearing CHP showed a specific induced aggregation with a galactose specific lectin, RCA<sub>120</sub>. These cell specific CHP would be utilized as an improved drug carrier with active targeting ability.

#### CHP modified by polyethylene oxide (PEO)

PEO has been widely utilized as a surface modifier to various biomaterials. Methoxy PEO amine (Mw=1100) was reacted with CHP as activated by *p*-nitrophenyl chloroformate. PEO chains (4.7, 9.4 and 24.5 per 100 glucose units) were introduced to CHP (PEO-X-CHP: X=4.7, 9.4, 24.5). Spherical particles of PEO-CHP were observed on a negatively stained electronmicrograph. The diameter of particles increased with increase in the number of PEO chain; (19 nm for PEO-4.7-CHP, 56 nm for PEO-9.4-CHP, 91 nm for PEO-24.5-CHP). PEO-CHP effectively coated liposomal surface and stabilized the liposome against external stimuli [1].

#### CHP modified by thermosensitive polymer, pluronic (PL)

Stimuli-responsive materials have much attention in modern materials science with respect to various applications. Poly(ethylene oxide)<sub>a</sub>-poly(propylene oxide)<sub>b</sub>-poly(ethylene oxide)<sub>a</sub> block copolymer (pluronic<sup>®</sup>; PL, Mw=1100, a:b=1:4) has a lower critical solution temperature (LCST) and plays a role as a thermosensitive device. To endow the thermosensitivity to CHP self-aggregate, we have synthesized a CHP derivative conjugated with PL (PL-CHP) [6]. Monodisperse and spherical particles of PL-CHP were observed on a negatively stained electronmicrograph, and its average diameter was approximately 30 nm. PL units of PL-CHP still maintain its original LCST at 35 °C even after the conjugation to CHP. The hydrophobic fluorescent probe complexed to the nanoparticle below CT dissociated when the temperature was raised up above CT. The PL-CHP self-aggregate is a unique thermosensitive and nanosize hydrogel of an amphiphilic polysaccharide.



R : -Cholesterol (CHP)

Fig.1 Structure of hydrophobized pullulan

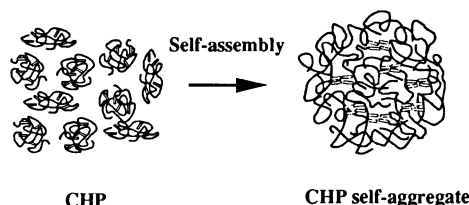


Fig.2 Schematic representation of self-assembly of CHP

#### REFERENCES

1. Akiyoshi K, Sunamoto J (1991) Physicochemical Characterization of cholesterol-bearing polysaccharides in solution. In: Friberg SE, Lindman B (eds) Organized Solutions. Marcel Dekker, inc New York, pp 289-304.
2. Akiyoshi K, Deguchi S, Moriguchi N, Yamaguchi S, Sunamoto J (1993) Self-aggregates of hydrophobized polysaccharides in water. Formation and characterization of nanoparticle. *Macromolecules* 26: 3062-3068.
3. Akiyoshi K, Deguchi S, Tajima H, Nishikawa T, Sunamoto J (1995) Self-assembly of hydrophobized polysaccharide: Structure of hydrogel nanoparticle and complexation with organic compounds. *Proc Japan Acad* 71, Ser. B: 15-19.
4. Akiyoshi K, Nagai K, Nishikawa T, Sunamoto J (1991) Self-aggregate of hydrophobized polysaccharide as a host for macromolecular guests. *Chem Lett* 1991: 1727-1730.
5. Nishikawa T, Akiyoshi K, Sunamoto J (1994) Supramolecular assembly between nanoparticles of hydrophobized polysaccharide and soluble protein: Complexation between the self-aggregate of cholesterol-bearing pullulan and  $\alpha$ -chymotrypsin. *Macromolecules* 27: 7654-7659.
6. Deguchi S, Akiyoshi K, Sunamoto J (1994) Solution property of hydrophobized pullulan conjugated with poly(ethylene oxide)-poly(propylene oxide)-poly(ethylene oxide) block copolymer: Formation of nanoparticle and their thermosensitivity. *Macromol Rapid Commun* 15: 705-711.

# NOVEL DESIGN OF SUPRAMOLECULAR-STRUCTURED BIODEGRADABLE POLYMER FOR DRUG DELIVERY

Nobuhiko Yui and Tooru Ooya

*School of Materials Science, Japan Advanced Institute of Science and Technology (JAIST)  
15 Asahidai, Tatsunokuchi, Ishikawa 923-12, Japan*

## SUMMARY

Biodegradable polymers with supramolecular structures were proposed as a novel candidate of substrates for temporal drug delivery. A biodegradable polyrotaxane was synthesized in which  $\alpha$ -cyclodextrins ( $\alpha$ -CDs) as drug carriers were threaded onto a poly(ethylene glycol) (PEG) chain capped at each terminal with L-phenylalanine (L-Phe) via peptide linkages. The release of  $\alpha$ -CDs from the biodegradable polyrotaxane was observed only when the terminal peptide linkages were hydrolyzed by papain. Further, the dethreading process of  $\alpha$ -CDs from PEG chains was also observed to be quite rapid. Therefore, it is suggested that  $\alpha$ -CD release from the biodegradable polyrotaxane was controlled by the hydrolysis of terminal peptide linkages.

**KEY WORDS:** Biodegradable polymers, Supramolecular structures, Polyrotaxanes, Temporal drug delivery.

## INTRODUCTION

Biodegradable polymers for controlled drug delivery have been extensively studied in the last two decades[1]. Recently, stimuli-responsive drug delivery systems have been achieved through surface-controlled degradation of hydrogels via specific internal signals[2]. However, degradation-controlled drug release cannot be guaranteed in these hydrogels because of high diffusivity of drugs through polymer matrices. Chemical modifications of drugs on hydrogel matrix or polymer backbone were still limited in terms of the amount of incorporated drugs, responsibility of drug release via degradation, and so on. Furthermore, pulsatile drug release has required in many clinical situations. From these perspectives, novel design of biodegradable hydrogels or polymeric systems which can deliver drugs in a pulsatile manner have been required.

Recently, it has been reported to form supramolecular assemblies such as polyrotaxanes in which many cyclic molecules are threaded onto a polymer chain: e.g.  $\alpha$ -cyclodextrins ( $\alpha$ -CDs) threaded onto a poly(ethylene glycol) (PEG) chain[4]. This paper deals with novel design of biodegradable polyrotaxane in which numerous  $\alpha$ -CDs as drug carriers are threaded onto a PEG chain capped by enzymatically degradable peptide bonds. For this system, drug-modified  $\alpha$ -CDs threaded onto the PEG chain will be released via the hydrolysis of the terminal peptide linkages (Fig.1).

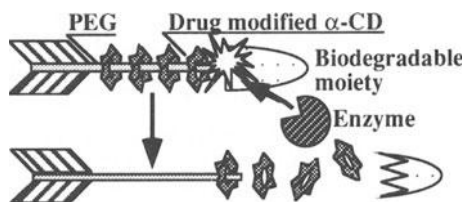


Fig.1 Strategy of drug release from biodegradable polyrotaxanes  
Drug modified  $\alpha$ -CDs will be released only when a biodegradable moiety is hydrolyzed.

## METHODS

Polyrotaxane consisting of  $\alpha$ -CDs and poly(ethylene glycol)-bisamine (PEG-BA) was prepared by simply mixing  $\alpha$ -CD and PEG-BA in aqueous solution[3]. The resulting inclusion complex was capped at each terminal with protected (*Z*-) L-phenylalanine (L-Phe) by condensation reaction, and then the *Z*-group of the compound was removed by catalytic reduction with palladium carbon under  $H_2$  atmosphere[4]. Finally, the product (biodegradable polyrotaxane) was purified by GPC on Sephadex G-25 with DMSO as an eluent. *In vitro* degradation of biodegradable polyrotaxane was examined by papain in citrate buffer containing mercapethanol (pH7.1) at 37°C[4]. The release of  $\alpha$ -CDs from the biodegradable polyrotaxane was monitored by 1-anilino-8-naphtalenesulfonic acid (ANS) fluorescence excited at 350nm and emitted at 500nm.

## RESULTS AND DISCUSSION

The introduction of L-Phe moiety to both ends of polyrotaxane was considered to be available for protecting to dethread  $\alpha$ -CDs from PEG chains because the benzyl group of L-Phe is bulky enough to prevent the  $\alpha$ -CDs from dethreading. The  $\alpha$ -CD dethreading from a PEG chain in the citrate buffer was completed within 8-10sec (Fig.2a). On the other hand, in the case of the biodegradable polyrotaxane, the concentration of  $\alpha$ -CDs in the presence of papain increased linearly during the first 5h although that of  $\alpha$ -CDs was quite low in the absence of papain (Fig.2b). These results indicate that  $\alpha$ -CDs were released only when the L-Phe moieties of the polyrotaxane were degraded by papain and that the process of peptide cleavages was the dominant step in  $\alpha$ -CD release from the polyrotaxane. Thus, it is concluded that supramolecular-structured biodegradable polymers can be a novel candidate as substrates for temporal drug delivery.

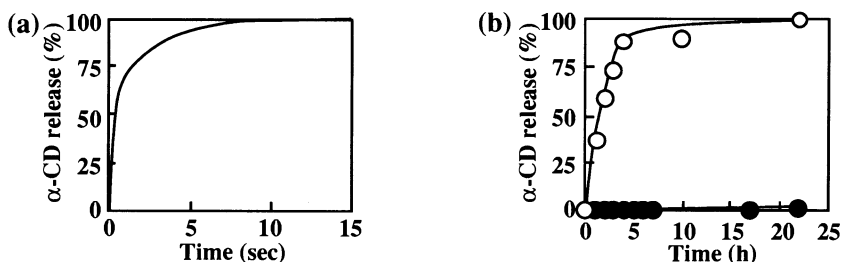


Fig.2  $\alpha$ -CD release from biodegradable polyrotaxane in citrate buffer (pH7.1)

(a)polyrotaxane at r.t. (b)L-Phe-polyrotaxane at 37°C with papain (O) and without papain (●).

## ACKNOWLEDGMENT

Prof. M. Terano and Dr. H. Mori, JAIST, are greatly acknowledged for their valuable discussions.

## REFERENCES

- [1] Baker RW (1987) Controlled release of biologically active agents. John Wiley, New York, pp 84-131
- [2] Okano T, Yui N, Yokoyama M, Yoshida R (1994) Advances in Polymeric Systems for Drug Delivery. Gordon & Breach Publishers, Yverdon, pp 106-145
- [3] Harada A, Kamachi M (1990) Complex formation between poly(ethylene glycol) and  $\alpha$ -cyclodextrin. Macromolecules. 23 : 2821-2823
- [4] Ooya T, Mori H, Terano M, Yui N (1995) Synthesis of a biodegradable polymeric supramolecular assembly for drug delivery. Macromol. Rapid Commun. 16 : in press

# INTERACTION OF POLY(ETHYLENE OXIDE)-BEARING LIPID RECONSTITUTED LIPOSOMES WITH MURINE B16 MELANOMA CELLS

Mamoru Haratake<sup>†</sup> and Junzo Sunamoto<sup>†,‡</sup>

<sup>†</sup>Surface Recognition Group, Supermolecules Project, Research Development Corporation of Japan Super Lab.Wing, Keihanna Plaza, Seika-cho 1-7, Souraku-gun, Kyoto 619-02, Japan.

<sup>‡</sup>Division of Synthetic Chemistry & Biological Chemistry, Graduate School of Engineering, Kyoto University, Yoshida-Hommachi, Sakyo-ku, Kyoto 606 Japan.

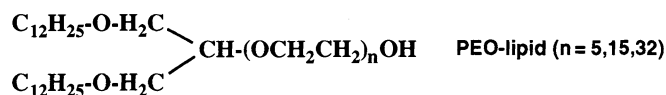
## SUMMARY

Interaction of poly(ethylene oxide)-bearing lipid(PEO-lipid( $n = X$ ),  $X$  = the average number of ethylene oxide units; 5, 15 and 32)-reconstituted egg PC liposomes with murine B16 melanoma cells was investigated. Water-soluble FITC-dextran (20 kDa) and lipophilic octadecyl rhodamine B (OD-RhoB) were incorporated into the liposomes to observe the actual modes of interaction by fluorescence microscopy. PEO-lipid-reconstituted liposomes used in this study were less interactive with the asynchronous cells. However when used PEO-lipid ( $n = 32$ , 20 mol%), both probes were introduced effectively into the mitotic cells even at 4°C and in the presence of cytochalasins B and D. Confocal fluorescence microscopy revealed that FITC-dextran and OD-RhoB, respectively, transferred cytosol and plasma membrane separately. These data suggested evidently the direct fusion between plasma membrane of mitotic cell and the liposome.

**KEY WORDS** : poly(ethylene oxide)-bearing lipid, liposome, murine B16 melanoma cell, confocal fluorescence microscopy, fusion

## INTRODUCTION

Introduction of biologically active foreign compounds into living cell is an important technique in experimental cell biology and medical field, especially gene therapy. Although endocytosis is one of major pathways for introducing the compounds into cell, labile substances are exposed to acidic medium in endosomes and subsequent almost complete enzymatic degradation in lysosome without showing their biological activity. It is, therefore, thought that a possible alternative pathway to deliver successfully into cytosol is direct membrane fusion through cell plasma membrane. From this point of view, Sunamoto and his co-workers have designed a novel fusogenic liposome reconstituted poly(ethylene oxide)(PEO)-bearing lipid on its outer leaflet. So far, our research groups have already examined the interaction of the proposed fusogenic liposomes with carrot protoplasts [1,2], HeLa cells [3] and Jurkat cells [4], and have demonstrated that the liposomes are capable of favorably transferring biologically liable plasmid and protein into the cell cytosol without losing their biological activity, as intended. The purpose of this work is to further extend our previous findings using murine B16 melanoma cell as a target and try to observe the actual modes of interaction of PEO-lipid-reconstituted liposomes with the cell by fluorescence microscopic techniques.



## MATERIALS AND METHODS

*Cells and cell culture* Murine B16 melanoma cells were maintained in Dulbecco's modified Eagle's medium(DMEM) supplemented with 10% fetal bovine serum at 37°C in humidified 5% CO<sub>2</sub>/95% air. Mitotic B16 melanoma cells were harvested by treatment with colcemid(40 ng/ml) for 3 hours [5].

*Preparation of liposomes* Large unilamellar liposomes were prepared by a slightly modified reverse-phase evaporation method. For embedding a lipophilic fluorescent probe, 15 mg of egg PC and 28 mg of octadecyl rhodamine B were dissolved in 0.6 ml of a mixture of diethyl ether and dichloromethane (56:44 by vol.). For a water-soluble probe FITC-dextran (20 kDa), 40 mg of the probe was dissolved in 0.2 ml of phosphate-buffered saline (PBS) and mixed with lipid emulsion. The obtained liposomal suspension was extruded through polycarbonate membrane (pore size 0.2  $\mu\text{m}$ ), followed by gel chromatography (Sephadex G-75,  $\phi 1.5 \times 30\text{cm}$ ) to remove unencapsulated FITC-dextran. For PEO-lipid reconstitution, liposome suspension was incubated with an ethanolic PEO-lipid solution at 37°C for 60 min. just before incubation with cells.

*Cell incubation with liposomes* After washing three times with PBS, cells ( $2 \times 10^5$  cells/ml) were incubated with liposome suspension at 37 or 4°C for 30 min. Final concentration of egg PC in incubation medium was always kept at 0.1 mM. After the incubation, cells were washed twice with DMEM and once with PBS, and then were subjected to fluorescence microscopic observation. After taking pictures, the number of fluorescent positive cells was counted on the pictures. Confocal fluorescence microscopy was performed with a Bio-Rad instrument (MRC-1000) equipped with air-cooled krypton/argon laser tube (15mW).

## RESULTS AND DISCUSSION

When the asynchronous cells in logarithmic-growing phase were incubated with PEO-lipid-reconstituted liposomes at 37°C, no significant introduction of the fluorescent probes was observed. Conventional liposome without PEO-lipids was internalized into the cells, but the uptake was completely inhibited when incubated at 4°C and in the presence of cytochalasins B and D (phagocytosis inhibitor). We tried to examine using the mitotic cells because of low endocytic activity [6] and higher membrane fluidity of plasma membrane [7,8]. For mitotic cells, internalization of conventional liposome was not observed at 37°C. Similarly, PEO-lipid (n = 5,15)-reconstituted liposomes were also less interactive with mitotic cells. Interestingly, in the case of PEO-lipid (n = 32, 20 mol%), about 40 to 50% of mitotic cells were dyed with both fluorescent probes. Additionally, the introduction of both probes were not prohibited even in the presence of cytochalasins B and D. , at 4°C, both fluorescent probes embedded into PEO-lipid (n = 32, 20 mol%)-reconstituted liposome was introduced simultaneously into about 20% of mitotic cells. In order to clarify the distribution of the two fluorescent probes in mitotic cells, we carried out the confocal laser scanning microscopic observation of mitotic cells treated with PEO-lipid (n = 32, 20 mol%)-reconstituted liposome at 4°C. Confocal laser scanning microscopy revealed that water-soluble and lipophilic probes were located separately on cytosol and cell plasma membrane, respectively. These supportive facts permit us to draw a conclusion that PEO-lipid (n = 32, 20 mol%)-reconstituted liposome fuses directly with the plasma membrane of mitotic B16 melanoma cells.

## REFERENCES

1. Tanaka K, Akiyoshi K, Sunamoto J, Sato T (1990) Fusion of PEG lipid-bearing liposome with plant protoplast. *Polymer Preprints, Japan* 39: 912
2. Sato T, Sunamoto J (1992) Recent aspects in the use of liposomes in biotechnology and medicine. *Prog.Lipid Res.* 31: 345-372
3. Okumura Y, Yamauchi M, Yamamoto M, Sunamoto J (1993) Interaction of a fusogenic liposome with HeLa cell. *Proc.Japan Acad.* 69(B): 45-50
4. Higashi N Sunamoto J (1994) Effective introduction of diphtheria toxin fragment A to Jurkat cell using a fusogenic liposome. *Polymer Preprints, Japan* 43: 3772-3773
5. Bhuyan BK, Adams EG, Badiner GJ, Trzos RJ (1987) Colcemid effects on B16 melanoma cell progression and aberrant mitotic division. *J.Cell.Physiol.* 132: 237-245
6. Berlin RD, Oliver JM (1980) Surface function during mitosis II. *J.Cell Biol.* 85:660-671
7. Lai C-S, Hopwood LE, Swartz HM (1980) Electron spin resonance studies of changes in membrane fluidity of chinese hamster ovary cells during the cell cycle. *Biochim.Biophys.Acta.* 602:117-126
8. Aszalos A, Yang GC, Gottesman MM (1986) Depolymerization of microtubules increases the motional freedom of molecular probes in cellular plasma membranes. *J.Cell Biol.* 100:1357-1362

# PHYSICAL STABILIZATION OF INSULIN THROUGH CHEMICAL MODIFICATION: SITE-SPECIFIC GLYCOSYLATION OR PEGYLATION

Miroslav Baudyš, Takashi Uchio, Soo Chang Song, Donald C. Mix and Sung Wan Kim

University of Utah, Department of Pharmaceutics and Pharmaceutical Chemistry / Center for Controlled Chemical Delivery, 570 Biomedical Polymers Research Building # 205, Salt Lake City, Utah 84112, USA

## ABSTRACT

The modification of human insulin by the covalent attachment of p-succinamidophenyl glucoside or monomethoxy monosuccinyl polyethylene glycol 600 and 2000 moieties to the protein remarkably alters the physical stability of insulin in solution. The synthesized derivatives were purified to homogeneity using ion exchange chromatography and then attachment site(s) were determined. The biological activity of the modified insulins was well preserved and covalent attachment of any hydrophilic group to any insulin amino group(s) improved insulin solution stability. However, the most significant impact on increased stability was the site-specific modification at PheB1 site. Moreover, as the number of groups attached to insulin increased, the solution stability of insulin derivatives also improved.

**KEY WORDS:** glycosylated insulin, PEG modified insulin, insulin physical stability, insulin aggregation

## INTRODUCTION

Insulin has a long history as being used as an essential protein pharmaceutical drug. As with any other biopharmaceutical protein, insulin is quite unstable compared to other drugs because of its complex physicochemical nature, which can lead to chemical and physical instability. The physical instability of protein is generally viewed as a two-step process: protein unfolding and subsequent aggregation [1]. The first step of protein unfolding is facilitated by hydrophobic forces (surfaces). We hypothesized that by hydrophilization of the surface of folded protein we could prevent or slow down this thermodynamically driven process of insulin aggregation (fibrillation). The covalent attachment of two hydrophilic moieties, glycosides or low  $M_r$  polyethylene glycols, to insulin amino groups (GlyA1, PheB1 and LysB29) and their effect on the kinetics of aggregation/fibrillation of insulin derivatives was studied.

## MATERIALS AND METHODS

To attach glucoside moieties, the amino group of p-aminophenyl glucoside was succinylated with succinic anhydride. The free carboxyl group of the resulting derivative (SAPG) was activated using mixed anhydride method to react with amino groups of insulin. In order to prepare PheB1 substituted insulin derivatives, monoBoc GlyA1 and diBoc GlyA1, LysB29 insulin derivatives were synthesized first from insulin using di-*tert*-butyl pyrocarbonate in DMSO. After attachment of SAPG group(s) to free amino groups, Boc groups were removed by TFA [2]. PEG insulin derivatives were synthesized in a similar manner. Monocarboxyl PEG derivatives were prepared from monomethoxy-PEG derivatives ( $M_r$  600 and 2000) by succinylation on the OH group in dry dioxane at 100 °C overnight. SAPG or PEG insulin derivatives were separated on a preparative Q-Sepharose column (7M urea, pH 7.8, 0 - 0.2M NaCl gradient). Final purification was achieved on S-Sepharose column (7M urea, 1M AcOH, 0 - 0.3M NaCl gradient). Purified derivatives were characterized by N-terminal group analysis (site(s) of attachment), carbohydrate content, UV and CD spectra (JASCO J-720). Biological activity of insulin derivatives (0.5 IU/kg i.v.) was determined using a rat blood glucose depression test (n=6), calculating the activities from AUC. The physical stability of insulin derivatives (0.5 mg/ml 0.01M PBS, pH 7.4) was evaluated in a

shaking test at 37 °C (5 ml vial, n=12-14, 1.2 ml filling volume, 100 strokes/min). Physical aggregation/fibrillation was monitored visually by periodical checks for precipitate formation and subsequent filtration (0.22 µm) and CD spectra recording (or RP HPLC, Vydac C<sub>4</sub> column) to determine residual insulin derivatives content.

## RESULTS AND DISCUSSION

The basic stability characteristics of glycosylated (SAPG) insulin derivatives and PEG insulin derivatives are shown in Table 1. It is obvious that site specific modification on PheB1 improves stability the most, and the number of SAPG groups coupled further correlates with stability. No conformational changes were detected by CD spectroscopy. Two PEGs with different M<sub>r</sub> were used - PEG 600 and PEG 2000. Since both PEG insulin derivatives gave similar results, only PEG 600 derivatives are shown in Table 1. It is evident that the same stability trend was preserved as for SAPG insulins; modification with PEG group on PheB1 caused a larger increase in stability, as the number of PEG moieties attached increased. It was suggested previously that conformational flexibility of insulin B-chain contributes to the fibrillation process. We found that PheB1 modification shifts monomer conformation into R-state, making it less flexible and thus more stable [2]. Also, as the number of hydrophilic SAPG groups attached increases, dimer/hexamer insulin derivative fraction decreases, but stability increases even further [2]. This apparently contradicts

Table 1: Characterization and Physical Stability of SAPG and PEG Insulin Derivatives.

Insulin Derivative	Biol. Activity ± SD (IU/mg)	Days to Fibrillation (±SD)
2Zn-Insulin	25.2 ± 4.7	0.5 (0.1)
Zn-free Insulin	NDA <sup>a</sup>	0.4 (0.1)
GlyA1-SAPG Insulin	22.2 ± 4.2	2.7 (1.5)
PheB1-SAPG Insulin	24.0 ± 4.0	12.4 (1.8)
GlyA1, LysB29-SAPG Insulin	16.8 ± 3.4	2.9 (0.9)
PheB1, LysB29-SAPG Insulin	30.2 ± 5.6	15.8 (4.1)
GlyA1, PheB1, LysB29-SAPG Insulin	19.9 ± 3.6	18.8 (4.0)
GlyA1-PEG 600 Insulin	22.0 ± 3.8	4.7 (0.4)
PheB1-PEG 600 Insulin	23.8 ± 3.5	22.0 (4.6)
GlyA1, PheB1-PEG 600 Insulin	16.2 ± 3.7	26.4 (2.6)
GlyA1, LysB29-PEG 600 Insulin	19.1 ± 4.1	8.4 (0.9)
GlyA1, PheB1, LysB29-PEG 600 Insulin	5.4 ± 1.8	35.9 (4.3)

<sup>a</sup> Not determined

an accepted view that the presence of insulin monomer and its conformational change at a hydrophobic interface triggers fibrillation [1]. This is explained by the increased hydrophilicity of insulin derivative monomer surface and/or steric hindrance by flanking PEG or SAPG moieties preventing formation of sufficiently large nucleation centers to trigger fibrillation.

## CONCLUSION

The covalent attachment of two different hydrophilic groups, succinamidophenyl glucopyranoside (SAPG) or polyethylene glycol (PEG), to any insulin amino group(s) had a beneficial effect on insulin physical stability. However, two trends were evident. First, site-specific attachment of one of the two moieties to PheB1 amino group of insulin increased stability the most. Second, as the number of hydrophilic groups coupled to insulin increased, the physical stability of insulin derivatives improved.

## REFERENCES

1. Costantino HR, Langer R, Klibanov AM. (1994) Solid-phase aggregation of proteins under pharmaceutically relevant conditions. *J. Pharm. Sci.* 83: 1662-1669
2. Baudys M, Uchio T, Mix D, Wilson, D, Kim SW. (1995) Physical stabilization of insulin by glycosylation. *J. Pharm. Sci.* 84: 28-33



# THERAPEUTIC EFFECTS OF THE SOYBEAN TRYPSIN INHIBITOR AND ITS GELATIN CONJUGATE ON THE PSEUDOMONAL ELASTASE INDUCED SHOCK IN GUINEA PIG

Young-Hee SHIN<sup>1</sup>, Takaaki AKAIKE<sup>2</sup> and Hiroshi MAEDA<sup>2</sup>

<sup>1</sup> College of Pharmacy, Kyungsoong University, Pusan 608-736, Korea.

<sup>2</sup> Deptment of Microbiology, Kumamoto University, School of Medicine, Kumamoto 860, Japan.

## ABSTRACT

We reported that bradykinin facilitate bacterial dessimination from the local site of infection as well as spreading exotoxin and endotoxin. However, very little studies have been carried out focusing on bacterial protease involved activation of kinin cascade, and septic shock, and hence intervention of the shock by appropriate inhibitors. In this study, we evaluated the therapeutic effects of the native SBTI and Suc-gel-SBTI which has about 6 times longer half-life than native SBTI, on the pseudomonal elastase induced sub-lethal septic shock model in guinea pigs in view of bradykinin.

**KEY WORD :** Kunitz-type soybean trypsin inhibitor (SBTI), SBTI-succinylated gelatin conjugate (Suc-gel-SBTI), pseudomonal elastase, bradykinin, shock model.

## INTRODUCTION

Kunitz-type Soybean trypsin inhibitor(SBTI), a typical serine protease inhibitor, has a most potent hibitory activity against kallikrein and its physicochemical and biochemical properties are well documented. Many reports described about its pharmacological effect and potential therapeutical possibilities. However, it exhibited very short half-life in vivo and hence therapeutic value was minimal. To enhance therapeutic value, we prepared the conjugated SBTI with succinylated gelatin(Suc-gel), and the conjugate possesses more larger than thereshold of renal clearance. We recently reported physicochemical, biopharmaceutical and pharmacological effects of both native and conjugated SBTI(Suc-gel-SBTI)[1]. Here, we report effect of the Suc-gel-SBTI and native SBTI on the Pseudomonas aeruginosa elastase induced sub-lethal shock model in guinea pigs.

## MATERIALS AND METHODS

Hartley strain albino guinea pigs of both sexes (320 - 380g) were used. Soybean trypsin inhibitor (SBTI), fragmented gelatin ( Mw of about 23,000), pseudomonal elastase , and bradykinin assay kit ( Markit M ) were used.

Synthesis of Suc-gel-SBTI :

SBTI was chemically modified with succinylated gelatin using carbodiimide. The reaction mixture was subjected for purification on a Sepacryl S-200 column, and ultrafiltered and then lyophilized[2].

Therapeutic effect on pseudomonal elastase induced sub-lethal shock model in guinea pigs :

(1) Measurement of mean systemic arterial blood pressure (MABP):

The jugular vein was cannulated for intravenous injection and the carotid artery was cannulated for the continuous measurement of MABP of guinea pig, through a pressure transducer(TP-200T, Nihon Koden, Japan)[3]. SBTI or Suc-gel-SBTI was administrated via jugular vein before injection of pseudomonal elastase intravenously and measurement of MABP continued.

(2) Bradykinin concentration in arterial blood of guinea pigs :

Treatment of guinea pigs was the same method as above. Pseudomonal elastase was iv injected and 3 min after, the arterial blood were removed and assayed using bradykinin assay kit(Markit M).

### (3) Effect of SBTI on vascular extravasation in the back skin of guinea pigs :

SBTI or Suc-gel-SBTI was pretreatment by iv injected and 1 min after 2.5% Evans blue saline solution was injected iv. Adequate time later, pseudomonal elastase was injected intradermally on the back skin of the guinea pigs. After 30 min, the guinea pig was sacrificed by decapitation, and the amount of extravasated Evans blue was quantified by the absorption at 620nm.

## RESULTS AND DISCUSSION

SBTI and Suc-gel-SBTI prevented guinea pig from hypotension. The preventive effect of native SBTI against decrease in blood pressure was not observed 3hrs after iv injection (Fig.). On the contrary, the effect of Suc-gel-SBTI remained effective, i.e. prevention of hypotension remained effective even 3hr after iv injection. Concordant results to this observation was that plasma concentration of bradykinin was maintained minimal for both native and Suc-gel-SBTI at one min after injection of SBTI, however, after 180min, effect of native SBTI was no longer significant, while that of Suc-gel SBTI remained effective(70% effective) even after 180min. Similarly, about 70% of extravasation of Evans-blue was suppressed upto 180min. After 6hrs, native has suppressed only 45% of extravasation while 60% was suppressed by Suc-gel-SBTI.

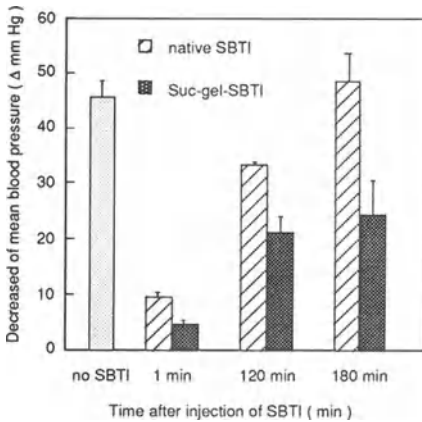


Fig. Effects of the pretreatment of native SBTI and Suc-gel-SBTI on the change of mean arterial blood pressure of guinea pigs caused by pseudomonal elastase induced sub-lethal shock model.

## CONCLUSION

Both SBTI and Suc-gel-SBTI showed significant suppression of generation of kinin after iv injection of pseudomonal elastase. Suc-gel-SBTI showed enhanced biological effect in vivo as revealed by three different parameters such as anti-hypotension, suppressed kinin formation and extravasation. These results suggest polymer conjugation of SBTI with such as biocompatible polymer as succinylated gelatin may lead us to develop a therapeutic with anti shock property.

## REFERENCE

1. Shin, Y. H., Kojima, Y., Otagiri, M. and Maeda, H. (1994): Conference of 10th Drug Delivery System. (Tokyo, Japan).
2. Kojima, Y., Haruta, A., Imai, T., Otagiri, M. and Maeda, H. (1993): Conjugation of Cu,Zn-superoxide dismutase with succinylated gelatin; Pharmacological activity and cell-lubricating function. *Bioconjugate Chemistry* 4, 490.
3. Khan, M. M. H., Yamamoto, T., Arki, H., Ijiri, Y., Shibuya, Y., Okamoto, M. and Kambara, T. (1993): Pseudomonal elastase injection causes low vascular resistant shock in guinea pigs. *Biochim. Acta* 1182, 83.

# THE PULSATILE RELEASE SYSTEM OF MACROMOLECULAR DRUGS FROM ALGINATE GEL BEADS

Minako Kawabuchi, Atsushi Watanabe and Masayasu Sugihara <sup>1)</sup>  
Akihiko Kikuchi, Yasuhisa Sakurai and Teruo Okano <sup>2)</sup>

1) Department of Pharmacy, Tokyo Women's Medical College Hospital  
2) Institute of Biomedical Engineering, Tokyo Women's Medical College  
8-1 Kawadacho, Shinjuku, Tokyo 162, JAPAN

## SUMMARY

We investigate the possible applicability of alginate gel beads for controlled release system of water-soluble macromolecular drugs, using Fluorescein Isothiocyanate Dextran (FITC-dex) as the model compound. Lower molecular weight dextran was released via the diffusion through alginate matrix, while alginate erosion strongly affected dex release with increasing molecular weight. For FITC-dex (MW: 145,000), pulsatile release was observed after a lag time of 90 min. The lag time could be controlled not only by molecular weight and concentration of alginate but also by particle size of beads. We have also succeeded to alter the release profile of FITC-dex (MW: 145,000) from pulsatile to sustained release by adding styrene-maleic anhydride copolymer (SMA) to alginate. These results suggest that alginate gel beads are utilized as vehicle for a delivery of bioactive compounds.

**KEYWORDS:** alginate gel bead, biodegradable polymer, pulsatile release, sustained release

## INTRODUCTION

It has a great impetus to establish the sustained release or the pulsatile release system for macromolecular bioactive compounds such as vaccines and polypeptide drugs. Especially, pulsatile release system is necessary for drugs which are subject to large metabolic degradation, or produce tolerance by repeated administrations, or have activity profiles influenced by circadian patterns, because the system allows fast and complete release of drugs after a predetermined lag time [1]. Biodegradable polymers have been used for the controlled release drug delivery systems [2]. Among the biodegradable polymers, alginate gel is useful for this purpose, because it can easily be formed in aqueous solution (no organic solvents) at room temperature and is biocompatible. In this paper, we investigate the possibility of sustained release as well as pulsatile release systems of Fluorescein Isothiocyanate Dextran (FITC-dex) as the model of water-soluble macromolecular drugs with alginate gel beads.

## MATERIALS AND METHODS

FITC-dex was dissolved to sodium alginate solution, and this solution was dropped into 0.1 M CaCl<sub>2</sub> solution using a syringe. These gels were cured for 2 days, and washed twice with distilled water. In this ways, alginate gel beads containing FITC-dex with molecular weight range of 9,400-145,000 were prepared. On the other hand, styrene-maleic anhydride (SMA)-alginate gel beads were prepared by mixing SMA with sodium alginate. The release of each component from alginate gel beads was determined using a JP 12 dissolution test apparatus (single basket method) in 500 ml phosphate buffered saline (PBS; pH7.4) at 37 ± 0.5°C with the basket rotation at 100 rpm. At scheduled time intervals, 5ml of solution was taken, and the amount of FITC-dex released was determined by measuring fluorescence with the excitation wavelength at 495 nm and the emission at 520nm, respectively. The amount of alginate released was determined according to the method reported by Murata, et al. [3,4]. The amount of released Ca<sup>2+</sup> as well as SMA were also determined by measuring atomic absorbance at 422.7nm and absorbance at 258nm, respectively.

## RESULTS AND DISCUSSION

Fig. 1 shows the effect of molecular weight of dextran on its release from alginate gel beads. As molecular weight of FITC-dex increased, FITC-dex release from alginate gel beads was retarded to show sigmoidal release profiles with initial lag time. Molecular weight of FITC-dex did not affect alginate release, and alginate was released rapidly after a lag time of 60-90min. For FITC-dex with

molecular weight 9,400 cumulative release is proportional to square root of time, indicating that release is mainly governed by diffusion through the matrix. FITC-dex with molecular weight 145,000 was released rapidly and completely after a lag time of 90 min, and its release profile was almost same to alginate release pattern. These results suggest that as molecular weight of FITC-dex increased, FITC-dex release was strongly influenced by the erosion of the alginate gel. Since FITC-dex release from alginate gel beads was retarded with decreasing the concentration of  $\text{Na}^+$  ion in the medium, the result indicates that complex-formed  $\text{Ca}^{2+}$  ion in alginate gel beads is exchanged with  $\text{Na}^+$  ion in the medium, and this exchange might affect the disintegration of beads and FITC-dex release. Furthermore, it was observed for release of FITC-dex with molecular weight 145,000, the bigger the particle size of beads, the longer was the lag time for the onset of pulsatile release without changing their release rates as shown in Fig. 2. It was also observed that the lag time became longer with increasing concentration as well as molecular weight of alginate. These results imply the possibility of the pulsatile release system for high molecular weight dextran using alginate gel beads with controlled onset time of dextran release.

We next modified alginate gel by adding SMA to alter the release profile of FITC-dex (MW: 145,000). By the addition of SMA, release profile of dextran was changed from sigmoidal to zero-order kinetic release. For 5% SMA-containing beads, sustained release of dextran was observed for up to 240 min. These results suggest that carboxyl group in SMA forms complex with  $\text{Ca}^{2+}$  ion to make hydrophobic domain. This complex formation would prevent alginate carboxyl group from binding with  $\text{Ca}^{2+}$  ion and thus alter the microstructure within the alginate gel beads.

In conclusion, pulsatile as well as sustained release of high molecular weight dextran were achieved using alginate gel beads. These results suggest that alginate gel bead is one of the promising devices for protein as well as peptide drugs.

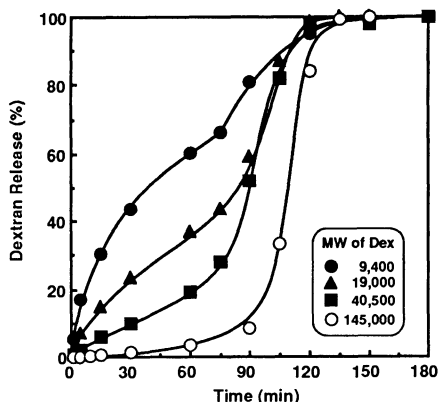


Fig.1 Cumulative release profiles of FITC-dex with various molecular weight from alginate gel beads in PBS

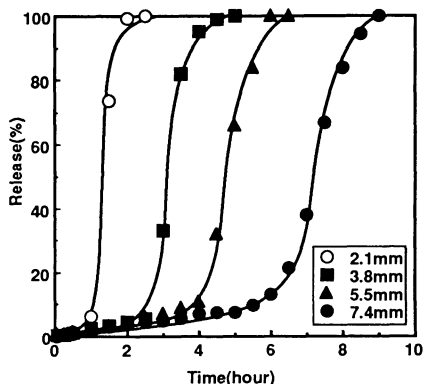


Fig.2 Effect of particle size on FITC-dex (MW:145K) release from alginate gel beads in PBS

## REFERENCES

1. Pozzi F, Furlani P, Gazzaniga A, Davis SS, Wilding IR (1994) The TIME CLOCK\* system: a new oral dosage form for fast and complete release of drug after a predetermined lag time. *J Controlled Release*, 31: 99-108
2. Okano T, Yui N, Yokoyama M, Yoshida R, (1994) *Advances in Polymeric Systems for Drug Delivery*. Gordon and Breach Science Publishers, Switzerland, pp106-120
3. Murata Y, Nakada K, Miyamoto E, Kawashima S, Seo SH (1993) Influence of erosion of calcium-induced alginate gel matrix on the release of Brilliant Blue. *J Controlled Release*, 23: 21-26
4. Murata Y, Kawashima S, Miyamoto E, Masauji N, Honda A (1990) Colorimetric determination of alginates and fragments thereof as the 2-nitrophenylhydrazides. *Carbohydr. Res*, 208: 289-292

# ALBUMIN RELEASE FROM BIOERODIBLE HYDROGELS BASED ON SEMI-INTERPENETRATING POLYMER NETWORKS COMPOSED OF POLY( $\epsilon$ -CAPROLACTONE) AND POLY(ETHYLENE GLYCOL) MACROMER

Jeong-Hun Ha<sup>1</sup>, Sung-Ho Kim<sup>1</sup>, and Chong-Su Cho<sup>2</sup>

<sup>1</sup>College of Pharmacy, Chosun University, Kwangju 501-759, Korea

<sup>2</sup>Department of Polymer Engineering, Chonnam National University, Kwangju 500-757, Korea

**ABSTRACT:** Poly(ethylene glycol) (PEG) macromers terminated with acrylate groups and semi-interpenetrating polymer networks (IPNs) composed of poly( $\epsilon$ -caprolactone) and PEG macromer were synthesized and characterized with the aim of obtaining a bioerodible hydrogel that could be used to release albumin. Polymerization of PEG macromer resulted in the formation of cross-linked gels due to the multifunctionality of macromer. Glass transition temperature ( $T_g$ ) and melting temperature ( $T_m$ ) of PEG network and PCL in the IPNs were shifted, indicating an interpenetration of PCL and PEG chains. Water content decreased with increasing PCL weight fraction due to the hydrophobicity of PCL. Albumin release from the IPNs can be controlled by the weight fraction of PEG in the IPNs, crosslinking density and the nature of PEG, and albumin loading content.

**KEY WORDS:** bioerodible, interpenetrating polymer networks (IPNs), macromer

## INTRODUCTION

One major advantage of using a biodegradable system is to eliminate surgical removal of an implanted delivery device after the delivery system is exhausted (1). Implantable delivery system by using the biodegradable polymers have been attempted for the peptide drugs because these drugs are rapidly degraded by proteolytic enzymes in the gastrointestinal tract (2). In this study, we are aiming to report albumin release from bioerodible hydrogel based on semi-interpenetrating polymer networks (IPNs) composed of poly( $\epsilon$ -caprolactone) (PCL) and poly(ethylene glycol) (PEG) macromer for the implantable system. PCL is one of the biodegradable polyesters which have attracted attention in a controlled drug delivery due to the non-toxicity. But the homopolymer itself is degraded very slowly. We decide to incorporate PEG macromer into PCL chains because PEG macromer is a hydrophilic segments which can be used to enhance the biodegradability of PCL.

## EXPERIMENTAL

### Synthesis of PCL/PEG semi-IPNs

The semi-IPNs were prepared by a method of simultaneous IPNs method. 10  $\mu$ l of the initiator solution was added to the methylene chloride solution of PCL and PEG macromer. The mixture solution was irradiated using a low-density of LWUV for 5 min, and the solvent was then evaporated to dryness at 4°C.

### In vitro degradation

The cutted dry IPNs were equilibrated in phosphate buffer saline (PBS) solution at pH 7.4 and incubated at 37°C. Weight loss was monitored gravimetrically at various intervals of time.

### In vitro release

Cutted disks of the drug loaded polymer were introduced into a vial with 5cm<sup>3</sup> of a phosphate buffer solution ( 0.1M, pH 7.4 ). The mixture was allowed to stir in a shaker whose temperature was maintained at 37°C. At predetermined time intervals, aliquots of 5cm<sup>3</sup> of the aqueous solution were withdrawn and another 5cm<sup>3</sup> of PBS was put into the vial. The concentration of albumin released was monitored using a UV spectrophotometer.

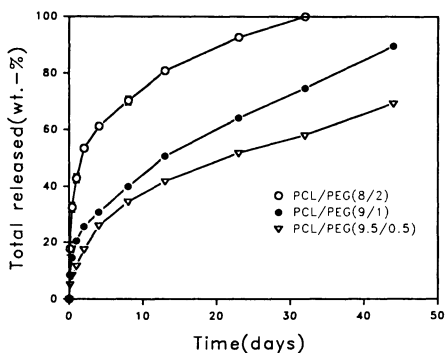


Fig.1 Released Albumin from the PCL/PEG IPNs against weight fraction of PEG

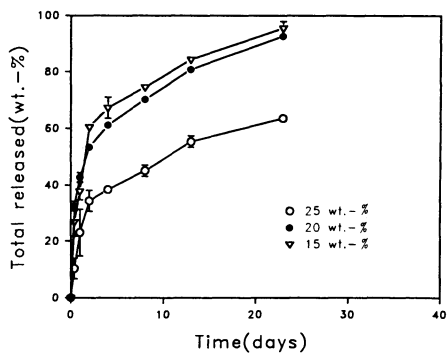


Fig.2 Released Albumin from the PCL/PEG (8/2)IPNs against conc. of PEG macromer

### RESULTS AND DISCUSSION

From the DSC studies, it was found that the glass transition temperature (  $T_g$  ) of PCL in the IPNs were inner-shifted whereas pure PCL has the glass transition around  $-52^\circ\text{C}$ . These results indicate the formation of the interpenetrating PCL and PEG chains (3).

From the total released of albumin from the PCL/PEG IPNs against weight fraction of PEG, it was found that the release of albumin from the IPNs rapidly increased with incorporation of PEG due to the increase of hydrophilicity of PEG in the IPNs(Fig. 1). From the total released of albumin from the PCL/PEG IPNs against concentration of PEG macromer in the IPNs preparation, it was found that the lower concentration of PEG macromer in the IPNs leads to a fast drug release than higher concentration of PEG macromer(Fig. 2). This was attributed to formation of the higher crosslink density of PEG gel in the higher concentration than lower one.

### REFERENCES

- (1) Heller J(1984) Bioerodible systems, In: Medical Application of Controlled Release, Langer RS, Wise DL(eds) CRC Press, Boca Raton, 39-90
- (2) Wary PY (1986) Insulin delivery by an implantable combined matrix system. Life Support Syst. 4: 380-382
- (3) Sperling LH (1981) Interpenetrating Polymer Networks and Related Materials. Plenum Press, New York, 85-105

# A NOVEL DRUG DELIVERY SYSTEM OF HEPATOCYTE GROWTH FACTOR (HGF): UTILIZATION OF HEPARIN-HGF COMPLEX

Yukio Kato<sup>a)</sup>, Ke-Xin Liu<sup>a)</sup>, Tetsuya Terasaki<sup>a)</sup>, Toshikazu Nakamura<sup>b)</sup>, and Yuichi Sugiyama<sup>a)</sup>

*a) Faculty of Pharmaceutical Sciences, University of Tokyo, 7-3-1 Hongo, Bunkyo-ku, Tokyo 113, Japan, Phone: 81-3-5802-2045, Fax: 81-3-5800-6949*

*b) Biomedical Research Center, Osaka University School of Medicine, Suita, Osaka 565, Japan*

## SUMMARY

Although hepatocyte growth factor (HGF) is most potent mitogen for mature hepatocytes and expected to be developed as a treatment for a liver diseases, its plasma residence time is very short, and therefore, a high dosage is needed to obtain pharmacological effect in vivo. To overcome such a problem, we designed heparin-HGF complex as a novel DDS for HGF and demonstrated that the complex exhibits a lower plasma clearance compared with that of HGF alone and retains the biological activity of HGF.

**KEY WORDS:** hepatocyte growth factor (HGF), heparin

## INTRODUCTION

Since HGF is a most potent mitogen for matured hepatocytes, it is expected to be used for the therapy of certain types of liver diseases [1,2]. However, the plasma half-life of HGF is short [3,4], and the large doses are necessary to show pharmacological effects in vivo. Therefore, it is essential to develop drug delivery system (DDS) which increases the plasma residence time of HGF in vivo with a minimal change in intrinsic biological activity. Since HGF is taken up by the liver via not only the receptor-mediated endocytosis, but also non-specific mechanism, which is probably related to the adsorption of HGF to heparin-like substance [3], we designed a heparin-HGF complex as a novel DDS of HGF, which is aimed to reduce such non-specific binding and result in the longer plasma residence time of HGF [5].

## MATERIALS AND METHODS [5]

(i) <sup>35</sup>S-heparin, fractionated on Sephadex G-100 and protamine Sepharose, was incubated with HGF (50 nM) for 50 min at 25 °C. Total and unbound concentration was determined by the ultrafiltration. (ii) Heparin with a high (18-23 kD) or low (4-6 kD) molecular weight was dissolved in saline and incubated with <sup>125</sup>I-HGF (5 μCi, 0.6 pmol/kg body wt). Heparin-<sup>125</sup>I-HGF complex thus obtained was administered intravenously to rats. The trichloroacetic acid (TCA)-precipitable radioactivities both in plasma and several tissues were chased. (iii) The mitogenic activity of heparin-HGF complex was measured by assessing <sup>125</sup>I-deoxyuridine incorporation in primary cultured rat hepatocytes.

## RESULTS [5]

Scatchard analysis of the binding between HGF and <sup>35</sup>S-heparin indicated the presence of saturable binding site for heparin on HGF molecule. The dissociation constant for the binding of <sup>35</sup>S-heparin (12-13 or 21-23 kD) was less than 1 nM, indicating that such binding has a strong affinity.

The TCA-precipitable radioactivity disappeared rapidly after the iv administration of tracer <sup>125</sup>I-HGF only, with the area under the plasma concentration curve from 0 to 30 min (AUC<sub>0-30</sub>) of 11.2 ± 0.0 (mean ± S. E. of at least three animals) % of dose·min/ml (Fig.1). On the other hand, the plasma concentration time profile was different after administration of a mixture of <sup>125</sup>I-HGF and heparin with a high Mw (Fig.1A). The AUC<sub>0-30</sub> values were 23.6±2.5, 25.7±0.1, and 33.4±0.2 % of dose·min/ml after iv administration of <sup>125</sup>I-HGF with 5, 10, and 20 mg heparin with high Mw, respectively. The effect of heparin with low Mw on the plasma disappearance of HGF was slightly smaller (Fig.1B), that is, the AUC<sub>0-30</sub> value was 25.0±0.0 % of dose·min/ml after the iv administration of <sup>125</sup>I-HGF with 20 mg of low Mw heparin. After the iv administration of <sup>125</sup>I-HGF only, the tissue-to-plasma concentration ratio (Kp) in the liver was 3.11 ± 0.15 ml/g liver and greater than those in other tissues. After the iv administration of <sup>125</sup>I-HGF with

Fig. 1 Plasma concentration-time profiles of heparin-<sup>125</sup>I-HGF complex

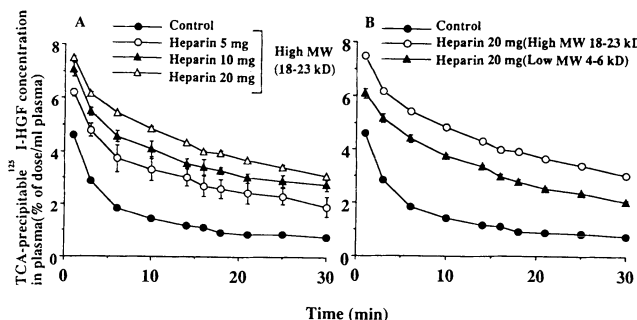
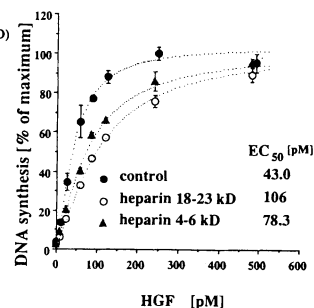


Fig. 2 HGF concentration dependence of mitogenic response in the presence and absence of heparin (1 mg/ml)



heparin, the  $K_p$  value was dropped to  $1.43 \pm 0.05$  ml/g liver. When the  $K_p$  values were converted to the distribution volume per kg body wt, the liver value was much greater than those in other tissues after the administration of either <sup>125</sup>I-HGF only or heparin-<sup>125</sup>I-HGF complex. These results suggested that heparin-HGF complex avoids its uptake to the liver and such avoidance of hepatic uptake contributes much to the decrease of HGF plasma clearance.

The HGF concentration dependence of mitogenic response was examined in the presence or absence of 1 mg/ml heparin. The half-effective concentration ( $EC_{50}$ ) was  $43.0 \pm 1.2$  pM in the absence of heparin, and  $106 \pm 4$  or  $78.3 \pm 2.5$  pM in the presence of heparin with a high or low Mw, respectively, while the maximal values of the mitogenic response was comparable in either case (Fig.2). Based on the binding parameters obtained, most (> 99.9%) of the binding site on HGF molecule was estimated to be occupied by heparin at any concentration of HGF (10-500 pM). These results suggested that heparin slightly decreases the affinity of HGF for its receptor, without any effect on its maximal activity.

## CONCLUSION

Heparin-HGF complex, which retained the biological activity of HGF, exhibited much lower clearances for hepatic uptake and plasma disappearance than HGF only. The heparin-HGF complex may thus be utilized as a novel DDS of HGF.

## REFERENCES

1. Matsumoto K, Nakamura T (1992) Hepatocyte growth factor: molecular structure, roles in liver regeneration, and other biological functions. *Crit. Rev. Oncogen.* 3: 27-54
2. Matsumoto K, and Nakamura T (1993) Roles of HGF as a pleiotropic factor in organ regeneration. In: Hepatocyte growth factor-Scatter Factor(HGF-SF) and the C-Met Receptor. Goldberg ID and Rosen EM (eds), Birkhauser Verlag, Basel, 1993; pp 225-249
3. Liu K, Kato Y, Narukawa M, Kim DC, Hanano M, Higuchi O, Nakamura T, Sugiyama Y (1992) The importance of the liver in the plasma clearance of hepatocyte growth factor in rats. *Am. J. Physiol.* 263: G642-G649
4. Liu K, Kato Y, Yamazaki M, Higuchi O, Nakamura T, Sugiyama Y (1993) Decrease in the hepatic uptake clearance of hepatocyte growth factor (HGF) in CCl<sub>4</sub>-intoxicated rats. *Hepatology* 17: 651-660
5. Kato Y, Liu K, Nakamura T, Sugiyama Y (1994) Heparin-hepatocyte growth factor complex with low plasma clearance and retained hepatocyte proliferating activity. *Hepatology* 20: 417-424



# NEW POLYMERIC HYDROGEL FORMULATIONS FOR THE CONTROLLED RELEASE OF PROTEIC DRUGS. DSC INVESTIGATION OF WATER STRUCTURE

E. E. Chiellini, E. Chiellini, D. Giannasi, E. Grillo Fernandes\*, R. Solaro

Department of Chemistry and Industrial Chemistry, University of Pisa, via Risorgimento 35, 56126 Pisa, Italy, Tel. (+39) 50-918299, Fax (+39) 50-28438

\*Instituto de Química, Universidade de São Paulo, São Paulo, SP (Brazil)

## SUMMARY

New hybrid matrices with strong hydrogel characteristics were prepared by combination of partial esters of the alternating copolymers of maleic anhydride with mono-O-methyloligoethylenglycol vinyl ethers with  $\alpha$ -interferon (IFN $\alpha$ ) or myoglobin dispersed in human serum albumin. The matrices were used for the formulation of ocular inserts for the controlled release of IFN $\alpha$ . Kinetics of hydration, weight loss, and protein release as well as amount of bound water were investigated in simulated tear fluid. Results are discussed in terms of synthetic matrix/protein interactions.

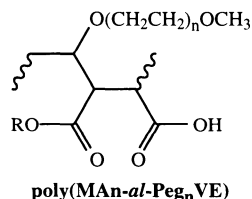
**KEY WORDS:** hybrid hydrogels,  $\alpha$ -interferon, controlled release, human serum albumin

## INTRODUCTION

Polypeptides and proteins are increasingly becoming an important class of therapeutic agents due to their extremely specific activity and high body tolerance<sup>1,2</sup>.

In the present contribution we describe a new approach in which the delivery of a protein of choice,  $\alpha$ -interferon (IFN $\alpha$ ), was pursued by using novel hydrophilic hybrid materials based on polymeric mixtures of human serum albumin (HSA) and partial esters of alternating copolymers of maleic anhydride with the vinyl ethers of mono-O-methyloligoethylenglycols (MAN-*al*-Peg<sub>n</sub>VE).

Hybrid matrices prepared by a novel low temperature casting method, were used for the formulation of ocular inserts for the controlled release of IFN $\alpha$ . Kinetics of hydration, weight loss, and protein release were investigated in simulated tear fluid. A preliminary differential scanning calorimetry study on the structure of water in the hydrogels is also reported.



## METHODS

Copolymers of poly(MAN-*al*-Peg<sub>n</sub>VE), n = 1-4, were converted into the corresponding partial esters by reaction with methanol, ethanol, 1-propanol, 1-butanol and 1-dodecanol in THF at reflux. Matrices containing IFN $\alpha$  were prepared by low temperature (-60°C) casting of a suspension of HSA/IFN $\alpha$  mixture in the acetone solution of poly(MAN-*al*-Peg<sub>n</sub>VE) partial esters. To evaluate these formulations as ophthalmic devices, the polymeric films thus obtained were cut into 3 mm diameter circular inserts weighing 2.7±0.1 mg, that were tested “*in vitro*” for dissolution rate, water uptake, weight loss, and protein release in isotonic buffer solution mimicking the tear fluid (pH 7.4, 1.33 mM).

Hybrid matrices based on the methyl esters of poly(MAN-*al*-Peg<sub>n</sub>VE), n = 1-3, and containing a mixture 1:4 myoglobin/human serum albumin have been also prepared by a room temperature casting method. The free water content of the resulting swollen gels was determined using differential scanning calorimetry (DSC). Hydrogels specimens (3-6 mg) were cut from the pre-equilibrated gels, placed in the appropriate aluminium pans, sealed, cooled from 30°C to -50°C at a rate of 10°C/min, and then heated up to 30°C at 5°C/min. The enthalpy of the melting peak observed at about 0°C was used to compute the amount of free water. Total water content was computed gravimetrically.

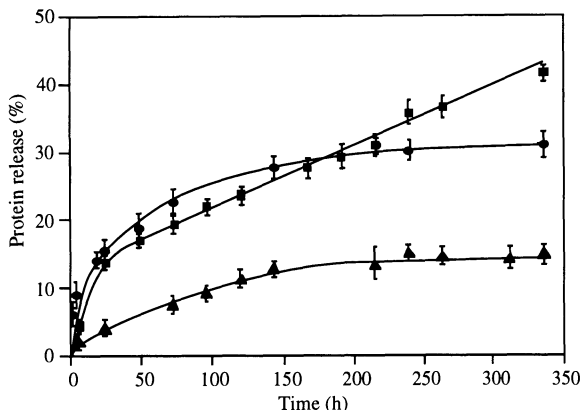


**Figure 1.** Kinetic profiles of protein release from inserts based on hemiesters of poly(MAN-*al*-PEG<sub>n</sub>VE) and HSA in isotonic phosphate buffer (pH 7.4) at 37°C.

● n = 1, methyl hemiester  
 ■ n = 1, butyl hemiester  
 ▲ n = 3, methyl hemiester

## RESULT AND DISCUSSION

Kinetic measurements indicated that water uptake was rapid, and a weight increase corresponding to about 90% of the final value was observed after 10-12 hours. The hydration process was accompanied by a substantial swelling corresponding to 15-30 times the sample initial weight, at saturation, while maintaining shape and integrity of the initial dry disk-like inserts. The inserts weight loss profiles were characterized by a 5-10% initial burst, most likely due to the loss of minute fragments, followed by an almost constant loss rate dependent upon the nature of the specimen.

"*In vitro*" release tests indicated that the percent of released protein was somehow dependent upon the polymer hydrophobic character (Fig. 1). This behavior was attributed to the strong interactions between hydrophilic portions of the polymer and protein molecules. Kinetic curves evidenced a fast protein release during the first 18 hours followed by an almost constant release for the next 10-15 days. During this period, about 40% of the protein virtual load was released by polymeric inserts based on the butyl hemiester of poly(MAN-*al*-Peg<sub>1</sub>VE), whereas only 30 and 15% release was detected for inserts based on the methyl hemiesters of poly(MAN-*al*-Peg<sub>1</sub>VE) and poly(MAN-*al*-Peg<sub>3</sub>VE), respectively.

Films obtained from methyl esters of poly(MAN-*al*-Peg<sub>n</sub>VE), n = 1-3, in combination with a 1:4 MYO/HSA<sub>α</sub> mixture by room temperature casting, showed an evident gel-like behavior with a high level of water uptake in the first 5-10 minutes. The bound water content of polymeric hemiesters, as evaluated by DSC measurements, increased with the number of oligooxyethylene units, suggesting a stronger interaction with water by more hydrophilic polymeric hemiesters. On the contrary, the bound water content of hybrid matrices, prepared by combination of the same polymeric hemiesters with proteins, slightly decreased with the number of oligooxyethylene units in the polymers.

This result has been tentatively attributed to the strong interactions occurring between proteins and the hydrophilic portions of the polymer, that could in principle reduce the amount of bound water. Final assessment and interpretation of this behavior need, however further investigation.

## ACKNOWLEDGMENTS

Part of this work has been performed under the Brite Euram Program – Contract BRE2.CT94.0530.

## REFERENCES

1. *Peptide and Protein Drug Delivery*, V.H.L. Lee, Ed., Marcel Dekker Inc., New York (1991)
2. *Stability of Protein Pharmaceuticals*, Part A & B, T.J. Ahern and M.C. Manning, Eds., Plenum Press, New York (1992)

# DEGRADATION MECHANISM OF AZO-CONTAINING POLYURETHANES BY THE ACTION OF INTESTINAL FLORA

Yoshiharu Kimura, Tetsuji Yamaoka, Tsutomu Ueda, Soon-In Kim<sup>†</sup> and Haruhide Sasatani<sup>†</sup>

*Department of Polymer Science and Engineering, Kyoto Institute of Technology, Matsugasaki, Kyoto 606, Japan*

<sup>†</sup> *Ono Pharmaceutical Co., Ltd., 3-1-1 Sakurai, Shimamoto-cho, Mishima-gun, Osaka 618, Japan*

## ABSTRACT

We have recently developed a colon specific drug delivery system by use of an ethanol-soluble segmented polyurethane comprising azo aromatic groups in the main chain. In the present study, two types of model compounds containing the azo aromatic group were synthesized, and their degradation kinetics in an anaerobic culture of intestinal flora was investigated for insight into the degradation mechanism of the polyurethane. A hydrophilic azo compound was readily reduced into its hydrazo form and then to amine form. The reduction rates from azo to hydrazo and from hydrazo to amine were comparable. In the case of a hydrophobic azo compound the reduction was stopped in the first step, and only the hydrazo form was produced. Since the polyurethane used for the coating is hydrophobic in nature, formation of hydrazo form was found without chain breakage.

**KEY WORDS** : azo reductase, intestinal flora, targeting the large intestine, segmented polyurethane, large-intestine-degradable polymer

## INTRODUCTION

A new drug delivery system (DDS) targeting the large intestine has recently been proposed by Saffran *et al.*<sup>1,2)</sup>. In their system a hydrophilic vinyl polymer crosslinked by an azo aromatic group was utilized as the coating material of drug pellets and capsules. It was thought that when the drug pellets and capsules coated with this polymer reach the large intestine, the azo groups are reduced to amines by the action of azo reductases which are liberated by intestinal floras and that the coating was solubilized to release the drug incorporated. However, the mechanism of the reduction and polymer degradation was not fully clarified. Furthermore, the preparation and coating of such a crosslinked polymer were found to be very difficult because of decreased solubility in solvents. More recently we have developed segmented polyurethanes comprising azo aromatic groups in the main chain, which can be degraded by the action of intestinal flora<sup>3)</sup>, and used for a new colon specific drug delivery system. The segmented polyurethanes were synthesized by reaction of isophorone diisocyanate (IPDI) with a mixture of *m,m'*-di(hydroxymethyl)azobenzene (DHMAB), poly(ethylene glycol) (PEG Mn=2000), poly(propylene glycol) (PPG) and propylene glycol (PG) having different compositions in feed. Their degradability can be readily controlled by changing the segment compositions. In the present paper, we report on the degradation mechanism of their polyurethanes based on the reactions of the model azo compounds.

## MATERIALS AND METHODS

Both DHMAB and *m,m'*-bis[(N-phenylcarbamoyl)oxy methyl]diazobenzene (PCMAB) were used as the model azo compounds. PCMAB was synthesized as follows. Two equivalent moles of phenyl isocyanate was added into a solution of 2.0 g of DHMAB in 20 ml of THF at 60 °C and stirred for 4 h. PCMAB was isolated and purified by the silica gel column chromatography using hexane/THF (1/1) as the eluent.

100 mg of water-soluble DHMAB and 10 mg of water-insoluble PCMAB were added to the aliquots of 30 ml of a flora culture. The mixtures were incubated for the predetermined days, and the products were extracted with a 20 ml of ethyl acetate 5 times. The extracts combined were analyzed by HPLC in which the azo, hydrazo, and amine compounds were detected at 254 nm.

## RESULTS AND DISCUSSION

Figure 1 shows the reaction profiles of DHMAB in the flora culture. The amine form of DHMAB increased with incubation time, while the azo form decreased. On the other hand, the hydrazo form rapidly increased, reached a maximum after 1 day, and then decreased. These profiles indicate that DHMAB was degraded to the *m*-hydroxymethyl aniline via the hydrazo form in a two-step process. The kinetic analysis revealed that the rate constants of the reductions from azo to hydrazo and hydrazo to amine are almost the same ( $1.2 \text{ day}^{-1}$ ).

Figure 2 shows the similar reaction profile of the water-insoluble PCMAB. Only the hydrazo form was formed and no amine form was detected even after 7 days of incubation, indicating that intestinal flora could not degrade the water-insoluble hydrazo compound to amine form.

When the polyurethane was incubated in the flora culture, the absorbance at  $\lambda_{\text{max}}=320 \text{ nm}$  which is characteristic of the azo aromatic chromophore, decreased with incubation time while its molecular weight did not change. Moreover, the absorbance was recovered by exposing the incubated polymer to air for 20 days. These results suggested that the polymer degradation proceeds with the reduction of the azo groups to the hydrazo groups during the bacterial treatment. Saffran *et al.*<sup>1,2)</sup> reported that the hydrophilic polymer gel crosslinked by an azo aromatic group was degraded by the conversion of the azo group into amine form. In our polymer, the azo groups were not converted into amine due to the hydrophobic nature of their surrounding. This should be a practical merit because neither toxic oligomer nor amine may not be produced *in vivo*.

## REFERENCES

1. M. Saffran, G. Kumar, C. Savariar, J. C. Burnham, F. Williams, and D. C. Neckers, A New Approach to the Oral Administration of Insulin and Other Peptide Drugs *Science*, **223**(1986)1081-1083
2. M. Saffran, C. Bedra, G. S. Kumar, and D. C. Neckers, Vasopressin: A Model for the Study of Effects of Additives on the Oral and Rectal Administration of Peptide Drugs *J. Pharm. Sci.*, **77**(1988)33-38
3. Y. Kimura, Y. Makita, T. Kumagai, H. Yamane, T. Kitao, H. Sasatani, and S. I. Kim, Degradation of azo-containing polyurethane by the action of intestinal flora : its mechanism and application as a drug delivery system *Polymer*, **33**(1992)5293

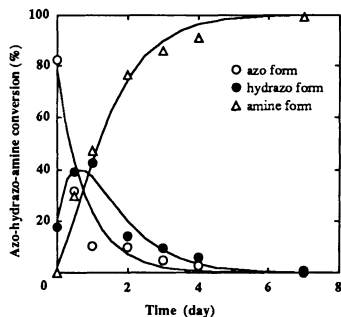


Figure 1. Azo-hydrazo-amine conversion of DHMAB in flora culture. Solid lines represent the calculated curves by fitting analysis.

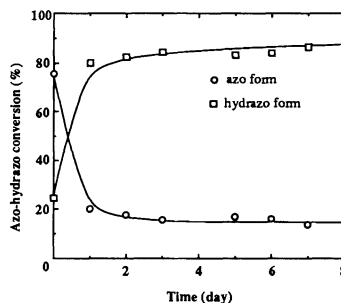


Figure 2. Azo-hydrazo conversion during the treatment of PCMAB with flora.

# NOVEL IMMUNOLIPOSOMES MODIFIED WITH AMPHIPATHIC POLYETHYLENEGLYCOLS CONJUGATED AT THEIR DISTAL TERMINALS TO MONOCLONAL ANTIBODIES

Kazuo Maruyama, Tomoko Takizawa, Motoharu Iwatsuru

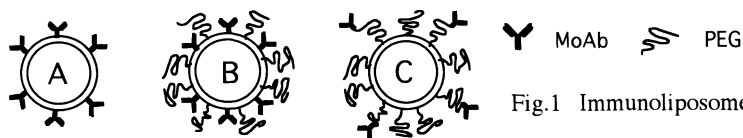
Department of Pharmaceutics, Faculty of Pharmaceutical Sciences, Teikyo University, Sagamiko, Tsukui-gun Kanagawa 199-01 (Japan)

## ABSTRACT

Distearoyl-N-(3-carboxypropionoyl polyethyleneglycol succinyl) phosphatidylethanolamine (DSPE-PEG-COOH) was newly synthesized and used to prepare novel immunoliposomes carrying monoclonal antibodies at the distal ends of the PEG chains (Type C). Liposomes were prepared from egg phosphatidylcholine (ePC) and cholesterol (CH) (2:1, m/m) containing 6 mol% of DSPE-PEG-COOH, and a monoclonal IgG antibody, 34A, which is highly specific to pulmonary endothelial cells, was conjugated to the carboxyl groups of DSPE-PEG-COOH to give various amounts of antibody molecules per liposome. Type C liposomes without antibodies showed prolonged circulation time and reduced reticuloendothelial system (RES) uptake owing to the presence of PEG. The degree of lung binding of 34A-Type C was about 1.3-fold higher than that of 34A-conventional immunoliposomes (34A-Type A), indicating that recognition by the antibodies attached to the PEG terminal was not sterically hindered and that the free PEG (i.e., that not carrying antibody) was effective in increasing the blood concentration of immunoliposomes by enabling them to evade RES uptake. Our approach provides a simple means of conjugating antibodies directly to the distal end of PEG which is already bound to the liposome membrane, and should contribute to the development of superior targetable drug delivery vehicles for use in diagnostics and therapy.

## INTRODUCTION

Drug delivery to specific cells by immunoliposomes represents a potentially attractive mode of therapy. However, though immunoliposomes are effective in specific binding to target cells *in vitro*, their targeting efficiency *in vivo* is relatively low [1]. Studies *in vivo* have revealed that coating liposomes with antibody (Type A in Fig. 1) leads to enhanced uptake of the immunoliposomes by the reticuloendothelial system (RES) and the immunotargetability depends on the antibody density on the surface. Thus, highly efficient target binding and a relatively low level of RES uptake of the immunoliposomes are apparently mutually exclusive. Recently, long-circulating liposomes have been prepared by coating the liposome surface with amphipathic polyethyleneglycol (PEG); this coating allows the liposomes to evade RES uptake and remain in the systemic circulation for a long period of time [2]. We proposed that antibodies could be attached to the distal ends of PEG chains which are already bound to the liposome membrane (Type C in Fig. 1)[3]. Since the binding of the antibody to the target cell should not be sterically hindered by the PEG chains in this situation, the immunoliposomes should show more efficient target binding. We have synthesized novel distearoyl phosphatidyl ethanolamine derivatives of PEG with terminal COOH groups for the preparation of Type C immunoliposomes. The targetability and biodistribution of Type C immunoliposomes were studied in mice in comparison with those of Type A and B immunoliposomes.



## METHOD

Distearoyl-N-(3-carboxypropionoyl polyethyleneglycol succinyl) phosphatidylethanolamine (DSPE-PEG-COOH) was newly synthesized and used to prepare Type C immunoliposomes. Liposomes were prepared from egg phosphatidylcholine (ePC) and cholesterol (CH) (2:1, m/m) containing 6 mol% of DSPE-PEG-COOH, and a monoclonal IgG antibody, 34A, which is highly specific to pulmonary endothelial cells, was conjugated to the carboxyl groups of DSPE-PEG-COOH to give various amounts of antibody molecules per liposome. Type A and Type B

immunoliposomes were prepared for comparison. The average molecular weight of PEG in Type B or C immunoliposomes was 2000.

## RESULTS and DISCUSSION

Type B and Type C liposomes without antibodies showed prolonged circulation time and low RES uptake owing to the presence of PEG. Three different types of 34A-immunoliposomes with 30-35 antibody molecules per vesicle were injected into mice to test the immunotargetability to the lung. 34A-Type A with an average of 35 antibody molecules per liposome accumulated 42.5 % of the injected dose in the lung at 30 min (Fig. 2). 34A-Type B which were prepared by incorporating DSPE-PEG with an average molecular weight of 2000 into Type A showed a lower level of target binding and a significantly higher blood level than those of Type A, suggesting that the steric hindrance of PEG chains reduced not only the immunospecific antibody-antigen binding, but also the RES uptake. Six h after injection, 43.7 % of the dose of 34A-Type B remained in the blood, a value much higher than that of the Type A. In the case of 34A-Type C with 30 antibody molecules per vesicle, the degree of target binding to the lung was 56.6 % of injected dose at 30 min, 1.3-fold higher than that of Type A (Fig. 2), indicating that recognition by the antibodies attached to the PEG terminal was not sterically hindered and that the free PEG (that not carrying antibody) was effective in increasing the blood concentration of immunoliposomes by enabling them to evade RES uptake. The latter phenomenon was confirmed by using nonspecific antibody-Type C, which showed a high blood level for a long time. Furthermore, 34A-Type C were better retained in the lung than the Type A at 6 h after injection (Fig. 2): 34A-Type C showed about 29 % dissociation of the bound immunoliposomes at 6 h, whereas 34A-Type A showed 41 % loss of the bound immunoliposomes over the same time period. As shown in Fig. 3, Type C showed higher immunotargetability than Type A and B at low antibody content (less than 30 antibody molecules per vesicle). Thus, Type C is accumulated more effectively in the lung than the other immunoliposomes, in spite of the low antibody content. At high antibody content, Type A also showed high level of target accumulation. Our approach provides a simple means of conjugating antibodies directly to the distal end of PEG which is already bound to the liposome membrane, and should contribute to the development of superior targetable drug delivery vehicles for use in diagnostics and therapy.

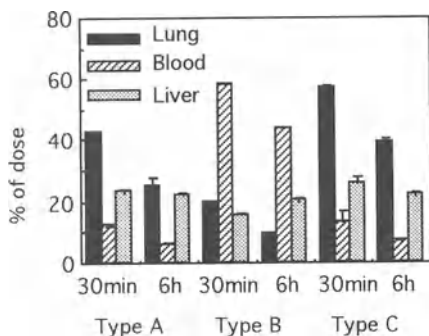


Fig.2 Immunotargetability and biodistribution of 34A-immunoliposomes at 30 min and 6 h after intravenous injection.

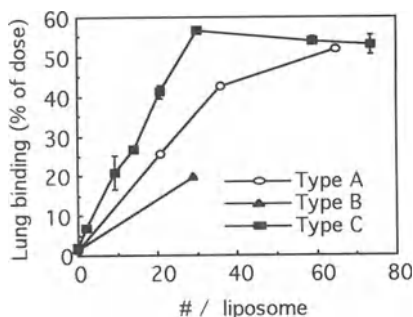


Fig.3 Comparison of target binding to the lung among the three types of 34A-immunoliposomes with various numbers of antibody molecules per liposome.

## REFERENCES

1. Maruyama K, Holmberg E, Kennel S, Klivanov A, Torchilin V and Huang L. (1990) Characterization of in vivo immunoliposome targeting to pulmonary endothelium. *J. Pharm. Sci.* 79: 978-984
2. Maruyama K, Yuda T, Okamoto A, Suginaka A and Iwatsuru M. Prolonged circulation time in vivo of large unilamellar liposomes composed of distearoyl phosphatidylcholine and cholesterol containing amphipathic poly(ethyleneglycol). (1992) *Biochim. Biophys. Acta* 1128: 44-49
3. Maruyama K, Takizawa T, Yuda T, Kennel S, Huang L and Iwatsuru M. Targetability of novel immunoliposomes modified with amphipathic polyethylene glycols conjugated at their distal terminals to monoclonal antibodies. (1995) *Biochim. Biophys. Acta* 1234:74-80

# PHOTO-INDUCED DRUG RELEASE FROM LIPOSOME USING PHOTOCROMIC LIPID HAVING SPIROPYRAN GROUP

Yuichi Ohya, Yukio Okuyama and Tatsuro Ouchi

Department of Applied Chemistry, Faculty of Engineering, Kansai University, Suita, Osaka 564, JAPAN

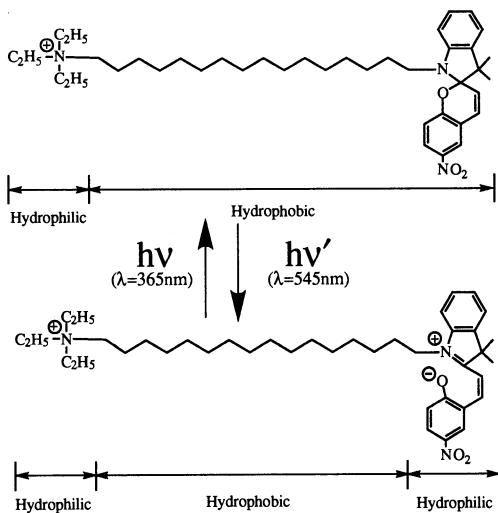
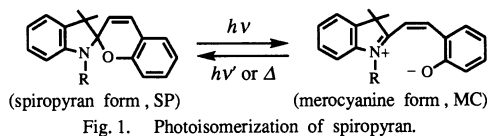
## SUMMARY

A novel photochromic lipid, SP-16A, having spiropyran group on its terminal was synthesized. It was confirmed that the obtained SP-16A molecule could form liposome with dipalmitoyl phosphatidylcholine (DPPC) by gel-filtration chromatography. The photo-induced isomerization of SP-16A by UV irradiation was confirmed UV-VIS spectra measurements in EtOH or in DPPC liposome. The photo-induced release behavior of carboxyfluorescein (CF) as a model drug from DPPC liposome containing SP-16A was investigated. After 1 min UV irradiation at 365nm, significance release of entrapped CF was observed. It is suggested that the perturbation of lipid membrane was induced by photoisomerization of SP-16A.

**KEY WORDS :** Spiropyran, Photochromic, Liposome, Photo-Induced Drug Delivery System

## INTRODUCTION

Molecules which can change their structures or physical properties in response to external stimuli or signals are expected to be applied for molecular devices or intelligent materials. There were many studies to apply some molecules which can isomerize reversibly in response to photon as photochromic materials. Spiropyran can isomerize reversibly by UV irradiation to form two different structures, spiropyran form (SP) without charge and zwitter ionic merocyanine form (MC) (Fig. 1). In recent years, structures and functions of supramolecular assembly have become topics in chemistry and biotechnology. Lipids are ones of the typical examples of such molecules, which can form various super structure such as micelle, Langmuir-Blodgett (LB) membrane or liposome. Liposomes have been studied as models of biomembrane or microcontainer of drugs for drugdelivery system (DDS). One of the object on the studies of liposomal drug delivery is the on-off switching of release of



substrates from liposome. Previously, photo-sensitive release behaviors from liposome using azobenzene group [1] or 2-nitrobenzyl ester group [2] were reported. In this study, to achieve photo-sensitive drug release from liposome by control of the aggregation state of lipid molecules by photo-irradiation, we synthesized a novel single chain photochromic lipid having terminal spiropyran group (SP-16A, Fig. 2) and investigated the photo-induced release behavior of model drugs from liposome containing the photochromic lipid.

## METHODS AND MATERIALS

The synthesis of photochromic lipid (SP-16A) was carried out based on the methods reported by Gruda [3]. The photo-induced isomerization of SP-16A molecule was confirmed by UV spectra measurements before and after UV irradiation at 365nm. Dipalmitoylphosphatidylcholine (DPPC) liposome containing 5-10 mol% of SP-16A were prepared by usual method using probe-type sonicator in HEPES buffer. The liposome formation of SP-16A with DPPC was confirmed by gel-filtration chromatography. Photo-induced release behavior of carboxyfluorescein (CF) entrapped in DPPC liposome containing SP-16A by photoisomerization of SP-16A was observed by fluorescence intensity at 525 nm (excitation at 470nm) after UV irradiation (365nm) at 30°C.

## RESULTS AND DISCUSSION

The photo-induced isomerization of SP-16A was observed by UV irradiation in EtOH. The increase of absorption at 545nm in UV-VIS absorption spectra of SP-16A by UV irradiation at 365nm was a evidence for isomerization to MC form. The isomerization from SP form to MC form was completed by 5 min UV irradiation at 365nm. It was also confirmed by UV-VIS spectra after keeping in the dark that the spontaneous reverse isomerization from MC to SP was very slow. The liposome formation of SP-16A molecules with DPPC was confirmed by gel-filtration chromatography. The elution profile of DPPC liposome containing SP-16A showed a sharp single peak at the same position of pure DPPC liposome, however, the free SP-16A showed a peak at lower molecular weight fraction. These results suggest that the SP-16A was incorporated into the DPPC liposome and they were located in lipid bilayer, but not in interior water phase of liposome. The photo-induced release behavior of CF from DPPC liposome containing 7 mol% of SP-16A was measured. After 1 min UV irradiation at 365nm, significance release of entrapped CF was observed. This phenomena was not observed when pure DPPC liposome. It is confirmed that the perturbation of lipid membrane was induced by photoisomerization of SP-16A. Moreover, the increase of fluorescence intensity was observed after bursting of the liposome by the addition of Triton X-100. These results suggest that the membrane perturbation was a passing phenomenon and the liposome kept its structure after isomerization of SP-16A.

## CONCLUSION

We could demonstrate photo-induced release behavior of model drug from liposome containing SP-16A. This photochromic lipid is expected to applied for photo-induced drug delivery system.

## REFERENCES

1. Morgan, C. G. *et al.* (1987). *Biochim. Biophys. Acta*, 903: 504.
2. Kutsumi, A. *et al.* (1989). *Chem. Lett.*, 1989: 433.
3. Gruda, I. and Leblanc, M. (1976). *Can. J. Chem.*, 54: 576.



# NEW STRUCTURALLY MODIFIED CYCLODEXTRINS FOR CONTROLLED RELEASE OF ANTIHYPERTENSIVE DRUGS

M. C. Breschi <sup>1</sup>, E. Chiellini <sup>2</sup>, F. Morganti <sup>2</sup>, R. Solaro <sup>2</sup>

<sup>1</sup> Faculty of Pharmacy, University of Pisa, Via Bonanno Pisano 6, 56126 Pisa, Italy

<sup>2</sup> Dept. of Chemistry and Industrial Chemistry, University of Pisa, via Risorgimento 35, 56126 Pisa, Italy

## SUMMARY

New  $\beta$ -cyclodextrin derivatives were prepared by grafting glycidyl ethers of alditols having an odd number of hydroxyl groups protected with isopropylidene groups. The modified  $\beta$ -cyclodextrins or commercially available hydroxypropyl- $\beta$ -cyclodextrin were used to prepare drug conjugates of antihypertensive drugs such as nifedipine, corynanthine and oxprenolol. Preliminary in vivo experiments indicate an improvement of drug absorption, bioavailability and antihypertensive efficacy.

**KEY WORDS:** modified cyclodextrins, antihypertensive drugs, controlled release, nifedipine, corynanthine, oxprenolol

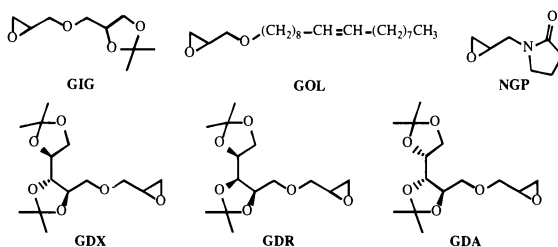
## INTRODUCTION

Over the years an investigation has been undertaken as aimed at the formulation of polymeric systems for controlled and targeted release of drugs<sup>1-4</sup>. More recently interest has been also directed to the formulation of conjugates of different drugs with modified  $\beta$ -cyclodextrin<sup>5,6</sup>, with the aim of increasing their bioavailability and possibly reduce side effects.

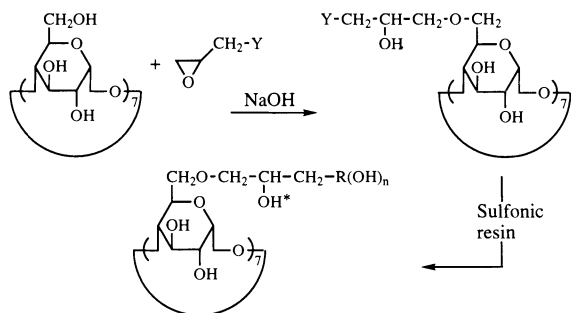
Cyclodextrins are cyclic oligomers of glucose constituted by 6, 7 and 8 glucose residues linked by  $\alpha(1-4)$  glycosyl bonds and are known as  $\alpha$ -,  $\beta$ -, and  $\gamma$ -cyclodextrin respectively. Topologically, they are represented by a toroid, where primary and secondary hydroxyl groups are placed on the smaller and the larger circumference, respectively. Due to the absence of hydroxyl groups, the toroid cavity has a pronounced hydrophobic character whereas the outer surface of the toroid is hydrophilic. This causes several lipophilic drugs to be included into the cavity, with potential improvement of solubility, stability and taste. However, the rather low solubility of cyclodextrins can limit the amount of drug that can be administered by normal tablets. Chemical modification of one or more hydroxyl groups present on the glucose residue appeared to be the best strategy to overcome this limitation<sup>7</sup>.

## FUNCTIONALIZED CYCLODEXTRINS

New functional derivatives of  $\beta$ -cyclodextrin were prepared by grafting the glycidyl ethers of the mono- and diacetonides of alditols consisting of 3 and 5 carbon atoms, N-glycidylpyrrolidone and fatty alcohols such as oleyl, cetyl and stearyl alcohols. Grafting reactions were carried out at 60 °C under alkaline conditions by using 1-2 moles of glycidyl ether per glucose residue. The reaction products, characterized by a content of 0.5-1.0 glycidyl residues per glucose unit, resulted in all cases soluble in chloroform. The isopropylidene groups of the grafted products were removed at 45 °C in methanol or in water/methanol in the presence of an acid



catalyst. By suitably tuning temperature and reaction time, it was possible to stop the reaction at various degrees of deprotection thus allowing for the realization of complex mixtures of cyclodextrin derivatives with interesting rheological behavior. The prepared derivatives, both partially protected or totally deprotected, were in any case amorphous in nature. Their solubility in water generally increased with increasing the degree of deprotection to reach values larger than 3 g/g, whereas their solubility in chloroform decreased from an upper value of more than 1.5 g/g to a practical insolubility at 100% deprotection.



Y = N-pyrrolidonyl, cetyl, oleyl, stearyl, isopropylidenglyceryl, diisopropylidenediisopropylidene-L-arabitolyl  
 R = N-pyrrolidonyl (n=0), cetyl (n=0), oleyl (n=0), stearyl (n=0), O-glyceryl (n=2), O-xylitolyl (n=4), O-L-arabitolyl (n=4), O-ribitolyl (n=4)

## $\beta$ -CYCLODEXTRIN DERIVATIVES / ANTIHYPERTENSIVE DRUGS CONJUGATES

New drug conjugates of antihypertensive drugs such as nifedipine, corynanthine and oxprenolol with some of the modified  $\beta$ -cyclodextrins or commercially available hydroxypropyl- $\beta$ -cyclodextrin (HP- $\beta$ CD) were prepared by thoroughly mixing different amounts of drugs and cyclodextrins in the presence of 5-15% water to promote complex formation. Some of the prepared formulations were preliminarily tested "in vivo" on spontaneously hypertensive rats. Improvement of drug absorption and bioavailability and an appreciable increase of antihypertensive efficacy was obtained when corynanthine and nifedipine were used as complexes with cyclodextrin derivatives (Fig. 1).

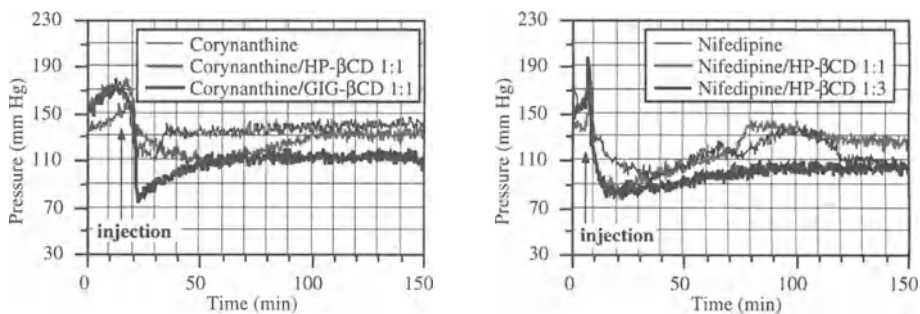


**Figure 1.** Variation of blood pressure in hypertensive rats by intraperitoneal administration of 5 mg of drug, alone or complexed with  $\beta$ -cyclodextrin derivatives.

## REFERENCES

1. M.F.Saettone, B.Giannaccini, P.Chetoni, G.Galli, E.Chiellini, in "Polymers in Medicine I Biomedical and Pharmacological Applications", E.Chiellini, P.Giusti, Eds., Plenum Press, New York, p. 187 (1983)
2. E.Chiellini, R.Solaro, G.Leonardi, R.Lisciani, G.Mazzanti, *Eur. Pat. Appl.* **92830172.0** (1992)
3. E.Chiellini, R.Solaro, G.Leonardi, D.Giannasi, *J. Bioact. Compat. Polym.*, **7**, 161 (1992).
4. E.Chiellini, R.Solaro, G.Leonardi, D.Giannasi, R.Lisciani, G.Mazzanti, *J. Controlled Release*, **22**, 273 (1992)
5. R.Solaro, S.D'Antone, L.Bemporad, E.Chiellini, *Eur. Pat. Appl.* **91830497.3** (1991)
6. R.Solaro, S.D'Antone, L.Bemporad, E.Chiellini, *J. Bioact. Compat. Polym.*, **8**, 236 (1993)
7. J.Pitha, J.Pitha, *J. Pharm. Sci.*, **74**, 987 (1985)

## DEVELOPMENT OF DELIVERY SYSTEMS FOR ANTISENSE OLIGONUCLEOTIDES

Yoshinobu Takakura, Ram I. Mahato, Takehiko Nomura, Kenzo Sawai, Mitsunobu Yoshida, Taro Kanamaru, and Mitsuru Hashida

*Department of Drug Delivery Research, Faculty of Pharmaceutical Sciences, Kyoto University, Sakyo-ku, Kyoto 606-01, JAPAN*

### SUMMARY

In order to construct the strategy for *in vivo* antisense oligonucleotide delivery systems, pharmacokinetic properties of a model antisense oligonucleotide, *c-myc* antisense 20-mer, were studied at organ level using organ perfusion experiments. In the liver, approximately 30-40 % of injected oligonucleotides were extracted by the organ during single passage. The hepatic uptake of the oligonucleotide was inhibited by the presence of various polyanions, suggesting that the hepatic uptake was non-specific. The kidney perfusion experiments showed that the oligonucleotide was reabsorbed by the tubule after glomerular filtration and a significant uptake by the tissue from the capillary side occurred. Competition experiments with polyanions suggested that the uptake from the capillary side was mediated by a scavenger receptor mechanism. After intratumoral injection into tissue-isolated tumor preparation of Walker 256 carcinoma, the oligonucleotide showed relatively rapid appearance in the venous outflow and was recovered in the leaked fluid from the tumor tissue. These findings will be useful information to design the carrier systems for antisense oligonucleotides.

**KEY WORDS:** antisense oligonucleotide, drug delivery system, pharmacokinetics, organ perfusion experiment, tissue-isolated tumor preparation

### INTRODUCTION

Recently, antisense oligonucleotides have attracted special interest as a novel class of chemotherapeutic agents for the treatment of cancer, viral infections and genetic disorders because of their ability to inhibit gene expression in a sequence-specific manner [1]. For an efficient chemotherapy with antisense oligonucleotides, however, there are many difficulties to be overcome, including stability against nucleases, cellular uptake characteristics, pharmacokinetic properties, etc. In order to improve the therapeutic potency, it is virtually necessary to develop delivery systems which can control the *in vivo* disposition characteristics of antisense oligonucleotides. Our previous *in vivo* study has demonstrated that the liver and kidney play important roles for the disposition of oligonucleotides in the body [2]. In the present paper, we studied pharmacokinetic properties of a model antisense oligonucleotides using isolated organ perfusion systems in order to construct the strategy for *in vivo* antisense oligonucleotide delivery systems.

### MATERIALS AND METHODS

**Materials.** We used an antisense oligonucleotide (20-mer) complimentary to the human *c-myc* proto-oncogene as the model. Three internucleotide linkages from the 3'-terminus of the oligonucleotide were phosphorothioated to enhance stability against 3'-exonucleases. The oligonucleotide was radiolabeled using a T4-kinase and [ $\gamma$ -<sup>32</sup>P]ATP.

***In Situ* Pharmacokinetic Study.** Organ perfusion experiments were carried out using isolated liver and kidney preparations of the rat [3,4]. These organs were selected as the sequestration organs of oligonucleotides. The [<sup>32</sup>P]oligonucleotide was bolusly introduced from the artery into the organs and the venous outflow perfusates were collected at appropriate time intervals. Bile and

urine samples were also collected in the isolated liver and kidney experiments, respectively. Moment analysis was applied to the venous outflow concentration-time profiles and moment and disposition parameters in the organs were derived. At the end of experiments, the tissues were excised and subjected to assay. In addition, pharmacokinetic characteristics of the oligonucleotide in its target organ was studied in the perfusion experiment using a tissue-isolated tumor preparations of Walker 256 carcinoma [5]. Radiolabeled oligonucleotide was injected directly into the perfused tumor preparation. During the perfusion experiment, the venous outflow and the exudate from the tumor were collected and the tissue was excised for radioactivity counting at the end of experiment.

## RESULTS AND DISCUSSION

### Liver perfusion experiments

In the liver, 30-40 % of injected oligonucleotides was extracted by the organ during a single passage while no significant radioactivity was detected in the bile. The hepatic uptake of the oligonucleotide was not significantly inhibited at a low temperature. However, the uptake was inhibited by the presence of various polyanions, suggesting that the hepatic uptake was non-specific.

### Kidney perfusion experiments

The oligonucleotide was shown to be reabsorbed by the tubule after glomerular filtration and urinary excretion was restricted. The experiments also demonstrated that a significant uptake of the oligonucleotide by the tissue from the capillary side occurred. Competition experiments using polyanions, such as dextran sulfate, poly [I], poly [C], and succinylated bovine serum albumin, suggested that the uptake from the capillary side was mediated by a scavenger receptor.

### Perfusion experiments using tissue-isolated tumors

After intratumoral injection into tissue-isolated tumor preparation, the oligonucleotide showed relatively rapid appearance in the venous outflow and was recovered in the leaked fluid from the tumor tissue. Approximately 30-60 % of injected oligonucleotides was remained in the tumor at 2 hr after injection.

## CONCLUSION

Basic pharmacokinetic characteristics of oligonucleotides were clarified by organ perfusion experiments. These findings will be useful information to design the carrier systems which can control the disposition of antisense oligonucleotides in the body.

## REFERENCES

1. Crooke ST. (1992) Therapeutic applications of oligonucleotides. *Annu Rev Pharmacol Toxicol* 32: 329-376
2. Miyao T, Takakura Y, Akiyama T, Yoneda F, Sezaki H, Hashida M. (1995) Stability and pharmacokinetic characteristics of oligonucleotides modified at terminal linkages in mice. *Antisense Res Develop* (in press)
3. Nishida K, Mihara K, Takino T, Nakane S, Takakura Y, Hashida M, Sezaki H. (1991) Hepatic disposition characteristics of electrically charged macromolecules in rat in vivo and in the perfused liver. *Pharm Res* 8: 437-444
4. Takakura Y, Mihara K, Hashida M. (1994) Control of the disposition profiles of proteins in the kidney via chemical modification. *J. Controlled Release* 28: 111-119
5. Imoto H, Sakamura Y, Ohkouchi K, Atsumi R, Takakura Y, Sezaki H, Hashida M. (1992) Disposition characteristics of macromolecules in the perfused tissue-isolated tumor preparation. *Cancer Res* 52: 4396-4401

# TRANSFECTION TO SMOOTH MUSCLE CELLS USING TERPLEX OF LDL, DNA, AND HYDROPHOBIZED CATIONIC POLYMERS

Atsushi Maruyama, Jin-Seok Kim<sup>1</sup>, Toshihiro Akaike, Sung Wan Kim<sup>1</sup>

Dept of Biomolecular Engineering, Tokyo Institute of Technology, Nagatsuta, Midori-ku, Yokohama 227, Japan

## ABSTRACT

Terplex of lipoprotein, hydrophobized poly(L-lysine) (H-PLL), and DNA was examined as gene carriers which were able to change their properties by enzymatic actions. Terplex with 200 nm in diameter was formed from H-PLL, LDL, and DNA, while considerably large aggregates were seen in the ter-mixtures containing unmodified PLL or mixtures without lipoprotein. The terplex with hydrophobized PLL exhibited the highest transfection efficacy, indicating that the terplex system had promising characteristics as a new type of gene carrier.

**KEY WORDS:** Transfection, Gene carrier, Lipoproteins, Smooth muscle cells, Terplex

## INTRODUCTION

Gene therapy has become a novel therapeutic entity for many human diseases which, by conventional medical intervention, were very difficult to be cured. Ideal synthetic carriers for gene have to possess the following properties; 1) formation of stable complexes, 2) protection of the genes from enzymatic degradations, 3) selective delivery to target cells (tissue permeability and selective attachment to target cells), 4) delivery of genes to cytoplasmic compartment in the cells, and so on. Low toxicity to cells is another important property that every carriers must possess in common.

In order for genes to be delivered inside target cells, the carriers first have to exhibit strong interactions with cell membranes. Such strong interactions, however, disturb the specific delivery of the pay-load to target cells because of the undesirable non-specific interactions with non-target cells and other biomolecules such as plasma proteins.

We have developed several synthetic gene carriers which are able to change their properties by partial degradation of the carriers through enzymatic actions or physical signals. These carriers are typically constructed with two major components. One is a gene-retaining compartment, which firmly retains genes and exhibits membrane permeable properties. The other is a degradable and/or protective compartment, which covers the gene-retaining compartment to minimize the non-specific interaction as well as self-aggregation of the complex. Degradation or detachment of these compartments from their original complex structure enables gene to transport through cell membranes. Some sensing (ligand) groups can also be conjugated to the protective compartment to attain the targetability.

In this study, hydrophobized poly(L-lysine) (H-PLL) and low density lipoproteins(LDL) were chosen as the retaining and protective compartments, respectively. Transfection to smooth muscle cells with non-covalent terplex of LDL, H-PLL and DNA is described here.

## MATERIALS AND METHODS

**Synthesis of hydrophobized PLL:** Stearyl or myristyl PLL was synthesized by reaction of PLL (Mw = 5.2 x 10<sup>4</sup> from Sigma) with stearyl bromide or myristyl bromide, respectively.

**Plasmid preparation:** pSV(from ProMega) containing a  $\beta$ -galactosidase encoding gene, SV40 promoter, and enhancer was amplified and purified from HB101 *E. Coli* culture.

**Cell culture and transfection:** Rat aorta smooth muscle cells, A7R5 (from ATCC), were grown in D-MEM supplemented with 10% FBS. Transfection to A7R5 was performed in multi-well plates. Twenty four hours

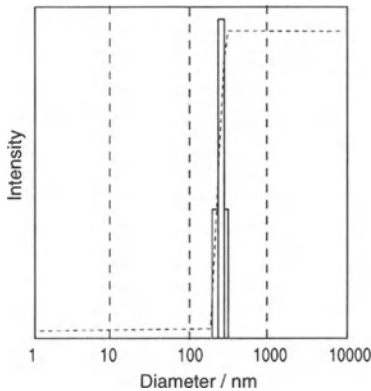


Fig. 1 DLS of terplex in D-PBS  
PLL modified with 5 mol % of stearyl bromide was mixed with DNA and LDL at weight ratio of 1:1:2.

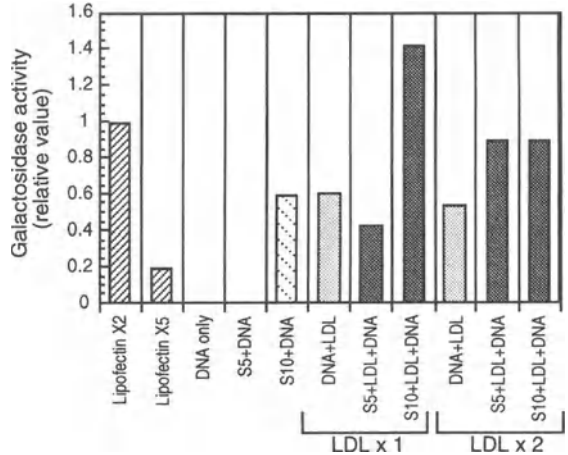


Fig. 2  $\beta$ -Galactosidase activity in the cell lysates  
Cells were incubated with the mixture for 6 hr in the absence of FBS, followed by additional 42 hr incubation in the presence of 10% FBS. Weight ratio of DNA/Polymer/LDL = 1/1/1(LDL x 1) or 1/1/2(LDL x 2). S5, S10: PLL modified with 5 or 10 mol % stearyl bromide.

prior to transfection, A7R5 cells were seeded at  $2 \times 10^4$  cells/well. To each well, 40  $\mu$ l of the complex solution containing 2  $\mu$ g of pSV plasmid was added and then incubated for additional 48 hr in a 5%  $\text{CO}_2$  incubator at 37°C. After lysing the cells,  $\beta$ -galactosidase activity in the cell lysate was assayed spectrophotometrically using o-nitrophenyl  $\beta$ -galactoside as a substrate.

## RESULTS AND DISCUSSION

### Characterization of terplex of LDL, H-PLL and DNA

Physico-chemical properties of gene complexes were characterized by turbidity measurement and dynamic light scattering (DLS) analysis. Considerably large aggregates of more than 1  $\mu$ m in diameter were formed when unmodified PLL was mixed with DNA. Similar aggregate formation was still observed when the complex was prepared in the presence of LDL. On the contrary, the size of complexes from H-PLL were much smaller in size than those observed with unmodified PLL. DLS measurements showed that the mean diameter of the aggregates prepared from H-PLL, LDL and DNA was about 200 nm (Fig.1). It is probable that hydrophobization of PLL enhanced the interaction between H-PLL and LDL, and the associated LDL suppressed the formation of the large aggregates which were usually observed for the complex of PLL derivatives and DNA.

### Transfection to SMC using terplex system

Results from transfection to SMC using a terplex system are shown in Fig. 2. Transfection efficacy was presented as a relative value to that obtained with Lipofectin™ reagent, a cationic lipid preparation. By changing LDL ratio, the terplex system showed the highest  $\beta$ -galactosidase activity among the mixtures of DNA and LDL, or DNA and H-PLL. It should be noted that smaller complex in size showed higher expression than larger one. The length and content of alkyl chains of H-PLL also affected transfection efficacy. Higher  $\beta$ -galactosidase activity observed with terplex system is presumably due to 1) the increase in effective DNA concentration by decreasing the aggregate size, 2) the enhanced interaction of complex with cells by receptor mediated manner, and 3) the enhanced membrane permeability by hydrophobized PLL.

In conclusion, the terplex system of LDL, DNA and H-PLL was found to possess several desirable properties which meet the requirements as a good gene carrier, and it seems promising to use this system as a new type of gene carrier.

# PREPARATION OF AMMONIO-TERMINATED POLYOXYETHYLENE/POLYDIMETHYLSILOXANE BLOCK COPOLYMER AND APPLICATION TO TRANSDERMAL PENETRATION ENHANCER

T. Aoyagi\*, T. Akimoto and Y. Nagase

Sagami Chemical Research Center, Sagamihara, Kanagawa 229, Japan

\* Present address; Institute of Biomedical Engineering, Tokyo Women's Medical College, Shinjuku, Tokyo 162, Japan

## SUMMARY

Polyoxyethylene(PEO)/polydimethylsiloxane (PDMS) block copolymers bearing ammonium group at the one side chain end was prepared and the enhancing activity on the drug permeation through the skin was investigated *in vitro*. The enhancing mechanism was discussed by simulating the permeation profile with a Fickian diffusion equation. These copolymers efficiently promoted the transdermal drug permeation and the activity considerably depended on the degree of polymerization of PEO and PDMS. Concerning the role of each part in the molecule, the compound consisting of all moieties, namely PEG, PDMS and cationic group showed highest enhancing activity. From the result of calculation of partition and diffusion parameters, it was revealed that these compound increased only drug partition from vehicle to the skin. Moreover, this materials scarcely showed the skin irritation.

## KEY WORDS

Polyoxyethylene / Polydimethylsiloxane / Transdermal Penetration / Enhancer / Partition

## INTRODUCTION

For the fabrication of the practical transdermal drug delivery, a certain penetration enhancing mode is necessary in order to overcome the difficulty of drug permeation through the skin. Inclusion of a penetration enhancer in the transdermal formulation is one of the most convenient methods. Many kinds of compounds have been investigated as the enhancer, however, it is probable that they will permeate into the skin and cause unfavorable side effects, such as inflammatory. We have been studying novel type of penetration enhancers that permeate into the skin with difficulty. These compounds compose of polymeric materials that the structures are similar to the surfactants. They are expected to function to only the skin surface and not be able to permeate into the skin because of the large bulkiness. The materials characteristically contain polydimethylsiloxane as hydrophobic part and ammonium or pyridinium groups as hydrophilic ones.[1, 2] In this study, other type of polymeric enhancer was prepared, that comprised polyoxyethylene(PEO)/polydimethylsiloxane(PDMS) block copolymer containing ammonium group at the one side chain end. The enhancing activity was investigated *in vitro* and the mechanism was sought by determining diffusion and partition parameters that was obtained by simulating the permeation profile with a Fickian diffusion equation.[3] Additionally, skin irritation test was carried out by Draize method.

## EXPERIMENTALS

**Preparation of Polymeric Enhancer:** Using the PEO containing hydroxydimethylsilyl group at the side chain end, the ring opening polymerization of hexamethylcyclo-trisiloxane(D<sub>3</sub>) was carried out followed by termination with 3-chloropropyl dimethylchlorosilane. After the substitution from the chloropropyl group to iodopropyl one using sodium iodide, the resulting block polymer was reacted with *N,N*-dimethylethylamine. The chemical structure is shown in Fig. 1.



Fig. 1 Chemical structure of polymeric enhancer.

**In Vitro Permeation Procedure:** The shaved abdominal skin that excised from rabbit was mounted between the two half diffusion cells with a water jacket. Suspension or solution of model drugs, antipyrine (ANP) or indomethacin (IND) containing enhancer was put in the donor compartment and

phosphate buffered solution adjusted to pH 7.4 was put in receptor one. The temperature was maintained at 37°C and the concentration of the drug permeated through the skin was determined by HPLC.

$$Q_t = (AP_1 C_0) \left[ P_2 t - \frac{1}{6} - \frac{2}{\pi^2} \sum_{n=1}^{\infty} \frac{(-1)^n}{n^2} \exp(-P_2 n^2 \pi^2 t) \right] \quad \text{eq. 1}$$

**Calculation of Partition and Diffusion Parameters:** The drug permeation through the skin was determined by curve-fitting data to Fickian diffusion equation as follows:

where  $Q_t$  is the cumulative amount of drug at time  $t$ ,  $A$  is effective surface area and  $L$  is the thickness of the skin barrier.  $K$  is the partition coefficient between skin and donor,  $C_v$  is the drug concentration in donor and  $D$  is the diffusion coefficient in the skin. Two parameters,  $K \cdot L$  and  $D/L^2$  are replaced with  $P_1$  and  $P_2$ , respectively, that were so-called 'partition and diffusion parameters'. The permeation profile was analyzed using a non-linear least squares computer program (MULTI), [4] that provided the two parameters.

## RESULTS AND DISCUSSION

The addition of the polymeric compounds surely promoted the permeation ANP, used as the model drug, and the enhancing activity depended on the degree of polymerization. To verify the role of PEO and PDMS segments and functional group in the molecule, the effect of addition of only PEO, ammonio-terminated PDMS that did not contained PEO segment, PEO/PDMS block copolymer that have no ammonium group were observed. In the case of ANP, the material composed of all parts, PEO, PDMS and ammonium group, showed most strong enhancing activity. On the other hand, concerning IND also used as the model drug, PEO segment apparently was not necessary to induce the activity. These results suggested that the polarity and/or chemical structure of the enhancer might closely relate to the enhancing activity.

The value of partition and diffusion parameters were calculated by the method described above. In the case of ANP, partition parameters became 10~50-fold larger than that of control, by addition of the polymeric enhancers. Contrary, the value of diffusion parameters lowered relative to that of control. Moreover, the same tendency was observed on IND. On the mechanism of the polymeric enhancer, the present results suggested as follows; these polymeric enhancers might adsorb onto the stratum corneum and form layer at the surface. The partition of drug to the adsorption layer increased more relative to no enhancer, as a result, the drug permeation increased. Perhaps, the cause of lowered diffusion parameter might be due to the formation of adsorbed layer on the skin surface. Thus, the enhancing mechanism is surely different from that of low-molecular-weight penetration enhancers.

The acute skin irritation of the polymeric enhancer that showed strongest enhancing activity was investigated by Draize test. The polymeric enhancer produced a primary irritation index of 1.3 according to the Draize classification scheme and no corrosive effects were observed.

In conclusion, polymeric penetration enhancer of the present study is very useful because of its safety and induction of high enhancing effect.

## REFERENCES

- [1] Aoyagi T, Takamura Y, Nakamura T, Yabuchi Y, Nagase Y (1992) Novel silicones for transdermal therapeutic system I: Synthesis of 1-methyl-4-pyridinio-terminated polydimethylsiloxane and the evaluation as transdermal penetration enhancer. *Polymer* 33: 2203-2207
- [2] Aoyagi T, Nakamura T, Yabuchi Y, Nagase Y (1992) Novel Silicones for Transdermal Therapeutic System III: Preparation of Pyridinio or Ammonio-terminated Poly-dimethylsiloxane and the Evaluation as Transdermal Penetration Enhancers. *Polym. J.* 24: 545-553
- [3] Calpena A, Lauroba J, Suriol M, Obach R, Domenech J (1994) Effect of d-limonene on the transdermal permeation of Nifedipine and domperidone. *Int. J. Pharm.* 103: 179-186
- [4] Yamaoka K, Tanigawara Y, Nakagawa T, Uno T (1981) A Pharmacokinetic Analysis Program (MULTI) for Microcomputer. *J. Pharm. Dyn.* 4: 879-885



# THEORETICAL DESIGN OF SKIN PENETRATION ENHANCEMENT VIA PRODRUG-ENHANCER COMBINATION BASED ON A DIFFUSION MODEL

Hiroto Bando, Fumiyoshi Yamashita, Yoshinobu Takakura, and Mitsuru Hashida.

Department of Drug Delivery Research, Faculty of Pharmaceutical Sciences, Kyoto University, 46-29 Yoshidashimoadachi-cho, Sakyou-ku, Kyoto 606-01, Japan,

## SUMMARY

We proposed prodrug-enhancer combination for effective penetration enhancement of various drugs in this study. Further, we hypothesized that skin permeation of drug could be enhanced the most effectively by synthesizing a prodrug with the optimal lipophilicity for an enhancer, which can be predicted by diffusion model. Next, the hypothesis was proved by synthesizing five types of acyclovir prodrugs and carrying out in vitro skin permeation study in rats, selecting 1-geranylazacycloheptan-2-one(GACH) as penetration enhancer. Among five prodrugs, as we expected, more lipophilic prodrugs (propionate, butyrate, valerate, and hexanoate) showed more largely enhanced penetration than that of hydrophilic one (acyclovir and acetate), when administrated in combination of GACH. Further we revealed that experimental values about enhancement ratio showed a good agreement with those we predicted. On the other hand, most of prodrugs appeared in a form of acyclovir in receptor phase without GACH but the appearance ratio of acyclovir to total flux decreased with an increasing the pretreatment dose with GACH.

**KEY WORDS :** prodrug-enhancer combination, percutaneous absorption, acyclovir

## INTRODUCTION

We have been developed several mathematical models to evaluate percutaneous absorption of drugs and its enhancement(1). The ultimate aim of these kinetic analyses is to predict and optimize the absorption of drug through the skin. In our previous study, we analyzed the action mechanism of a penetration enhancer, 1-geranylazacycloheptan-2-one (GACH), based on a two-layer skin diffusion model with polar and nonpolar routes in the stratum corneum, revealing that this enhancer shows the most extensive effect on a drug with octanol/water partition coefficient(PCoet/w) of about 0.5. Therefore, we hypothesized that skin permeation of a drug might be most enhanced if a prodrug with the adequate lipophilicity was synthesized(2). In the present study, we investigated the possibility of designing the prodrug/enhancer combination based on a skin diffusion model. We synthesized ester-type prodrugs of acyclovir and evaluated their in vitro rat skin penetration in the presence of GACH. Further, we analyzed penetration profiles of the prodrugs based on a diffusion model considering metabolic process in the skin, in order to confirm the theoretical basis of prodrug/enhancer combination.

## METHODS

### Simulation of prodrug design

Based on a two-layer skin diffusion model(1), we simulated the relationship between PCoet/w of drugs and the penetration amounts through the skin with/without GACH, using the parameters previously determined. In this simulation, the partition coefficient to the nonpolar route was related to PCoet/w based on a linear free-energy relationship.

### Synthesis of acyclovir esters

Esterification of acyclovir was carried out in dimethylformamide with acetyl chloride and dimethylaminopyridine at room temperature for 48 hr. After the crude crystals were obtained in cold NaOH solution (pH 9.0±0.2), they were purified by recrystallization from ethanolic solution(2).

## In vitro skin permeation study

The excised rat skin was mounted on a flow-through type diffusion cell and pretreated with an ethanolic solution containing different dose of enhancer. After ethanol was evaporated 6 hr later, the suspension of prodrugs was applied to the donor chamber. The receptor fluid was collected every hour for 12 hr(3). The determination of prodrugs was carried out using HPLC.

## Data analysis

We considered that the skin is composed of the stratum corneum with two parallel pathways and the viable layer, and that prodrugs are hydrolyzed by esterases distributing in the second layer homogeneously based on first-order kinetics. Based on this model, Laplace transforms for the amounts of prodrug and parent drug appearing in the receptor across the skin were derived. Penetration parameters were estimated by curve-fitting to penetration profiles using a nonlinear

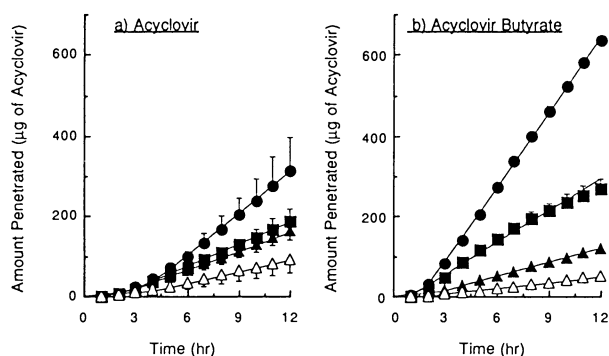


Fig.1 Time courses of total acyclovir amount penetrated through rat skin pretreated with ethanolic solution of 0 ( $\Delta$ ), 6.4 ( $\blacktriangle$ ), 12.7 ( $\blacksquare$ ), and 25.5 ( $\bullet$ )  $\mu$ mol of GACH. The data represent the sum of acyclovir and acyclovir butyrate in the case of the prodrug application. Each point represents the mean  $\pm$  S.D. values of at least three experiments (from reference 2).

regression program combined with a fast inverse Laplace transform algorithm (MULTI(FILT)).

**RESULTS AND DISCUSSION**

Without GACH, even for hexanoate with a PCoct/w value larger than acyclovir by about 300-fold, its skin permeability was only about twice. Because lipophilicity of all prodrugs is not high enough to distribute into nonpolar route, the contribution of the polar route, where the penetration is independent on lipophilicity of drugs, on total penetration process is still large. This indicates that skin permeation of acyclovir could not be improved only by a prodrug approach. On the other hand, the permeation of acyclovir was only 3.4-fold enhanced, while that of acyclovir butyrate with a PCoct/w of 0.4 was remarkably enhanced by a factor of about 12 (Fig1). The experiments using other prodrugs revealed that the enhancement effect due to GACH on five prodrugs was in good agreement with the hypothesis predicted based on a diffusion model. Further, the ratio of regenerated acyclovir to total amount appearing in the receptor was decreased with an increase in preloading dose of GACH. The analysis based on a skin diffusion/bioconversion model found that GACH mainly affects the parameters of drugs in the nonpolar route, and extensively increases their partition parameter with an increase in GACH dose, while the diffusion parameters did not change so much. These findings were in the same manner as reported for the model drugs which were little metabolized in the skin (1). Furthermore, GACH significantly decreased bioconversion of all the prodrugs as compared to the control condition. In conclusion, a two-layer diffusion model with parallel routes can totally explain the absorption behavior of drugs including prodrugs and the prodrug/enhancer combination would offer an effective and rational way to increase the transdermal delivery of wide range of drugs.

## REFERENCES

1. Yamashita F, Yoshioka T, Koyama Y, Okamoto H, Sezaki H, and Hashida M. (1993) Analysis of skin penetration enhancement based on a two-layer skin diffusion model with polar and nonpolar routes in the stratum corneum: Dose-dependent effect of 1-geranylazacycloheptan-2-one on drugs with different lipophilicities. *Biol. Pharm. Bull.* 16: 690-697.
2. Bando H, Yamashita F, Takakura Y, and Hashida M. (1994) Skin penetration enhancement of acyclovir by prodrug-enhancer combination. *Biol. Pharm. Bull.* 17: 1141-1143.
3. Yamashita F, Bando H, Koyama Y, Kitagawa S, Takakura Y, and Hashida M. (1994) In vivo and in vitro analysis of skin penetration enhancement based on a two-layer diffusion model with polar and nonpolar routes in the stratum corneum. *Pharm. Res.* 11: 185-191.

# PREPARATION OF BIODEGRADABLE MICROSPHERES CONTAINING WATER-SOLUBLE DRUG, $\beta$ -LACTAM ANTIBIOTIC

Jin Hee Kim<sup>\*†</sup>, Ick Chan Kwon<sup>\*</sup>, Yong Hee Kim<sup>\*</sup>, Young Taek Sohn<sup>†</sup>, SeoYoung Jeong<sup>\*</sup>

<sup>\*</sup>Biomedical Research Center, Korea Institute of Sci. & Tech., P.O. Box 131 Cheongryang, Seoul, Korea, <sup>†</sup>Duksung Women's University, 419 Ssangmoon-Dong, Dobong-Ku, Seoul, Korea

## SUMMARY

The biodegradable poly(l-lactide), PLLA, microspheres containing hydrophilic ampicillin sodium (AMP-Na) was prepared by W/O/W emulsion - evaporation method. The preparation parameters of PLLA microspheres and *in vitro* release pattern of AMP-Na from PLLA microspheres were discussed.

## KEYWORDS

poly(l-lactide), biodegradation, local delivery system

## INTRODUCTION

The antibiotic delivery systems utilizing biodegradable polylactide as a polymer matrix have been extensively studied.[1-4] However, most of the studies have been performed with hydrophobic antibiotics due to the hydrophobic characteristic of polylactide. The purpose of this study was to develop biodegradable poly(l-lactide), PLLA, microspheres containing hydrophilic Ampicillin Sodium (AMP-Na) and to target them to local inflammatory regions such as otitis media or sinusitis for 3-4 week period. The preparation parameters of PLLA microspheres and *in vitro* release pattern of AMP-Na from PLLA microspheres were discussed.

## METHODS

A saturated solution of Amp-Na in distilled water was emulsified in a  $\text{CH}_2\text{Cl}_2$  solution containing PLLA (0.7g/5 ml) and Span 80 by ultrasonication for 30 min to form w/o emulsion. The resulting emulsion was added into an aqueous polyvinylalcohol (PVA) solution through a 21G-needle to form w/o/w emulsion followed by a 5 min stirring with homogenizer to stabilize the emulsion. To evaporate organic solvent,  $\text{CH}_2\text{Cl}_2$ , the w/o/w emulsion was then heated to 35 °C for 2 hours. The microspheres were filtered with 0.45  $\mu\text{m}$  membrane filter, washed with distilled water and vacuum-dried over a few days. The stability of primary emulsion (W/O) was studied by various combination of surfactants in water and oil phase. The turbidity of emulsion was measured at 450nm by UV/VIS spectrophotometer. *In vitro* release experiments were performed with approximately 300 mg of microspheres in 30 ml of PBS solution (pH 7.4) as a release media. The microspheres were contained in a stainless steel basket and the temperature of release media was kept at 37°C in a shaking bath. The amount of released AMP-Na was determined with UV spectrophotometer.

## RESULTS AND DISCUSSION

(1) Preparation of PLLA Microspheres : Microspheres were prepared at various combination of each preparation parameters such as polymer concentration, combination of surfactants, amount of stabilizer (PVA), and stirring rate and time. Among the combination of surfactants, Span 80 showed the highest stability as shown in Fig. 1 ~ Fig. 3. When Span 80 was used as a surfactant for primary emulsion, the loading efficiency of AMP-Na in microspheres was enhanced with the increase of the concentration of PLLA as well as the amount of surfactant (span 80) in organic phase. The size of microspheres were mainly influenced by the stirring rate and time, and the

amount of surfactant. The amount of PVA, as a stabilizer, also affected the loading efficiency of AMP-Na and size of microspheres, however, it was not as significant as other factors.

(2) Release Studies : The release experiments were performed with 200-350  $\mu\text{m}$  PLLA microspheres containing AMP-Na. at 16 w/w%. As shown in Fig. 4, 40% AMP-Na was released during the first 4 days and the release rate of AMP-Na was relatively constant afterward. The release of AMP-Na and the degradation of PLLA microspheres was rapid although high molecular weight ( $M_w$  100,000) PLLA is used as a polymer matrix. This rapid degradation may result from the highly porous inner structure of microspheres.

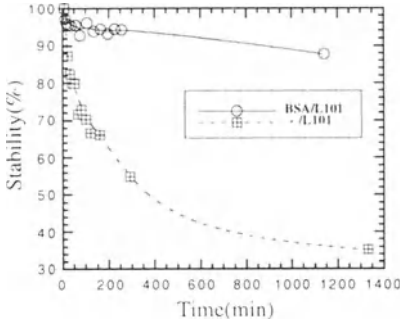


Fig. 1. The dependence of emulsion stability on the surfactants (BSA/water phase, Pluronic L101/oil phase).

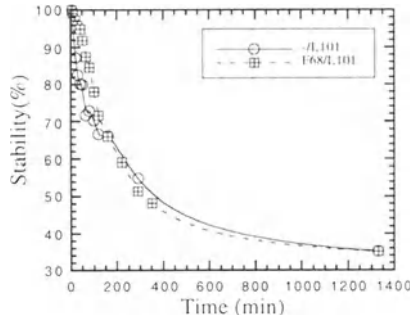


Fig. 2. The dependence of emulsion stability on the surfactants (Pluronic F68 /water phase, Pluronic L101/oil phase).

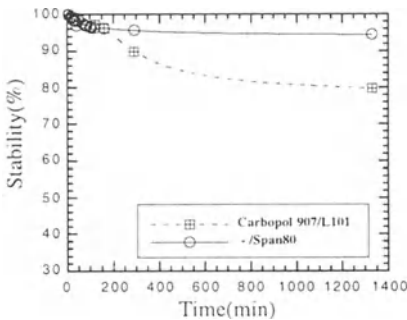


Fig. 3. The dependence of emulsion stability on the surfactants (Carbopol 907 /water phase, Pluronic L101, Span 80 /oil phase).

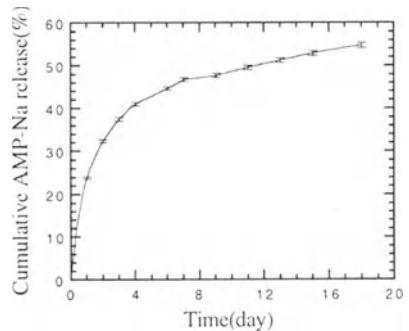


Fig. 4. AMP-Na release from PLLA microspheres in PBS 7.4 at 37°C.

## REFERENCES

- [1] Arshady R.(1990) Microspheres and microparticles, a survey of manufacturing techniques: Part III: Solvent evaporation. *Polymer Eng. & Sci.* 30:915-924
- [2] Jeffery H., Davis S.S., and O'Hagan D.T.1991 The preparation and characterization of poly(lactide-co-glycolide) microparticles. I: Oil-in-water emulsion solvent evaporation. *International J. Pharmaceutics* 77: 169-175
- [3] Ogawa Y., Yamamoto M., Okada H., Yashiki T., and Shimamoto T.(1988) A new technique to efficiently entrap leuprolide acetate into microcapsules of polylactic acid or copoly(lactic/glycolic) acid. *Chem. Pharm. Bull.* 36:1095-1103
- [4] Wang H.T., Schmitt E., Flanagan D.R., and Linhardt R.J.(1991) Influence of formulation methods on the in vitro controlled release of protein from polyester microspheres. *J. Controlled Release* 17:23-32

# EFFECT OF MICROPORE STRUCTURE ON DRUG RELEASE FROM SELF-SETTING CALCIUM PHOSPHATE CEMENT CONTAINING ANTI-CANCER AGENT

Makoto Otsuka,<sup>a</sup> Yoshihisa Matsuda,<sup>a</sup> Jer Hsu,<sup>b</sup> Jeffrey L. Fox<sup>b</sup> and William I. Higuchi<sup>b</sup>

Department of Pharmaceutical Technology,<sup>a</sup> Kobe Pharmaceutical University, Higashi-Nada, Kobe 658, Japan, phone +81-78-441-7531, FAX +81-78-441-7532

<sup>b</sup>Department of Pharmaceutics and Pharmaceutical Chemistry, University of Utah, Salt Lake City, Utah 84112, U.S.A.

## Introduction

The delivery of chemotherapeutic agents to bone via systemic routes of administration is problematic because of the serious side effects of these agents and the poor circulation to the bone. Hence, local delivery is an attractive option for these compounds.

Polymethylmethacrylate cements have demonstrated clinical success as a combination bone filler and local drug delivery system for fixing non-bioactive prostheses to the surrounding bone.<sup>1</sup> However, this cement has several clinical problems for long-term application.<sup>2</sup> On the other hand, hydroxyapatite (HAP) has an excellent bioaffinity with the hard tissues<sup>3</sup> and would therefore be a viable candidate for long term use. This has led us to investigate drug delivery systems for several drugs<sup>4-12</sup> which is transformed from metastable calcium phosphates into HAP. In the present study, we test the hypothesis that drug release can be controlled by factors within the anti-cancer drug, 6-mercaptopurine (6-MP)-containing cement such as its porosity and geometrical structure.

## Materials and Methods

**Materials** Tetracalcium phosphate (TTCP,  $\text{Ca}_4(\text{PO}_4)_2\text{O}$ ) and dicalcium phosphate dihydrate (DCPD,  $\text{CaHPO}_4 \cdot 2\text{H}_2\text{O}$ ) powders were obtained from Kyoritsu Ceramic Co., Japan and Nakalai Tesque Co., Japan. The HAP used as seed crystals was synthesized by a precipitation method<sup>13</sup> at 105°C. The bulk powder of calcium phosphate cement was prepared according to the procedure described by Brown and Chow.<sup>11</sup> The cement powder system was an equimolar mixture of TTCP and DCPD with added HAP seed crystals. (40%). Bulk 6-MP powder (lot No. 908) was obtained from Nihon Bulk Pharm. Co., Osaka, Japan. All other reagents were of analytical grade.

**Procedures for cement formation** Preparation of cement for release from a planar surface loaded on the bone: calcium phosphate cement powder (0.5 g) was mixed with 0.125-0.325 ml of 20 mM  $\text{H}_3\text{PO}_4$  for 1 min, then the drug powder (25 mg) was mixed with the paste. This mixture was then placed in a mold (8.5 mm in diameter, 3 mm in thickness) and stored at 37°C and 100% relative humidity for 24 h. The hardened cement pellet with the mold was mounted in a dissolution apparatus, so that the pellet surface (1.13 cm<sup>2</sup>) was exposed.

**Drug release test** Release profiles from all cement pellets containing the drug were measured as follows: A sample cement was introduced into 25 ml of simulated body fluid (SBF)<sup>14</sup> containing 142 mM of  $\text{Na}^+$ , 5.0 mM of  $\text{K}^+$ , 1.5 mM of  $\text{Mg}^{2+}$ , 147.8 mM of  $\text{Cl}^-$ , 2.5 mM  $\text{Ca}^{2+}$ , 4.2 mM of  $\text{HCO}_3^-$ , 0.5 mM of  $\text{SO}_4^{2-}$  and 1.0 mM  $\text{HPO}_4^{2-}$  (pH 7.25) in a 50 ml capped test tube. The tube was fixed on the sample holder in a thermostatically regulated water bath maintained at  $37.0 \pm 0.1^\circ\text{C}$  and shaken horizontally at 90 strokes/min. During the release test, the entire dissolution medium was replaced with fresh buffer at various intervals. The concentrations of 6-MP were measured spectrophotometrically (UV 160A, Shimadzu Co., Kyoto, Japan) at 321 nm. The data represents the average of 2 measurements from the independent experiments.

## Results and Discussion

The results of the effect of mixing solution volume on the drug release profiles from the surface of the cement systems containing 5% 6-MP in pH 7.25 SBF at 37°C suggested as follows: The drug release rates from both cements increased with increasing mixing solution volume, indicating that the volume determined the drug release rate, since the porosity of the cement matrix also depended on the volume. As reported previously,<sup>7-10</sup> the drug release profiles from the planar surface of homogeneous drug loaded calcium phosphate cement systems followed the Higuchi equation:<sup>15</sup>

$$M_t = AM_0 \sqrt{C_s \frac{D_i \epsilon}{\tau} (2C_d - \epsilon C_s) t} \quad \text{eq. 1}$$

where  $M_t$  is the amount of drug released from the cement at time  $t$ ,  $M_0$  is the total amount of drug,  $A$  is the surface area of the tablet,  $D$  is the diffusion coefficient of the drug,  $C_s$  is the solubility,  $C_d$  is the concentration of drug,  $\tau$  is the tortuosity and  $\epsilon$  is the porosity.

Therefore, the drug release was determined by the porosity and tortuosity of the cement pore.

The results of Higuchi plot (Fig. 1) for the drug release profiles from various kind of calcium phosphate cement suggested as follows: The drug release profiles from the drug loaded-cement matrix systems were analyzed by using equations 1, and the kinetic parameters were estimated using the least-squares computer program. The calculated values were in good agreement with the observed values under all drug release conditions. This result suggested that drug diffusion in the cement micro-pores determined the drug release rate from these cement systems.

The relationship between the mixing solution volume and the drug release rate constants for drug release from the surface of the calcium phosphate cements suggested as follows: The drug release rate constants from the cements increase linearly with increasing mixing solution volume, indicating that it was possible to control the drug release by varying the mixing solution volume.

## Conclusion

The drug release rate from homogeneous drug loaded calcium phosphate cements containing 6-MP increased with increasing mixing solution volume. The drug release profiles from the surface of the cement followed the Higuchi equation. Drug release rates were a function of the mixing solution volume. These results suggest that self-setting calcium phosphate cement skeletal drug-delivery systems could be developed into an effective treatment for localized bone cancers in patients following surgery.

## References

1. Salvati EA, Callaghan JJ, Brause BD, Klein RF, Small RD [1986] *Clin. Orthop.* 207: 83-93.
2. Petty W, Florida G [1978] *Bone J Jt Surg Am*, 60A: 752-757.
3. Aoki H [1991] "Science and medical applications of hydroxyapatite", p.137-163, Takayama Press, Tokyo
4. Otsuka M, Matsuda Y, Yu D, Wong J, Fox JL, Higuchi WI [1990] *Chem Pharm Bull*, 38: 3500-3502.
5. Yu D, Wong J, Matsuda Y, Fox JL, Higuchi WI, Otsuka M [1992] *J Pharm Sci*, 81: 529-531.
6. Otsuka M, Matsuda Y, Suwa Y, Fox JL, Higuchi WI [1994] *J Pharm Sci*, 83: 259-263.
7. Otsuka M, Matsuda Y, Suwa Y, Fox JL, Higuchi WI [1994] *Pharm Pharmacol Lett*, 3: 173-175.
8. Otsuka M, Matsuda Y, Fox JL, Higuchi WI [1994] *Pharm Pharmacol Lett*, 3: 183-185.
9. Otsuka M, Matsuda Y, Suwa Y, Fox JL, Higuchi WI [1994] *J Pharm Sci*, 83: 611-615.
10. Otsuka M, Matsuda Y, Suwa Y, Fox JL, Higuchi WI [1994] *J. Pharm. Sci.* 83: 255-258.
11. Brown, WE, Chow CL, U.S. Patent 4,612,053 [1986].
12. Takezawa Y, Doi Y, Shibata S, Uno K, Horiguchi T, Wakamatsu N, Kamezizu H, Gyotoku T, Adachi M, Moriawaki Y, Yamamoto K, Haeuchi Y [1989] *Jpn J Oral Biology*, 31: 240-247.
13. Wong J, Otsuka M, Higuchi WI, Powell GL, Fox JL [1990] *J Pharm Sci*, 79: 510-514.
14. Kokubo T, Yoshiwara S, Nishimura N, Yamamuro T [1991] *J Am Ceram Soc*, 74: 1739-1741.
15. Higuchi T [1963] *J Pharm Sci*, 52: 1145-1149.

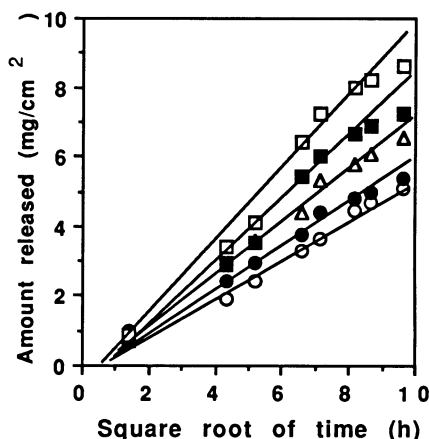


Fig. 1. Higuchi plot for drug release from 5% 6-MP-loaded calcium phosphate cements.  
 O, 0.25 ml/g; ●, 0.35 ml/g; △, 0.45 ml/g;  
 ■, 0.55 ml/g; □, 0.65 ml/g.

# AMINE EFFECT ON CONTROLLED RELEASE OF INSULIN FROM PHENYLBORONIC ACID GEL IN PHYSIOLOGICAL pH

Daijiro Shiino<sup>1,2)</sup>, Kazuo Matsuyama<sup>1,2)</sup>, Yoshiyuki Koyama<sup>2,3)</sup>, Kazunori Kataoka<sup>2,4)</sup>, Yasuhisa Sakurai<sup>2,5)</sup>, Teruo Okano<sup>2,5)</sup>

(1) NOF Corporation; Tokodai 5-10, Tsukuba-shi, Ibaraki 300-26, Japan

(2) International Center for Biomaterials Science; Yamazaki 2669-1, Noda, Chiba 278, Japan

(3) Otsuma Women's University; Sanbancyo 12, Chiyoda-ku, Tokyo 162, Japan

(4) Science University of Tokyo; Yamazaki 2641, Noda-shi, Chiba 278, Japan

(5) Tokyo Women's Medical College; Kawada-cho 8-1, Shinjuku-ku, Tokyo 162, Japan

## SUMMARY

An insulin delivery system comprising phenylboronic acid (PBA) hydrogel was investigated for efficacy at physiological pH by an addition of amino moiety. Release of gluconated insulin from hydrogel beads having PBA group responded to glucose concentration was strongly affected by the incorporation of amine group in the beads under physiological pH. Released G-Ins indicates 17600 mIU/cm<sup>3</sup>·day, that value is practical for in vivo application. These results indicate the feasibility of insulin delivery system consisting of PBA and amino groups at physiological conditions.

## KEY WORDS

Drug delivery, controlled release, insulin, glucose, phenylboronic acid

## INTRODUCTION

In recent years, there has been a great interest to introduce stimuli-responsive functions into synthetic polymers to realize so-called "intelligent materials". We have proposed that a totally-synthetic polymer hydrogel containing phenylboronic acid (PBA) moiety could be utilized as glucose recognition to achieve glucose responsive insulin release [1,2]. However this hydrogel is difficult to use in controlled release system in physiological pH = 7.4, because of unstable nature of the complex. In this study, amine effect was discussed on controlled release of insulin from amine containing PBA hydrogel beads in physiological pH.

## METHODS

A reversible type of suspension polymerization was utilized to make hydrogel beads of poly(acrylamidophenylboronic acid-co-N,N-dimethylaminopropylacrylamide-co-acrylamide-co-N,N'-methylene-bis(acrylamide)) (BAP). Measurements of released G-Ins from the polymerized beads were achieved using liquid chromatography system. BAP was swollen in phosphate buffer solution (pH = 7.4), then gluconated insulin (G-Ins) [1] was added to the beads. These beads were packed into a liquid chromatography column. Eluent solutions were alternatively cycled between the phosphate buffer solution and the glucose containing phosphate buffer solution at 0.2 ml/min. The concentrations of eluted G-Ins and glucose was monitored using a fluorescent detector (Ex = 275 nm, Em = 304 nm) and refractive meter, respectively.

## RESULTS AND DISCUSSION

The size of BAP diameter was determined with a microscope as a range of 100  $\mu\text{m}$  - 400  $\mu\text{m}$ . Plasma emission spectrometry and conductivity titration indicated the boron content:  $1.8 \times 10^{-4}$  mol/g and amine content:  $11.7 \times 10^{-4}$  mol/g. Figure 1 shows the concentration changes of glucose and G-Ins from BAP in physiological pH = 7.4. The release of G-Ins from BAP considerably correlated to the change in glucose concentration without delay. The amount of responded release of G-Ins was preferably maintained in spite of its multiple releasing. In other words, BAP showed less gradual decrease in the amount of release of G-Ins than PBA-system without amino group in physiological pH = 7.4. These results suggest that the addition of amino group in this PBA system strengthen the complex formation and the release response of G-Ins in physiological pH. Figure 2 describes the conceptional mechanism of this study using a polymer having PBA and amino groups.

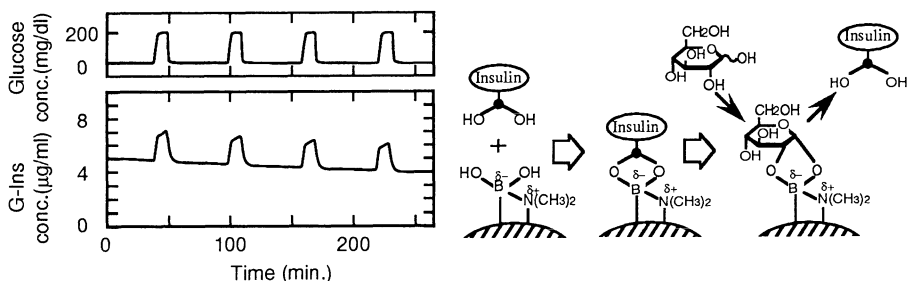


Fig.1 Release of G-Ins from BAP at pH = 7.4 Fig.2 Release mechanism of G-Ins from BAP

Makino et.al. has reported a microcapsule self-regulating delivery system for insulin using glucose sensitive protein of Con A. This system could release 3 mIU/cm<sup>3</sup>·day of succinyl-amidophenyl-glucopyranoside insulin [3]. On the other hand, our system has released 17,600 mIU/cm<sup>3</sup>·day of G-Ins. If a simplifying assumption can be made that one example need 24 IU/day, Con A-system needs about 8000 cm<sup>3</sup>, however, our system needs only 1.36 cm<sup>3</sup>. This value indicates that this amine containing PBA system is much more practical for in vivo application.

Further studies in the presence of the other compositions, such as plasma proteins and the other saccharides, and further studies on this polymer-based structure for the selectivity against glucose will provide completely chemical responsive on-off drug release with the goal of achieving a novel, promising totally synthetic artificial pancreas.

## REFERENCES

- [1] Shiino D, Murata Y, Kataoka K, Koyama Y, Yokoyama M, Okano T, Sakurai Y (1994) Preparation and characterization of a glucose-responsive insulin-releasing polymer device. *Biomaterials* 15: 121-128
- [2] Shiino D, Kataoka K, Koyama Y, Yokoyama M, Okano T, Sakurai Y (1994) A self-regulated insulin delivery system using boronic acid gel. *Journal of intelligent material systems and structures* 5: 311-314
- [3] Makino K, Mack EJ, Okano T, Kim SW (1990) A microcapsule self-regulating delivery system for insulin. *J. Control. Release*, 12: 235-239



# DRUG RELEASING MECHANISM FROM REDOX ACTIVE MICELLES

Yukikazu Takeoka\*, Takashi Aoki\*, Kohei Sanui\*, Naoya Ogata\*,  
Teruo Okano\*\*, Yasuhisa Sakurai\*\*, Masayoshi Watanabe\*\*\*

\* Department of Chemistry, Faculty of Science and Technology, Sophia University,  
7-1, Kioi-cho, Chiyoda-ku, Tokyo 102, Japan,

\*\*Institute of Biomedical Engineering, Tokyo Women's Medical College, 1-8 Kawada-cho,  
Shinjuku-ku, Tokyo 162, Japan

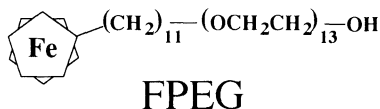
\*\*\*Department of Chemistry, Yokohama National University, 156 Tokiwadai, Hodogaya-ku,  
Yokohama 240, Japan

## SUMMARY

Electrochemical reaction of FPEG is coupled with the preceding disassembled reaction of micelles in aqueous solution. The change in diffusion species from the micelles to the monomers at cmc in the concentration gradient in diffusion layers appeared in case of bulk electrolysis of FPEG. The drug releasing mechanism from the redox active micelles were clarified.

## INTRODUCTION

The redox active non-ionic surfactant (FPEG) which has a ferrocenyl group as redox active site forms micelles. The micelles are disrupted by oxidation of the redox active sites [1]. We have shown that the electrochemical control of drug release from the micelles was achieved by using this system [2]. However, the releasing mechanism of drugs from the micelles has remained unclarified. The aim of this study is to clarify the electrode reaction of the redox active surfactant, and further, the drug releasing mechanism, for the ideal molecular design of this kind of drug carriers.



## MATERIALS AND METHODS

FPEG was purchased from Dojin Co. and used without further purification. All solutions of FPEG were prepared by normal saline solution. Cyclic voltammetry (CV) and chronoamperometry (CA) were conducted as electrochemical experiments. Glassy carbon electrode and SSCE were used as working electrode and reference electrode, respectively.

## RESULTS AND DISCUSSION

### CV

CV of FPEG showed concentration dependence in peak potentials (Fig. 1). CV analysis showed that electrochemical reaction of FPEG micelles was coupled with a preceding reaction [3]. According to the theory of Nicholson and Shain [4], FPEG is not electro-active as the micelles, while it is electro-active in monomer state dissociated from the micelles. This is understandable by considering that the micellar diameter is 80Å and ferrocenyl group is located in the hydrophobic core, because the possible distance for the electron transfer reaction between electrodes and substrates is normally less than 10Å [5-8]. Accordingly, the driving force to disrupt the micelle is the shifting of the micellar formation-disruption equilibrium by the electrochemical oxidation of FPEG (Fig. 2).

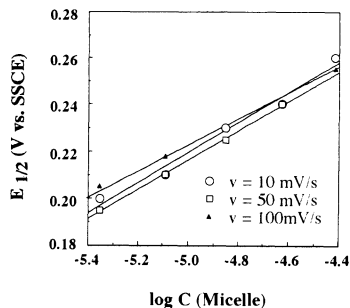


Fig. 1 Plots of formal potential of FPEG versus  $\log C$  ( $C$ : concentration of micelle)  $C = (C_m - cmc) / n$  ( $C_m$ : concentration of FPEG,  $n$ : aggregation number)

## CA

Furthermore, the disruption of the FPEG micelles to the monomer before the electrode reaction is clearly shown under the diffusion controlled condition, when, the concentration of FPEG at the electrode surface is zero. This condition was realized when the electrode potential was kept higher than the redox potential of FPEG in order to release drugs from the micelles. Specific diffusion layer was formed for the redox active surfactants [9] (Fig. 3). The hydrophobic drugs solubilized into the micelles were released at the area (AE) away from the electrode (Fig. 3). However, critical micelle concentration (cmc) of FPEG, in case of including the hydrophobic drug, is decreased because of the interaction between FPEG and the hydrophobic drugs. Therefore, the diffusion layer in case of including the hydrophobic drugs is changeable because of the change of cmc and aggregation number of micelles.

## CONCLUSION

It can be concluded that micelle-monomer equilibrium precedes the electrochemical reaction of FPEG. The electrochemical disruption of the micelle can be achieved due to the formation of the specific diffusion layer during the electrolysis.

## REFERENCES

- [1] Saji T, (1988) Electrochemical formation of a phthalocyanine thin film by disruption of micellar aggregates. *Chem. Lett.*, 693-696
- [2] Takeoka Y, Aoki T, Sanui K, Ogata N, Yokoyama M, Okano T, Sakurai Y (1995) Electrochemical control of drug release from redox-active micelles. *J. Controlled Release*, 33: 79-87
- [3] Takeoka Y, Aoki T, Sanui K, Ogata N, Watanabe M, Electrochemical studies of a redox-active surfactants. Correlation between electrochemical responses and dissolved states. *Langmuir*, submitted.
- [4] Nicholson R S, Shain I (1964) Theory of stationary electrode polarography. *Anal. Chem.* 36: 706-723
- [5] Marcus R A (1963) On the theory of oxidation-reduction reactions involving electron transfer. V. Comparison and properties of electrochemical and chemical rate constants. *J. Phys. Chem.* 67: 853-857
- [6] Marcus R A (1964) Chemical and electrochemical electron-transfer theory. *Annu. Rev. Phys. Chem.* 15: 155-196
- [7] Marcus R A (1965) On the theory of electron-transfer reactions. VI. Unified treatment for homogeneous and electrode reactions. *J. Chem. Phys.* 43: 679-701
- [8] Marcus R A, Sutin N (1985) *Biochem. Biophys. Acta.* 811: 265
- [9] Saji T, Hoshino K, Aoyagui S (1985) Reversible formation and disruption of micelles by control of the redox state of the head group. *J. Am. Chem. Soc.* 107: 6865-6868

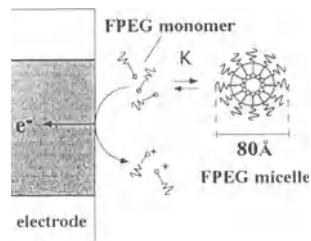


Fig. 2 Electrode reaction of the redox active surfactant in the case of forming micelle. K: micelle disruption equilibrium coefficient

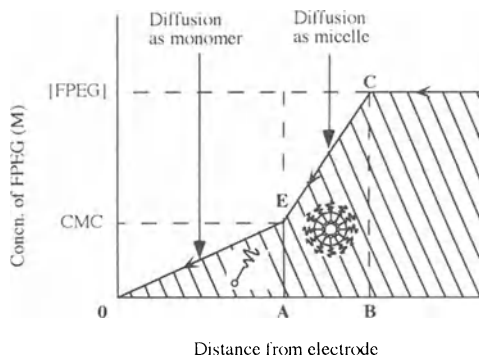


Fig. 3 Specific diffusion layer composed of redox active surfactants under diffusion controlled condition

# Author Index

- Abdellaoui, K. 57  
Abe, K. 257  
Akaike, Takaaki 339  
Akaike, Toshihiro 173, 215,  
287, 359  
Akashi, M. 183, 211, 219, 259,  
301  
Akatsuka, Y. 259  
Akimoto, T. 361  
Akiyoshi, K. 239, 331  
Akutsu, T. 247  
Anderson, J.M. 163  
Aoki, T. 263, 295, 371  
Aoyagi, T. 361  
Armitage, G.C. 106  
Arvanitoyannis, I. 241
- Babukutty, Y. 217  
Bahulekar, R. 223  
Bando, H. 363  
Barsotti, G. 299  
Baudys, M. 337  
Boustta, M. 57  
Brazel, C.S. 3  
Breschi, M.C. 355  
Britland, S. 158  
Bruil, A. 38
- Cammas, S. 325  
Castner, D.G. 142  
Chang, P.C.-T. 137  
Chang, Y. 249  
Chen, G.H. 62, 315  
Chiellini, E. 28, 299, 347,  
355  
Chiellini, E.E. 347  
Chiu, Y.-T. 249  
Cho, C.-S. 173  
Cho, C.-S. 287, 343  
Chowdhury, S.M. 179  
Cooper, S.L. 198
- Crommelin, D.J.A. 111  
Crommen, J. 81  
Curtis, A. 158
- DeFife, K.M. 163  
Deguchi, S. 331  
Ding, J.-L. 285  
Ding, Z.L. 62, 315  
Doi, Y. 229  
Dossi, E. 299
- Ekimoto, H. 327  
Endo, M. 273  
Esaki, A. 307
- Feijen, J. 38  
Fernandes, E.G. 347  
Fox, J.L. 367  
Fritzinger, B.K. 106  
Fujimoto, K. 231  
Fukushima, S. 327  
Furukawa, M. 283  
Furuzono, T. 183, 211
- Gakumazawa, H. 231  
Ge, S. 243  
Ghanem, A.-H. 111  
Giannasi, D. 299, 347  
Giovannetti, S. 299  
Glück, G. 279  
Gong, J. 8  
Goto, Masamitsu 275  
Goto, Mitsuaki 173, 287  
Grainger, D.W. 142
- Ha, J.-H. 343  
Hagiwara, K. 247  
Hara, Y. 255
- Harada, A. 317  
Haratake, M. 335  
Hashida, M. 86, 357, 363  
Hayashi, K. 241  
Hayashi, T. 289  
Heller, J. 106  
Herron, J.N. 111  
Higuchi, W.I. 111, 367  
Hirao, A. 261  
Hirayama, C. 307  
Hiroto, M. 297  
Hisamitsu, I. 281  
Hodgson, A.J. 309  
Hoffman, A.S. 38, 62, 237, 293,  
313, 315  
Horie, T. 257  
Hsiue, G.-H. 137  
Hsu, H.-L. 249  
Hsu, J. 367  
Hubbell, J.A. 179
- Ihara, H. 307  
Iijima, M. 205  
Ikada, Y. 168  
Imanishi, Y. 265  
Inada, Y. 297  
Inomata, Y. 231  
Inoue, H. 227  
Ishihara, K. 213, 227  
Ito, H. 207  
Ito, Y. 265  
Iwata, T. 307  
Iwatsuru, M. 351
- Jenney, C. 163  
Jeong, B.J. 188  
Jeong, S.Y. 365  
Jikihara, A. 237  
John, M.J. 309  
Jozefonvicz, J. 147  
Jozefowicz, M. 147

- Kaang, S.Y. 62  
 Kabra, B. 62  
 Kajiyama, T. 243  
 Kanamaru, T. 357  
 Kaneko, Y. 23, 303  
 Kano, J. 223  
 Kanzaki, Y. 313  
 Kao, C.-Y. 137  
 Kao, W.J. 163  
 Kasuya, Y. 231  
 Kataoka, K. 96, 205, 207, 225,  
 263, 281, 315, 317, 319, 321,  
 323, 325, 327, 329, 369  
 Katayose, S. 319  
 Kato, M. 205, 207, 323  
 Kato, S. 301  
 Kato, Y. 121, 345  
 Kawabuchi, M. 341  
 Kawaguchi, H. 231  
 Kawasaki, N. 241  
 Kelso, M. 309  
 Kido, T. 247, 261  
 Kikuchi, A. 23, 263, 267, 295,  
 303, 341  
 Kim, J.-H. 365  
 Kim, J.-S. 359  
 Kim, S.-H. 343  
 Kim, S.-I. 349  
 Kim, S.W. 126, 337, 359  
 Kim, Y.Ha 247  
 Kim, Yong Hee 365  
 Kim, Yong-Hee 111  
 Kimura, Y. 209, 349  
 Kinomura, K. 237, 293  
 Kishida, A. 183, 211, 219, 259,  
 301  
 Knutson, K. 116  
 Kobayashi, A. 173, 287  
 Kobayashi, K. 173, 215  
 Kodama, M. 217, 221, 223,  
 255  
 Kodera, Y. 297  
 Kogoma, M. 217  
 Kojo, K. 243  
 Kopeček, J. 91  
 Kopečková, P. 91  
 Kotani, S. 289  
 Koyama, Y. 369  
 Kuboyama, M. 239  
 Kugo, K. 233  
 Kuo, S.M. 269  
 Kurita, K. 227  
 Kuroda, S. 247  
 Kusumoto, S. 289  
 Kwon, G.S. 329  
 Kwon, I.C. 365  
 La, S.B. 321  
 Lee, H.B. 188  
 Lee, J.H. 188  
 Lee, S.-D. 137  
 Li, S.K. 111  
 Lin, H.-B. 198  
 Liu, K.-X. 345  
 Lu, J.-H. 249  
 Luttrell, A.S. 3  
 Maeda, H. 101, 339  
 Maeda, M. 235  
 Mahato, R.I. 357  
 Makino, K. 305  
 Makino, Y. 71  
 Manfait, M. 57  
 Mao, G. 142  
 Maruyama, A. 173, 359  
 Maruyama, I. 183, 211, 259  
 Maruyama, K. 351  
 Matsuda, T. 153, 253  
 Matsuda, Y. 367  
 Matsukata, M. 23, 295  
 Matsumoto, T. 183, 211  
 Matsushima, A. 297  
 Matsushita, H. 245  
 Matsutani, K. 233  
 Matsuura, T. 255  
 Matsuyama, K. 369  
 Mazzanti, G. 299  
 McNally, A.K. 163  
 Milstein, S. 51  
 Mix, D.C. 337  
 Miyata, T. 237, 313  
 Miyazaki, H. 225  
 Mlynek, G.M. 67  
 Mongia, N.K. 3  
 Morganti, F. 355  
 Morimoto, S. 307  
 Morishita, I. 71  
 Morishita, M. 71  
 Morjani, H. 57  
 Mu, G. 255  
 Nabeshima, Y. 315  
 Nagai, T. 71  
 Nagao, Y. 263  
 Nagasaki, Y. 205, 207, 323, 325  
 Nagase, Y. 361  
 Naito, M. 329  
 Nakabayashi, N. 193, 213, 227  
 Nakahama, S. 261  
 Nakamae, K. 237, 293, 313  
 Nakamura, M. 271  
 Nakamura, Takao 211  
 Nakamura, Teruo 323  
 Nakamura, Toshikazu 345  
 Nakayama, A. 241  
 Nakayama, Y. 253  
 Negishi, N. 245  
 Nishikawa, M. 86  
 Nishimura, H. 297  
 Nishino, J. 233  
 Nishino, T. 293  
 Nizuka, T. 313  
 Nojiri, C. 247, 261  
 Nomiyama, H. 217  
 Nomura, T. 357  
 Nozaki, Mikihiro 251  
 Nozaki, Motohiro 245  
 Ogata, N. 23, 32, 263, 295, 371  
 Ogura, F. 267  
 Ohmura, K. 301  
 Ohno, J. 245  
 Ohshima, H. 305  
 Ohya, Y. 353  
 Okahata, Y. 273  
 Okano, T. 23, 207, 225, 229,  
 251, 257, 263, 267, 281, 295,  
 303, 305, 321, 325, 327, 329,  
 341, 369, 371  
 Okazaki, S. 217  
 Okuhara, M. 267  
 Okumura, M. 237, 293  
 Okumura, Y. 275, 279, 285, 291  
 Okuyama, Y. 353  
 Omelyanenko, V. 91  
 Ooya, T. 333  
 Osada, Y. 8  
 Otsuka, M. 367  
 Ottenbrite, R.M. 51, 285  
 Ouchi, T. 353  
 Park, K.D. 247  
 Park, K.-H. 287  
 Peppas, N.A. 3  
 Randeri, K. 62  
 Rao, S.S. 106  
 Robinson, J.R. 67  
 Roskos, K.V. 106  
 Saiki, Y. 293  
 Saishin, M. 255  
 Sakai, H. 229

- Sakai, K. 23, 303  
 Sakai, K. 247  
 Sakamoto, N. 219  
 Sakata, M. 307  
 Sakurai, Y. 23, 207, 225, 229,  
     251, 257, 263, 267, 281, 295,  
     303, 305, 321, 325, 327, 329,  
     341, 369, 371  
 Sanui, K. 263, 295, 371  
 Sasatani, H. 349  
 Sato, T. 273  
 Sawa, T. 285  
 Sawai, K. 357  
 Schacht, E. 81  
 Senshu, K. 247, 261  
 Seto, T. 327  
 Seymour, L. 81  
 Shih, C.-C. 249  
 Shiiba, T. 283  
 Shiino, D. 369  
 Shin, Y.-H. 339  
 Sohn, Y.T. 365  
 Solaro, R. 28, 299, 347, 355  
 Song, S.C. 337  
 Suda, Y. 289  
 Sugawara, M. 257  
 Sugihara, M. 341  
 Sugimura, K. 301  
 Sugiyama, Y. 121, 345  
 Sunamoto, J. 76, 239, 271, 275,  
     277, 279, 285, 291, 331, 335  
 Sung, H.W. 249  
 Suzuki, Kazuya 219  
 Suzuki, Ken 207, 251, 257,  
     305  
 Suzuki, Ken-ichi 275  
 Suzuki, Y. 71  
 Taenaka, A. 207  
 Taira, H. 315  
 Takada, H. 289  
 Takagi, M. 235  
 Takahara, A. 243  
 Takakura, Y. 86, 357, 363  
 Takebe, Y. 209  
 Takemoto, K. 18  
 Takemura, N. 251  
 Takeoka, Y. 371  
 Takizawa, T. 351  
 Tamura, T. 289  
 Taniguchi, I. 331  
 Terada, E. 263  
 Terada, S. 251  
 Terasaki, T. 345  
 Terlingen, J.G.A. 38  
 Toda, T. 245  
 Tsai, S.W. 269  
 Tsujii, K. 271  
 Tsuruta, T. 315  
 Tsuruta, Teiji 43, 207  
 Uchio, T. 337  
 Ueda, Takehiko 239, 277  
 Ueda, Tsutomu 349  
 Ueno, Y. 259  
 Umeno, D. 235  
 Uragami, T. 237, 313  
 Usui, T. 215  
 Vakkalanka, S. 3  
 Vanderpe, J. 81  
 Vert, M. 57  
 Wallace, G.G. 13, 309  
 Wang, B. 255  
 Wang, Y.J. 269  
 Wang, Z. 221  
 Watanabe, A. 341  
 Watanabe, M. 371  
 West, J.L. 179  
 Yamada, N. 229, 263  
 Yamamoto, N. 241  
 Yamaoka, T. 209, 349  
 Yamashita, F. 363  
 Yamashita, S. 261  
 Yamauchi, A. 255  
 Yang, B. 116  
 Yokoyama, M. 327, 329  
 Yoneto, K. 111  
 Yoshida, M. 357  
 Yoshida, R. 303  
 Yoshida, Y. 293  
 Yui, N. 333  
 Yura, H. 173  
 Zhang, Z. 221  
 Zhao, R. 51  
 Zheng, J. 265  
 Zhou, Z. 291

# Key Word Index

- AB block copolymer 321, 329  
Ablation 253  
Acetonitrile 205  
Acetylcholinesterase 275  
Acrylamide 217  
Actin 163  
Acyclovir 363  
Adhesion factor 265  
Adhesion of tumor cells 273  
Adhesive tablet 71  
Adoptive immunotherapy 225  
Adriamycin 96, 327  
Adsorbed protein layer 251, 261  
Affinity chromatography 271  
Affinity latex 231  
Affinity separation 235  
Albumin 309  
 $\alpha$ -interferon 347  
Alginate gel bead 341  
1-alkyl-2-pyrrolidones 111  
Amino acid interactions 13  
Amino group 281  
Amphiphilic polysaccharide 331  
Anion-exchange capacity 307  
Anionic polymerization 205  
Anticoagulant activity 219  
Antihypertensive drugs 355  
Antisense oligonucleotide 121, 357  
Antithrombogenicity 217  
Antithrombogenic material 257  
Antitumor activity 327  
Aramid 211  
Artificial boundary lipid 271, 279  
Artificial cornea 137  
Artificial skin 245  
Artificial substrates 223  
Artificial thymus 245  
Artificial vitreous body 255  
Asialoglycoprotein 173  
Atmospheric plasma glow (APG) discharge 217  
Atomic force microscopy (AFM) 243  
Azo reductase 349  
Bacterial cell 289  
Band 3 275  
Binding activity 277  
Biocompatibility 193, 253, 255  
Bioconjugate 32, 235  
Biodegradable hydrogels M 91  
Biodegradable polymer 179, 241, 333, 341  
Biodegradation 81, 209, 365  
Bioerodible 343  
Bioerosion 106  
Biological patch 249  
Biological reaction 249  
Biomatrix 269  
Biomedical material 193  
Biomimetic glycopolymers 173  
Biomolecule conjugates 23  
Biorecognition of polymers 91  
Bioseparation 231  
Biospecificity random polystyrene derivatives 147  
4-{bis(trimethylsilyl)methyl}styrene 207  
Block copolymer 96, 207, 251, 317  
Block copolymer micelle 329  
Blood cell 227  
Blood compatibility 183  
11B-NMR 281  
Boronic acid 281  
Boundary lipid 277  
Bradykinin 339  
BSA 295  
Buccal delivery 116  
<sup>13</sup>C-Labeling 291  
Calcitonin delivery 126  
Capillary formation 263  
Cell activation 158  
Cell adhesion 188, 211  
Cell attachment 209, 223, 229  
Cell behaviour 158  
Cell culture 229, 263, 265  
Cell detachment 267  
Cell fusion 227

- Cell metabolism 267  
 Cell seeding 168  
 Cell spreading 273  
 Cell-polymer interaction 301  
 Cellulose 259  
 Cellulose membrane 213  
 Chaperones 51, 67  
 Chemical incorporation 327  
 Chemical modification 297  
 Chemomechanical 283  
 Cholesterol 331  
 Chromophore 239  
 Chronic uraemia therapy 299  
 Collagen 153, 269  
 Comb-shaped copolymer 297  
 Comb-type grafted hydrogel 303  
 Complement activation 213  
 Complexation 239  
 Computerized transmission electron microscopic image analysis 257  
 Concanavalin A 237  
 Conducting electroactive polymers 13  
 Conducting polymers 309  
 Confocal fluorescence microscopy 163, 335  
 Conformational transition 43  
 Controlled release 309, 347, 355, 369  
 Cooperativity 8  
 Corona discharge 188  
 Corynanthine 355  
 Cross-linking characteristics 249  
 Cyanomethylpotassium 205  
 Cyclodextrin derivatives 28  
 Cytokine 301
- Deprotection 207  
 Dialyzer 259  
 Diffusion 116  
 Dimethylsulfoxide 239  
 Dissolution rate 321  
 DNA-like antigen 147  
 Doxorubicin 329  
 Drug delivery 369  
 Drug delivery system (DDS) 76, 121, 321, 325, 357  
 Drug loading 325  
 Drug release 28, 106
- Electro-osmosis 305  
 Electrostatic interaction 8, 317  
 Emulsion 76  
 Endothelial cell 153, 198, 263  
 Endotoxin 307  
 Enhancement factor 111  
 Enhancer 361  
 Enzyme 32
- Epidermal growth factors 3, 121  
 Epifluorescent video microscopy 247  
 Epithelium 137  
 Epoxy compound 249  
 $\epsilon$ -caprolactone 241  
 ePTFE 221  
 Erythrocyte 275  
 Excimer laser 253  
 Extracellular matrix 153
- Factor VIII-like antigen 147  
 Faster deswelling 303  
 Fibrinolytic 179  
 Fibrinolytic enzymes 3  
 Fibroblast 285, 287  
 Fibronectin 233  
 Fluorescence anisotropy 111  
 Fluorescent labelling 57  
 Fluorination 38  
 Foreign body giant cell 163  
 FTIR ATR 233  
 Functional polymeric micelles 325  
 Fusion 335
- Galactose receptor 86  
 Galactose-carrying polystyrene 173  
 $\gamma$ -irradiation 255  
 Gel 8, 281  
 Gene carrier 359  
 Gene vector 319  
 Glow discharge treatment 38  
 Glucose 369  
 Glucose transporter 173  
 Glucose-sensitivity 237  
 Glucoside polymer 219  
 Glucosyloxyethylmethacrylate 293  
 Glycoconjugates 263  
 Glycolipid 273, 289  
 Glycophorin A 291  
 Glycosylated insulin 337  
 Gold 142  
 Gradient surfaces 188  
 Graft copolymers 315  
 Grafted substrate 229  
 Growth factor 265  
 Growth promotion 285  
 Guided tissue regeneration 209
- Healing 179  
 HEMA-St ABA type block copolymer 257  
 HEMA/styrene block copolymer 261  
 Hemodialysis membrane 213  
 Heparin 51, 247, 345

- Heparin delivery 315  
Heparinoid 219  
Hepatocyte growth factor (HGF) 121, 345  
Hepatocytes 173  
Heterobifunctional PEO/PBLA block copolymers 325  
Heterobifunctional poly(ethylene glycol) 323  
Human growth hormone 67  
Human serum albumin 347  
Human thrombomodulin 259  
Hyaluronic acid 18  
Hybrid graft 153  
Hybrid hydrogels 347  
Hydrogel 23, 28, 193, 237, 255, 299, 331  
Hydrogel composite 309  
Hydrogel containing phosphate groups 313  
Hydrolysis 241  
Hydrophilic/hydrophobic surface property changes 267  
Hydrophilicity 217  
Hydrophobic interaction 8  
Hydrophobized polysaccharide 239  
Hydroxyl containing polycarbonates 28  
Hydroxyl containing polyesters 28
- IL-2 225  
Immobilization 259, 265  
In vivo 221  
Indomethacin 321  
Inert surface 43  
Insulin 265, 369  
Insulin aggregation 337  
Insulin delivery 126, 281  
Insulin physical stability 337  
Insulin receptor 277  
Integrin 231  
Interferon 51  
Interleukin-4 163  
Interleukin-6 289  
Interpenetrating polymer networks (IPNs) 343  
Intestinal flora 349  
Intracellular uptake 57  
Ion exchange mechanism 313  
Ionic gel 283  
Ionic interactions 13  
Ionic strength 307
- Keratinocytes 245  
Killer cell 225  
Kunitz-type soybean trypsin inhibitor (SBTI) 339
- L-asparaginase 297
- $\lambda$  phage DNA 235  
Lactate dehydrogenase 293  
Lactide 241  
Langmuir-Blodgett(LB) film 287  
Large-intestine-degradable polymer 349  
Laser-Microspectrofluorometry (L-MSF) 57  
Leukocyte adhesion 38  
Lipoproteins 359  
Liposomal vaccine 76  
Liposome 76, 271, 275, 279, 335, 353  
Local delivery system 365  
Long-circulating carrier 96  
Lymphocyte proliferation 225  
Lysozyme 317  
Lysozyme release 313
- MACDA 285  
Macromer 343  
Macromolecular drug delivery 126  
Macromolecular prodrug 57  
Macrophage 301  
Mammalian cells 13  
Materials design 43  
Melting curve 319  
Membrane lung 207  
Membrane protein 271, 279  
Membrane protein transfer 275  
2-Methacryloyloxyethyl phosphorylcholine 193  
Methyl group 291  
Micelle forming polymeric drug 327  
Micro-separated structure 287  
Microdomain structure 43, 251  
Microfabrication 158  
Microporous 221  
Microprocessing 253  
Microspheres 71  
Mitogen 225  
Mitomycin C 81  
Modified cyclodextrins 355  
Molecular design 86  
Molten globular state 67  
Monolayer 279  
mRNA expression 301  
Multiblock copolymer 183, 211  
Murine B16 melanoma cell 335
- Nano-associates 317  
Nanofabrication 158  
Nanoparticle 331  
Nasal powder 71  
Natural polymer 289  
Neocarzinostatin 239  
Nifedipine 355  
Non-enzymatic cell detachment 229



- Nonthrombogenicity 193, 227  
 Nucleic acid base 18  
 Nylon 269
- Optical resolution 32  
 Oral delivery of proteins 91  
 Oral drug delivery 51  
 Organ perfusion experiment 357  
 Organosilane monolayer 243  
 Oxidized polysaccharides 299  
 Oxprenolol 355  
 Oxygen permeability 183  
 Ozone-induced graft copolymerization 247
- Partition 361  
 PEG modified insulin 337  
 Penetrating keratoplasty 137  
 PEO-chymotrypsin conjugates 91  
 PEO-dextran conjugates 91  
 Peptides 198  
 Percutaneous absorption 363  
 Periodontitis 106  
 Permeation 116  
 pH-sensitive 315  
 pH-sensitive gels 3  
 Pharmacokinetics 357  
 Phase-separated structure 243  
 Phenylboronic acid 225, 263, 369  
 Phospholipid 193, 273  
 Phospholipid polymer 213, 227  
 Photo-induced drug delivery system 353  
 Photochromic 353  
 Photocrosslinking of proteins 91  
 Physical incorporation 327  
 Pilot molecule 323  
 Plasma 269  
 Plasma immobilization 38  
 Plasma induced grafted polymerization 137  
 Platelet adhesion 213, 227  
 Platelet plasma membrane glycocalyx 257  
 Platelet ultrastructure 257  
 Poly(acrylamides) 223  
 Poly(dimethylsiloxane) 183, 211, 361  
 Poly( $\epsilon$ -N-benzyloxycarbonyl-L-lysine) 233  
 Poly(ethylene glycol) 179, 297, 317  
 Poly(ethylene oxide) 188, 205, 329  
 Poly(ethylene oxide)-bearing lipid 335  
 Poly(L amino acid) 329  
 Poly(L-lactide) 365  
 Poly(lactic acid) (PLLA) 209  
 Poly(*N*-isopropylacrylamide) 23, 32, 229, 235, 267, 295, 303, 305  
 Poly(ortho ester) 106  
 Poly(siloxanes) 142
- Polyamine copolymers 43  
 Polyamino acid 18  
 Polyanion polymer 285  
 Polyelectrolyte 8  
 Polyester 241  
 Polyethyleneimine 18  
 Polyion complex 96, 227, 319  
 Polylysine 319  
 Polymer micelle 96, 321  
 Polymer scaffold 168  
 Polymer with pendant glucose groups 237  
 Polymers 158  
 Polyoxyethylene 361  
 Polyphosphazenes 81  
 Polypyrrole 309  
 Polyrotaxanes 333  
 Polysaccharide analogue 219  
 Polystyrene 233  
 Polyurethanes 163, 198, 221, 283  
 Porosity 307  
 Potassium naphthalene 205  
 Prodrug-enhancer combination 363  
 Protein adsorption 188, 193, 211, 213, 227, 243  
 Protein drug 76  
 Protein transfer 277, 279  
 Proteinoid microspheres 51  
 Proteinoids 67  
 Pseudomonas elastase 339  
 Pulsatile release 341  
 PVA 255
- Quartz-crystal microbalance (QCM) 273, 277
- Rapid conformational changes 303  
 Receptor-mediated endocytosis 86, 121, 323  
 Reducing monosaccharide residue 323  
 Retained activity 293  
 RGD 209  
 RGD binding 198  
 RGDS 231  
 RT-PCR 301
- Safe polymer 71  
 SBTI-succinylated gelatin conjugate (Suc-gel-SBTI) 339  
 Secondary structure 233, 291  
 Segmented polyurethane 349  
 Selective removal 307  
 Self-assembled biomimetic membrane 193  
 Self-assembly 142, 331  
 Semitelechelic oligomer 295  
 Serum-free culture 285

- Shock model 339  
Short chain n-alkanols 111  
Silicone rubber membrane 137  
Skin immunology 245  
Small vascular graft 251  
Smooth muscle cells 359  
Soft surfaces 305  
Spacer 231  
Spiropyran 353  
Stability 325  
Stability of enzyme 293  
Stabilization of enzyme 297  
Stimuli-sensitivity 313  
Stratum corneum lipid liposomes 111  
Stress proteins 67  
Sugar residues 223  
Sugar-PEG 323  
Sulfonated polyurethane 247  
Superoxide dismutase 86  
Supramolecular structure of polymers in solution 91  
Supramolecular structures 333  
Surface analysis 183  
Surface gelation 253  
Surface modification 23, 142, 213, 247  
Surface restructuring 261  
Surface structure control 243  
Sustained release 341  
Swellable polymers 3
- Targetable polymeric prodrugs 91  
Targeting 86  
Targeting the large intestine 349  
Taste receptor 271
- Teflon-like surfaces 38  
Temperature-responsibility 23  
Temperature-responsible surfaces 267  
Temperature-responsive bioconjugate 295  
Temperature-sensitive 315  
Temperature-sensitive gels 3  
Temporal drug delivery 333  
Terplex 359  
Tetracycline 106  
Thermosensitivity 303  
Thermosensitive hydrogels 126  
Thymopoietin II 245  
Tissue engineering 168  
Tissue regeneration 168  
Tissue substitution 168  
Tissue-isolated tumor preparation 357  
Transbuccal 116  
Transdermal penetration 361  
Transfection 359  
Transmission electron microscopy 261  
Transport mechanisms 116  
Trypsin 32, 293  
Tumor necrosis factor- $\alpha$  289
- Ultrathin films 142  
Urea up-take 299
- Vascular graft 221, 261
- Water interactions 13  
Water solubility 18